Large Scale Integration of Micro-Generation to Low Voltage Grids

Contract No: ENK5-CT-2002-00610

WORK PACKAGE E

Deliverable DE2

PROTECTION GUIDELINES FOR A MICROGRID

Final Draft

June 2005

Document Information

Title	Protection Guidelines for a MicroGrid
Date	June 2005
Version	Final Draft
Task(s)	TE4, TE5

Coordination: Prof. Nick Jenkins nick.jenkins@manchester.ac.uk

Authors:
Xueguang Wu w.xueguang@manchester.ac.uk
Nilanga Jayawarna t.jayawarna@postgrad.manchester.ac.uk
Yibin Zhang zhangyb@epri.ac.cn
João Peças Lopes jpl@fe.up.pt
Carlos Moreira cmoreira@inescporto.pt
André Madureira agm@inescporto.pt
Jose Pereira da Silva jls@fe.up.pt

Access:	
Project Consortium (for the actual version)	
European Commission, PUBLIC (for final version)	
Status:	
	Draft Version
	Final Version (internal document)
X	Submission for Approval (deliverable)
	Final Version (deliverable, approved on.)

Contents

Chapter 1 Introduction

A MicroGrid consists of a cluster of micro sources, energy storage systems (e.g. flywheel) and loads, operating as a single controllable system. The voltage level of the MicroGrid is 400 Volts or less. The architecture of the MicroGrid is formed to be radial with a number of feeders. The MicroGrid often provides both electricity and heat to the local area. The MicroGrid can be operated in both grid-connected mode and islanded mode

The micro sources are usually made of many new technologies, e.g. micro gas turbine, fuel cell, photovoltaic system and several kinds of wind turbines. The energy storage system often is a flywheel system. The micro sources and flywheel are not suitable for supplying energy to the grid directly [Barsali, 2002]. They have to be interfaced with the grid through an inverter stage. The use of power electronic interfaces in the MicroGrid thus leads to a series of challenges in the design and operation of the MicroGrid. One of the major challenges is protection design of the MicroGrid to comply with the relevant national Distribution Codes and to maintain the safety and stability of the MicroGrid during both grid-connected mode and islanded mode.

The MicroGrid is also subject to the same safety and stability requirements as any other utility electric power system. The basic principles of the protection are the reliability, selectivity, speed and cost. The protection of the MicroGrid must respond to both main network and MicroGrid faults. If a fault is on the main network, the desired response may be to isolate the MicroGrid from the main network as rapidly as necessary to protect the MicroGrid loads. If a fault is within the MicroGrid, the protection system may only isolate the smallest possible faulted section of the MicroGrid to eliminate the fault.

However, the inverter based MicroGrid can not normally provide the required levels of short circuit current. In extreme cases, the fault current contribution from the micro sources may only be twice load current or less [Wall, 2001]. Some overcurrent sensing devices will not even respond to this level of overcurrent. In addition, the

over/under voltage and frequency protection may fail to detect faults on the MicroGrid due to the voltage and frequency control of the MicroGrid.

The unique nature of the MicroGrid requires a fresh look into the design and operation of the protection. One approach is to develop a real-time fault location technique that will identify the exact location of the fault. This is likely to be costly, as fast communication is needed between the protection devices installed at different locations. Lower cost approaches such as distance protection and differential protection show promise. Although these methods are not in common use on distribution networks, they can provide the functions required by the MicroGrid. In addition, the protection of the MicroGrid can be achieved by using conventional overcurrent-based protection devices if the flywheel supplies 3-5p.u fault current during islanded mode. However, to meet coordination of the protection systems, the protection on the main network may take seconds to respond to the fault on the network, rather than the fraction of a second that is necessary for the safety and stability of the MicroGrid operated in islanded mode. The MicroGrid may be unstable due to a long fault clearance time taken by such protection. Thus, to maintain the stability of the MicroGrid, faster protection (e.g. differential protection) is needed to protect the main network.

The control of the micro sources and the flywheel is very important to maintain the safety and stability of the MicroGrid during all times. For basic operation of the MicroGrid, the controllers should use only local information to control the flywheel and micro sources. Hence, fault communication between the micro sources and the flywheel is unnecessary. For a micro source, the inverter should have plug and play capabilities [Lasseter, 2002]. Plug and play implies that a micro source can be added to the MicroGrid without any changes to the control of the units, which are already a part of the network. For the flywheel, the inverter should be able to respond to the change of load in a predetermined manner automatically.

The possible control strategies of the micro sources and the flywheel are: (a) PQ control (fixed active and reactive power control), (b) Droop control and (c) Frequency/Voltage control. The MicroGrid may be unstable if the flywheel uses PQ control at all times. In this case, the flywheel can't supply dynamic active and reactive

power compensation to the MicroGrid during islanded mode due to its constant output power. PQ control is adopted only when the micro sources and the flywheel need to run on constant power output. The electricity, generated by the micro source, may be constant because of the need of the associated thermal load. The output power of the flywheel can be fixed at zero when the MicroGrid is operated in parallel with the main network, grid-connected mode. During islanded mode, the stability of the MicroGrid can be improved by using Droop control or Frequency/Voltage control of the flywheel. With Droop control, the output active and reactive powers of the flywheel are regulated according to their droop settings. With Frequency/Voltage control, the frequency and voltage of the MicroGrid are restored to normal values (e.g. f=50Hz and V=1.0p.u).

In this report, Chapter 2 proposes the possible protection schemes for a MicroGrid. For a fault on the main distribution network, overcurrent relay protection and balanced earth fault (BEF) protection can be installed at the grid side of the circuits between the main distribution network and the MicroGrid, with the capability of intertripping the MicroGrid. To maintain the stability of the MicroGrid, fast protection (e.g. differential protection) can be used on the main distribution network. For a fault on the MicroGrid, overcurrent relay protection and residual current device (RCD) are used to protect the feeder from the fault. During the fault, the flywheel supplies a high fault current (e.g. 3 p.u based on its rating or above) if the MicroGrid is operated in islanded mode. After the fault, the protection disconnects the faulty feeder from the MicroGrid and has the capability of inter-tripping all the micro sources on the feeder at the same time. Discrimination of the protection can be achieved by using a time delay. For a fault at the residential consumer, a short circuit protection device (SCPD), e.g. a miniature circuit breaker (MCB) or fuses, and a RCD can be installed at the grid side of the residential consumer. The SCPD is used to protect the residential consumer against the phase-to-phase and phase-to-neutral faults. The RCD is used for the phase-to-ground fault (earth fault).

Chapter 3 investigates the stability of a MicroGrid. Three control strategies, (a) PQ control, (b) Droop control and (c) Frequency/Voltage control, of the MicroGrid are described and tested. Based on the three control schemes, three representations, (1) synchronous generator representation, (2) STATic Synchronous Shunt COMpensator

with battery energy storage, STATCOM-BES, representation, and (3) controllable AC or DC voltage source representation, of the MicroGrid are implemented and tested in PSCAD/EMTDC. For different characteristics of load, locations of fault and inertia constants of motor, the stability (critical clearing time, CCT) of the MicroGrid is investigated. Finally, a traditional method (undervoltage load shedding) is used to improve the stability of the MicroGrid. Simulations of the stability of the MicroGrid are demonstrated and discussed with supporting PSCAD/EMTDC results.

1.1 UK perspective

Protection and operation of a MicroGrid in the UK must comply with the Distribution Code [Ofgem, 2004]. The Distribution Code specifies standards for the design and operation of Public Electricity Supplier (PES) - owned distribution networks. The Distribution Code requires users of distribution networks, such as MicroGrids, to provide certain information about new loads and generator installations in the network. The Distribution Code also specifies arrangements for the design of the MicroGrid connections to PES networks, and certain requirements for the protection of the MicroGrid. The protection of the MicroGrid must co-ordinate properly with the protection on the PES network.

To connect embedded generation to distribution networks, the UK Electricity Association published an engineering recommendation G59/1 (G59) [G59, 1991] and an engineering technical report 113 (ETR 113) [ETR 113, 1995]. G59 strictly applies only to generation under 5MW and connected at 20kV or below. The protection introduced in G59 is also fitted for all MicroGrid connections. ETR 113 provides further advice on the protection arrangements stated in G59. The title of ETR 113 is "Notes of Guidance for the Protection of Embedded Generating Plant up to 5MW for Operation in Parallel with Public Electricity Suppliers' Distribution Systems". The essential objective of G59 and ETR 113 is to safeguard the network and the connection of distributed generation. It is noted that the protection of a MicroGrid is owned and operated by the MicroGrid. The MicroGrid is therefore given the responsibility for the protection of the distribution network. The interface protection between the distribution network and the MicroGrid is required to protect the network from the fault current flowing into or out of the MicroGrid.

Chapter 2 Protection of a MicroGrid

In a traditional distribution system, the protection systems are designed assuming unidirectional power flow and are usually based on overcurrent relays with discriminating capabilities. For any fault situation, Distributed Generation sources (DG) connected to the system are tripped off. In other words, islanded operation of DG sources is not allowed.

The MicroGrid is a system designed to operate when interconnected to the distribution system as well as when disconnected from it. These two operating modes introduce a challenge in protection of a MicroGrid. When the MicroGrid is connected to the main grid, the grid sources provide high fault currents that can be used to detect faults. However, we cannot expect such large fault current contribution from the MicroGrid, which is dominated by power electronic interfaces. And then, using conventional overcurrent protection in the MicroGrid is not promising due to this low short circuit current of the MicroGrid, especially, when it is operated in islanded mode. It is quite obvious that alternate means of detecting an event within an isolated MicroGrid must be studied and new protection systems have to be devised.

The ideal protection systems of the MicroGrid should possess the following features:

a. Must respond both to distribution system and MicroGrid faults,
b. For a fault on the main grid, isolate the MicroGrid as quickly as possible,
c. For a fault within the MicroGrid, isolate the smallest possible section of the radial feeder carrying the fault to get rid of the fault,
d. Effective operation of customers' protection

From the above, points a and b are clear enough. Point c indicates that if a fault occurs within the MicroGrid, the protection should only isolate the faulted feeder from the MicroGrid and have the capability of intertripping all micro sources on the feeder. Point d requires coordination of protection of the MicroGrid with the customers' protection. The protection of the MicroGrid should follow the same principles as the electrical protection in the conventional network.

2.1 Principles of the protection of a MicroGrid

The basic principles of the electrical protection of the network are [Gers, 1998]:

(1) **Reliability**, the ability of the protection to operate correctly. Under the occurrence of a fault or abnormal condition, the protection must detect the problem quickly in order to isolate the affected section. The rest of the system should continue in service and limit the possibility of damage to other equipment.

(2) **Selectivity**, maintaining continuity of supply by disconnecting the minimum section of the network necessary to isolate the fault.

(3) **Speed**, minimum-operating time to clear a fault in order to avoid damage to equipment and maintain stability.

(4) **Cost**, maximum protection at the lowest cost possible.

The principles above show that it is practically impossible to satisfy all the above mentioned points simultaneously. A compromise is required to obtain the optimum protection system for a MicroGrid.

2.2 Main protection schemes in distribution network

Generally, the main electrical protection schemes in distribution networks are overcurrent protection, differential protection, distance protection and zero sequence protection.

2.2.1 Overcurrent protection

Overcurrent protection detects the fault from a high value of the fault current. The common types of overcurrent protection are thermomagnetic switches, moulded-case circuit breakers (MCCB), fuses and overcurrent relays. A typical overcurrent relay protection scheme is shown in Figure 2.1.

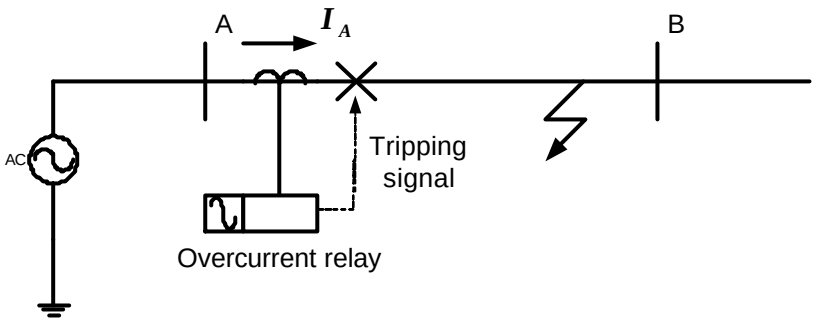

Figure 2.1 Overcurrent relay protection

A typical setting of an overcurrent relay is 50% of the maximum short-circuit current at the point of connection of the relay or 6-10 times the maximum circuit rated current. The relay measures the line current using a current transformer (CT). If the current is above the setting, the relay operates to trip the circuit breaker on the line.

According to the characteristics of the overcurrent relay, it can be classified into three groups: (1) definite current relay; (2) definite time relay; and (3) inverse time relay, as shown in Figure 2.2 (a), (b) and (c) [Gers, 1998].

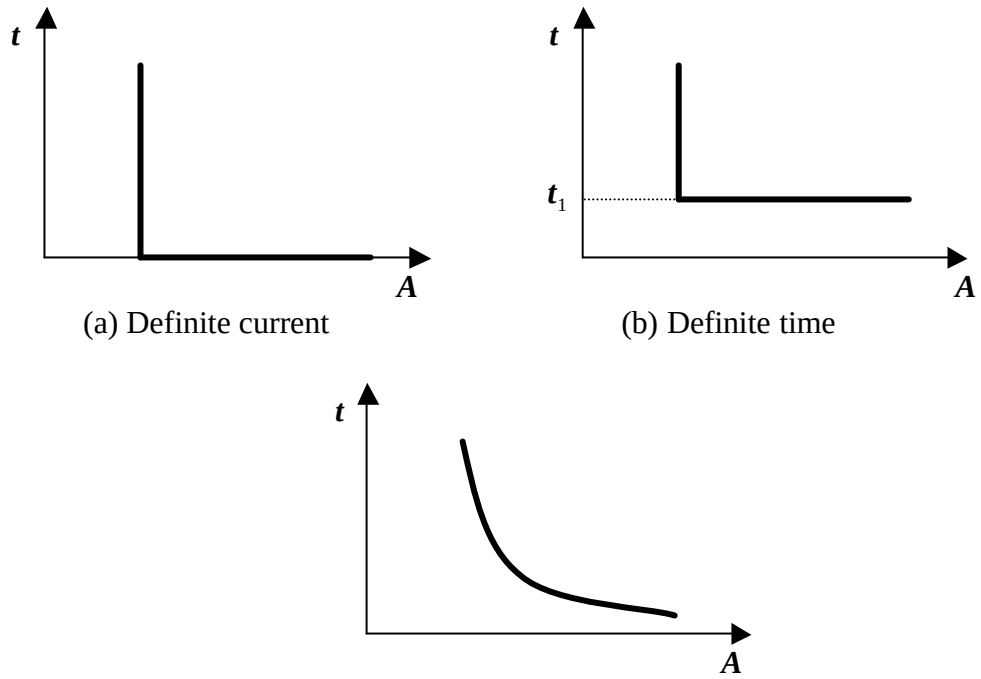

(a) Definite current

(b) Definite time

(c) Inverse time

Figure 2.2 Time/current operating characteristics of the overcurrent relay

The definite current relay operates instantaneously when the current reaches a predetermined value. This type of relay has little selectivity. If the settings of the relay

are based on the maximum fault level conditions, the settings may not be appropriate for a low fault level. However, if a lower value of fault level is used for settings, some protection devices may operate unnecessarily, leading to nuisance tripping.

The definite time relay operates in a certain time. The setting can be adjusted to cope with different levels of current by using different operating times. The disadvantage of this type of relay is that the faults, which are near to the main source, may be cleared in a relatively long time.

The inverse time relay operates in a time, which is inversely proportional to the fault current. The advantage of this type of relay is that the higher the fault current, the shorter is the tripping time. The inverse time relay provides improved protection selectivity.

2.2.2 Differential protection

Differential protection operates when the vector difference of two or more similar electrical magnitudes exceeds a predetermined value (setting). The most common type of differential protection is the overcurrent relay differential protection. A simple overcurrent relay differential protection is shown in Figure 2.3.

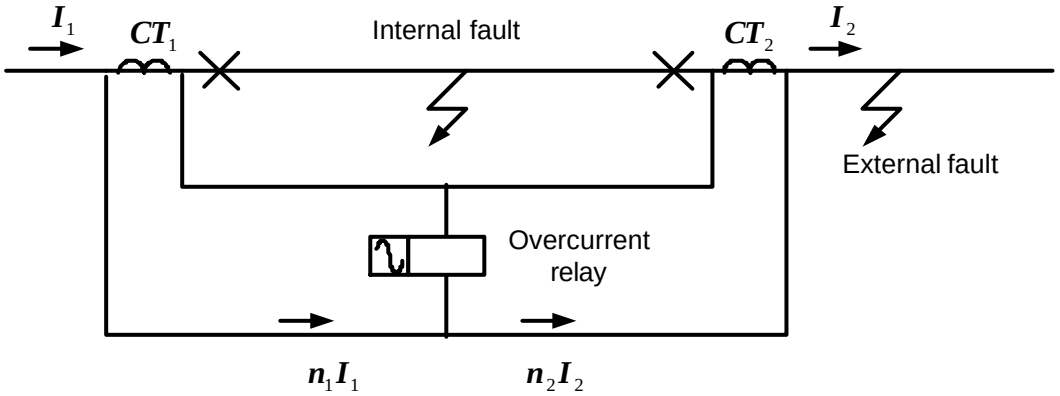

Figure 2.3 A simple overcurrent relay based differential protection

Figure 2.3 shows that an overcurrent relay is connected to the secondary sides of the current transformers CT1 and CT2. The protection zone is between CT1 and CT2. Under normal load condition or when there is a fault outside of the protection zone

(external fault), the secondary currents $\boldsymbol{n}_1\boldsymbol{I}_1$ and $\boldsymbol{n}_2\boldsymbol{I}_2$ would circulate between CT1 and CT2. In other words, the current $\boldsymbol{n}_1\boldsymbol{I}_1$ is equal to $\boldsymbol{n}_2\boldsymbol{I}_2$. There is no current flowing through the overcurrent relay. However, if a fault occurs in the section between CT1 and CT2 (internal fault), the fault currents would flow towards the faulted point from both sides of the element. The current flowing through the overcurrent relay is the sum of the secondary currents, $\boldsymbol{n}_1\boldsymbol{I}_1+\boldsymbol{n}_2\boldsymbol{I}_2$. In all cases the current in the overcurrent relay is proportional to the vector difference between the currents, which enter and leave the protected element. If the current flowing through the overcurrent relay exceeds the setting, the overcurrent relay will operate and send a signal to trip the circuit breakers at two terminals of the element. As a result, the faulted section is isolated from the network.

For an application of differential protection to an extensive network, the relays should be located at the terminals of the protected element to monitor the electrical quantities (e.g. the line currents) required for the trip decision of the protection. The data relating to the state of the network must be transferred from the remote terminal(s) to the local terminal and then compared with data obtained at the local terminal. This requires the use of a communication system for data transfer. Ideally, the communication system should instantaneously transfer all the data required for the protection between the relays. Usually, the communication system can use metallic conductors (pilot wires), optical fibres, or free space via radio or microwave as its communication medium.

The main advantage of differential protection is its high selectivity. The differential protection scheme only operates in the case of an internal fault. However, the requirement for separate back-up protection and the additional cost of the communication system may limit the application of differential protection in the MicroGrid.

2.2.3 Distance protection

Distance protection uses an impedance measured by the distance relay to detect the faults on the network. The distance relay compares the fault current against the

voltage at the relay location to calculate the impedance from the relay to the faulty point.

Figure 2.4 shows a distance protection scheme. The distance relay is located at busbar A. The line current $\boldsymbol{I}$ and busbar voltage $\boldsymbol{V}$ are used to evaluate the impedance $\boldsymbol{Z} = \boldsymbol{V}/\boldsymbol{I}$. The value of measured impedance of the distance relay is $\boldsymbol{Z}_{\boldsymbol{AF}1}$ for a fault F1 and $(\boldsymbol{Z}_{\boldsymbol{AB}} + \boldsymbol{Z}_{\boldsymbol{BF}2})$ for a fault F2.

The zones of the distance protection normally consist of Zone 1, Zone 2 and Zone 3. It is usual for Zone 1 to be 80-85% length of the protected line. Zone 2 is 150%, covering 100% length of the protected line plus 50% next shortest adjacent line. Zone 3 is 225%, covering 100% length of the protected line plus 100% second longest line, plus 25% shortest next line.

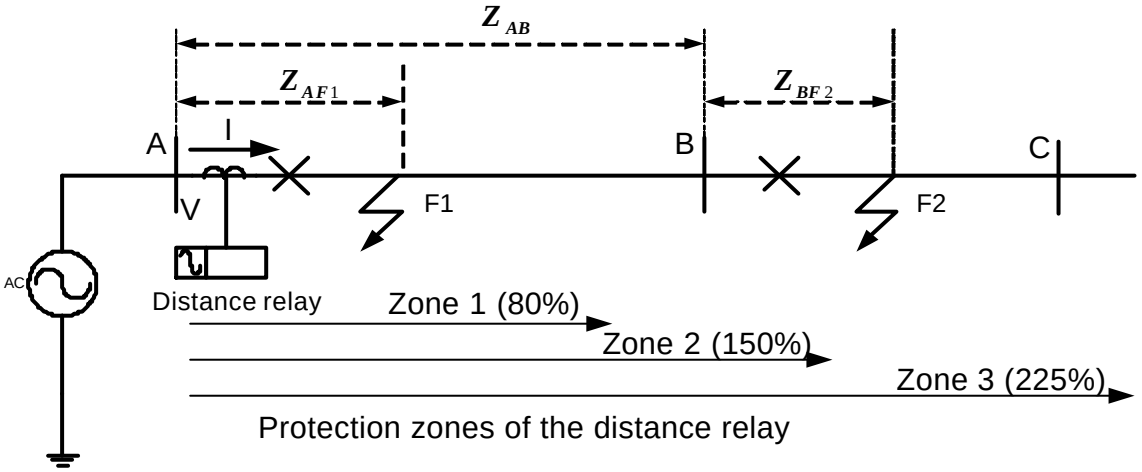

Figure 2.4 A typical distance protection scheme for the faults on the network

On the plane of the resistance (R) and reactance (X), the distance relay could be classified into the impedance relay, directional relay, reactance relay, mho relay, completely polarised mho relay and combined relay, etc. The impedance relay is a basic type of the distance relay. It operates in a circular impedance characteristic with its centre at the origin of the co-ordinates and a radius equal to the setting of the distance relay in ohms. Figure 2.5 shows the typical characteristics of the impedance relay.

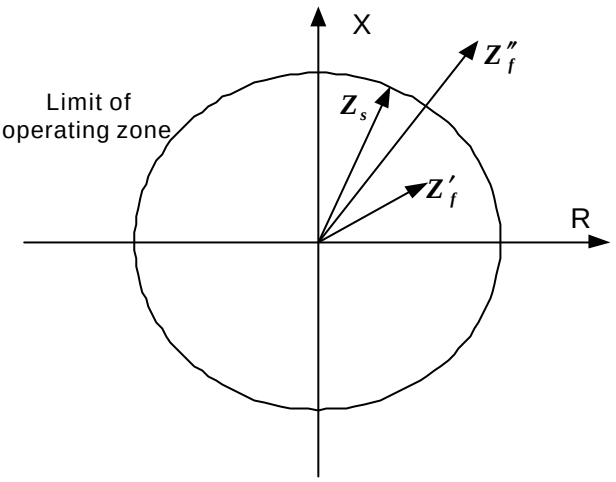

Figure 2.5 The characteristics of the impedance relay

In Figure 2.5, the area in the circle is the operating zone of the impedance relay. The radius Z_s of the circle is the setting of the impedance relay. If a fault occurs in the operating zone of the relay, the measured impedance Z'_f is less than the setting. The relay operates to trip the circuit breaker. When a fault is outside of the zone, the measured impedance Z''_f is larger than the setting Z_s. The relay remains in its normal condition.

The advantage of the distance protection is the zones of protection (e.g. Zone1, Zone2 and Zone3). The zones only depend on the impedance of the protected line. The line impedance is constant and independent of the magnitudes of the voltage and current. In contrast, the zones of overcurrent protection vary with the system operating conditions.

However, the disadvantages of the distance protection may be:

(a) It is affected by the infeeds (DG or loads). The measured impedance of the distance relay is a function of infeed currents.
(b) It is also affected by the fault arc resistance.
(c) It is sensitive to oscillations on the power system. During a power system oscillation, the voltage and current, which feed the distance relay, vary with time. As a result, the distance relay would see an impedance that is varying with time. The variation of measured impedance might cause the relay to operate incorrectly.

2.2.4 Zero sequence protection

Concerning the type of protection, which could be used to detect the faults on the MicroGrid, the results in [Pereira da Silva, 2004] show how the zero sequence protection can be used to protect the MicroGrid. The operation of the zero sequence protection is shown in Table 2.1.

Solid Faults	Detection by
PH-G, PH-PH-G	$> U_o$
PH-N, PH-PH-N	$> U_o$ difficult , $< U$
PH-PH, PH-PH-PH	$< U$
Resistive Faults	
PH-G	$< U_o$
PH-PH-G	$> I_o$
PH-N, PH-PH-N	$> I_{on}$

Table 2.1 Fault detection
(*Copied from reference [Pereira da Silva, 2004]*)

Table 2.1 shows how the zero sequence voltage based, under voltage based and zero sequence current based protection can be used to detect faults on the MicroGrid. The zero sequence voltage-based protection is used to detect the phase-to-ground and double-phase-to ground solid faults. The under voltage based protection is used to detect the phase-to-neutral, double-phase-to-neutral, phase-to-phase and three-phase solid faults. The zero sequence current-based protection is used to detect the double-phase-to ground, phase-to-neutral, double-phase-to-neutral resistive faults.

However, to identify the location of the faults on the MicroGrid precisely, the zero sequence protection technique may need fast communication between the protection devices installed at different places. The cost of the zero sequence protection may be very high.

2.3 Possible protection schemes for a MicroGrid

To investigate various protection schemes of the MicroGrid, a simple MicroGrid is used and shown in Figure 2.6. Three faults (F1, F2 and F3) are located at three different places.

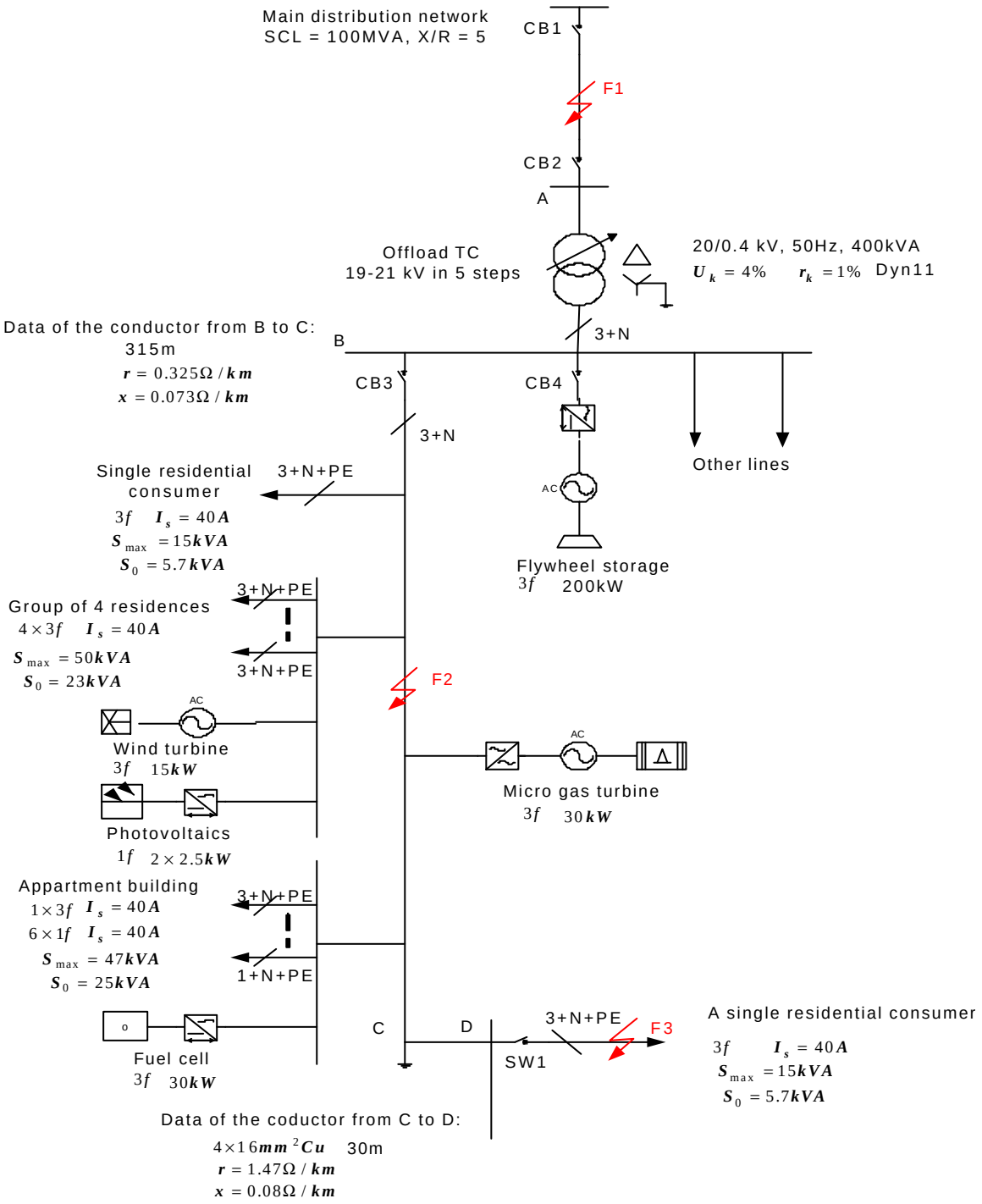

Figure 2.6 A simple MicroGrid with three faults (F1, F2 and F3) located at different places

In Figure 2.6, the main distribution network is assumed to have a short circuit level of 100MVA and a X/R ratio of 5. The MicroGrid consists of a flywheel storage system with a rating of 200kW, a number of micro sources and a group of residential consumers. A feeder of the MicroGrid is interconnected with the main distribution network through the circuit breaker CB3. The main transformer is rated at 20/0.4 kV, 400kVA.

The earthing system of the MicroGrid is assumed to be a TN-C-S system. The transformer neutral is directly earthed. The MicroGrid feeder uses a TN-C system, where the neutral conductor and the earth conductor are combined. The earthing arrangement in the installations (consumers) is TN-S, with separate neutrals and earth conductors.

Two scenarios (Case 1 and Case 2) of the MicroGrid are investigated. In Case 1, the MicroGrid is connected to the main network. In Case 2, the MicroGrid is operating in islanded mode. Three different faults (F1, F2 and F3) were applied to the MicroGrid. Fault F1 is on the main distribution network. Fault F2 is on the MicroGrid network. Fault F3 is at a single residential consumer.

For faults F1 and F3, the energies ($\boldsymbol{E} = \left(3\boldsymbol{I}^2\boldsymbol{R}\right)\cdot\boldsymbol{t}$) supplied by the flywheel are calculated and shown in Table 2.2.

Table 2.2 Energy supplied by the flywheel to faults F1 and F3

Fault	V (kV)	R (ohms)	$\boldsymbol{I}_{f\_flywheel} = 3\boldsymbol{p.u}$, based on 200kW			$\boldsymbol{I}_{f\_flywheel} = 5\boldsymbol{p.u}$, based on 200kW		
			P (kW)	E (kJ) in the time of		P (kW)	E (kJ) in the time of	
				0.5sec.	1.0sec.		0.5sec.	1.0sec.
F1	20	10.00	9.00	4.50	9.00	24.99	12.50	25.00
F3	0.4	0.146	328.51	164.25	328.51	912.53	456.26	912.53

Table 2.2 shows the energies supplied by the flywheel for faults F1 and F3. The fault currents of the flywheel were assumed as 3 per unit and 5 per unit, based on its rating.

R is a resistance between flywheel (at busbar B) and the fault point. For fault F1, the energy supplied by the flywheel in 1 second are 9.00 kilo Joules and 25.00 kilo Joules under the fault currents of 3 p.u and 5 p.u. For fault F3, the energy supplied by the flywheel in 1 second are 328.51 kilo Joules and 912.53 kilo Joules. The fault current contribution from the flywheel is above 3p.u. if the energy supplied by the flywheel is larger than 300 kilo Joules. Thus, for a flywheel with capacity of 4MJ (supplying a 200kW active power in 20 seconds continually) installed in the MicroGrid, the flywheel is able to supply 3-5 p.u fault current to any point in the MicroGrid.

Based on the assumptions above, the electrical protection of the MicroGrid can be investigated and shown as follows:

(1) For a fault F1 on the main distribution network

Considering a fault F1 on the main distribution network, a simplified MicroGrid is shown in Figure 2.7.

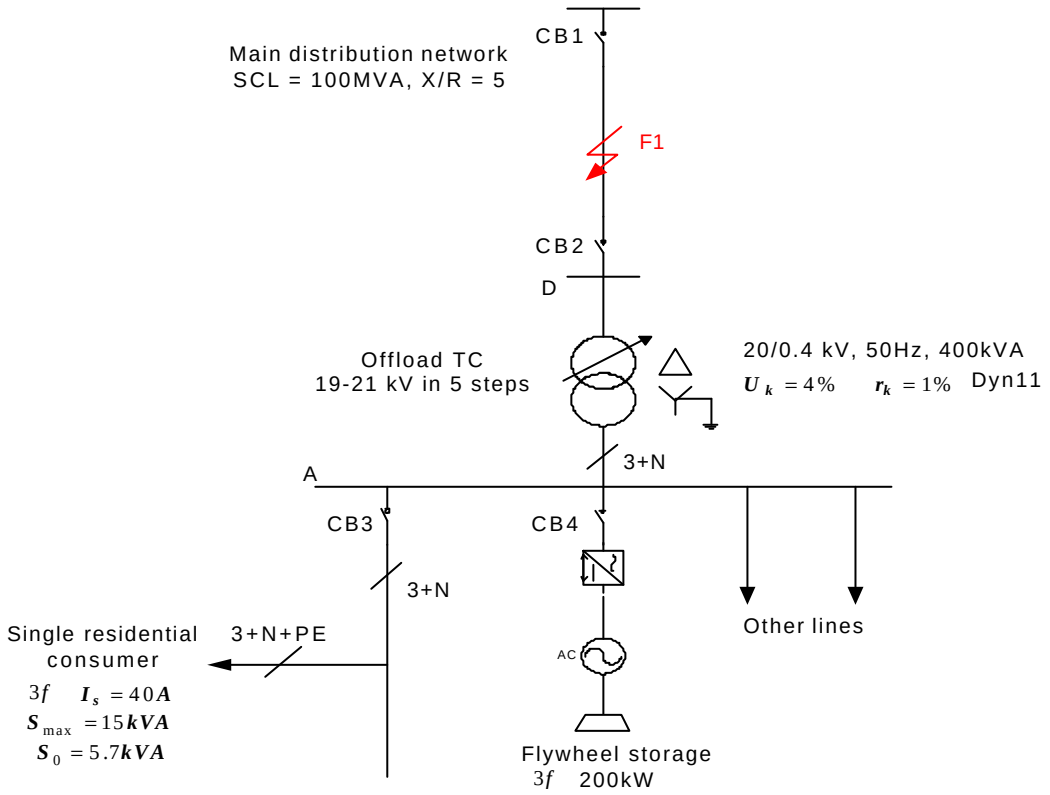

Figure 2.7 A simplified MicroGrid with a fault F1 on the main distribution network

Fault F1 may be a phase-to-phase fault (three-phase short circuit or two-phase short circuit) or a phase-to-ground fault (single-phase to ground or two-phase to ground).

The action of the protection against fault F1 should trip the circuit breakers CB1 and CB2 rapidly.

During the fault, the main distribution network supplies a large current to the fault point, flowing through the circuit breaker CB1. However, the fault current contribution from the MicroGrid passing through the circuit breaker CB2 may be very low. Further, the voltage and frequency may be maintained within an acceptable range by the control functions of the MicroGrid.

Therefore, the options of the protection scheme against fault F1 are:

(a) Option 1 is to install an overcurrent relay protection and a balanced earth fault (BEF) protection at CB1, with a capability of inter-tripping CB2. The overcurrent relay protects the main grid line against the phase-to-phase faults. The BEF detects the earth faults on the main distribution network. After CB1 is opened, the inter-tripping signal is sent to CB2 to disconnect the MicroGrid from the main network.

(b) Option 2 is to install an overcurrent relay protection scheme and a BEF protection scheme at CB1 and a distance relay protection at CB2. The overcurrent relay protection operates to trip CB1 when the fault current is above the setting of the relay. The BEF protects the grid line against the earth faults on the main distribution network. The distance protection operates to trip CB2, according to the measured impedance of the distance relay.

(c) Option 3 is to use a differential protection system between CB1 and CB2. In this solution, a communications system is necessary for the data transmission between two terminals. The cost of the differential protection may be high due to the additional communication devices.

(2) For a fault F2 on the MicroGrid

Considering a fault F2 on the MicroGrid, a simplified MicroGrid is shown in Figure 2.8.

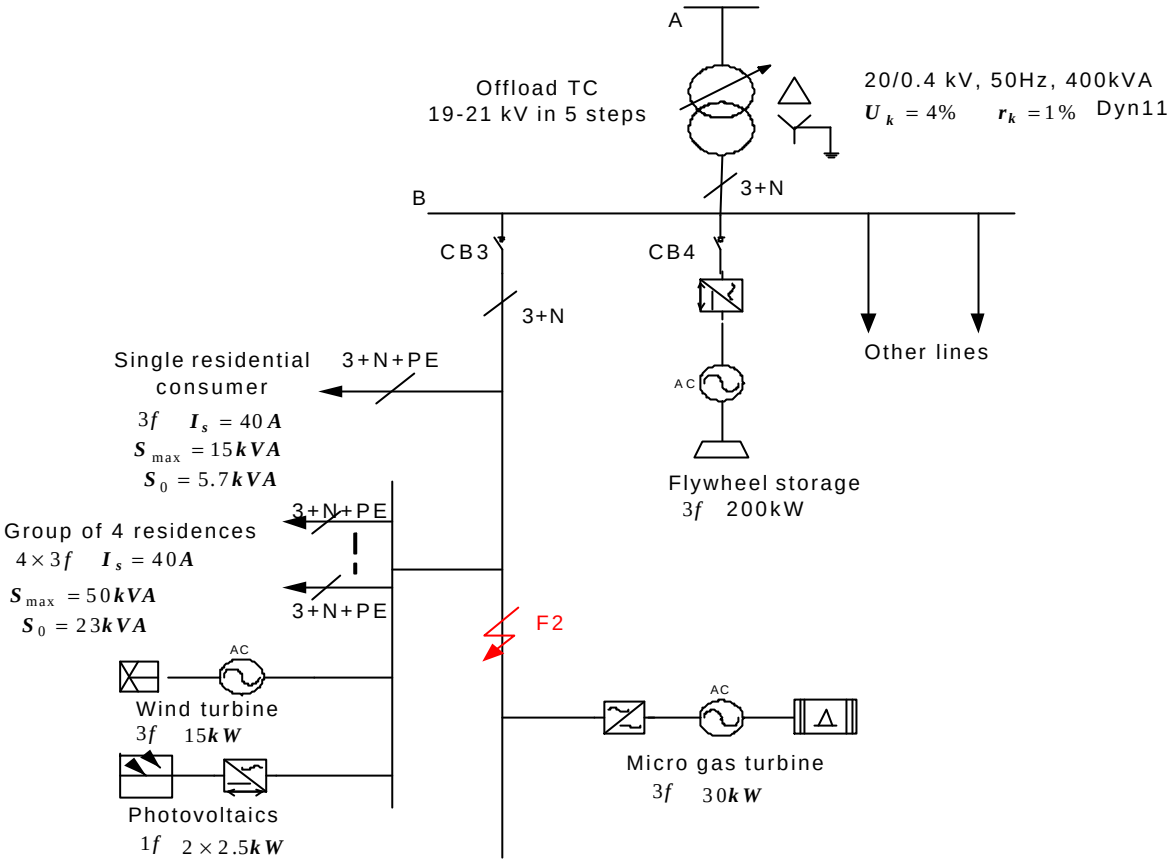

Figure 2.8 A simplified MicroGrid with a fault F2 on the MicroGrid

Fault F2 may be a phase-to-phase fault, a phase-to-neutral fault or a phase-to-ground fault. The action of the protection against fault F2 should trip the circuit breaker CB3 and shut down the faulted feeder quickly. According to UK reliability data, approximately 22 faults per 100km occur in LV networks annually. This means only 1 fault would take place in a MicroGrid spanning 1 km in 5 years. So, we do not need to section each feeder.

During the fault, in Case 1, the main distribution network supplies a large fault current to fault F2, flowing through the circuit breaker CB3. However, in Case 2, the fault current contribution from the MicroGrid may be low.

Therefore, the options of the protection scheme against fault F2 are:

(a) to install an overcurrent relay protection scheme and a residual current device (RCD) at CB3, with a capability of intertripping all micro sources on the MicroGrid. The overcurrent relay protection is mainly used to protect the MicroGrid against the phase-to-phase faults and phase-to-neutral faults. In Case 1

(grid-connected operation), the overcurrent relay protection can operate correctly due to the large fault current contribution from the main network. However, in Case 2 (islanded operation), the overcurrent relay protection may only operate correctly when the flywheel supplies a high fault current (3 - 5 p.u. based on its rating). The RCD is used to detect the earth faults on the MicroGrid. The cost of intertripping all micro sources on the MicroGrid, using the existing slow communication system between the MicroGrid control centre and the micro sources or the information of the voltage and frequency variation when the micro sources use fixed PQ control, may be reasonable. Discrimination of the overcurrent relay protection will be achieved by grading the upstream protection at CB1 and the protection at CB3 on a time delay.

(2) For a fault F3 at the residential consumer

Considering a fault F3 at the residential consumer, a simplified MicroGrid is shown in Figure 2.9.

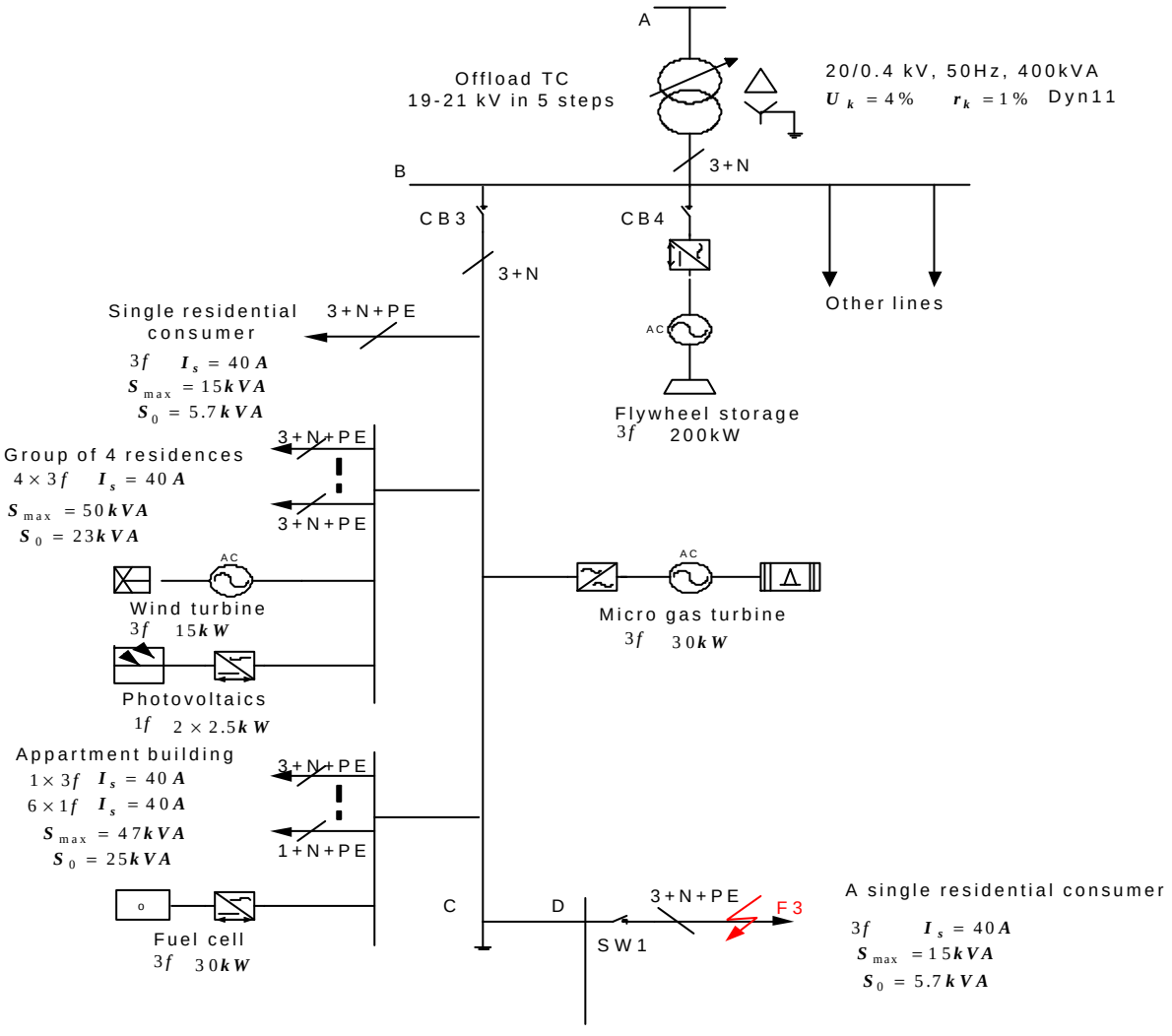

Figure 2.9 A simplified MicroGrid with a fault F3 at the residential consumer

Fault F3 may be also a phase-to-phase fault, a phase-to-neutral fault or a phase-to-ground fault. The action of the protection against fault F3 should automatically disconnect the part of the MicroGrid affected by the fault.

Therefore, the option of the protection scheme against fault F3 is:

(a) to install a short circuit protection device (SCPD), e.g. a miniature circuit breaker (MCB) or fuses, and a RCD at SW1 (grid side of the residential consumer). The SCPD is used to protect the residential consumer against the phase-to-phase and phase-to-neutral faults. To make the SCPD operate correctly in Case2, the flywheel should supply a high fault current (e.g. 3-5p.u. based on its capacity) during the fault. The RCD is used to protect residential consumer against the phase-to-ground fault (earth fault). Discrimination of the protection at CB3 and SW1 will be achieved by using a time delay.

Consequently, the possible electrical protection schemes for a MicroGrid are summarised and shown in Table 2.3.

Table 2.3 Possible electrical protection schemes for a MicroGrid

Case		**Possible electrical protection schemes for a MicroGrid**							
		O/C	**SCPD**	**RCD**	**U/V**	**F**	**Z**	**D**	V_0 / I_0
1. MicroGrid connected	F1	√	×	×	×	×	√	√+£	×
	F2	√	√	√	×	×	×	×	√+ff
	F3	√	√	√	×	×	×	×	√+ff
2. MicroGrid islanded	F1	√	×	×	×	×	√	√+£	×
	F2	√+Ifly	√+Ifly	√	×	×	×	×	√+ff
	F3	√+Ifly	√+Ifly	√	×	×	×	×	√+ff

Notes:

(1) ***O/C*** *is overcurrent protection; SCPD is a short circuit protection device (e.g. MCB or fuses);* ***RCD*** *is a residual current device;* ***U/V*** *is under-voltage protection;* ***F*** *is frequency protection;* ***Z*** *is distance protection;* ***D*** *is differential protection;* $\boldsymbol{V}_0 / \boldsymbol{I}_0$ *is zero sequence based protection.*

(2) *The mark "´" is that the protection cannot operate correctly; the mark "Ö" is that the protection can operate correctly; the mark "Ö+Ifly" is that the protection can operate correctly if the flywheel supplies a high fault current (3-5p.u. based on its capacity); the mark "Ö+£" is that the protection can operate correctly, but may be expensive; the mark "Ö+££" is that the protection can operate correctly, but may be very expensive.*

Table 2.3 shows that the undervoltage, frequency protection schemes may fail to trip faults F1, F2 and F3 in both grid-connected and islanded cases due to the voltage and frequency control of the MicroGrid. The distance protection scheme may fail to protect the MicroGrid from faults F2 and F3 because of the effect of multiple infeeds on distance relays. The differential protection scheme installed on the main distribution network against fault F1 may be expensive. The zero sequence protection may be too expensive to be implemented on the MicroGrid due to a high cost of the communication equipment. It may fail to detect the faults F2 and F3 precisely.

Therefore, for a fault F1 on the main distribution network, the possible electrical protection scheme is to install an overcurrent relay protection and a BEF protection at CB1, with a capability of inter-tripping CB2. Alternatively, to maintain the stability of the MicroGrid, fast protection (e.g. differential protection) is necessary between CB1 and CB2.

For a fault F2 on the MicroGrid, it is possible to install an overcurrent relay protection and a RCD at CB3. This protection system possesses the capability of intertripping all micro sources in the MicroGrid. To make the overcurrent relay protection operate correctly in islanded model of the MicroGrid, the flywheel should supply a high fault current (e.g. 3-5p.u. based on its capacity) during the fault. Discrimination of the protection will be achieved by comparing the setting of the upstream protection at CB1 with the setting of the protection at CB3 using a time delay.

For a fault F3 at the residential consumer, a possible electrical protection scheme is to install a SCPD (using MCB or fuses) and a RCD at SW1 (grid side terminal of the residential consumer). Similarly, to make the SCPD operate correctly in islanded mode of the MicroGrid, the flywheel should supply a high fault current with a value of 3-5p.u, based on its capacity, during the fault. The protection only disconnects the residential consumer affected by the fault. Discrimination of the protection at SW1 and CB3 can be achieved by using a time delay.

2.4 Design of the protection of a MicroGrid

Based on a simple MicroGrid, shown in Figure 2.6, and starting from the data which is given there, the design of the electrical protection schemes of the MicroGrid is carried out. Take into account the following considerations:

(a) For fault F1, the protection schemes at CB1 are an overcurrent relay and a BEF protection, with a capability of inter-tripping CB2. For fault F2, the protection schemes at CB3 are an overcurrent relay and a RCD. For fault F3, the protection schemes at SW1 are the fuses and a RCD.
(b) The overcurrent relays associated with breaker CB1 and CB3 are the definite time type.
(c) The standard secondary current of current transformers (CTs) is 5A.
(d) The rating of the flywheel is 200kW. In Case 1 (grid-connected mode), CB2 is closed. The injecting current of the flywheel is zero. In Case 2 (islanded mode), CB2 is open. The flywheel supplies 3p.u or 5p.u fault currents (based on its rating) during the fault.
(e) The normal capacity of the feeder is 200kVA. The maximum load of the residential consumer is 15kVA.
(f) The per unit impedances of equivalent network are calculated on the bases:

$$S_{base} = 100MVA,\ I_{base} = \frac{S_{base}}{\sqrt{3}V_{base}},\ Z_{base} = \frac{V^{2}_{base}}{S_{base}}.$$

(1) Calculation of equivalent impedance

The short circuit level of the main distribution network at 20kV is 100MVA. Using this, the equivalent impedances of the network in per unit are calculated and shown in Figure 2.10.

$$\boldsymbol{Z}_{source\_p.u} = \left(\cos\left(\boldsymbol{tg}^{-1}5.0\right) + \boldsymbol{j}\sin\left(\boldsymbol{tg}^{-1}5.0\right)\right) \times \frac{\boldsymbol{S}_{base}}{\boldsymbol{S}_{source}} = (0.19 + \boldsymbol{j}0.98) \times \frac{100}{100} = 0.19 + \boldsymbol{j}0.98$$

$$\boldsymbol{Z}_{transf\_p.u} = (0.01 + \boldsymbol{j}0.04) \times \frac{\boldsymbol{S}_{base}}{\boldsymbol{S}_{transfe}} = (0.01 + \boldsymbol{j}0.04) \times \frac{100}{0.4} = 2.50 + \boldsymbol{j}10.00$$

$$\boldsymbol{Z}_{line\_p.u} = (0.146 + \boldsymbol{j}0.025) \times \frac{\boldsymbol{S}_{base}}{\boldsymbol{V}^{2}_{base}} = (0.146 + \boldsymbol{j}0.025) \times \frac{100}{0.4^{2}} = 91.25 + \boldsymbol{j}15.62$$

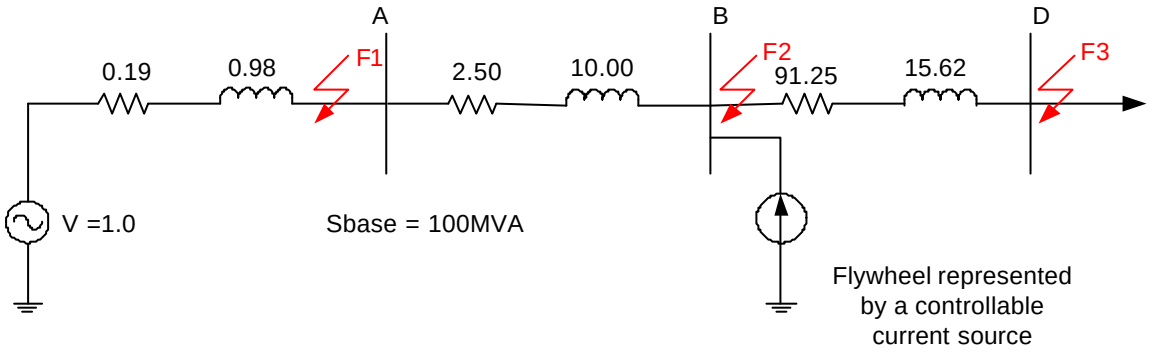

Figure 2.10 Positive-sequence equivalent impedance network for a MicroGrid shown in Figure 2.6

(2) Calculation of normal currents

The normal current of an element is the current passing through the element under normal operation. The normal current of the MicroGrid can be calculated according to the capacity of the transformer at the substation. Similarly, the normal current of a residential consumer can be obtained by the maximum capacity of the load. Therefore, the normal currents passing through CB1, CB3 and SW1 are as followers:

$$\boldsymbol{I}_{norm\_CB1} = \frac{\boldsymbol{S}_{trans}}{\sqrt{3} \times \boldsymbol{V}} = \frac{400}{\sqrt{3} \times 20} = 11.54\boldsymbol{A}\text{, referred to 20kV;}$$

$$\boldsymbol{I}_{norm\_CB3} = \frac{\boldsymbol{S}_{feeder}}{\sqrt{3} \times \boldsymbol{V}} = \frac{200}{\sqrt{3} \times 0.4} = 288.68\boldsymbol{A}\text{, referred to 0.4kV}$$

$$\boldsymbol{I}_{norm\_SW1} = \frac{\boldsymbol{S}_{load}}{\sqrt{3}\times\boldsymbol{V}} = \frac{15}{\sqrt{3}\times 0.4} = 21.65\boldsymbol{A}$$, referred to 0.4kV

(3) Calculation of fault currents

From the equivalent circuit of the network (see Figure 2.10), the magnitudes of the fault currents for three-phase faults F1, F2 and F3 have been calculated as follows:

(a) For fault F1

$$\begin{aligned}\boldsymbol{I}_{faultF1} &= \left|\frac{1.0\angle 0^\circ}{0.19+\boldsymbol{j}0.98}\right|\times\frac{\boldsymbol{S}_{base}}{\sqrt{3}\times\boldsymbol{V}_{base}}\times 1000\\ &= \left|\frac{1.0\angle 0^\circ}{0.19+\boldsymbol{j}0.98}\right|\times\frac{100}{\sqrt{3}\times 20}\times 1000\\ &= 2891.90\boldsymbol{A}\end{aligned}$$

(b) For fault F2

The MicroGrid operates in interconnected mode:

$$\begin{aligned}\boldsymbol{I}_{faultF2\_grid-connected} &= \left|\frac{1.0\angle 0^\circ}{(0.19+2.50)+\boldsymbol{j}(0.98+10.00)}\right|\times\frac{\boldsymbol{S}_{base}}{\sqrt{3}\times\boldsymbol{V}_{base}}\times 1000\\ &= \left|\frac{1\angle 0^\circ}{2.69+\boldsymbol{j}10.98}\right|\times\frac{100}{\sqrt{3}\times 0.4}\times 1000\\ &= 12768.28\boldsymbol{A}\end{aligned}$$

The MicroGrid operates in islanded mode:

$$\boldsymbol{I}_{faultF2\_islanded\_3p.u} = 3.0\times\frac{\boldsymbol{S}_{flywheel}}{\sqrt{3}\times\boldsymbol{V}} = 3.0\times\frac{200}{\sqrt{3}\times 0.4} = 866.05\boldsymbol{A}$$

$$\boldsymbol{I}_{faultF2\_islanded\_5p.u} = 5.0\times\frac{\boldsymbol{S}_{flywheel}}{\sqrt{3}\times\boldsymbol{V}} = 5.0\times\frac{200}{\sqrt{3}\times 0.4} = 1443.42\boldsymbol{A}$$

(c) For fault F3

The MicroGrid operates in interconnected mode:

$$I_{faultF3\_grid-connected} = \left| \frac{1.0\angle 0^\circ}{(0.19+2.50+91.25)+j(0.98+10.00+15.62)} \right| \times \frac{S_{base}}{\sqrt{3}\times V_{base}} \times 1000$$
$$= \left| \frac{1\angle 0^\circ}{93.94+j26.60} \right| \times \frac{100}{\sqrt{3}\times 0.4} \times 1000$$
$$= 1478.40A$$

The MicroGrid operates in islanded mode:

$$I_{faultF3\_islanded\_3p.u} = 3.0 \times \frac{S_{flywheel}}{\sqrt{3}\times V} = 3.0 \times \frac{200}{\sqrt{3}\times 0.4} = 866.05A$$

$$I_{faultF2\_islanded\_5p.u} = 5.0 \times \frac{S_{flywheel}}{\sqrt{3}\times V} = 5.0 \times \frac{200}{\sqrt{3}\times 0.4} = 1443.42A$$

(4) Choice of CT transformer ratios

The transformation ratio of a CT is determined by the larger of the two following values [Gers, 1998]:

(a) normal current I_{norm};

(b) maximum short-circuit current without saturation being present.

Therefore, $I_{sc}(5/X) \le 100A$ so that $X \ge (5/100)I_{sc}$, where I_{sc} is the short-circuit current.

Table 2.4 summarises the CT ratio calculations for the overcurrent relay protection at CB1 and CB3.

Table 2.4 Selection of the CT ratios

Breaker	I_{norm} (A)	I_{sc} (A)	$(5/100)I_{sc}$ (A)	CT ratio	Type of device	Supplier
CB1	11.54	2891.90	144.59	200/5	ASTW6-200/5	Moeller, 2004
CB3	288.68	12768.28	638.41	800/5	ASTW12-800/5	Moeller, 2004

(5) Calculation of settings of the protection

Settings of the overcurrent protection consist of the setting of pick-up current and the setting of instantaneous tripping current.

The setting of the pick-up current is determined by allowing a margin (a safety factor, e.g. 2.0) for overload above the normal current, as in the following expression [Gers, 1998]:

$$\boldsymbol{I}_{\boldsymbol{pick-up}} = 2.0 \times \boldsymbol{I}_{\boldsymbol{norm}} \times (1/\boldsymbol{CTR}) \qquad (2\text{-}1)$$

where, CTR is the ratio of CT transformation.

The setting of the instantaneous tripping current is usually decided by 50% of maximum short-circuit current at the point of installation of the protection, as shown in the following equation [Gers, 1998]:

$$\boldsymbol{I}_{\boldsymbol{inst-trip}} = 0.5 \times \boldsymbol{I}_{\boldsymbol{sc}} \times (1/\boldsymbol{CTR}) \qquad (2\text{-}2)$$

According to equations (2-1) and (2-2), the settings of the protection at SW1, CB3 and CB1 are calculated as follows.

Protection at SW1

The protection at SW1 consists of overcurrent protection (using MCB or fuses) and RCD. The rating of the fuse is:

$\boldsymbol{I}_{\boldsymbol{fuse\_pick-up\_SW1}} = 2.0 \times \boldsymbol{I}_{\boldsymbol{nom\_SW1}} = 2.0 \times 21.65 = 43.36\boldsymbol{A}$, rating = 45A .

To make the protection operate correctly in both grid-connected operation and islanded operation, the fault current $\boldsymbol{I}_{\boldsymbol{sc}}$ in equation (2-2) should be the minimum value of the fault currents in both grid-connected operation and islanded operation.

Therefore, the setting of instantaneous element should be minimum value of these:

(a) In grid-connected mode

$\boldsymbol{I}_{\boldsymbol{fuse\_inst-trip\_SW1}} = 0.5 \times \boldsymbol{I}_{\boldsymbol{faultF3}} = 0.5 \times 1478.40 = 739.20\boldsymbol{A}$, setting = 750A.

(b) In islanded mode, the flywheel supplies 3p.u fault current during the fault

$I_{fuse\_inst-trip\_SW1} = 0.5 \times I_{faultF3\_islanded\_3p.u} = 0.5 \times 866.05 = 433.02A$, setting = 450A.

(c) In islanded mode, the flywheel supplies 5p.u fault current during the fault

$I_{fuse\_inst-trip\_SW1} = 0.5 \times I_{faultF3\_islanded\_5p.u} = 0.5 \times 1443.42 = 721.71A$, setting = 750A.

So, the setting of instantaneous-trip of the overcurrent protection at SW1 is 450A.

The sensitivity of RCD is set to 30mA, with the normal operating voltage 400V a.c. and current 25A.

Operating time of the protection is: $T_{SW1} = 0.2\text{sec}$. (minimum)

Protection at CB3:

The protection at CB3 consists of the overcurrent relay protection and RCD. The setting of pick-up current of the overcurrent relay is:

$I_{relay\_pick-up\_CB3} = 2.0 \times I_{nom\_CB3} \times (1/CTR) = 2.0 \times 288.68 \times (5/800) = 3.61A$;

setting = 4A.

So, the setting at primary side of CT is: $4 \times 800/5 = 640A$.

Similarly, the setting of instantaneous element is also the minimum value of these:

(a) In grid-connected mode

$I_{relay\_inst-trip\_CB3} = 0.5 \times I_{faultF2} \times (1/CTR) = 0.5 \times 12768.28 \times (5/800) = 39.9A$; setting = 40A. The setting at primary side of CT is: $40 \times 800/5 = 6400A$.

(b) In islanded mode, the flywheel supplies 3p.u fault current during the fault

$I_{relay\_inst-trip\_CB3} = 0.5 \times I_{faultF2\_islanded\_3p.u} \times (1/CTR) = 0.5 \times 866.05 \times (5/800) = 2.7A$;

setting = 3A. The setting at primary side of CT is: $3 \times 800/5 = 480A$.

(c) In islanded mode, the flywheel supplies 5p.u fault current during the fault,

$I_{relay\_inst-trip\_CB3} = 0.5 \times I_{faultF3\_islanded\_5p.u} \times (1/CTR) = 0.5 \times 1443.42 \times (5/800) = 4.5A$;

setting = 5A. The setting at primary side of CT is: $5 \times 800/5 = 800A$.

So, the setting of instantaneous-trip of the overcurrent protection at CB3 is 480A.

However, this setting is less than the pick-up setting of 640A. Therefore, the pick-up setting of the overcurrent relay should be changed from 640A to 480A. Consequently, there is no instantaneous-trip setting for the overcurrent relay protection at CB3.

The sensitivity of RCD is set to 300mA, with the normal operating voltage 400V a.c. and current 300A.

Operating time of the protection is: $\boldsymbol{T}_{\boldsymbol{CB}3} = \boldsymbol{T}_{\boldsymbol{SW}1} + 0.5\text{sec.} = 0.7\,\text{sec}$.

Protection at CB1:

The protection at CB1 consists of the overcurrent relay protection plus intertripping CB2. The settings of pick-up current of the overcurrent relay are as follows:

$\boldsymbol{I}_{\boldsymbol{relay\_pick-up\_CB}1} = 2.0 \times \boldsymbol{I}_{\boldsymbol{norm\_CB}1} \times (1/\boldsymbol{CTR}) = 2.0 \times 11.54 \times (5/200) = 0.57\boldsymbol{A}$;

setting = 1A.

So, the setting at primary side of CT is: $1 \times 200/5 = 40\boldsymbol{A}$.

$\boldsymbol{I}_{\boldsymbol{relay\_inst-trip\_CB}1} = 0.5 \times \boldsymbol{I}_{\boldsymbol{faultF}1} \times (1/\boldsymbol{CTR}) = 0.5 \times 2891.90 \times (5/200) = 36.15\boldsymbol{A}$;

setting = 40A.

So, the setting at primary side of CT is: $40 \times 200/5 = 1600\boldsymbol{A}$.

Operating time of the overcurrent protection is: $\boldsymbol{T}_{\boldsymbol{CB}1} = \boldsymbol{T}_{\boldsymbol{CB}3} + 0.5\text{sec.} = 1.2\text{sec}..$ This setting of the time delay looks like too long to maintain the stability of the MicroGrid. Thus, faster protection (e.g. differential protection) may be needed on the main distribution network against fault F1.

The setting of the BEF protection is set for 70% of available phase-to-earth fault current. A setting of 70% allows for a 30% margin to detect bolted phase-to-earth faults. The BEF can operate instantaneously in the time of 0.2sec. (minimum). The

BEF doesn’t need to co-ordinate with the earth fault protection in the MicroGrid due to the delta connection of primary side winding of the transformer at substation.

Table 2.5 shows the settings of the overcurrent-based protection at SW1, CB1 and CB3

Table 2.5 The settings of the overcurrent based protection for a MicroGrid

Protection position	Protection scheme	Normal voltage (kV)	Normal current (A)	Setting of pick-up $I_{pick-up\_prim}$ (A)	Setting of instantaneous $I_{inst-trip\_prim}$ (A)	CT ratio	Time (sec.)	Approximate Price of unit (Euro)	Type of device and Supplier
CB1	Overcurrent relay + intertripping CB2	20	11.54	40	1600	200/5	1.20	165.5	70POCR, [RS, 2004] BROYCE CONTROL
	BEF	20	70% I_{phef}				0.20	166.7	AREVA
CB3	Overcurrent relay	0.4	288.68	480		800/5	0.70	165.5	70POCR, [RS, 2004] BROYCE CONTROL
	RCD			Sensitivity: 300mA; Operating voltage: 400V; Operating current: 300A				166.7	70POCR, [RS, 2004] BROYCE CONTROL
SW1	MCB (or Fuses)	0.4	21.65	45	450		0.20	2.9	HRC, gG/500V – 25 ABB [ABB, 2004b]
	RCD			Sensitivity: 30mA; Operating voltage: 400V; Operating current: 25A				74.4	F364-25/0-03, ABB [RS, 2004]

Notes:

(a) I_{phef} is an available phase-to-earth fault current.

From Table 2.5, the co-ordinated curves of the overcurrent protection associated with SW1, CB3 and CB1 are shown in Figure 2.11. Fuses were chosen for the overcurrent protection at SW1. The time-current characteristic of the fuse (25A rating) was obtained from ABB HRC fuse link catalogue [ABB, 2004]. The setting values of overcurrent relay at CB1 were referred to 0.4kV.

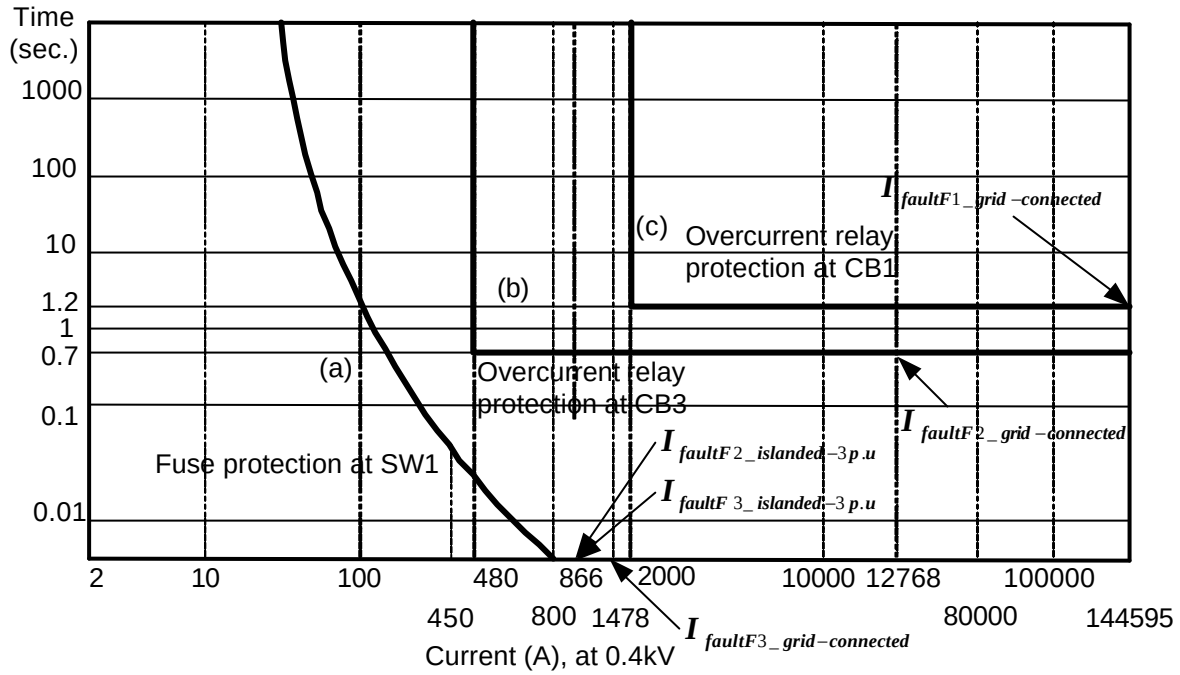

Figure 2.11 Co-ordination curves of the overcurrent protection for a MicroGrid

Figure 2.11 shows the co-ordination performances of the overcurrent protection in the MicroGrid. Curve (a) is a time-current characteristic of the fuse at SW1. Curve (b) is a definite time characteristic of the overcurrent relay at CB3. Curve (c) is also a definite time characteristic of the overcurrent relay at CB1. The fault currents of the MicroGrid are shown in Figure 2.11. Clearly, discrimination of the overcurrent protection at SW1, CB3 and CB1 has been achieved by using a time delay with grading of 0.5 second.

2.5 Validation of co-ordination of the protection in PSCAD/EMTDC

To validate the settings of the protection above, the overcurrent protection schemes were implemented into a simple MicroGrid model in PSCAD/EMTDC, as shown in Figure 2.12.

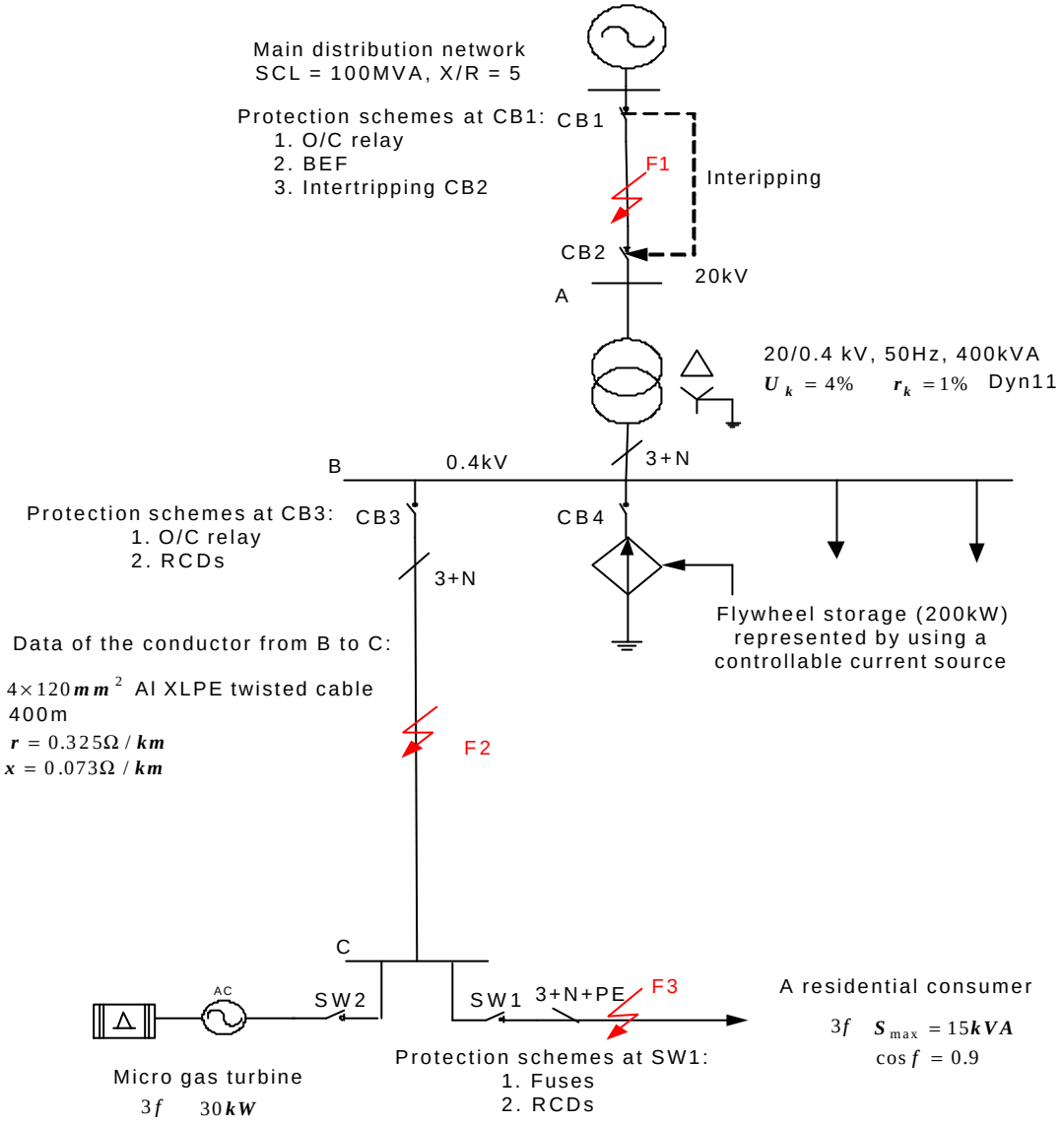

Figure 2.12 A simple MicroGrid model in PSCAD/EMTDC

In Figure 2.12, the circuit breakers CB1, CB2, CB3 and switchgear SW1 and SW2 are controlled by their protection relays. The flywheel is represented by a controllable current source and connected to the 0.4kV busbar through a circuit breaker CB4. The maximum load of the residential consumer is 15kVA. The residential consumer is controlled by switchgear SW1. The micro source in MicroGrid is a 30kW gas turbine synchronous generator. The generator is directly connected to the MicroGrid through switchgear SW2.

(1) For a fault F1

A solid three-phase fault is applied on the main distribution network at 30 seconds. The operating time of the overcurrent protection at CB1 is 1.2 seconds.

Figure 2.13 shows that the fault is correctly cleared up by opening CB1 and CB2 in 1.2 seconds after the fault. The states of CB1 and CB2 are changed from “0” (closing state) to “1” (opening state). The states of CB3, CB4, SW1 and SW2 are still retained at “0”. However, the operating time of the protection at CB1 takes too long to maintain the stability of the MicroGrid after disconnection from the main distribution network. Therefore, a further investigation is required to study the stability of the MicroGrid operating as an island.

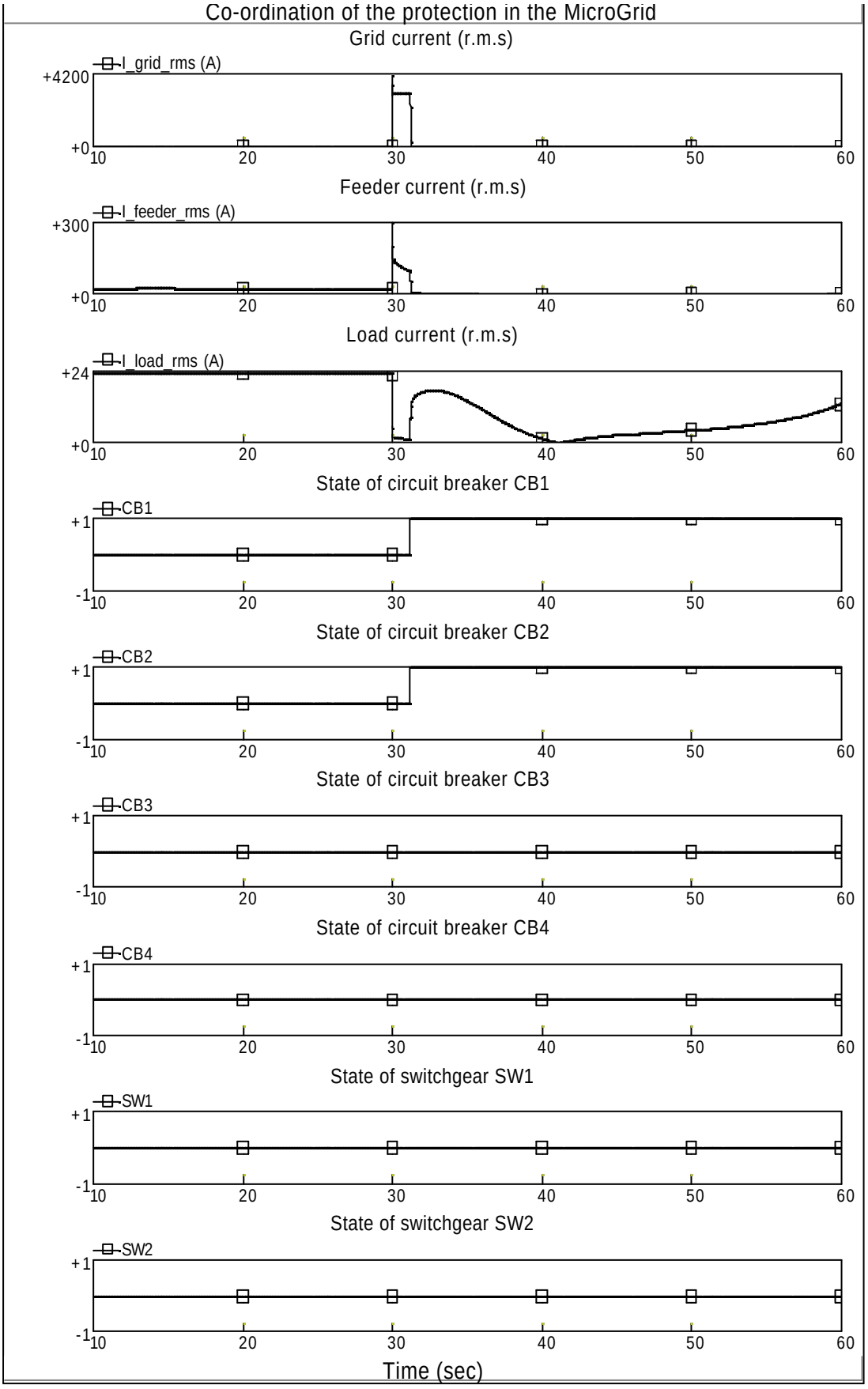

Figure 2.13 The circuit currents and states of the circuit breakers and switchgears (for fault F1)

(2) For a fault F2

Similarly, a solid three-phase fault is applied on the MicroGrid at 30 seconds. The operating time of the overcurrent protection at CB3 is 0.7 second.

Figures 2.14 and 2.15 show the fault is tripped off by opening CB3 and SW2 in 0.7 second after the fault in both grid-connected mode and islanded. The states of CB3 and SW2 are changed from “0” to “1”. The states of CB1, CB2, CB4 and SW1 are still retained at “0”.

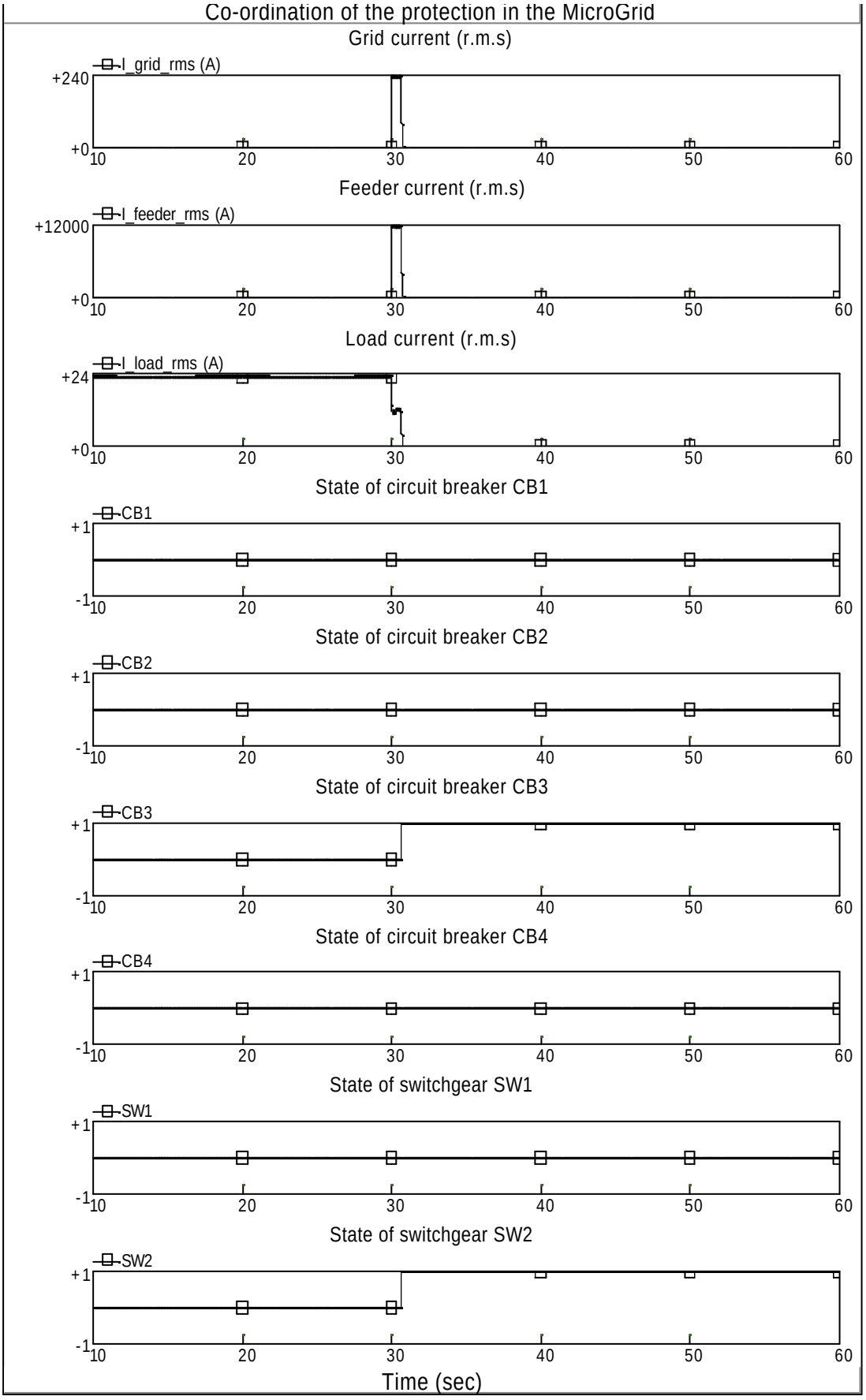

Figure 2.14 The circuit currents and states of the circuit breakers and switchgears (For fault F2, the MicroGrid is operated in grid-connected mode)

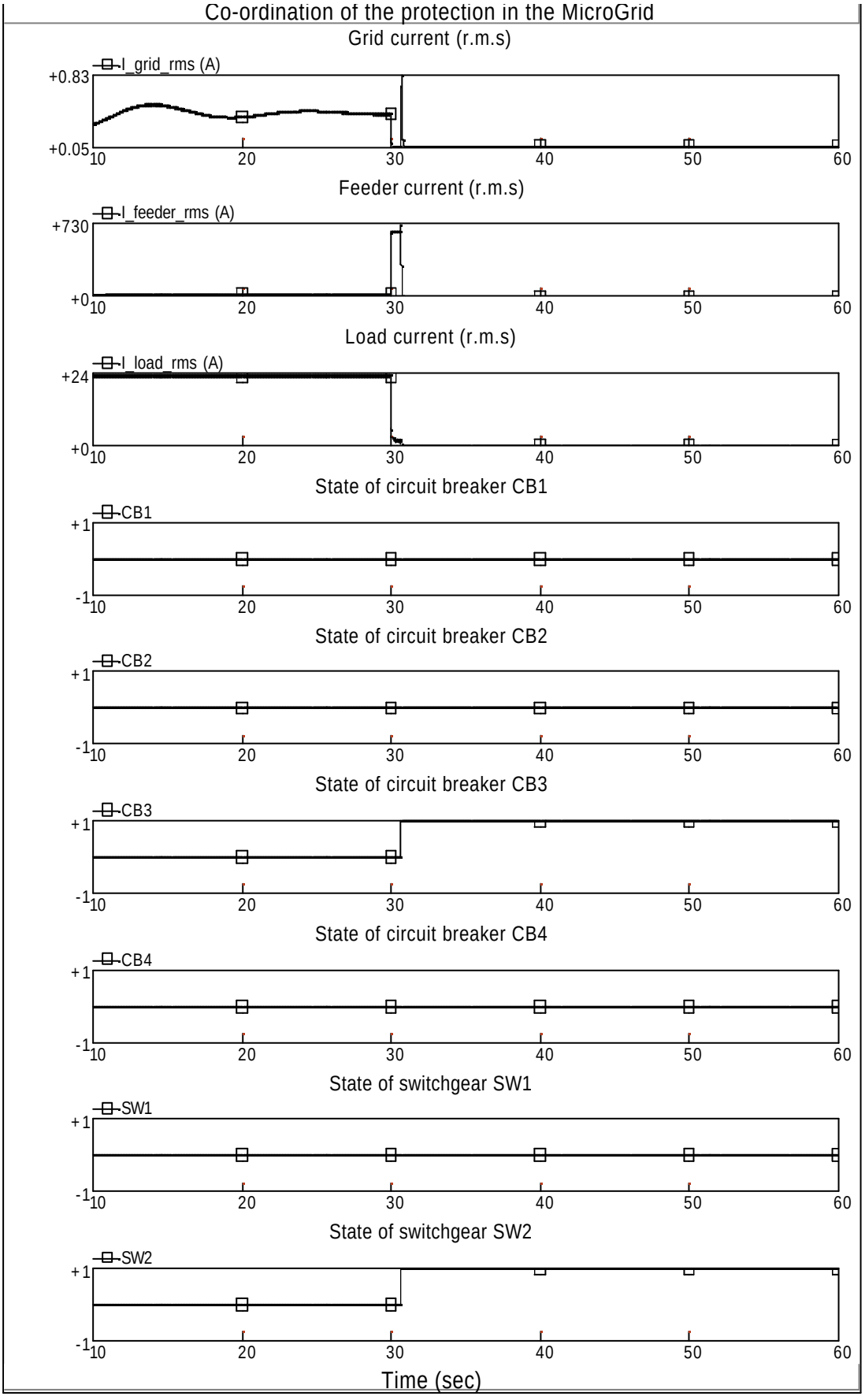

Figure 2.15 The circuit currents and states of the circuit breakers and switchgears (For fault F2, the MicroGrid is operated in islanded mode)

(3) For a fault F3

A solid three-phase fault is also applied on the residential consumer at 30 seconds. The operating time of the overcurrent protection at SW1 is 0.2 second.

Figures 2.16 and 2.17 show that, in both grid-connected mode and islanded mode, the fault is correctly taken off by tripping the switchgear SW1 in 0.2 second after the fault. The state of SW1 is changed from “0” to “1”, while the states of CB1, CB2, CB3, CB4 and SW2 are still retained at “0”.

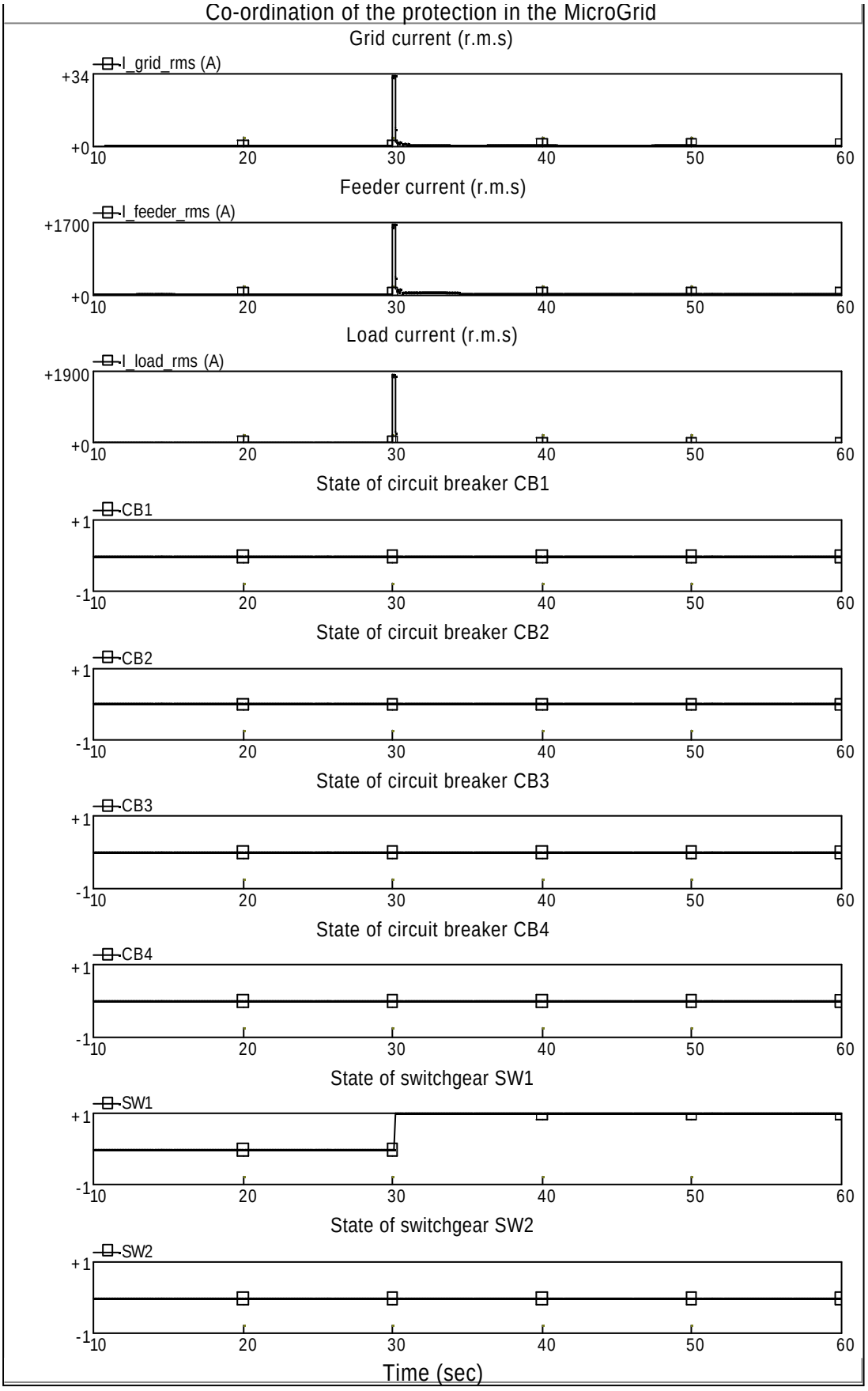

Figure 2.16 The circuit currents and states of the circuit breakers and switchgears (For fault F3, the MicroGrid is operated in grid-connected mode)

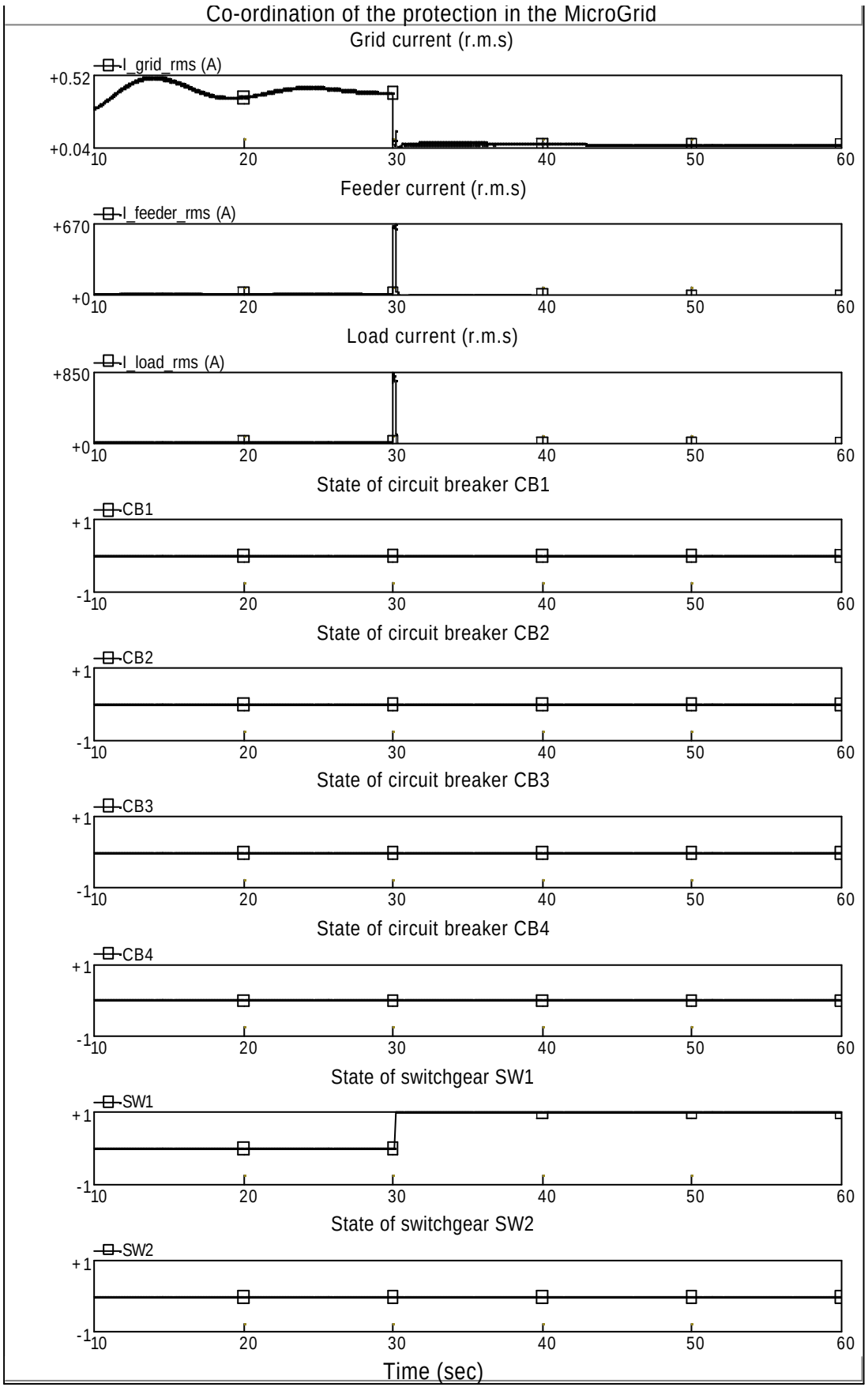

Figure 2.17 The circuit currents and states of the circuit breakers and switchgears (For fault F3, the MicroGrid is operated in islanded mode)

2.6 Summaries of Chapter 2

The unique nature of the MicroGrid requires the electrical protection systems to trip the faults on the network correctly and rapidly. Therefore, the possible electrical protection schemes for a MicroGrid are:

(1) for a fault F1 on the main distribution network, to use an overcurrent relay protection scheme and a balanced earth fault (BEF) protection device at CB1, with a capability of intertripping CB2. An alternative is to install an overcurrent protection and a BEF protection at CB1 and distance protection at CB2. Further, to maintain the stability of the MicroGrid, fast protection (e.g. differential protection) is needed to protect the main distribution network against fault F1.

(2) for a fault F2 on the MicroGrid, to install an overcurrent relay protection and a RCD at CB3. During islanded operation of the MicroGrid, the flywheel should supply a high fault current (e.g. 3p.u based on its rating). The protection should have a capability of intertripping all the micro sources in the MicroGrid. Discrimination of the protection can be achieved by using a time delay.

(3) for a fault F3 at the residential consumer, to install a SCPD (using MCB or fuses) and a RCD at the grid side of the residential consumer. The SCPD, using the fuses, trips the fault quickly if there is a high fault current contribution from the flywheel. The protection should only disconnect the consumer affected by the fault. Discrimination of the protection can be also achieved by using a time delay.

In practice, the protection schemes of the MicroGrid should not only satisfy the requirements of the protection systems but also maintain the stable operation of the MicroGrid. Thus, the stability of the MicroGrid should be investigated deeply.

Chapter 3 Stability of a MicroGrid

In principle, a MicroGrid is also subject to the same safety and stability requirements as any other utility electric power system. The control of the micro sources and the flywheel is very important to maintain the safety and stability of the MicroGrid during both grid-connected mode and islanded mode. To maintain the stability of the MicroGrid, three possible control strategies are PQ control, Droop control and Frequency/Voltage control. Based on the three control strategies, three representations (synchronous generator representation, STATCOM-BES representation and controllable AC or DC voltage source representation) of the MicroGrid are compared and tested in PSCAD/EMTDC. Considering the MicroGrid characteristic of power electronic devices based interface with grid, the major factors influencing the stability of the MicroGrid are investigated by using the STATCOM-BES representation. Finally, a traditional undervoltage load shedding method is used to improve the stability of the MicroGrid.

The MicroGrid will be unstable if the flywheel uses PQ control all the time. In this case, the flywheel can't supply dynamic active and reactive power compensation to the MicroGrid during islanded mode due to its constant output power. PQ control is only adopted when the micro sources and the flywheel need to run on constant power output. The electricity, generated by the micro source, may be constant because of the need of the associated thermal load. The power output of the flywheel can be fixed at zero when the MicroGrid is operated in parallel with the main network, grid-connected mode.

After disconnection of the MicroGrid from the main network, operating in islanded mode, the control scheme of the flywheel can be changed from PQ control to Droop control or Frequency/Voltage control. With Droop control of the flywheel, the frequency and voltage of the MicroGrid will be controlled to their steady state values determined by the droop characteristics. With Frequency/Voltage control of the flywheel, the frequency and voltage of the MicroGrid can be brought back to their normal values after a disturbance.

3.1 Control strategies of a MicroGrid

The possible control strategies of the MicroGrid are: (a) PQ control, (b) Droop control and (c) Frequency/Voltage control.

3.1.1 PQ control

Using this control, the outputs of the micro sources and the flywheel are fixed at their constant values (settings). PQ control consists of a P controller and a Q controller.

The P controller adjusts the frequency-droop characteristic of the generator up or down to maintain the active power output of the generator at a constant value (Pdes, desired active power) when the frequency changes. Figure 3.1 shows the effect of frequency-droop characteristic adjustment. A typical droop of the frequency characteristic is about 4% [Kundur, 1994].

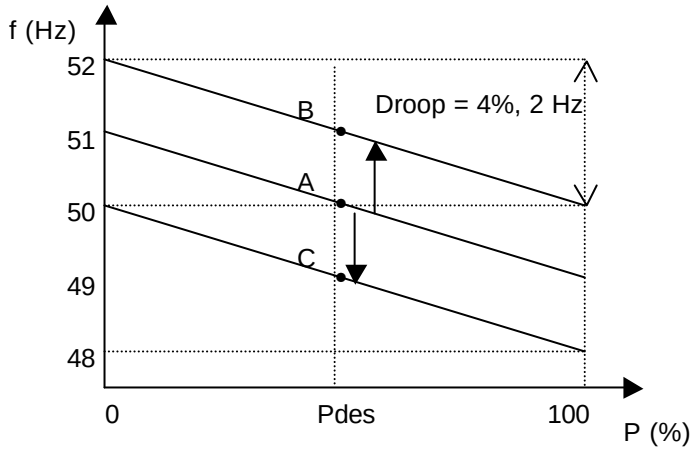

Figure 3.1 Effect of the frequency-droop characteristic adjustment

At output Pdes, characteristic A corresponds to 50Hz frequency of the grid, characteristic B corresponds to 51Hz frequency of the grid and characteristic C corresponds to 49Hz frequency of the grid. For a frequency change, the power output of the generator can be maintained at the desired value by moving the droop characteristic up or down.

Similarly, the Q controller adjusts the voltage-droop characteristic of the generator by moving the droop lines upon or down to maintain the reactive power output of the generator at a constant value (Qdes, desired reactive power) when the voltage is changed. Figure 3.2 shows the effect of voltage-droop characteristic adjustment. A typical droop of voltage characteristic is about 10% [Kundur, 1994].

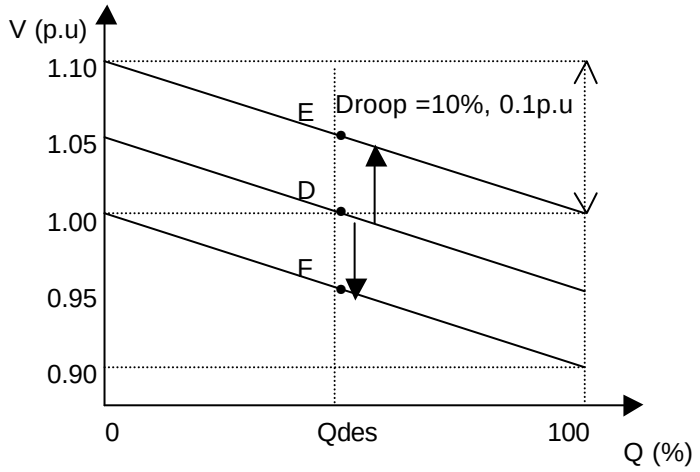

Figure 3.2 Effect of the voltage-droop characteristic adjustment

At output Qdes, characteristic D corresponds to 1.00 pu voltage of the network, characteristic E corresponds to 1.05 pu voltage of the grid and characteristic F corresponds to 0.95 pu voltage of the grid. For a voltage change, the reactive power output of the generator is maintained at the desired value Qdes by shifting the voltage-droop characteristic up or down.

3.1.2 Droop control

When the MicroGrid is operated in islanded mode, the control scheme of the micro sources is still PQ control. However, the control scheme of the flywheel needs to be changed to enable local frequency control. With Droop control of the flywheel, the power output of the flywheel is regulated according to the predetermined droop characteristics. Droop control consists of a frequency-droop controller and a voltage-droop controller. Figure 3.3 shows a frequency-droop characteristic, which would be used in the frequency-droop controller.

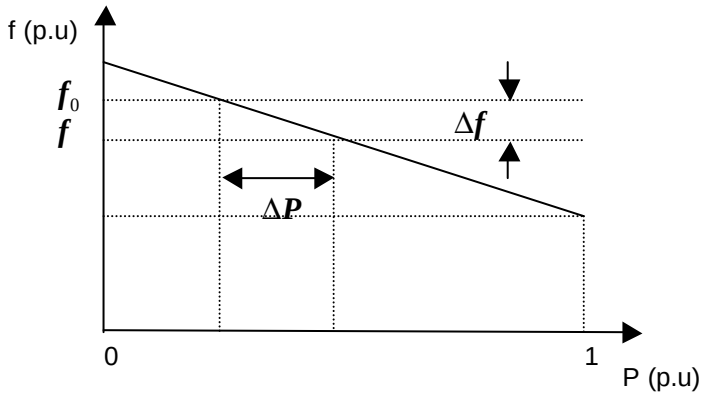

Figure 3.3 A typical frequency-droop characteristic

The value of droop R_f is the ratio of frequency deviation Δf to change in active power output ΔP. It can be expressed in percentage terms as in equation (3-1).

$$R_f = \frac{\Delta f(p.u)}{\Delta P(p.u)} \times 100\% \qquad (3\text{-}1)$$

Figure 3.4 shows a typical voltage-droop characteristic used in the voltage-droop controller.

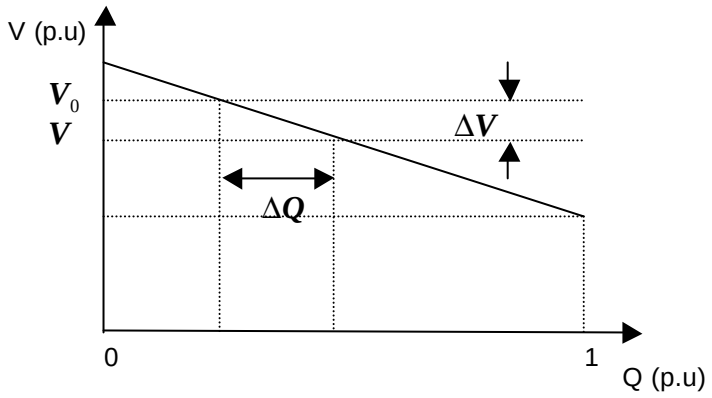

Figure 3.4 A typical voltage -droop characteristic

The value of droop R_V is a ratio of voltage deviation ΔV to change in reactive power output ΔQ. It can be expressed in percentage terms as in equation (3-2).

$$R_V = \frac{\Delta V(p.u)}{\Delta Q(p.u)} \times 100\% \qquad (3\text{-}2)$$

3.1.3 Frequency/Voltage control

With droop control action, a load change in the MicroGrid will result in steady-state frequency and voltage deviations, depending on the droop characteristics and Frequency/Voltage sensitivity of the load. The flywheel will contribute to the overall change in generation. Restoration of the Frequency/Voltage of the MicroGrid to their normal values requires a supplementary action to adjust the output of the flywheel. The basic means of the local frequency control of the MicroGrid is through regulating the output of the flywheel. As the load of the MicroGrid changes continually, it is necessary to automatically change the output of the flywheel.

The objective of the frequency control is to restore the frequency to its normal value. This is accomplished by moving the frequency-droop characteristic left or right to maintain the frequency at a constant value. The frequency control adjusts the output of the flywheel to restore the frequency of the MicroGrid to normal (e.g. 50Hz). Figure 3.5 shows the effect of this adjustment.

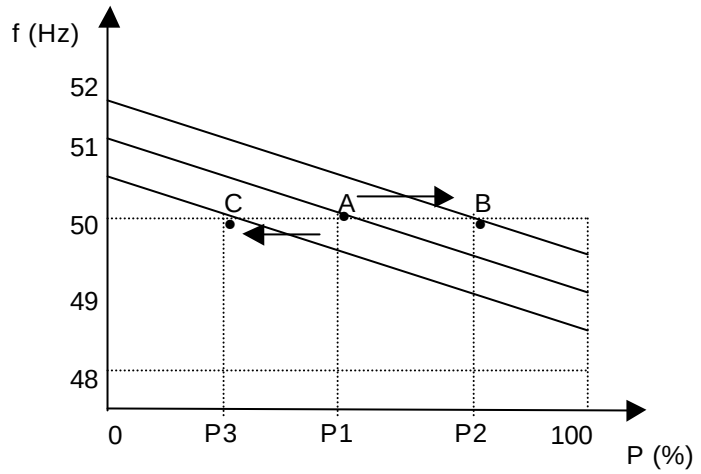

Figure 3.5 Effect of the adjustment on the frequency-droop characteristic

At 50Hz, characteristic A corresponds to P1 active power output of the flywheel, characteristic B corresponds to P2 active power output and characteristic C corresponds to P3 active power output. The frequency of the MicroGrid is fixed at a constant value (50Hz) by moving the frequency-droop characteristic left or right.

Similarly, the voltage control adjusts the voltage-droop characteristic left or right to maintain a constant voltage when the voltage of the MicroGrid is changed. Thus, the

voltage of the MicroGrid is fixed at a desired value (e.g. 1.0p.u). The effect of this adjustment is shown in Figure 3.6.

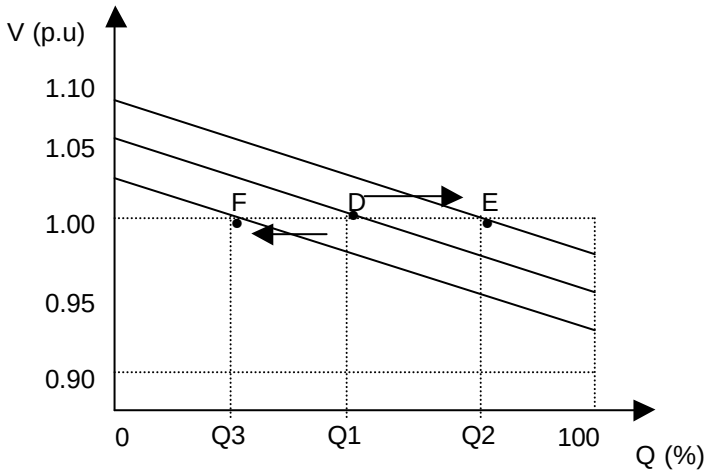

Figure 3.6 Effect of the adjustment on the voltage-droop characteristic

At 1.0 p.u voltage, characteristic D corresponds to Q1 reactive power output of the flywheel, characteristic E corresponds to Q2 reactive power output and characteristic F corresponds to Q3 reactive power output. The voltage of the MicroGrid is fixed at a constant value (1.0 p.u) by moving the voltage-droop characteristic left or right.

3.2 Implementation of the control strategies

3.2.1 With synchronous generator representation

For this representation of the MicroGrid, all micro sources and the flywheel are represented by synchronous generators. The control schemes of the MicroGrid are implemented as follows:

(1) PQ control

The function of moving droop characteristic of PQ controller is similar to the speed control of a synchronous generator with a supplementary control loop, as shown in Figure 3.7.

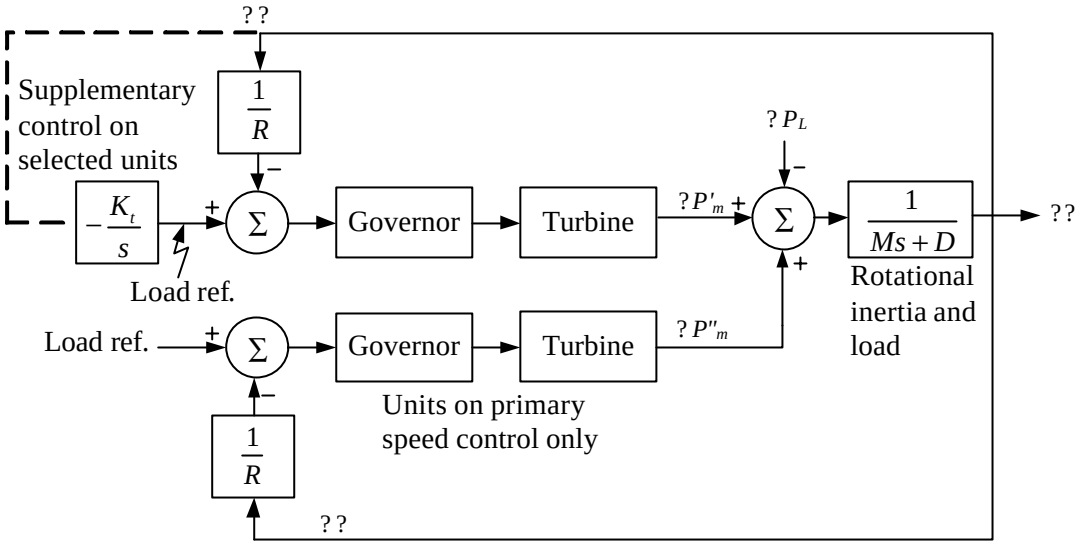

Figure 3.7 Speed control of synchronous generator with a supplementary control loop [Kundur, 1994]

The movement of the characteristic is achieved through adding an integral control loop, which acts on the load reference settings, to the speed droop control of the generator. The integral control action ensures that the output power of the generator is fixed at a constant value (setting).

Figure 3.8 shows the configuration of P controller for a synchronous generator representation of the MicroGrid.

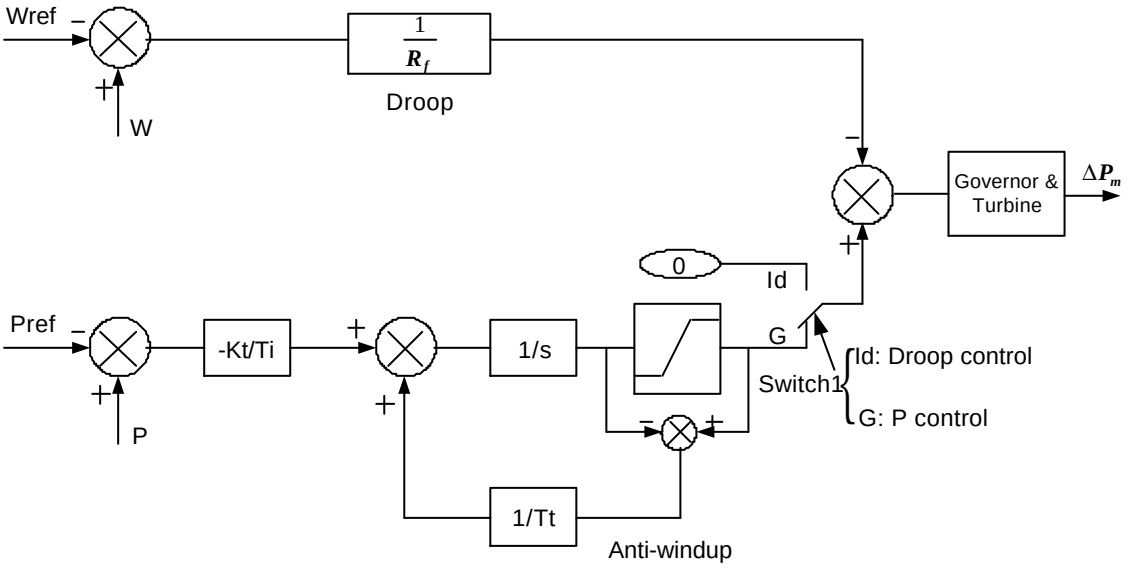

Figure 3.8 Configuration of P controller for synchronous generator representation

Figure 3.9 shows the implementation of Q controller for a synchronous generator representation.

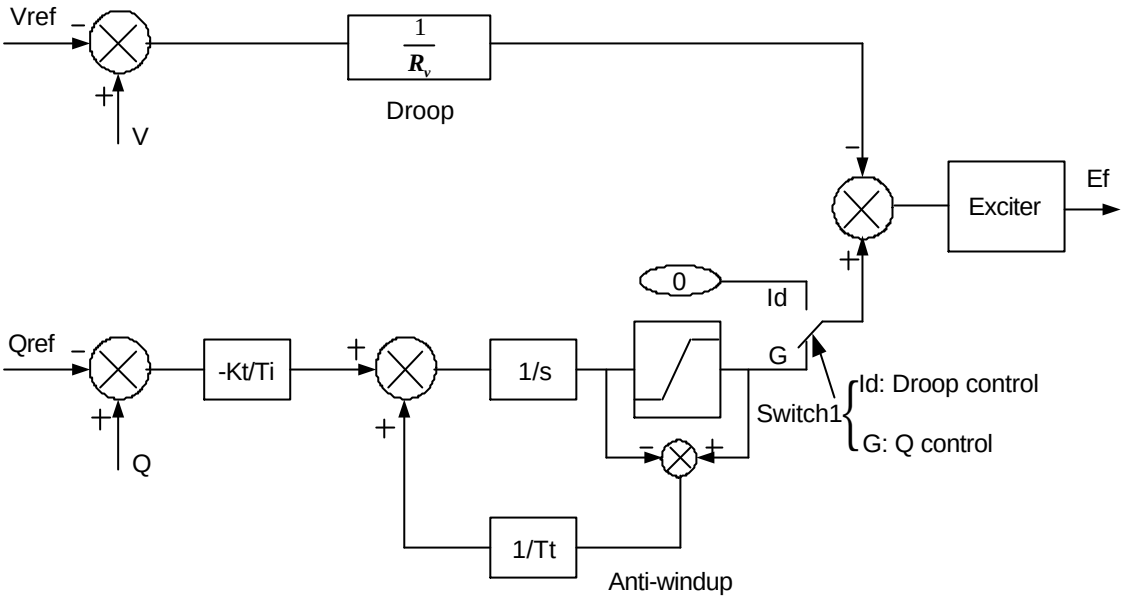

Figure 3.9 Implementation of Q controller for synchronous generator representation

(2) Droop control

The implementation of Droop control can be easily achieved by changing the position of Switch 1 from G to Id, as shown in Figures 3.8 and 3.9.

(3) Frequency/Voltage control

The implementation of Frequency control is similar to P control in Figure 3.8. However, the connection of the supplementary control loop needs to be changed from position Gp of Switch 2 to If and from Id of Switch 1 to G.

Figure 3.10 shows the layout of Frequency control for a synchronous generator representation.

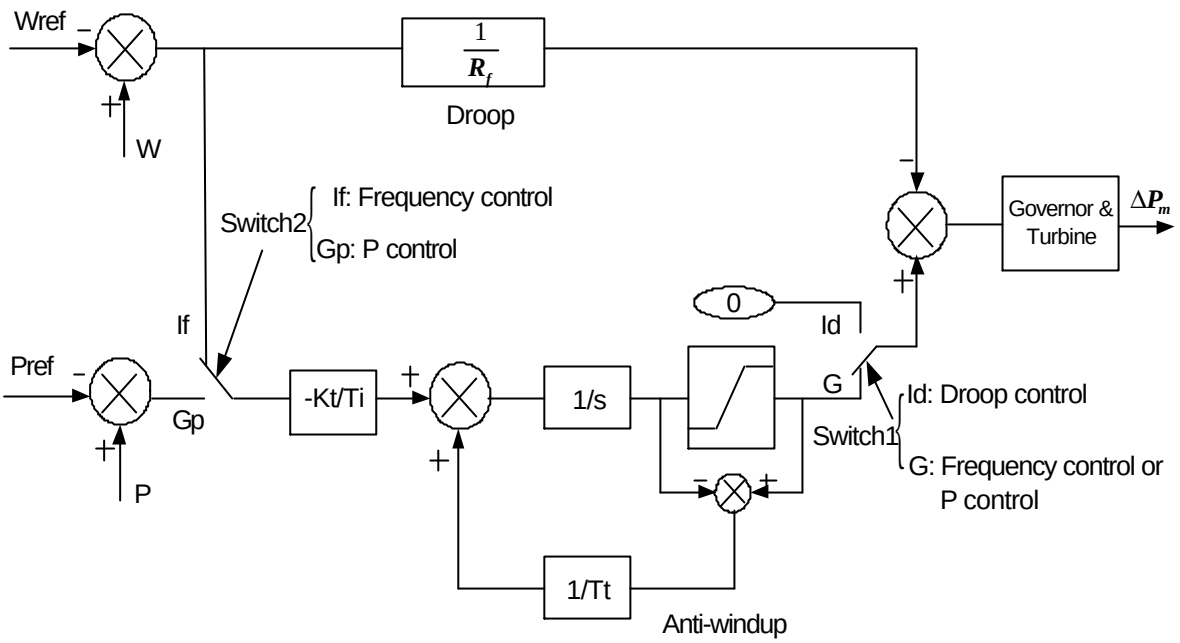

Figure 3.10 Layout of Frequency control for synchronous generator representation

Similarly, Figure 3.11 shows the implementation of Voltage control for a synchronous generator representation.

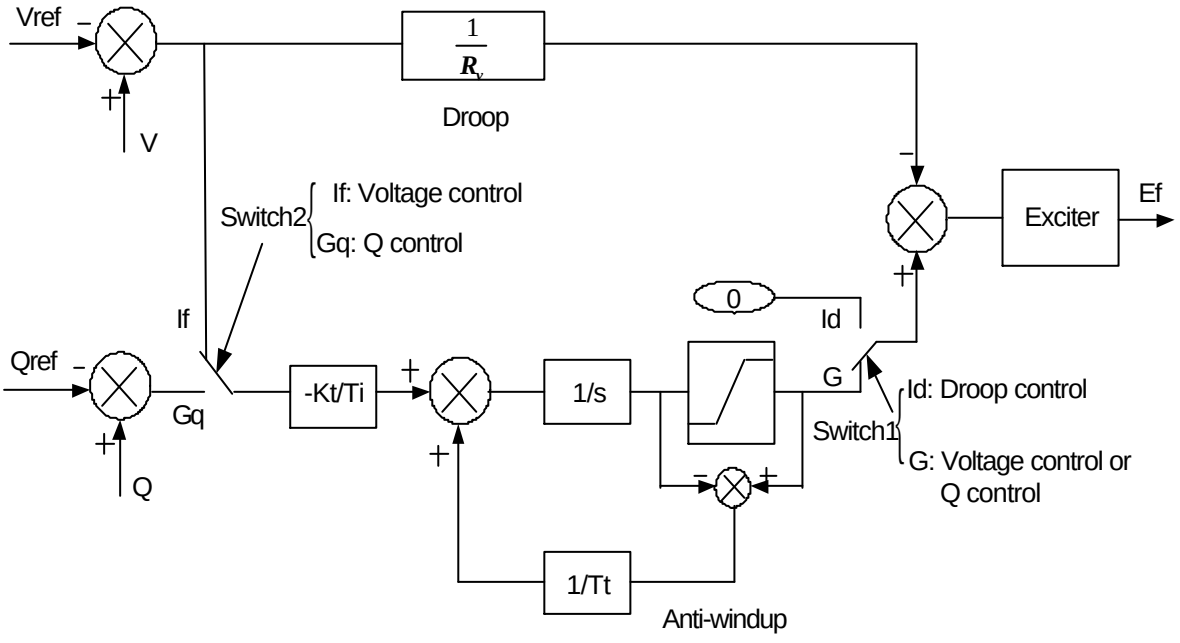

Figure 3.11 Implementation of Voltage control for synchronous generator representation

3.2.2 With STATCOM-BES representation

In this representation, the micro sources and flywheel of the MicroGrid are represented by STATCOM-BES. The control schemes of the MicroGrid consist of PQ control, Droop control and Frequency/Voltage. Figure 3.12 shows the implementation of these control strategies of the flywheel in STATCOM-BES representation.

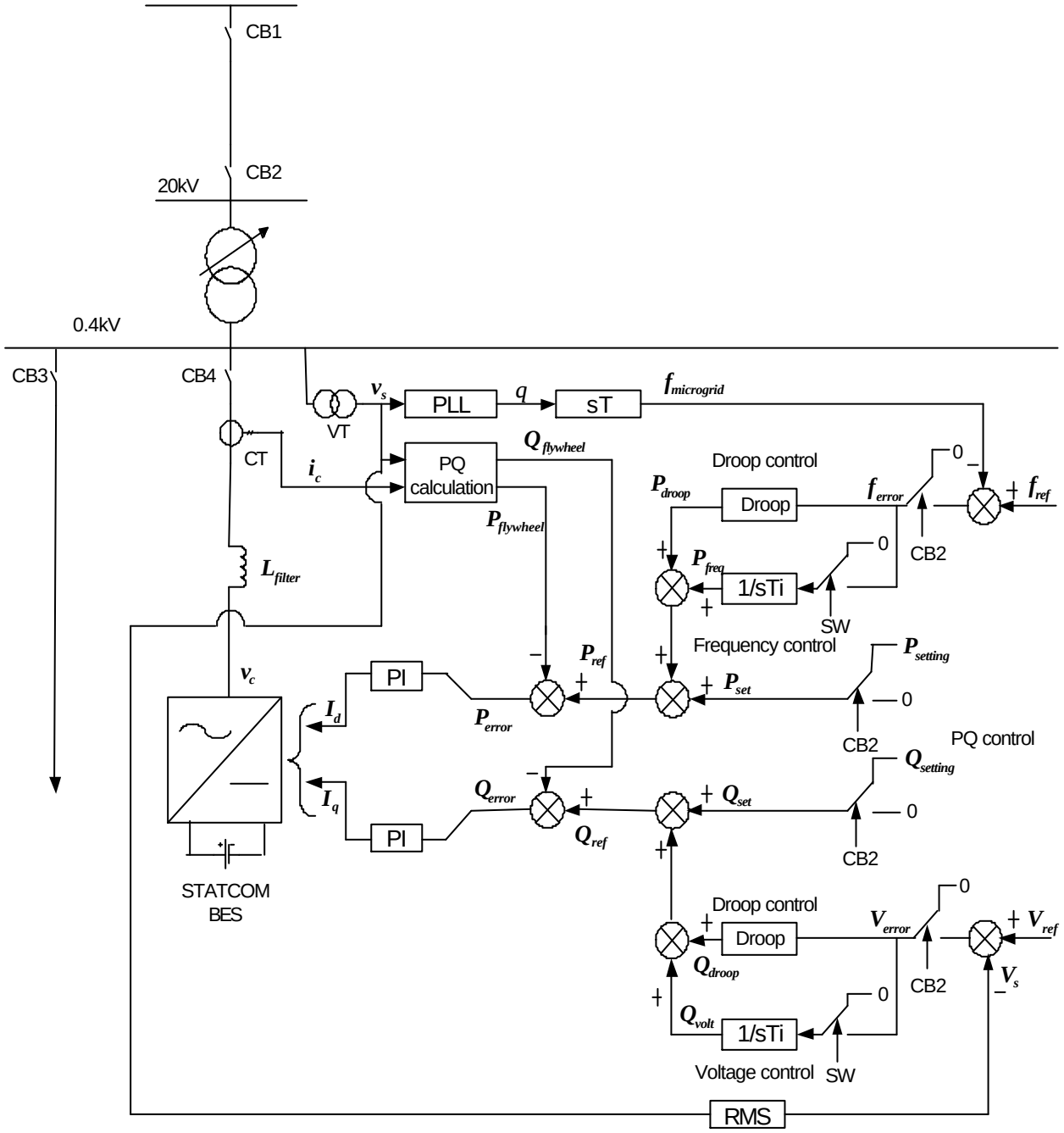

Figure 3.12 Control schemes of the flywheel represented by STATCOM-BES

During grid-connected mode, the state of circuit breaker CB2 is closed. The control scheme of the flywheel is PQ control. The output P_{droop} and Q_{droop} of Droop control are zero. The output P_{freq} and Q_{volt} of Frequency/Voltage control are also zero. The output P_{set} and Q_{set} of PQ control are set to $P_{setting}$ and $Q_{setting}$. The reference values of active powers P_{ref} and reactive power Q_{ref} of the STATCOM-BES are $P_{setting}$ and $Q_{setting}$.

After disconnection of the MicroGrid from the main network, during islanded mode, CB2 is open. The outputs P_{set} and Q_{set} of PQ control are set to zero by a state signal coming from CB2. The reference values of active power P_{ref} and reactive power Q_{ref} are P_{droop} and Q_{droop}. The integral control loops are switched to zero by SW. The control scheme of the flywheel is thus changed from PQ control to Droop control.

If the integral control loops are added to Droop control by SW, the reference value of the active power P_{ref} is the sum of P_{droop} and P_{freq}. The reference value of the reactive power Q_{ref} is also the sum of Q_{droop} and Q_{volt}. Finally, the control scheme of the flywheel is switched from PQ control to Frequency/Voltage control.

3.2.3 With controllable AC or DC voltage source representation

To simplify modelling of the flywheel, two simple representations of the flywheel are presented by using controllable AC or DC voltage sources. The control schemes of the flywheel are still PQ control, Droop control and Frequency/Voltage control, which are similar to that in the STATCOM-BES representation.

Figures 3.13 and 3.14 show the implementations of the control schemes of the flywheel represented by the AC and DC controllable voltage sources.

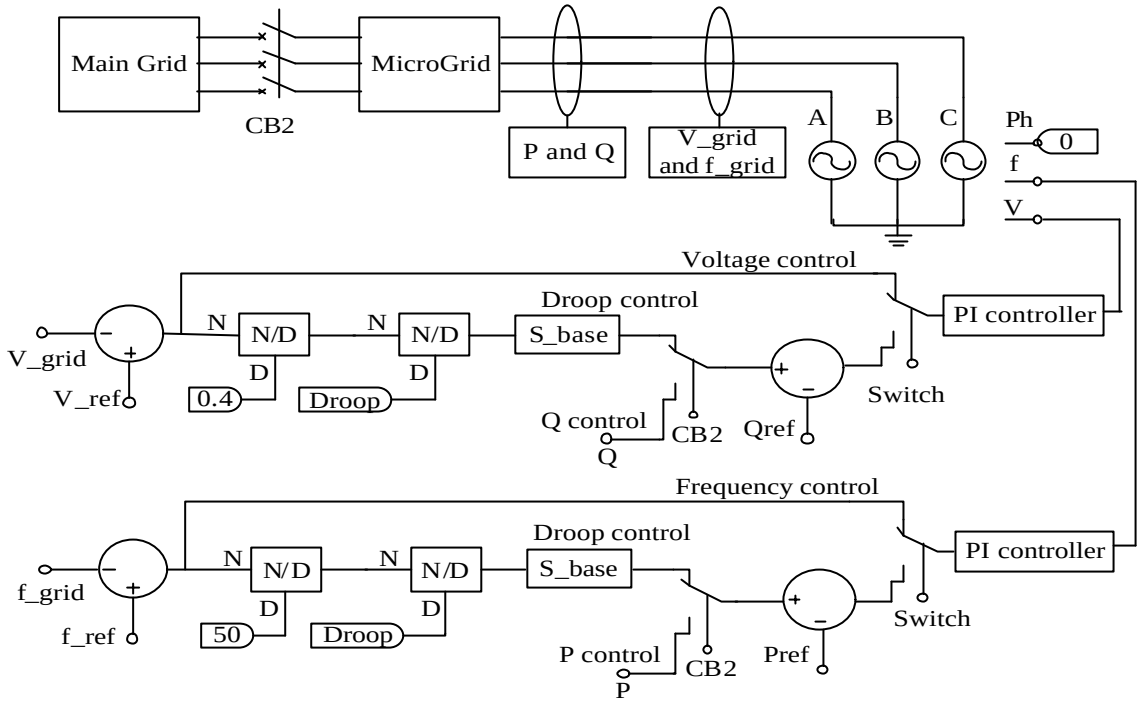

Figure 3.13 Control schemes of the flywheel represented by a controllable AC voltage source

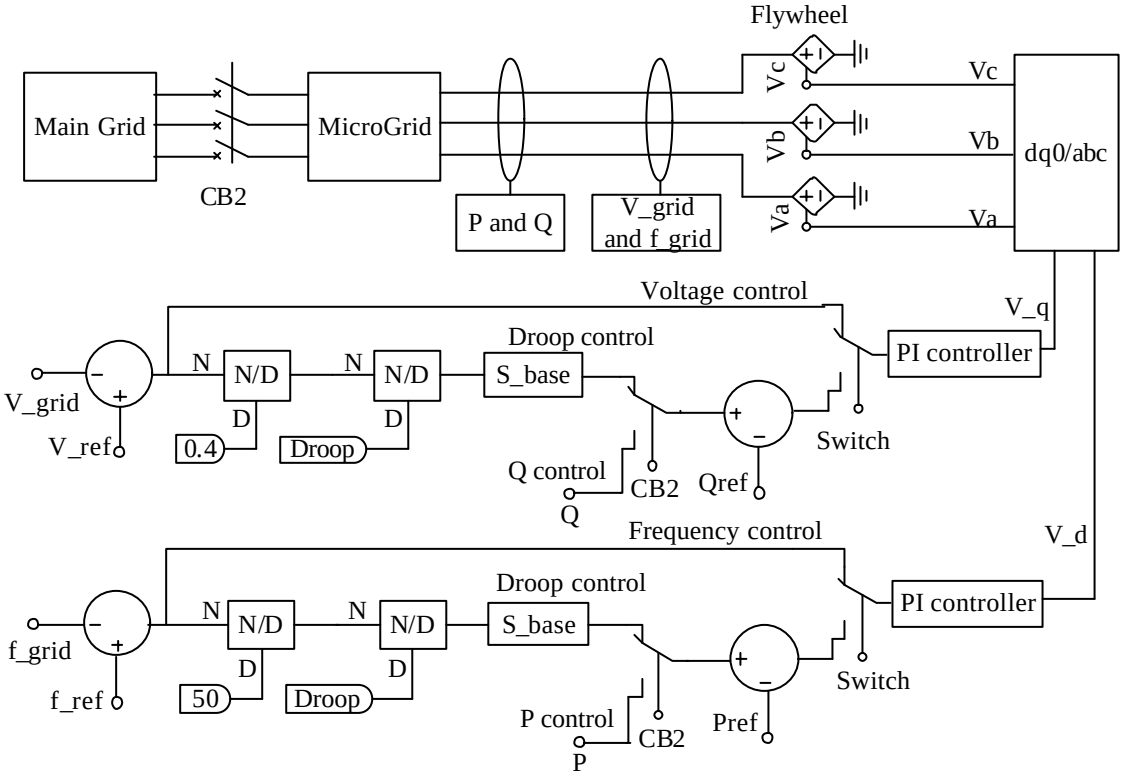

Figure 3.14 Control schemes of the flywheel represented by a controllable DC voltage source

3.3 Comparison of the three representations of a MicroGrid

3.3.1 Modelling of a simple MicroGrid in PSCAD/EMTDC

In this study, it is assumed that the micro sources and the flywheel of the MicroGrid are represented by the three representations (synchronous generator representation, STATCOM-BES representation and controllable AC and DC voltage source representation). The three representation modes of the MicroGrid are implemented in PSCAD/EMTDC and shown in Figures 3.15, 3.16 and 3.17.

Figure 3.15 shows a simple MicroGrid model, in which the micro source and the flywheel are represented by synchronous generators.

Figure 3.16 shows a simple MicroGrid model, in which the micro source and the flywheel are represented by STATCOMs-BES.

Figure 3.17 shows a simple MicroGrid model, in which the micro source and the flywheel are represented either by controllable AC or DC voltage sources.

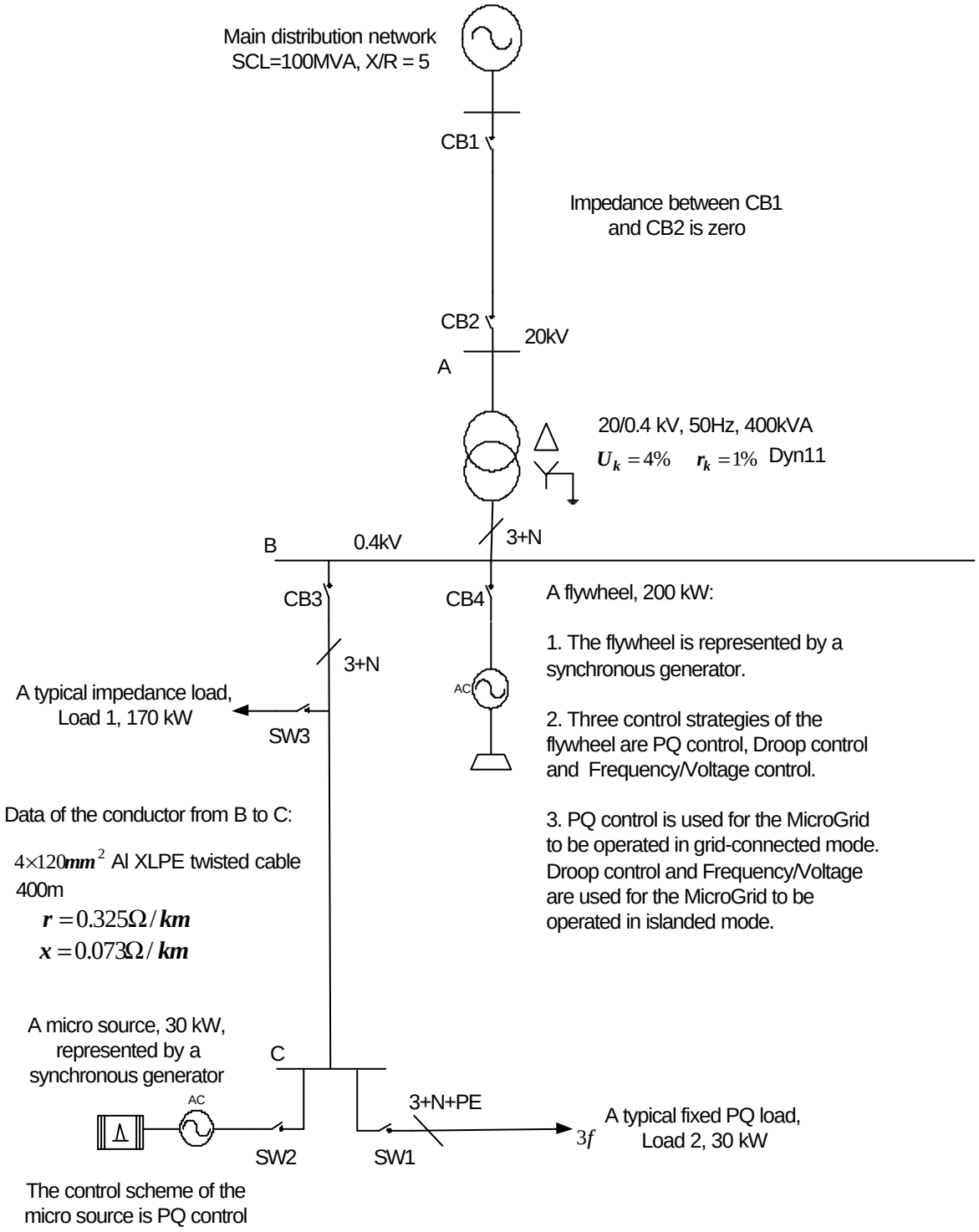

Figure 3.15 A simple MicroGrid model represented by synchronous generators

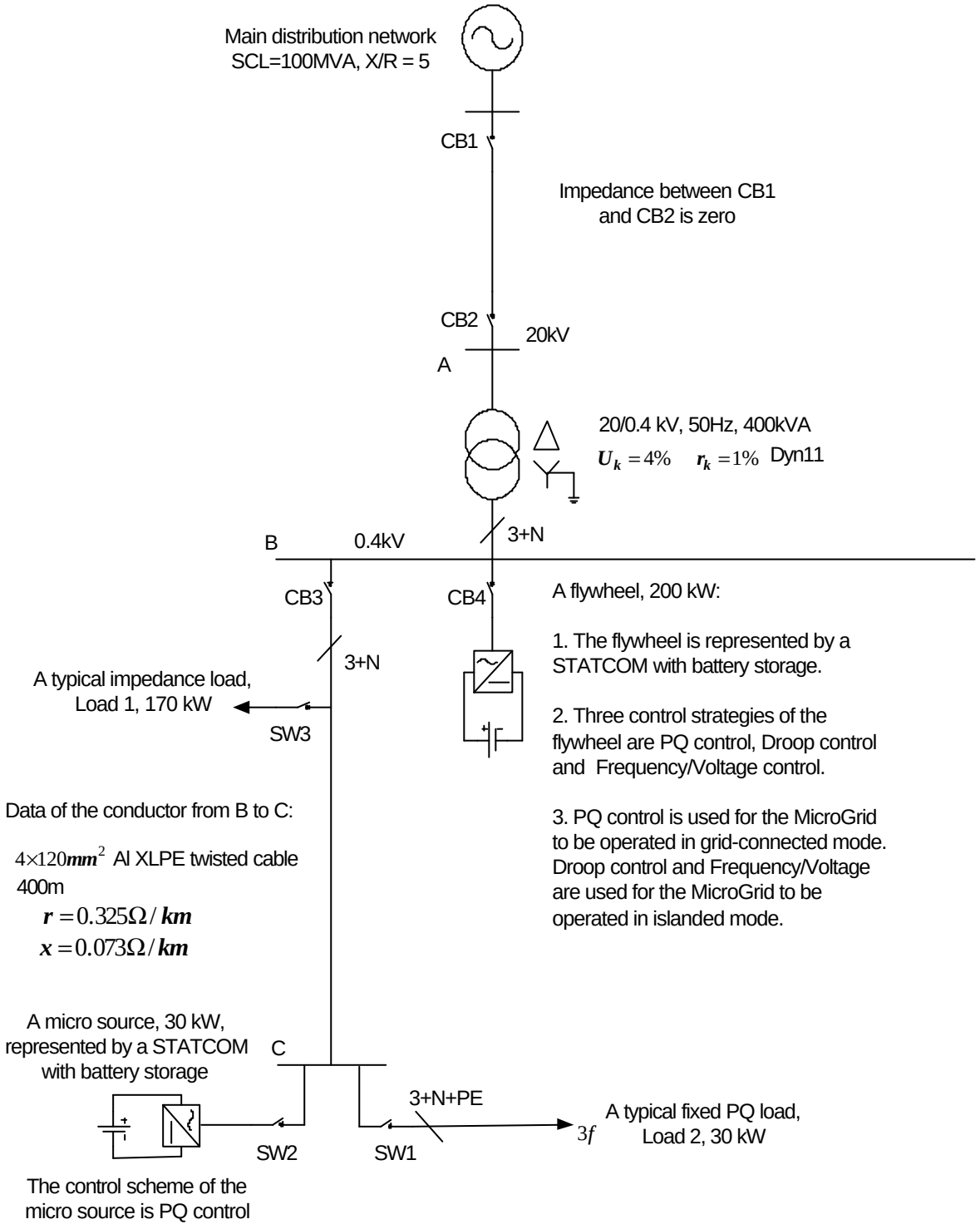

Figure 3.16 A simple MicroGrid model represented by STATCOM-BES

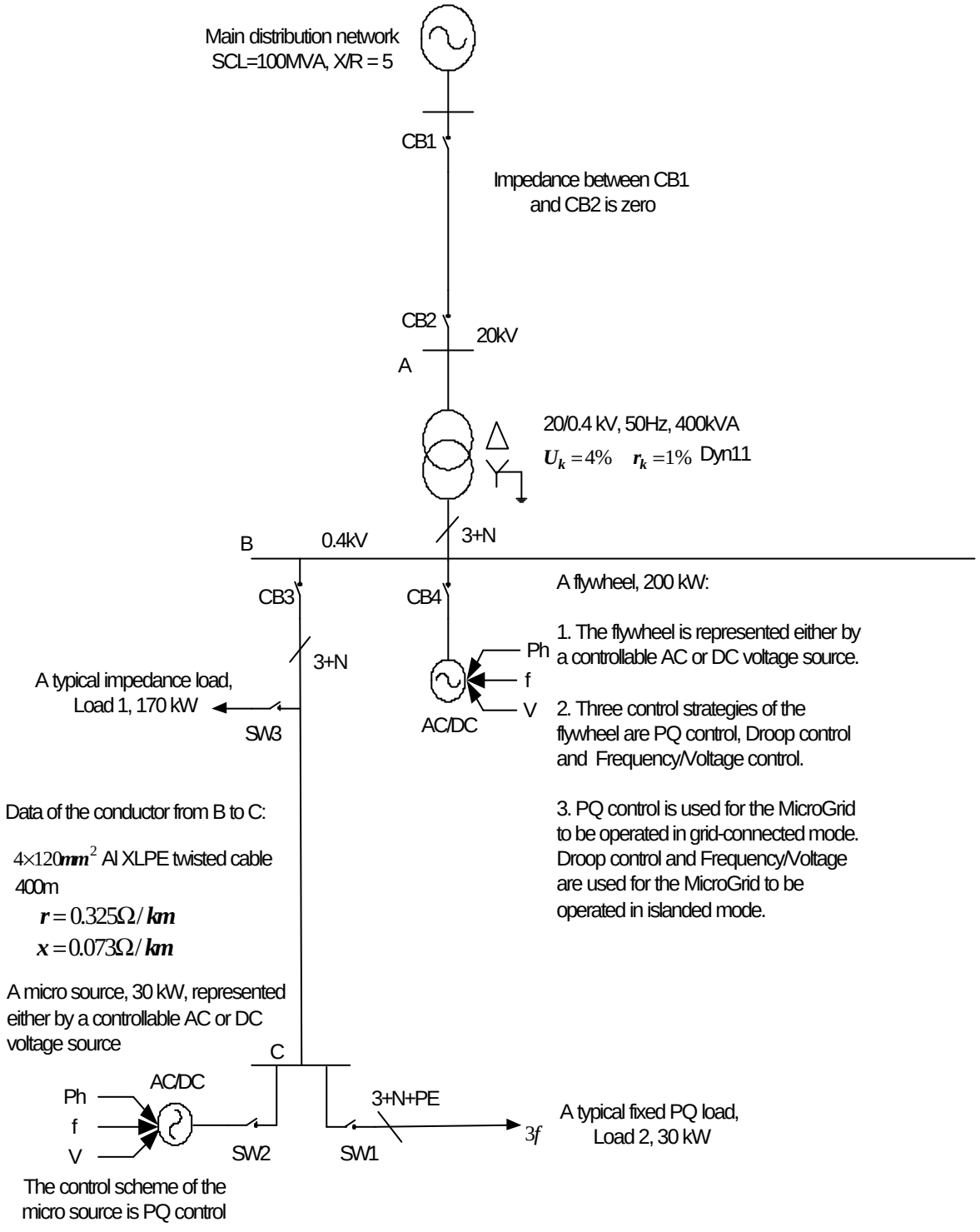

Figure 3.17 A simple MicroGrid model represented either by controllable AC or DC voltage source

In the three representations of the MicroGrid, the fault level at the 20kV main distribution network is 100MVA, with a X/R ratio of 5. One transformer (400kVA, 20/0.4kV) is installed at the substation between the main network and the MicroGrid. The impedance of the transformer is 0.01+j0.04 p.u. The MicroGrid consists of a flywheel and a feeder. The flywheel is connected to the 0.4kV busbar, which is near to the substation. The capacity of the flywheel is 200kW (assuming the flywheel supplies 4MJ energy for 20 seconds continuously). The feeder is connected to a micro source and two loads (Load 1 and Load 2) through 400 meters of ALXLPE twisted cable ($4\times120mm^2$). The impedance of the cable is 0.325+j0.073 ohms per kilometre [Bungay, 1990]. The capacity of the micro source is 30kW. Load 1 is an impedance load, with capacity of 170kW. Load 2 is a fixed PQ load, with capacity of 30kW.

In the synchronous generator representation, the parameters of the synchronous generators are the typical average values of the synchronous turbine generator constants [Glover, 2002]:

- Synchronous d-axis reactance (X_d): 1.10 [p.u];
- Synchronous q-axis reactance (X_q): 1.08 [p.u];
- Transient d-axis reactance (X'_d): 0.23 [p.u];
- Transient q-axis reactance (X'_q): 0.23 [p.u];
- Sub-transient d-axis reactance (X''_d): 0.12 [p.u];
- Sub-transient q-axis reactance (X''_q): 0.15 [p.u];
- Negative sequence reactance (X_2): 0.13 [p.u];
- Zero sequence reactance (X_0): 0.05 [p.u];
- Stator armature resistance (R_a): 0.005 [p.u];
- Transient time constant (T'_{do}): 5.60 [sec.];
- Sub- transient time constant ($T''_d = T''_q$): 0.035 [sec.];
- Inertia constant (H): 1.05 [MW/MVA].

In the STATCOM-BES and controllable AC or DC voltage source representations, the ratings of the STATCOMs-BES and the voltage sources are the same as the capacities of the micro source and flywheel, 30kW and 200kW.

The control scheme of the micro source is PQ control at all times. The control strategies of the flywheel are PQ control, Droop control or Frequency/Voltage control. The flywheel uses PQ control only when the MicroGrid is operated in grid-connected mode. During islanded mode, the control of the flywheel is switched from PQ control to Droop control or Frequency/Voltage control.

3.3.2 Simulation results

Based on the three representations of the MicroGrid (synchronous generator representation, STATCOM-BES representation, and controllable AC or DC voltage source representation), the dynamic performance of the MicroGrid was investigated and demonstrated in PSCAD/EMTDC under three control strategies (PQ control, Droop control and Frequency/Voltage control) of the flywheel. In all cases, circuit breaker CB2 is tripped at 10 seconds without a fault on the network. Following the trip of CB2, the MicroGrid is disconnected from the main network and operated in islanded mode.

(1) Synchronous generator representation

In this representation, the micro sources and flywheel in the MicroGrid are represented by synchronous generator representation, as shown in Figure 3.15. The control scheme of the micro source is PQ control all time. The control strategies of the flywheel are PQ control, Droop control and Frequency/Voltage control. For the three control schemes of the flywheel, simulation results are as follows:

(a) PQ control

Figure 3.18 shows the dynamic performance of the MicroGrid when the flywheel uses PQ control during islanded mode. The control schemes of the micro source and the flywheel are PQ control. The implementation of PQ control is shown in Figures 3.8 and 3.9.

Obviously, the flywheel makes no contribution to the local frequency and voltage control of the MicroGrid. The frequency and voltage of the MicroGrid are unstable

after disconnection of the MicroGrid from the main network. The frequency and voltage of the MicroGrid collapse so that the MicroGrid can not be operated in islanded mode.

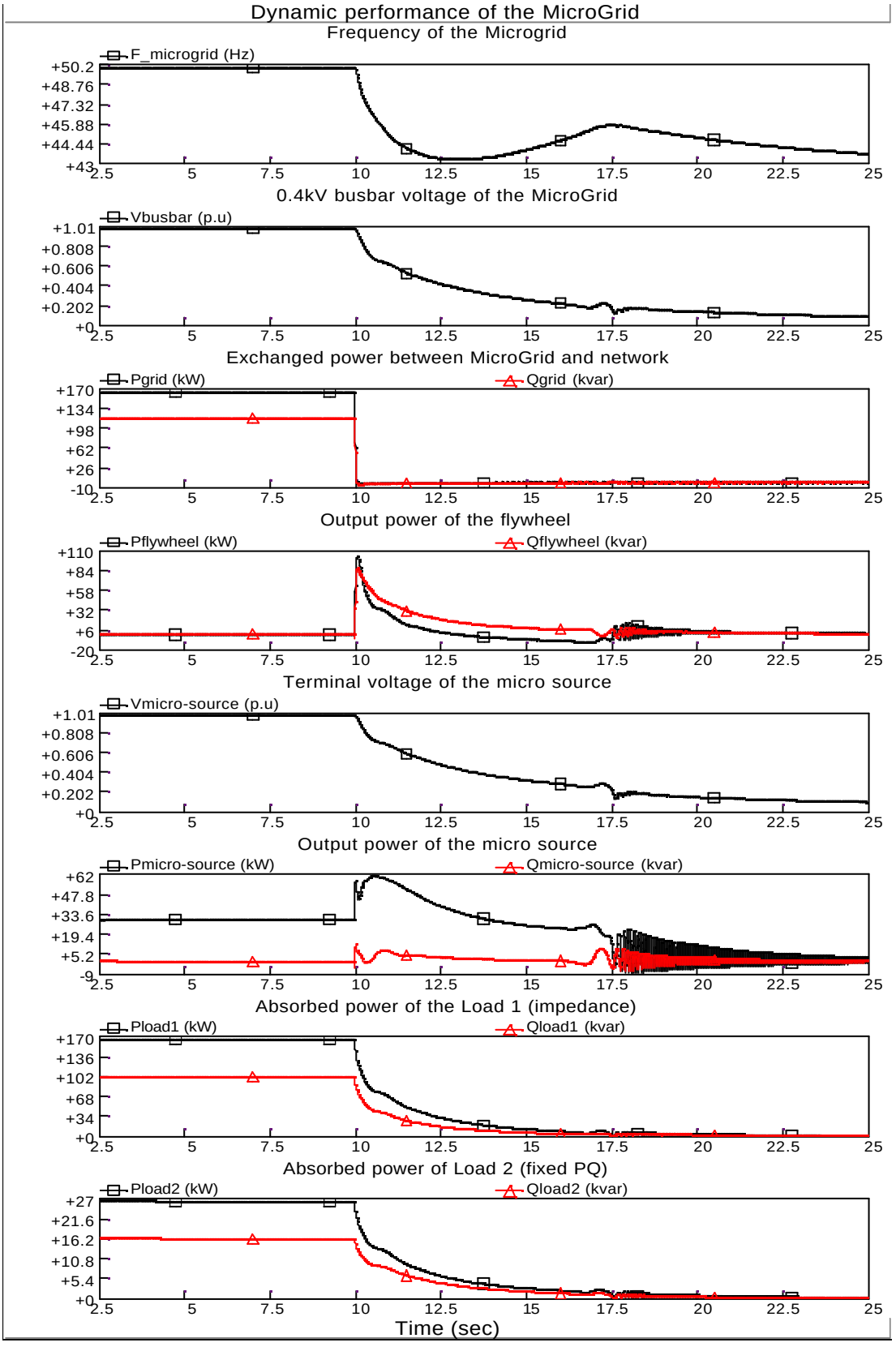

Figure 3.18 Dynamic performance of the MicroGrid (synchronous generator representation) when the flywheel uses PQ control during islanded mode

(b) Droop control

Figure 3.19 shows the dynamic performance of the MicroGrid when the flywheel uses Droop control (shown in Figures 3.8 and 3.9, changed position of Switch 1 from G to Id) during islanded mode. The control scheme of the micro source is still PQ control.

After disconnection of the MicroGrid from the main network, the output of the micro source is still retained at 30kW. But, the output of flywheel is changed from zero to the value of 149kW+j110kVar according to the droop settings ($\boldsymbol{R}_f = 4\%$ and $\boldsymbol{R}_v = 10\%$). Thus, the frequency and voltage of the MicroGrid drop to their steady state values (48.35Hz and 0.9325p.u) associated with the droop characteristics.

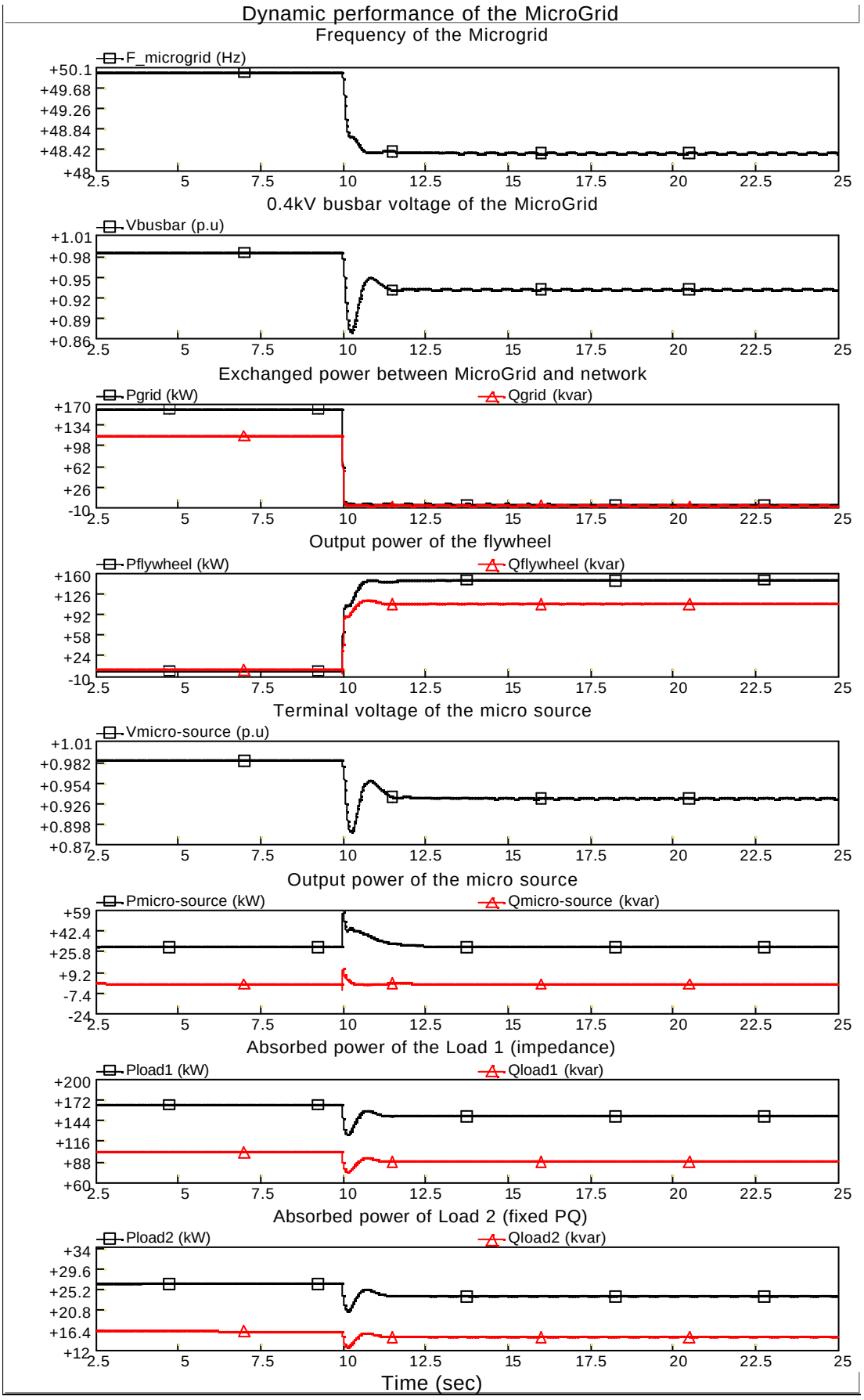

Figure 3.19 Dynamic performance of the MicroGrid (synchronous generator representation) when the flywheel uses Droop control during islanded mode

(c) Frequency/Voltage control

Figure 3.20 shows the dynamic performance of the MicroGrid when the flywheel uses Frequency/Voltage control (shown in Figures 3.10 and 3.11) during islanded mode. The control of the micro source is PQ control all time. The control of the flywheel is switched from PQ control to Frequency/Voltage.

During islanded mode of the MicroGrid, the output of the micro source is maintained at a constant value of 30kW. However, the output of the flywheel is changed from zero to the value of 171kW+j127kVar. Consequently, the frequency and voltage of the MicroGrid are both brought back to the normal values (50Hz and 1.0p.u). It should be noted that the energy export of the flywheel using Frequency/Voltage control is larger than when using Droop control.

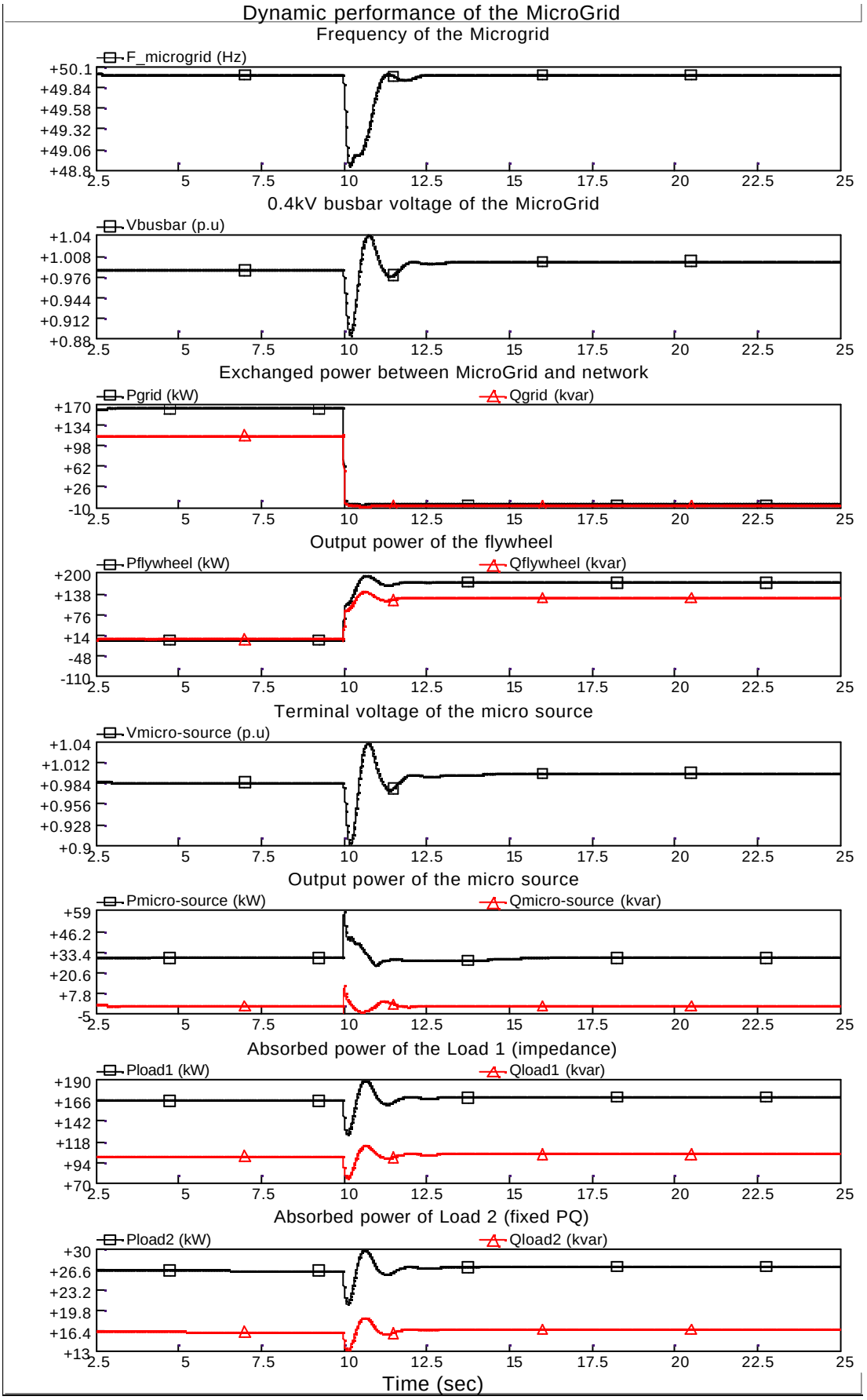

Figure 3.20 Dynamic performance of the MicroGrid (synchronous generator representation) when the flywheel uses Frequency/Voltage control during islanded mode

(2) STATCOM-BES representation

Figures 3.21, 3.22 and 3.23 show the dynamic performances of the MicroGrid represented by STATCOM-BES when the flywheel uses PQ control, Droop control and Frequency/Voltage control during islanded mode. The deviations of the frequency and voltage depend on the mismatch between generation and demand in the MicroGrid.

Comparisons with Figures 3.18, 3.19 and 3.20 show that the simulation results of the STATCOM-BES representation are similar to the synchronous generator representation. However, after a disturbance, the dynamic response of the frequency and voltage of the STATCOM-BES representation MicroGrid is faster than the synchronous generator representation due to the zero inertia value of the STATCOM-BES.

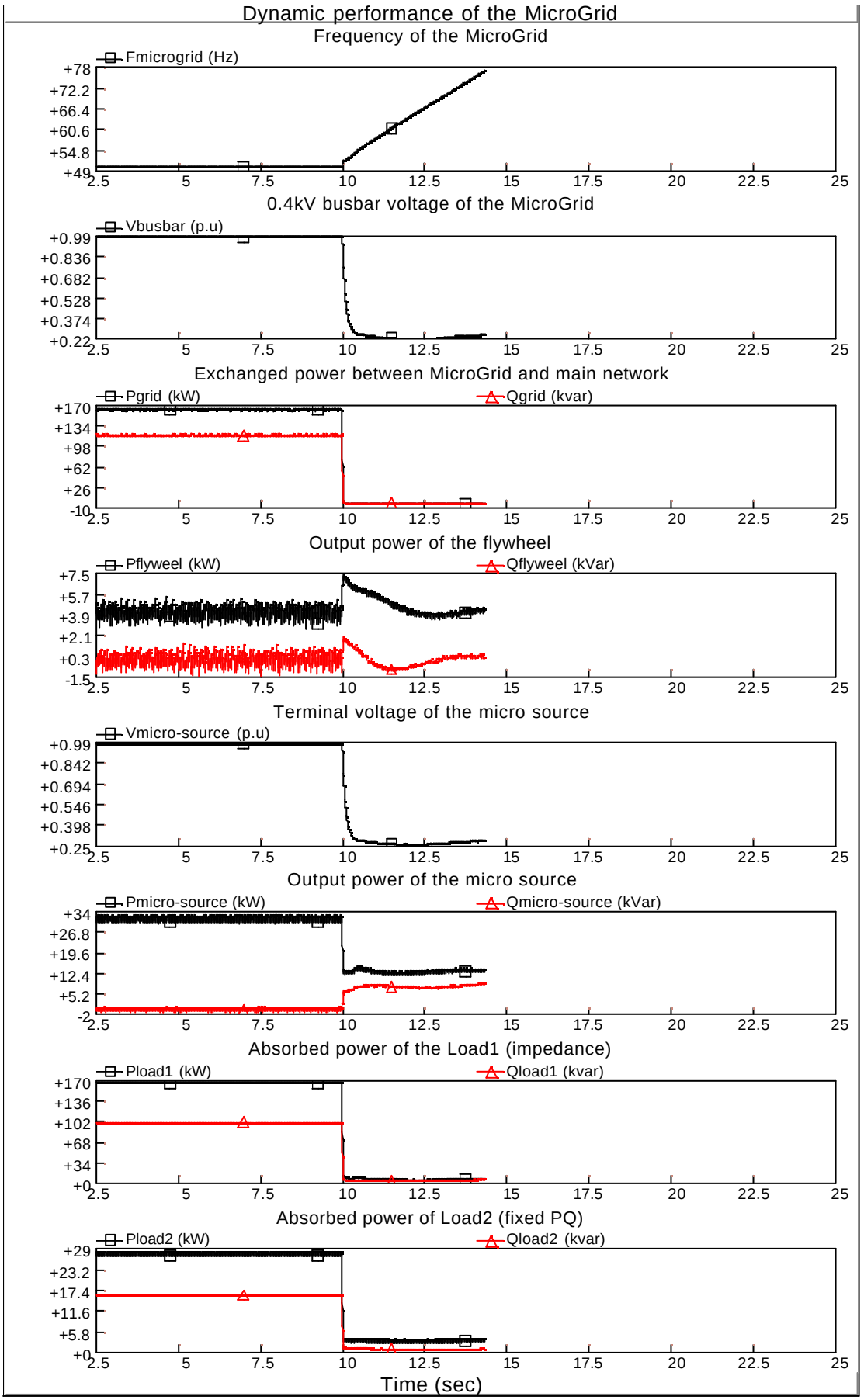

Figure 3.21 Dynamic performance of the MicroGrid (STATCOM-BES representation) when the flywheel uses PQ control during islanded mode

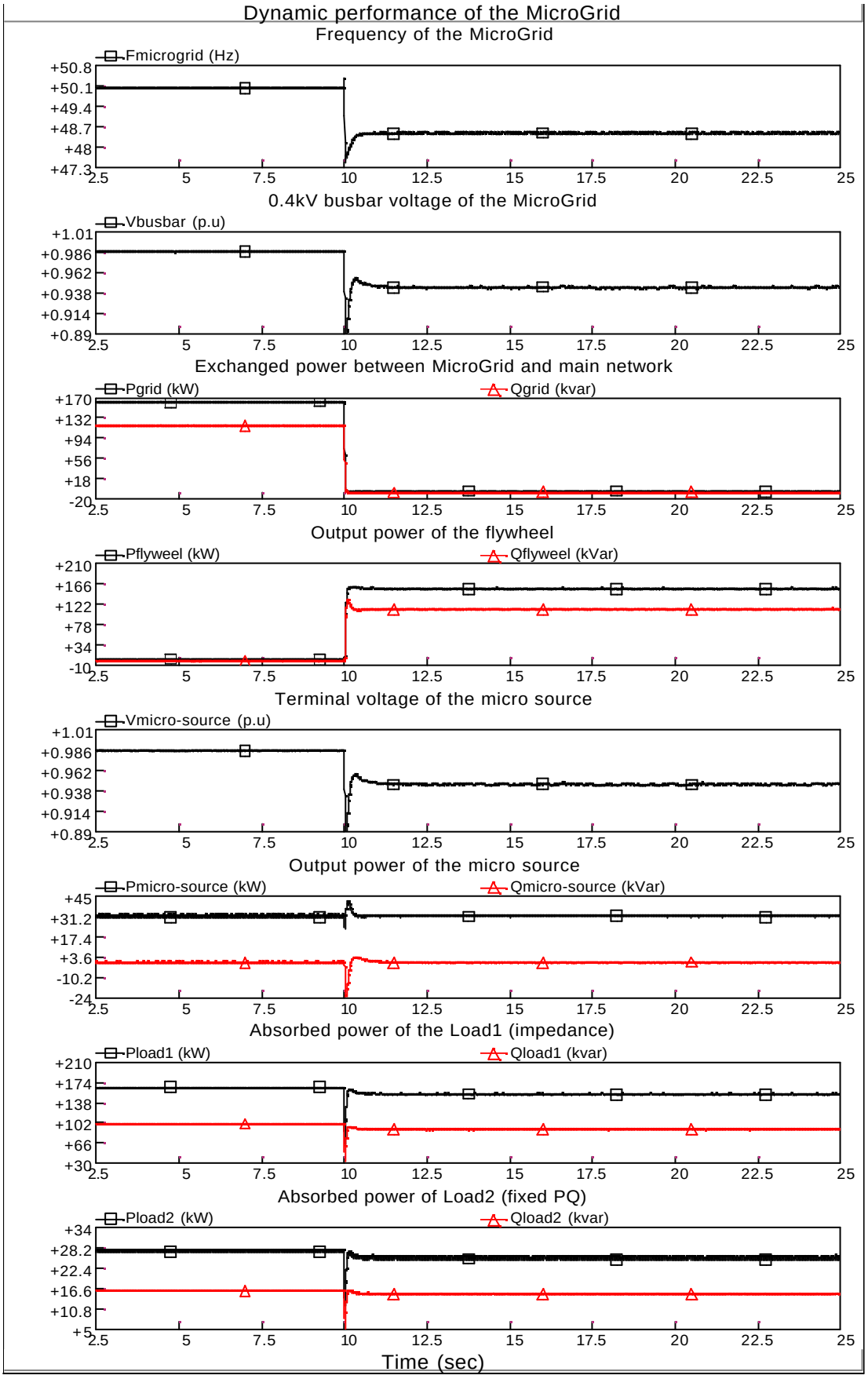

Figure 3.22 Dynamic performance of the MicroGrid (STATCOM-BES representation) when the flywheel uses Droop control during islanded mode

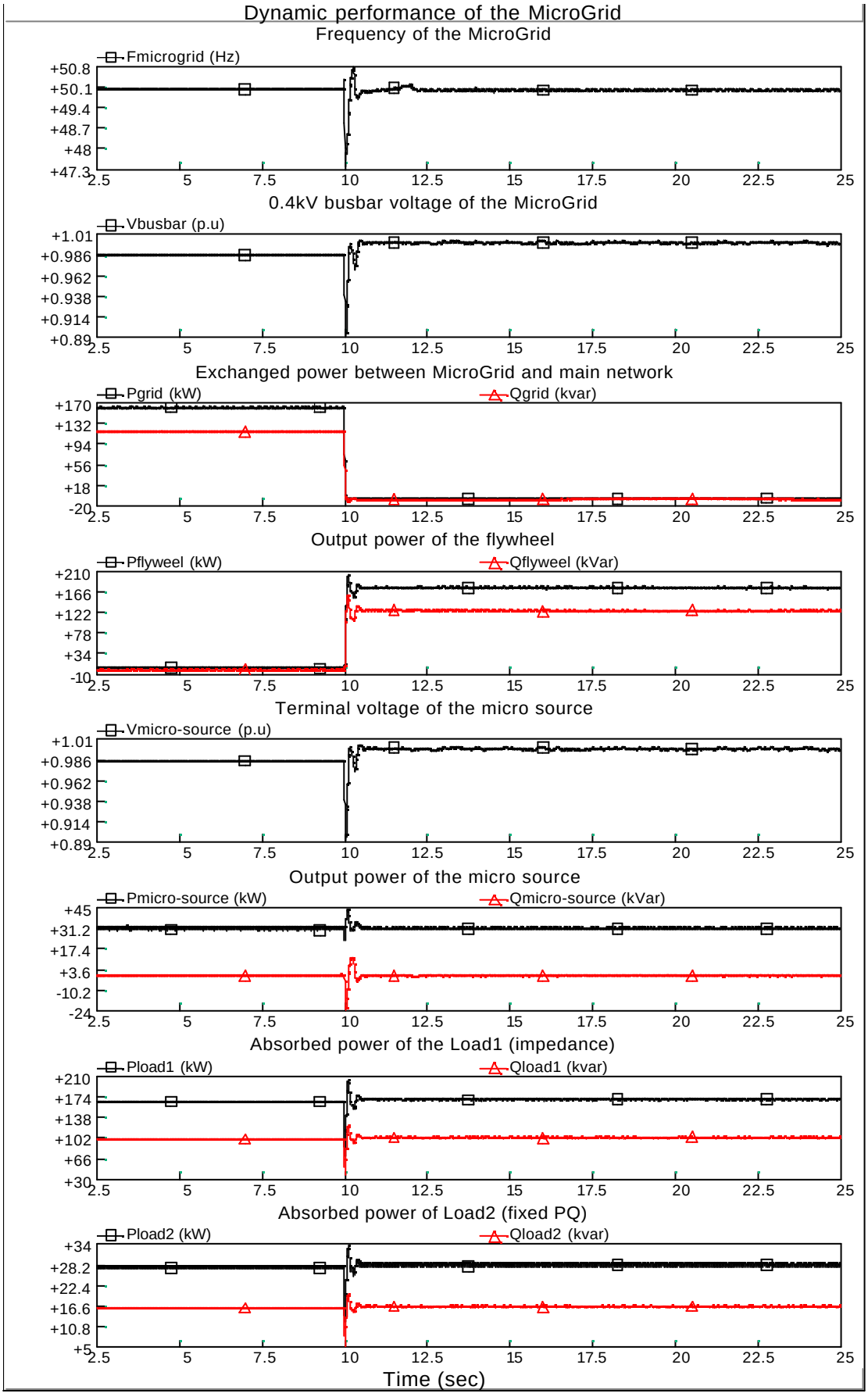

Figure 3.23 Dynamic performance of the MicroGrid (STATCOM-BES representation) when the flywheel uses Frequency/Voltage control during islanded mode

(3) Controllable AC and DC voltage source representations

The MicroGrid model used in this study is shown in Figure 3.17. The flywheel is represented either by the controllable AC or DC voltage sources. The control strategies of the flywheel are implemented and shown in Figures 3.13 and 3.14. Simulation results produced in PSCAD/EMTDC are shown in Figures 3.24, 3.25, 3.26 and 3.27.

Figure 3.24 shows the dynamic performance of the MicroGrid when the flywheel, represented by a controllable AC voltage source, uses Droop control during islanded mode. The control scheme of the flywheel is switched from PQ control to Droop control after disconnection of the MicroGrid from the main network.

Figure 3.25 shows the dynamic performance of the MicroGrid when the flywheel, represented by a controllable AC voltage source, uses Frequency/Voltage during islanded mode. The control scheme of the flywheel is switched from PQ control to Frequency/Voltage control after disconnection of the MicroGrid from the main network.

Similarly, Figures 3.26 and 3.27 show the dynamic performance of the MicroGrid when the flywheel, represented by a controllable DC voltage source, uses Droop control and Frequency/Voltage control during islanded mode.

Simulation results show that the dynamic performances of the MicroGrid produced from the simple controllable AC and DC voltage source representations of the flywheel are similar to that from the full STATCOM-BES model. For a simple application of the flywheel to the MicroGrid, the flywheel can be represented either by a controllable AC voltage source or a controllable DC voltage source.

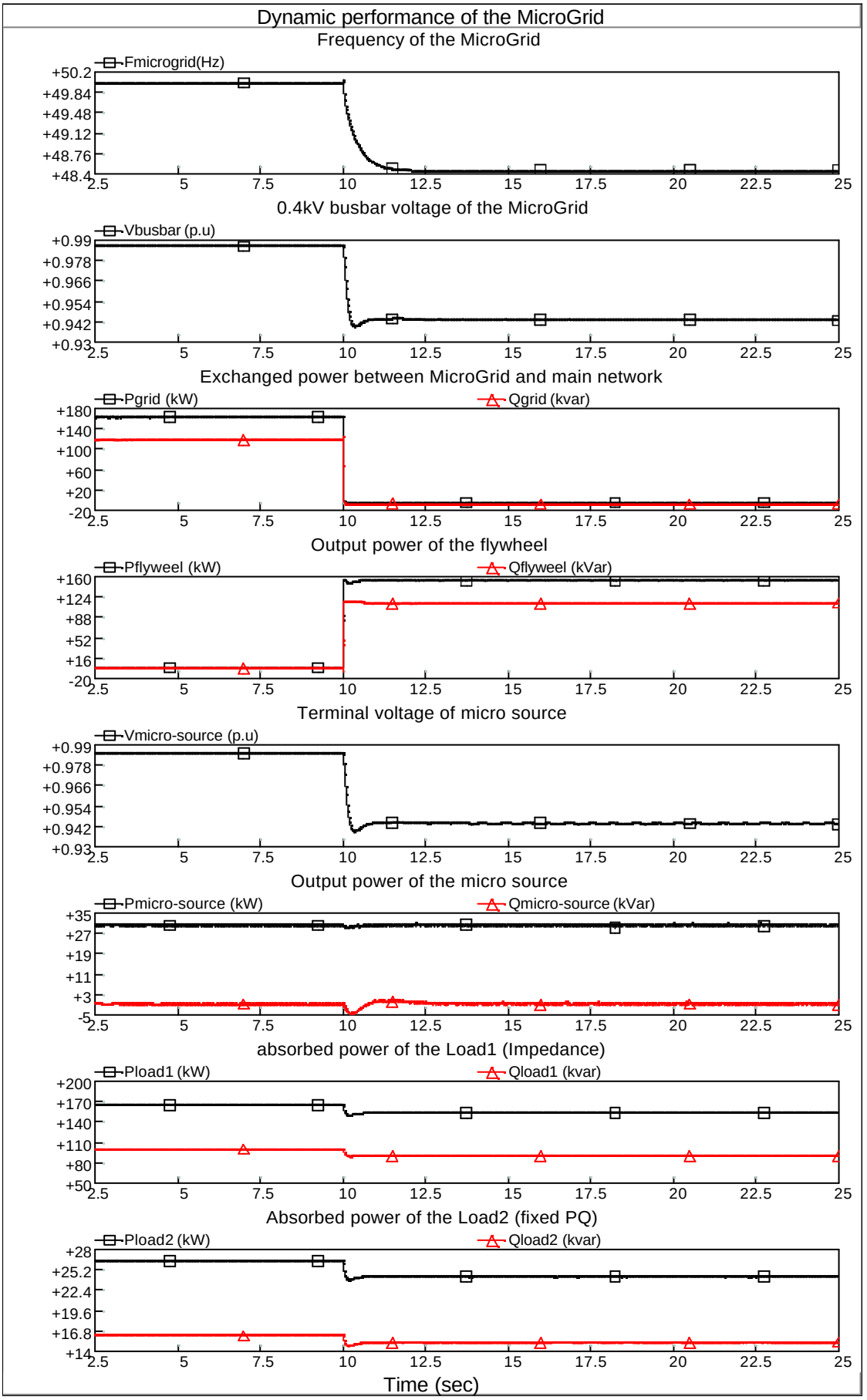

Figure 3.24 Dynamic performance of the MicroGrid when the flywheel, represented by a controllable AC voltage source, uses Droop control during islanded mode

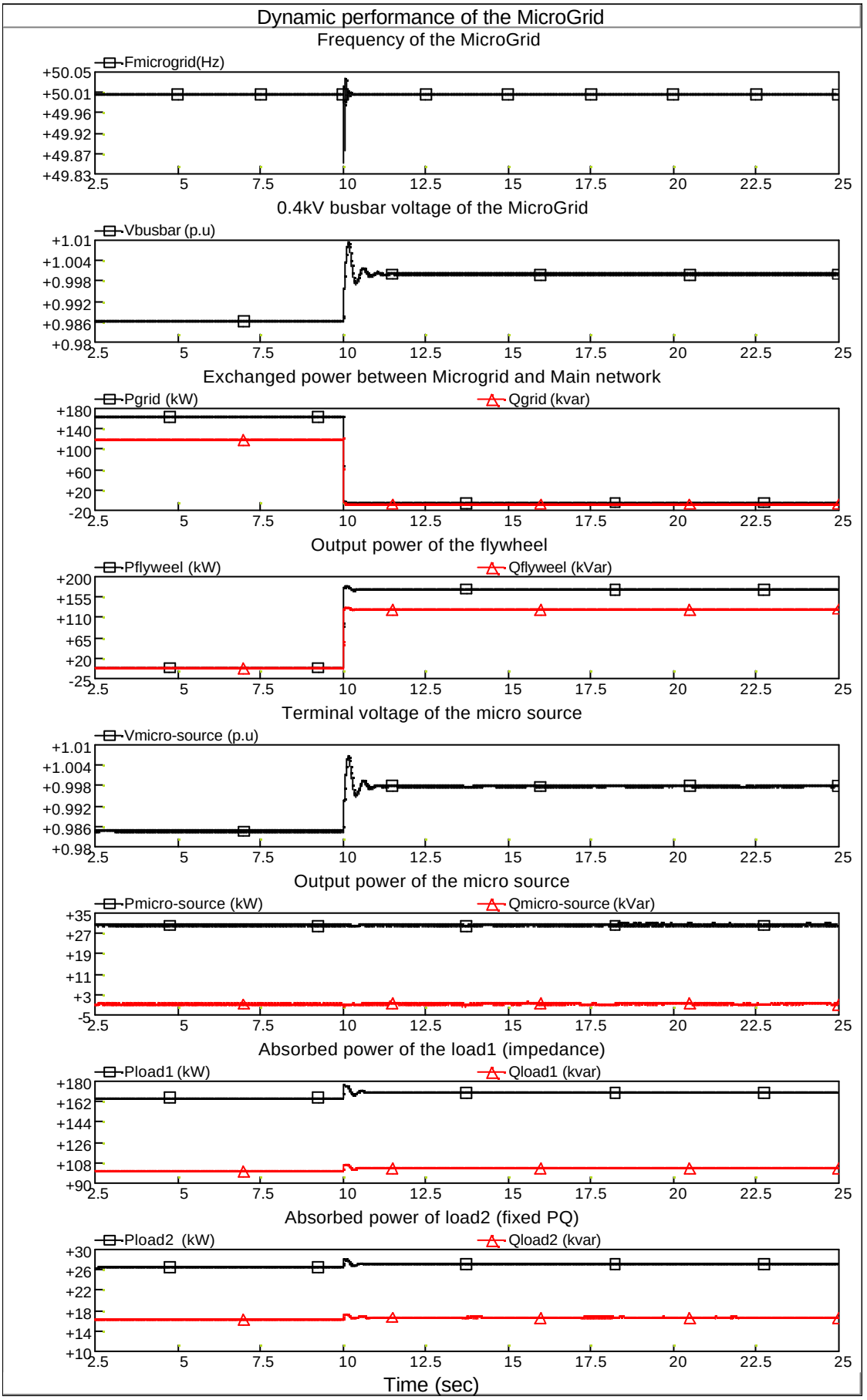

Figure 3.25 Dynamic performance of the MicroGrid when the flywheel, represented by a controllable AC voltage source, uses Frequency/Voltage control during islanded mode

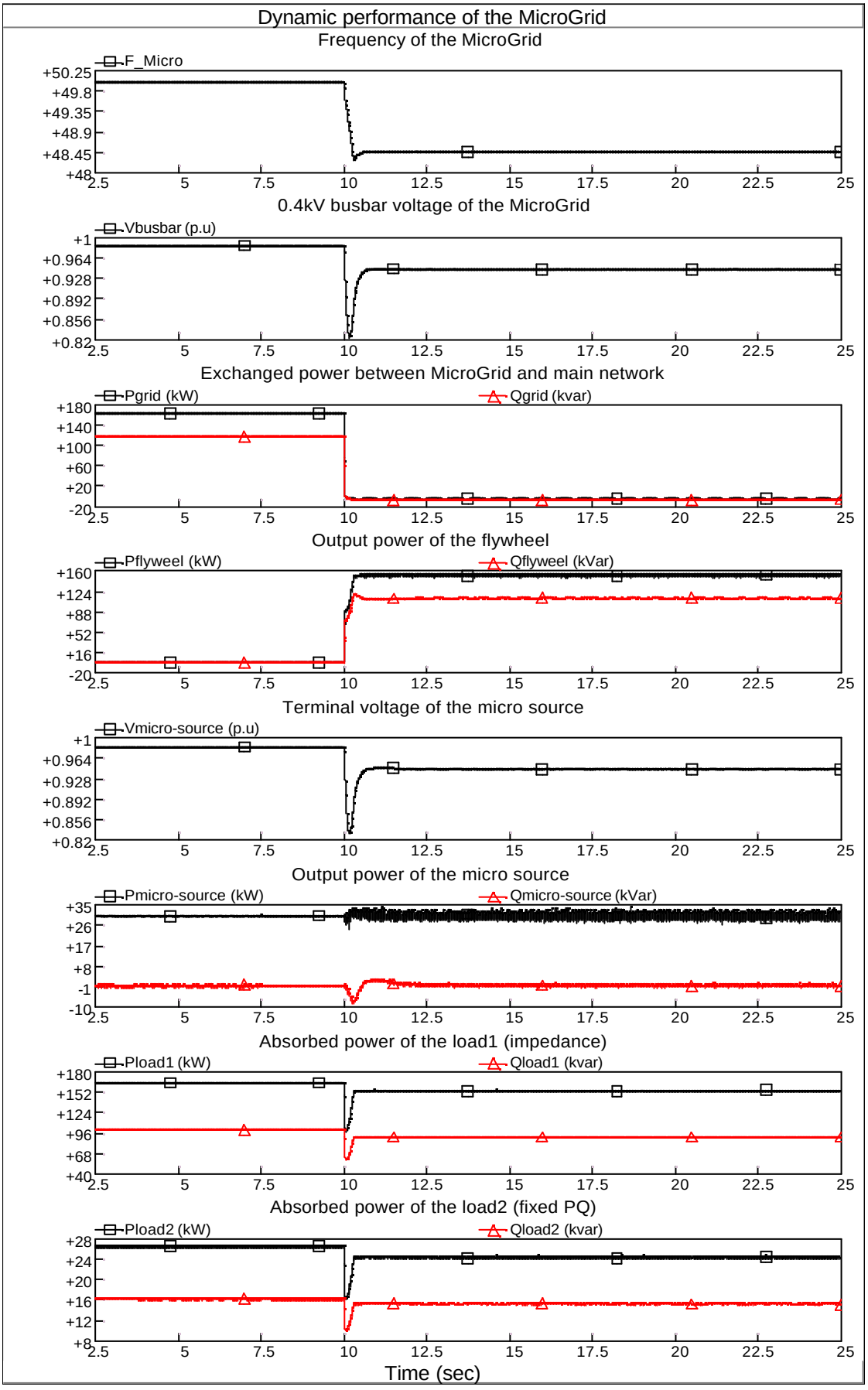

Figure 3.26 Dynamic performance of the MicroGrid when the flywheel, represented by a controllable DC voltage source, uses Droop control during islanded mode

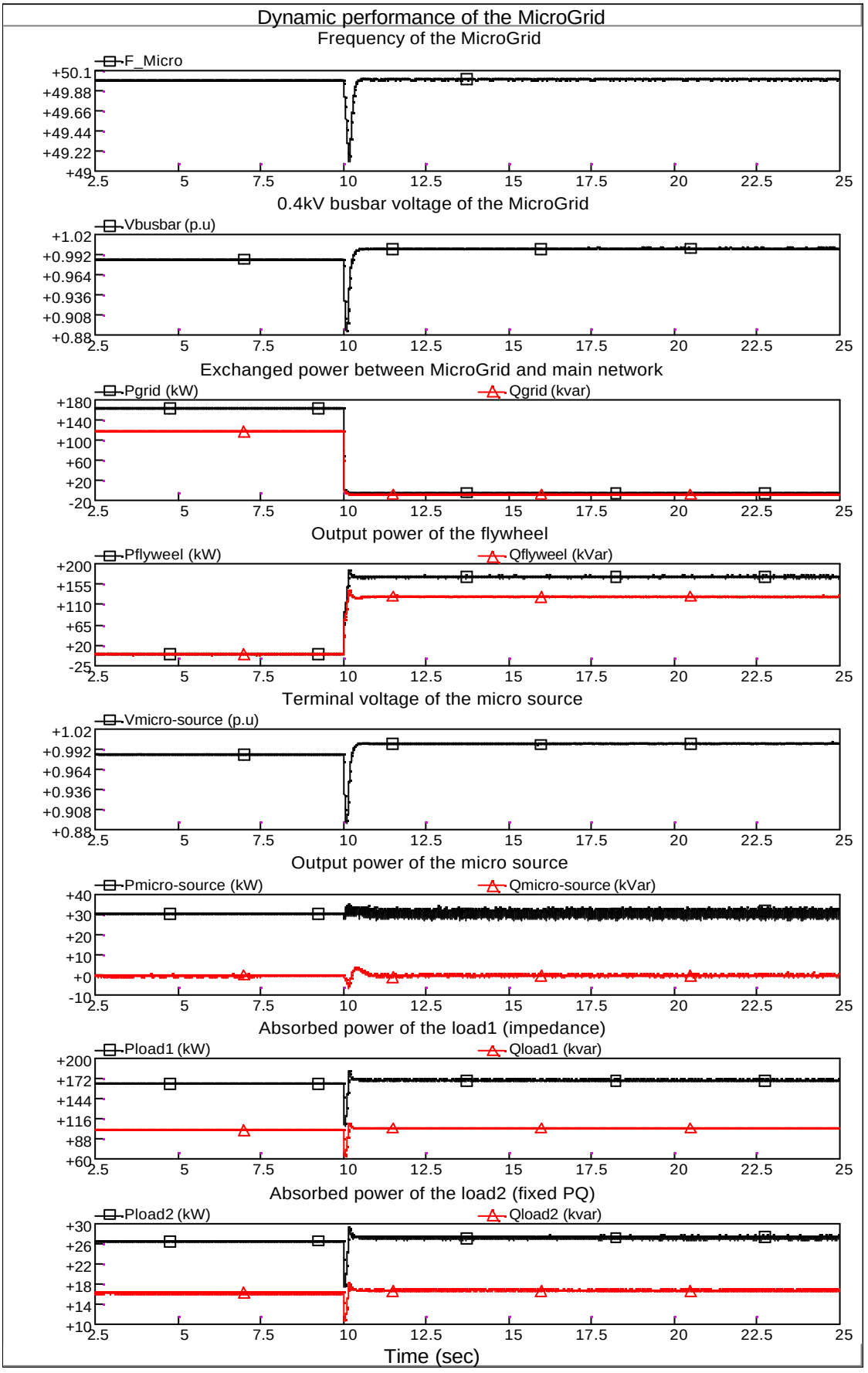

Figure 3.27 Dynamic performance of the MicroGrid when the flywheel, represented by a controllable DC voltage source, uses Frequency/Voltage control during islanded mode

3.4 Investigation of the stability of a MicroGrid

The stability of a MicroGrid is defined as a property of the MicroGrid that enables it to remain in a state of operating equilibrium under normal operating condition and to regain an acceptable state of equilibrium after being subjected to a disturbance. Being similar to the stability of the conventional system [Kundur, 1994], the stability of the MicroGrid may be divided into two components, namely, small signal stability and transient stability

The MicroGrid is small signal stable if, following small disturbances, it maintains a steady state operating condition. The dynamic simulation results of the MicroGrid produced in PSCAD/EMTDC show no evidences of small signal instability of the MicroGrid. The micro sources and flywheel are interfaced with the MicroGrid through power electronic devices. They are completely decoupled from the MicroGrid by the inverters. Normally, the length of the MicroGrid is short (less than 500meters). In summary, the MicroGrid has not demonstrated small stability problem.

The MicroGrid is transiently stable under large disturbances if, following that disturbance, it reaches an acceptable steady state operating condition. The large disturbance usually considered is a severe contingency, causing a large deviation of the operating state of the MicroGrid (e.g. a three-phase fault on the feeder). Instability of the MicroGrid may result in voltage and/or frequency collapse.

The major factors influencing the stability of the MicroGrid include the control strategies of the MicroGrid, types of load in the MicroGrid and inertia constants of the motor. The control schemes of the MicroGrid are PQ control, Droop Control and Frequency/Voltage control. The micro sources and the flywheel use PQ control only when the MicroGrid is operated in grid-connected mode. After disconnection of the MicroGrid from the main network, the control of the flywheel is switched from PQ control to Droop control or Frequency/Voltage control. The types of load in the MicroGrid are fixed PQ, impedance and motor. The absorbed power of the fixed PQ load is constant at all time. The power taken by impedance loads is a function of the frequency and voltage of the MicroGrid. The motor is a rotating machine with a value of inertia.

To indicate the stability of the MicroGrid, a critical clearing time (CCT) is used in the study. The CCT is defined as a maximum fault clearing time, such that when the fault is cleared before this value the MicroGrid is stable. If the CCT is larger than the actual fault clearing time, the MicroGrid is determined to be stable; otherwise, the MicroGrid is unstable. The difference between these two values is an index of stability of the MicroGrid. The larger the CCT is, the higher the stability of the MicroGrid has.

Figure 3.28 shows a simple MicroGrid represented by STATCOM-BES. To investigate the stability of the MicroGrid, it is implemented in PSCAD/EMTDC.

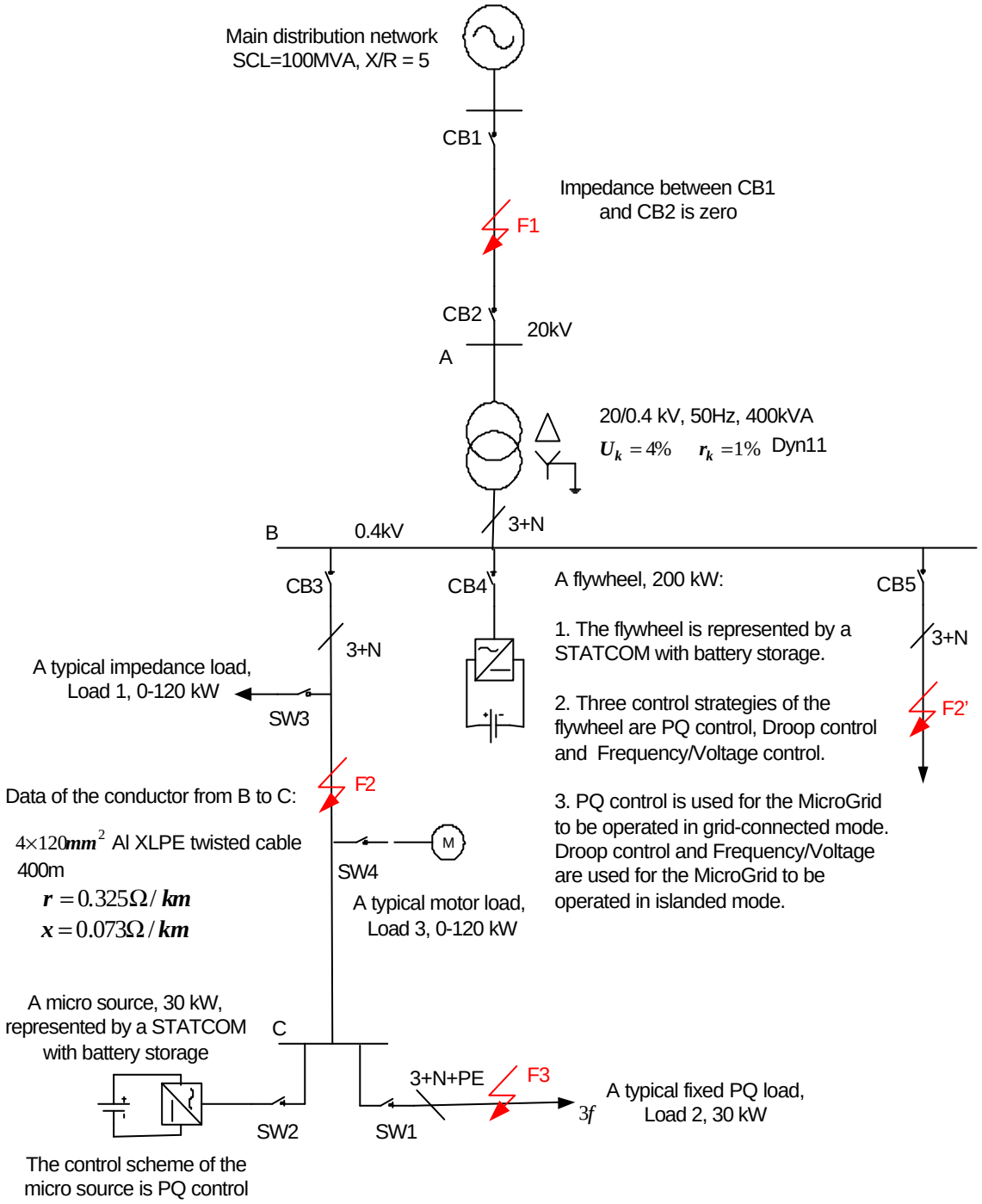

Figure 3.28 A simple MicroGrid model represented by STATCOM-BES

In Figure 3.28, the flywheel and micro source are represented by STATCOM-BES. The parameters of the MicroGrid are the same as that described in Section 3.3. Load 3 is a typical squirrel induction motor. The parameters of the motor are as follows [Smith, 1993]:

- Rated capacity: 100 [kW]
- Rated voltage: 0.4 [kV]
- No. of Poles: 4;
- Power factor: 0.8;
- Stator resistance (R_s): 0.0267 [p.u];
- Stator unsaturated leakage reactance (X_s): 0.0990 [p.u];
- Mutual unsaturated reactance (X_m): 3.7380 [p.u];
- Rotor resistance (R_r): 0.0126 [p.u];
- Rotor unsaturated mutual reactance (X_r): 0.0665 [p.u];
- Inertia constant (H): 0.6600 [kW sec./kVA].

3.4.1 Impact of types of load in the MicroGrid

Based on a simple MicroGrid model shown in Figure 3.28, the impact of three types of load (fixed PQ load, impedance load and motor load) on the stability of the MicroGrid is tested in PSCAD/EMTDC. A three-phase fault was applied at F1 at 10 seconds. Following the fault, the MicroGrid was disconnected from the main network and operated in islanded mode when the circuit breaker CB2 was open.

(1) Fixed PQ load

In this case, the type of load in the MicroGrid is a fixed PQ load, with a capacity of 200kW. Figure 3.29 shows the dynamic performance of the MicroGrid subjected to a long-term (5 seconds) disturbance of the fault at F1. It can be seen that the MicroGrid has no stability problem. During the fault, the voltage of the MicroGrid drops to zero. The frequency of the MicroGrid increases continuously due to the difference of active power between generation and demand in the MicroGrid. Although the frequency of the MicroGrid is high during the fault, it has no influence on the load as the absorbed power of the load is zero during the fault. The load is de-energised during the fault as the applied voltage is zero. After the fault, the MicroGrid is stable. The voltage and frequency of the MicroGrid are both brought back to their normal values.

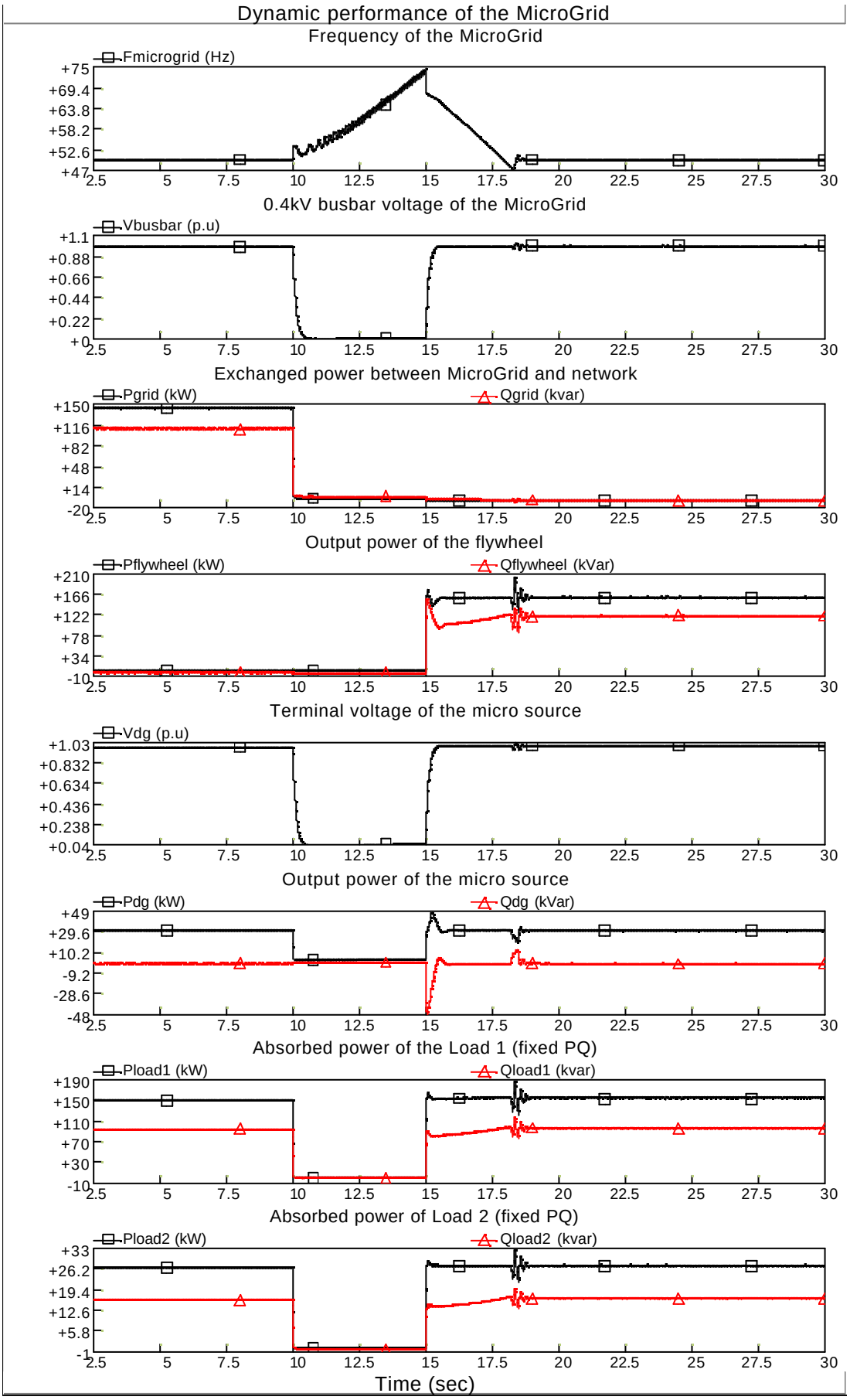

Figure 3.29 Dynamic performance of the MicroGrid for a type of fixed PQ load

(2) Impedance load

Similarly, the MicroGrid has also no stability problem for the impedance load.

(3) Motor load

In this case, the type of load in the MicroGrid is a squirrel induction motor, with a capacity of 200kW. Figure 3.30 shows the dynamic performance of the MicroGrid for a fault at F1 with a clearing time of 0.025 seconds. During the fault, the speed of the motor decreases. After the fault, it can be seen that the speed of the motor reduces continuously, and then, the motor is stalled. The motor tends to absorb large reactive power from the MicroGrid. The MicroGrid is unstable. The voltage of the MicroGrid collapses while the frequency of the MicroGrid is normal. This is a typical transient voltage instability (voltage collapse) of the MicroGrid.

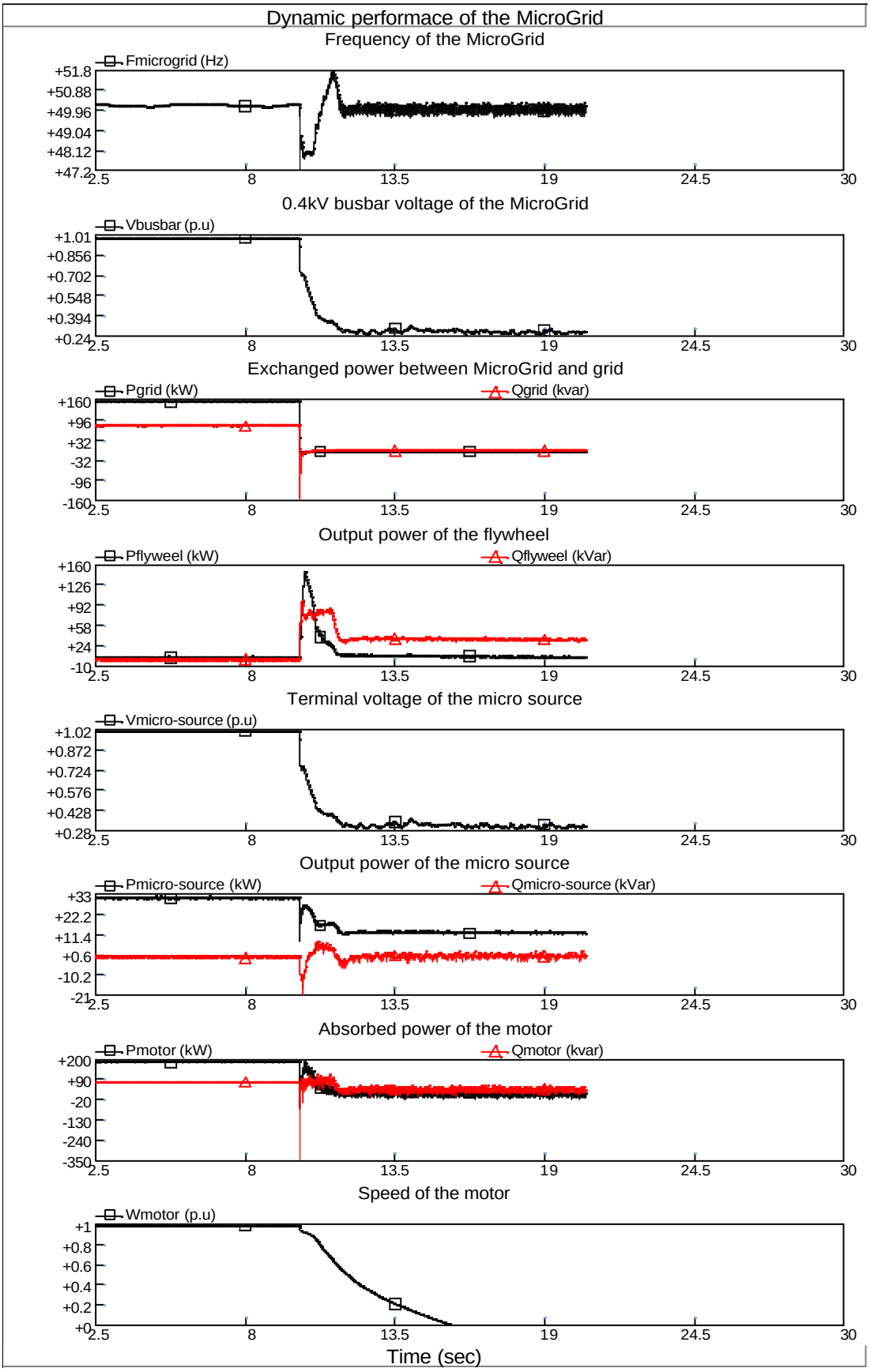

Figure 3.30 Dynamic performance of the MicroGrid for a type of motor load

Therefore, the stability of the MicroGrid mainly depends on the motor load in the MicroGrid. The larger the capacity of the motor in the MicroGrid, the lower the stability of the MicroGrid. Instability of the MicroGrid is usually due to voltage collapse.

3.4.2 Impact of locations of fault in the MicroGrid

In this study, a combined type load (15% fixed PQ, Load 1; 25% impedance, Load 2; and 60% motor, Load 3) is used in the MicroGrid. A three-phase fault is applied at three different places: F1, F2' and F3 separately, as shown in Figure 3.28.

(1) Fault F1

For fault F1, the MicroGrid is disconnected from the main network after the fault. The MicroGrid is operated in islanded mode when the circuit breaker CB2 is open. The control scheme of the flywheel is switched from PQ control to Frequency/Voltage. The control of the micro source is still PQ control. Simulation results produced in PSCAD/EMTDC indicate the MicroGrid has stability problem. The critical clearing time of the MicroGrid mainly depends on the characteristic of the motor load in the MicroGrid. Figure 3.31 shows the CCT characteristic of the MicroGrid for the capacity of the motor load changed from 50kW to 120kW.

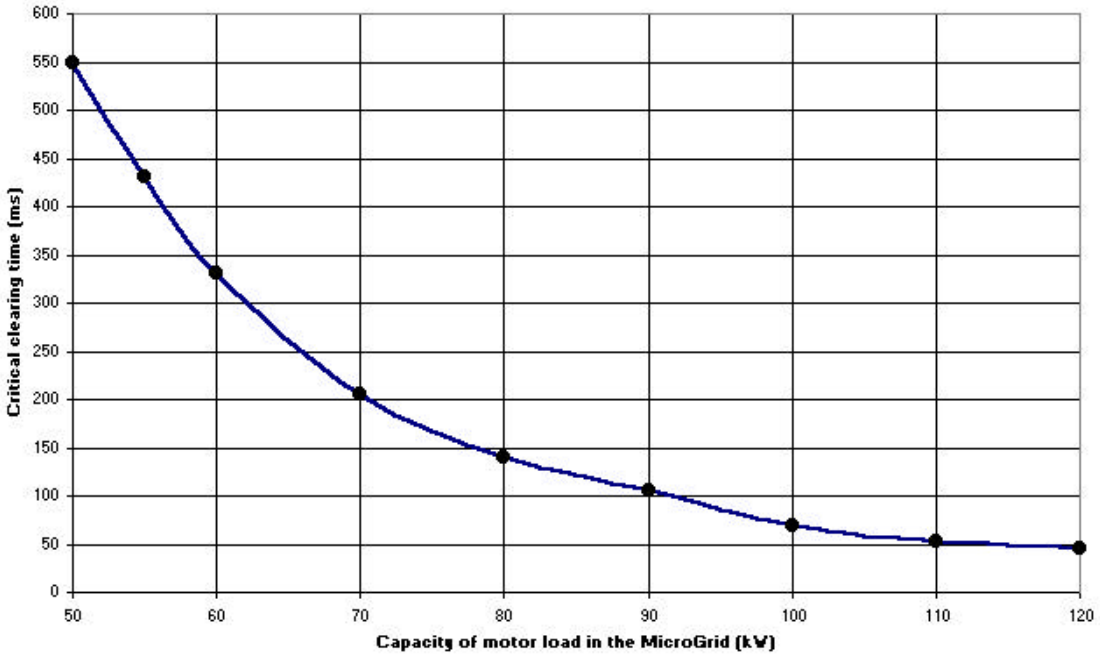

Figure 3.31 CCT characteristic of the MicroGrid for fault F1

(2) Faults F2' and F3 (grid-connected mode)

For faults F2' and F3, the circuit breaker CB2 is closed at all times. The MicroGrid is still operated in grid-connected mode after the fault. The control schemes of the micro source and flywheel are PQ control. Simulation results show that the MicroGrid has no stability problem. The main network supplies enough active and reactive power to compensate requirements of the MicroGrid. The voltage and frequency of the MicroGrid are brought back to their normal values. The speed of the motor load is also restored to normal.

(3) Faults F2' and F3 (islanded mode)

However, for faults F2' and F3, the MicroGrid may be unstable if the MicroGrid is already being operated in islanded mode. During the islanded mode, the flywheel compensates the extra power unbalance between generation and demand in the MicroGrid. The compensation capability of the flywheel is limited by its capacity.

Figure 3.32 shows the CCT characteristics of the MicroGrid operated in islanded mode for faults F2' and F3. The control scheme of the flywheel is Frequency/Voltage control. The rating of the flywheel is 200kW. The capacity of the motor load in the MicroGrid is changed from 50kW to 120kW.

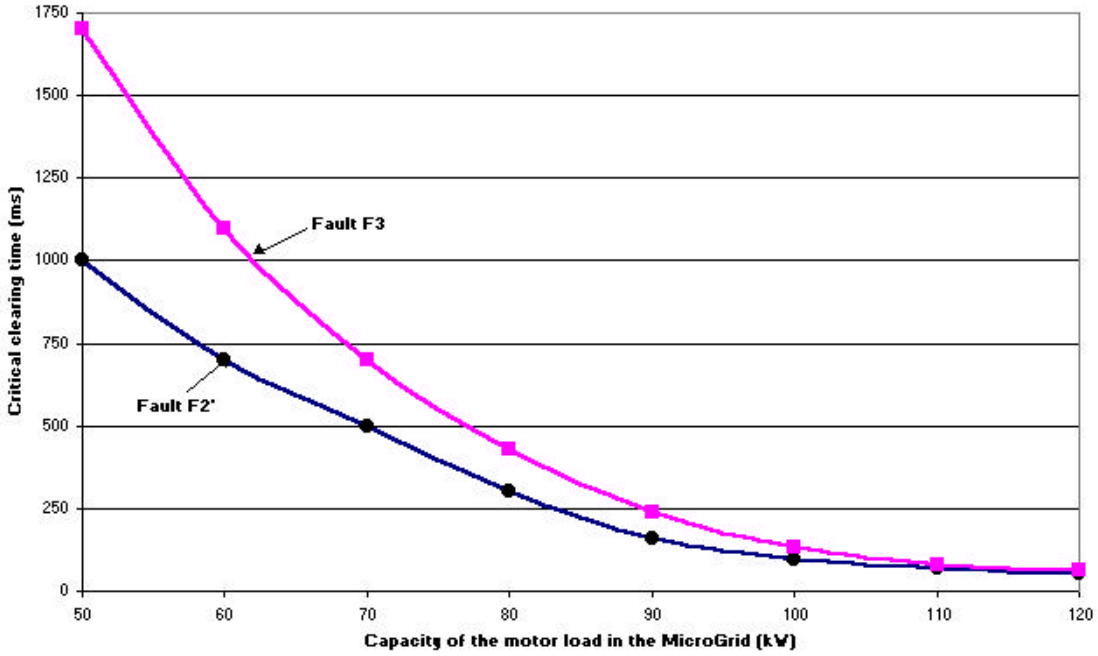

Figure 3.32 CCT characteristics of the MicroGrid operated in islanded mode for fault F2' and F3

Figure 3.32 shows that for faults F3 and F2', the CCTs of the MicroGrid operated in islanded mode decrease when the capacity of the motor in the MicroGrid increases. The stability of the MicroGrid for fault F2' is more sensitive than for fault F3. However, the CCTs of the MicroGrid are almost the same when the capacity of the motor increases and reaches to a value of 120kW.

Considering the stability of the MicroGrid at different locations of the faults (F1, F2' and F3), the fault at F1 is the severest case to maintain the stable operation of the MicroGrid after the fault. For fault F1, the MicroGrid will be disconnected from the main network and operated in islanded mode. The control strategy of the flywheel is switched from PQ control to Droop control or Frequency/Voltage control. The CCTs of the MicroGrid are quite low when a fault happens at F1. Thus, to maintain the stability of the MicroGrid after the fault, transition to islanded mode, fast protection (e.g. differential protection) is needed for fault F1.

3.4.3 Impact of inertia constants of the motor

In this study, three types of loads (Load 1, 15% fixed PQ; Load 2, 25% impedance; and Load3, 60% motor) are used in the MicroGrid. The capacity of the motor load (Load 3) is changed from 50kW to 120kW. A three-phase fault is applied at F1 on the main network, as shown in Figure 3.28. After the fault, the MicroGrid is operated in islanded mode. The control scheme of the micro source is PQ control. The control strategy of the flywheel is switched from the PQ control to Frequency/Voltage control.

Figure 3.33 shows the CCT characteristics of the MicroGrid for different inertia constants of the motor.

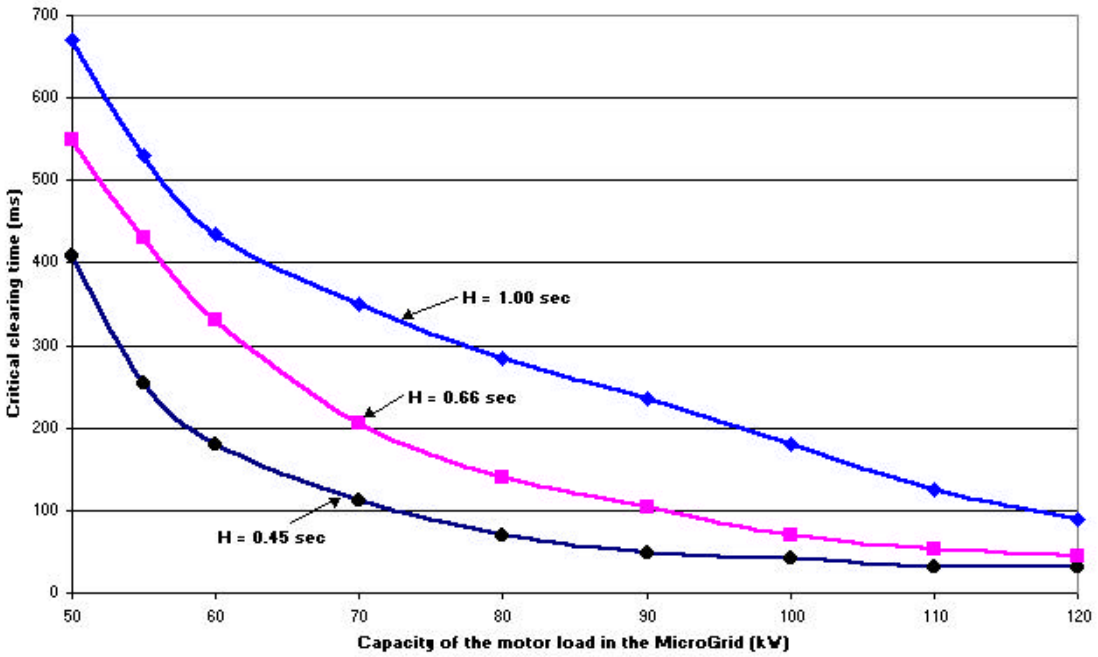

Figure 3.33 The CCT characteristics of the MicroGrid for different inertia constants of the motor in the MicroGrid

In Figure 3.33, the three curves correspond to the three inertia constants (H = 0.45sec., 0.66se. and 1.00sec.) of the motor load. It can be seen that the inertia constant of the motor load has a significant influence on the stability of the MicroGrid. The stability of the MicroGrid is high when the inertia constant of the motor load is large.

3.5 Evaluation of MicroGrid stability for different types and locations of disturbances – INESC Porto contribution

A simulation platform under the *MatLab*® *Simulink*® environment was developed in order to evaluate the dynamic behaviour of several microsources operating together in a MicroGrid network under pre-specified conditions including interconnected and autonomous operation of the MicroGrid.

This simulation platform, including dynamic models of MicroGrid components with control and management systems, has been introduced in deliverable DD1 [Pecas Lopes,2004].

3.5.1 Dynamic Models

All the microsource models used for dynamic simulation were detailed in Deliverable DD1 [Pecas Lopes, 2004] and earlier in Deliverable DA1 [Kariniotakis, 2003] and, for that reason, will not be described here. In addition, some devices (such as synchronous and induction generators, loads, breakers, buses and lines) were modelled using the *MatLab® Simulink®* library *SimPowerSystems.*

Inverter models were developed independently and will be discussed here in detail since their development holds the basis for the control strategies adopted for an efficient MicroGrid operation. These control strategies will be explained in a later chapter.

3.5.1.1 Inverter

Habitually, there are two ways of operating an inverter. Two inverter models were derived from the implementation of the control strategies presented by INESC Porto in deliverable DD1. More details on inverter operation can be found in [Barsali, 2002].

The first model is based on a PQ Inverter control logic, where the inverter is used to supply a given active and reactive power set-point. This model differs from the original PQ version of the inverter presented in deliverable DD1 [Pesas Lopes, 2004].

The second model uses a Voltage Source Inverter (VSI) control logic, where the inverter is controlled in order to "feed" the load a pre-defined value for voltage and frequency. The VSI real and reactive power output is defined based on the load connected to it.

This type of inverter modelling based on their respective control functions assumes several simplifications such as neglecting fast transients, harmonic content and active power losses.

3.5.1.1.1 PQ Inverter

A PQ inverter is based on a control scheme of a current-controlled voltage source.

A method for calculating single-phase active and reactive powers is presented in [Engler, 2002] and was adapted for the PQ inverter developed. The instantaneous active and reactive components of inverter current are computed, with the active component in phase with the voltage and the reactive component with a 90º phase-shift lagging, both of them limited to the [-1, 1] interval. The active component is then used to control the DC link voltage and inherently the inverter active power output, balancing microsource and inverter active power levels since all microsource power variations imply a voltage variation on the DC link, which is corrected using a PI regulator. Simultaneously, the reactive component controls the inverter reactive power output. A PQ inverter can be operated using a unit power factor (corresponding to Set Point = 0 in Fig. 3.34) or receiving a reactive power set-point from the MGCC.

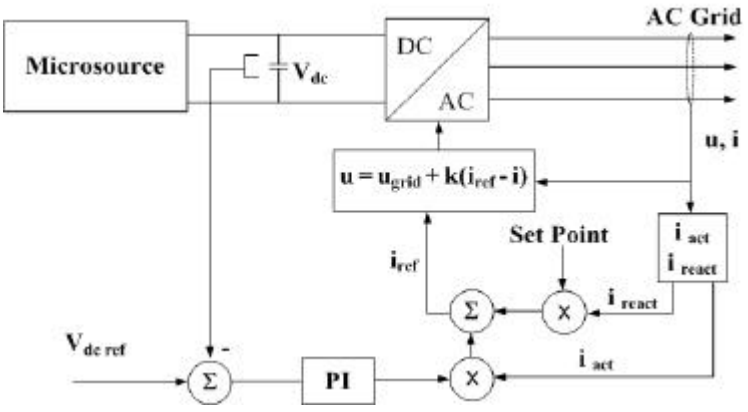

Fig 3.34 PQ inverter control system

3.5.1.1.2 Voltage Source Inverter

A VSI utilizes a control concept similar to frequency and voltage control for a conventional synchronous machine.

For a VSI operating in parallel with an AC system with angular frequency ?grid? (as it can be seen in Fig. 3.35), the VSI output power is defined through the droop equation derived. In order to change the VSI output power, the idle frequency (? $_0$) is altered. When the AC system is not available, the VSI output power depends only on network load levels and droop settings so that the frequency can reach a new value. The active power is shared amongst all inverters present at the new frequency value. Similar considerations can be made for the voltage/reactive power control [Chandorkar, 1993].

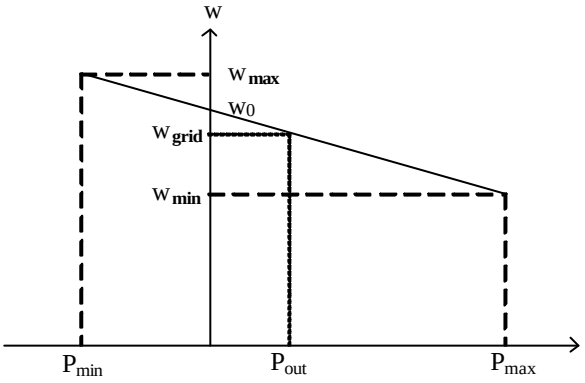

Fig 3.35 Frequency/Active Power droop

A three-phase balanced model of a VSI including the droop concepts was derived from a single-phase version presented in [Engler, 2002] and is shown in Fig. 3.36.

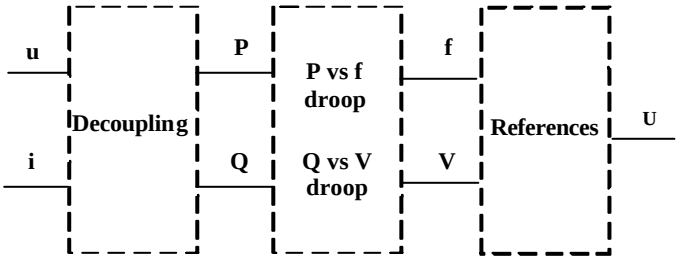

Fig. 3.36 VSI control system

From the control scheme it can be seen that VSI voltages and currents are measured and used to compute active and reactive power levels and that a delay is introduced for decoupling purposes. Frequency and voltage are then computed through the droop

equations and used as references for a switching sequence for the VSI, using a PWM technique.

3.5.1.1.3 Inverter Behavior Under Short-Circuit Conditions

In conventional power systems containing synchronous machines directly connect to the network, these devices are capable of providing high short-circuit currents that are essential for quick and efficient fault detection and elimination. In a MicroGrid, however, most generating devices are connected to the network through power electronic converters and are not capable of providing such high current values.

According to the MicroGrid protection procedures [Jayawarna, 2004], a protection scheme based on over-current protection will be difficult to implement for islanded operation due to the low short-circuit to load current ratio. The power electronic devices used are usually selected based on voltage, current carrying capability (for a defined switching frequency and under certain cooling conditions) and safe operating areas. Based on these factors, short-circuit handling capability of a power electronic device can be increased only by increasing the respective power rating. The following considerations are made in accordance to the previous points:

- The VSI should be up-rated in order to provide an adequate contribution to short-circuit currents (from 3 to 5 times the nominal current value);
- The PQ inverters can only provide a small total of short-circuit current (around 1.5 pu regarding its nominal current).

During and after the short-circuit, the time interval for which large current values are admissible in the VSI and value of the current itself are strongly dependent on motor load characteristics and asynchronous generator dynamics. The correct dimensioning of the storage capacity available is a very important issue in order to fully benefit from the main features of dispersed generation.

A control scheme developed for PQ inverters enables the control of the inverter current output under short-circuit conditions. In face of a short-circuit, there is a voltage drop at the inverter, leading to an active power output reduction.

Consequently, there is an increase of the DC link voltage and a PI controller forces the increase of active current output of the inverter. By limiting the total gain of the PI controller, the output current of the inverter can also be limited. An increase in the DC link voltage will also be experienced.

Acting as a voltage source, the output current of the inverter is usually very high under fault conditions (similarly to conventional synchronous machines). A control scheme such as the one presented in Fig. 3.34 is used in order to limit the output current. The main difference lays in the fact that now the current reference has a maximum peak value that depends on the switching devices characteristics and the frequency is imposed by the inverter frequency/active power droop. The output current is continuously monitored and, whenever its value rises above the maximum value, the control scheme is switched in accordance. After fault elimination, the VSI returns to voltage control mode.

3.5.2 Operation and Control Modes

This subsection describes the different control modes developed and tested and the main strategies chosen in order to achieve good performance for MicroGrid dynamic behaviour.

For a MicroGrid operating in emergency mode, i.e. in islanded mode, the inverters must be responsible for providing means to control frequency and also voltage. If not, the MicroGrid could experience voltage and/or reactive power oscillations [Lasseter, 2000].

While the MicroGrid is being operated in interconnected mode, all inverters can be operated as PQ inverters since a frequency and voltage reference is available from the main MV system. However, a disconnection from the main power source would lead to the loss of the MicroGrid as the frequency and voltage references would be lost and there could be no matching for load/generation imbalances. Then, the VSI must provide these requirements. Using VSI control capabilities by adjusting droop

settings, a VSI can be operated in parallel with the main power grid without injecting active or reactive power. When disconnection from the main grid occurs, the VSI output is automatically defined by the load/generation deviation within the MicroGrid. This is a key solution for MG islanded operation. Based on this, two main control strategies are achievable [Madureira, 2005]:

- Single Master Operation – in which a VSI or a synchronous machine connected to the grid (using a diesel engine as the prime mover, for example) is used as voltage reference when the main power supply is lost; all other inverters present can be operated in PQ mode;
- Multi Master Operation – in which more than one inverter is operated as a VSI, corresponding to a scenario with dispersed storage devices; eventually, other PQ inverters may also coexist.

The VSI reacts to power system disturbances (for example, load-following situations or wind fluctuations) based only on information available locally [Chandorkar, 1993]. In order to promote adequate secondary control for restoring frequency to the nominal value of 50 Hz after a disturbance, two main strategies can be followed: local secondary control, using a local PI controller located at each microsource, or centralized secondary control mastered by the MGCC, providing set-points for active power outputs of the primary energy sources [Engler, 2005].

These two control strategies were presented in deliverable DD1 [Pecas Lopes, 2004], and their respective detailed implementation can be found there.

3.5.3 Simulation in *MatLab® Simulink®*

This subsection introduces the Low Voltage test system used for simulation purposes considered in this document.

The study case LV network defined by NTUA was the base for the simulation platform that was developed, with some modifications that were later introduced. A single-line diagram of this network can be seen in Fig. 3.37.

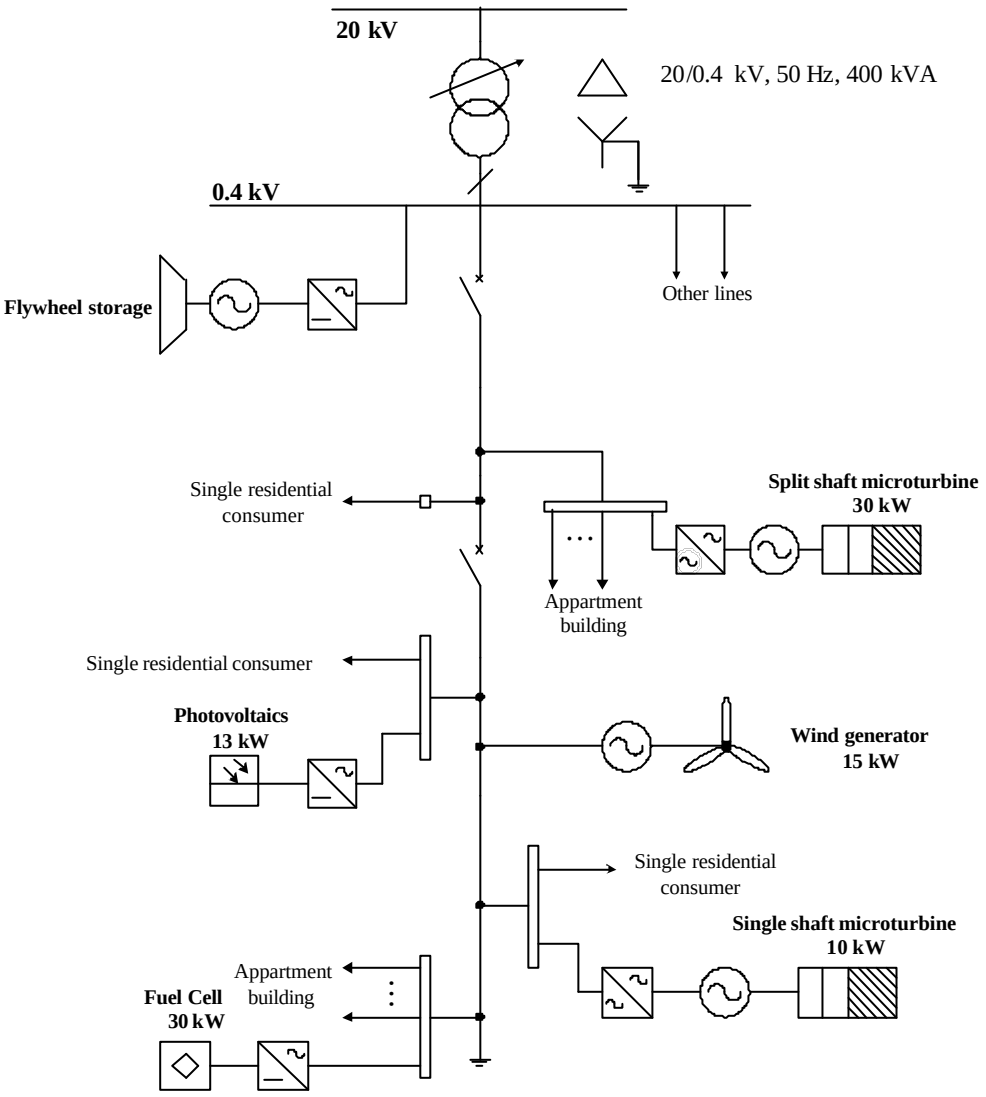

Fig. 3.37 – Study case LV network

Fig 3.38 depicts the LV test network under the *MatLab*® *Simulink*® environment.

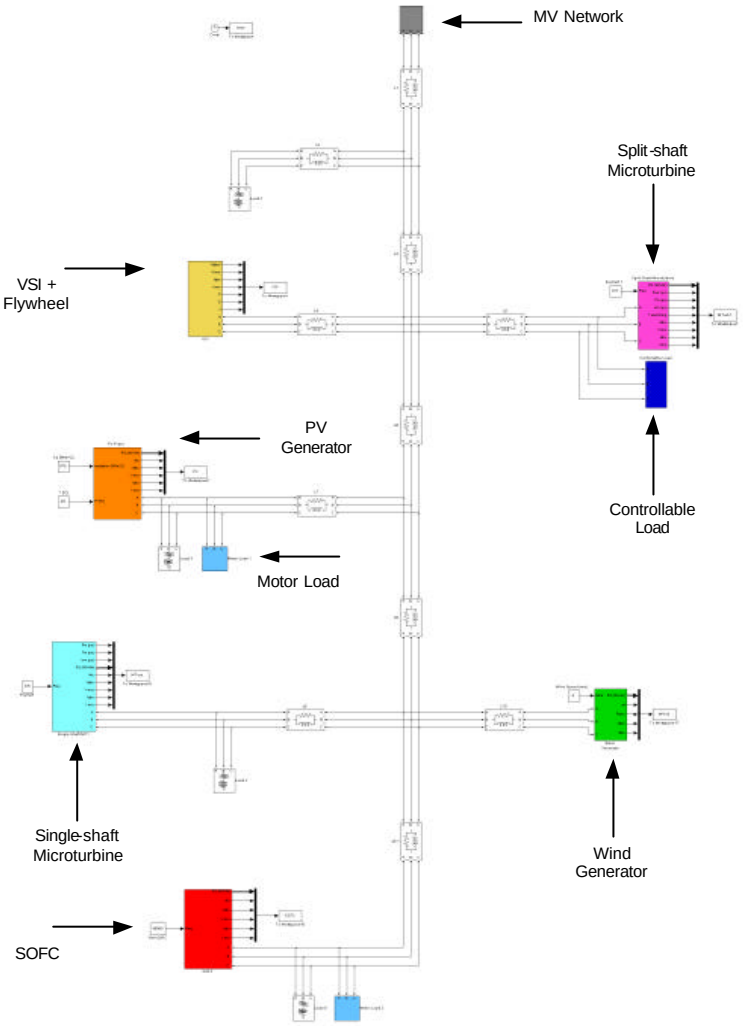

Fig 3.38 Study case LV network under the *MatLab*® *Simulink*® environment

For simplification of the simulation procedure, namely concerning computational execution times, several smaller networks based on the study case network were developed. The structure of these networks will be detailed in the corresponding chapter.

3.5.4 Simulation Results

This subsection introduces some of the most interesting results obtained from a large number of simulations performed. The main variables under analysis will be presented and a critical review of the results will be made.

For simulation purposes, two different operating scenarios were considered: In Scenario 1 the Microgrid is connected to the main MV network and in Scenario 2 the Microgrid is operating in islanded mode. Plus, two different fault locations were considered: In Case A a fault on the main MV network was considered and in Case B a fault was applied to the MicroGrid network. Several fault elimination times were considered for the presented situations.

Also, the impact of load types on the dynamic behaviour of the MicroGrid was evaluated.

In addition, for the scenarios and cases described, a comparison between the dynamic behaviour of the MicroGrid with and without the possibility of load-shedding was tested.

For the simulation platform considered, under the *MatLab*® *Simulink*® environment, only symmetrical three-phase faults were applied.

The control strategy chosen to operate the MicroGrid was the Single Master approach.

3.5.4.1 Impact of Types of Loads

It has been observed that constant impedance load types have no significant influence on the dynamic behaviour of the MicroGrid. However, motor loads have very serious implications on the stability of the MicroGrid under fault conditions. The influence of motor loads is due to the fact that the speed of the motor reduces significantly leading to the stalling of the motor. In such a case, the motor absorbs large portions of reactive power which causes voltage stability problems in the MicroGrid that often lead to Voltage Collapse. Consequently, the stability of the MicroGrid depends on the percentage and characteristics (namely the inertia) of the motor loads present.

3.5.4.2 Impact of Fault Locations

The simulation was performed using a simplified network, shown in Fig. 3.39, based on the one presented in Fig. 3.37. The simplified network includes a Solid Oxide Fuel-Cell (SOFC), a Single-shaft Microturbine, a Flywheel system with a VSI and several loads (30% of motor loads and 70% of constant impedance loads). The total load of the MicroGrid is around 40 kW.

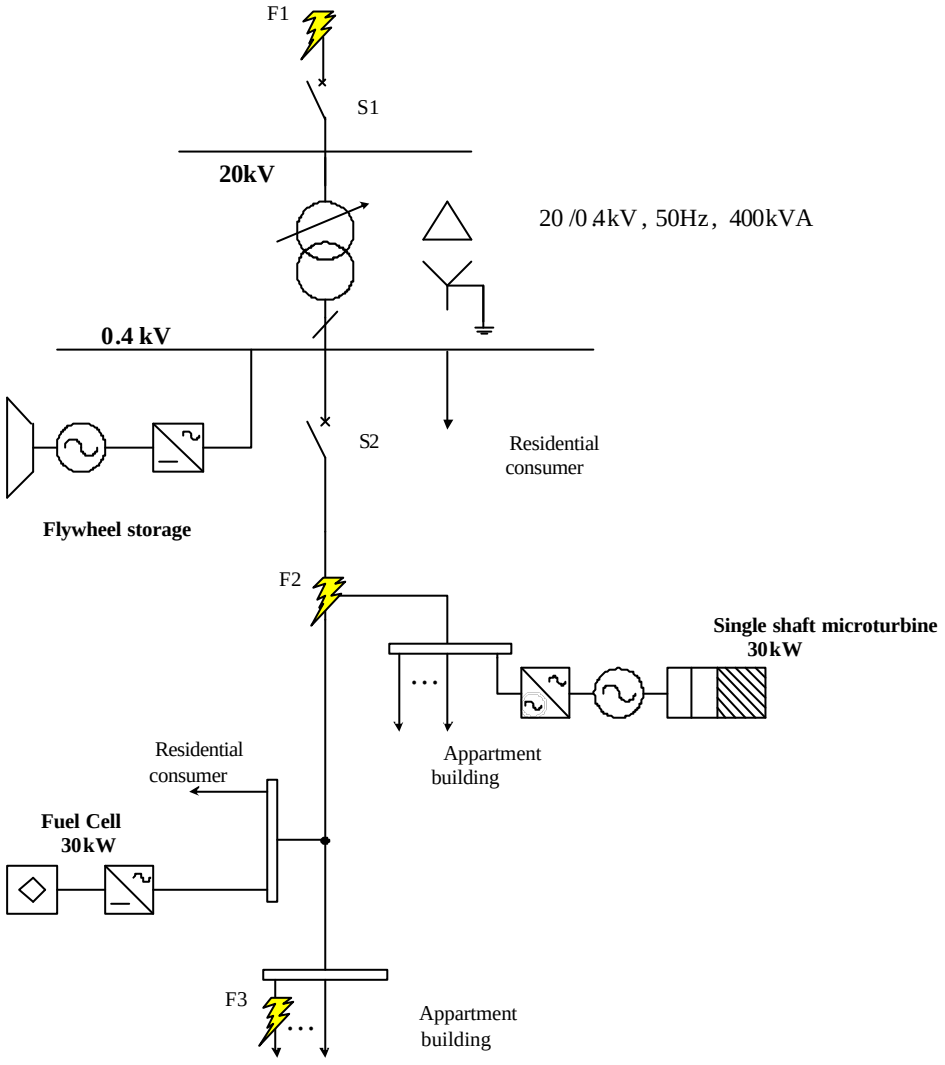

Fig. 3.39 Simplified study case LV network

Fig. 3.40 shows the LV test network under the *MatLab*® *Simulink*® environment.

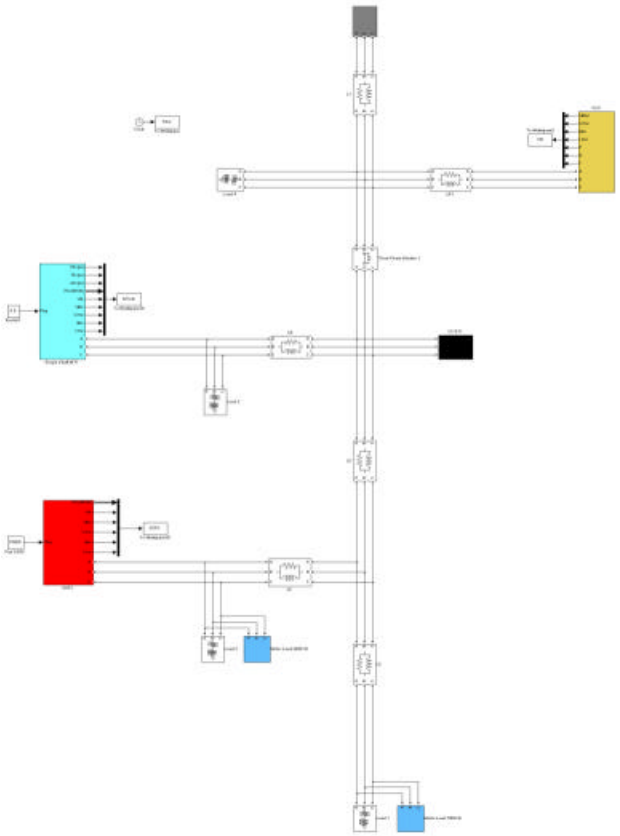

Fig. 3.40 Simplified study case LV network under the *MatLab® Simulink®* environment

3.5.4.2.1 Fault on the Main MV Network

A three-phase fault (F1) is considered to be applied at t = 10 seconds. The MicroGrid is operating in interconnected mode prior to the fault – Scenario 1. The successful elimination of the fault takes 100 milliseconds after the occurrence of the fault, causing the islanding of the MicroGrid. The MicroGrid is importing active power (around 10 kW) from the main MV network prior to the occurrence of the fault. The simulation results are presented for the main electrical variables.

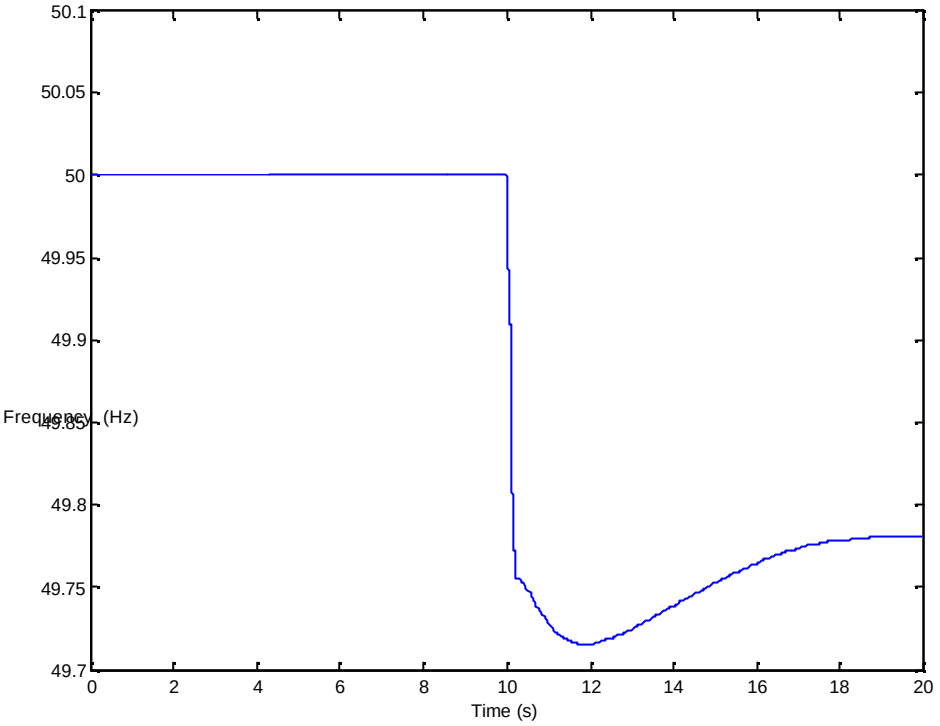

Fig. 3.41 MicroGrid frequency for a F1 fault

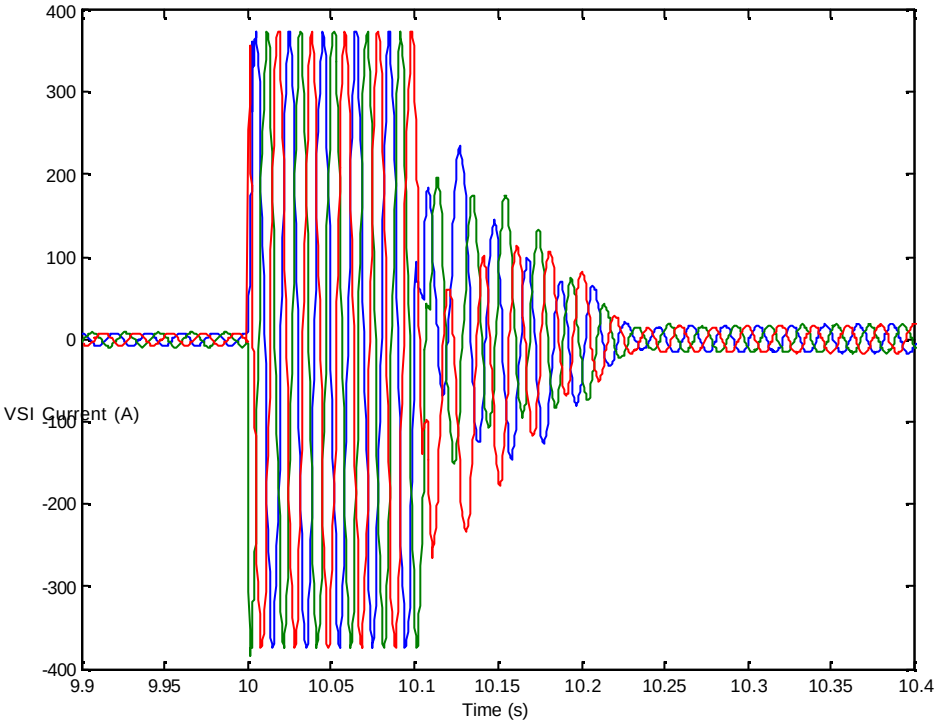

Fig. 3.42 VSI current for a F1 fault

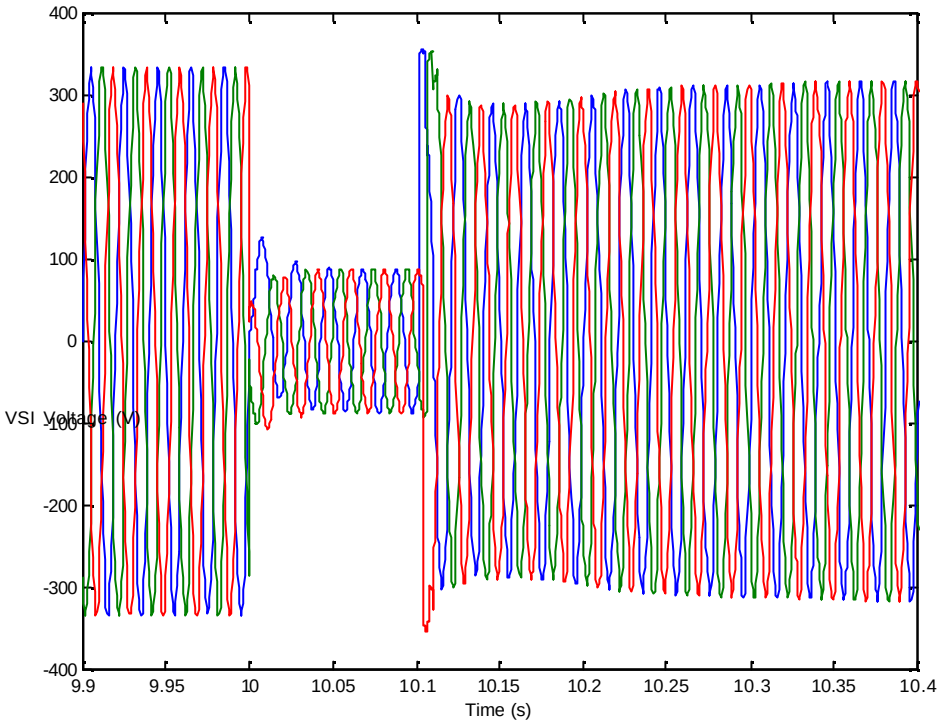

Fig. 3.43 VSI voltage for a F1 fault

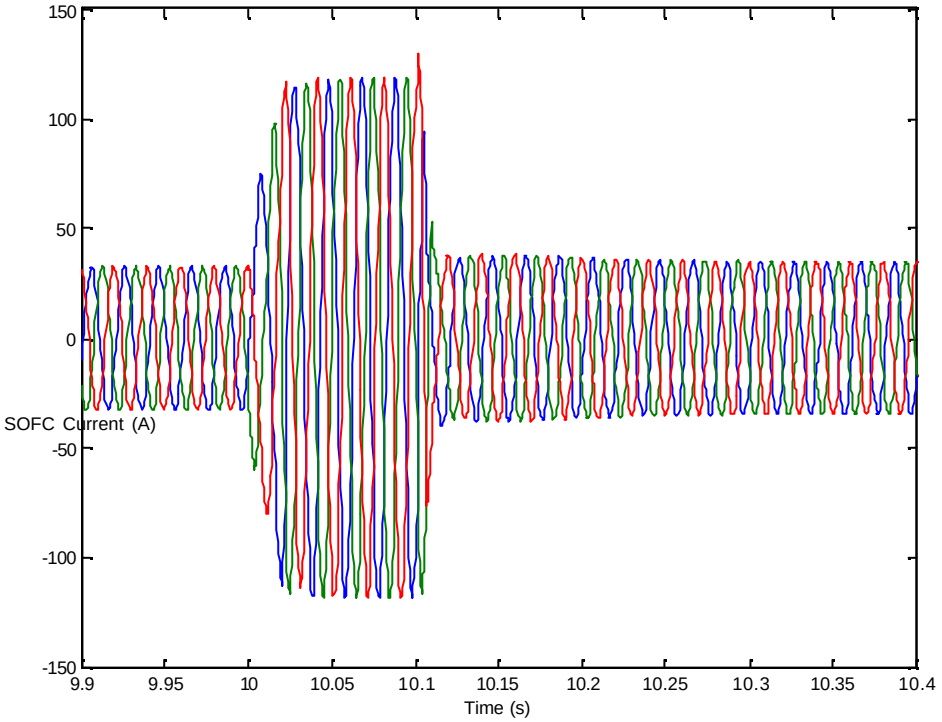

Fig. 3.44 SOFC current for a F1 fault

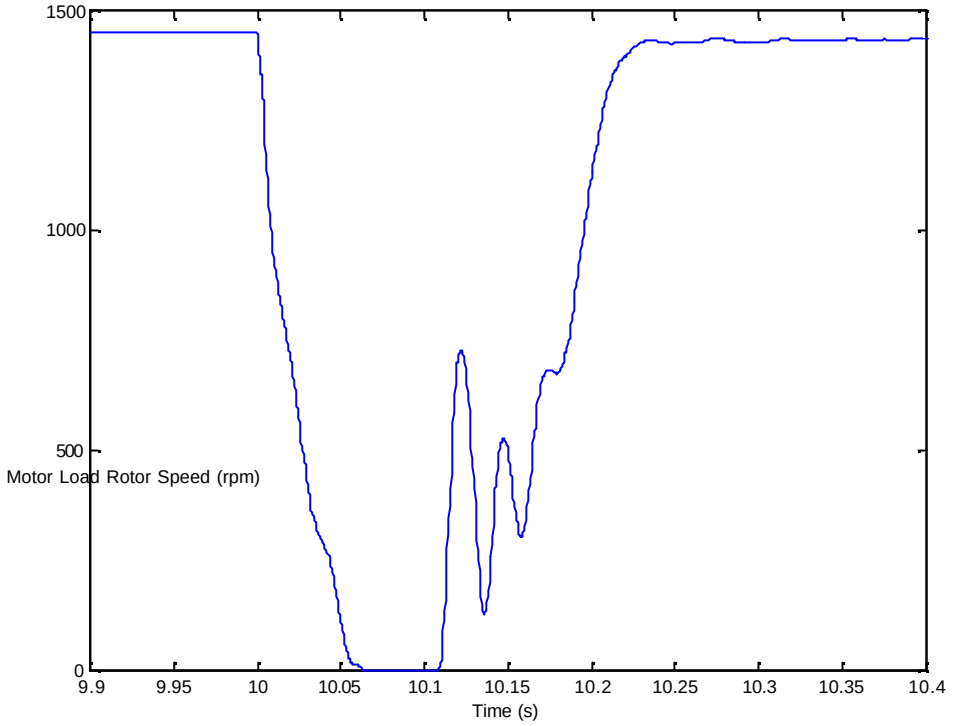

Fig. 3.45 Rotor speed of a motor load for a F1 fault

As can be observed, the stability of the MicroGrid is not lost in face of a F1 fault with an elimination time of 100 milliseconds. The frequency (Fig. 3.41) stabilizes with an offset because secondary control was not yet activated. It can be noticed that, even though stability is preserved, the rotation speed of the motor loads drops leading to the stall of the motors (Fig. 3.45). The motors will then restart after the fault has been eliminated. Current and voltage waveforms (Fig. 3.42 and Fig.3.43, respectively) appear distorted due to the dynamic behaviour of the motor loads during and especially after fault elimination.

The restart of the motor loads is possible even though zero rotation speed is reached due to the speed-torque characteristic of the motors used in this case (data from the *SimPowerSystems* library available in *MatLab*® *Simulink*® was adopted for these motors). This characteristic that can be observed in Fig. 3.46 is mainly dependent on the size and constructive characteristics of the motors. As can be seen, the electromagnetic torque (Te) is always higher than the mechanical torque (Tm) and therefore the motor is able to restart in any situation.

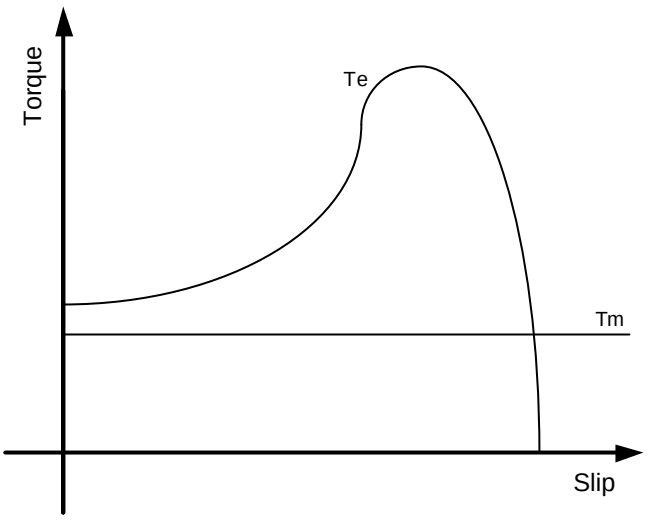

Fig. 3.46 Speed-Torque Characteristic of the motor loads used

3.5.4.2.2 Fault on the MicroGrid Network

A three-phase fault (F2) is applied at t = 10 seconds. The MicroGrid is operating in islanded mode prior to the fault – Scenario 2. The operating time of protection S2 in the MicroGrid is 100 milliseconds. The simulation results are presented for the main electrical quantities.

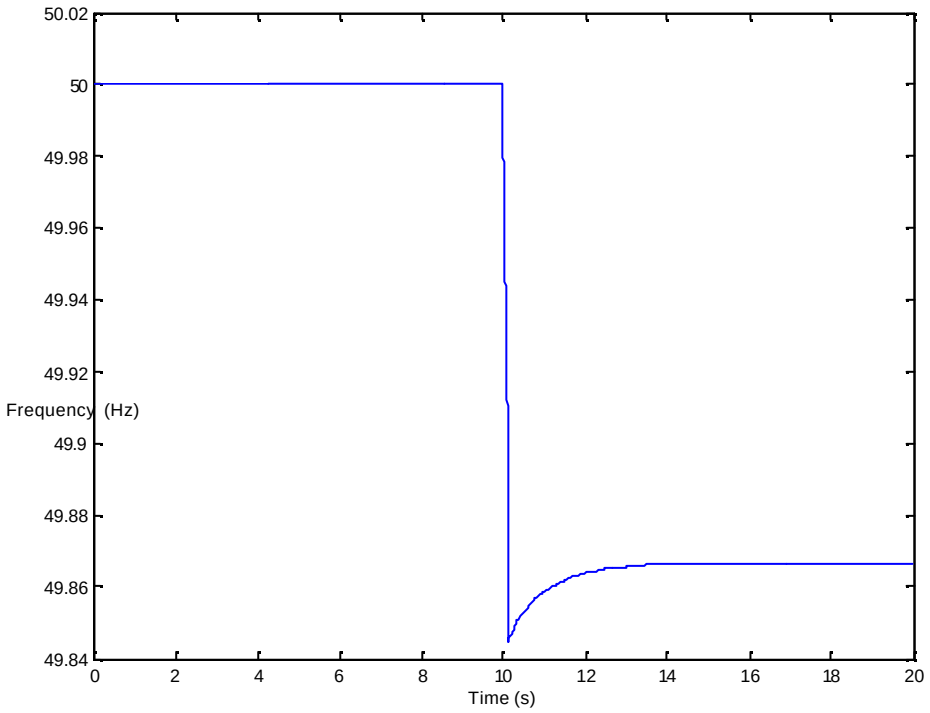

Fig. 3.47 MicroGrid frequency for a F2 fault

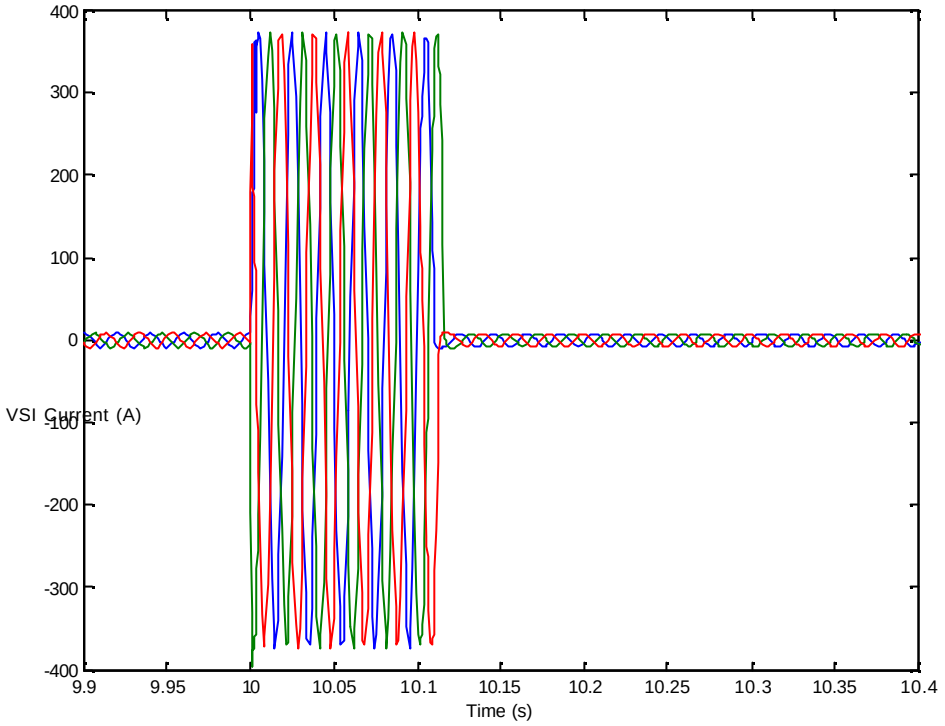

Fig. 3.48 VSI current for a F2 fault

As can be seen in Fig. 3.47 and Fig. 3.48, the fault did not cause instability to the node where the VSI and the load are connected. The branch of the MicroGrid containing the fault was isolated by the tripping of S2 and all microsources on that branch were safely disconnected.

Another situation was tested, involving a fault near a consumer. For this case, a three-phase fault (F3) is applied at t = 10 seconds. The MicroGrid is operating in islanded mode prior to the occurrence of the fault – Scenario 2. The operating time of the protection located at the load is 100 milliseconds. The main simulation results obtained are presented next.

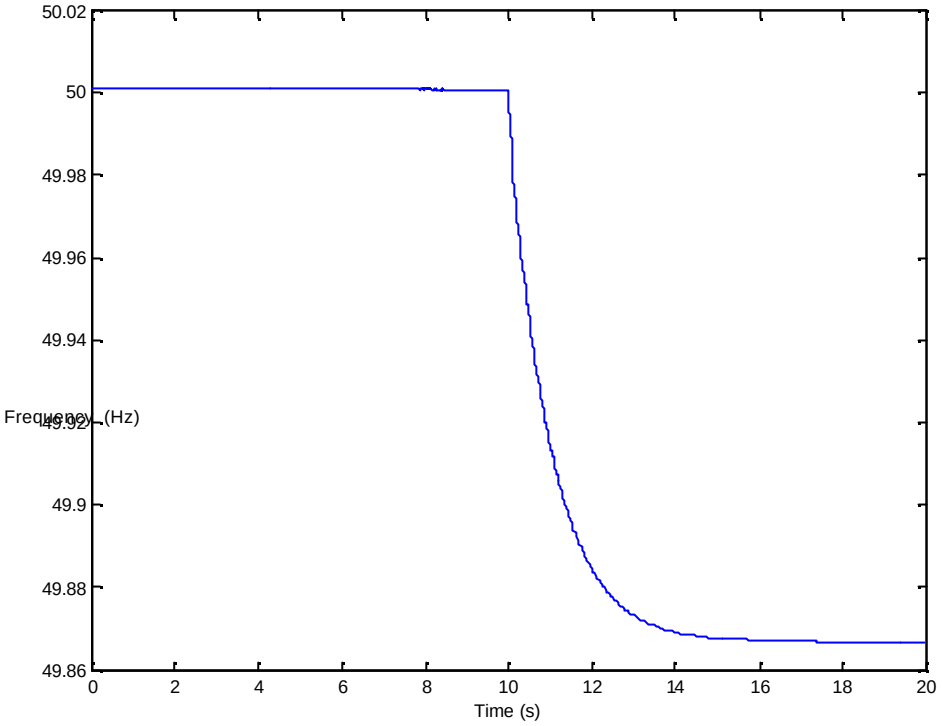

Fig. 3.49 MicroGrid frequency for a F3 fault

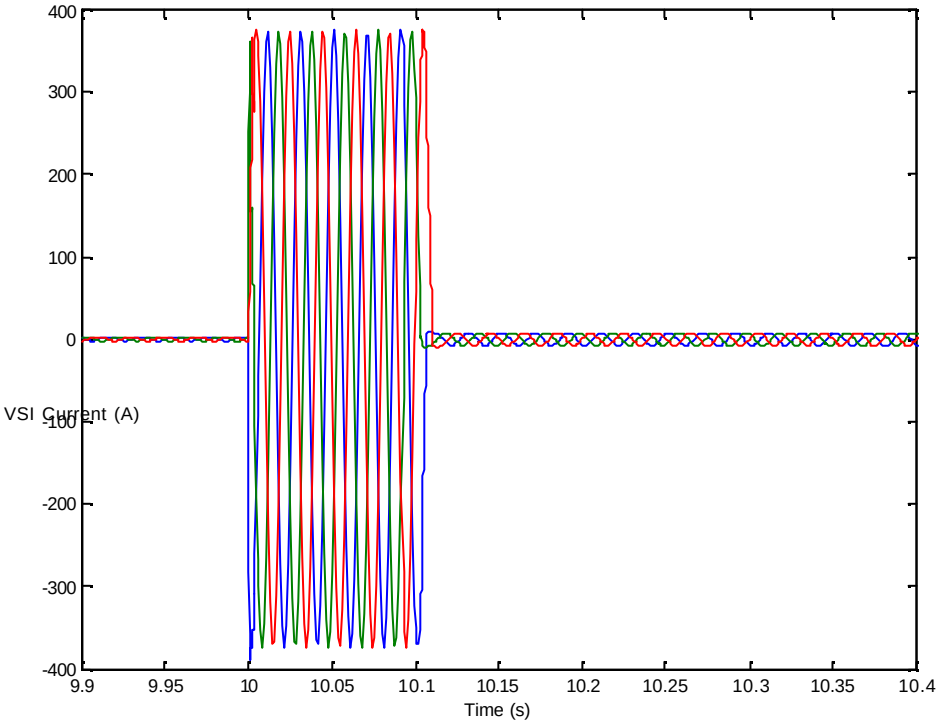

Fig. 3.50 VSI current for a F3 fault

As can be seen, the stability of the MicroGrid is not significantly affected by the fault.

3.5.4.3 Impact of the Inclusion of Load-Shedding Mechanisms

Load-shedding strategies should be considered as an important resource against severe fault situations. The influence of this control option is confirmed in this section.

The simulation platform used in this section is the same of Section 3.5.4.2. A situation considering a F1 fault with an elimination time of 100 milliseconds and Scenario 1 was simulated in order to compare the dynamic behaviour of the MicroGrid with and without the possibility of load-shedding.

Fig. 3.51 shows the frequency deviation for the two cases: with the action of a load-shedding mechanism and without that possibility.

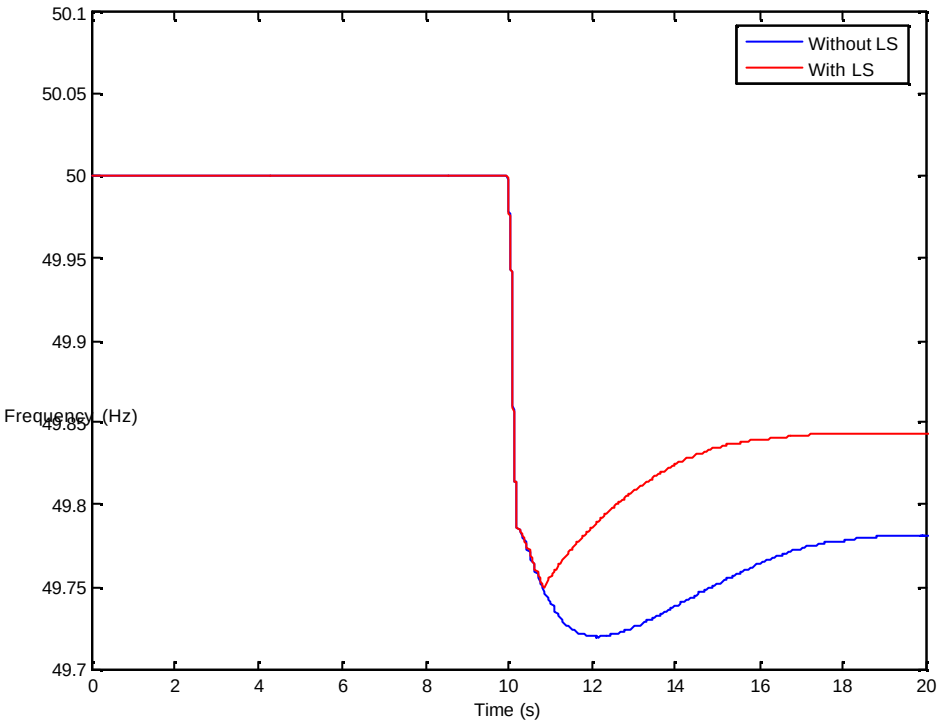

Fig. 3.51 Frequency of the MicroGrid with and without Load-Shedding (LS) actions

As it can be observed, there is an improvement on the stability of the MicroGrid when using load-shedding. Using this procedure, it is possible to reduce significantly the frequency deviation caused mainly by the islanding of the MicroGrid after the well-

succeeded elimination of the fault. If the load-shedding procedure is furthermore optimized, it will lead to more robust MicroGrid operation.

3.5.4.4 Impact of Storage Capacity Sizing

An adequate sizing of the storage capacity can be a decisive issue for maintaining MicroGrid stability after fault occurrence.

The simulation platform used in this section is the same of Section 3.5.4.2. A situation based on Scenario 1, considering a F1 fault with an elimination time of 100 milliseconds, was simulated in order to compare the dynamic behaviour of the MicroGrid with two different values of storage capacity of the flywheel system, by adjusting the slope of the frequency droop of the set VSI + flywheel.

Fig. 3.52 shows the frequency deviation for two cases, considering two different values for the frequency droop of the VSI.

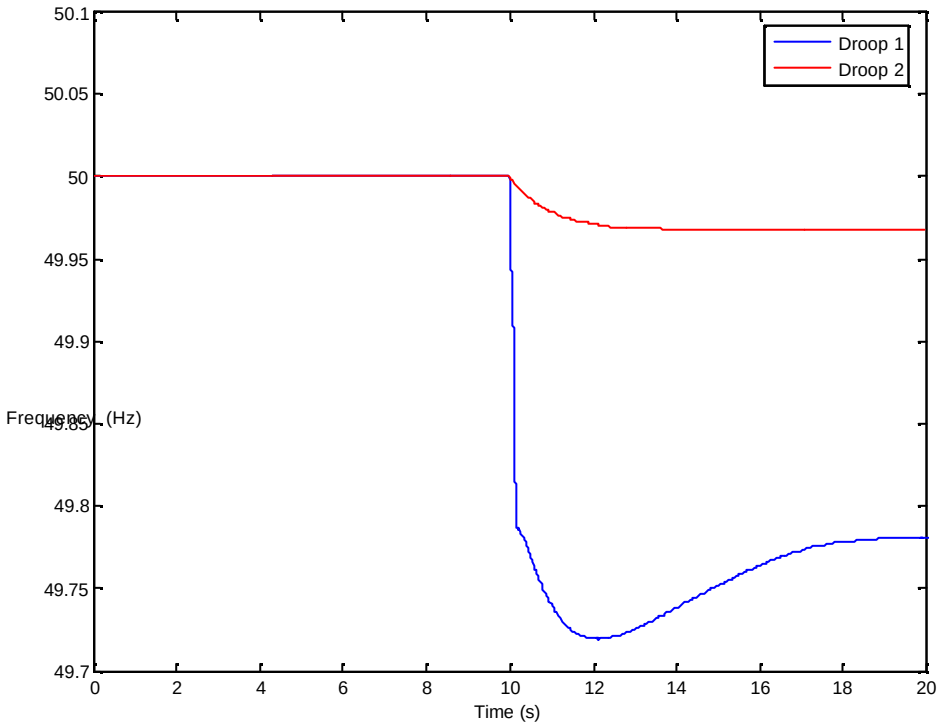

Fig. 3.52 Frequency of the MicroGrid for different frequency droop values

The slope of the frequency is given by the following equation:

$$K_p = \frac{\Delta w}{P_{nom}}$$

Where ?? is the frequency deviation admitted and P_{nom} is the nominal active power of the storage device.

In Fig. 3.52, Droop 1 = 2.094e-4, considering a deviation of 1 Hz; Droop 2 = 2.094e-5, considering a deviation of 0.1 Hz.

The figure shows that the frequency deviation can be drastically reduced, acting on the slope of the frequency droop.

Therefore, by combining an adequate sizing of the storage capacity and an efficient load-shedding strategy, it is possible to guarantee a major improvement on the dynamic behaviour of the MicroGrid following the occurrence of faults.

3.5.4.5 Impact of Large Fault Clearance Times

Several simulations were performed in order to illustrate the influence of a high percentage of motor loads combined with large fault clearance times on MicroGrid stability.

The simulation platform used in this section is the same of Section 3.5.4.2. A situation, using Scenario 1 and considering a F1 fault with several different elimination times, was simulated in order to analyse the dynamic behaviour of the MicroGrid.

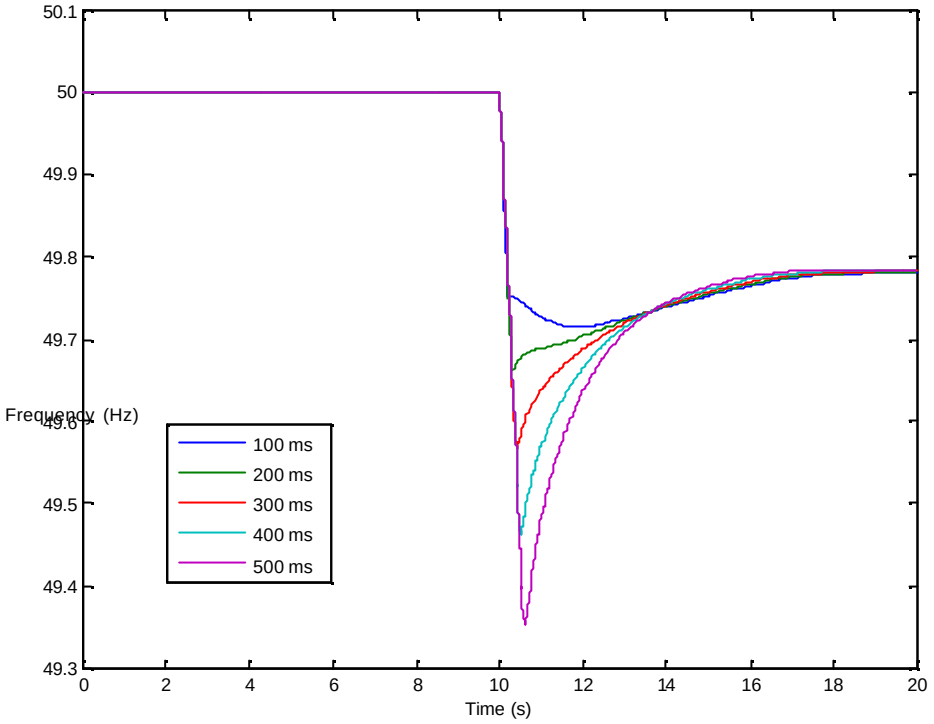

Fig. 3.53 – Frequency of the MicroGrid for different fault elimination times

It can be observed in Fig. 3.53 that, considering fault elimination times up to 500 ms, the stability of the MicroGrid is not lost. The maximum frequency deviation observed does not exceed a reference value of 1 Hz.

If the speed-torque characteristic of the motors is not favourable as the one of the motors used in this case, the motors will not be able to have a direct restart and stability would be lost.

3.5.4.6 Impact of Fault Resistance

Several simulations were performed in order to show the influence of fault resistance on MicroGrid stability.

The simulation platform used in this section is the same of Section 3.5.4.2. A situation, using Scenario 1 and considering a F1 fault with two different values for fault resistance (Rd), was simulated in order to analyse MicroGrid dynamic behaviour.

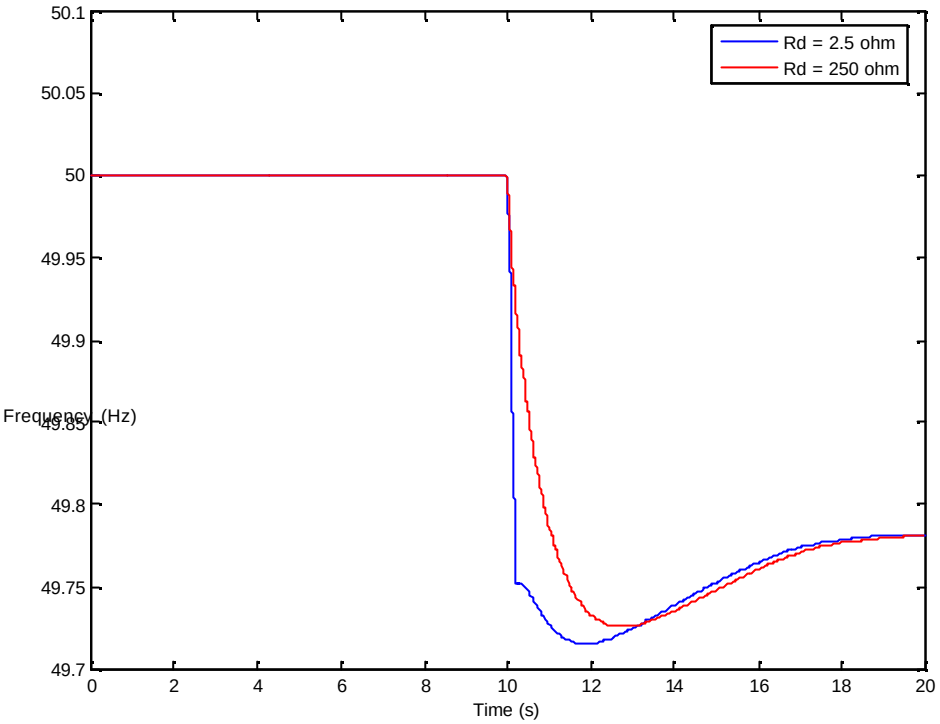

Fig. 3.54 Frequency of the MicroGrid for different fault resistance values (Rd)

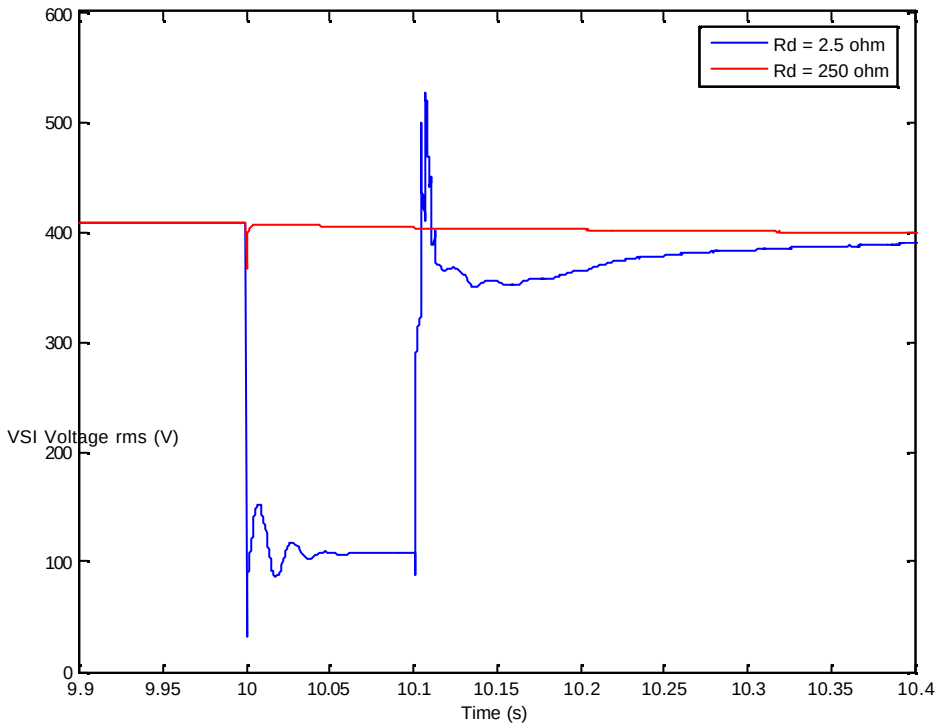

Fig. 3.55 VSI voltage for different fault resistance values (Rd)

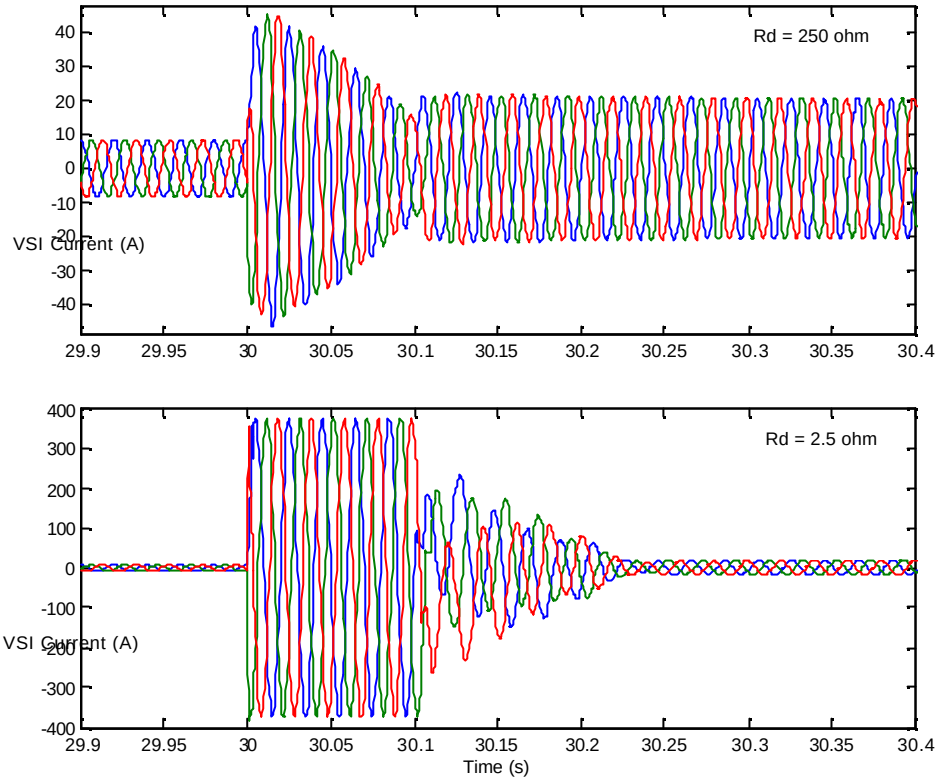

Fig. 3.56 VSI current for different fault resistance values (Rd)

It can be observed from Fig. 3.54 that the frequency fall is much faster considering a small value for the fault resistance, as expected. The amplitude of the frequency deviation, however, is not significantly different.

The voltage drop during the fault was significant for a small value of the fault resistance but almost insignificant for a high value of fault resistance (Fig. 3.55). The current value is extremely low for a fault with a small resistance value, as can be seen in Fig. 3.56, endangering an adequate fault detection and elimination.

3.5.5 Conclusions

It has been seen that the stability of the MicroGrid is largely influenced by a number of factors, such as:

- The control strategies adopted for the MicroGrid;
- The location of the fault and the operating mode;
- The percentage of motor loads present;

- The inclusion of control strategies such as load-shedding mechanisms;
- The capacity of the storage devices.

Results indicate that a F1 fault appears to be a rather severe fault, not only due to the effects of the fault itself but also due to the islanding of the MicroGrid in order to eliminate the fault. Thus, the severity of the impact on the dynamic behaviour of the MicroGrid is mainly related to the imbalance between generation and consumption at the moment of the islanding procedure.

Results also suggest that a F2 fault with large elimination time endangers the stability of the MicroGrid. This is due to the fact that, when the MicroGrid is already operating in islanded mode, any disturbance can cause large frequency and/or voltage oscillations given the global low inertia of this type of power system.

It has been shown that the implementation of a load-shedding mechanism in the MicroGrid can have a positive impact on the stability of this type of networks.

It has also been shown that a correct sizing of the storage capacity available in the MicroGrid can be very helpful in order to reduce significantly the frequency deviation resulting from the elimination of the fault.

Finally, simulation results suggest that the presence of a large number of motor loads, in particular those with little inertia may be a risk to MicroGrid stability after the occurrence of a fault, especially if the fault elimination time is large.

A recommendation can be issued such that fault elimination must be as fast as possible in order to guarantee MicroGrid stability. However, faults with high resistance values in the LV network lead to large fault elimination times (due to low short-circuit currents) using fuses, which may provoke stability problems in the MicroGrid.

3.6 Improvement of the stability of a MicroGrid

The investigation of the stability of the MicroGrid shows the main issues influencing the stable operation of the MicroGrid are the control strategy of the flywheel and the type of load used in the MicroGrid, particularly motor load. The control scheme of the flywheel is PQ control when the MicroGrid is operated in grid-connected mode. During islanded mode, the control of the flywheel needs to be switched from PQ control to Droop control or Frequency/Voltage. The motors will be stalled when their speeds decrease significantly. The motors will be unstable when the operating point of the motor is beyond its pull-out point, corresponding to the maximum electrical torque of the motor. The motors absorb large reactive power from the MicroGrid during stalling operation. Thus, the voltage of the MicroGrid will collapse. However, the stability of the MicroGrid can be improved by using undervoltage load shedding to trip some less important motor loads in the MicroGrid.

Undervoltage load shedding method is a traditional approach to improve the stability of conventional power systems. The undervoltage load shedding measure can be easily implemented on the motor loads in the MicroGrid. The motor loads are divided into a number of groups according to their importance to the customers. Then undervoltage load shedding devices, with their setting values (e.g. V< 0.7p.u), are installed on the motor loads in the least important group. If the voltage of the MicroGrid is below 0.7 per unit, the undervoltage load shedding devices trip the less important motor loads in a time delay of 150ms automatically.

In this study, a simple MicroGrid model (see Figure 3.28) is used. A three-phase fault was applied at F1. The loads in the MicroGrid comprise Load 1, Load 2 and Load 3. Load 1 is a fixed PQ load, with a capacity of 30kW. Load 2 is an impedance load, with capacity of 50kW. Load 3 is a motor load. The inertia constant of the motor is 0.66 seconds. The function of undervoltage load shedding is installed on Load 3. Based on three capacities of the motor load (80kW, 100kW and 120kW), the improvement of the stability of the MicroGrid was investigated using the undervoltage load shedding method. The CCT characteristics of the MicroGrid were calculated in PSCAD/EMTDC.

Figure 3.57 shows the stability improvement of the MicroGrid by applying the undervoltage load shedding measure on the motor load.

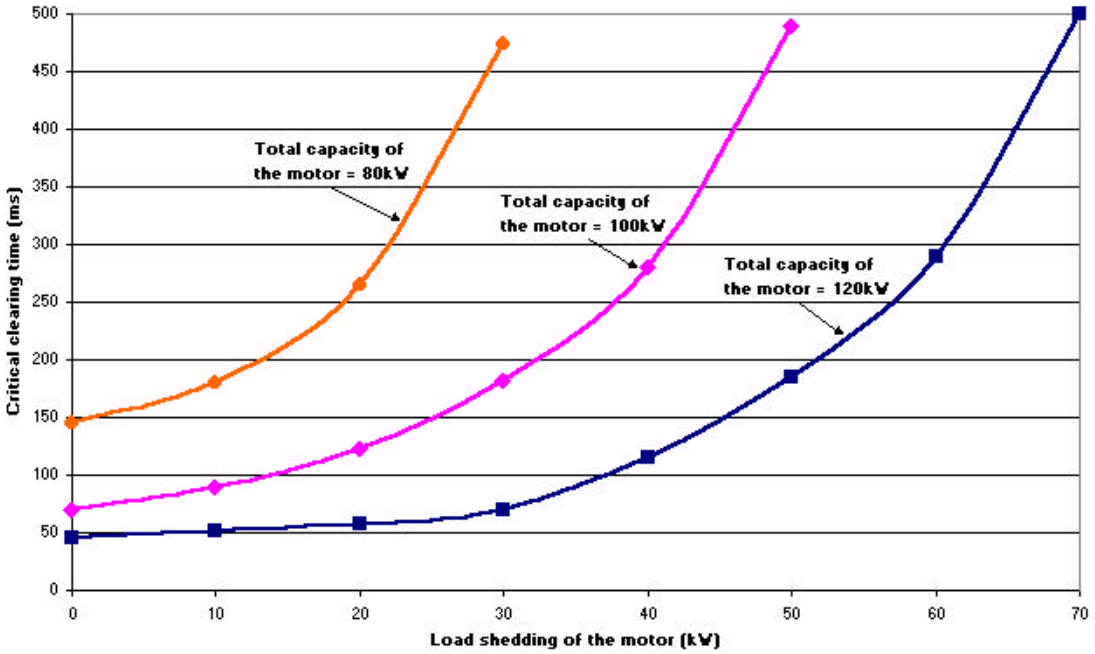

Figure 3.57 Stability improvement of the MicroGrid through using undervoltage load shedding on the motor load

From Figure 3.57, the results show that the stability of the MicroGrid is improved significantly by using the undervoltage load shedding on the motor load. For a 200kW motor in the MicroGrid, the CCT of the MicroGrid increases from 45ms to 500ms when the capacity of the motor load shed varies from zero to 70kW. For a 100kW and a 80kW motors, the improvement of stability of the MicroGrid has similar results. Therefore, larger the capacity of the motor load that is shed in the MicroGrid, higher the stability of the MicroGrid.

Chapter 4 Conclusions and Recommendations

With increasing penetration levels of the DGs, a number of MicroGrids will exist in the distribution network system in the future. The safety and reliability of the MicroGrid is becoming more and more important. The unique nature of the MicroGrid requires the protection of the MicroGrid to comply with the relevant national Distribution Codes and to maintain stable operation of the MicroGrid in both grid-connected mode and islanded mode.

The possible electrical protection schemes for a MicroGrid are:

(1) for a fault F1 on the main distribution network, to install an overcurrent relay protection and a balanced earth fault (BEF) protection at CB1, with a capability of intertripping CB2. An alternative is to install an overcurrent protection and a BEF protection at CB1 and distance protection at CB2. Further, to maintain the stability of the MicroGrid, fast protection (e.g. differential protection) is needed to protect the main distribution against fault F1.

(2) for a fault F2 on the MicroGrid, to install an overcurrent relay protection scheme and a RCD at CB3. During islanded operation of the MicroGrid, the flywheel should supply a high fault current (e.g. 3p.u based on its rating). The protection should have a capability of intertripping all the micro sources in the MicroGrid. Discrimination of the protection can be achieved by using a time delay.

(3) for a fault F3 at the residential consumer, to install a SCPD (using MCB or fuses) and a RCD at the grid side of the residential consumer. The SCPD, using the fuses, trips the fault quickly if there is a high fault current contribution from the flywheel. The protection should only disconnect the consumer affected by the fault. Discrimination of the protection can be also achieved by using a time delay.

The stable operation of the MicroGrid can be obtained through the control of the flywheel and using load-shedding measures on the motor load in the MicroGrid. The possible control schemes of the MicroGrid are: (a) PQ control, (b) Droop control and (c) Frequency/Voltage control. The major factors influencing the stability of the MicroGrid are the control strategies of the flywheel, types of loads, locations of the

fault and inertia constants of the motors. A traditional undervoltage load shedding method can be used to improve the stability of the MicroGrid.

The flywheel uses PQ control only when the MicroGrid is operating in grid-connected mode. The active and reactive power outputs of the flywheel are then fixed at the constant values (e.g. zero). After disconnection of the MicroGrid from the main network, during islanded mode, the control of the flywheel should be switched from PQ control to Droop control or Frequency/Voltage control. The output power of the flywheel is regulated automatically according to the predetermined droop characteristics (Droop control) or errors of the frequency and voltage of the MicroGrid (Frequency/Voltage control).

The fixed PQ and impedance loads have no effect on the stability of the MicroGrid. The motor load introduces instability to the MicroGrid as it absorbs large amounts of reactive power from the MicroGrid during its stalled operation. The instability mechanism of the MicroGrid is likely to be voltage collapse.

In three different location faults (F1, F2' and F3) on the MicroGrid, the fault at F1 is the severest case to maintain the stable operation of the MicroGrid. Under fault F1, the MicroGrid is disconnected from the main network and operated in islanded mode after the fault. The control strategy of the flywheel is switched from PQ control to Droop control or Frequency/Voltage control during islanded operation. The CCTs of the MicroGrid have the lowest values when the fault occurs at F1.

The inertia constants of the motor loads have significant influence on the stability of the MicroGrid. The motors with high inertia constants used in the MicroGrid will enhance the stability of the MicroGrid.

The stability of the MicroGrid can be improved by using traditional undervoltage load shedding on the motors that are less important loads in the MicroGrid. The larger the capacity of the motor loads that is shed in the MicroGrid the better would be the stability of the MicroGrid.

Chapter 5 References

ABB (2004), Low Voltage Products – FuseLine HRC Fuse Links (Catalogue), www.abb/lvswitches.

Barsali S., et al. (2002), Control Techniques of Dispersed Generators to Improve the Continuity of Electricity Supply, Power Engineering Society Winter Meeting, 2002, IEEE, Volume: 2, 27-37 January 2002.

Bungay E., McAllister D. (1990), Electric Cables Handbook (second edition), BSP Professional Books, Blackwell Scientific Publication Ltd..

Engineering Recommendation 59/1 (1991), Recommendations for the Connection of Embedded Generating Plant to the Public Electricity Supplier's Distribution Systems, (2nd amendment 1995), Electricity Association.

Engineering Technical Report 113 (1995), Notes of Guidance for the Protection of Embedded Generating Plant up to 5MW for Operation in Parallel with Public Electricity Suppliers' Distribution Systems, Electricity Association.

Gers J.M and Holmes E.J (1998), Protection of Electricity Distribution Network (book), The Institution of Electrical Engineers, London, United Kingdom.

Glover J.D., Sarma M.S. (2002), Power System Analysis and Design (third edition), Brooks/Cole, Thomson Learning.

Kundur P. (1994), Power System Stability and Control (book), McGraw-Hill, Inc..

Lasseter R.H. (2002), MicroGrids, Power Engineering Society Winter Meeting, 2002. IEEE, Volume: 1, 27-31 January.

Ofgem (2004), The Distribution Code of Great Britain, www.dcode.org.uk.

Pereira da Silva J.L., Moreira Carlos (2004), Evaluation of the Discriminating Capability of Zero Sequence Protection, MicroGrid Project internal report (WPE_TE4_DV11), INESC Porto, January.

RS (2004), Electrical & Automation (Catalogue), March -September, http://rswww.com.

Smith J.R., Chen M.J. (1993), Three-Phase Electrical Machine Systems- computer simulation (book), Research Studies Press LTD.

Wall S.R. (2001), Performance of Inverter Interfaced Distributed Generation, Transmission and Distribution Conference and Exposition, 2001 IEEE/PES, Volume: 2, 28 Oct. – 2 Nov. 2001, Pages: 945 – 950.

Peças Lopes J. et al (2004), DD1 – Emergency Strategies and Algorithms, MicroGrids project deliverable

Kariniotakis G. et al (2003), DA1 – Digital Models for Microsources, MicroGrids project deliverable

Engler A. (2002), Regelung von Batteriestromrichtern in modularen und erweiterbaren Inselnetzen, Ph.D. dissertation

Chandorkar M., et al (1993), Control of Parallel Connected Inverters in Standalone ac Supply Systems, IEEE Transactions on Industry Applications, Vol. 29, No 1, 1993

Jayawarna N., et al (2004), Task TE2 – Fault Current Contribution from Converters, MicroGrids draft report for task TE2,

Lasseter R., Piagi P. (2000), Providing Premium Power through Distributed Resources, Proc. of the 33rd Hawaiian International Conference on System Science, Vol. 4, 2000

Peças Lopes J., Moreira C., Madureira A. (2005), Defining Control Strategies for Analysing MicroGrids Islanded Operation, St. Petersburg PowerTech SPPT'05, accepted for publication

Madureira A., Moreira C., Peças Lopes J. (2005), Secondary Load-Frequency Control for MicroGrids in Islanded Operation, Proc. of the International Conference on Renewable Energy and Power Quality ICREPQ'05, 2005

Engler A., et al (2005), DC1 – Evaluation of the Local Controller Strategies, MicroGrids project deliverable

Appendix List of reports contributing to DE2

Title of the Report	Authors	DE2-Appendixes
Protection Issues of a MicroGrid	Nilanga Jayawarna Xueguang Wu (UMIST)	DE2-Appendix I
Evaluation of the Discriminating Capability of Zero Sequence Protection	J L Pereira da Silva Carlos Moreira	DE2-Appendix II
Electrical Protection Schemes for a MicroGrid	Xueguang Wu Nilanga Jayawarna Nick Jenkins (UMIST)	DE2-Appendix III
Local frequency control of a MicroGrid	Xueguang Wu Nilanga Jayawarna Yibin Zhang Nick Jenkins (UMIST)	DE2-Appendix IV
Stability of a MicroGrid	Xueguang Wu Yibin Zhang Nick Jenkins (UMIST)	DE2-Appendix V
Evaluation of MicroGrid stability for different types and locations of disturbances	Joao Pecas Lopes Carlos Moreira Andre Madureira	DE2-Appendix VI

Large Scale Integration of Micro-Generation to Low Voltage Grids

Contract No: ENK-CT-2002-00610

WORK PACKAGE E

APPENDICES

Document Information

Title	Protection Issues of a Microgrid
Date	20th April 2004
Version	Draft Issue No 1
Task(s)	

Authors:	Nilanga Jayawarna Xueguang Wu

Access:	
Project Consortium (for the actual version) European Commission , PUBLIC (for final version)	
Status:	
	Draft Version Final Version (internal document) **X** Submission for Approval (deliverable) Final Version (deliverable, approved on.)

DE2-Appendix I

MICROGRIDS

Large Scale Integration of Micro-Generation
To Low Voltage Grids

WORK PACKAGE E

PROTECTION ISSUES OF A MICROGRID

DRAFT Issue No 1

20th April 2004

Nilanga Jayawarna
Xueguang Wu

UMIST

Protection Issues of a MicroGrid

In a traditional distribution system, the protection systems are designed assuming unidirectional power flow and are usually based on overcurrent relays with discriminating capabilities. For any fault situation, Distributed Generation sources (DG) connected to the system are tripped off. In other words islanding operation of DG sources is not allowed.

A MicroGrid is designed to operate when interconnected to the distribution system as well as when disconnected from it. These two operating scenarios introduce a host of new issues in protection of a MicroGrid. When the MicroGrid is connected to the main grid, the grid sources could provide high fault currents that could be used to detect faults. But we cannot expect fault currents that are much larger than load currents in an islanded MicroGrid dominated by power electronic interfaces. Therefore using conventional overcurrent protection in a MicroGrid is not promising due to this low short circuit capability of a MicroGrid, especially when it is islanded. It is quite obvious that alternate means of detecting an event within an isolated microgrid must be studied and new protection systems devised.

Our MicroGrid concept is based on a capacity of around 1 MVA with an approximate geographical span of 1 km. Appendix 1 presents the single line diagram of a feeder in a typical MicroGrid (the study case LV network proposed by NTUA).

The ideal protection system of a MicroGrid should possess the following features

I. Must respond both to distribution system and MicroGrid faults
II. For a fault on the main grid, isolate the MicroGrid as quickly as possible
III. For a fault within the MicroGrid, isolate the smallest possible section of the radial feeder carrying the fault to get rid of the fault
IV. Effective operation of customers' protection

From the above, points I and II are clear enough. Point III could be expanded according to the two operating scenarios. If a fault occurs within the MicroGrid when operating interconnected to the distribution system, the MicroGrid should isolate from

the main grid first and then try to isolate the faulty feeder within. If a fault occurs in an already islanded MicroGrid, the protection system should try to sectionalise the MicroGrid in order to get rid of that fault.

Sectionalising of a MicroGrid would involve complex protection and control schemes and incurring greater costs. There are two operating principles open to a MicroGrid in this regard.

1. To sectionalise the MicroGrid by isolating the smallest possible section of the feeder carrying the fault.
2. To shut down the complete MicroGrid for any fault within it.

The decision will depend on the needs of the MicroGrid customers and whether the cost involved could be justified for the benefits gained through sectionalising.

According to system reliability index figures, approximately 22 faults per 100 km occur in a LV network (overhead lines + power cables) annually in the UK. This implies that less than 3 faults will take place in a typical MicroGrid spanning 1 km in a decade. We have to address the question whether it is really worthwhile to consider sectionalising of a MicroGrid in this scenario.

An islanded MicroGrid presents the biggest challenges to our protection problem. Therefore we need to have a clear understanding of the needs of an isolated MicroGrid. Some of the characteristics of a MicroGrid in islanded mode, which influence its protection needs are as follows

- Low fault level. (What kind of a margin of fault level could we expect?)
- Bi-directional power flow
- Low system inertia
- Extensive use of converters

When trying to understand the protection needs of a MicroGrid, we have to address the following initial issues at first.

1. What are the possibilities of failure / fault conditions?
2. What are the consequences due to these faults?
3. What are the protection functions required in a MicroGrid?

4. Which of the above issues (in 3) could use existing techniques and which of them need new approaches?
5. What are the benefits that the MicroGrid would gain through rapid sectionalising?
6. How to determine when to form an islanded MicroGrid?

Then we have to answer the more technical questions of

I. What are the present regulations/ statutory requirements?
II. What are the suitable protection schemes and their operating times?
III. How to earth the MicroGrid and what is its impact on protection arrangements?
IV. What are the protection requirements for generators within the MicroGrid?
V. What are the requirements for network protection?
VI. What is the impact of network protection operation on transient stability of generators?
VII. How does the operating principal of a MicroGrid (sectionalise or not?) impact the choice of protection?
VIII. When you detect a fault how does the tripping work?
IX. How to provide the islanded MicroGrid with sufficient coordinated fault protection?
X. What is the best possible way to synchronise and reconnect with the grid after clearing a fault?

Appendix 1: LV Feeder with LV DG sources

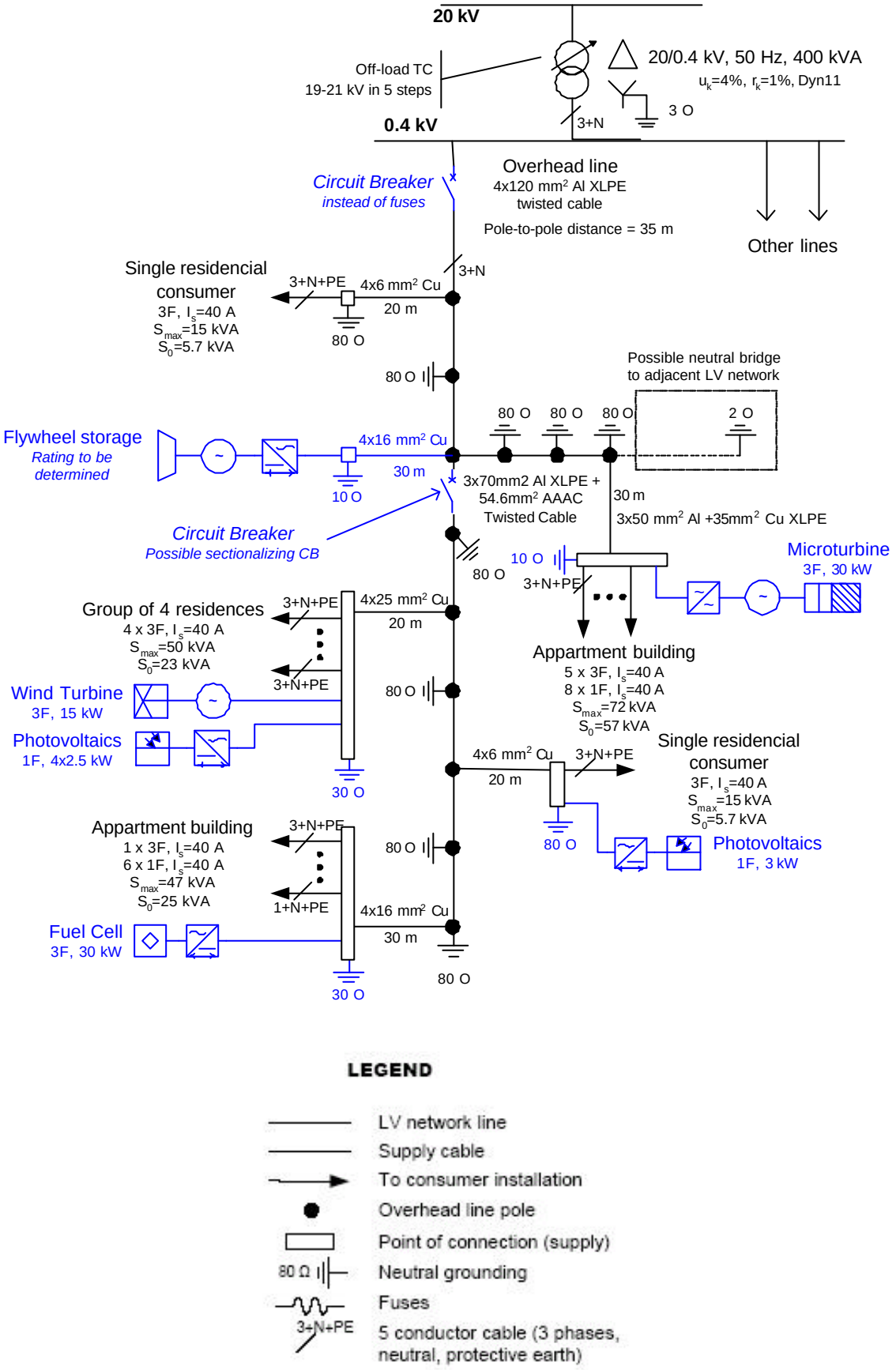

January 2004

Project funded by the European Commission under the 5th (EC) RTD Framework Programme (1998-2002) within the thematic programme "Energy, Environment and Sustainable Development"

Project MICROGRIDS

Contract No. ENK-CT-2002-00610

Report for Work Package E, Task E4

Evaluation of the Discriminating Capability of Zero Sequence Protections

Document Type: Draft Version 1.1

Authors: J. L. Pereira da Silva, Carlos Moreira

Company/Institution: INESC Porto

Address: Campus da FEUP

Rua Dr. Roberto Frias, 378

4200-465 Porto

Portugal

Tel.: +351.22.2094230

Fax:

E-mail: jls@fe.up.pt; cmoreira@inescporto.pt

Further Authors:

Document Information

Document Name: WPE_TE4_DV11.pdf

Rev. Date: January 2004

Classification:

Status: Draft Version 1.1

Project MICROGRIDS

Contract No. ENK-CT-2002-00610

Evaluation of the Discriminating Capability of Zero Sequence Protections

Table of Contents

1. Introduction

The interconnection of the distributed generation sources to the microgrid is mainly done by power electronic interfaces, usually named as VSC (voltage source converters). The VSC can provide fast control to balance generation and load; they can also provide a suitable synchronization strategy, allowing a smooth transition from the island operation mode to the interconnected operation mode.

These devices are very sensitive to faults that may occur in the network. So it is necessary to evaluate efficiency of several protection devices commonly used in electrical networks, such as minimum phase voltage relays, zero sequence voltage relays and zero sequence current relays. These relays should detect faults and in coordination with circuit breakers, provide good clearing capability, shutting down the VSC, if their security is in risk.

2. Mathematical Models

The fault analysis in the study case low voltage network was based on the assumption that electrical system network components are symmetrical. The system elements of interest are electric machines (transformers, induction machines), transmission lines and loads (each load is assumed as an equivalent load connected in Y configuration). Unbalanced systems currents and voltages only depend on the asymmetry introduced by loads, VSC or the fault itself. In this case, the method of symmetrical components is used, since positive, negative and zero sequence components are decoupled.

2.1. VSC

VSC are assumed to behave during the fault as current sources. In this approach it is possible to consider three current sources for each inverter, modelling positive, negative and zero sequence injected currents.

Figure 1: Fault and inverter model

In general, $A_{sk}^{f} = [\ A_{+k}^{f}\ \ A_{-k}^{f}\ \ A_{0k}^{f}\ ]^{T}$ represents the vector of the symmetrical components of node k variable 'A', during the fault(f).

I_{sm}^{Th} represents the vector of symmetrical components of the Thévenin current injected by the inverter connected to node *m*. The procedure explained above requires this vector to be known for each inverter connected to the network.

An alternative model based on an equivalent positive, negative and zero sequence impedances and a voltage or current source, could be adopted. In such a procedure, the equivalent impedances would be included in the impedance matrix of the network.

As there is no theoretical information based on models that describes the VSC behavior during faults, namely those impedances values, this procedure was not followed. The model based on current source that inject a fix current was adopted because, from experimental results, inverters' manufactures say VSC behave like current sources.

2.2. Electrical Machines and Loads

The HV/LV transformer (Δ - Yg connection) is represented as usually by its positive, negative and zero sequence impedances (leakage impedances), and neutral-ground resistance. The induction machine coupled to the wind turbine is assumed to be delta connected (open zero sequence circuit) and is represented by its positive and negative subtransient impedances.

Concerning the electrical loads, they are assumed to be Y-connected with the Y common point connected to the neutral conductor. Loads are regarded as impedances, calculated after a power flow study. This is a reasonable approach, since this is a low voltage network and loads are mainly of impedance type. In this way, the positive, negative and zero sequence impedances are very similar (in this case, are assumed to be equal). So, they are included in the symmetrical components impedance matrix of the system

2.3. Transmission Lines

Low voltage cables can be regarded as short length transmission lines; in this case, the π model is valid with great accuracy. This model can be simplified to the series impedance model, since in low voltage networks, the shunt capacitance in not very important. This is the conventional model that was adopted for the positive and negative sequences, since in these cases the neutral current is zero and the neutral and earth potential are equal.

Since the neutral conductor is connected to the earth in several points of the network, a more detailed model was considered to represent the zero sequence components. For the zero sequence impedances, two cases were considered:

- earth faults, involving one or more phase conductors and the earth;
- neutral faults, involving one or more phase conductors and the neutral.

2.3.1. Faults Involving the Earth

Let us consider a fault involving one or more phase conductors and earth. As it can be seen in the following picture, the main current path is through phase conductors and the earth.

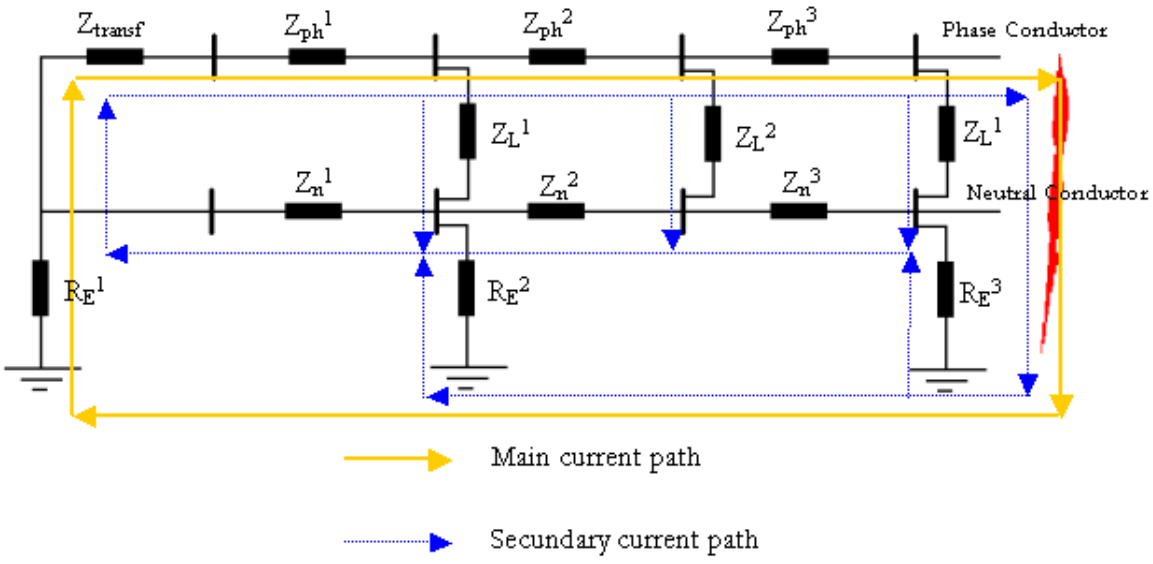

Figure 2: Current distribution in a phase to ground fault

As R_E^1 (the transformer neutral resistance) is much lower then the other neutral resistances, the major part of the phase to ground fault current passes through phase conductors and R_E^1; the current that flows by the neutral conductor and loads is much lower than the one that flows by the transformer neutral resistance.

At this point, some simplifications are taken. The cable neutral impedances are included in an equivalent zero sequence cable impedance, assuming a return circuit by earth and fourth (neutral) conductor. Data for low voltage cables zero sequence impedances were obtained from IEC 909-2 Technical Report " Electrical equipment – Data for short-circuit current calculations in accordance with IEC 909" as function of their positive sequence impedances.

As a consequence of that assumption, the neutral potential is assumed to be constant along the zero sequence equivalent circuit. Then, for earth faults, zero sequence equivalent circuits are represented as defined in the following picture.

The phase to neutral voltages in each phase (V_{an}, V_{bn}, V_{cn}) can be calculated using the phase to earth voltages in the same node (V_a, V_b, V_c) as follows:

$$\begin{cases} V_{an} = V_a + 3 \times I_0^f \times R_e^{eq} \\ V_{bn} = V_b + 3 \times I_0^f \times R_e^{eq} \\ V_{cn} = V_c + 3 \times I_0^f \times R_e^{eq} \end{cases}$$

being R_e^{eq} the equivalent neutral to earth resistance (parallel of R_E^1, R_E^2 and R_E^3)

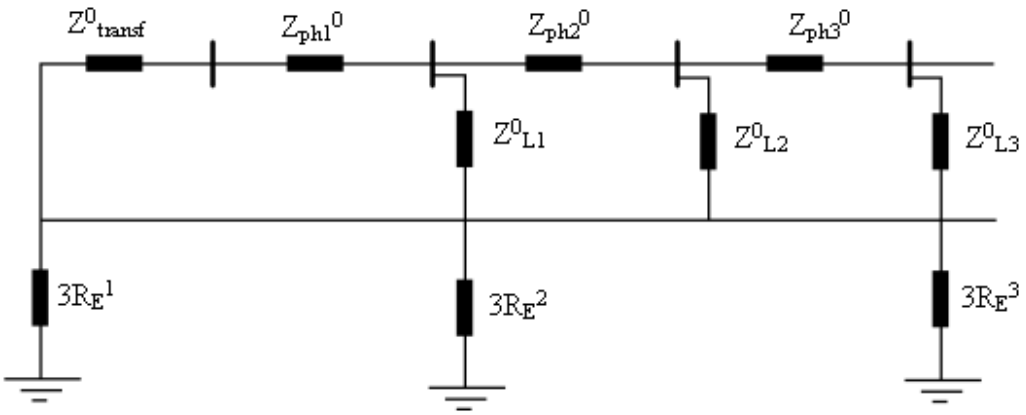

Figure 3: Zero sequence equivalent circuit for faults involving the earth

2.3.2. Faults Involving the Neutral Conductor

A similar approach needs to be made in what concerns with faults that involves one ore more phase conductors and the neutral. The cables impedances are much lower than the other ones, then, as it can be regarded in the following picture, the majority part of the fault current is in a mesh that contains the faulted phase and the neutral.

At this point, again some simplifications are taken. The cable neutral impedances are included in an equivalent zero sequence cable impedance, assuming a return circuit only by fourth (neutral) conductor. Data for low voltage cables zero sequence impedances were also obtained from IEC 909-2 Technical Report as function of their positive sequence impedances. As a consequence of that assumption the neutral potential of the zero sequence equivalent circuit will be constant and the grounding point can be neglected.

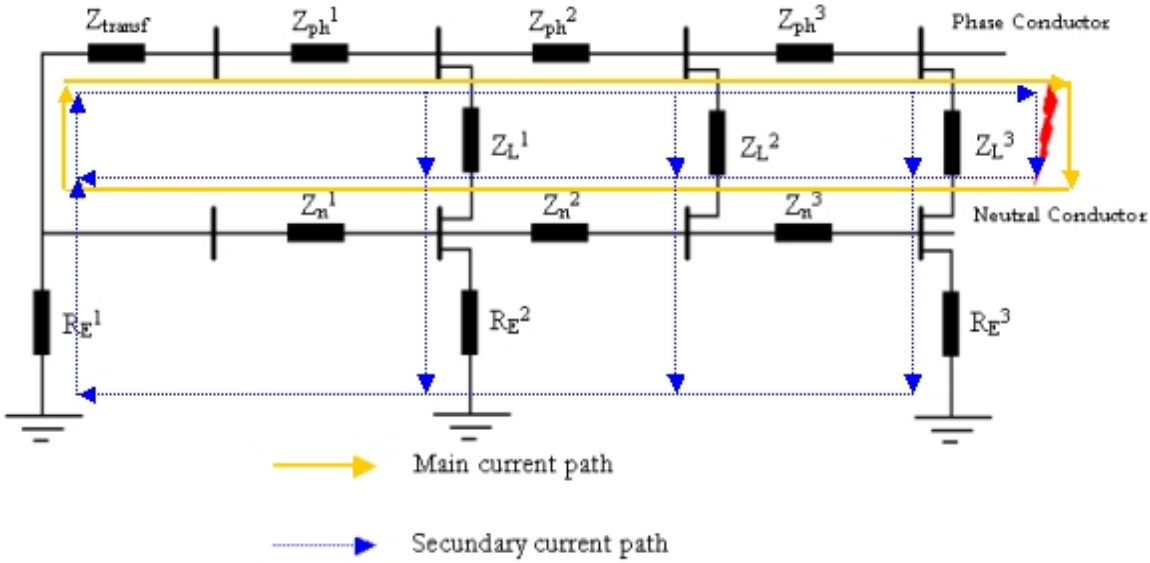

Figure 4: Current distribution in a phase to neutral ground fault

These approaches lead to the definition of the following zero sequence equivalent circuit for faults involving the neutral conductor:

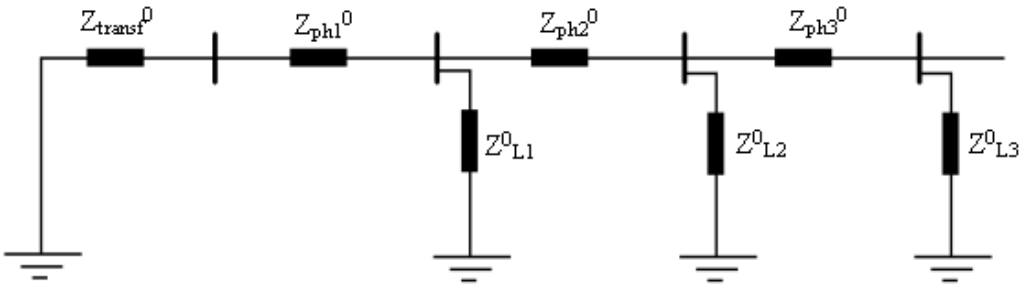

Figure 5: Zero sequence equivalent circuit for faults involving the neutral conductors

2.4. Network Equations

Taking node *j* as the faulted one and, for simplicity, lets consider only one inverter connected to the network at node *m*. Using the symmetrical components impedance matrix of the system $\mathbf{Z_s}$ and superposition theorem, the following equations stands (superscript *0* means pre-fault values and superscript *f* means post-fault quantities):

$$V_s^f = V_s^0 + Z_s I_s^f$$

$$\begin{bmatrix} V_{s1}^f \\ \vdots \\ V_{sj}^f \\ \vdots \\ V_{sn}^f \end{bmatrix} = \begin{bmatrix} V_{s1}^0 \\ \vdots \\ V_{sj}^0 \\ \vdots \\ V_{sn}^0 \end{bmatrix} + \begin{bmatrix} Z_{s11} & \dots & Z_{s1j} & \dots & Z_{s1n} \\ \dots & \dots & \dots & \dots & \dots \\ Z_{sj1} & \dots & Z_{sjj} & \dots & Z_{sjn} \\ \dots & \dots & \dots & \dots & \dots \\ Z_{sn1} & \dots & Z_{snj} & \dots & Z_{snn} \end{bmatrix} \times \begin{bmatrix} 0 \\ \vdots \\ -I_{sj}^f \\ 0 \\ \vdots \\ I_{sm}^{Th} \\ 0 \end{bmatrix}$$

being the matrix Z_{sij} given by:

$$Z_{sij} = \begin{bmatrix} Z_{+ij} & 0 & 0 \\ 0 & Z_{-ij} & 0 \\ 0 & 0 & Z_{0ij} \end{bmatrix}$$

For a generic node *i* and for a set of *p* inverters connected to network nodes, we have:

$$V_{si}^{\ f} = V_{si}^{\ 0} + \left(-Z_{sij} I_{sj}^{\ f} + \sum_{p} Z_{sim} I_{sm}^{\ Th} \right)$$

and at node *j* (faulted node):

$$V_{sj}^{\ f} = V_{sj}^{\ 0} + \left(-Z_{sij} I_{sj}^{\ f} + \sum_{p} Z_{sjm} I_{sm}^{\ Th} \right)$$

Assuming the fault at node *j* represented by the symmetrical component fault admittance matrix $Y_s^{\ f}$ the fault current in this node will be given by:

$$I_{sj}^{\ f} = Y_s^{\ f} V_{sj}^{\ f}$$

From the above equations, it is possible to obtain the general voltage equation at node *j* during the fault:

$$V_{sj}^{\ f} = \left[I + Z_{sjj} Y_s^{\ f} \right]^{-1} \times \left[V_{sj}^{\ 0} + \sum_{p} Z_{sjm} I_{sm}^{\ Th} \right]$$

Concerning the last equation, it is important to note that:

- If the vector $\left[V_{sj}^{\ 0} + \sum_{p} Z_{sjm} I_{sm}^{\ Th} \right]$ has only positive sequence component, it is only necessary to know the first column of $\left[I + Z_{sjj} Y_{s}^{\ f} \right]^{-1}$; otherwise, all the elements of this matrix need to be known;
- If the pre-fault load scenario is unbalanced or if the currents injected by the inverts are unbalanced, it is necessary to obtain the general expression of that matrix for each fault type.

Regarding the simulation of several types of faults in a node, the phase impedances Z_a, Z_b, Z_c and the neutral impedance Z_g are used to model each type of fault (for example Z_a=Z_g=0 and Z_b=Z_c=∞, represents phase a to ground solid fault).

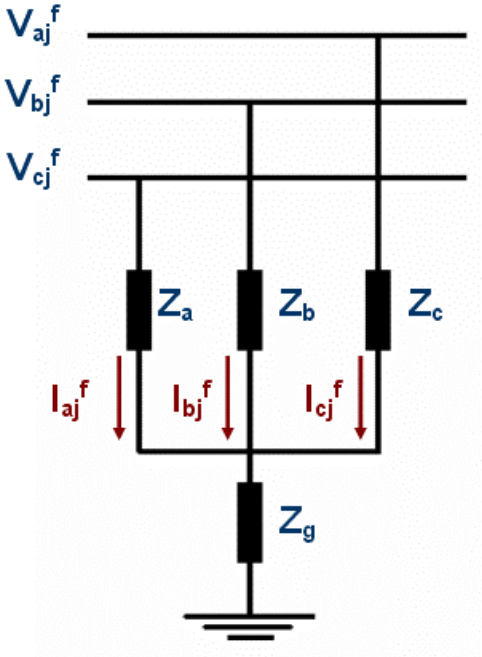

Figure 6: Fault model

The phase to earth voltages can be written as:

$$\begin{cases} V_{aj}^{f} = I_{aj}^{f} Z_a + (I_{aj}^{f} + I_{bj}^{f} + I_{cj}^{f}) Z_g \\ V_{bj}^{f} = I_{bj}^{f} Z_b + (I_{aj}^{f} + I_{bj}^{f} + I_{cj}^{f}) Z_g \\ V_{cj}^{f} = I_{aj}^{f} Z_c + (I_{aj}^{f} + I_{bj}^{f} + I_{cj}^{f}) Z_g \end{cases}$$

or in a more compact form (matricial form):

$$\begin{bmatrix} V_{aj}^{f} \\ V_{bj}^{f} \\ V_{cj}^{f} \end{bmatrix} = \begin{bmatrix} Z_a + Z_g & Z_g & Z_g \\ Z_g & Z_b + Z_g & Z_g \\ Z_g & Z_g & Z_c + Z_g \end{bmatrix} \times \begin{bmatrix} I_{aj}^{f} \\ I_{bj}^{f} \\ I_{cj}^{f} \end{bmatrix} \Leftrightarrow \left[V_{pj}^{f} \right] = \left[Z^{f} \right] \times \left[I_{pj}^{f} \right]$$

Using the transformation matrix between phase symmetrical components and phase quantities, *T*:

$$[T] \times \left[V_{sj}^{f} \right] = \left[Z^{f} \right] \times [T] \times \left[I_{sj}^{f} \right] \Leftrightarrow \left[V_{sj}^{f} \right] = [T]^{-1} \times \left[Z^{f} \right] \times [T] \times \left[I_{sj}^{f} \right] = \left[Z_{s}^{f} \right] \times \left[I_{sj}^{f} \right]$$

Finally, the symmetrical components of the fault current can be obtained by:

$$\left[I_{sj}^{f} \right] = \left[Y_{s}^{f} \right] \times \left[V_{sj}^{f} \right]$$

3. Developed Studies

Up to now, the "correct" inverter behaviour during a fault is not completely known. Thus, it was assumed that the currents injected by the inverters before and during the fault are balanced, as well as their difference (Thévenin current injection).

Also some assumptions were made regarding inverter behaviour accordingly fault impedance severity. As an example, considering that fault current in a phase to neutral

solid fault is high and bigger than in a phase-to-ground solid fault, it was assumed that inverter currents injected during the fault will be different. Then in a phase to neutral solid fault, the current injected by the inverters is set to be twice their rated current, and in a phase to ground solid fault, the current injected by the inverters is set to be 30% bigger than its rated value.

Assuming the microgrid connected to the main grid, several fault analysis were made for the study case low voltage network, involving different types of solid and non solid faults: three phase faults, single line-neutral and single line-ground faults, line-line faults and line–line-neutral and line-line-ground faults.

These fault analyses were performed, and results compared, assuming two different scenarios: microsources out of service or connected to the microgrid.

The main variables that were analyzed are the zero sequence voltage and the minimum phase voltage results in the nodes where the inverters are connected. In particular as faults were simulated at all the nodes of the microgrid, those results were analysed by checking their variation regarding the fault location.

Now we are trying to model and check some of the assumptions made, using the same methodology, in order to perform the fault analysis during islanding operation of the study case microgrid.

4. Numerical Results

Some results are presented here considering in all cases only two scenarios. In the first one the distributed generation sources are assumed disconnected from the grid; in the second one the distributed generation sources are assumed connected to the grid through power electronic interfaces that were modeled as stated in previous sections. Faults in the upstream medium voltage network were not yet considered and only the interconnected operation was analysed. However, this is an exploratory work mainly limited by the model adopted for the VSC.

The studies were made under the study case LV network defined by NTUA. At

this stage some modifications were made: the photovoltaic panels are not considered, because these devices are connected through single phase VSC.

The single line diagram of the study case LV network is represented in figure 7:

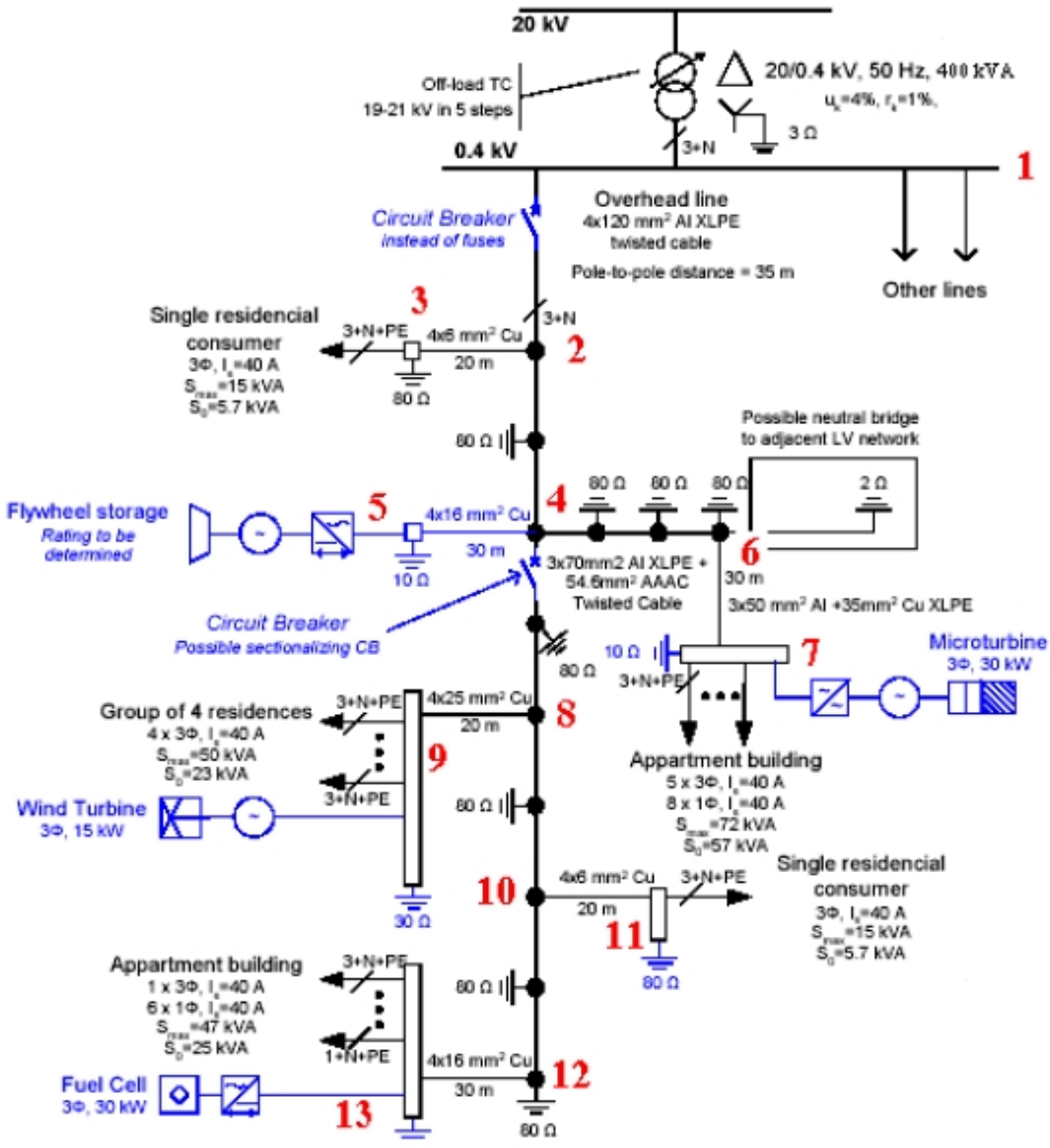

Figure 7: Single line diagram of the study case low voltage network

4.1. Phase to Ground Solid Fault

A phase to ground solid fault was simulated in each node and the zero sequence components of the phase to ground and phase to neutral voltages in nodes 7 and 13 are depicted in the following pictures:

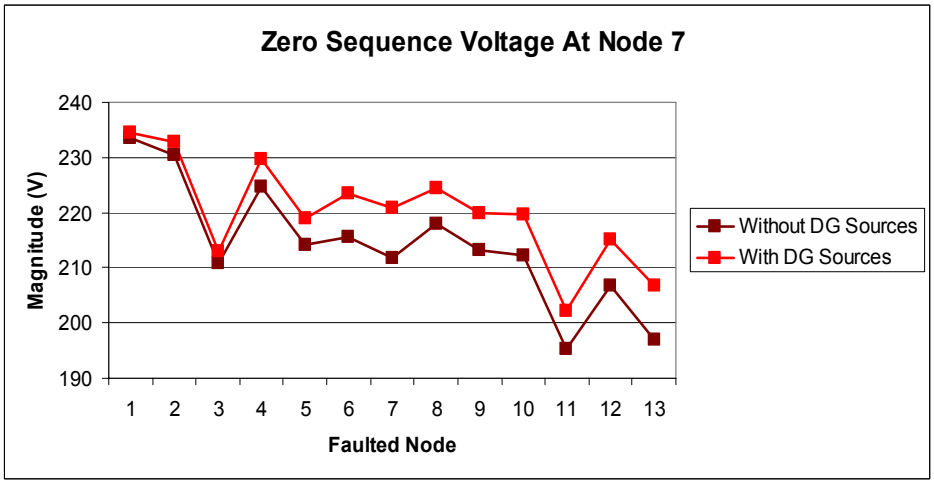

Figure 8: Zero sequence component of phase to ground voltage at node 7

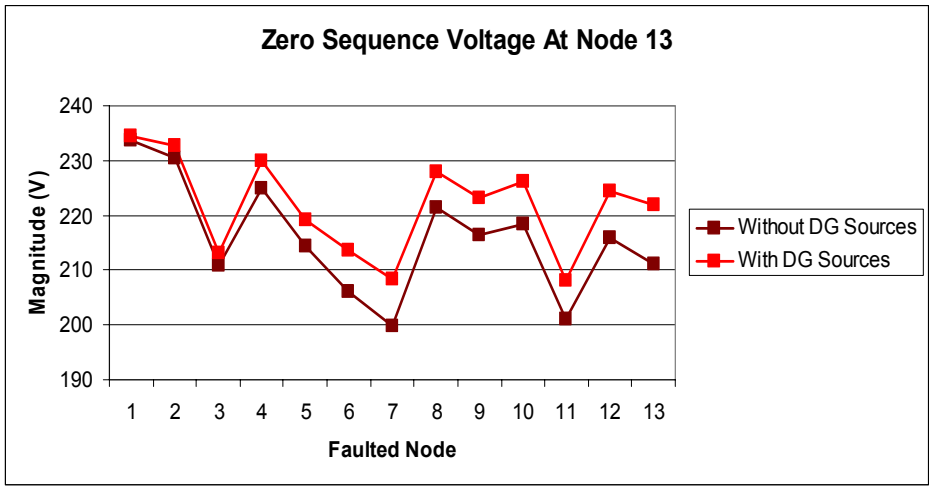

Figure 9: Zero sequence component of phase to ground voltage at node 13

As it can be easily observed, and according the VSC model adopted, the values of the zero sequence voltages as a function of the fault location is not significantly influenced by the distributed generation sources.

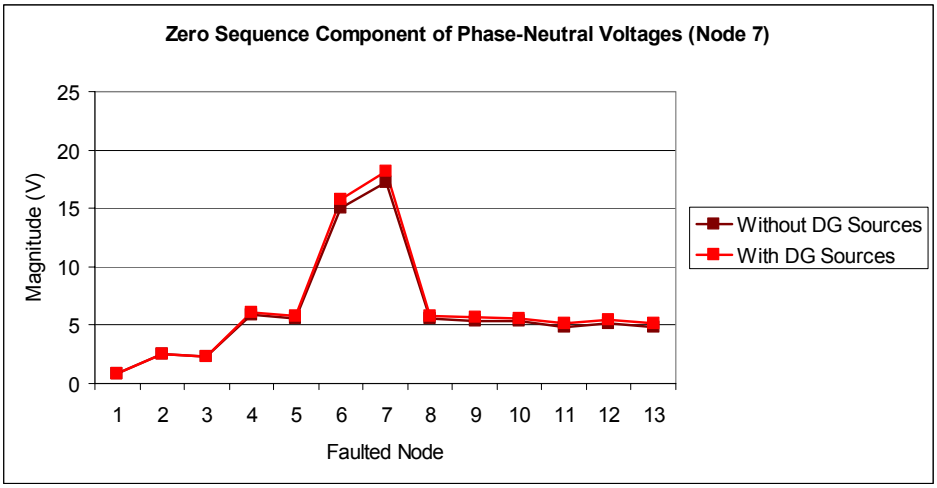

Figure 10: Zero sequence component of phase to neutral voltage at node 7

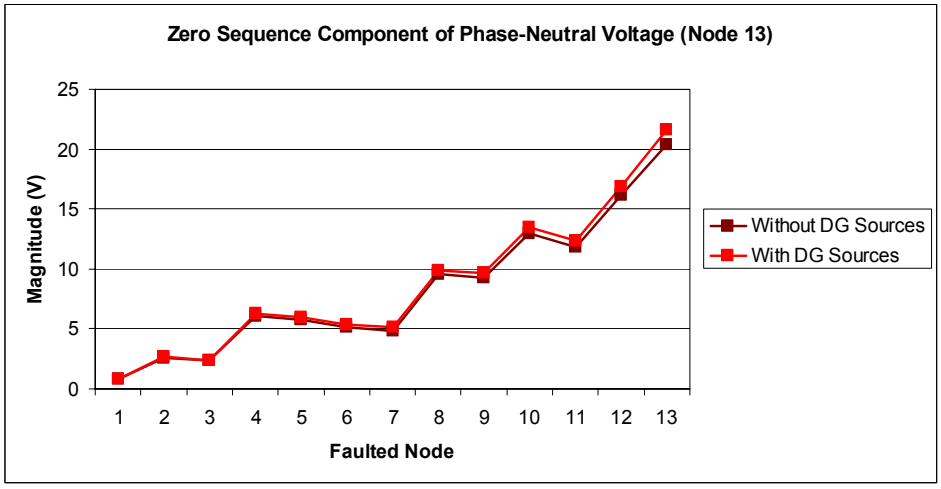

Figure 11: Zero sequence component of phase to neutral voltage at node 13

When the phase to neutral voltages are considered, the zero sequence component of the phase to neutral voltages are not very significant; if the fault location is electrically far way from the inverter (high impedance path between the inverter and the fault location) these voltages can not be used to detect this kind of faults.

As a conclusion, it can be pointed out that phase to ground solid faults can be easily detected if near the inverter zero sequence component of the phase to ground voltages are measured.

4.2. Phase to Ground Resistive Fault

In this kind of network (overhead conductors – XLPE twisted cables), it is almost impossible to happen a phase to ground solid fault. Even if a phase conductor touches the earth, there is always a contact resistance. So phase to earth resistive faults were simulated (the impedance between a phase and earth is set to be 5 Ω).

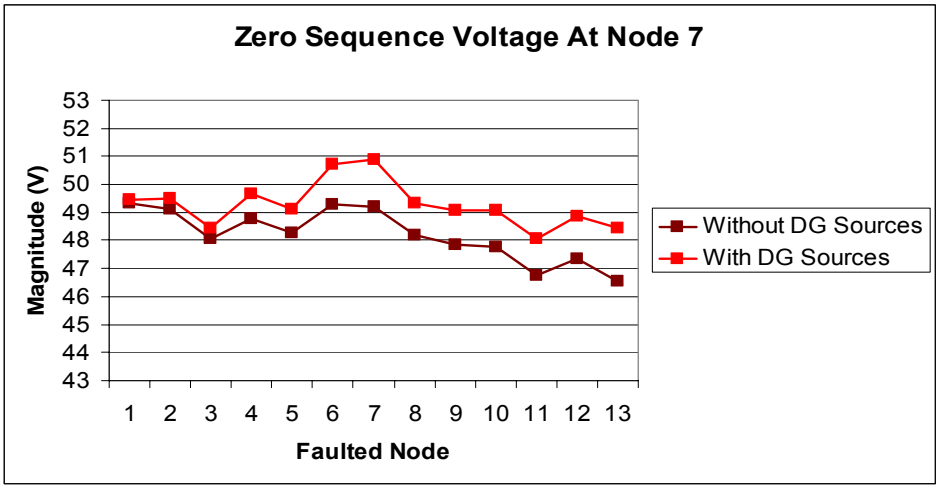

Figure 12: Zero sequence component of phase to ground voltage at node 7

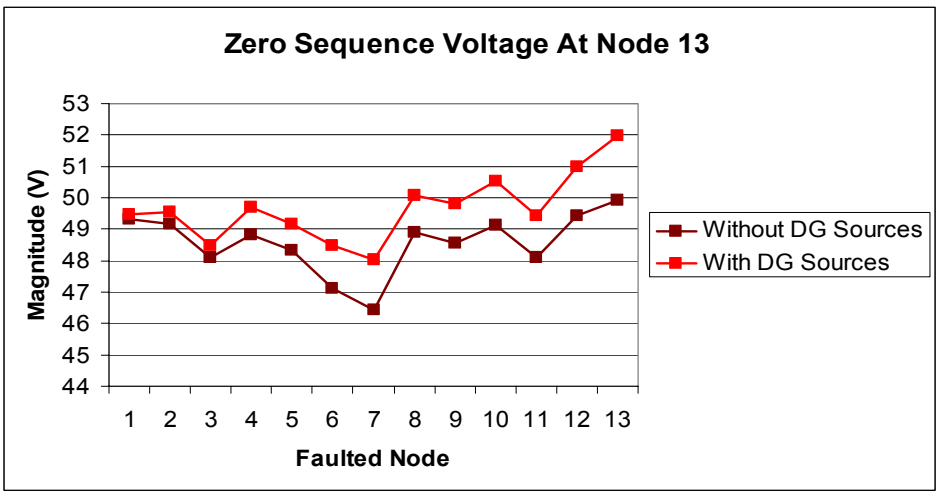

Figure 13: Zero sequence component of phase to ground voltage at node 13

In this case, the zero sequence component of phase to ground is much lower than in the previous case. This kind of faults cannot be detected by using the zero sequence component of phase to neutral voltages because their values are not significant.

Again, only the zero sequence component of phase to ground voltages can be used to detect phase to ground resistive faults.

4.3. Phase to Neutral Solid Fault

Regarding the models adopted, a phase to neutral solid fault was simulated in each bus of the network; zero sequence voltages at nodes 7 and 13 are depicted in the following pictures regarding the fault location.

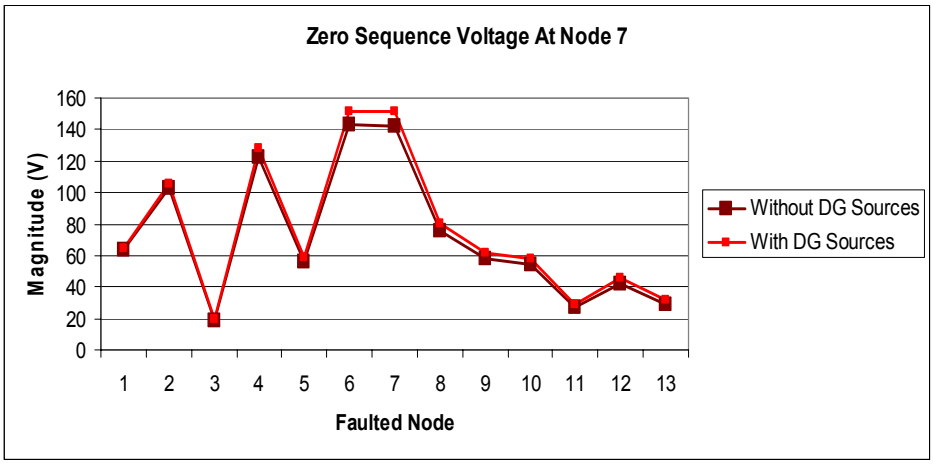

Figure 14: Zero sequence component of phase to neutral voltage at node 7

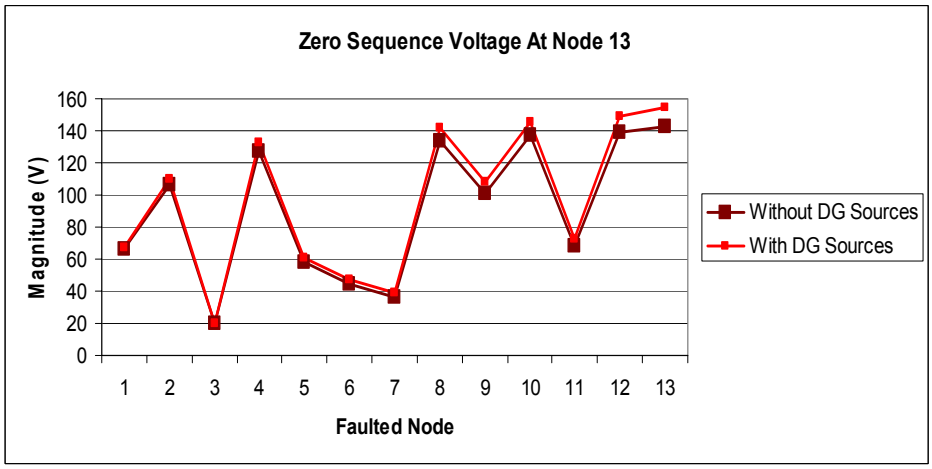

Figure 15: Zero sequence component of phase to neutral voltage at node 13

There are some cases where the zero sequence voltages are relatively small. However distribution networks do not operate with high unbalances and knowing the maximum unbalance in normal operation a zero sequence protection could be implemented.

4.4. Phase to Neutral Resistive Fault

Phase to neutral resistive faults were simulated in each node of the network, being the fault impedance 5 Ω. Zero sequence voltage protections cannot be used because zero sequence voltages are very low. If the fault occurs near the inverter, a zero sequence current protections can be used to detect the fault.

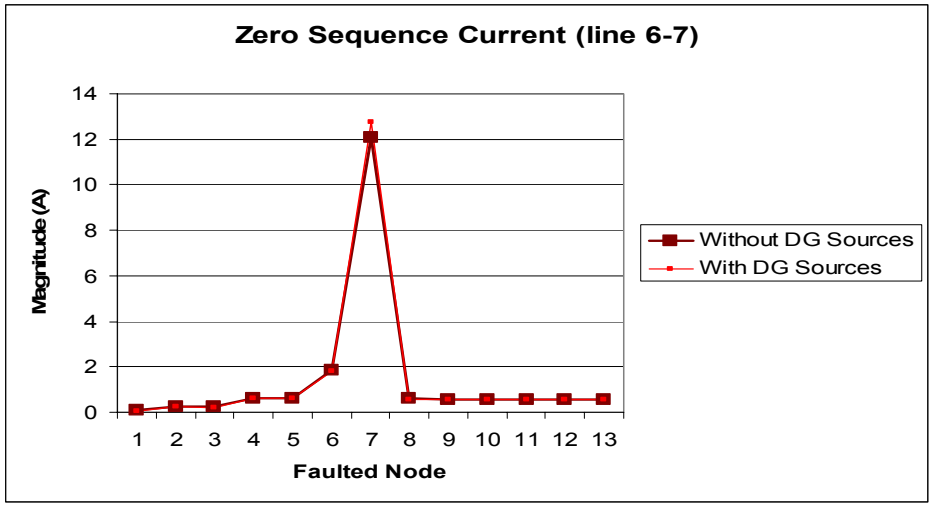

Figure 16: Zero sequence current at line 6-7

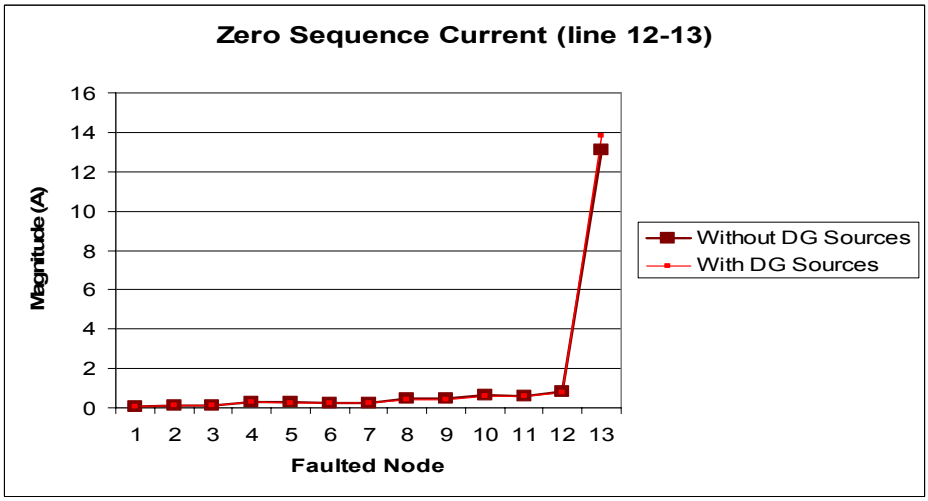

Figure 17: Zero sequence current at line 12-13

4.5. Phase to Phase Solid Fault

In phase-to-phase faults no zero sequence components exists. However, voltage sags can be used to provide disconnection of the inverters, as can be seen in the following pictures.

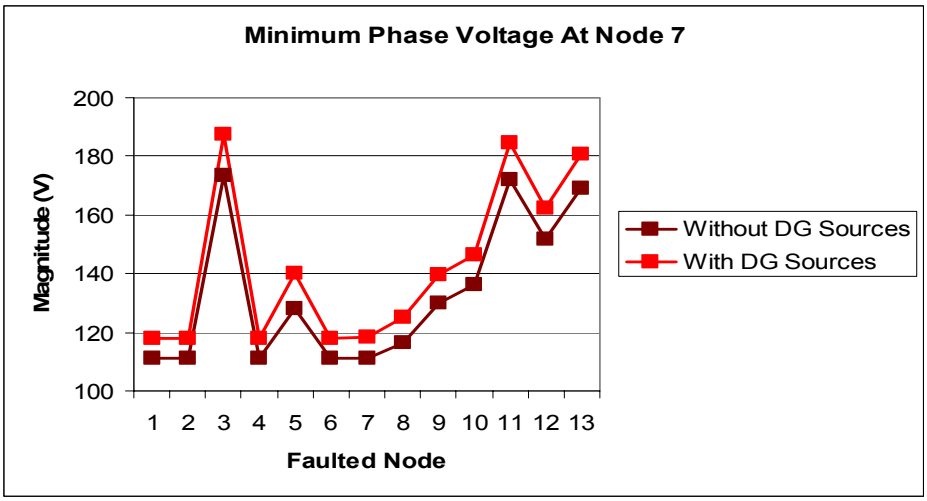

Figure 18: Minimum phase voltage at node 7

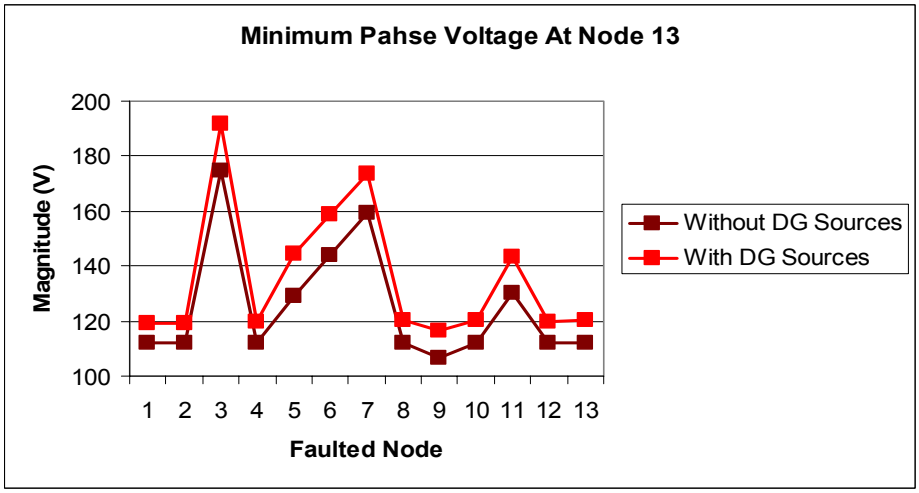

Figure 19: Minimum phase voltage at node 13

5. Conclusions

Several types of faults were simulated in the network. From the obtained results a set of general conclusions can be pointed out concerning the type of protection that could be used in order to disconnect from operation the inverters if a fault occur in the network. These conclusions are synthesized in the following table.

Solid Faults	Detection by
PH-G, PH-PH-G	$> U_o$
PH-N, PH-PH-N	$> U_o$ difficult , $< U$
PH-PH, PH-PH-PH	$< U$
Resistive Faults	
PH-G	$< U_o$
PH-PH-G	$> I_o$
PH-N, PH-PH-N	$> I_{on}$

Table 1: Fault detection

Unbalanced solid faults that involve one ore more phase conductors and the earth can be easily detected using overvoltage zero sequence protections (zero sequence component of the phase to ground voltages).

If this kind of faults is resistive, zero sequence voltages are much lower than in solid faults. Further development is necessary to decide between overvoltage zero sequence protections or overcurrent zero sequence protections.

Other types of unbalanced resistive faults are very difficult to detect. However if the fault occurs near the point where the inverter is connected an overcurrent zero

sequence protection can be adopted to detect the fault.

Phase to neutral solid faults, phase-phase-neutral solid faults, phase to phase solid faults and three phase solid faults can be easily detected by undervoltage protection; in these kind of faults, phase currents are very big and voltage sag in the node were the inverter is connected can be used as a parameter to regulated minimum phase voltage protections.

Notice that the presented fault analysis approach assumes that the Thévenin current injected by each inverter during the fault is known.

In the steady state fault analysis electrical quantities are regarded as phasors. The phase angles of the inverters injected currents are not known, being assumed to be equal to the ones that are obtained from the power flow study.

In what concerns the fault analysis in islanding operation, this kind of procedure is not suitable because doing this the network behavior is being forced. In fact, current faults and voltages are very dependent on the injected current specified.

The presented fault analysis approach can easily handle unbalanced operation of inverters, even if these devices are represented as current injections or as equivalent impedances of voltage or current sources.

Document Information

Title	Electrical Protection Schemes for a Microgrid
Date	20th July 2004
Version	Draft Issue No 2
Task(s)	

Authors:	Xueguang Wu, Nilanga Jayawarna, Nick Jenkins

Access:	
Project Consortium (for the actual version) European Commission , PUBLIC (for final version)	
Status:	
	Draft Version Final Version (internal document) **X** Submission for Approval (deliverable) Final Version (deliverable, approved on.)

DE2-Appendix III

MICROGRIDS

Large Scale Integration of Micro-Generation
To Low Voltage Grids

WORK PACKAGE E

TASK TE4

Electrical Protection Schemes for a MicroGrid

Draft Issue No 2

20th July 2004

Xueguang Wu, Nilanga Jayawarna, Nick Jenkins

UMIST

Contents

1. Basic principles of electrical protection in the power system

The electrical protection for any power system must take into account the following basic principles:

(1) **Reliability**, the ability of the protection to operate correctly. Under the occurrence of a fault or abnormal condition, the protection must detect the problem quickly in order to isolate the affected section. The rest of the system should continue in service and limit the possibility of damage to other equipment.

(2) **Selectivity**, maintaining continuity of supply by disconnecting the minimum section of the network necessary to isolate the fault.

(3) **Speed**, minimum operating time to clear a fault in order to avoid damage to equipment and maintain stability.

(4) **Cost**, maximum protection at the lowest cost possible.

Obviously, it is practically impossible to satisfy all the above mentioned points simultaneously. A compromise is required to obtain the optimum protection system.

2. Main electrical protection schemes in the distribution network

The main electrical protection schemes in the distribution network are overcurrent protection, differential protection, and distance protection.

(1) Overcurrent protection

Overcurrent protection is a device that detects the fault from a high value of the fault current. The common types of the overcurrent protection are the thermomagnetic switches, moulded-case circuit breakers (MCCB), fuses and overcurrent relays. A typical overcurrent relay protection is shown in Figure 1.

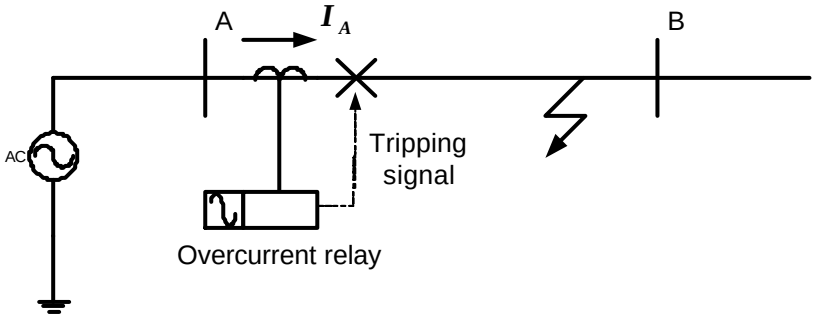

Figure 1 Overcurrent relay protection

A typical setting of an overcurrent relay is, say, 50% of the maximum short-circuit current at the point of connection of the relay or 6-10 times the maximum circuit rating. The relay measures the line current using a current transformer (CT). If the current is above the setting, the relay operates to trip the circuit breaker on the line.

According to the characteristics of an overcurrent relay, it can be classified into three groups: (1) definite current relay; (2) definite time relay and (3) inverse time relay, as shown in Figure 2(a), Figure 2(b) and Figure 2(c), respectively [Gers, 1998].

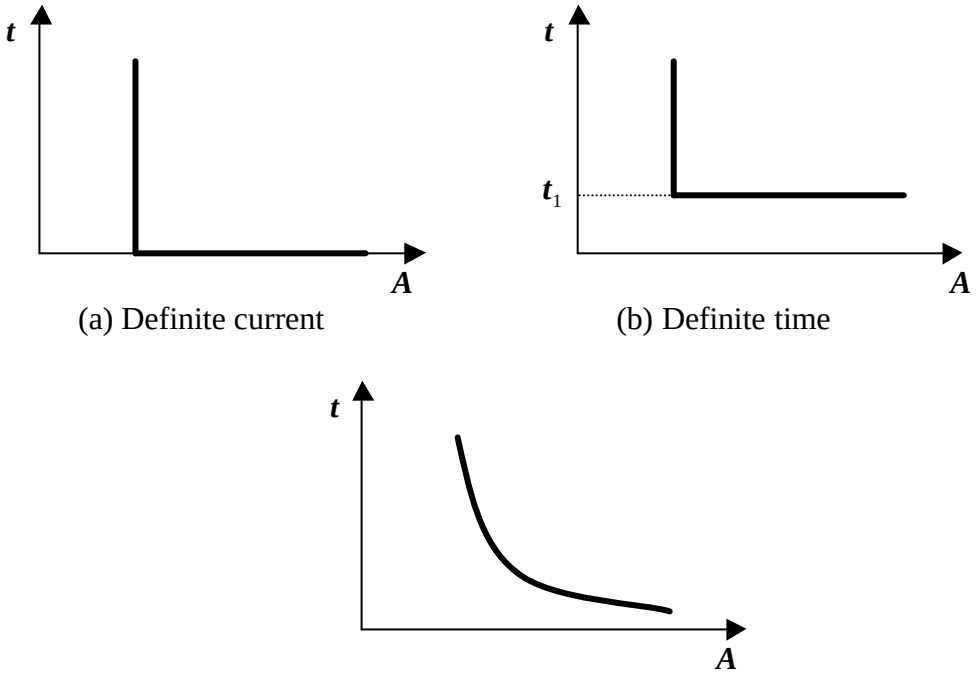

(a) Definite current (b) Definite time

(c) Inverse time

Figure 2 Time/current operating characteristics of the overcurrent relay

The definite current relay operates instantaneously when the current reaches a predetermined value. This type of relay has little selectivity. If the settings of the relay are based on the maximum fault level conditions, the settings may not be appropriate for a low fault level. However, if a lower value of fault level is used for settings, some breakers may operate unnecessarily, leading to nuisance tripping.

The definite time relay operates in a certain time. The setting can be adjusted to cope with different levels of current by using different operating times. The disadvantage

of this type of relay is that the faults, which are near to the main source, may be cleared in a relatively long time.

The inverse time relay operates in a time, which is inversely proportional to the fault current. The advantage of this type of relay is that the higher the fault current, the shorter is the tripping time. Generally, the inverse time relay provides improved protection selectivity.

(2) Differential protection

Differential protection operates when the vector difference of two or more similar electrical magnitudes exceeds a predetermined value (setting). The most common type of differential protection is the overcurrent relay differential protection. A simple overcurrent relay differential protection is shown in Figure 3.

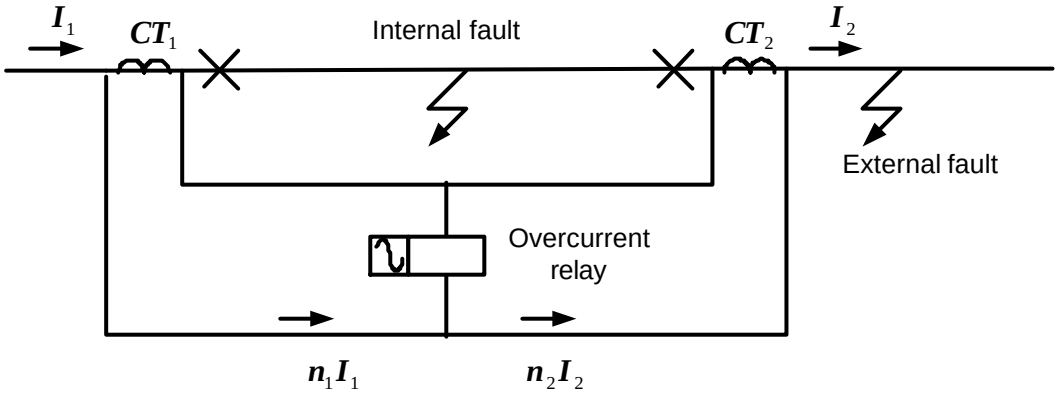

Figure 3 A simple overcurrent relay differential protection

In Figure 3, an overcurrent relay is connected to the secondary sides of the current transformers CT1 and CT2. The protection zone is between CT1 and CT2. Under normal load condition or when there is a fault outside of the protection zone (external fault), the secondary currents $n_1 I_1$ and $n_2 I_2$ would circulate between CT1 and CT2. In other words, the current $n_1 I_1$ is equal to $n_2 I_2$. There is no current flowing through the overcurrent relay. However, if a fault occurs in the section between CT1 and CT2 (internal fault), the fault currents would flow towards the faulted point from both sides of the element. The current flowing through the overcurrent relay is the sum of the secondary currents, $n_1 I_1 + n_2 I_2$. In all cases the current in the overcurrent relay is proportional to the vector difference between the currents, which enter and leave the

protected element. If the current flowing through the overcurrent relay exceeds the setting, the overcurrent relay will operate and send a signal to trip off the circuit breakers at two terminals of the element. As a result, the faulted section will be isolated from the network.

For application of differential protection in an extensive network, the relays should be located at the terminals of the protected element to monitor the electrical quantities (e.g. the line currents) required for the trip decision of the protection. The data relating to the state of the network must be transferred from the remote terminal(s) to the local terminal and then compared with data obtained at the local terminal. This requires the use of a communication system for data transfer. Ideally, the communication system should instantaneously transfer all the data required for the protection between the relays. The communication system can use metallic conductors (pilot wires), optical fibres, or free space via radio or microwave as its communication medium.

With development of the digital relay, a digital data voice-frequency grade communication channel can be used to provide the communication between the relays. A simplified representation of the differential protection based on the digital data voice-frequency communication was proposed [Redfern, 1994], as shown in Figure 4.

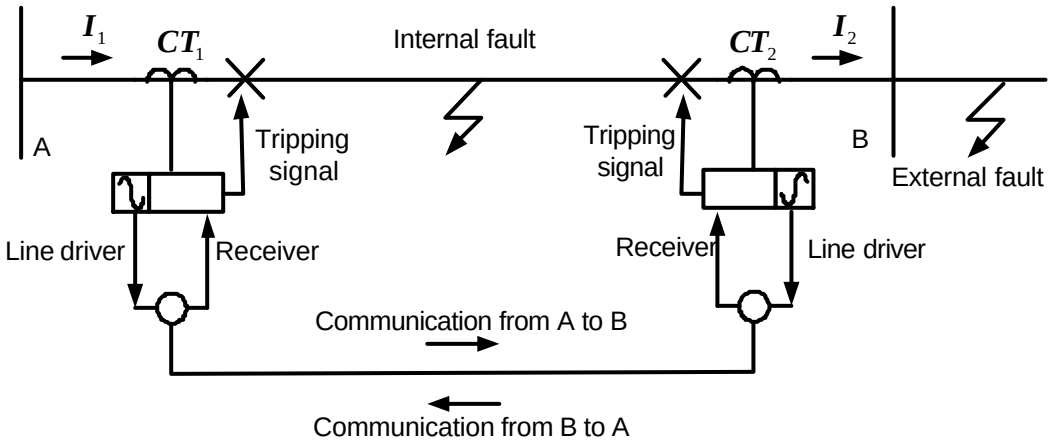

Figure 4 A communication based differential protection

Voice-frequency grade communication channels are commonly used for telephone communications. They usually operate with a 4kHz bandwidth. Since the available bandwidth of the voice-frequency communication channel is limited, the volume of data, which can be handled, is also limited. The standard data rates cover a wide range varying from 75 bits/sec to 14.4kbits/sec operating in full or half duplex.

The relationship between the rate of data transfer and maximum tripping time was investigated in reference [Li, 2002]. For a full duplex digital data voice-frequency communication channel with a capacity of 2400 bits/sec, the typical maximum tripping time of the differential protection was about 50 milliseconds [Redfen, 1994]. Using a moulded data reduction algorithm, the capacity of the channel can be increased. The tripping time will be decreased.

The main advantage of differential protection is its high selectivity. The differential protection only operates in the case of an internal fault. However, the requirement for separate back-up protection and the additional cost of the communication system may limit the application of differential protection in the MicroGrid.

(3) Distance protection

Distance protection uses the impedance measured by the distance relay to detect the faults. Essentially, the distance relay compares the fault current against the voltage at the relay location to calculate the impedance from the relay to the faulty point. For a distance protection scheme shown in Figure 5, the distance relay is located at busbar A. The line current $\boldsymbol{I}$ and busbar voltage $\boldsymbol{V}$ were used to evaluate the impedance $\boldsymbol{Z} = \boldsymbol{V}/\boldsymbol{I}$. The value of measured impedance of the distance relay would be $\boldsymbol{Z}_{\boldsymbol{AF}1}$ for a fault F1 and $\left(\boldsymbol{Z}_{\boldsymbol{AB}} + \boldsymbol{Z}_{\boldsymbol{BF}2}\right)$ for a fault F2. The protection zones of the distance relay are Zone1 (80-85% length of the protected line), Zone2 (150%, covering 100% length of the protected line plus 50% next shortest adjacent line) and Zone3 (225%, covering 100% length of the protected line plus 100% second longest line, plus 25% shortest next line).

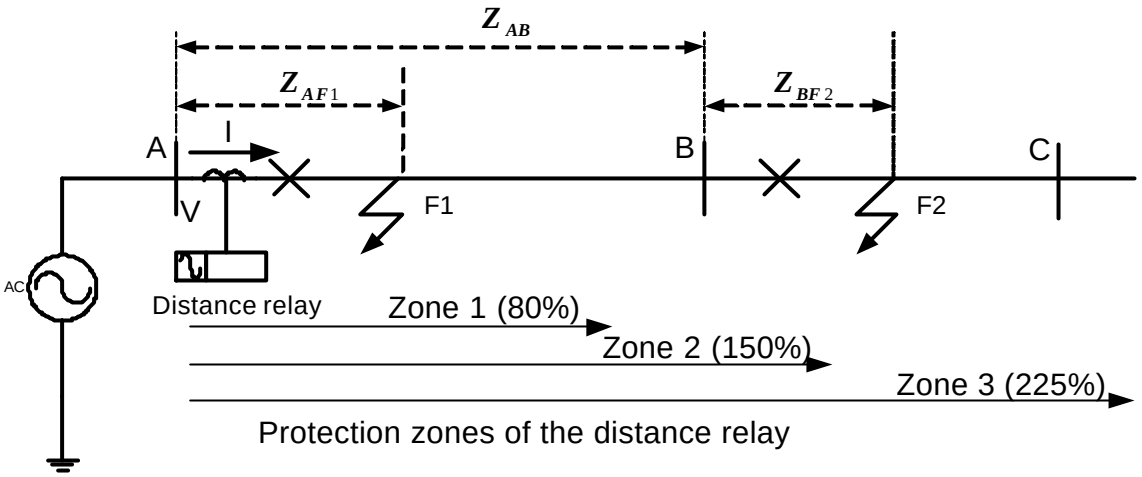

Figure 5 Measured impedance of the relay for the faults on the network

On the R-X plane, the distance relay could be classified into the impedance relay, directional relay, reactance relay, mho relay, completely polarised mho relay and combined relay, etc. The impedance relay is a basic type of the distance relay. It operates in a circular impedance characteristic with its centre at the origin of the co-ordinates and a radius equal to the setting of the distance relay in ohms. Figure 6 shows the typical characteristics of an impedance relay.

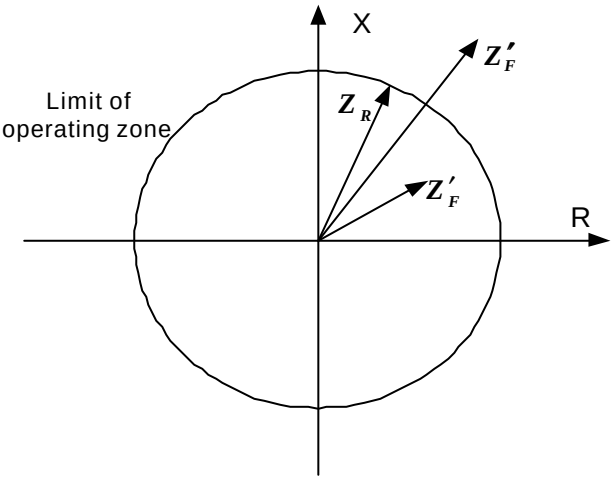

Figure 6 Typical characteristics of the impedance relay

In Figure 6, the area in the circle is the operating zone of the impedance relay. The radius Z_R of the circle is the setting of the impedance relay. If a fault occurs in the operating zone of the relay, the measured impedance Z'_F is less than the setting. The relay operates to trip the circuit breaker. When a fault is outside of the zone, the

measured impedance Z_F'' is larger than the setting Z_R. The relay remains in its normal condition.

The advantage of the distance protection is the zones of protection (e.g. Zone1, Zone2 and Zone3). The zones only depend on the impedance of the protected line. The line impedance is constant and independent of the magnitudes of the voltage and current. In contrast to, the zones of overcurrent protection vary with the system operating conditions.

However, the disadvantages of the distance protection are:

(a) It is affected by the infeeds (DG or loads). The measured impedance of distance relay is a function of infeed currents. The distance relay may over reach if the infeeds are disconnected.
(b) It is also be affected by the fault arc resistance.
(c) It is sensitive to oscillations on the power system. During a power system oscillation, the voltage and current, which feed the distance relay, vary with time. As a result, the distance relay would see an impedance that is varying with time. The variation of measured impedance might cause the relay to operate incorrectly. Therefore, a power-swing blocking unit is necessary for the distance protection in transmission system.

(4) GPS based adaptive protection

The protection systems in distribution networks are often based on the fact the network is radial in nature. Each protection system co-ordinates with the immediate upstream and/or downstream section protection. After connecting distributed generation (DG), part of the distribution network may no longer be radial. The co-ordination of the protection systems may not hold.

To solve this problem, a GPS based adaptive protection scheme for a distribution network with high penetration of the DG was proposed in [Brahma, 2004]. Basically, the distribution network was divided into a number of zones (e.g. Z_1, Z_2, Z_3, Z_4, Z_5 and Z_6) by the breakers ($B_{s\text{-}1}$, $B_{1\text{-}2}$, $B_{2\text{-}3}$, $B_{2\text{-}5}$, $B_{3\text{-}5}$, $B_{4\text{-}5}$ and $B_{5\text{-}6}$), according to a reasonable balance of the DG and local loads, as shown in Figure 7.

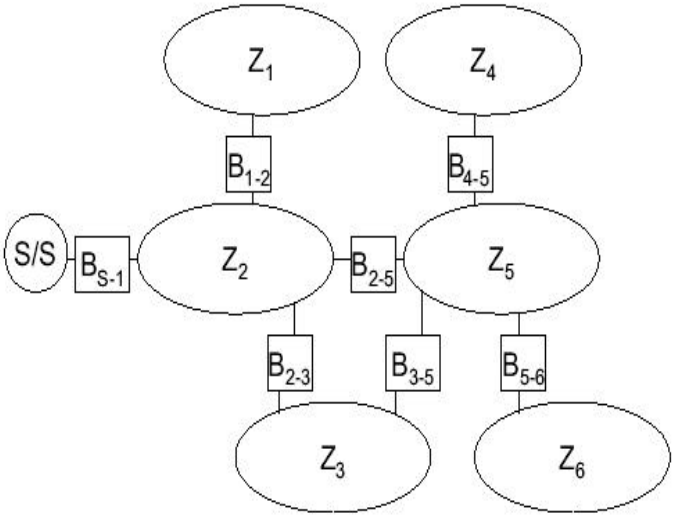

Figure 7 a typical distribution network divided in breaker-separated zones
(copied from reference [Brahma, 2004])

In each zone, the capacity of the DG is a little higher than the load. At least one DG has load frequency control capability in the zone. The breakers between the zones are equipped with check-synchronisation function. The main relay (close to substation) is capable of storing and analysing large amounts of data and communicating with the zone breakers and the DG.

The measurements of the GPS based adaptive protection are the synchronised current vectors of all three phases from every DG and the main source and, in addition, the current directions of the zone-breakers. The synchronised vectors are obtained using a global positioning system (GPS) based phase measurement unit. The current direction indicates whether the fault is in the zone or outside of the zone.

The current phasors from the main source and all DG are continuously available. In normal operating conditions, the sum of all these current phasors would be equal to the total load in the network. In the case of a fault in the network, this sum would be significantly larger than the total load. This is similar to current differential protection. Once a fault in the network is sensed, the total fault current in each phase can be determined using a simple equation as follows:

$$\boldsymbol{I}_{fabc} = \sum_{i=1}^{n} \boldsymbol{I}_{fabc\_i} \qquad (1)$$

where, $\boldsymbol{I}_{fabc}$ is the total fault current in three phases; $\boldsymbol{I}_{fabc\_i}$ is the fault current contribution in three phases from the source *i*; n is total number of the sources, including the main source and all DG.

From equation (1), according to the magnitudes of the fault current in each phase, the fault type and phase involved in the fault can be immediately determined. Since the fault contribution from each source is also available from the measurements, it is possible to identify the faulted section through checking each source fault current contribution with its fault current distribution on the section.

From the fault point, every source can be represented as a voltage source behind Thevnin impedance. If the fault point shifts from one busbar to the adjoining busbar, for a given type of fault, the Thevnin impedance to a given source can increase or decrease. In other words, if the fault point shifts over a section (i-j) from busbar i to busbar j, for a given type of fault, the fault current contribution from any given source k can either continuously increase (from $\boldsymbol{I}_{f\min}$ to $\boldsymbol{I}_{f\max}$) or decrease (from $\boldsymbol{I}'_{f\max}$ to $\boldsymbol{I}'_{f\min}$), as shown in Figure 8.

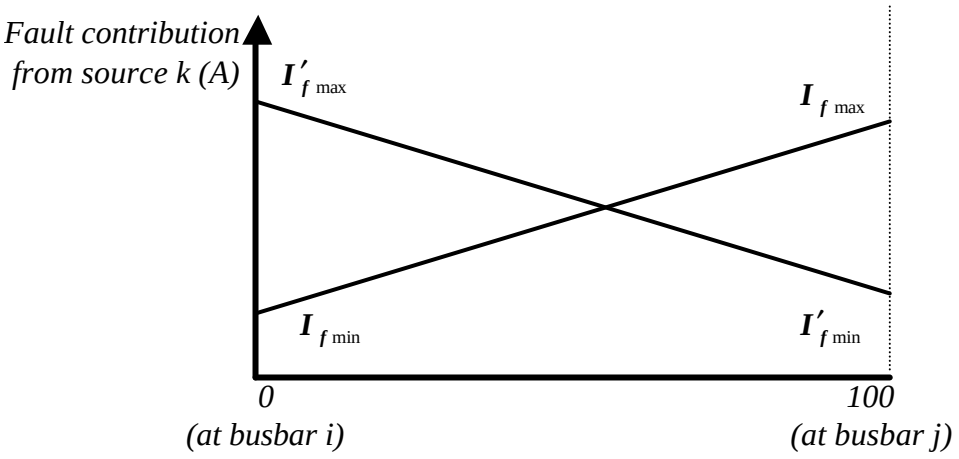

Figure 8 Characteristics of fault contribution from a source k for a given type of fault on a line section between busbar i and busbar j

Thus, the fault current contribution from source k, for a given type of fault occurring at any point between busbar i and busbar j, will lie between the contributions from source k to the same type of fault on busbar i and busbar j.

Fault current contribution from each source for every type of fault for all busbars can be obtained from offline short-circuit analysis. The results of fault current calculation are stored in a database to form a look-up table containing fault current contributions from each source for each type of fault at each busbar. From looking up the table, the faulted section can be identified if the measured fault contribution from each source lies between the calculated fault contribution at the two busbars connected to this section from the same source for a given type of fault.

It is claimed that the GPS based adaptive protection scheme could be effective when there are a number of distributed generators (DGs) in the distribution network. The accuracy of the GPS based adaptive protection is shown in Table 1 [Brahma, 2004].

Table 1 Accuracy of the GPS based adaptive protection.

DG connected in system	Accuracy L-L-L %	Accuracy L-L %	Accuracy L-L-G %	Accuracy L-G %
none	30.5	26.6	26.6	26.6
one	61.8	52.7	52.7	52.7
two	77.8	65.5	65.5	65.5
three	94.4	83.0	83.0	83.0
four	95.1	86.1	86.1	86.1
five	97.9	93.9	93.9	93.9

** Copied from reference [Brahma, 2004].*

Table 1 shows the dependence of accuracy of the GPS based adaptive protection on number of the DG connected in the network. The accuracy of the adaptive protection is proportional to the number of DGs in the network. If there is no DG in the network, the accuracy of the adaptive protection is about 30%. If there are five DGs in the network, the accuracy of the adaptive protection is above 90%.

The advantage of the adaptive protection scheme is that a look-up table, containing the fault current contribution from each source for a given type of fault, can be formed using offline short-circuit analysis. The scheme is adaptive to temporary as well as

permanent changes in the distribution network. The region of the scheme would be extended to more than one feeder.

However, the disadvantage of the adaptive protection scheme is the use of GPS measurements and communication between DGs and substation. The installation of measurement and communication equipment may produce a high cost.

(5) Zero sequence protection

Concerning the type of protection, which could be used to detect the faults on the MicroGrid, the results in [Pereira da Silva, 2004] show how the protection can be used to protect the MicroGrid. The operation of the protection is shown in Table 2.

Solid Faults	Detection by
PH-G, PH-PH-G	$> U_o$
PH-N, PH-PH-N	$> U_o$ difficult , $< U$
PH-PH, PH-PH-PH	$< U$
Resistive Faults	
PH-G	$< U_o$
PH-PH-G	$> I_o$
PH-N, PH-PH-N	$> I_{on}$

Table 2 Fault detection
(*Copied from reference [Pereira da Silva, 2004]*)

Table 2 shows how the zero sequence voltage based, under voltage based and zero sequence current based protection can be used to detect the faults on the MicroGrid. The zero sequence voltage-based protection is used to detect the phase-to-ground and double-phase-to ground solid faults. The under voltage based protection is used to detect the phase-to-neutral, double-phase-to-neutral, phase-to-phase and three-phase solid faults. The zero sequence current-based protection is used to detect the double-phase-to ground, phase-to-neutral, double-phase-to-neutral resistive faults. However, to identify the location of the faults on the MicroGrid precisely, the zero sequence protection technique may need fast communication between the protection devices

installed at different places. The cost of the zero sequence-based protection may be very high.

3. Major issues of the MicroGrid

A MicroGrid comprises a low voltage (LV) distribution system with distributed energy sources (e.g. micro-turbines, fuel cells, PV, etc.) together with storage devices (flywheels, energy capacitor and batteries). The MicroGrid offers more benefits when a lot of micro sources are installed in the system. The benefits from the MicroGrid are not only for residential consumers, but also for hotels, hospitals and large industries with many micro sources. The advantages of the MicroGrid are summarised as follows [Nara, 2002]:

(a) Diversification of power sources;
(b) Reduction of power distribution loss;
(c) Reduction of reactive power resources;
(d) Enhancement of power supply ability and reliability;

The MicroGrid can be operated in a non-autonomous way if interconnected to the network or in an autonomous way (islanded) if disconnected from the main grid. The control of the MicroGrid is considerably complex, particularly, if islanded operation is allowed. A typical MicroGrid control architecture is shown in Figure 9.

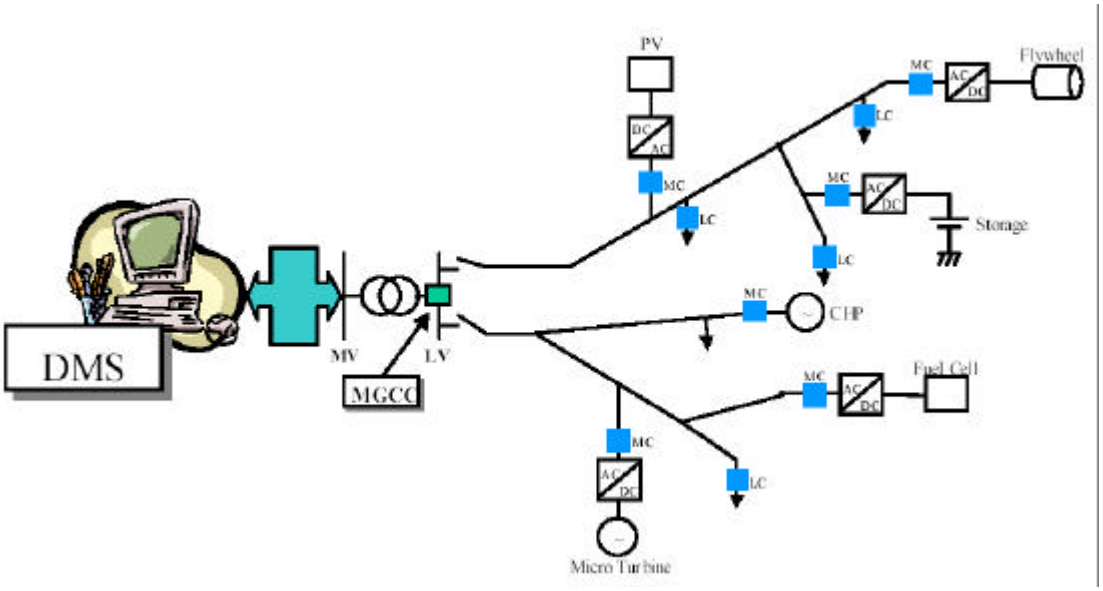

Figure 9 A typical MicroGrid control architecture

Figure 9 shows three control levels of the MicroGrid: (1) local micro source controllers (MC) and load controllers (LC); (2) micro grid system central controllers (MGCC); and (3) distribution management system (DMS).

The MC is to be housed within the power electronic interface of the micro source. It uses local information and the instructions from the MGCC to control the micro source during all events. The LC is installed at the controllable loads. The LC provides load control capabilities following instructions from the MGCC. To control the MicroGrid, a communication system is needed to interface with MC, LC and MGCC. The MGCC is responsible for providing system load forecast and controlling the MicroGrid to operate in an optimal state. The defined optimised-operating scenario can be achieved by controlling the micro sources and loads in the MicroGrid. The DMS is an enhanced distribution system management system with new operating features of the MicroGrid. It exchanges information with the MGCC.

The MicroGrid is subject to the same safety requirements as any other utility electric power system. The protection scheme of the MicroGrid must respond to both system and MicroGrid faults. If a fault is on the network, the desired response may be to isolate the MicroGrid from the main grid as rapidly as necessary to protect the MicroGrid loads. If a fault is within the MicroGrid, the protection system should only isolate the smallest possible faulted section to eliminate the fault.

The power electronic based MicroGrid can not normally provide the required levels of short circuit current. The micro sources may only be capable of supplying twice load current or less to a fault. Some conventional overcurrent sensing devices may not even respond to this fault current level. In addition, undervoltage and frequency protection may fail to detect the faults due to the voltage and frequency control in the MicroGrid.

Therefore, the electrical protection schemes for the MicroGrid have to make a trade-off between technical requirements and economic aspects.

4. Possible electrical protection schemes for the MicroGrid

A detailed analysis of the electrical protection schemes for the MicroGrid is required due to its unique nature in design. In order to investigate various protection schemes for the MicroGrid, a typical MicroGrid was considered with the faults located at different places as shown in Figure 10.

The main distribution network is assumed to have a short circuit level of 100MVA and a X/R ratio of 5. The MicroGrid consists of a flywheel storage (200kW), a number of micro sources and a group of residential consumers. A feeder of the MicroGrid is interconnected with the main distribution network through the circuit breaker CB3 and a transformer (20/0.4 kV, 400kVA).

The earthing system of the MicroGrid is assumed to be a TN-C-S system. The transformer neutral is earthed. The supply feeder consists of a TN-C system, where the neutral conductor and the earth conductor are combined. The earthing arrangement in the installations (consumers) is TN-S, with separate neutrals and earth conductors.

In this study, two scenarios (Case 1 and Case 2) of the MicroGrid were investigated. In Case 1, the MicroGrid is connected to the main network. In Case 2, the MicroGrid is operating in islanded mode. Three different faults (F1, F2 and F3) were applied to the MicroGrid. Fault F1 is on the main distribution network. Fault F2 is on the MicroGrid network. Fault F3 is at a single residential consumer.

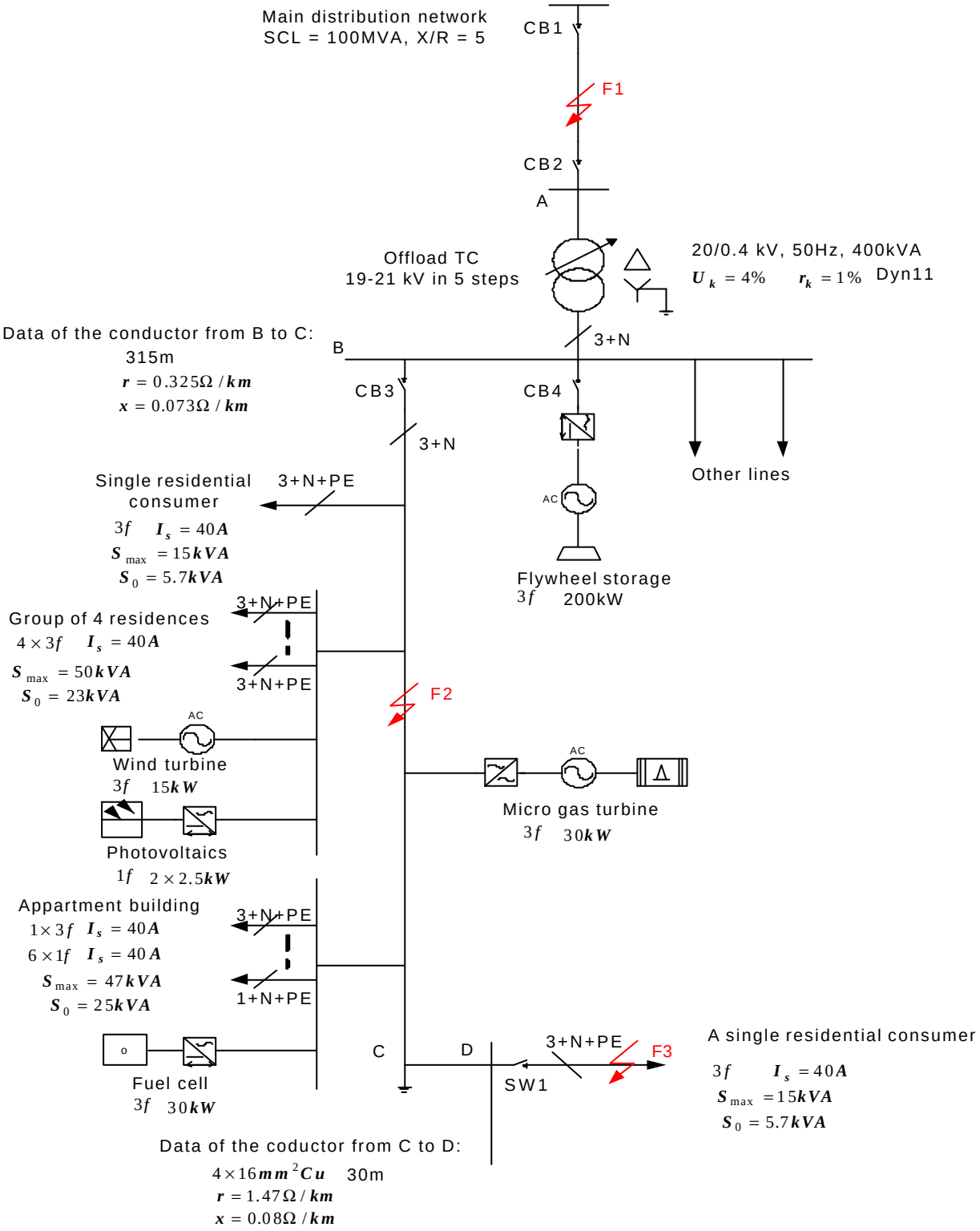

Figure 10 A typical MicroGrid with faults (F1, F2 and F3) located at different places

Based on the data (shown in Figure 10), for the faults F1 and F3, the energies ($\boldsymbol{E} = (3\boldsymbol{I}^2\boldsymbol{R})\cdot\boldsymbol{t}$) supplied by the flywheel were calculated and shown in Table 2. The fault currents of the flywheel were assumed as 3 per unit and 5 per unit, based on its rating. $\boldsymbol{R}$ is a resistance between flywheel (at busbar B) and the faulty point.

Table 2 Supply energies of the flywheel to faults F1 and F3

Case	Voltage (kV)	R (ohms)	$\boldsymbol{I}_{f\_flywheel} = 3\boldsymbol{p.u}$, based on 200kW				$\boldsymbol{I}_{f\_flywheel} = 5\boldsymbol{p.u}$, based on 200kW			
			P (kW)	E (kJ) in the time of			P (kW)	E (kJ) in the time of		
				0.3sec.	0.5sec.	1.0sec.		0.3sec.	0.5sec.	1.0sec.
F1	20	10.00	9.00	2.50	4.50	9.00	24.99	7.50	12.50	25.00
F3	0.4	0.146	328.51	98.55	164.25	328.51	912.53	273.76	456.26	912.53

Table2 shows the supply energies of the flywheel to faults F1 and F3. The supply energy of the flywheel to fault F1 is considerably less than that to fault F3.

For fault F1, the energy supplied by the flywheel in 1 second (refereed to 20kV) are 9.00 kilo Joules and 25.00 kilo Joules under the fault currents 3 p.u. and 5 p.u. (based on its capacity 200kW), respectively. For fault F3, the energy supplied by the flywheel in 1 second (refereed to 0.4kV) are 328.51 kilo Joules and 912.53 kilo Joules, respectively. The energy supplied by the flywheel is larger than 300 kilo Joules if the fault current contribution from the flywheel is above 3p.u, based on its rating. Therefore, for a flywheel with capacity of 4MJ installed in the MicroGrid, the flywheel is able to supply 3-5 p.u fault current (based on its rating) to any point in the MicroGrid in a certain time.

The electrical protection schemes for the MicroGrid may be different, according to the fault location and type. For faults F1, F2 and F3 (in Figure 10), the possible electrical protection schemes for the MicroGrid will be investigated separately.

(1) Fault F1 on the main distribution network

Considering a fault F1 on the main distribution network, a simplified MicroGrid is shown in Figure 11.

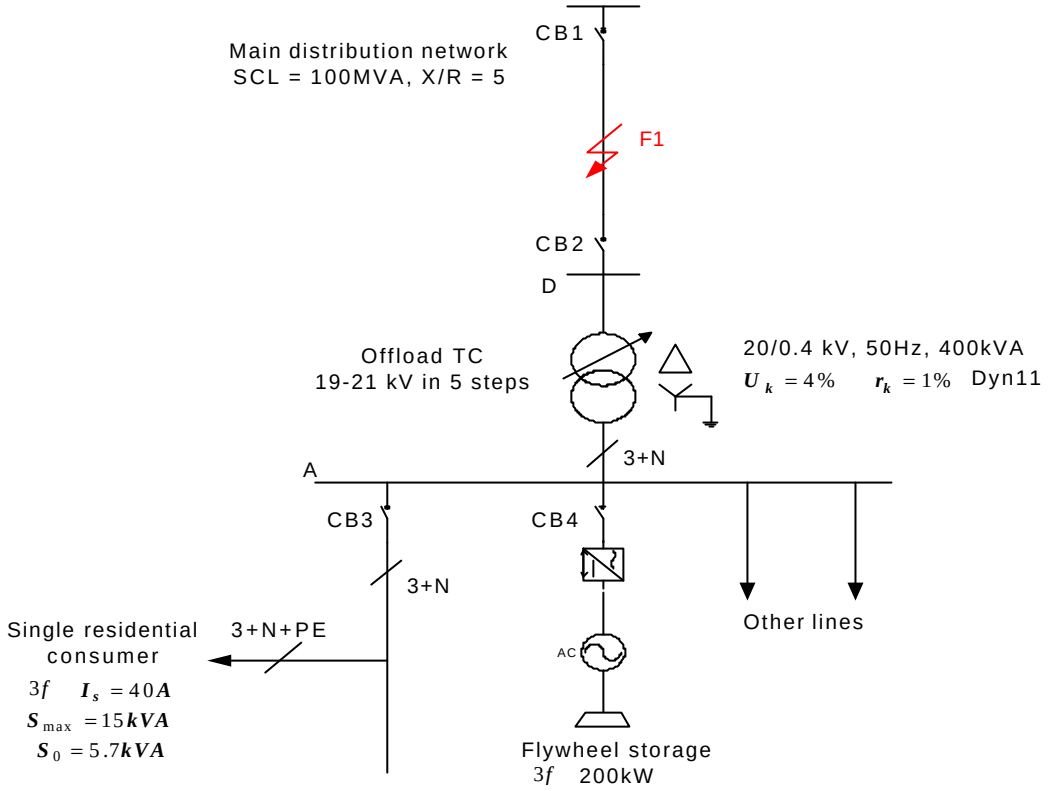

Figure 11 A simplified MicroGrid with a fault F1 on the main distribution network

The fault F1 may be a phase-to-phase fault (three-phase short circuit or two-phase short circuit) or a phase-to-ground fault (single-phase to ground or two-phase to ground). The action of the protection against fault F1 should trip the circuit breakers CB1 and CB2 rapidly.

During the fault, the main distribution network supplies a large current to the fault point, flowing through the circuit breaker CB1. However, the fault current contribution from the MicroGrid passing through the circuit breaker CB2 may be very low. Further, the voltage and frequency may be maintained within an acceptable range by the control functions of the MicroGrid.

Therefore, the possible options of the protection scheme against fault F1 are:

(a) Option 1 is to install an overcurrent relay protection and a balanced earth fault (BEF) protection at CB1, with a capability of inter-tripping CB2. The overcurrent relay protects the main grid line against the phase-to-phase faults. The BEF

detects the earth faults on the main distribution network. After CB1 is opened, the inter-tripping signal is sent to CB2 to disconnect the MicroGrid from the main network.

(b) Option 2 is to install an overcurrent relay protection and a BEF protection at CB1 and a distance relay protection at CB2. The overcurrent relay protection operates to trip CB1 when the fault current is above the setting of the relay. The BEF protects the grid line against the earth faults on the main distribution network. The distance protection operates to trip CB2, according to the measured impedance of the distance relay.

(c) Option 3 is to install the GPS based adaptive protection at CB1 and CB2. In this solution, an amount of GPS measurements and communications is necessary. The cost of the GPS based protection may be high.

(2) Fault F2 on the MicroGrid

Considering a fault F2 on the MicroGrid, a simplified MicroGrid is shown in Figure 12.

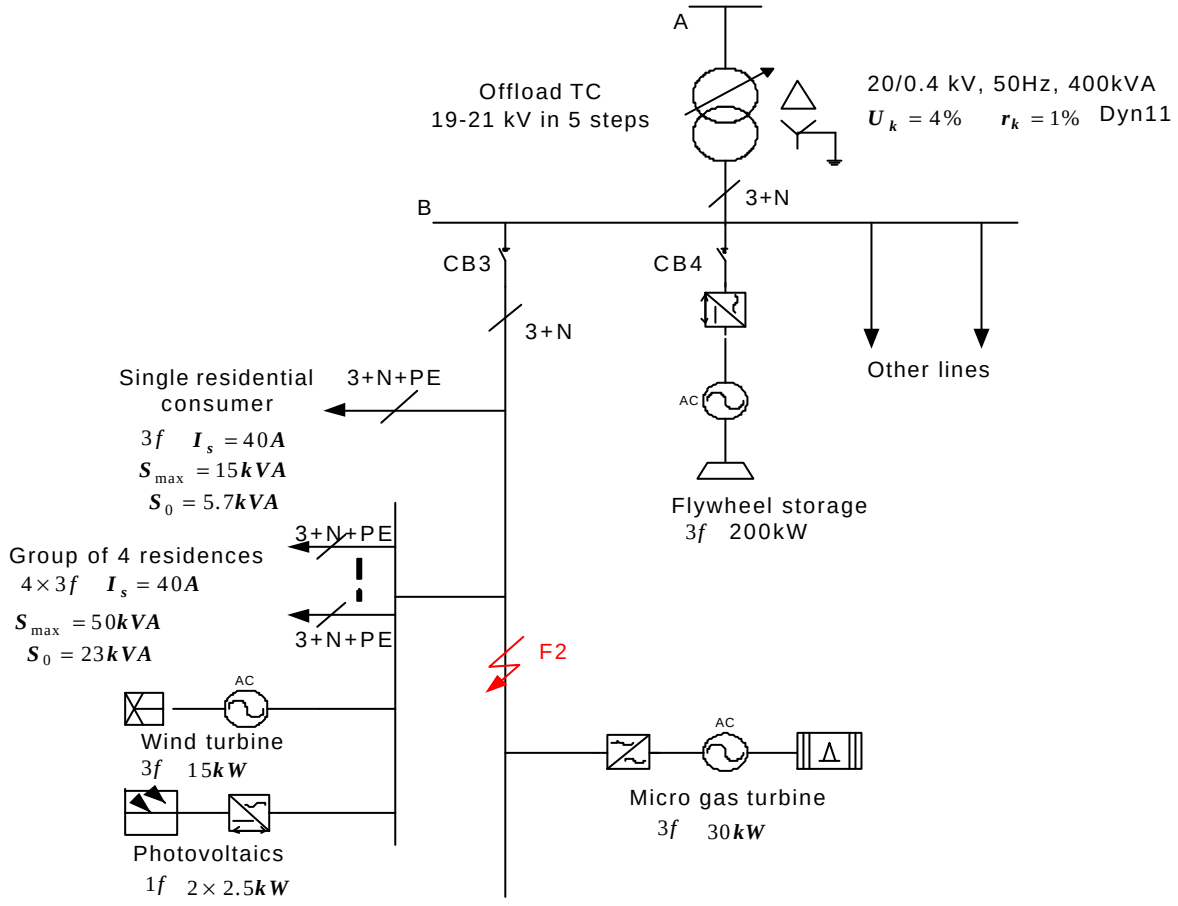

Figure 12 A simplified MicroGrid with a fault F2 on the MicroGrid

Fault F2 may be a phase-to-phase fault, a phase-to-neutral fault or a phase-to-ground fault. The action of the protection against fault F2 should trip the circuit breaker CB3 and shut down the whole MicroGrid quickly. According to UK reliability data, approximately 22 faults per 100km occur in LV networks annually. This means only 1 fault would take place in a MicroGrid spanning 1 km in 5 years.

During the fault, in Case 1, the main distribution network supplies a large fault current to fault F2, flowing through the circuit breaker CB3. However, in Case 2, the fault current contribution from the MicroGrid may be low.

Therefore, the possible options of the protection scheme against fault F2 may be:

(a) to install an overcurrent relay protection and a residual current device (RCD) at CB3, with a capability of intertripping all micro sources on the MicroGrid. The overcurrent relay protection is mainly used to protect the MicroGrid against the phase-to-phase faults and phase-to-neutral faults. In addition, the synchronisation between the MicroGrid and the main network may be necessary if a recloser is installed at CB3. In Case 1 (grid-connected operation), the overcurrent relay protection can operate correctly due to the large fault current contribution from the main network. However, in Case 2 (islanded operation), the overcurrent relay protection may only operate correctly when the flywheel supplies a high fault current (3 - 5 p.u. based on its rating). The RCD is used to detect the earth faults on the MicroGrid. The cost of intertripping all micro sources on the MicroGrid, using the pilot wires, may be reasonable. Discrimination of the overcurrent relay protection will be achieved by grading the upstream protection at CB1 and the protection at CB3 on a time delay.

(2) Fault F3 at the residential consumer

Considering a fault F3 at the residential consumer, a simplified MicroGrid is shown in Figure 13.

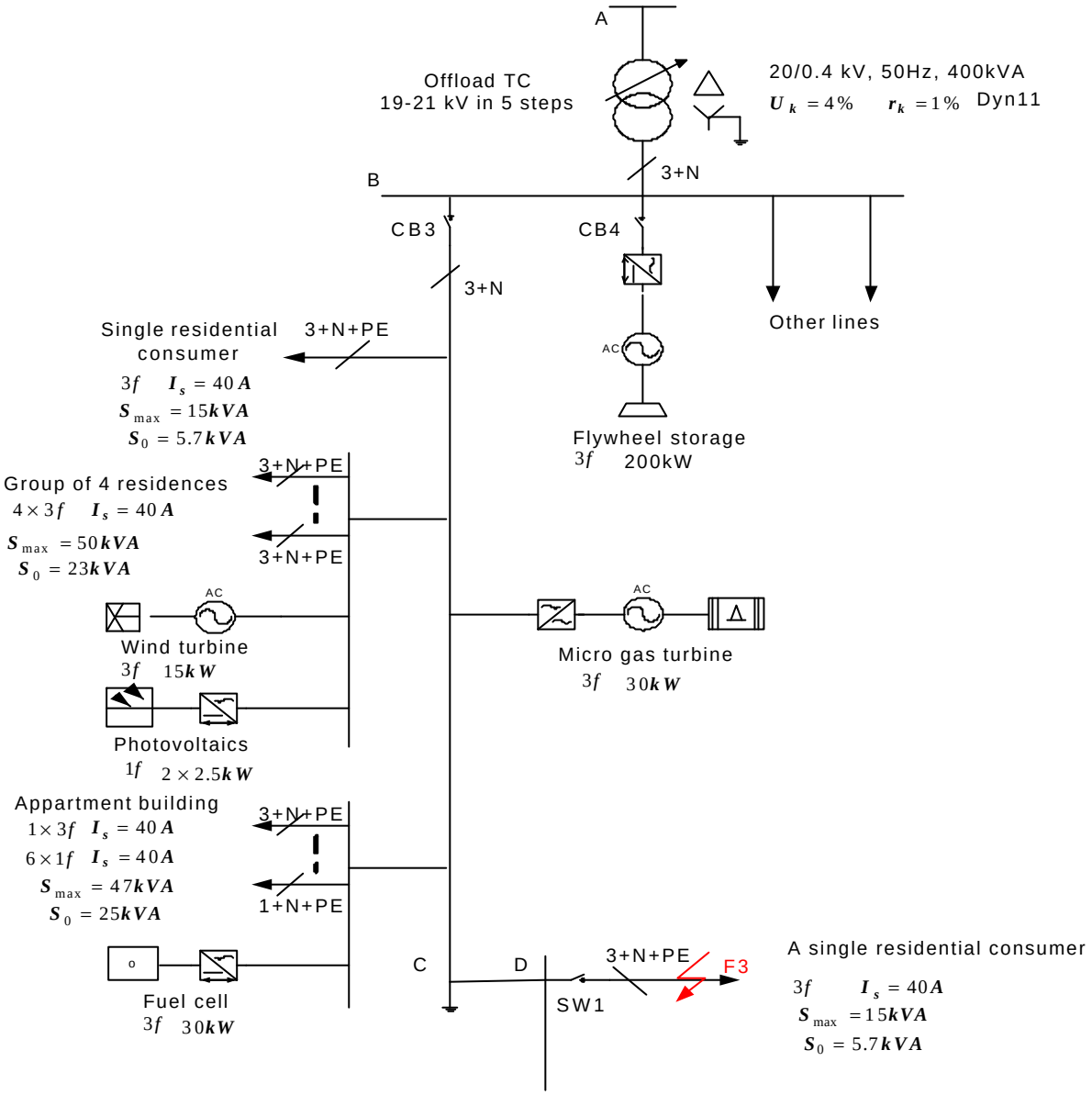

Figure 13 A simplified MicroGrid with a fault F3 at the residential consumer

The fault F3 may be a phase-to-phase fault, a phase-to-neutral fault or a phase-to-ground fault. The action of the protection against fault F3 should automatically disconnect the part of the MicroGrid affected by the fault.

Therefore, the possible options of the protection scheme against fault F3 may be:

(a) to install a short circuit protection device (SCPD), e.g. a miniature circuit breaker (MCB) or fuses, and a RCD at SW1 (grid side of the residential consumer). The SCPD is used to protect the residential consumer against the phase-to-phase and

phase-to-neutral faults. However, to make the SCPD operate correctly in Case2, the flywheel should supply a high fault current (e.g. 3-5p.u. based on its capacity) during the fault. The RCD is used to protect residential consumer against the phase-to-ground fault (earth fault). Discrimination of the protection at CB3 and SW1 will be achieved by using a time delay.

The possible electrical protection schemes for a MicroGrid are summarised and shown in Table 3.

Table 3 Possible electrical protection schemes for a MicroGrid

Case		**Possible electrical protection schemes for a MicroGrid**								
		O/C	**SCPD**	**RCD**	**U/V**	**F**	**Z**	**D**	**GPS**	V_0 / I_0
1. MicroGrid connected	F1	√	×	×	×	×	√	√+£	√+ ££	×
	F2	√	√	√	×	×	×	√+£	×	√+ ££
	F3	√	√	√	×	×	×	×	×	√+ ££
2. MicroGrid islanded	F1	√	×	×	×	×	×	√+£	√+ ££	×
	F2	√+Ifly	√+Ifly	√	×	×	×	√+£	×	√+ ££
	F3	√+Ifly	√+Ifly	√	×	×	×	×	×	√+ ££

Notes:

(1) The mark "´" is fail to operate; the mark "Ö" is correct to operate; the mark "Ö+Ifly" is correct to operate, and the flywheel should supply a high fault current (3-5p.u. based on its capacity); the mark "Ö+£" is correct to operate, but expensive; the mark "Ö+ ££" is correct to operate, but may be very expensive.

*(2) **O/C** is overcurrent protection; SCPD is a short circuit protection device (e.g. MCB or fuses); **RCD** is a residual current device; **U/V** is under-voltage protection; **F** is frequency protection; **Z** is distance protection; **D** is differential*

protection; ***GPS*** *is GPS based adaptive protection.* $\boldsymbol{V}_0 / \boldsymbol{I}_0$ *is zero sequence based protection.*

Table 3 shows that the undervoltage, frequency protection schemes may fail to trip faults F1, F2 and F3 in both grid-connected and islanded cases. During the fault, the voltage and frequency of the MicroGrid may be controlled within the acceptable ranges. The distance protection scheme may fail to protect the MicroGrid from faults F2 and F3 due to the effect of multiple infeeds on distance relays. The differential protection scheme installed on the MicroGrid looks likely to be quite expensive. It may fail to protect residential consumers against fault F3.

The GPS based protection scheme is too expensive to be implemented on the MicroGrid. It may fail to detect the faults F2 and F3. Similarly, the high cost of the communication equipment may limit the application of the zero sequence protection to the MicroGrid.

Therefore, for a fault F1 on the main distribution network, the possible electrical protection scheme may be to install an overcurrent protection and a BEF protection at CB1, with a capability of inter-tripping CB2.

For a fault F2 on the MicroGrid, it is possible to install an overcurrent relay protection and a RCD at CB3. The protection should possess the capability of intertripping all micro sources in the MicroGrid. To make the overcurrent relay protection operate correctly in islanded model of the MicroGrid, the flywheel should supply a high fault current (e.g. 3-5p.u. based on its capacity) during the fault. Discrimination of the protection will be achieved by comparing the setting of the upstream protection at CB1 with the setting of the protection at CB3 and using a time delay.

For a fault F3 at the residential consumer, a possible electrical protection scheme is to install a SCPD (using MCB or fuses) and a RCD at SW1 (grid side terminal of the residential consumer). To make the SCPD operate correctly in islanded mode of the MicroGrid, the flywheel should supply a high fault current with a value of 3-5p.u., based on its capacity, during the fault. The protection only disconnects the residential

consumer affected by the fault. Discrimination of the protection at SW1 and CB3 can be achieved by using a time delay.

5. Design of the electrical protection schemes of the MicroGrid

For the MicroGrid shown in Figure 10, and starting from the data which is given there, the design of the electrical protection schemes of the MicroGrid is carried out. Take into account the following considerations:

(1) For fault F1, the protection schemes at CB1 are an overcurrent relay and a BEF protection, with a capability of inter-tripping CB2. For fault F2, the protection schemes at CB3 are an overcurrent relay and a RCD. For fault F3, the protection schemes at SW1 are the fuses and a RCD.

(2) The overcurrent relays associated with breaker CB1 and CB3 are the definite time type.

(3) The standard secondary current of current transformers (CTs) is 5A.

(4) The rating of the flywheel is 200kW. In Case 1 (grid-connected mode), CB2 is closed. The injecting current of the flywheel is zero. In Case 2 (islanded mode), CB2 is open. The flywheel supplies 3p.u or 5p.u fault currents (based on its rating) during the fault.

(5) The normal capacity of the feeder is 200kVA. The maximum load of the residential consumer is 15kVA.

(6) The per unit impedances of equivalent network are calculated on the bases:

$$\boldsymbol{S}_{base} = 100\boldsymbol{MVA}\ ,\ \boldsymbol{I}_{base} = \frac{\boldsymbol{S}_{base}}{\sqrt{3}\boldsymbol{V}_{base}}\ ,\ \boldsymbol{Z}_{base} = \frac{\boldsymbol{V}^{2}{}_{base}}{\boldsymbol{S}_{base}}\ .$$

Calculation of equivalent impedance

The short-circuit level of the main distribution network at 20kV is 100MVA. Using this, the equivalent impedances of the network in per unit are calculated and shown in Figure 14.

$$\boldsymbol{Z}_{source\_p.u} = \left(\cos\left(\boldsymbol{tg}^{-1}5.0\right) + \boldsymbol{j}\sin\left(\boldsymbol{tg}^{-1}5.0\right)\right) \times \frac{\boldsymbol{S}_{base}}{\boldsymbol{S}_{source}} = \left(0.19 + \boldsymbol{j}0.98\right) \times \frac{100}{100} = 0.19 + \boldsymbol{j}0.98$$

$$\boldsymbol{Z}_{transf\_p.u} = \left(0.01 + \boldsymbol{j}0.04\right) \times \frac{\boldsymbol{S}_{base}}{\boldsymbol{S}_{transfe}} = \left(0.01 + \boldsymbol{j}0.04\right) \times \frac{100}{0.4} = 2.50 + \boldsymbol{j}10.00$$

$$\boldsymbol{Z}_{line\_p.u} = (0.146 + \boldsymbol{j}0.025) \times \frac{\boldsymbol{S}_{base}}{\boldsymbol{V}^{2}_{base}} = (0.146 + \boldsymbol{j}0.025) \times \frac{100}{0.4^{2}} = 91.25 + \boldsymbol{j}15.62$$

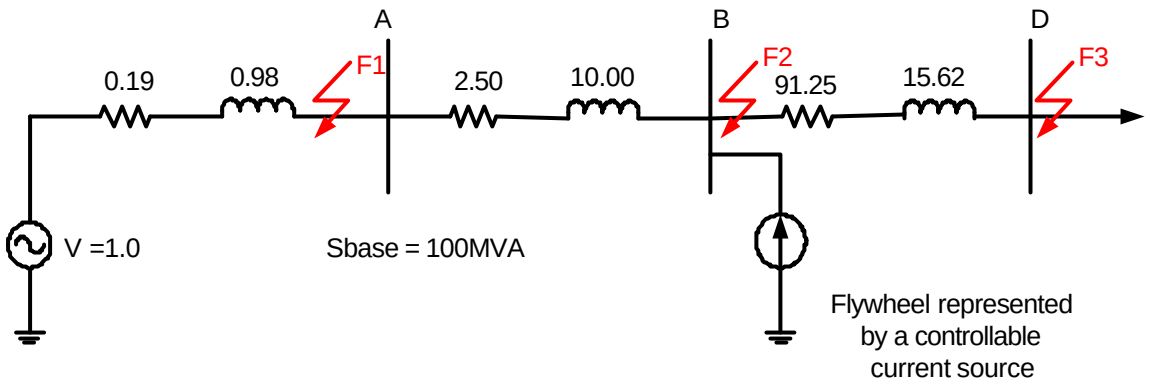

Figure 14 Positive-sequence equivalent impedance network
for the MicroGrid in Figure 10

Calculation of normal currents

Generally, the normal current of an element is the current passing through the element under normal operation. The normal current of the MicroGrid can be calculated according to the capacity of the transformer at the substation. Similarly, the normal current of a residential consumer can be obtained by the maximum capacity of the load. Therefore, the normal currents passing through CB1, CB3 and SW1 are as followers:

$$\boldsymbol{I}_{norm\_CB1} = \frac{\boldsymbol{S}_{trans}}{\sqrt{3} \times \boldsymbol{V}} = \frac{400}{\sqrt{3} \times 20} = 11.54\boldsymbol{A}$$, referred to 20kV;

$$\boldsymbol{I}_{norm\_CB3} = \frac{\boldsymbol{S}_{feeder}}{\sqrt{3} \times \boldsymbol{V}} = \frac{200}{\sqrt{3} \times 0.4} = 288.68\boldsymbol{A}$$, referred to 0.4kV

$$\boldsymbol{I}_{norm\_SW1} = \frac{\boldsymbol{S}_{load}}{\sqrt{3} \times \boldsymbol{V}} = \frac{15}{\sqrt{3} \times 0.4} = 21.65\boldsymbol{A}$$, referred to 0.4kV

Calculation of fault currents

From the equivalent circuit of the network (see Figure 14), the magnitudes of the fault currents for the faults F1, F2 and F3 have been calculated as follows:

(1) For fault F1

$$\boldsymbol{I}_{\boldsymbol{faultF1}} = \left|\frac{1.0\angle 0^{\circ}}{0.19+\boldsymbol{j}0.98}\right| \times \frac{\boldsymbol{S}_{\boldsymbol{base}}}{\sqrt{3}\times \boldsymbol{V}_{\boldsymbol{base}}} \times 1000$$
$$= \left|\frac{1.0\angle 0^{\circ}}{0.19+\boldsymbol{j}0.98}\right| \times \frac{100}{\sqrt{3}\times 20} \times 1000$$
$$= 2891.90\boldsymbol{A}$$

(2) For fault F2

The MicroGrid operates in the interconnected mode:

$$\boldsymbol{I}_{\boldsymbol{faultF2\_grid-connected}} = \left|\frac{1.0\angle 0^{\circ}}{(0.19+2.50)+\boldsymbol{j}(0.98+10.00)}\right| \times \frac{\boldsymbol{S}_{\boldsymbol{base}}}{\sqrt{3}\times \boldsymbol{V}_{\boldsymbol{base}}} \times 1000$$
$$= \left|\frac{1\angle 0^{\circ}}{2.69+\boldsymbol{j}10.98}\right| \times \frac{100}{\sqrt{3}\times 0.4} \times 1000$$
$$= 12768.28\boldsymbol{A}$$

The MicroGrid operates in the islanded mode:

$$\boldsymbol{I}_{\boldsymbol{faultF2\_islanded\_3p.u}} = 3.0\times \frac{\boldsymbol{S}_{\boldsymbol{flywheel}}}{\sqrt{3}\times \boldsymbol{V}} = 3.0\times \frac{200}{\sqrt{3}\times 0.4} = 866.05\boldsymbol{A}$$

$$\boldsymbol{I}_{\boldsymbol{faultF2\_islanded\_5p.u}} = 5.0\times \frac{\boldsymbol{S}_{\boldsymbol{flywheel}}}{\sqrt{3}\times \boldsymbol{V}} = 5.0\times \frac{200}{\sqrt{3}\times 0.4} = 1443.42\boldsymbol{A}$$

(3) For fault F3

The MicroGrid operates in the interconnected mode:

$$\boldsymbol{I}_{\boldsymbol{faultF3\_grid-connected}} = \left|\frac{1.0\angle 0^{\circ}}{(0.19+2.50+91.25)+\boldsymbol{j}(0.98+10.00+15.62)}\right| \times \frac{\boldsymbol{S}_{\boldsymbol{base}}}{\sqrt{3}\times \boldsymbol{V}_{\boldsymbol{base}}} \times 1000$$
$$= \left|\frac{1\angle 0^{\circ}}{93.94+\boldsymbol{j}26.60}\right| \times \frac{100}{\sqrt{3}\times 0.4} \times 1000$$
$$= 1478.40\boldsymbol{A}$$

The MicroGrid operates in the islanded mode:

$$\boldsymbol{I}_{\boldsymbol{faultF3\_islanded\_3p.u}} = 3.0\times \frac{\boldsymbol{S}_{\boldsymbol{flywheel}}}{\sqrt{3}\times \boldsymbol{V}} = 3.0\times \frac{200}{\sqrt{3}\times 0.4} = 866.05\boldsymbol{A}$$

$$\boldsymbol{I}_{\boldsymbol{faultF2\_islanded\_5p.u}} = 5.0\times \frac{\boldsymbol{S}_{\boldsymbol{flywheel}}}{\sqrt{3}\times \boldsymbol{V}} = 5.0\times \frac{200}{\sqrt{3}\times 0.4} = 1443.42\boldsymbol{A}$$

Choice of CT transformer ratios

The transformation ratio of a CT is determined by the larger of the two following values [Gers, 1998]:

(1) normal current I_{norm};

(2) maximum short-circuit current without saturation being present.

Therefore, $I_{sc}(5/X) \leq 100A$ so that $X \geq (5/100)I_{sc}$, where I_{sc} is the short-circuit current.

Table 4 summarises the CT ratio calculations for the overcurrent relay protection at CB1 and CB3.

Table 4 Selection of the CT ratios

Breaker	I_{norm} (A)	I_{sc} (A)	$(5/100)I_{sc}$ (A)	CT ratio	Type of device	Supplier
CB1	11.54	2891.90	144.59	200/5	ASTW6-200/5	Moeller, 2004
CB3	288.68	12768.28	638.41	800/5	ASTW12-800/5	Moeller, 2004

Calculation of settings of the protection

Settings of the overcurrent protection consist of the setting of pick-up current and the setting of instantaneous tripping current.

The setting of the pick-up current is determined by allowing a margin (a safety factor, e.g. 2.0) for overload above the normal current, as in the following expression [Gers, 1998]:

$$I_{pick-up} = 2.0 \times I_{norm} \times (1/CTR) \qquad (2)$$

where, CTR is the ratio of CT transformation.

The setting of the instantaneous tripping current is usually decided by 50% of maximum short-circuit current at the point of installation of the protection, as shown in the following equation [Gers, 1998]:

$$I_{inst-trip} = 0.5 \times I_{sc} \times (1/CTR) \quad (3)$$

According to equations (1) and (2), the settings of the protection at SW1, CB3 and CB1 are calculated as follows.

Protection at SW1

The protection at SW1 consists of overcurrent protection (using MCB or fuses) and RCD. The rating of the fuse is:

$I_{fuse\_pick-up\_SW1} = 2.0 \times I_{nom\_SW1} = 2.0 \times 21.65 = 43.36A$, rating = 45A .

To make the protection operate correctly in both grid-connected operation and islanded operation, the fault current I_{sc} in equation (3) should be the minimum value of the fault currents in both grid-connected operation and islanded operation.

Therefore, the setting of instantaneous element should be minimum value of these:

(1) In grid-connected mode

$I_{fuse\_inst-trip\_SW1} = 0.5 \times I_{faultF3} = 0.5 \times 1478.40 = 739.20A$,

setting = 750A.

(2) In islanded mode, the flywheel supplies 3p.u fault current during the fault

$I_{fuse\_inst-trip\_SW1} = 0.5 \times I_{faultF3\_islanded\_3p.u} = 0.5 \times 866.05 = 433.02A$,

setting = 450A.

(3) In islanded mode, the flywheel supplies 5p.u fault current during the fault

$I_{fuse\_inst-trip\_SW1} = 0.5 \times I_{faultF3\_islanded\_5p.u} = 0.5 \times 1443.42 = 721.71A$,

setting = 750A.

So, the setting of instantaneous-trip of the overcurrent protection at SW1 is 450A.

The sensitivity of RCD is set to 30mA, with the normal operating voltage 400V a.c. and current 25A.

Operating time of the protection is: $\boldsymbol{T}_{\boldsymbol{SW}1} = 0.2\text{sec}.$ (minimum)

Protection at CB3:

The protection at CB3 consists of the overcurrent relay protection and RCD. The setting of pick-up current of the overcurrent relay is:

$\boldsymbol{I}_{\boldsymbol{relay\_pick-up\_CB}3} = 2.0 \times \boldsymbol{I}_{\boldsymbol{nom\_CB}3} \times (1/\boldsymbol{CTR}) = 2.0 \times 288.68 \times (5/800) = 3.61\boldsymbol{A}$;

setting = 4A.

So, the setting at primary side of CT is: $4 \times 800/5 = 640\boldsymbol{A}$.

Similarly, the setting of instantaneous element is also the minimum value of these:

(1) In grid-connected mode

$\boldsymbol{I}_{\boldsymbol{relay\_inst-trip\_CB}3} = 0.5 \times \boldsymbol{I}_{\boldsymbol{faultF}2} \times (1/\boldsymbol{CTR}) = 0.5 \times 12768.28 \times (5/800) = 39.9\boldsymbol{A}$;

setting = 40A. The setting at primary side of CT is: $40 \times 800/5 = 6400\boldsymbol{A}$.

(2) In islanded mode, the flywheel supplies 3p.u fault current during the fault

$\boldsymbol{I}_{\boldsymbol{relay\_inst-trip\_CB}3} = 0.5 \times \boldsymbol{I}_{\boldsymbol{faultF}2\_\boldsymbol{islanded}\_3\boldsymbol{p.u}} \times (1/\boldsymbol{CTR}) = 0.5 \times 866.05 \times (5/800) = 2.7\boldsymbol{A}$;

setting = 3A. The setting at primary side of CT is: $3 \times 800/5 = 480\boldsymbol{A}$.

(3) In islanded mode, the flywheel supplies 5p.u fault current during the fault,

$\boldsymbol{I}_{\boldsymbol{relay\_inst-trip\_CB}3} = 0.5 \times \boldsymbol{I}_{\boldsymbol{faultF}3\_\boldsymbol{islanded}\_5\boldsymbol{p.u}} \times (1/\boldsymbol{CTR}) = 0.5 \times 1443.42 \times (5/800) = 4.5\boldsymbol{A}$;

setting = 5A. The setting at primary side of CT is: $5 \times 800/5 = 800\boldsymbol{A}$.

So, the setting of instantaneous-trip of the overcurrent protection at CB3 is 480A.

However, this setting is less than the pick-up setting of 640A. Therefore, the pick-up setting of the overcurrent relay should be changed from 640A to 480A. Consequently, there is no instantaneous-trip setting for the overcurrent relay protection at CB3.

The sensitivity of RCD is set to 300mA, with the normal operating voltage 400V a.c. and current 300A.

Operating time of the protection is: $\boldsymbol{T}_{\boldsymbol{CB}3} = \boldsymbol{T}_{\boldsymbol{SW}1} + 0.5\text{sec}. = 0.7\,\text{sec}.$

Protection at CB1:

The protection at CB1 consists of the overcurrent relay protection plus intertripping CB2. The settings of pick-up current of the overcurrent relay are as follows:

$\boldsymbol{I}_{\boldsymbol{relay\_pick\text{-}up\_CB1}} = 2.0 \times \boldsymbol{I}_{\boldsymbol{norm\_CB1}} \times (1/\boldsymbol{CTR}) = 2.0 \times 11.54 \times (5/200) = 0.57\boldsymbol{A}$;

setting = 1A.

So, the setting at primary side of CT is: $1 \times 200/5 = 40\boldsymbol{A}$.

$\boldsymbol{I}_{\boldsymbol{relay\_inst\text{-}trip\_CB1}} = 0.5 \times \boldsymbol{I}_{\boldsymbol{faultF1}} \times (1/\boldsymbol{CTR}) = 0.5 \times 2891.90 \times (5/200) = 36.15\boldsymbol{A}$;

setting = 40A.

So, the setting at primary side of CT is: $40 \times 200/5 = 1600\boldsymbol{A}$.

Operating time of the overcurrent protection is: $\boldsymbol{T}_{\boldsymbol{CB1}} = \boldsymbol{T}_{\boldsymbol{CB3}} + 0.5\text{sec.} = 1.2\text{sec}$.

The setting of the BEF protection is set for 70% of available phase-to-earth fault current. A setting of 70% allows for a 30% margin to detect bolted phase-to-earth faults. The BEF can operate instantaneously in the time of 0.2sec. (minimum). The BEF doesn't need to co-ordinate with the earth fault protection in the MicroGrid due to the delta connection of primary side winding of the transformer at substation.

Table 5 summarises the settings of the protection at SW1, CB1 and CB3

Table 5 Summary of settings of the protection for the MicroGrid

Protection position	Protection scheme	Normal voltage (kV)	Normal current (A)	Setting of pick-up $I_{pick-up\_prim}$ (A)	Setting of instantaneous $I_{inst-trip\_prim}$ (A)	CT ratio	Time (sec.)	Price of unit (£)	Type of device and Supplier
CB1	Overcurrent relay + intertripping CB2	20	11.54	40	1600	200/5	1.20	99.28	70POCR, [RS, 2004] BROYCE CONTROL
	BEF	20	70% I_{phef}				0.20	?	AREVA
CB3	Overcurrent relay	0.4	288.68	480		800/5	0.70	99.28	70POCR, [RS, 2004] BROYCE CONTROL
	RCD			Sensitivity: 300mA; Operating voltage: 400V; Operating current: 300A				?	?
SW1	MCB (or Fuses)	0.4	21.65	45	450		0.20	1.76	HRC, gG/500V – 25 ABB [ABB, 2004b]
	RCD			Sensitivity: 30mA; Operating voltage: 400V; Operating current: 25A				44.65	F364-25/0-03, ABB [RS, 2004]

Notes:

(1) I_{phef} is an available phase-to-earth fault current.

From Table 5, the co-ordinated curves of the overcurrent protection associated with SW1, CB3 and CB1 are shown in Figure 15. Fuses were chosen for the overcurrent protection at SW1. The time-current characteristic of the fuse (25A rating) was obtained from ABB HRC fuse link catalogue (see Appendix-A). The setting values of overcurrent relay at CB1 were referred to 0.4kV.

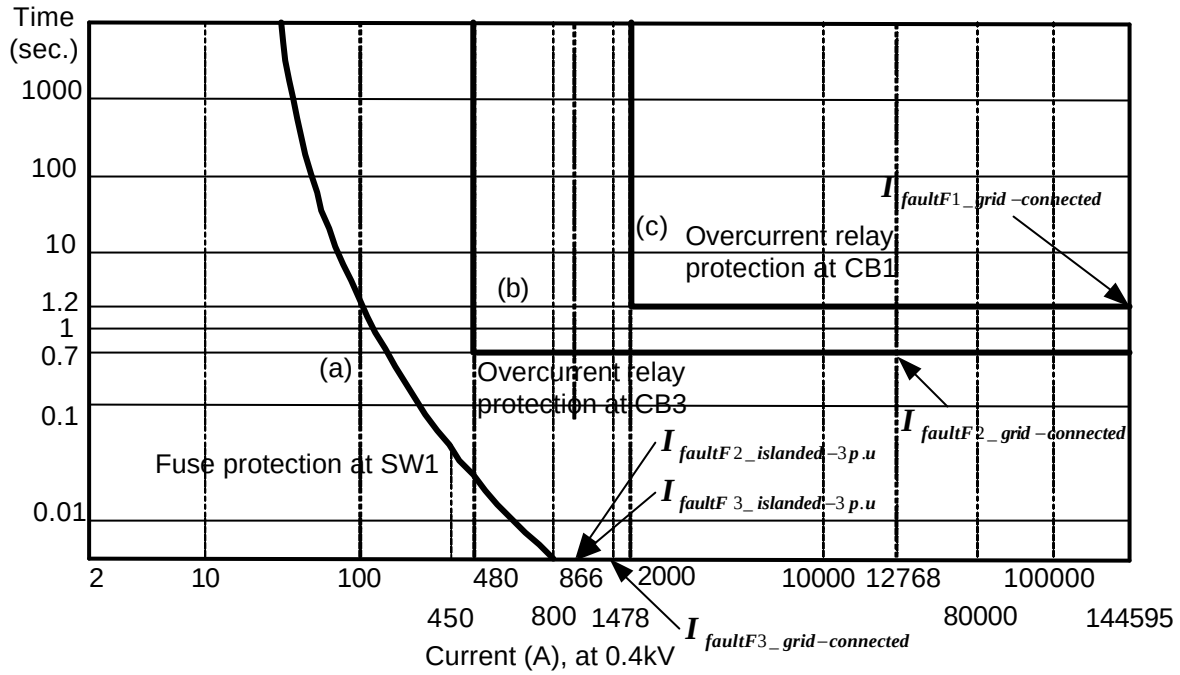

Figure 15 Co-ordination curves of the overcurrent protection for the MicroGrid

Figures 15 shows the co-ordination performances of the overcurrent protection in the MicroGrid. Curve (a) is a time-current characteristic of the fuse at SW1. Curve (b) is a definite time characteristic of the overcurrent relay at CB3. Curve (c) is also a definite time characteristic of the overcurrent relay at CB1. There are no cross characteristics among the curves (a), (b) and (c). Clearly, discrimination of the overcurrent protection at SW1, CB3 and CB1 has been achieved by using a time delay with grading of 0.5 second.

6. Validation of co-ordination of the protection in PSCAD/EMTDC

To validate the settings of the overcurrent protection above, the overcurrent protection schemes were implemented into a simple MicroGrid model in PSCAD/EMTDC, as shown in Figure 16.

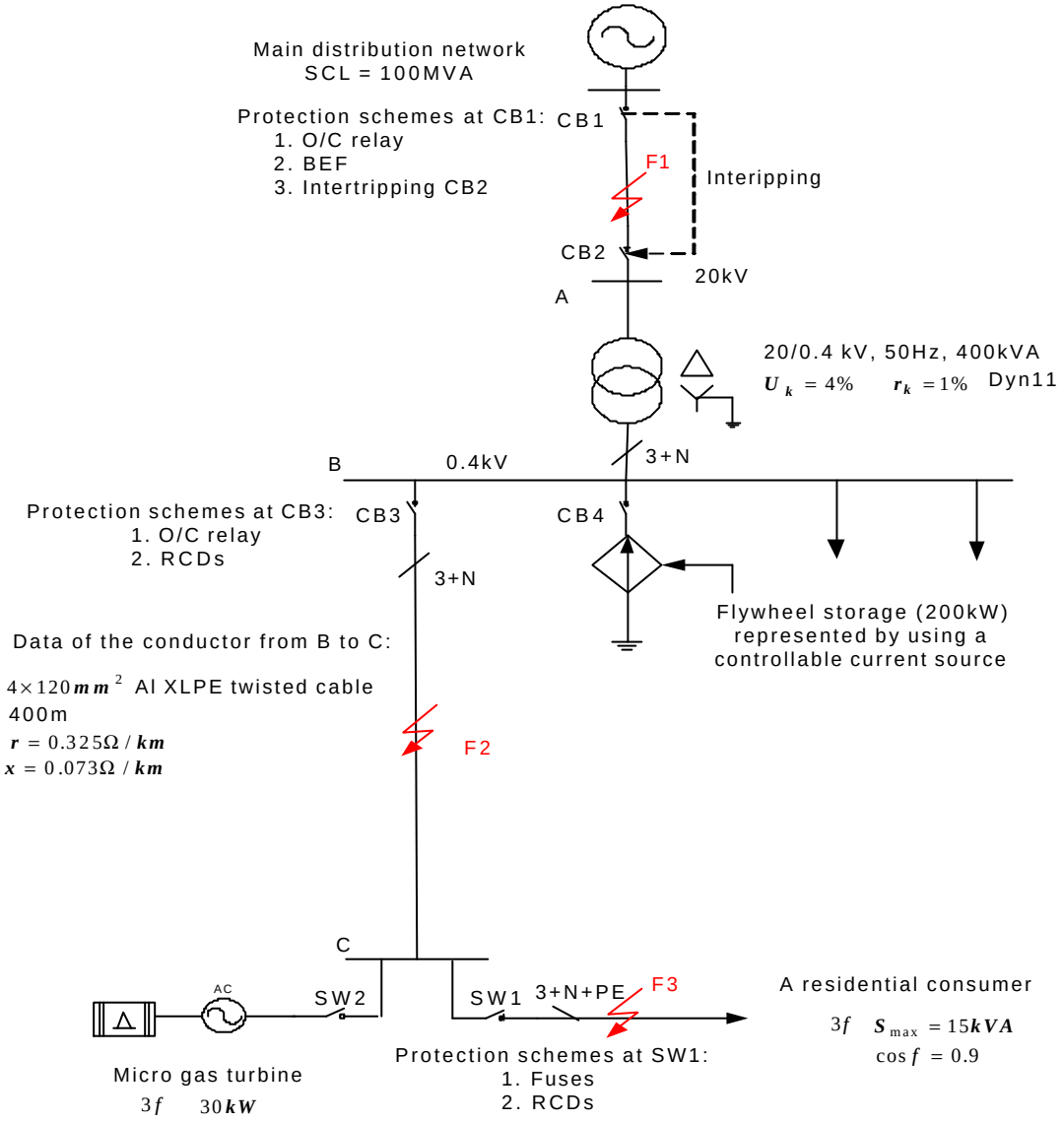

Figure 16 A simple MicroGrid model in PSCAD/EMTDC

In Figure 16, the circuit breakers CB1, CB2, CB3 and switchgear SW1 and SW2 are controlled by their protection relays. The flywheel is represented by a controllable current source and connected to 0.4kV busbar through a circuit breaker CB4. The maximum load of residential consumer is 15kVA. The residential consumer is controlled by switchgear SW1. The micro source in MicroGrid is a 30kW gas turbine synchronous generator. The generator is directly connected to the MicroGrid through switchgear SW2.

(1) For a fault F1

A solid three-phase-to-ground fault is applied on the main distribution network at 30 seconds. The operating time of the overcurrent protection at CB1 is 1.2 seconds.

Figure 17 shows that the fault is correctly cleared up by opening CB1 and CB2 in 1.2 seconds after the fault. The states of CB1 and CB2 are changed from “0” (closing state) to “1” (opening state). The states of CB3, CB4, SW1 and SW2 are still retained at “0”. However, the operating time of the protection at CB1 looks like too long to maintain the stability of the MicroGrid after disconnection from the main distribution network. Therefore, a further investigation is required to study the stability of the MicroGrid operating as an island.

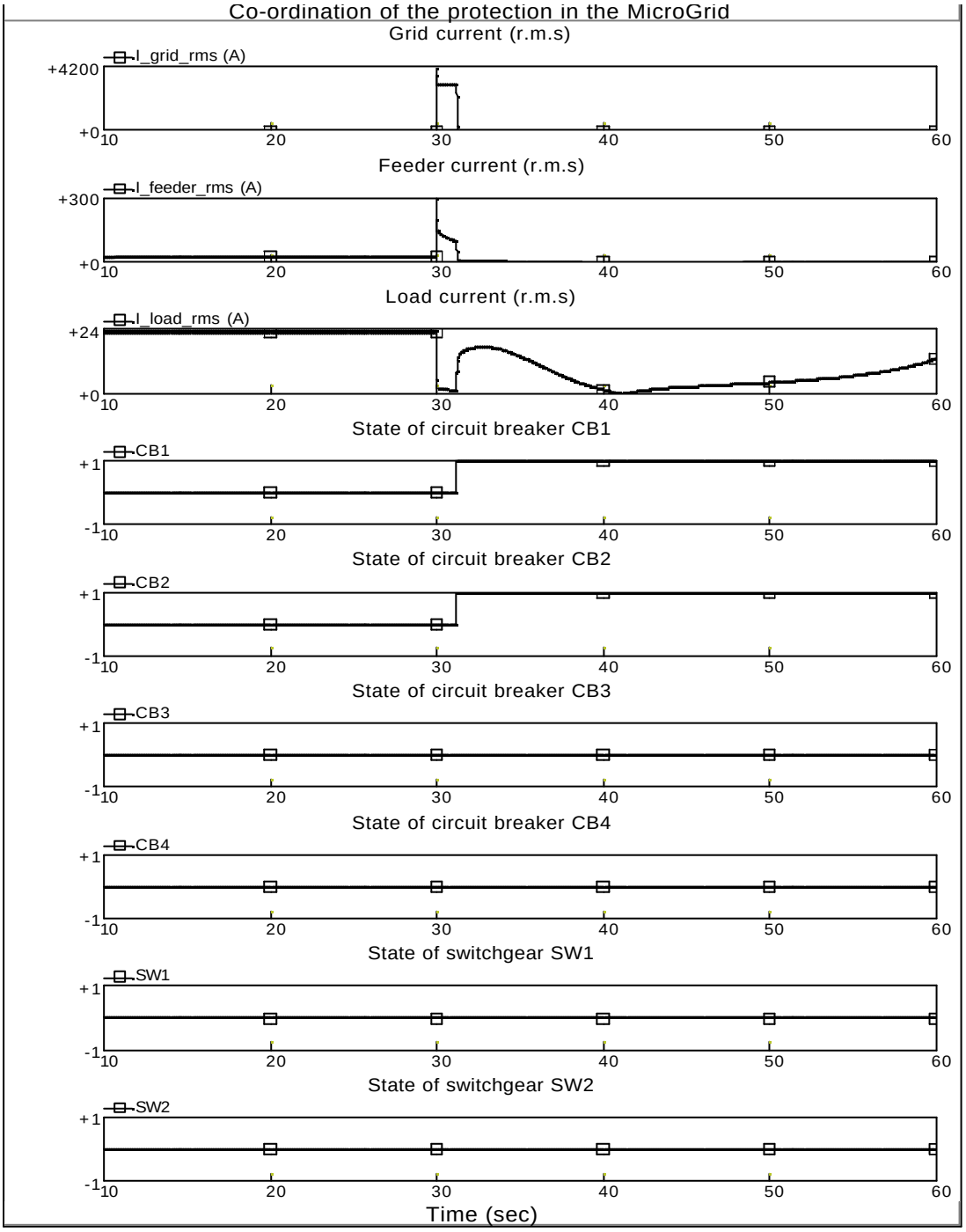

Figure 17 The r.m.s values of the circuit currents and states of the circuit breakers and switchgears (for fault F1)

(2) For a fault F2

Similarly, a solid three-phase-to-ground fault is applied on the MicroGrid at 30 seconds. The operating time of the overcurrent protection at CB3 is 0.7 second.

Figures 18 and 19 show the fault is tripped off by opening CB3 and SW2 in 0.7 second after the fault in both grid-connected mode and islanded. The states of CB3 and SW2 are changed from “0” to “1”. The states of CB1, CB2, CB4 and SW1 are still retained at “0”.

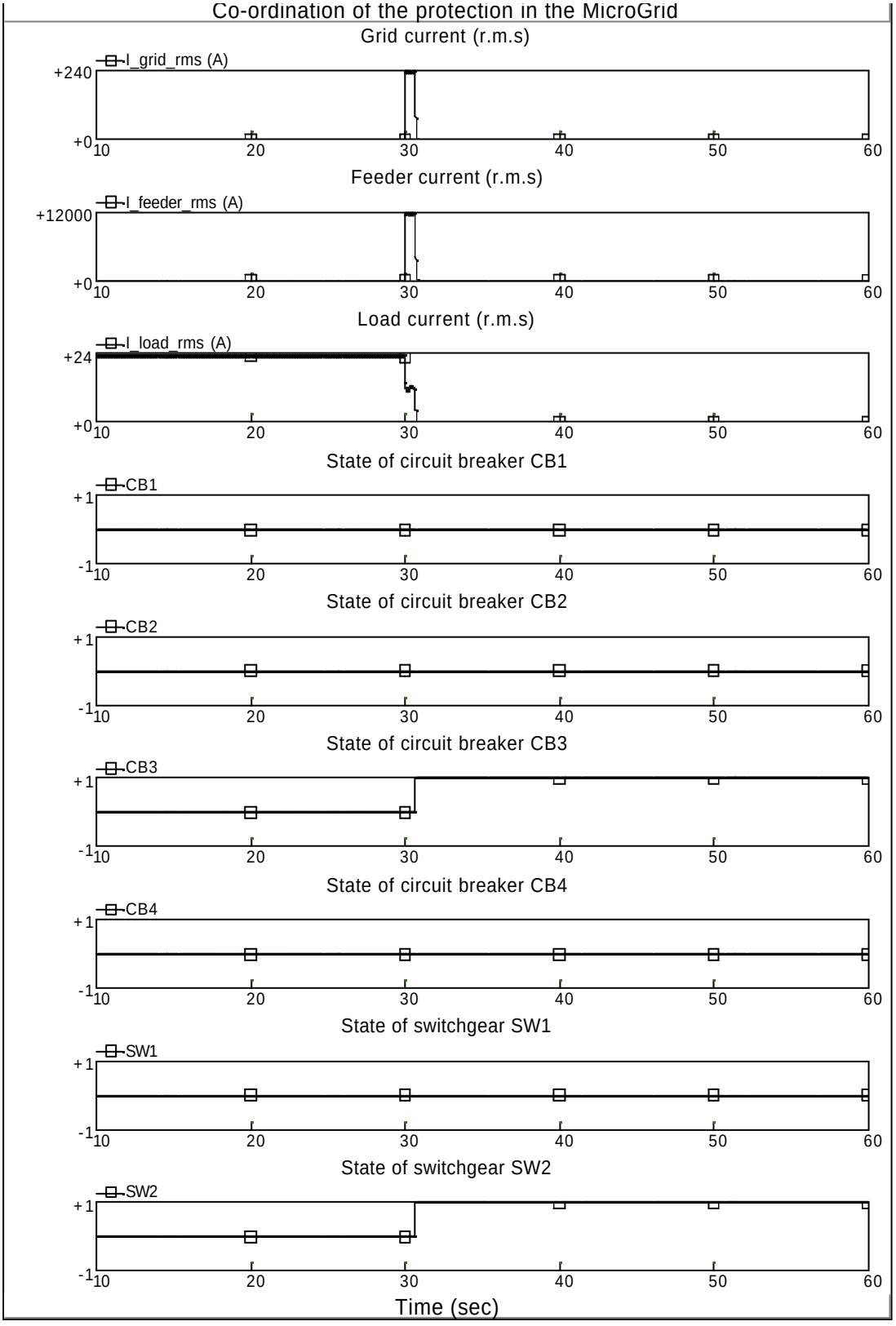

Figure 18 The r.m.s values of the circuit currents and states of the circuit breakers and switchgears
(For fault F2, the MicroGrid is operated in grid-connected mode)

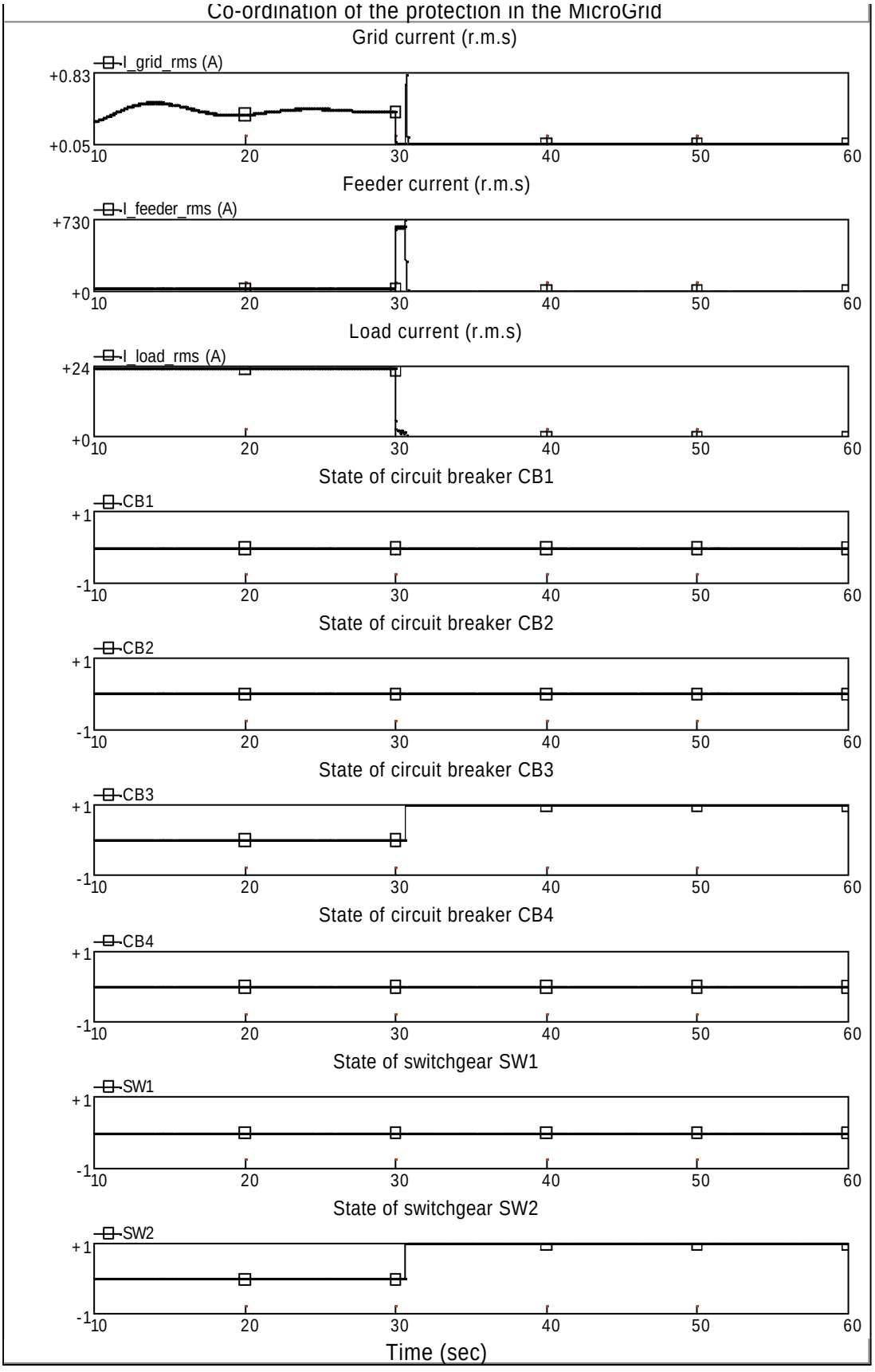

Figure 19 The r.m.s values of the circuit currents and states of the circuit breakers and switchgears
(For fault F2, MicroGrid is operated in islanded mode)

(3) For a fault F3

A solid three-phase-to-ground fault is also applied on the residential consumer at 30 seconds. The operating time of the overcurrent protection at SW1 is 0.2 second.

Figures 20 and 21 show that, in both grid-connected mode and islanded mode, the fault is correctly taken off by tripping the switchgear SW1 in 0.2 second after the fault. The state of SW1 is changed from “0” to “1”, while the states of CB1, CB2, CB3, CB4 and SW2 are still retained at “0”.

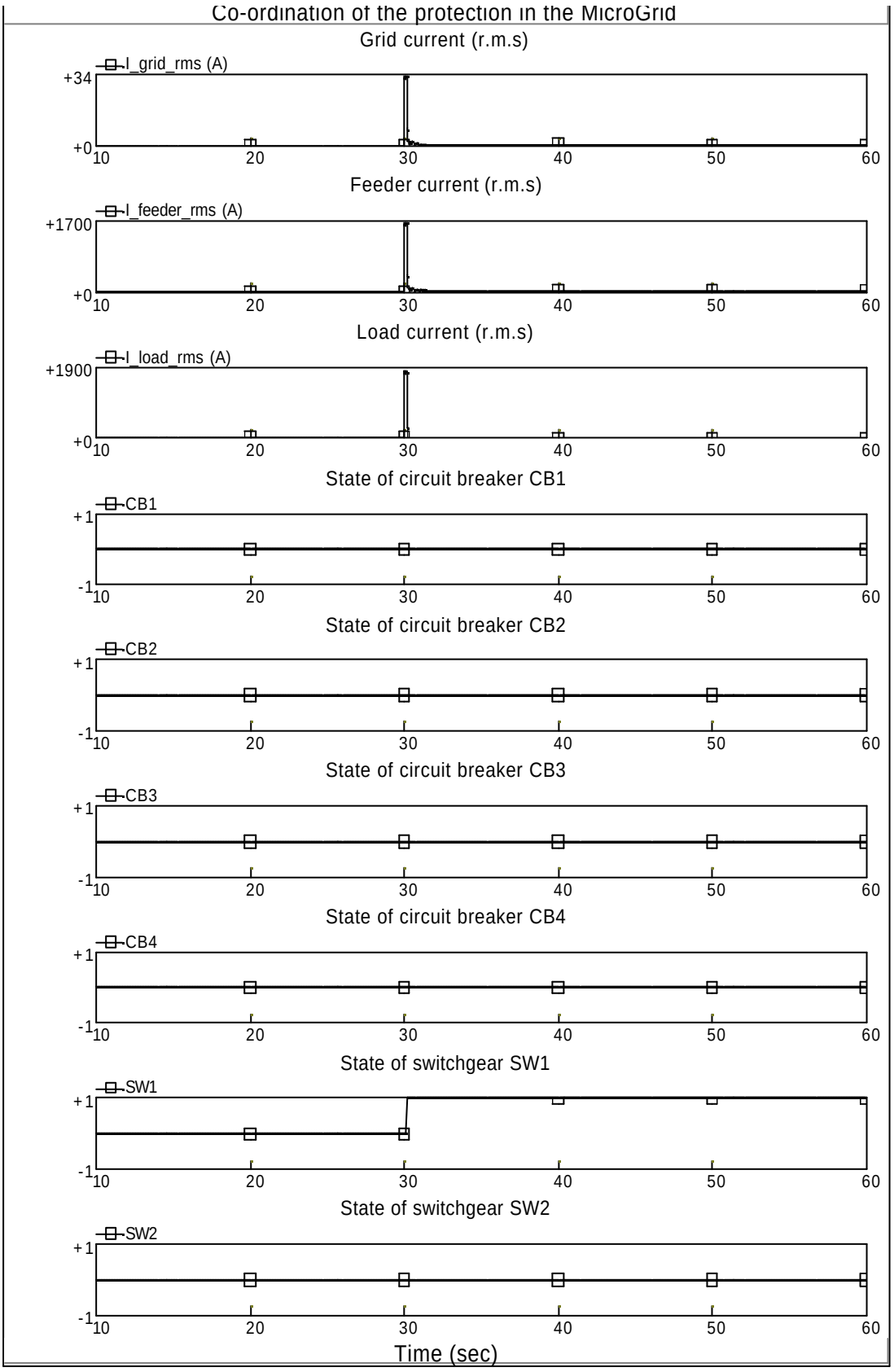

Figure 20 The r.m.s values of the circuit currents and states of the circuit breakers and switchgears
(For fault F3, MicroGrid is operated in grid-connected mode)

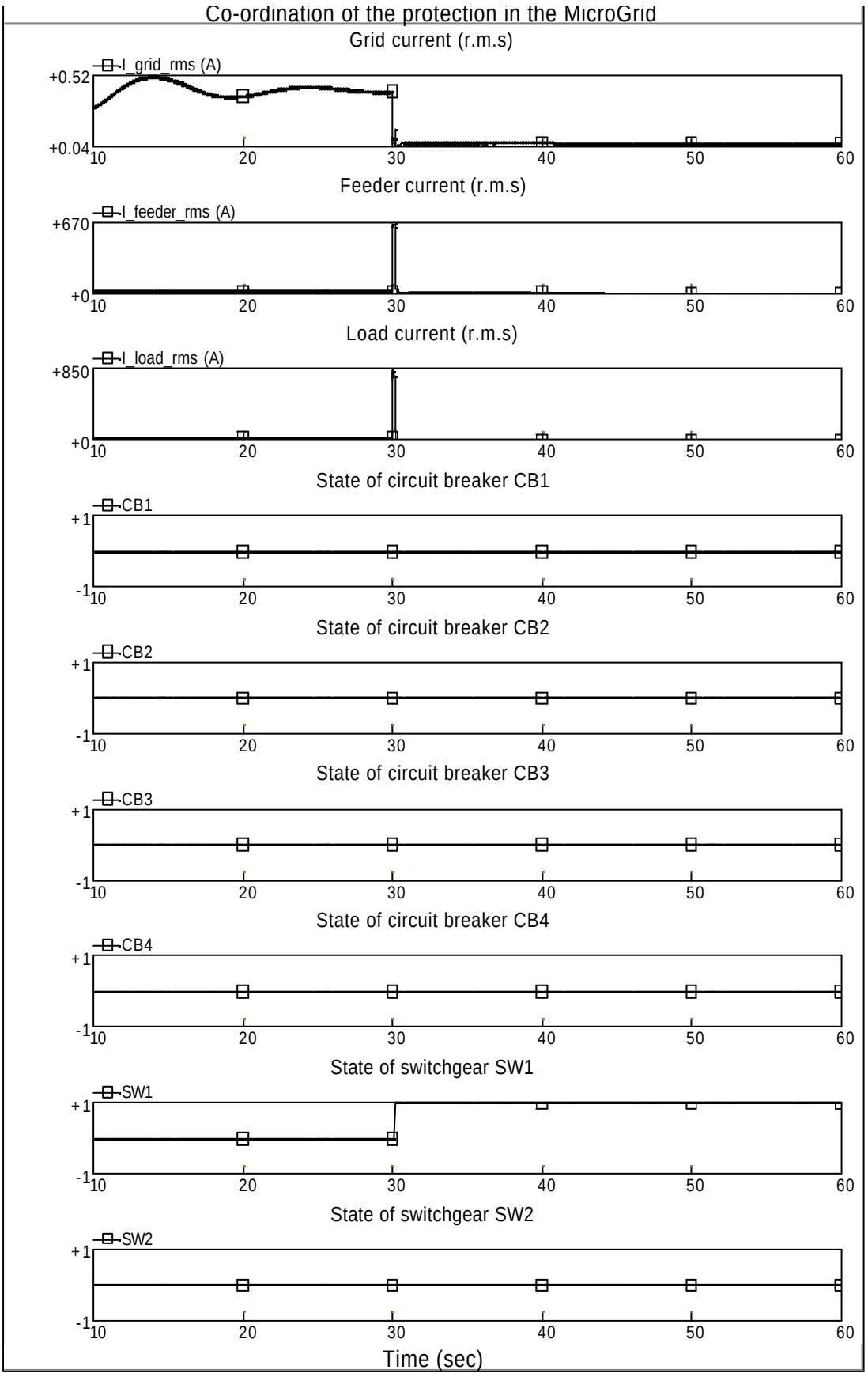

Figure 21 The r.m.s values of the circuit currents and states of the circuit breakers and switchgears
(For fault F3, MicroGrid is operated in islanded mode)

7. Conclusions

With increasing penetration levels of the DGs, a number of MicroGrids will exist in the distribution network system in the near future. The safety and reliability of the MicroGrid are becoming more and more important. The unique nature of the MicroGrid requires the electrical protection to trip faults on the MicroGrid correctly and rapidly. The possible electrical protection schemes for the MicroGrid are as follows:

(1) for fault F1 on the main distribution network, to install an overcurrent relay protection and a balanced earth fault (BEF) protection at CB1, with a capability of intertripping CB2. An alternative is to install an overcurrent protection and a BEF protection at CB1 and distance protection at CB2.

(2) for fault F2 on the MicroGrid, to install an overcurrent relay protection and a RCD at CB3. During islanded operation of the MicroGrid, the flywheel should supply a high fault current (e.g. 3p.u based on its rating). The protection should have a capability of intertripping all the micro sources in the MicroGrid. Discrimination of the protection can be achieved by using a time delay.

(3) for fault F3 at the residential consumer, to install a SCPD (using MCB or fuses) and a RCD at the grid side of the residential consumer. The SCPD, using the fuses, trips the fault quickly if there is a high fault current contribution from the flywheel. The protection should only disconnect the consumer affected by the fault. Discrimination of the protection can be also achieved by using a time delay.

Based on the possible electrical protection schemes of the MicroGrid, the settings of the protection have been calculated and validated in PSCAD/EMTDC.

7. References

Moeller (2004), Current Transformers (Catalogue), http://catalog.moeller.net

ABB (2004), Low Voltage Products – FuseLine HRC Fuse Links (Catalogue), www.abb/lvswitches.

Gers J.M and Holmes E.J (1998), Protection of Electricity Distribution Network (book), The Institution of Electrical Engineers, London, United Kingdom.

Brahma S.M and Girgis A.A (2004), Development of Adaptive Protection Scheme for Distribution Systems with High Penetration of Distributed Generation, IEEE Transactions on Power Delivery, Vol. 19, No. 1, January, Pages: 56-63.

Li, H.Y and Crossley P.A (2002), Optimal Message Transfer Rate for Distribution Feeder Protection Operating Over Switched Telephone Networks, IEEE Transactions on Power Delivery, Vol. 17, No. 2, April, Pages: 353-358.

Lorentzou M., Papathanassiou S., Hatziargyriou N. (2004), Review of Earthing Practices in LV Networks and Installations, ICCS/NTUA –WP E, MicroGrids Project internal report, January.

Nara, K. (2002), Enabler of Introducing Distributed Generators and its Effect to Power Distribution Systems, Transmission and Distribution Conference and Exhibition 2002: Asia Pacific. IEEE/PES, Vol.1, 6-10 Oct. 2002, Pages: 584-589.

Pereira da Silva J.L., Moreira Carlos (2004), Evaluation of the Discriminating Capability of Zero Sequence Protection, MicroGrid Project internal report (WPE_TE4_DV11), INESC Porto, January.

Redfern M.A Chiwaya A.A (1994), A New Approach to Digital Differential Protection for low and Medium Voltage Feeder Circuits Using a Digital Voice-Frequency Grade Communications Channel, IEEE Transactions on Power Delivery, Vol. 9, No. 3, July, Pages: 1352-1358.

RS (2004), Electrical & Automation (Catalogue), March -September, http://rswww.com.

8. Appendix - A

ABB, HRC Fuse links, type gG – fuses, time-current characteristics:

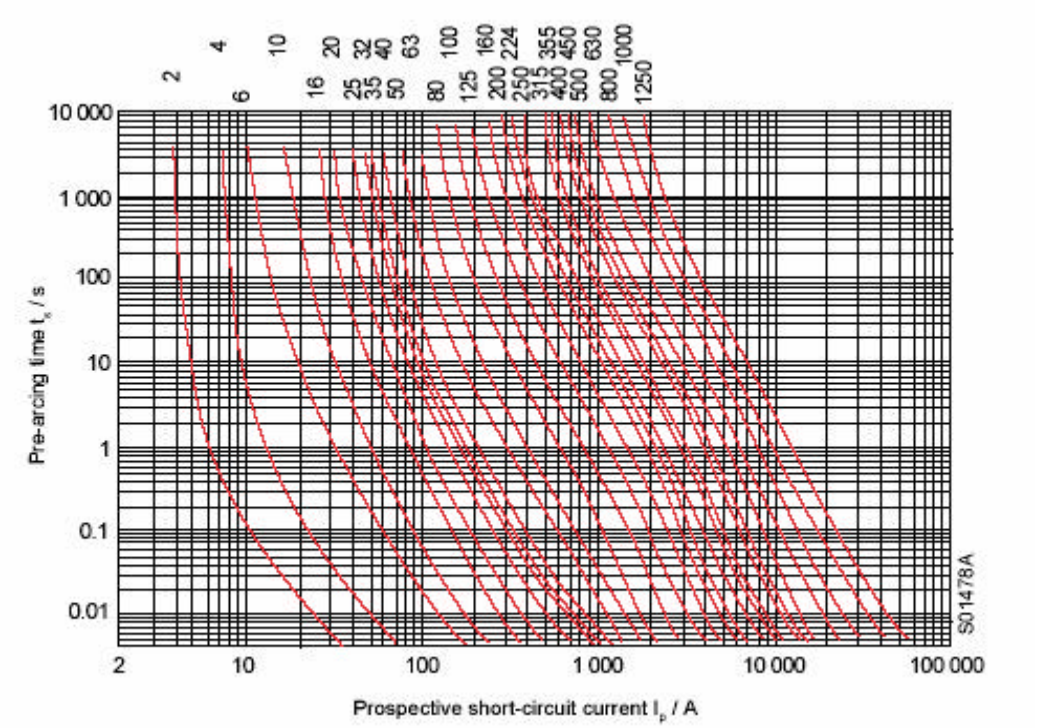

Document Information

Title	Stability of a Microgrid
Date	18th November 2004
Version	Draft Issue No 1
Task(s)	

Authors:	Xueguang Wu, Yibin Zhang, Nick Jenkins

Access:	
Project Consortium (for the actual version) European Commission , PUBLIC (for final version)	
Status:	
	Draft Version Final Version (internal document) **X** Submission for Approval (deliverable) Final Version (deliverable, approved on.)

Document Information

Title	Local Frequency Control of a Microgrid
Date	30th September 2004
Version	Draft Issue No 1
Task(s)	

Authors:	Xueguang Wu, Nilanga Jayawarna, Yibin Zhang, Nick Jenkins

Access:	
Project Consortium (for the actual version) European Commission , PUBLIC (for final version)	
Status:	
	Draft Version Final Version (internal document) **X** Submission for Approval (deliverable) Final Version (deliverable, approved on.)

DE2-Appendix I

MICROGRIDS

Large Scale Integration of Micro-Generation
To Low Voltage Grids

WORK PACKAGE E

PROTECTION ISSUES OF A MICROGRID

DRAFT Issue No 1

20th April 2004

Nilanga Jayawarna
Xueguang Wu

UMIST

Protection Issues of a MicroGrid

In a traditional distribution system, the protection systems are designed assuming unidirectional power flow and are usually based on overcurrent relays with discriminating capabilities. For any fault situation, Distributed Generation sources (DG) connected to the system are tripped off. In other words islanding operation of DG sources is not allowed.

A MicroGrid is designed to operate when interconnected to the distribution system as well as when disconnected from it. These two operating scenarios introduce a host of new issues in protection of a MicroGrid. When the MicroGrid is connected to the main grid, the grid sources could provide high fault currents that could be used to detect faults. But we cannot expect fault currents that are much larger than load currents in an islanded MicroGrid dominated by power electronic interfaces. Therefore using conventional overcurrent protection in a MicroGrid is not promising due to this low short circuit capability of a MicroGrid, especially when it is islanded. It is quite obvious that alternate means of detecting an event within an isolated microgrid must be studied and new protection systems devised.

Our MicroGrid concept is based on a capacity of around 1 MVA with an approximate geographical span of 1 km. Appendix 1 presents the single line diagram of a feeder in a typical MicroGrid (the study case LV network proposed by NTUA).

The ideal protection system of a MicroGrid should possess the following features

I. Must respond both to distribution system and MicroGrid faults
II. For a fault on the main grid, isolate the MicroGrid as quickly as possible
III. For a fault within the MicroGrid, isolate the smallest possible section of the radial feeder carrying the fault to get rid of the fault
IV. Effective operation of customers' protection

From the above, points I and II are clear enough. Point III could be expanded according to the two operating scenarios. If a fault occurs within the MicroGrid when operating interconnected to the distribution system, the MicroGrid should isolate from

the main grid first and then try to isolate the faulty feeder within. If a fault occurs in an already islanded MicroGrid, the protection system should try to sectionalise the MicroGrid in order to get rid of that fault.

Sectionalising of a MicroGrid would involve complex protection and control schemes and incurring greater costs. There are two operating principles open to a MicroGrid in this regard.

1. To sectionalise the MicroGrid by isolating the smallest possible section of the feeder carrying the fault.
2. To shut down the complete MicroGrid for any fault within it.

The decision will depend on the needs of the MicroGrid customers and whether the cost involved could be justified for the benefits gained through sectionalising.

According to system reliability index figures, approximately 22 faults per 100 km occur in a LV network (overhead lines + power cables) annually in the UK. This implies that less than 3 faults will take place in a typical MicroGrid spanning 1 km in a decade. We have to address the question whether it is really worthwhile to consider sectionalising of a MicroGrid in this scenario.

An islanded MicroGrid presents the biggest challenges to our protection problem. Therefore we need to have a clear understanding of the needs of an isolated MicroGrid. Some of the characteristics of a MicroGrid in islanded mode, which influence its protection needs are as follows

- Low fault level. (What kind of a margin of fault level could we expect?)
- Bi-directional power flow
- Low system inertia
- Extensive use of converters

When trying to understand the protection needs of a MicroGrid, we have to address the following initial issues at first.

1. What are the possibilities of failure / fault conditions?
2. What are the consequences due to these faults?
3. What are the protection functions required in a MicroGrid?

4. Which of the above issues (in 3) could use existing techniques and which of them need new approaches?
5. What are the benefits that the MicroGrid would gain through rapid sectionalising?
6. How to determine when to form an islanded MicroGrid?

Then we have to answer the more technical questions of

I. What are the present regulations/ statutory requirements?
II. What are the suitable protection schemes and their operating times?
III. How to earth the MicroGrid and what is its impact on protection arrangements?
IV. What are the protection requirements for generators within the MicroGrid?
V. What are the requirements for network protection?
VI. What is the impact of network protection operation on transient stability of generators?
VII. How does the operating principal of a MicroGrid (sectionalise or not?) impact the choice of protection?
VIII. When you detect a fault how does the tripping work?
IX. How to provide the islanded MicroGrid with sufficient coordinated fault protection?
X. What is the best possible way to synchronise and reconnect with the grid after clearing a fault?

Appendix 1: LV Feeder with LV DG sources

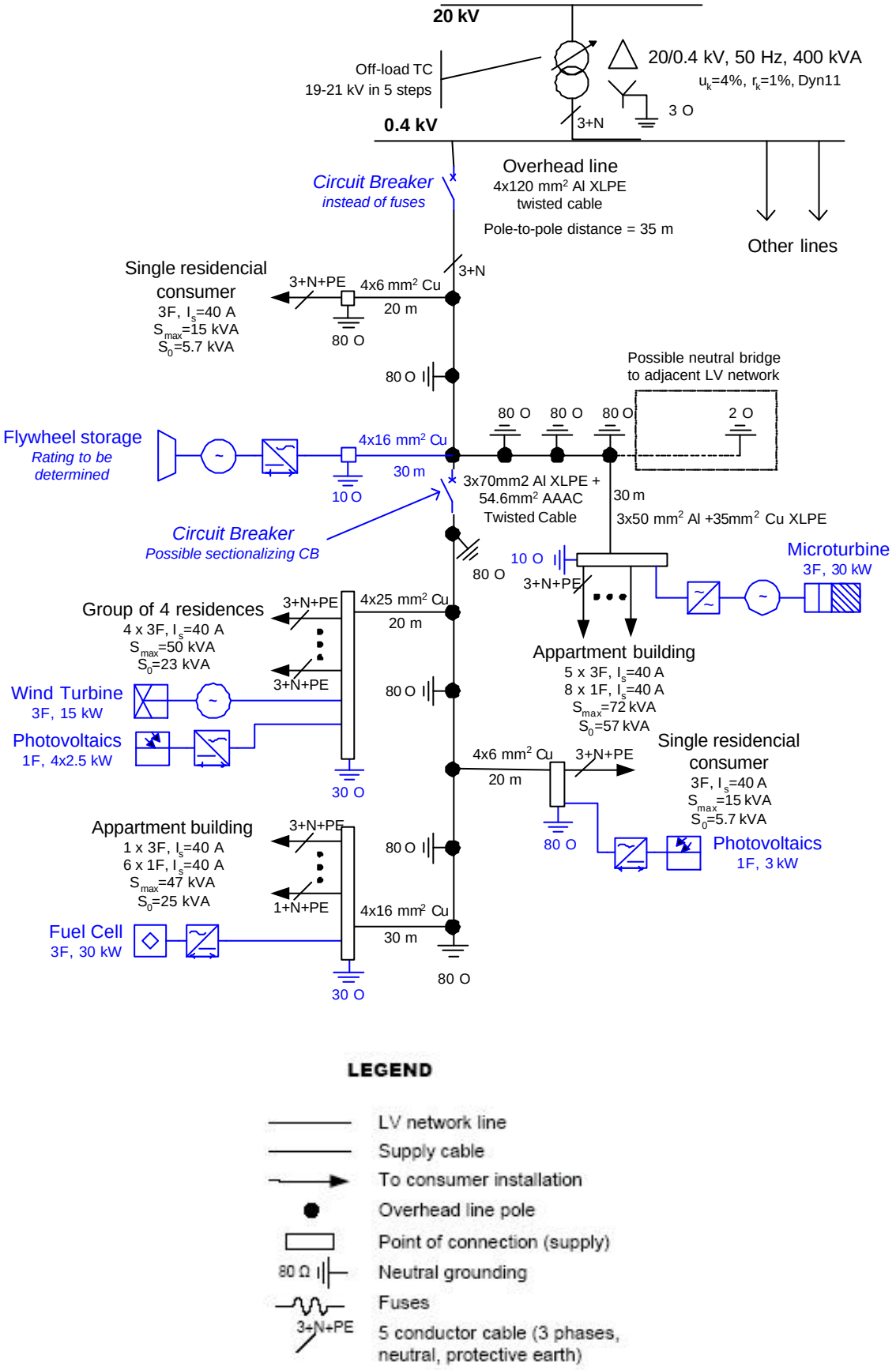

Document Information

Title	Protection Issues of a Microgrid
Date	20th April 2004
Version	Draft Issue No 1
Task(s)	

Authors:	Nilanga Jayawarna Xueguang Wu

Access:	
Project Consortium (for the actual version) European Commission , PUBLIC (for final version)	
Status:	
	Draft Version Final Version (internal document) **X** Submission for Approval (deliverable) Final Version (deliverable, approved on.)

DE2-Appendix IV

MICROGRIDS

Large Scale Integration of Micro-Generation

To Low Voltage Grids

WORK PACKAGE D

TASK TD2

Local Frequency Control of a MicroGrid

Draft Issue No 1

30 September 2004

Xueguang Wu, Nilanga Jayawarna, Yibin Zhang, Nick Jenkins

UMIST

Contents

1. Introduction

Micro-scale distributed generators (DGs), or micro sources, are being applied increasingly to provide electricity for the expanding energy demands in the network. The development of micro DGs also helps to reduce greenhouse gas emissions and increase energy efficiency.

The MicroGrid usually consists of a cluster of micro DGs, energy storage systems (e.g. flywheel) and loads, operating as a single controllable system. The voltage level of the MicroGrid at the load is about 400 Volts or less. The architecture of the MicroGrid is formed to be radial with a few feeders. It often provides both electricity and heat to the local area. It can be operated in both grid-connected mode and islanded mode

The micro DGs existing in the distribution network mainly use rotating machines. They are directly connected to the grid to supply electric power. However, the new technologies (e.g. micro gas turbine, fuel cells, photovoltaic system and several kinds of wind turbines) proposed to be used in MicroGrid are not suitable for supplying energy to the grid directly [Barsali, 2002]. They have to be interfaced with the grid through an inverter stage. Thus, the use of power electronic interfaces in the MicroGrid leads to a series of challenges in the design and operation of the MicroGrid. One of the main challenges is local frequency control of the MicroGrid operated in islanded mode.

It is well known that frequency has a strong coupling with active power in the network [Kundur, 1994]. The value of the frequency is a function of the difference between generation and demand plus network losses. If demand increases, the frequency will fall unless there is a matching increase in generation. If generation increases, the frequency will rise unless there is a matching increase in demand. The rate of change of frequency depends on the inertia of the system. The larger the inertia, the smaller the rate of change. During a disturbance, the frequency of the MicroGrid may change rapidly due to the low inertia (or zero inertia) present in the MicroGrid. In grid-connected mode, the frequency of the MicroGrid is maintained within a tight range (50±0.2Hz) by the main network. However, in islanded mode,

with relatively few micro sources, the local frequency control of the MicroGrid is not straightforward.

Obviously, the control of the micro sources and the flywheel is very important to maintain the frequency of the MicroGrid during islanded operation. The controllers of the micro sources and flywheel inverters respond in milliseconds. For basic operation of the MicroGrid, the controllers should use only local information to control the flywheel and micro sources. Communication between the micro sources and flywheel is unnecessary. For a micro source, the inverter should have plug and play capabilities [Lasseter, 2002]. Plug and play implies that a micro source can be added to the MicroGrid without any changes to the control of the units, which are already a part of the network. For the flywheel, the inverter should be able to respond to the change of load in a predetermined manner automatically.

Possible control strategies of the micro sources and the flywheel may be: (a) PQ control (fixed power control), (b) Droop control and (c) Frequency/Voltage control. PQ control is adopted so that the micro sources and the flywheel run on constant power output. The electricity, generated by the micro source, may be constant because of the need of the associated thermal load. In addition, the power output of the flywheel may be fixed at zero when the MicroGrid is operated in grid-connected mode. However, as PQ control delivers a fixed power output, it makes no contribution to local frequency control of the MicroGrid.

Therefore, the control scheme of the flywheel has to be changed from PQ control to Droop control or Frequency/Voltage control during islanded operation. Droop control is similar to the function of Primary frequency control in a conventional synchronous generator. The frequency of the MicroGrid can be restored to a steady state value determined by the droop characteristic. Frequency/Voltage control is similar to the function of Secondary frequency control in the conventional synchronous generator. The frequency and voltage of the MicroGrid can be brought back to the normal values (e.g. f = 50Hz and V = 1.0 p.u.) after a disturbance.

In this report, three control strategies (PQ control, Droop control and Frequency/Voltage control) for the local frequency control of the MicroGrid are

proposed. Based on two MicroGrid models (synchronous generator representation and STATic Synchronous Shunt COMpensator with battery energy storage, STATCOM-BES, representation) in PSCAD/EMTDC, these control schemes are implemented and tested. Simulations are demonstrated and discussed with supporting PSCAD/EMTDC results.

2. Local frequency control of the MicroGrid

The unique nature of the MicroGrid determines that the local frequency control of the MicroGrid may be: (a) PQ control (fixed active and reactive power control), (b) Droop control and (c) Frequency/Voltage control. In modelling of the MicroGrid, the micro sources and flywheel could be represented by the synchronous generators or STATCOM-BES. Thus, for different representation of the MicroGrid, the implementation of the control schemes may be different.

(1) MicroGrid represented by the synchronous generator

In this representation, the micro sources and flywheel of the MicroGrid are represented by synchronous generators. The local frequency control scheme of the MicroGrid is as follows:

(a) PQ control

Using this control, the outputs of the micro sources and the flywheel are fixed at their constant values (settings). The PQ control consists of a P controller and a Q controller.

The P controller adjusts the frequency-droop characteristic of the generator up or down to maintain the active power output of the generator at a constant value (Pdes, desired active power) when the frequency is changed. Figure 1 shows the effect of frequency-droop characteristic adjustment.

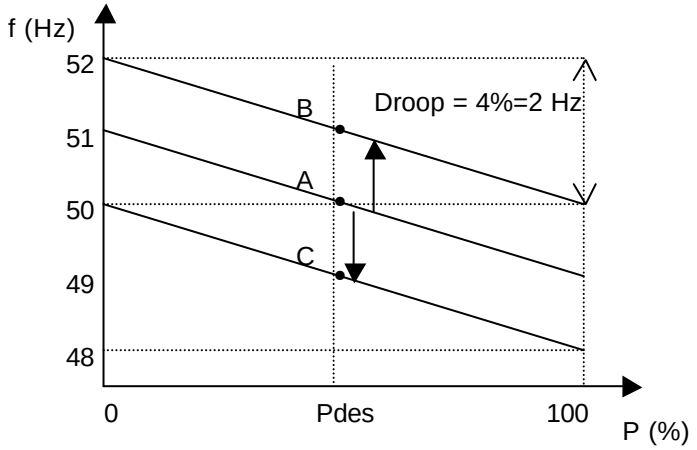

Figure 1 Effect of the frequency-droop characteristic adjustment

At output Pdes, characteristic A corresponds to 50Hz frequency of the grid, characteristic B corresponds to 51Hz frequency of the grid and characteristic C corresponds to 49Hz frequency of the grid. For a frequency change, the power output of the generator can be maintained at the desired value by moving the droop characteristic up or down. A typical droop of the frequency characteristic is about 4% [Kundur, 1994].

The function of a P controller is similar to the speed control of a synchronous generator with a supplementary control loop, as shown in Figure 2.

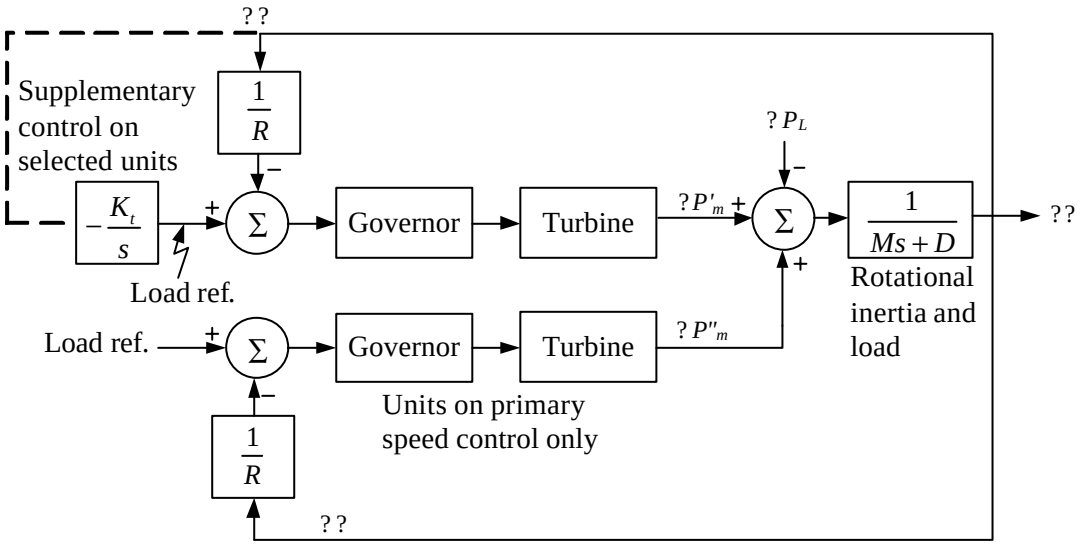

Figure 2 Speed control of synchronous generator with a supplementary control loop [Kundur, 1994]

The movement of the characteristic is achieved through adding an integral control loop, which acts on the load reference settings, to the speed droop control of the generator. The integral control action ensures that the output power of the generator is fixed at a constant value (setting).

Figure 3 shows the configuration of P controller for a synchronous generator representation of the MicroGrid.

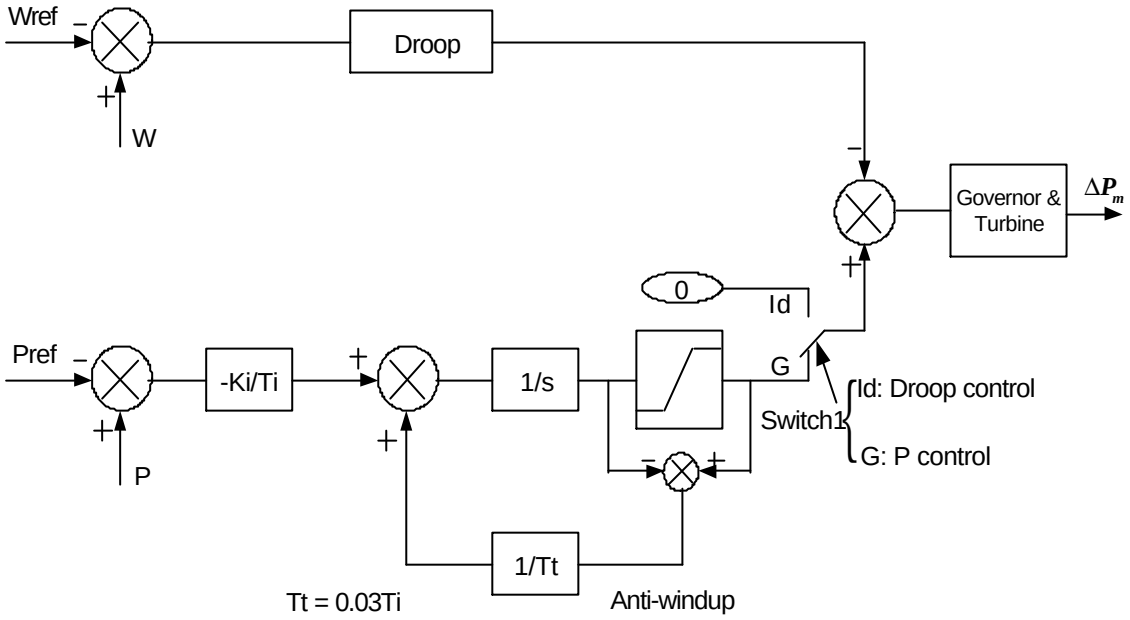

Figure 3 Configuration of P controller for a synchronous generator representation

Similarly, the Q controller adjusts the voltage-droop characteristic of the generator by moving the droop lines upon or down to maintain the reactive power output of the generator at a constant value (Qdes, desired reactive power) when the voltage is changed. Figure 4 shows the effect of voltage-droop characteristic adjustment.

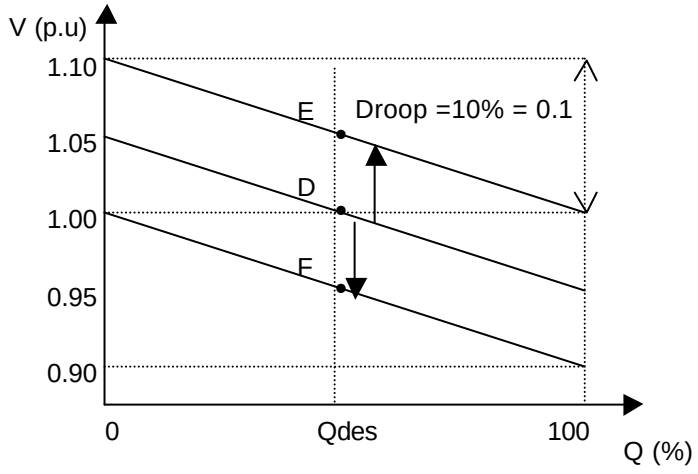

Figure 4 Effect of the voltage-droop characteristic adjustment

At output Qdes, characteristic D corresponds to 1.00 voltage of the network, characteristic E corresponds to 1.05 voltage of the grid and characteristic F corresponds to 0.95 voltage of the grid. For a voltage change, the reactive power output of the generator is maintained at the desired value Qdes by shifting the voltage-droop characteristic up or down. A typical droop of voltage characteristic is about 10% [Kundur, 1994].

Figure 5 shows the implementation of Q controller for a synchronous generator representation.

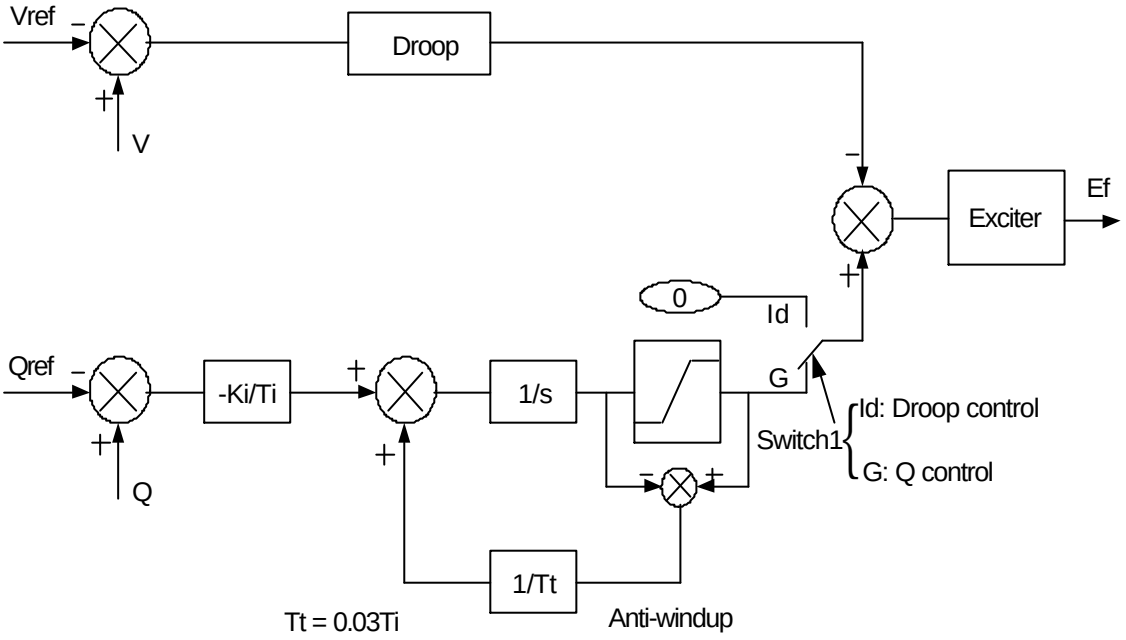

Figure 5 Implementation of Q controller for a synchronous generator representation

(b) Droop control

When the MicroGrid is operated in islanded mode, the control scheme of the micro sources is still PQ control. However, the control scheme of the flywheel should be changed to enable local frequency control. The flywheel may use Droop control. The power output of the flywheel is regulated according to the predetermined droop characteristics. Droop control consists of a frequency-droop controller and a voltage-droop controller.

Figure 6 shows a frequency-droop characteristic, which would be used in frequency-droop controller.

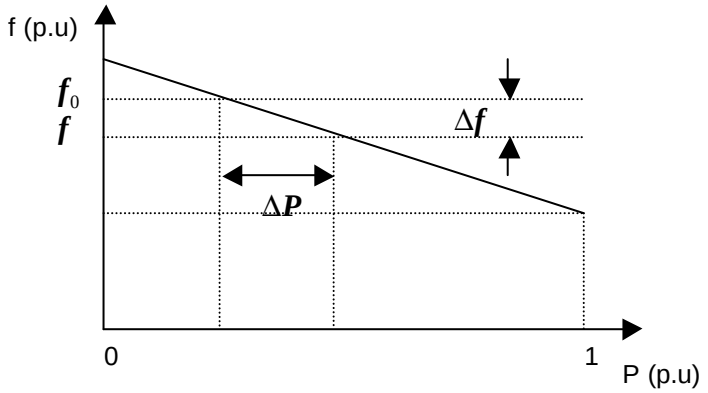

Figure 6 A typical frequency-droop characteristic

The value of droop R_f is a ratio of frequency deviation Δf to change in active power output ΔP. It can be expressed in percentage as equation (1).

$$R_f = \frac{\Delta f(p.u)}{\Delta P(p.u)} \times 100\% \qquad (1)$$

Figure 7 also shows a typical voltage-droop characteristic used in the voltage-droop controller.

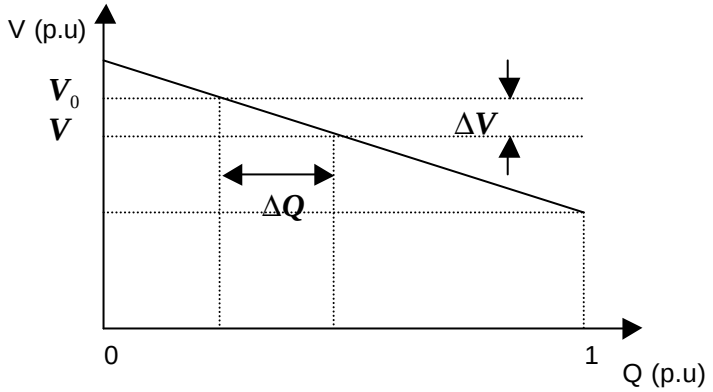

Figure 7 A typical voltage-droop characteristic

The value of droop R_V is a ratio of voltage deviation ΔV to change in reactive power output ΔQ. It can be expressed in percentage as equation (2).

$$R_V = \frac{\Delta V(p.u)}{\Delta Q(p.u)} \times 100\% \qquad (2)$$

The implementation of Droop control can be achieved by changing Switch1 from G to Id in Figures 3 and 5.

(c) Frequency/Voltage control

With droop control action, a load change in the MicroGrid will result in steady-state frequency and voltage deviations, depending on the droop characteristics and Frequency/Voltage sensitivity of the load. The flywheel will contribute to the overall change in generation. Restoration of the Frequency/Voltage of the MicroGrid to their normal values requires a supplementary action to adjust the output of the flywheel. The basic means of the local frequency control of the MicroGrid is through regulating the output of the flywheel. As the load of the MicroGrid changes continually, it is necessary to automatically change the output of the flywheel.

The objective of the frequency control is to restore the frequency to its normal value. This is accomplished by moving the frequency-droop characteristic left or right to maintain the frequency at a constant value. The frequency control adjusts the output of the flywheel to restore the frequency of the MicroGrid to normal (e.g. 50Hz). Figure 8 shows the effect of this adjustment.

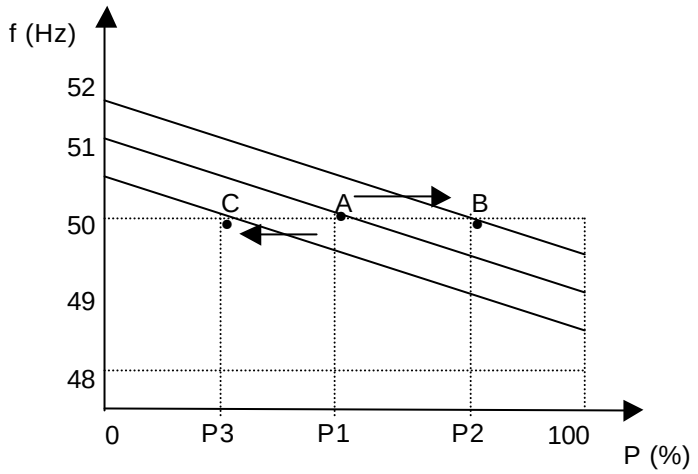

Figure 8 Effect of the adjustment on the frequency-droop characteristic

At 50Hz, characteristic A corresponds to P1 active power output of the flywheel, characteristic B corresponds to P2 active power output and characteristic C corresponds to P3 active power output. The frequency of the MicroGrid is fixed at a constant value (50Hz) by moving the frequency-droop characteristic left or right.

The implementation of Frequency control is similar to P control in Figure 3. But, the connection of the supplementary control loop needs to be changed from Gp of

Switch2 to If and from Id of Switch1 to G. Figure 9 shows the layout of Frequency control for a synchronous generator representation.

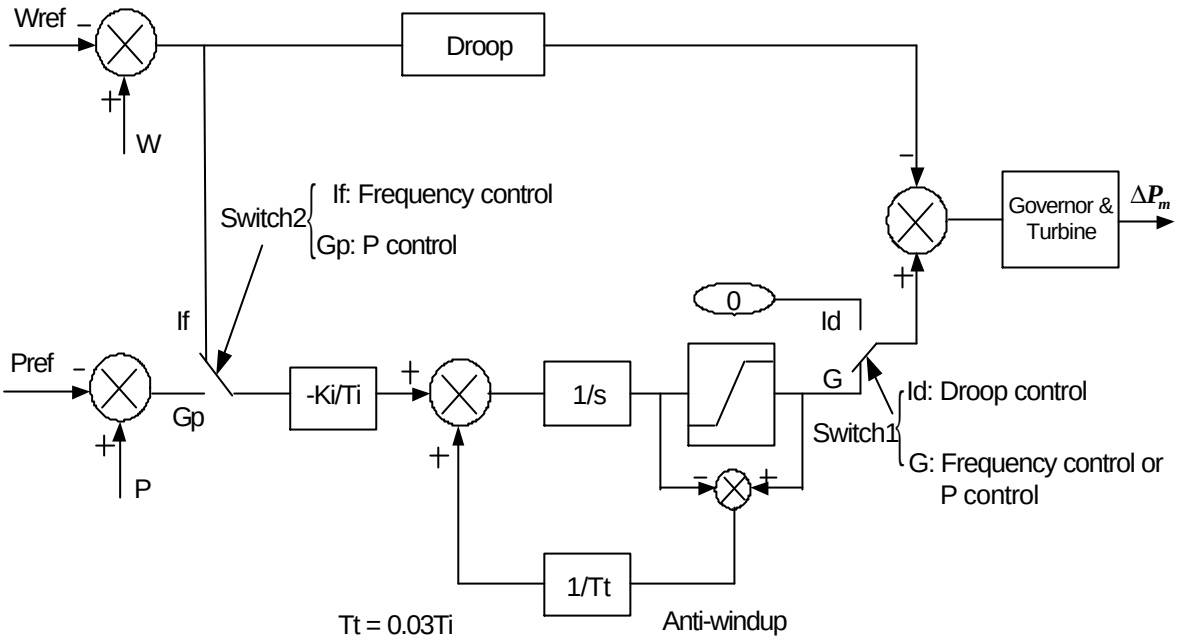

Figure 9 Layout of Frequency control for a synchronous generator representation

Similarly, the voltage control adjusts the voltage-droop characteristic left or right to maintain a constant voltage when the voltage of the MicroGrid is changed. Thus, the voltage of the MicroGrid is fixed at a desired value (e.g. 1.0p.u). The effect of this adjustment is shown in Figure 10.

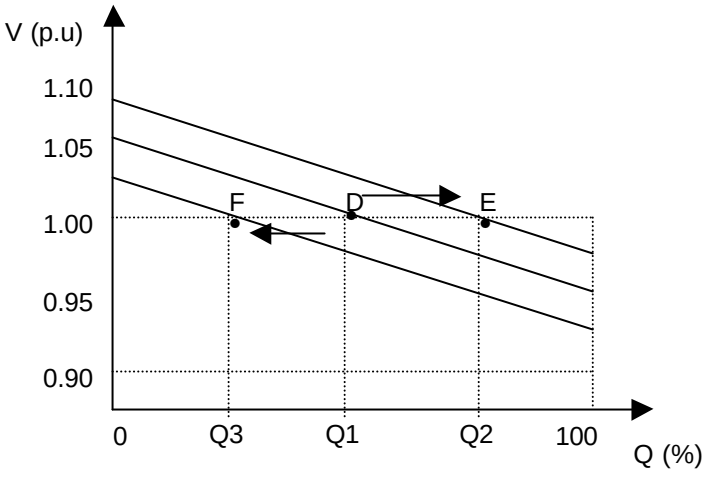

Figure 10 Effect of the adjustment on the voltage-droop characteristic

At 1.0 p.u voltage, characteristic D corresponds to Q1 reactive power output of the flywheel, characteristic E corresponds to Q2 reactive power output and characteristic F corresponds to Q3 reactive power output. The voltage of the MicroGrid is fixed at a constant value (1.0 p.u) by moving the voltage-droop characteristic left or right.

Figure 11 shows the implementation of Voltage control for a synchronous generator representation.

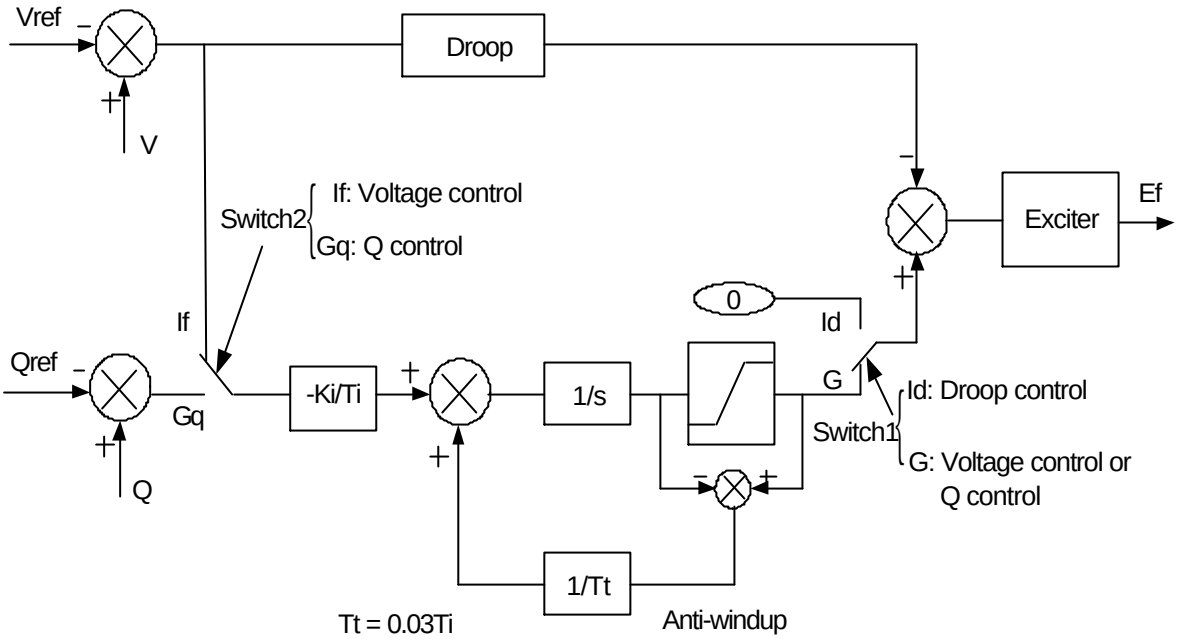

Figure 11 Implementation of Voltage control for a synchronous generator representation

(2) MicroGrid represented by the STATCOM-BES

In this representation, the micro sources and flywheel of the MicroGrid are represented by the STATCOM-BES. The local frequency control schemes of the MicroGrid are PQ control, Droop control and Frequency/Voltage. Figure 12 shows the implementation of these control strategies of the flywheel in a STATCOM-BES.

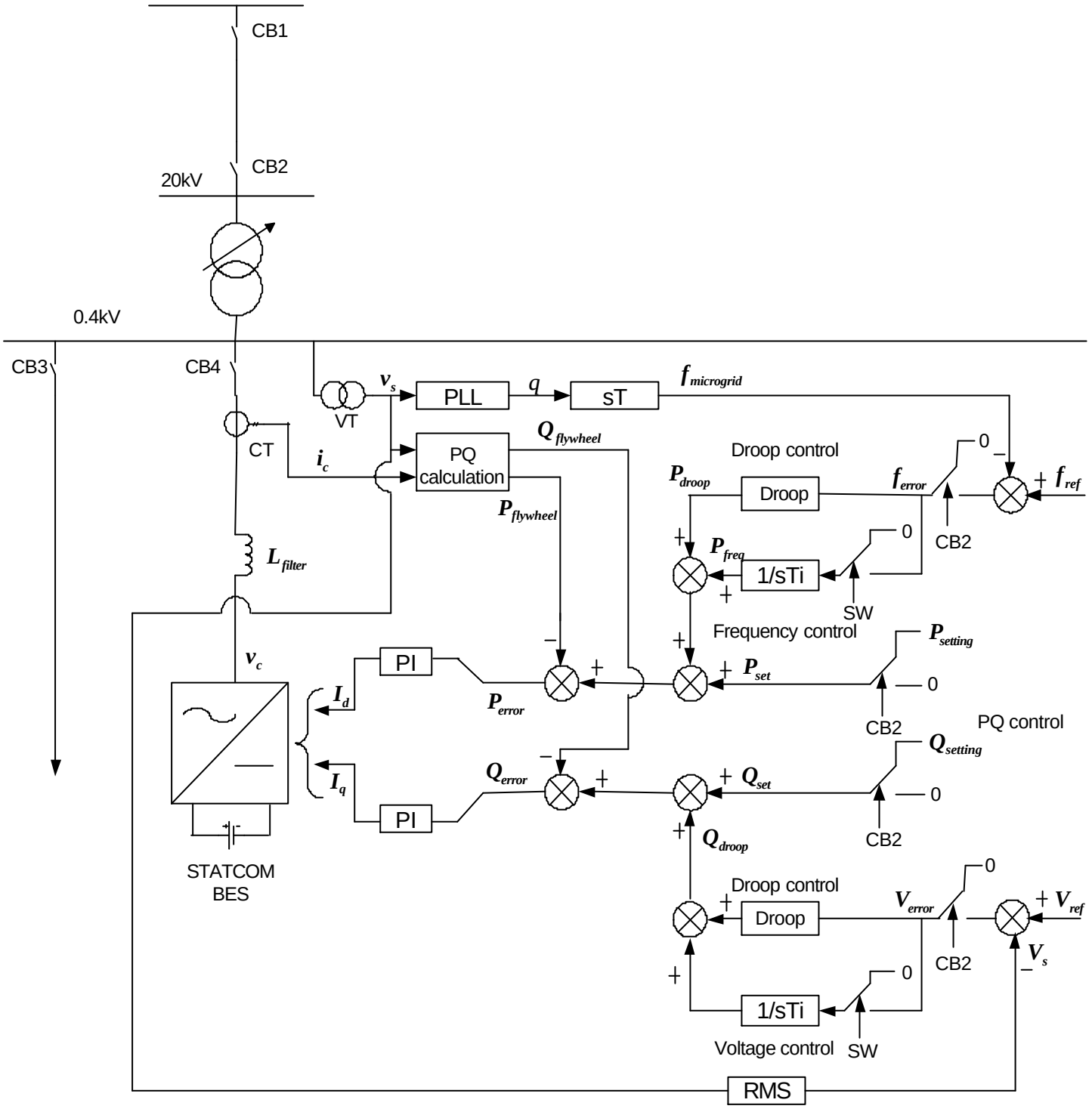

Figure 12 Control schemes of the flywheel represented by a STATCOM-BES

During grid-connected mode, the state of circuit breaker CB2 is closed. The control schemes of the micro source and flywheel are PQ control. The droop output P_{droop} and Q_{droop} of Droop control are zero. Thus, the reference values of the active and reactive powers are $P_{set} = P_{setting}$ and $Q_{set} = Q_{setting}$, acting on PQ control.

After disconnection of the MicroGrid from the main network, during islanded mode, CB2 is open. The outputs P_{set} and Q_{set} of the PQ control loop are set to zero. The reference values of the active and reactive powers are P_{droop} and Q_{droop}, acting on Droop control. The control scheme of the flywheel is thus switched from PQ control to Droop control.

If the inputs of PI controllers of the STATCOM are taken from the errors of the frequency and voltage ($f_{error} = f_{ref} - f_{microgrid}$ and $V_{error} = V_{ref} - V_s$), the control scheme of the flywheel will be Frequency/Voltage control.

3. Assumptions in this study

It is assumed that the micro sources and the flywheel of the MicroGrid are represented by the synchronous generators and the STATCOM-BES, respectively. Two representation modes of the MicroGrid are implemented in PSCAD/EMTDC and shown in Figures 13 and 14.

Figure 13 shows a simple MicroGrid mode, in which the micro source and the flywheel are represented by the synchronous generators.

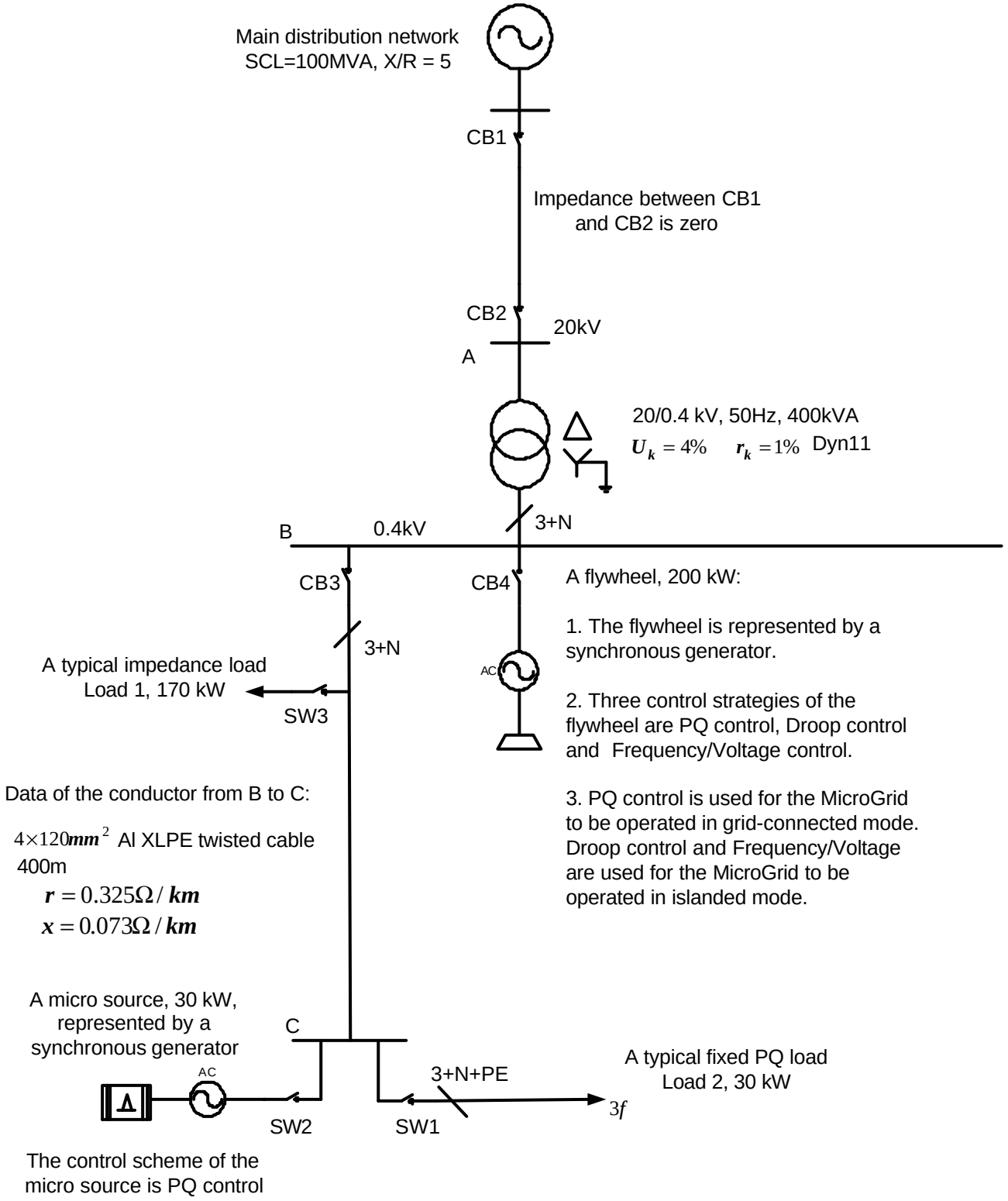

Figure 13 A simple MicroGrid model represented by the synchronous generators

Figure 14 shows a simple MicroGrid mode, in which the micro source and the flywheel are represented by the STATCOM-BES.

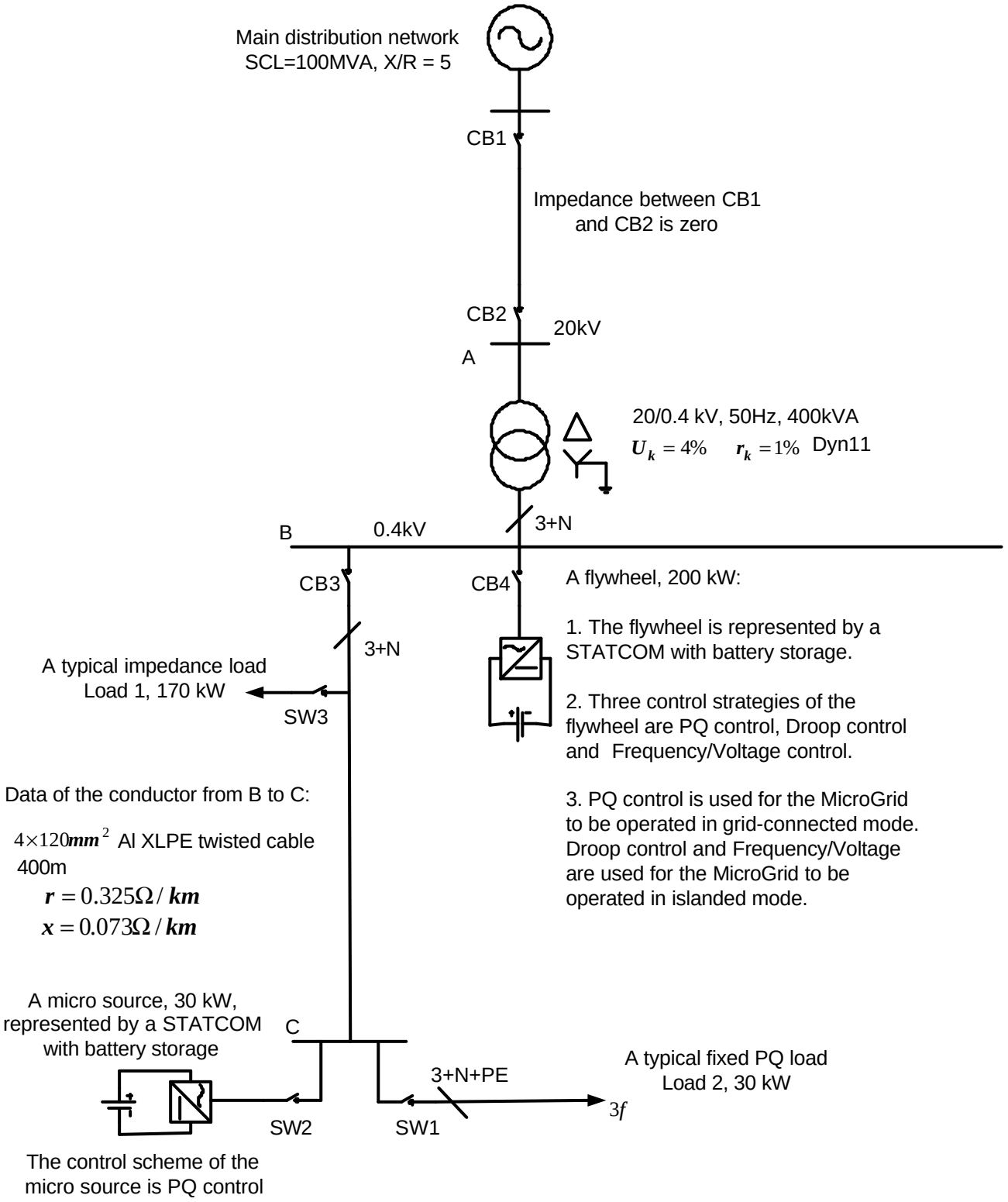

Figure 14 A simple MicroGrid model represented by the STATCOM-BES

For both representations of the MicroGrid above, the fault level at the 20kV main distribution network is 100MVA, with a X/R ratio of 5. One transformer (400kVA, 20/0.4kV) is installed at the substation between the main network and the MicroGrid. The impedance of the transformer is 0.01+j0.04 p.u. The MicroGrid consists of a flywheel and a feeder. The flywheel is connected to 0.4kV busbar, which is near to the substation. The capacity of the flywheel is 200kW (assuming the flywheel supplies 4MJ energy for 20 seconds continuously). The feeder is connected to a micro source and two loads (Load 1 and Load 2) through 400 meters of ALXLPE twisted cable ($4\times120mm^2$). The impedance of the cable is 0.325+j0.073 ohms per kilometre [Bungay, 1990]. The capacity of the micro source is 30kW. Load 1 is an impedance load, with capacity of 170kW. Load 2 is a fixed PQ load, with capacity of 30kW.

In the synchronous generator representation, the parameters of the synchronous generators are the typical average values of the synchronous turbine generator constants [Glover, 2002]:

- Synchronous d-axis reactance (X_d): 1.10 [p.u];
- Synchronous q-axis reactance (X_q): 1.08 [p.u];
- Transient d-axis reactance (X'_d): 0.23 [p.u];
- Transient q-axis reactance (X'_q): 0.23 [p.u];
- Sub-transient d-axis reactance (X''_d): 0.12 [p.u];
- Sub-transient q-axis reactance (X''_q): 0.15 [p.u];
- Negative sequence reactance (X_2): 0.13 [p.u];
- Zero sequence reactance (X_0): 0.05 [p.u];
- Stator armature resistance (R_a): 0.005 [p.u];
- Transient time constant (T'_{do}): 5.60 [sec.];
- Sub- transient time constant ($T''_d = T''_q$): 0.035 [sec.];
- Inertia constant (H): 1.05 [MW/MVA].

In the STATCOM-BES representation, the ratings of the STATCOMs-BES are the same as the capacities of the micro source and flywheel, 30kW and 200kW.

The control scheme of the micro source is PQ control at all times. The control strategies of the flywheel are PQ control, Droop control or Frequency/Voltage control. The flywheel uses PQ control only when the MicroGrid is operated in grid-connected mode. During islanded mode, the control of the flywheel is switched from PQ control to Droop control or Frequency/Voltage control.

4. Simulation results

Based on two representations of the MicroGrid (synchronous generator representation and STATCOM-BES representation), the dynamic performances of the MicroGrid are investigated and demonstrated in PSCAD/EMTDC under three control strategies (PQ control, Droop control and Frequency/Voltage control) of the flywheel. In all cases, circuit breaker CB2 is tripped at 10 seconds. Following the trip of CB2, the MicroGrid is disconnected from the main network and operated in islanded mode.

(1) For the synchronous generator representation

The MicroGrid mode, used in PSCAD/EMTDC modelling, is shown in Figure 13. The control scheme of the micro source is PQ control. The control strategies of the flywheel are PQ control, Droop control and Frequency/Voltage control.

(a) PQ control

Figure 15 shows the dynamic performance of the MicroGrid when the flywheel uses PQ control during islanded mode. The control schemes of the micro source and the flywheel are PQ control. The implementation of PQ control is shown in Figures 3 and 5.

Obviously, the flywheel makes no contribution to the local frequency control of the MicroGrid. The frequency and voltage of the MicroGrid are unstable. The voltage of the MicroGrid collapses so that the MicroGrid can not be operated in islanded mode.

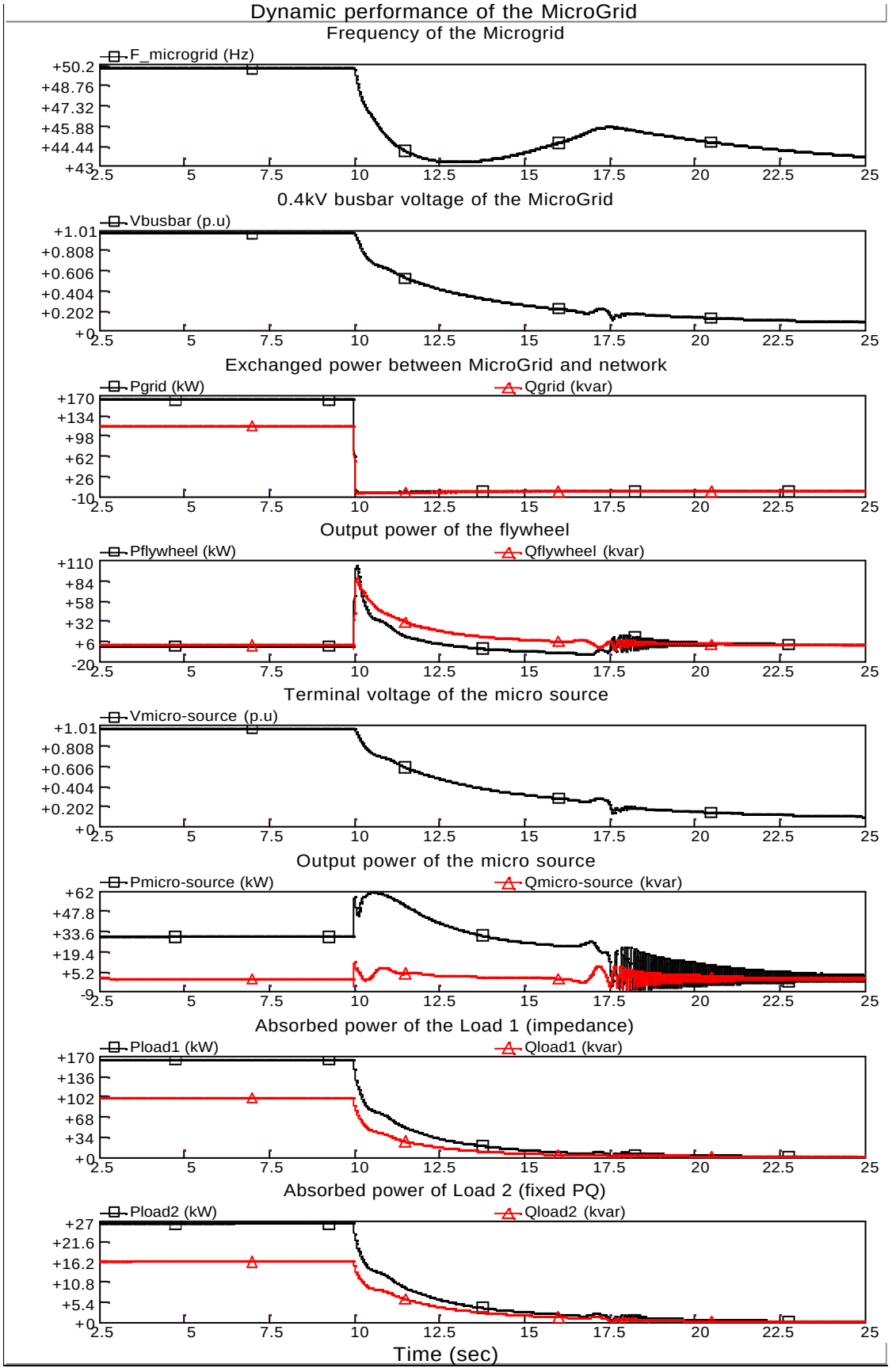

Figure 15 Dynamic performance of the MicroGrid (using synchronous generator representation) when the flywheel uses PQ control during islanded mode

(b) Droop control

Figure 16 shows the dynamic performance of the MicroGrid when the flywheel uses Droop control (shown in Figures 3 and 5, changes Switch1 from G to Id) during islanded mode. The control scheme of the micro source is still PQ control.

After disconnection of the MicroGrid from the main network, the output of the micro source is still retained at 30kW. But, the output of flywheel is changed from zero to the value of 149kW+j110kVar according to the droop settings ($\boldsymbol{R}_f = 4\%$ and $\boldsymbol{R}_v = 10\%$). Thus, the frequency and voltage of the MicroGrid are restored to the steady state values (48.35Hz and 0.9325p.u), associated with the droop characteristics.

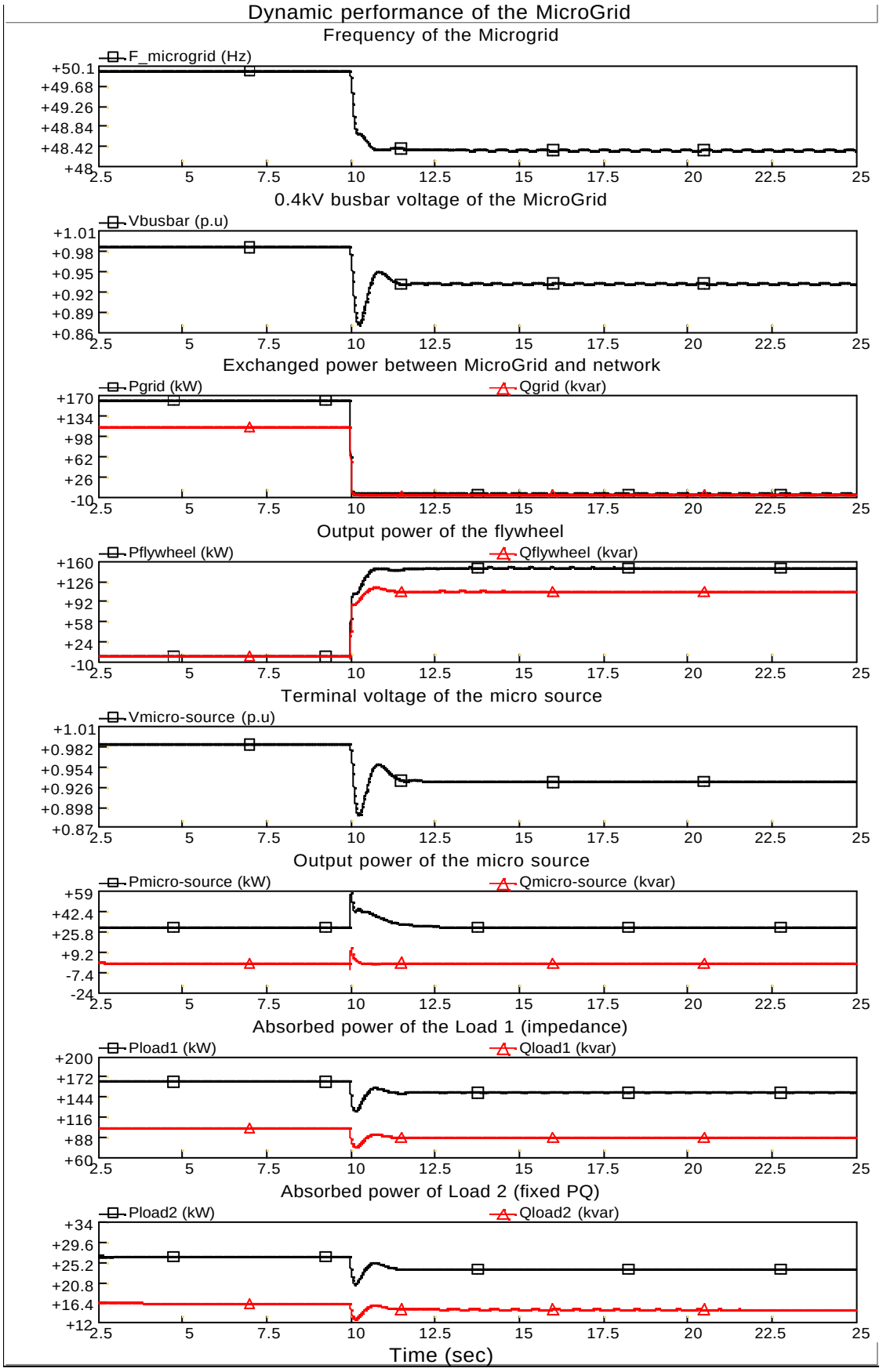

Figure 16 Dynamic performance of the MicroGrid (using synchronous generator representation) when the flywheel uses Droop control during islanded mode

(c) Frequency/Voltage control

Figure 17 shows the dynamic performance of the MicroGrid when the flywheel uses Frequency/Voltage control (shown in Figures 9 and 11) during islanded mode. The control of the micro source is still PQ control. The control of the flywheel is switched from PQ control to Droop control.

During islanded mode of the MicroGrid, the output of the micro source is maintained at a constant value of 30kW. However, the output of the flywheel is changed from zero to the value of 171kW+j127kVar. Consequently, the frequency and voltage of the MicroGrid are both brought back to the normal values (50Hz and 1.0p.u). It should be noted that the energy export of the flywheel using Frequency/Voltage control is larger than using Droop control.

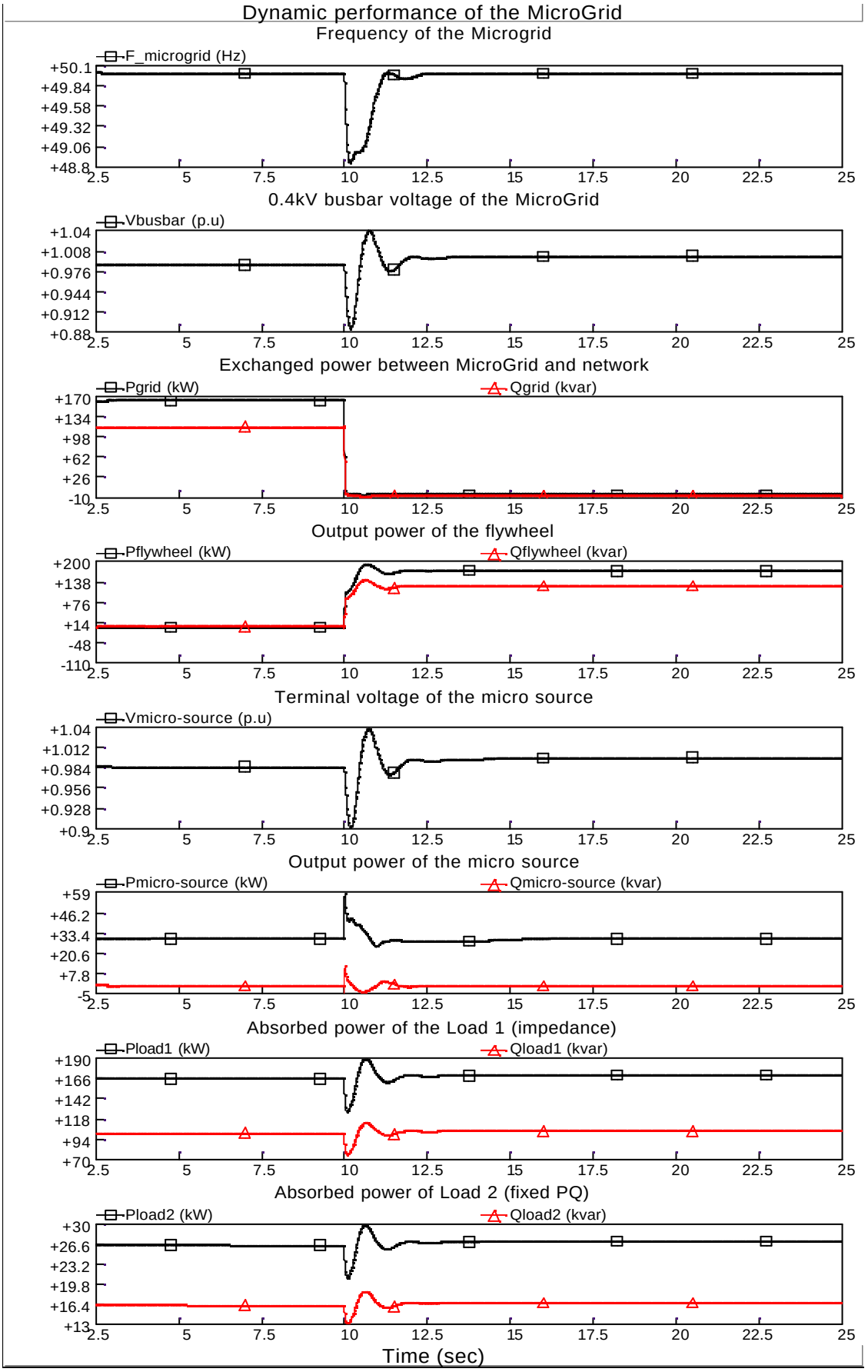

Figure 17 Dynamic performance of the MicroGrid (using synchronous generator representation) when the flywheel uses Frequency/Voltage control during islanded mode

(2) For the STATCOM-BES representation

The MicroGrid mode, used in PSCAD/EMTDC modelling, is a STATCOM-BES representation, as shown in Figure 14. The implementation of three control schemes (PQ control, Droop control and Frequency/Voltage control) is shown in Figure 12.

Figures 18, 19 and 20 show the dynamic performances of the MicroGrid when the flywheel uses PQ control, Droop control and Frequency/Voltage control during islanded mode, respectively. The deviations of the frequency and voltage depend on the mismatch between generation and demand in the MicroGrid.

Comparisons with Figures 15, 16 and 17 show that the simulation results of the STATCOM-BES representation are similar to the synchronous generator representation. However, after a disturbance, the dynamic response of the frequency and voltage of the STATCOM-BES representation MicroGrid is faster than the synchronous generator representation due to a low or zero inertia value of the STATCOM- BES.

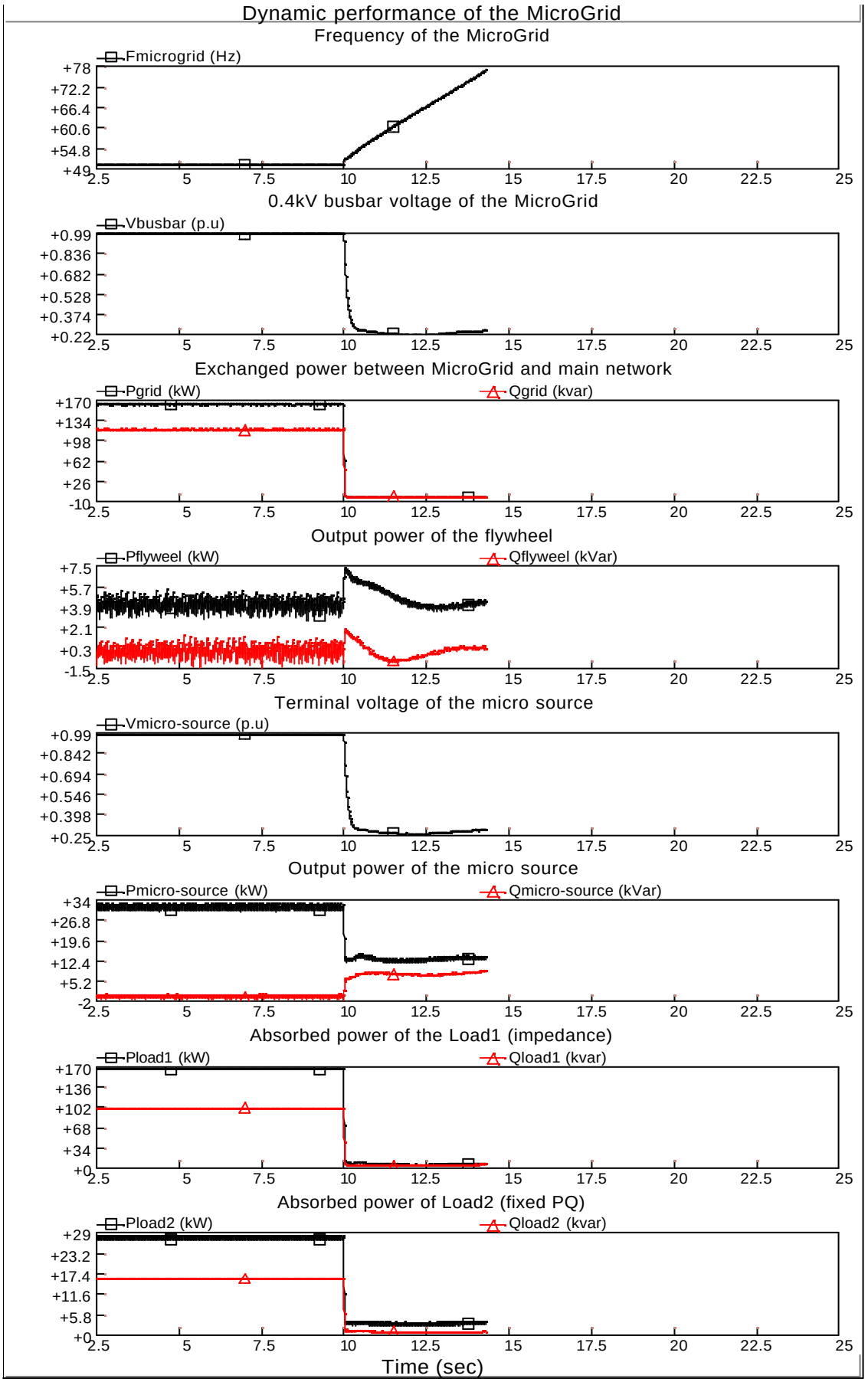

Figure 18 Dynamic performance of the MicroGrid (using STATCOM-BES representation) when the flywheel uses PQ control during islanded mode

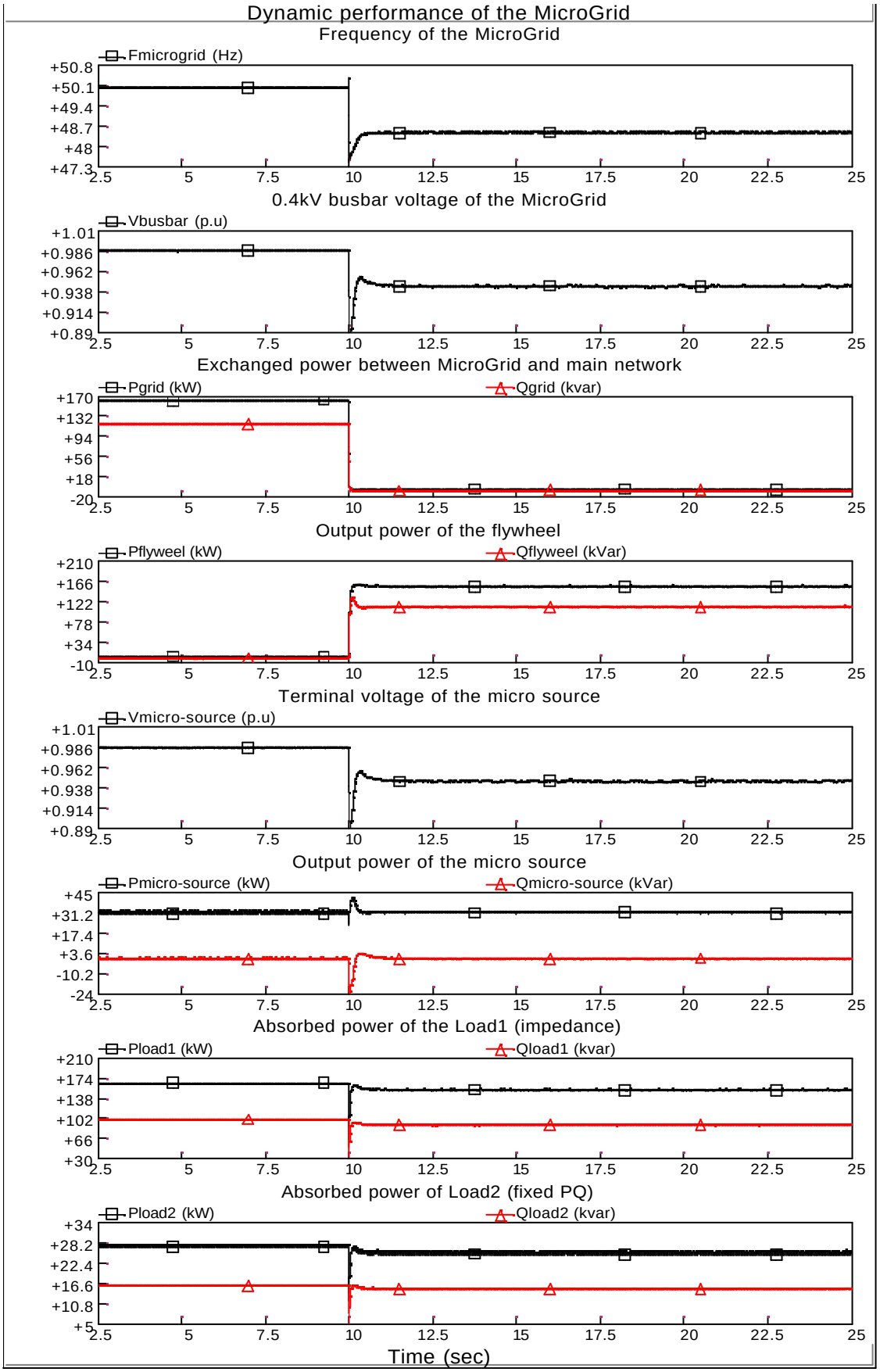

Figure 19 Dynamic performance of the MicroGrid (using STATCOM-BES representation) when the flywheel uses Droop control during islanded mode

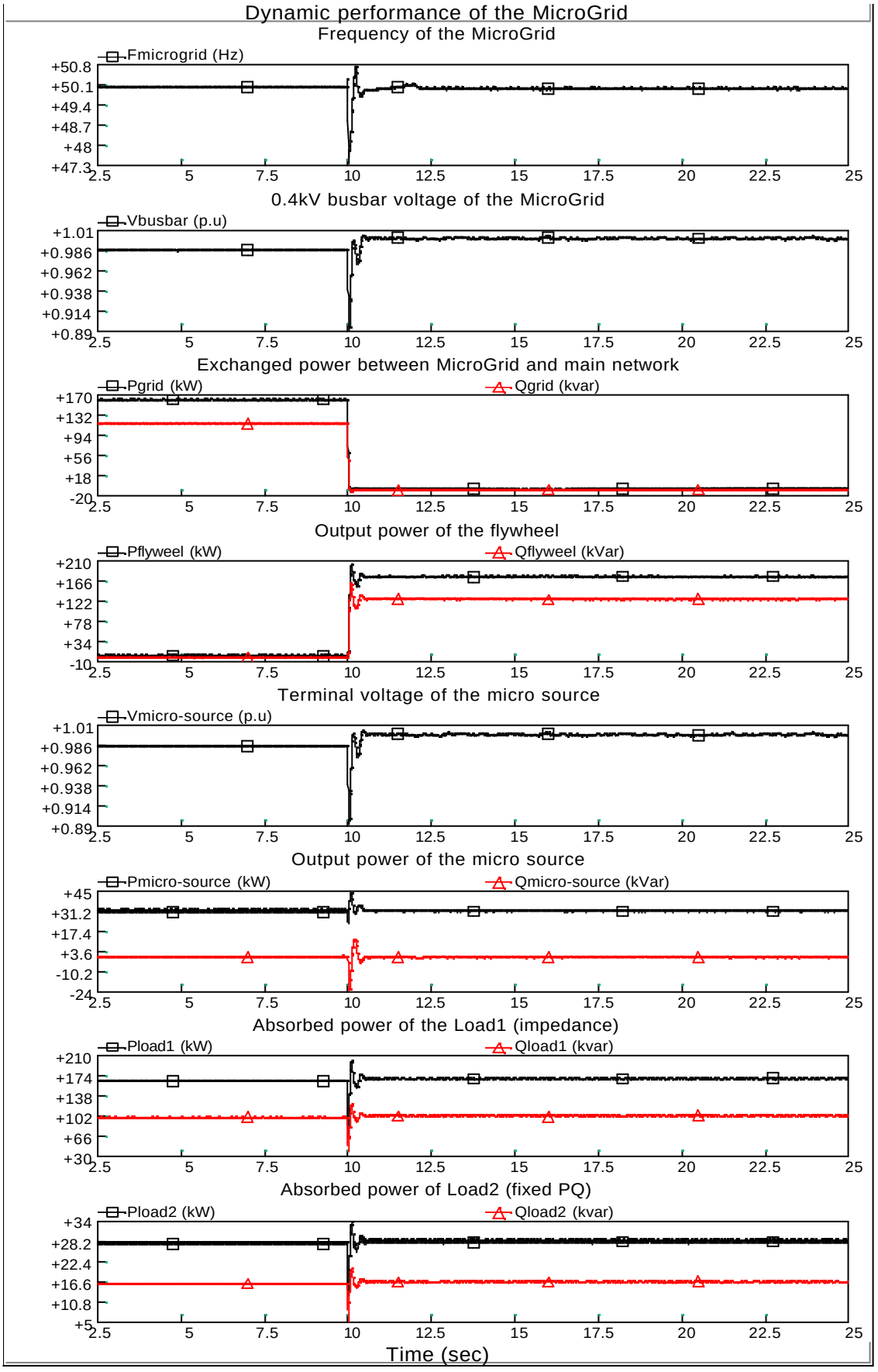

Figure 20 Dynamic performance of the MicroGrid (using STATCOM-BES representation) when the flywheel uses Frequency/Voltage control during islanded mode

5. Conclusions

With increasing penetration levels of the DGs, a number of MicroGrids will exist in the distribution network system in the near future. The safety and reliability of the MicroGrid are becoming more and more important. The unique nature of the MicroGrid requires local frequency control of the MicroGrid. The local frequency control of the MicroGrid can be mainly achieved through control of the flywheel. The possible control schemes of the flywheel for this purpose are PQ control, Droop control and Frequency/Voltage control. The control schemes are implemented in both synchronous generator representation and STATCOM-BES representation of the MicroGrid.

PQ control is only used by the flywheel while the MicroGrid is operating in grid-connected mode. The PQ control of the flywheel makes no contribution to the local frequency control of the MicroGrid due to its fixed active and reactive power outputs. After disconnection of the MicroGrid from the main network, during islanded mode, the control of the flywheel has to be switched from PQ control to Droop control or Frequency/Voltage control.

Droop control is similar to the Primary frequency control of a conventional synchronous generator. For a change of frequency in the MicroGrid, the active power output of the flywheel is regulated automatically according to a predetermined frequency-droop characteristic. The frequency of the MicroGrid can be restored to a steady state value determined by the droop.

Frequency/Voltage control is similar to the Secondary frequency control of a conventional synchronous generator. It controls the frequency and voltage of the MicroGrid at the normal values (e.g. f = 50Hz and V = 1.0 p.u.). The frequency and voltage of the MicroGrid can be brought back to their normal values after the disturbance. The frequency and voltage of the MicroGrid in which the flywheel uses Frequency/Voltage control are better than the flywheel use Droop control. However, it should be noted that the flywheel using Frequency/Voltage control has to supply higher active and reactive powers to the MicroGrid than using Droop control. The control capability of the flywheel in practice may be limited by its available capacity.

6. References

Barsali S., et al. (2002), Control Techniques of Dispersed Generators to Improve the Continuity of Electricity Supply, Power Engineering Society Winter Meeting, 2002, IEEE, Volume: 2, 27-37 January 2002.

Bungay E., McAllister D. (1990), Electric Cables Handbook (second edition), BSP Professional Books, Blackwell Scientific Publication Ltd..

Glover J.D., Sarma M.S. (2002), Power System Analysis and Design (third edition), Brooks/Cole, Thomson Learning.

Kundur P. (1994), Power System Stability and Control (book), McGraw-Hill, Inc..

Lasseter R.H. (2002), MicroGrids, Power Engineering Society Winter Meeting, 2002. IEEE, Volume: 1, 27-31 January 2002

Appendix

1. Simple representation of the flywheel in the MicroGrid

To simplify modelling of the flywheel, two simple representations of the flywheel are presented by using controllable AC and DC voltage sources. The control schemes of the flywheel are still PQ control, Droop control and Frequency/Voltage control, as described in Chapter 2 of this report.

Figures A1 and A2 show the implementations of the control schemes of the flywheel represented by the AC and DC controllable voltage sources, respectively.

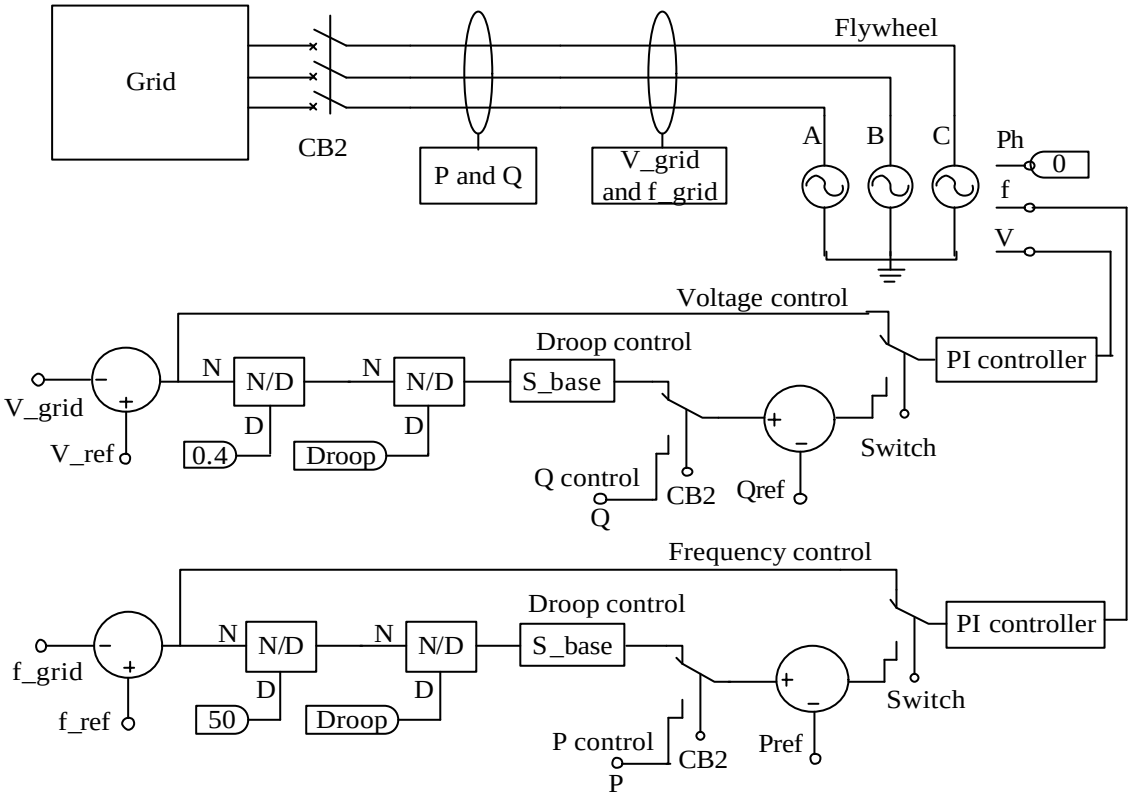

Figure A1 Control schemes of the flywheel represented by a controllable AC voltage source

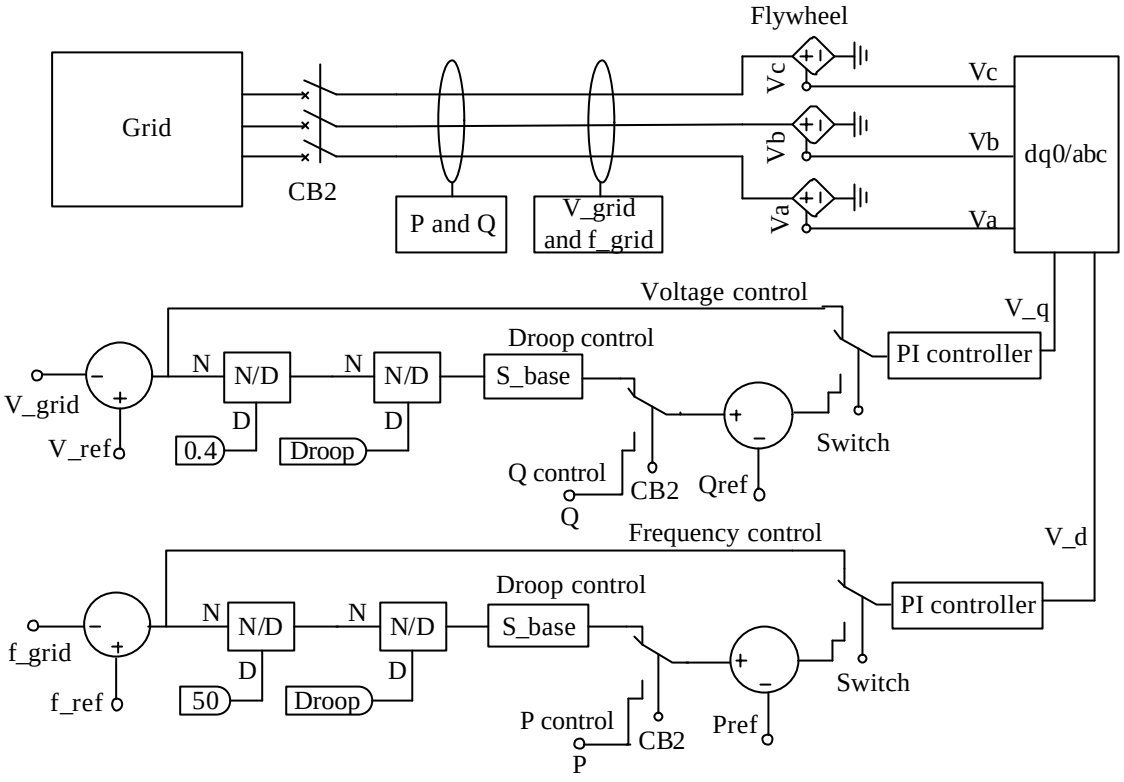

Figure A2 Control schemes of the flywheel represented by a controllable DC voltage source

2. Simulation results

The MicroGrid model used in this study is shown in Figure 14. The flywheel is represented either by a controllable AC voltage source or a controllable DC voltage source. Control strategies of the flywheel are PQ control, Droop control and Frequency/Voltage control. The flywheel uses PQ control only when the MicroGrid is operated in grid-connected mode. After disconnection of the MicroGrid from the main network at 10 seconds, during islanded mode, the control scheme of the flywheel is switched from PQ control to Droop control or Frequency/Voltage control. Simulation results produced in PSCAD/EMTDC are shown in Figures A3, A4, A5 and A6.

Figure A3 shows the dynamic performance of the MicroGrid when the flywheel, represented by a controllable AC voltage source, uses Droop control during islanded mode. The control scheme of the flywheel is switched from PQ control to Droop control after disconnection of the MicroGrid from the main network.

Figure A4 shows the dynamic performance of the MicroGrid when the flywheel, represented by a controllable AC voltage source, uses Frequency/Voltage during islanded mode. The control scheme of the flywheel is switched from PQ control to Frequency/Voltage control after disconnection of the MicroGrid from the main network

Similarly, Figures A5 and A6 show the dynamic performance of the MicroGrid when the flywheel, represented by a controllable DC voltage source, uses Droop control and Frequency/Voltage control during islanded mode.

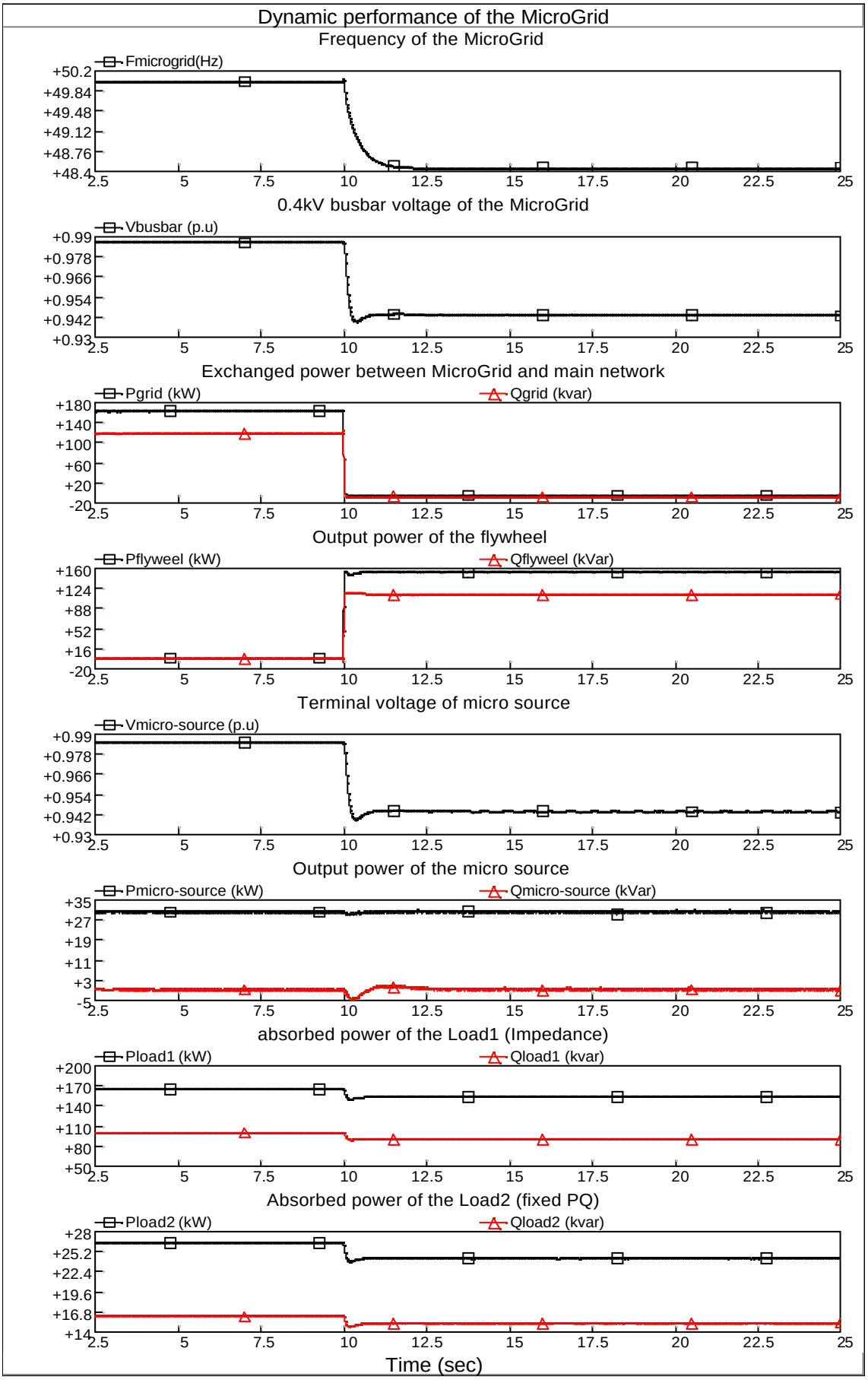

Figure A3 Dynamic performance of the MicroGrid when the flywheel, represented by a controllable AC voltage source, uses Droop control during islanded mode

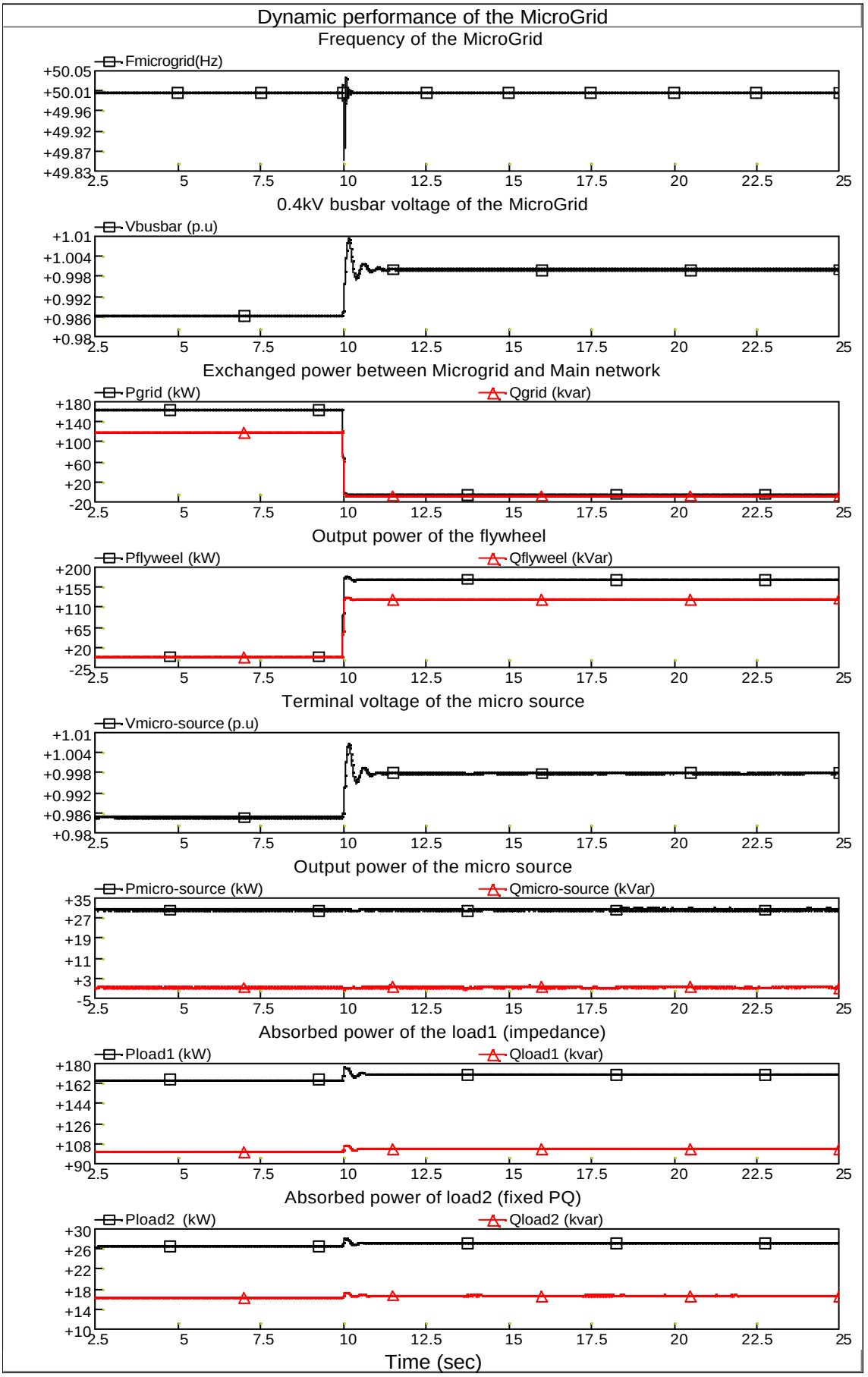

Figure A4 Dynamic performance of the MicroGrid when the flywheel, represented by a controllable AC voltage source, uses Frequency/Voltage control during islanded mode

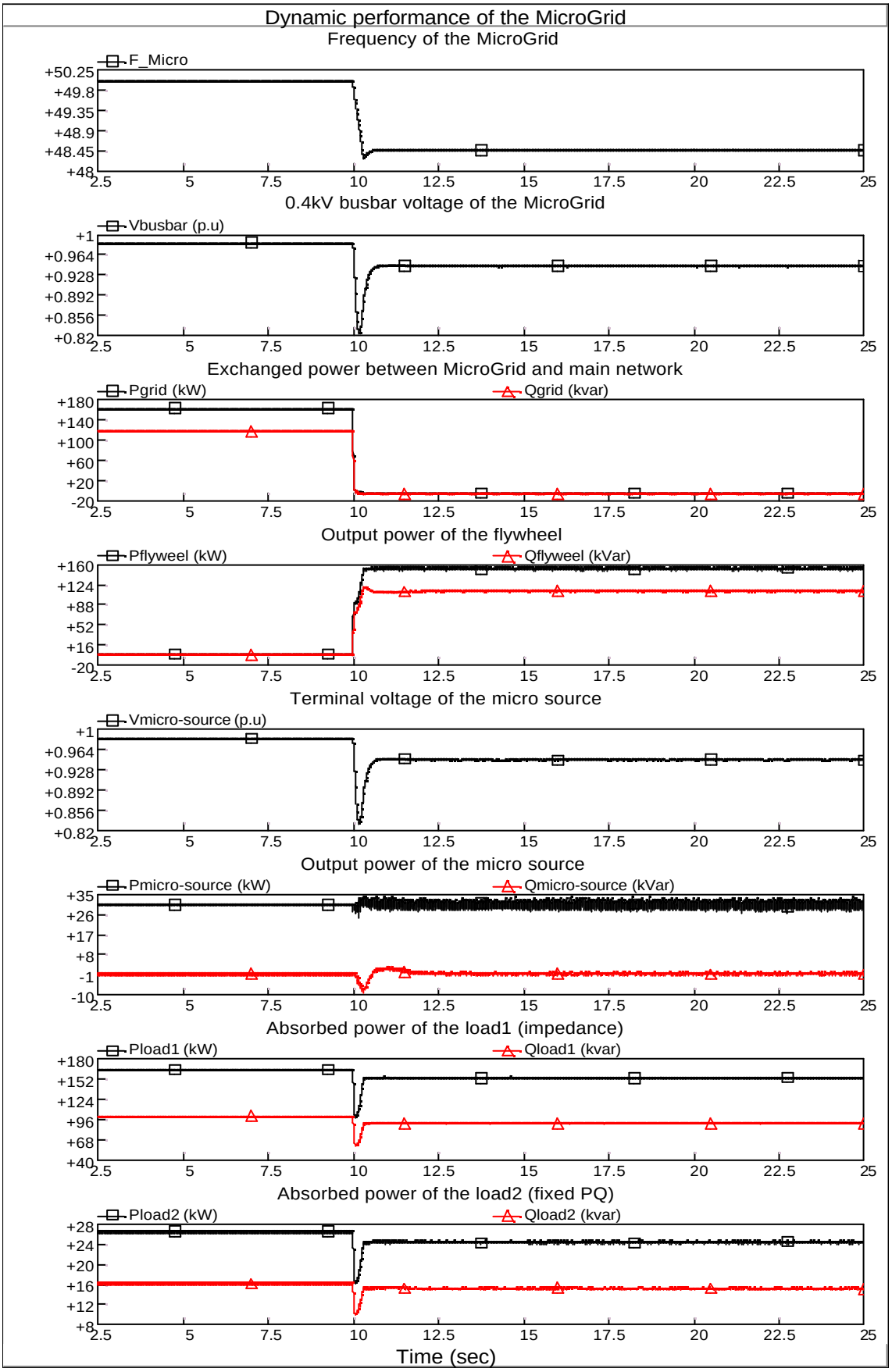

Figure A5 Dynamic performance of the MicroGrid when the flywheel, represented by a controllable DC voltage source, uses Droop control during islanded mode

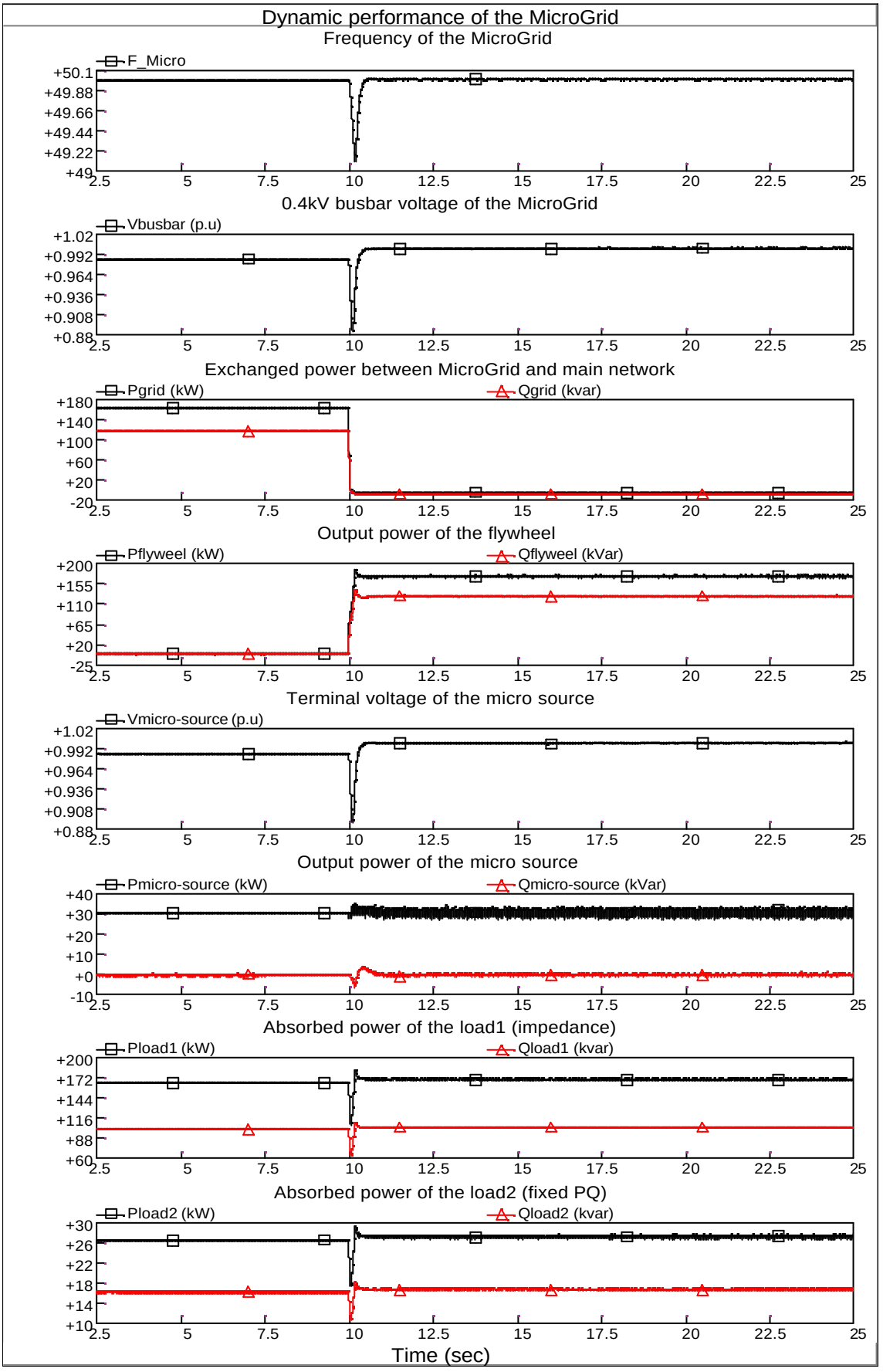

Figure A6 Dynamic performance of the MicroGrid when the flywheel, represented by a controllable DC voltage source, uses Frequency/Voltage control during islanded mode

3. Conclusions

Simulation results show that the dynamic performances of the MicroGrid produced from the simple controllable AC and DC voltage source representations of the flywheel are similar to that from the full STATCOM-BES model. For a simple application of the flywheel to the MicroGrid, the flywheel can be represented by a controllable AC voltage source or a controllable DC voltage source.

Document Information

Title	Local Frequency Control of a Microgrid
Date	30th September 2004
Version	Draft Issue No 1
Task(s)	

Authors:	Xueguang Wu, Nilanga Jayawarna, Yibin Zhang, Nick Jenkins

Access:	
Project Consortium (for the actual version) European Commission , PUBLIC (for final version)	
Status:	
	Draft Version Final Version (internal document) **X** Submission for Approval (deliverable) Final Version (deliverable, approved on.)

DE2-Appendix IV

MICROGRIDS

Large Scale Integration of Micro-Generation

To Low Voltage Grids

WORK PACKAGE D

TASK TD2

Local Frequency Control of a MicroGrid

Draft Issue No 1

30 September 2004

Xueguang Wu, Nilanga Jayawarna, Yibin Zhang, Nick Jenkins

UMIST

Contents

1. Introduction

Micro-scale distributed generators (DGs), or micro sources, are being applied increasingly to provide electricity for the expanding energy demands in the network. The development of micro DGs also helps to reduce greenhouse gas emissions and increase energy efficiency.

The MicroGrid usually consists of a cluster of micro DGs, energy storage systems (e.g. flywheel) and loads, operating as a single controllable system. The voltage level of the MicroGrid at the load is about 400 Volts or less. The architecture of the MicroGrid is formed to be radial with a few feeders. It often provides both electricity and heat to the local area. It can be operated in both grid-connected mode and islanded mode

The micro DGs existing in the distribution network mainly use rotating machines. They are directly connected to the grid to supply electric power. However, the new technologies (e.g. micro gas turbine, fuel cells, photovoltaic system and several kinds of wind turbines) proposed to be used in MicroGrid are not suitable for supplying energy to the grid directly [Barsali, 2002]. They have to be interfaced with the grid through an inverter stage. Thus, the use of power electronic interfaces in the MicroGrid leads to a series of challenges in the design and operation of the MicroGrid. One of the main challenges is local frequency control of the MicroGrid operated in islanded mode.

It is well known that frequency has a strong coupling with active power in the network [Kundur, 1994]. The value of the frequency is a function of the difference between generation and demand plus network losses. If demand increases, the frequency will fall unless there is a matching increase in generation. If generation increases, the frequency will rise unless there is a matching increase in demand. The rate of change of frequency depends on the inertia of the system. The larger the inertia, the smaller the rate of change. During a disturbance, the frequency of the MicroGrid may change rapidly due to the low inertia (or zero inertia) present in the MicroGrid. In grid-connected mode, the frequency of the MicroGrid is maintained within a tight range (50±0.2Hz) by the main network. However, in islanded mode,

with relatively few micro sources, the local frequency control of the MicroGrid is not straightforward.

Obviously, the control of the micro sources and the flywheel is very important to maintain the frequency of the MicroGrid during islanded operation. The controllers of the micro sources and flywheel inverters respond in milliseconds. For basic operation of the MicroGrid, the controllers should use only local information to control the flywheel and micro sources. Communication between the micro sources and flywheel is unnecessary. For a micro source, the inverter should have plug and play capabilities [Lasseter, 2002]. Plug and play implies that a micro source can be added to the MicroGrid without any changes to the control of the units, which are already a part of the network. For the flywheel, the inverter should be able to respond to the change of load in a predetermined manner automatically.

Possible control strategies of the micro sources and the flywheel may be: (a) PQ control (fixed power control), (b) Droop control and (c) Frequency/Voltage control. PQ control is adopted so that the micro sources and the flywheel run on constant power output. The electricity, generated by the micro source, may be constant because of the need of the associated thermal load. In addition, the power output of the flywheel may be fixed at zero when the MicroGrid is operated in grid-connected mode. However, as PQ control delivers a fixed power output, it makes no contribution to local frequency control of the MicroGrid.

Therefore, the control scheme of the flywheel has to be changed from PQ control to Droop control or Frequency/Voltage control during islanded operation. Droop control is similar to the function of Primary frequency control in a conventional synchronous generator. The frequency of the MicroGrid can be restored to a steady state value determined by the droop characteristic. Frequency/Voltage control is similar to the function of Secondary frequency control in the conventional synchronous generator. The frequency and voltage of the MicroGrid can be brought back to the normal values (e.g. f = 50Hz and V = 1.0 p.u.) after a disturbance.

In this report, three control strategies (PQ control, Droop control and Frequency/Voltage control) for the local frequency control of the MicroGrid are

proposed. Based on two MicroGrid models (synchronous generator representation and STATic Synchronous Shunt COMpensator with battery energy storage, STATCOM-BES, representation) in PSCAD/EMTDC, these control schemes are implemented and tested. Simulations are demonstrated and discussed with supporting PSCAD/EMTDC results.

2. Local frequency control of the MicroGrid

The unique nature of the MicroGrid determines that the local frequency control of the MicroGrid may be: (a) PQ control (fixed active and reactive power control), (b) Droop control and (c) Frequency/Voltage control. In modelling of the MicroGrid, the micro sources and flywheel could be represented by the synchronous generators or STATCOM-BES. Thus, for different representation of the MicroGrid, the implementation of the control schemes may be different.

(1) MicroGrid represented by the synchronous generator

In this representation, the micro sources and flywheel of the MicroGrid are represented by synchronous generators. The local frequency control scheme of the MicroGrid is as follows:

(a) PQ control

Using this control, the outputs of the micro sources and the flywheel are fixed at their constant values (settings). The PQ control consists of a P controller and a Q controller.

The P controller adjusts the frequency-droop characteristic of the generator up or down to maintain the active power output of the generator at a constant value (Pdes, desired active power) when the frequency is changed. Figure 1 shows the effect of frequency-droop characteristic adjustment.

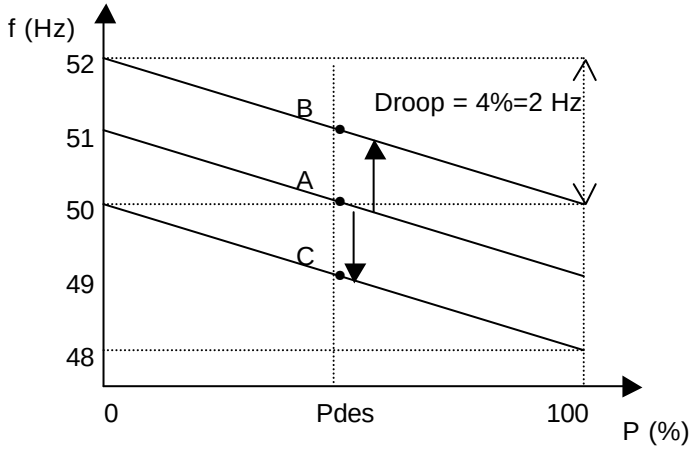

Figure 1 Effect of the frequency-droop characteristic adjustment

At output Pdes, characteristic A corresponds to 50Hz frequency of the grid, characteristic B corresponds to 51Hz frequency of the grid and characteristic C corresponds to 49Hz frequency of the grid. For a frequency change, the power output of the generator can be maintained at the desired value by moving the droop characteristic up or down. A typical droop of the frequency characteristic is about 4% [Kundur, 1994].

The function of a P controller is similar to the speed control of a synchronous generator with a supplementary control loop, as shown in Figure 2.

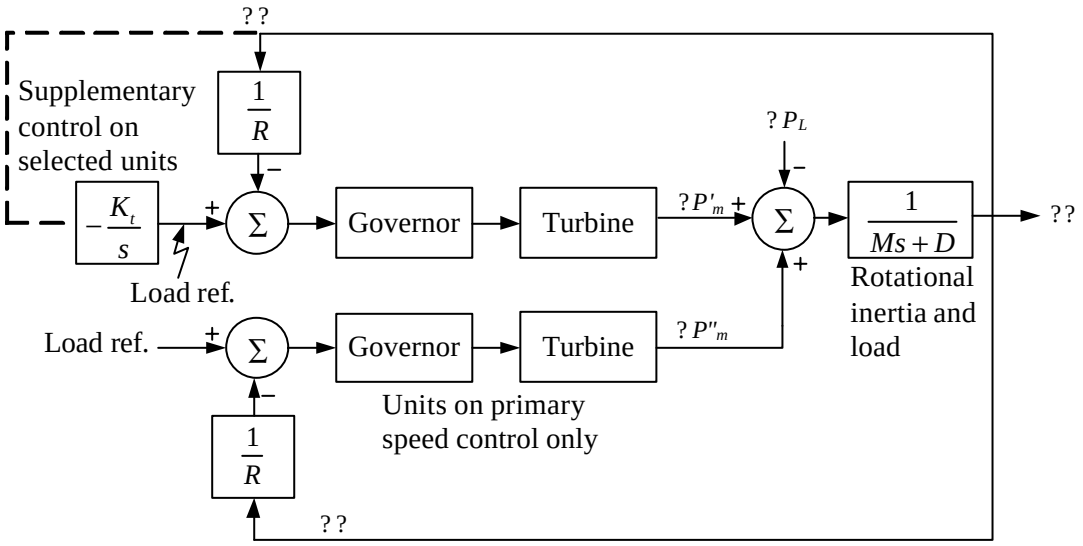

Figure 2 Speed control of synchronous generator with a supplementary control loop [Kundur, 1994]

The movement of the characteristic is achieved through adding an integral control loop, which acts on the load reference settings, to the speed droop control of the generator. The integral control action ensures that the output power of the generator is fixed at a constant value (setting).

Figure 3 shows the configuration of P controller for a synchronous generator representation of the MicroGrid.

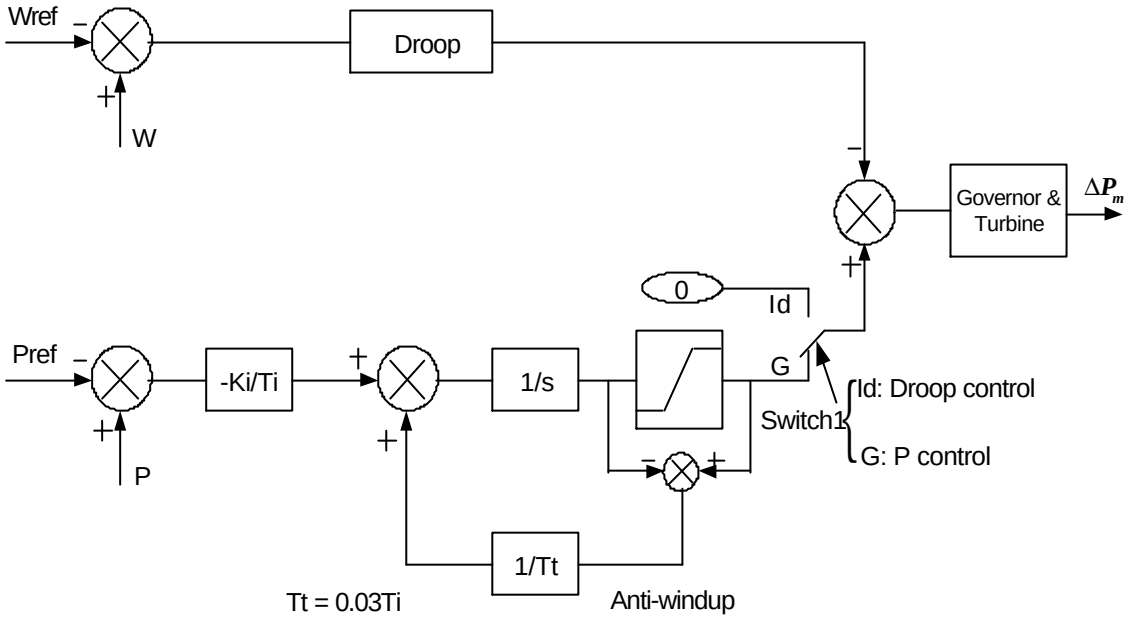

Figure 3 Configuration of P controller for a synchronous generator representation

Similarly, the Q controller adjusts the voltage-droop characteristic of the generator by moving the droop lines upon or down to maintain the reactive power output of the generator at a constant value (Qdes, desired reactive power) when the voltage is changed. Figure 4 shows the effect of voltage-droop characteristic adjustment.

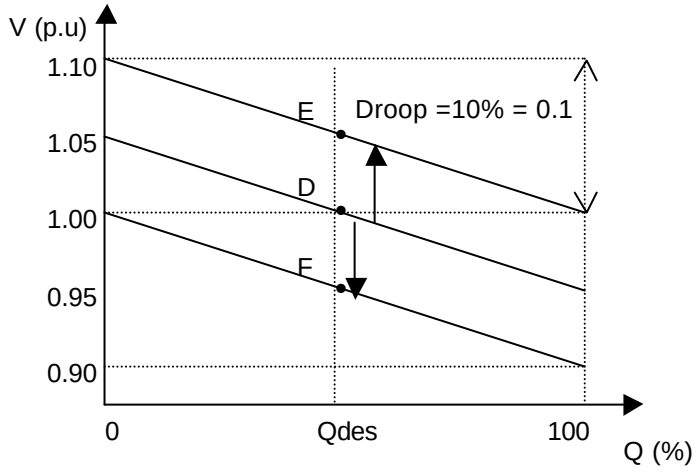

Figure 4 Effect of the voltage-droop characteristic adjustment

At output Qdes, characteristic D corresponds to 1.00 voltage of the network, characteristic E corresponds to 1.05 voltage of the grid and characteristic F corresponds to 0.95 voltage of the grid. For a voltage change, the reactive power output of the generator is maintained at the desired value Qdes by shifting the voltage-droop characteristic up or down. A typical droop of voltage characteristic is about 10% [Kundur, 1994].

Figure 5 shows the implementation of Q controller for a synchronous generator representation.

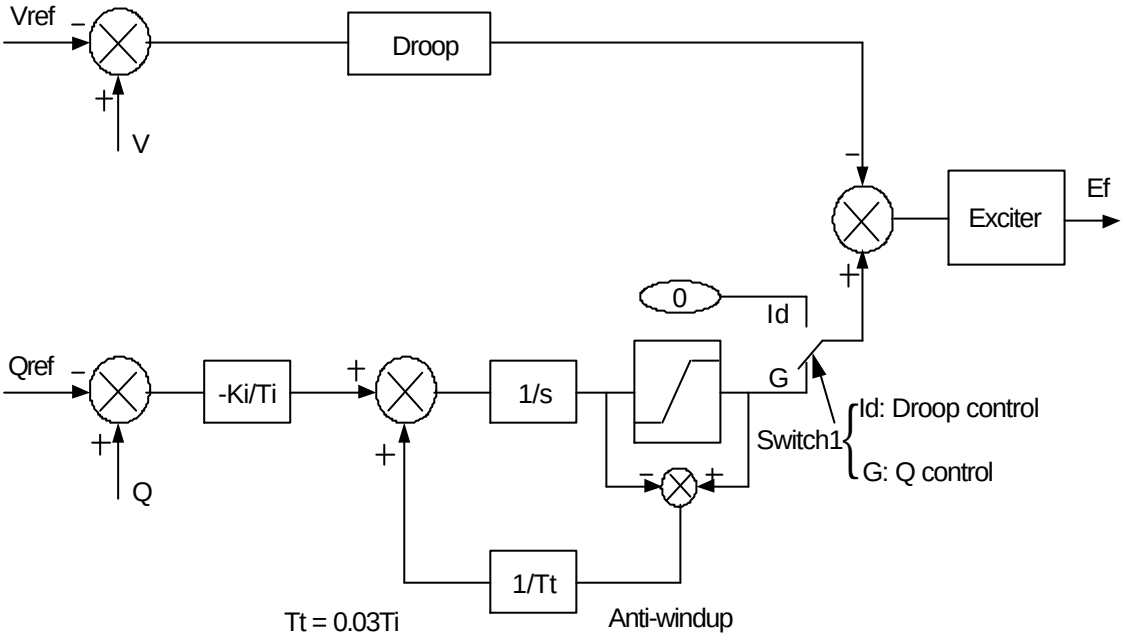

Figure 5 Implementation of Q controller for a synchronous generator representation

(b) Droop control

When the MicroGrid is operated in islanded mode, the control scheme of the micro sources is still PQ control. However, the control scheme of the flywheel should be changed to enable local frequency control. The flywheel may use Droop control. The power output of the flywheel is regulated according to the predetermined droop characteristics. Droop control consists of a frequency-droop controller and a voltage-droop controller.

Figure 6 shows a frequency-droop characteristic, which would be used in frequency-droop controller.

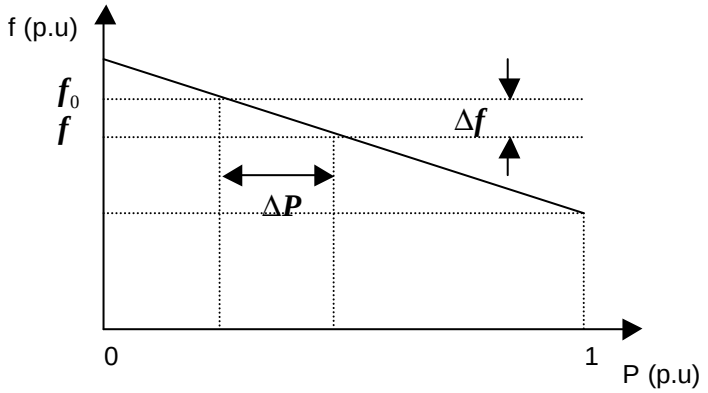

Figure 6 A typical frequency-droop characteristic

The value of droop R_f is a ratio of frequency deviation Δf to change in active power output ΔP. It can be expressed in percentage as equation (1).

$$R_f = \frac{\Delta f(p.u)}{\Delta P(p.u)} \times 100\% \qquad (1)$$

Figure 7 also shows a typical voltage-droop characteristic used in the voltage-droop controller.

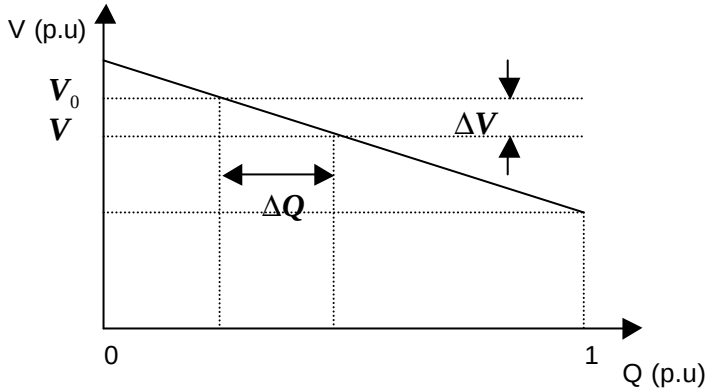

Figure 7 A typical voltage-droop characteristic

The value of droop R_V is a ratio of voltage deviation ΔV to change in reactive power output ΔQ. It can be expressed in percentage as equation (2).

$$R_V = \frac{\Delta V(p.u)}{\Delta Q(p.u)} \times 100\% \qquad (2)$$

The implementation of Droop control can be achieved by changing Switch1 from G to Id in Figures 3 and 5.

(c) Frequency/Voltage control

With droop control action, a load change in the MicroGrid will result in steady-state frequency and voltage deviations, depending on the droop characteristics and Frequency/Voltage sensitivity of the load. The flywheel will contribute to the overall change in generation. Restoration of the Frequency/Voltage of the MicroGrid to their normal values requires a supplementary action to adjust the output of the flywheel. The basic means of the local frequency control of the MicroGrid is through regulating the output of the flywheel. As the load of the MicroGrid changes continually, it is necessary to automatically change the output of the flywheel.

The objective of the frequency control is to restore the frequency to its normal value. This is accomplished by moving the frequency-droop characteristic left or right to maintain the frequency at a constant value. The frequency control adjusts the output of the flywheel to restore the frequency of the MicroGrid to normal (e.g. 50Hz). Figure 8 shows the effect of this adjustment.

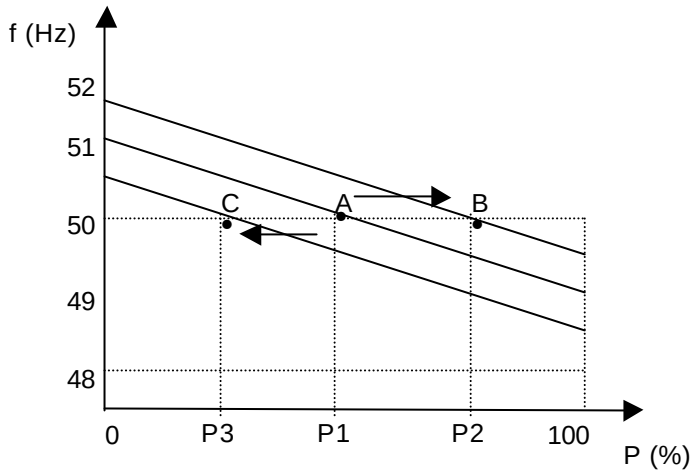

Figure 8 Effect of the adjustment on the frequency-droop characteristic

At 50Hz, characteristic A corresponds to P1 active power output of the flywheel, characteristic B corresponds to P2 active power output and characteristic C corresponds to P3 active power output. The frequency of the MicroGrid is fixed at a constant value (50Hz) by moving the frequency-droop characteristic left or right.

The implementation of Frequency control is similar to P control in Figure 3. But, the connection of the supplementary control loop needs to be changed from Gp of

Switch2 to If and from Id of Switch1 to G. Figure 9 shows the layout of Frequency control for a synchronous generator representation.

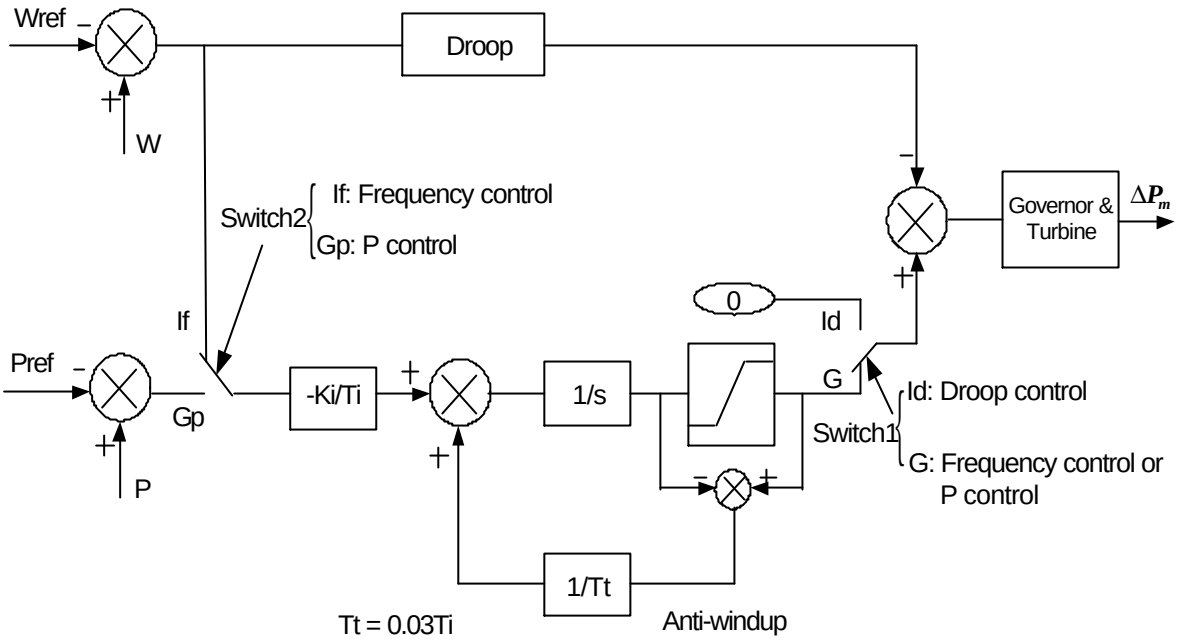

Figure 9 Layout of Frequency control for a synchronous generator representation

Similarly, the voltage control adjusts the voltage-droop characteristic left or right to maintain a constant voltage when the voltage of the MicroGrid is changed. Thus, the voltage of the MicroGrid is fixed at a desired value (e.g. 1.0p.u). The effect of this adjustment is shown in Figure 10.

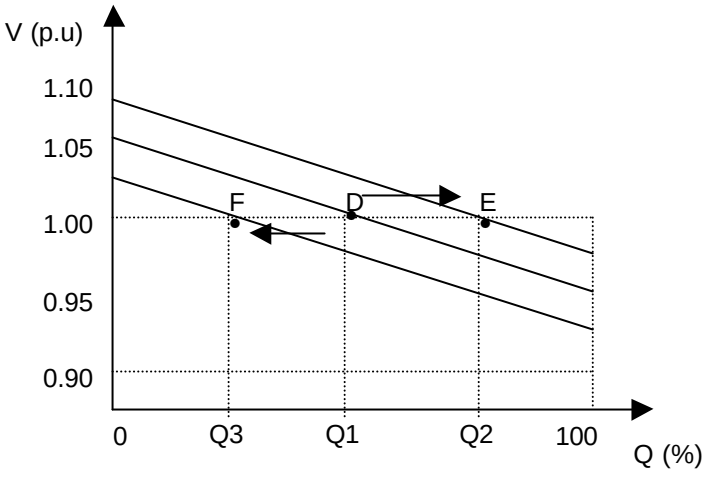

Figure 10 Effect of the adjustment on the voltage-droop characteristic

At 1.0 p.u voltage, characteristic D corresponds to Q1 reactive power output of the flywheel, characteristic E corresponds to Q2 reactive power output and characteristic F corresponds to Q3 reactive power output. The voltage of the MicroGrid is fixed at a constant value (1.0 p.u) by moving the voltage-droop characteristic left or right.

Figure 11 shows the implementation of Voltage control for a synchronous generator representation.

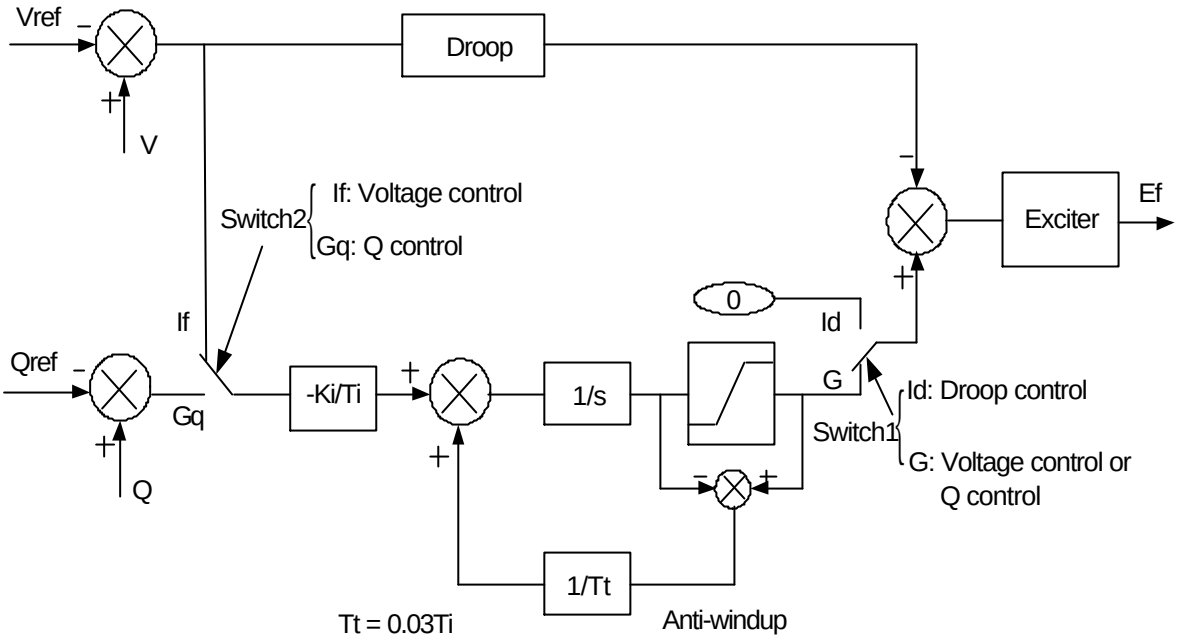

Figure 11 Implementation of Voltage control for a synchronous generator representation

(2) MicroGrid represented by the STATCOM-BES

In this representation, the micro sources and flywheel of the MicroGrid are represented by the STATCOM-BES. The local frequency control schemes of the MicroGrid are PQ control, Droop control and Frequency/Voltage. Figure 12 shows the implementation of these control strategies of the flywheel in a STATCOM-BES.

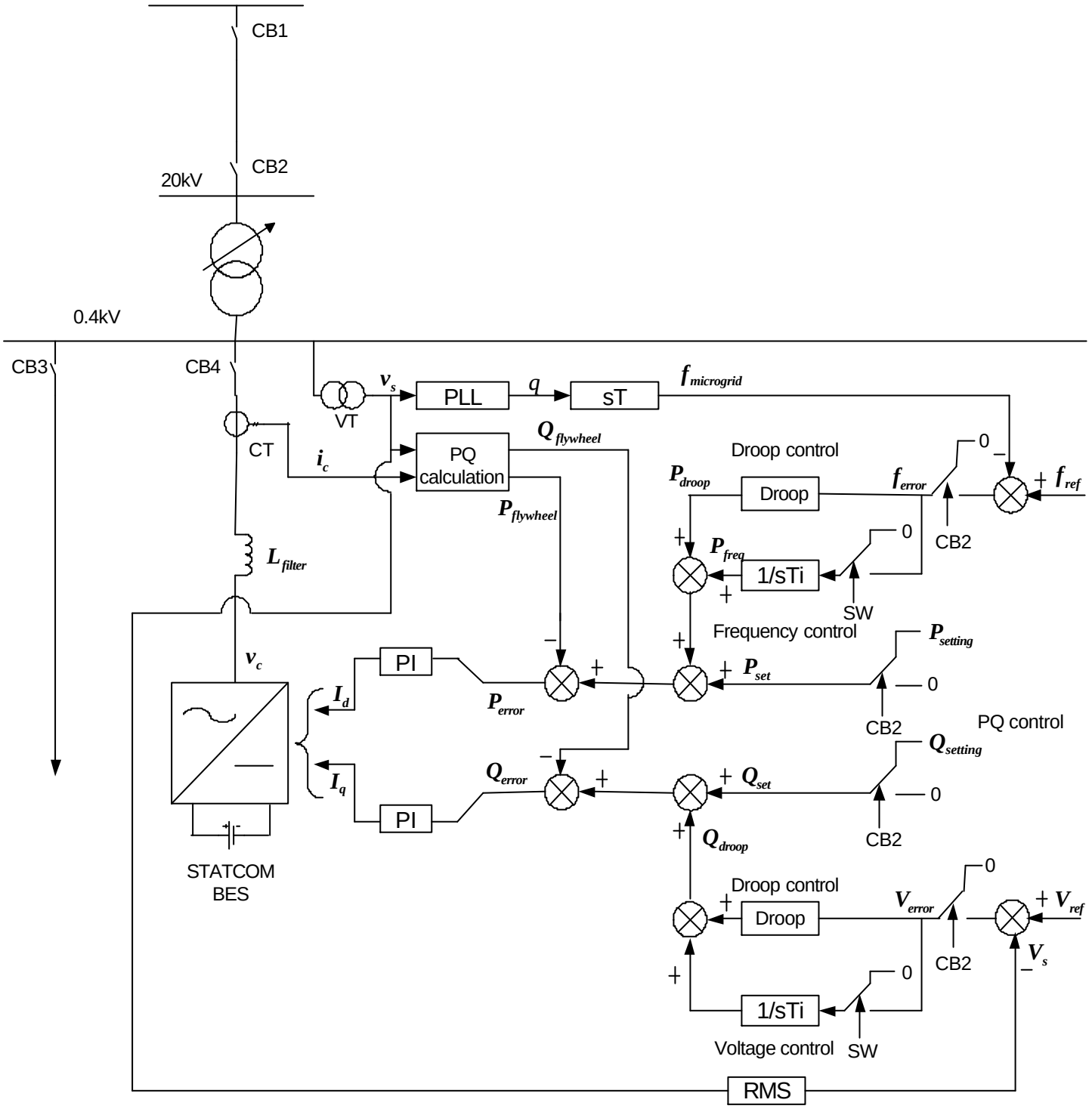

Figure 12 Control schemes of the flywheel represented by a STATCOM-BES

During grid-connected mode, the state of circuit breaker CB2 is closed. The control schemes of the micro source and flywheel are PQ control. The droop output P_{droop} and Q_{droop} of Droop control are zero. Thus, the reference values of the active and reactive powers are $P_{set} = P_{setting}$ and $Q_{set} = Q_{setting}$, acting on PQ control.

After disconnection of the MicroGrid from the main network, during islanded mode, CB2 is open. The outputs P_{set} and Q_{set} of the PQ control loop are set to zero. The reference values of the active and reactive powers are P_{droop} and Q_{droop}, acting on Droop control. The control scheme of the flywheel is thus switched from PQ control to Droop control.

If the inputs of PI controllers of the STATCOM are taken from the errors of the frequency and voltage ($f_{error} = f_{ref} - f_{microgrid}$ and $V_{error} = V_{ref} - V_s$), the control scheme of the flywheel will be Frequency/Voltage control.

3. Assumptions in this study

It is assumed that the micro sources and the flywheel of the MicroGrid are represented by the synchronous generators and the STATCOM-BES, respectively. Two representation modes of the MicroGrid are implemented in PSCAD/EMTDC and shown in Figures 13 and 14.

Figure 13 shows a simple MicroGrid mode, in which the micro source and the flywheel are represented by the synchronous generators.

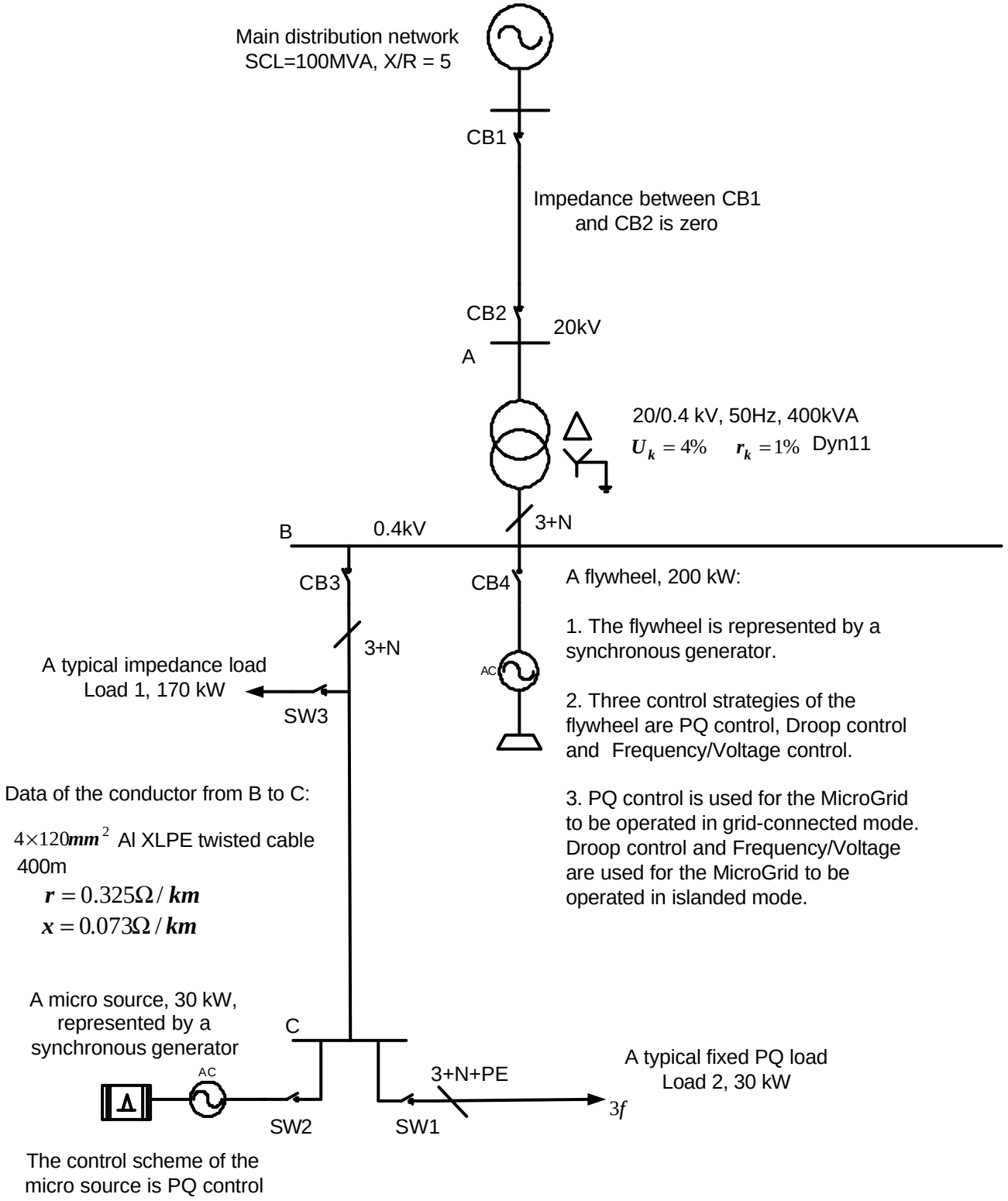

Figure 13 A simple MicroGrid model represented by the synchronous generators

Figure 14 shows a simple MicroGrid mode, in which the micro source and the flywheel are represented by the STATCOM-BES.

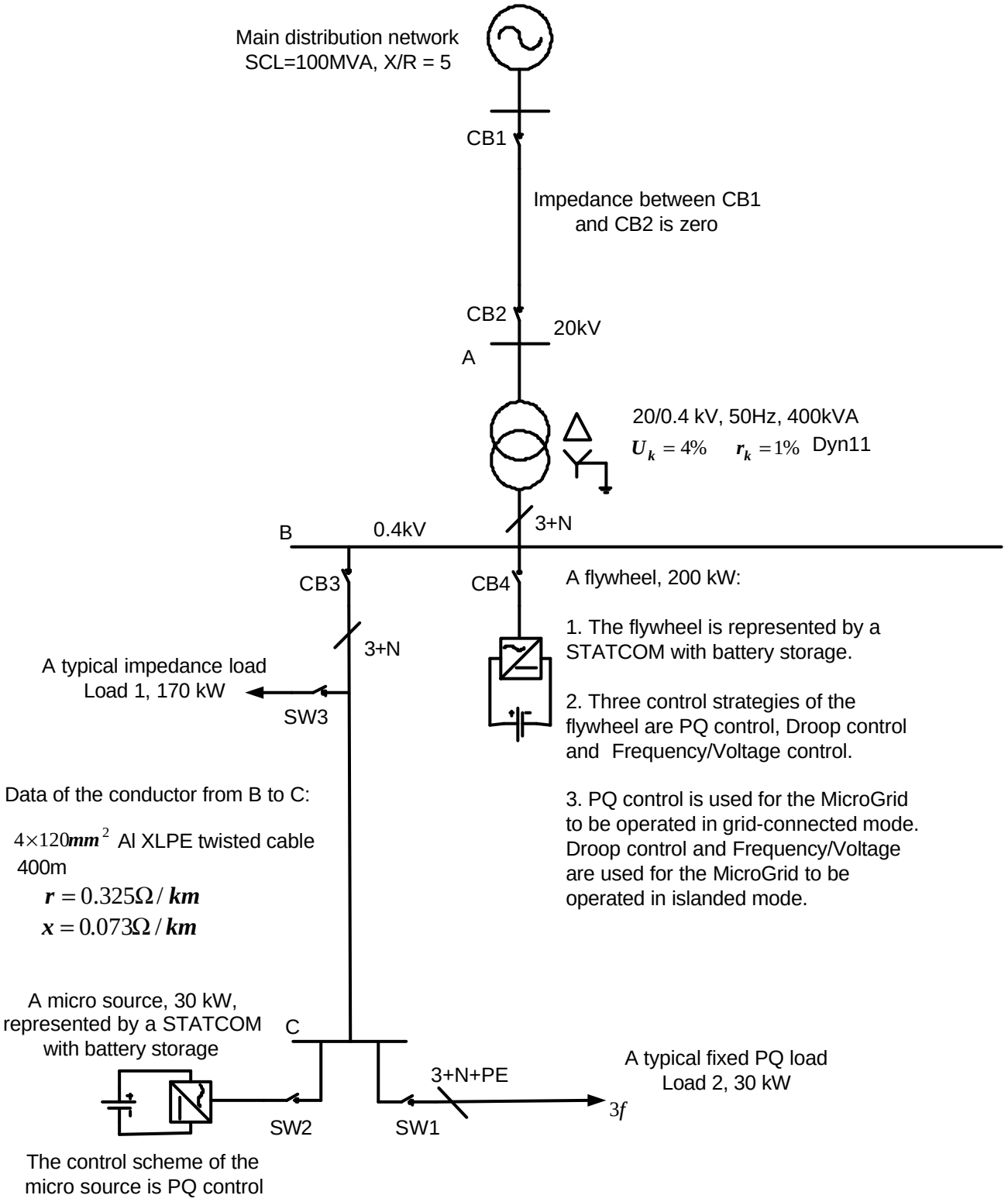

Figure 14 A simple MicroGrid model represented by the STATCOM-BES

For both representations of the MicroGrid above, the fault level at the 20kV main distribution network is 100MVA, with a X/R ratio of 5. One transformer (400kVA, 20/0.4kV) is installed at the substation between the main network and the MicroGrid. The impedance of the transformer is 0.01+j0.04 p.u. The MicroGrid consists of a flywheel and a feeder. The flywheel is connected to 0.4kV busbar, which is near to the substation. The capacity of the flywheel is 200kW (assuming the flywheel supplies 4MJ energy for 20 seconds continuously). The feeder is connected to a micro source and two loads (Load 1 and Load 2) through 400 meters of ALXLPE twisted cable ($4\times120mm^2$). The impedance of the cable is 0.325+j0.073 ohms per kilometre [Bungay, 1990]. The capacity of the micro source is 30kW. Load 1 is an impedance load, with capacity of 170kW. Load 2 is a fixed PQ load, with capacity of 30kW.

In the synchronous generator representation, the parameters of the synchronous generators are the typical average values of the synchronous turbine generator constants [Glover, 2002]:

- Synchronous d-axis reactance (X_d): 1.10 [p.u];
- Synchronous q-axis reactance (X_q): 1.08 [p.u];
- Transient d-axis reactance (X'_d): 0.23 [p.u];
- Transient q-axis reactance (X'_q): 0.23 [p.u];
- Sub-transient d-axis reactance (X''_d): 0.12 [p.u];
- Sub-transient q-axis reactance (X''_q): 0.15 [p.u];
- Negative sequence reactance (X_2): 0.13 [p.u];
- Zero sequence reactance (X_0): 0.05 [p.u];
- Stator armature resistance (R_a): 0.005 [p.u];
- Transient time constant (T'_{do}): 5.60 [sec.];
- Sub- transient time constant ($T''_d = T''_q$): 0.035 [sec.];
- Inertia constant (H): 1.05 [MW/MVA].

In the STATCOM-BES representation, the ratings of the STATCOMs-BES are the same as the capacities of the micro source and flywheel, 30kW and 200kW.

The control scheme of the micro source is PQ control at all times. The control strategies of the flywheel are PQ control, Droop control or Frequency/Voltage control. The flywheel uses PQ control only when the MicroGrid is operated in grid-connected mode. During islanded mode, the control of the flywheel is switched from PQ control to Droop control or Frequency/Voltage control.

4. Simulation results

Based on two representations of the MicroGrid (synchronous generator representation and STATCOM-BES representation), the dynamic performances of the MicroGrid are investigated and demonstrated in PSCAD/EMTDC under three control strategies (PQ control, Droop control and Frequency/Voltage control) of the flywheel. In all cases, circuit breaker CB2 is tripped at 10 seconds. Following the trip of CB2, the MicroGrid is disconnected from the main network and operated in islanded mode.

(1) For the synchronous generator representation

The MicroGrid mode, used in PSCAD/EMTDC modelling, is shown in Figure 13. The control scheme of the micro source is PQ control. The control strategies of the flywheel are PQ control, Droop control and Frequency/Voltage control.

(a) PQ control

Figure 15 shows the dynamic performance of the MicroGrid when the flywheel uses PQ control during islanded mode. The control schemes of the micro source and the flywheel are PQ control. The implementation of PQ control is shown in Figures 3 and 5.

Obviously, the flywheel makes no contribution to the local frequency control of the MicroGrid. The frequency and voltage of the MicroGrid are unstable. The voltage of the MicroGrid collapses so that the MicroGrid can not be operated in islanded mode.

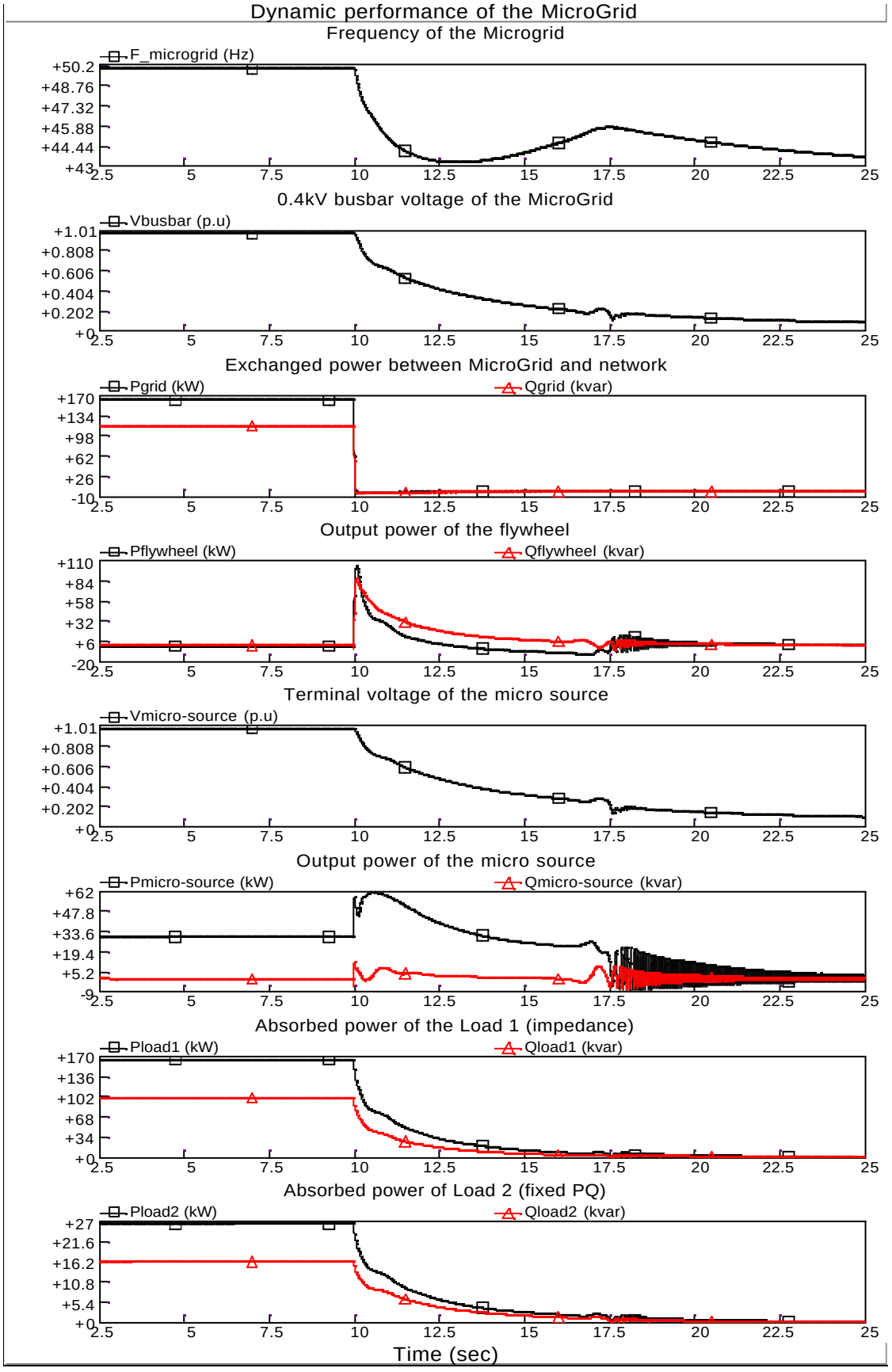

Figure 15 Dynamic performance of the MicroGrid (using synchronous generator representation) when the flywheel uses PQ control during islanded mode

(b) Droop control

Figure 16 shows the dynamic performance of the MicroGrid when the flywheel uses Droop control (shown in Figures 3 and 5, changes Switch1 from G to Id) during islanded mode. The control scheme of the micro source is still PQ control.

After disconnection of the MicroGrid from the main network, the output of the micro source is still retained at 30kW. But, the output of flywheel is changed from zero to the value of 149kW+j110kVar according to the droop settings ($\boldsymbol{R}_f = 4\%$ and $\boldsymbol{R}_v = 10\%$). Thus, the frequency and voltage of the MicroGrid are restored to the steady state values (48.35Hz and 0.9325p.u), associated with the droop characteristics.

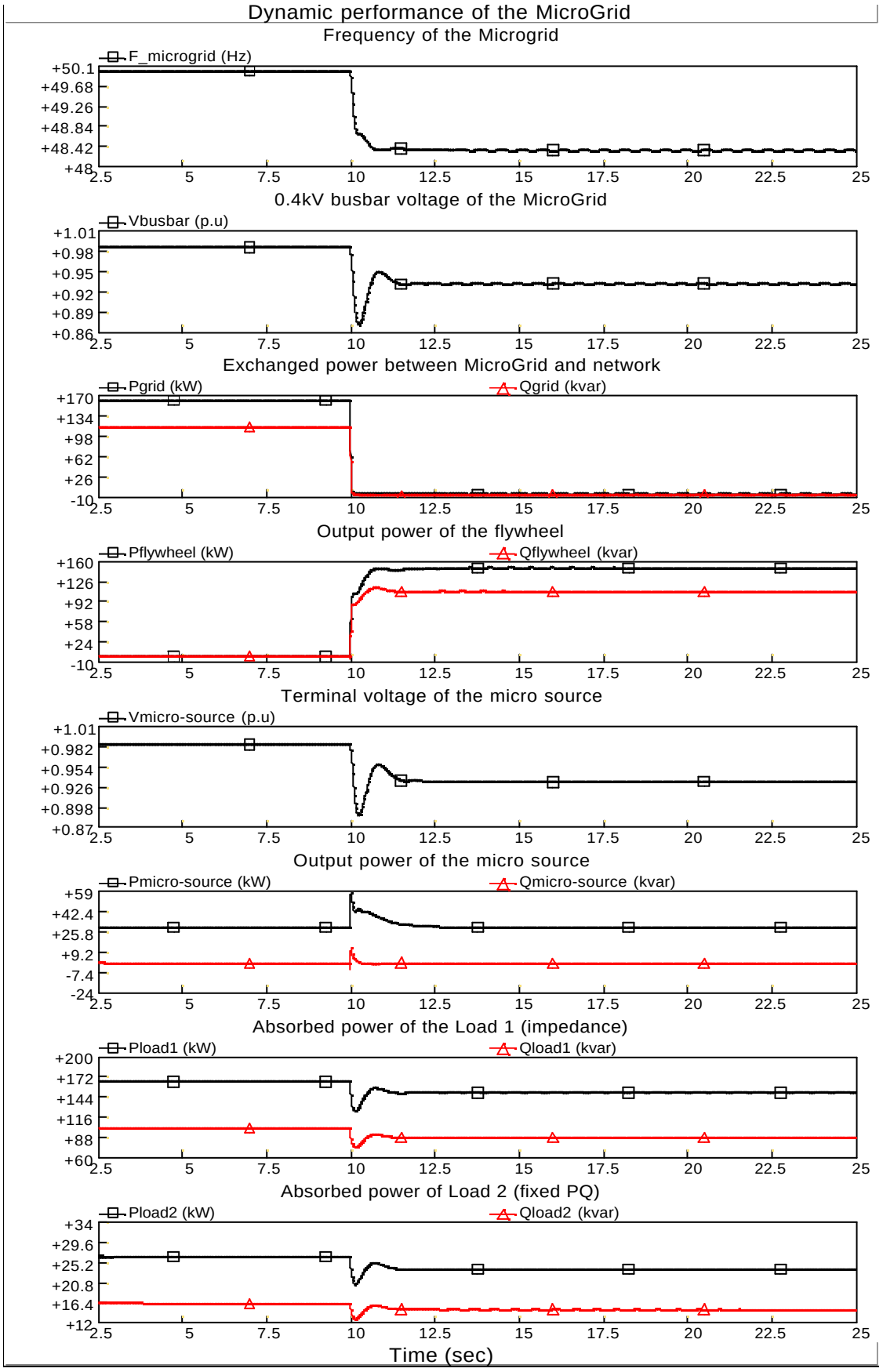

Figure 16 Dynamic performance of the MicroGrid (using synchronous generator representation) when the flywheel uses Droop control during islanded mode

(c) Frequency/Voltage control

Figure 17 shows the dynamic performance of the MicroGrid when the flywheel uses Frequency/Voltage control (shown in Figures 9 and 11) during islanded mode. The control of the micro source is still PQ control. The control of the flywheel is switched from PQ control to Droop control.

During islanded mode of the MicroGrid, the output of the micro source is maintained at a constant value of 30kW. However, the output of the flywheel is changed from zero to the value of 171kW+j127kVar. Consequently, the frequency and voltage of the MicroGrid are both brought back to the normal values (50Hz and 1.0p.u). It should be noted that the energy export of the flywheel using Frequency/Voltage control is larger than using Droop control.

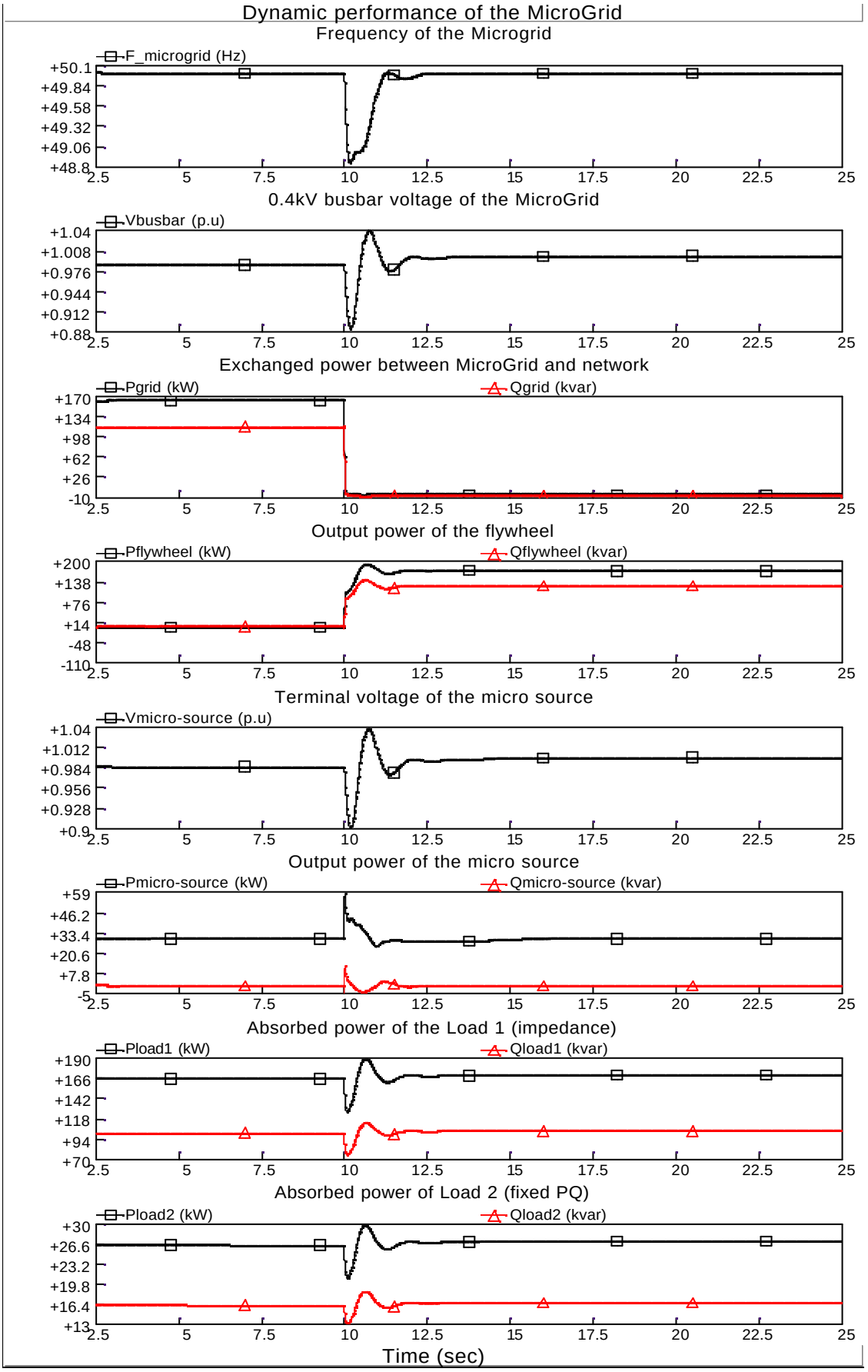

Figure 17 Dynamic performance of the MicroGrid (using synchronous generator representation) when the flywheel uses Frequency/Voltage control during islanded mode

(2) For the STATCOM-BES representation

The MicroGrid mode, used in PSCAD/EMTDC modelling, is a STATCOM-BES representation, as shown in Figure 14. The implementation of three control schemes (PQ control, Droop control and Frequency/Voltage control) is shown in Figure 12.

Figures 18, 19 and 20 show the dynamic performances of the MicroGrid when the flywheel uses PQ control, Droop control and Frequency/Voltage control during islanded mode, respectively. The deviations of the frequency and voltage depend on the mismatch between generation and demand in the MicroGrid.

Comparisons with Figures 15, 16 and 17 show that the simulation results of the STATCOM-BES representation are similar to the synchronous generator representation. However, after a disturbance, the dynamic response of the frequency and voltage of the STATCOM-BES representation MicroGrid is faster than the synchronous generator representation due to a low or zero inertia value of the STATCOM- BES.

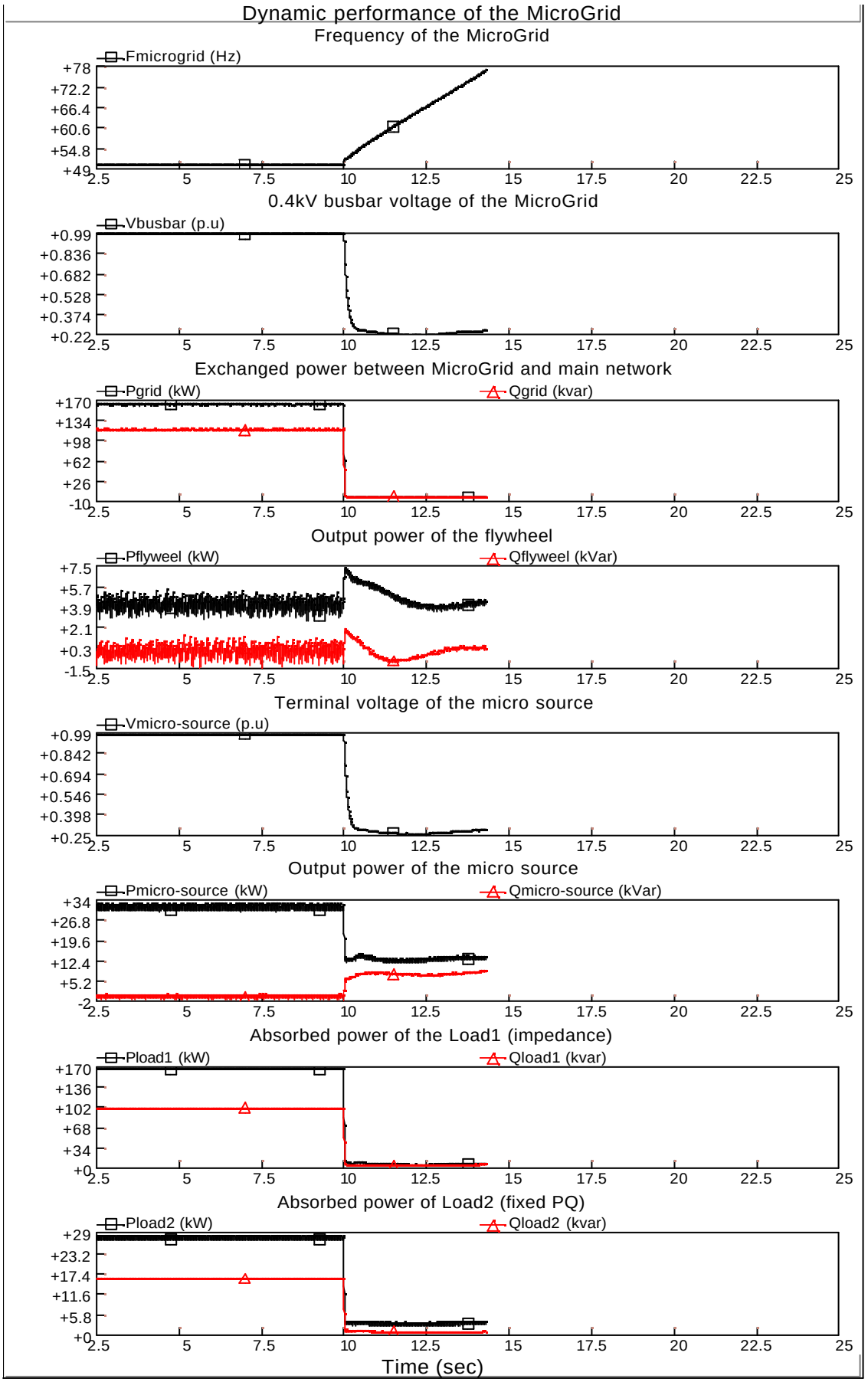

Figure 18 Dynamic performance of the MicroGrid (using STATCOM-BES representation) when the flywheel uses PQ control during islanded mode

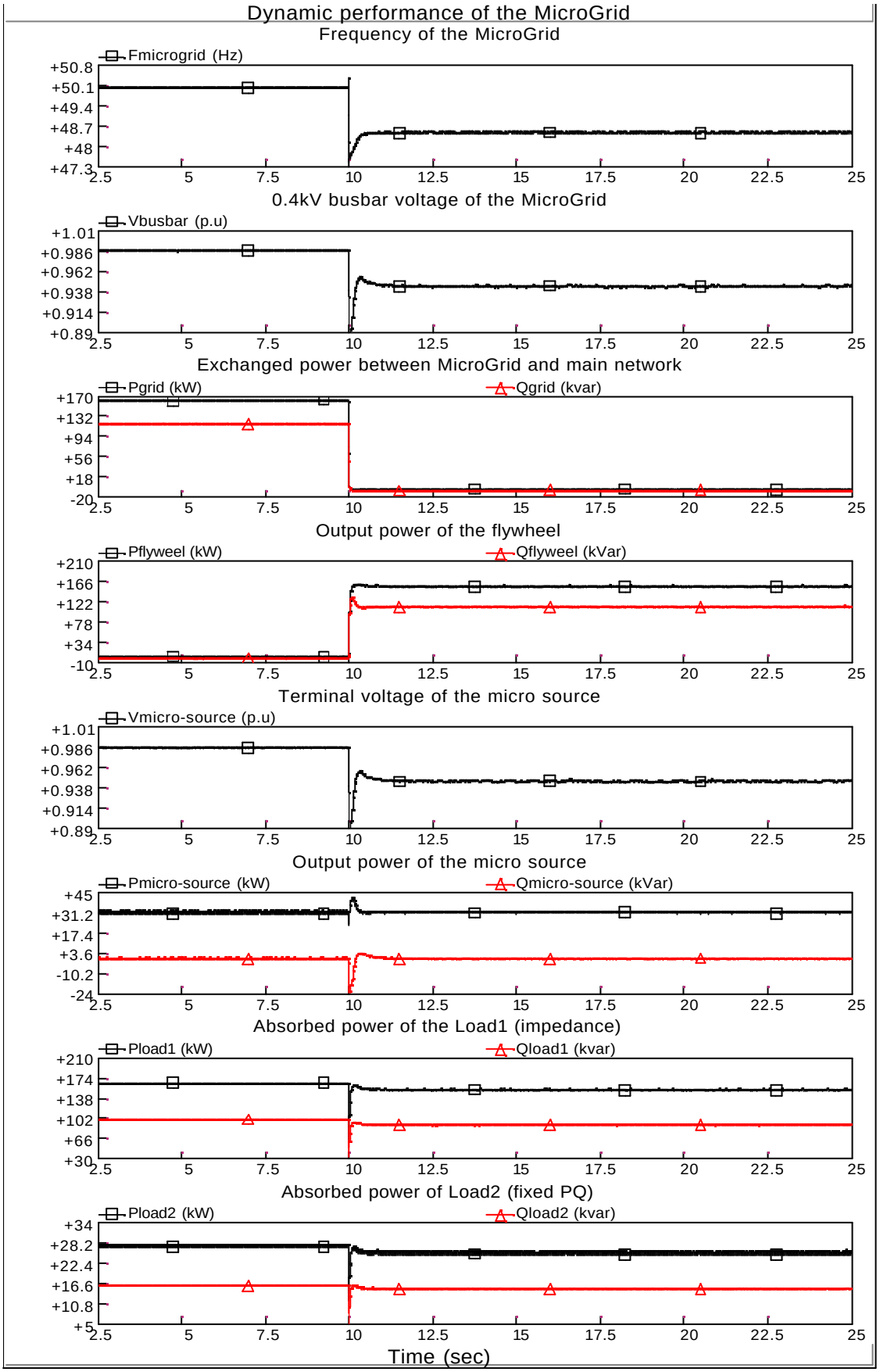

Figure 19 Dynamic performance of the MicroGrid (using STATCOM-BES representation) when the flywheel uses Droop control during islanded mode

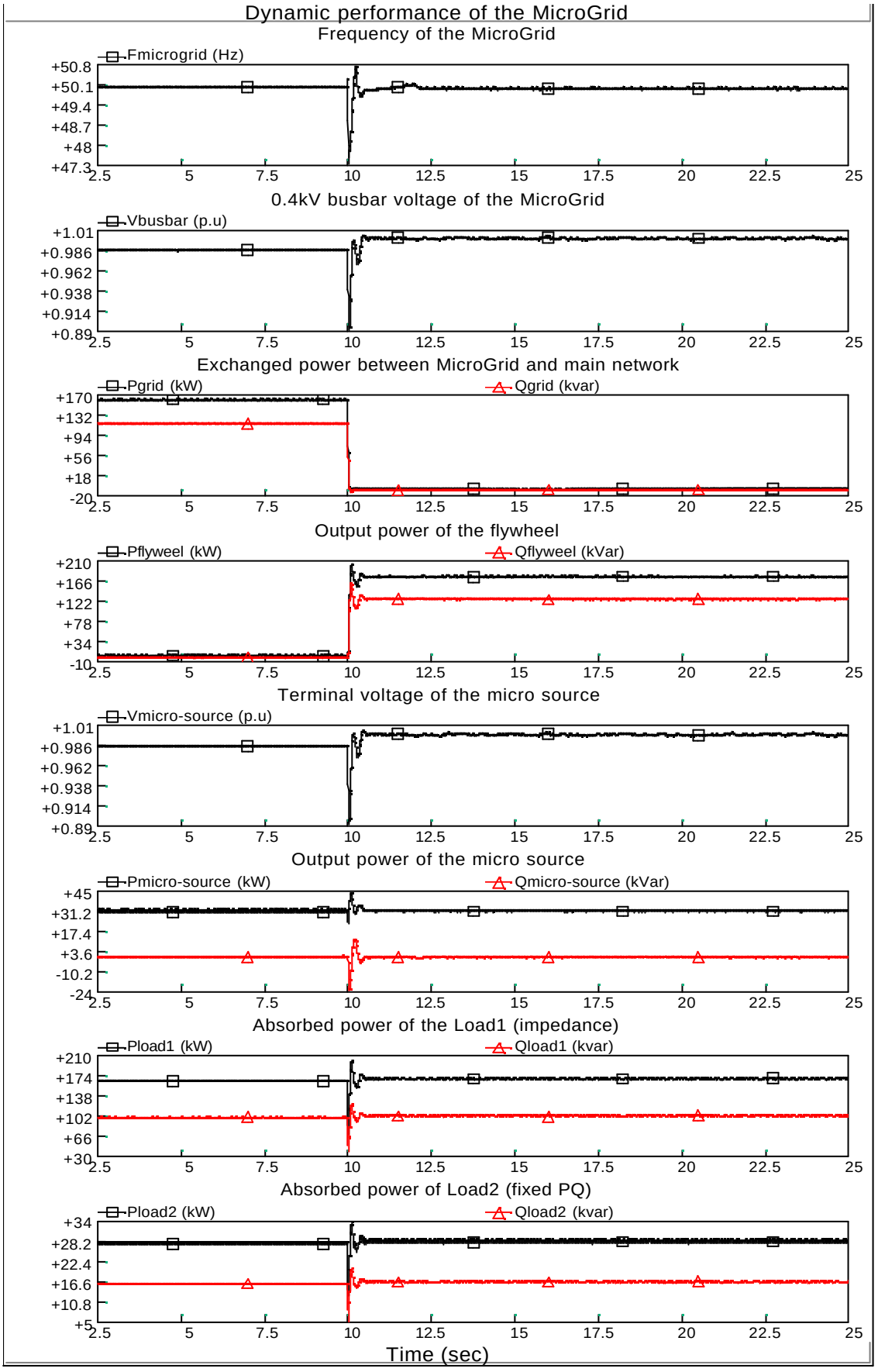

Figure 20 Dynamic performance of the MicroGrid (using STATCOM-BES representation) when the flywheel uses Frequency/Voltage control during islanded mode

5. Conclusions

With increasing penetration levels of the DGs, a number of MicroGrids will exist in the distribution network system in the near future. The safety and reliability of the MicroGrid are becoming more and more important. The unique nature of the MicroGrid requires local frequency control of the MicroGrid. The local frequency control of the MicroGrid can be mainly achieved through control of the flywheel. The possible control schemes of the flywheel for this purpose are PQ control, Droop control and Frequency/Voltage control. The control schemes are implemented in both synchronous generator representation and STATCOM-BES representation of the MicroGrid.

PQ control is only used by the flywheel while the MicroGrid is operating in grid-connected mode. The PQ control of the flywheel makes no contribution to the local frequency control of the MicroGrid due to its fixed active and reactive power outputs. After disconnection of the MicroGrid from the main network, during islanded mode, the control of the flywheel has to be switched from PQ control to Droop control or Frequency/Voltage control.

Droop control is similar to the Primary frequency control of a conventional synchronous generator. For a change of frequency in the MicroGrid, the active power output of the flywheel is regulated automatically according to a predetermined frequency-droop characteristic. The frequency of the MicroGrid can be restored to a steady state value determined by the droop.

Frequency/Voltage control is similar to the Secondary frequency control of a conventional synchronous generator. It controls the frequency and voltage of the MicroGrid at the normal values (e.g. f = 50Hz and V = 1.0 p.u.). The frequency and voltage of the MicroGrid can be brought back to their normal values after the disturbance. The frequency and voltage of the MicroGrid in which the flywheel uses Frequency/Voltage control are better than the flywheel use Droop control. However, it should be noted that the flywheel using Frequency/Voltage control has to supply higher active and reactive powers to the MicroGrid than using Droop control. The control capability of the flywheel in practice may be limited by its available capacity.

6. References

Barsali S., et al. (2002), Control Techniques of Dispersed Generators to Improve the Continuity of Electricity Supply, Power Engineering Society Winter Meeting, 2002, IEEE, Volume: 2, 27-37 January 2002.

Bungay E., McAllister D. (1990), Electric Cables Handbook (second edition), BSP Professional Books, Blackwell Scientific Publication Ltd..

Glover J.D., Sarma M.S. (2002), Power System Analysis and Design (third edition), Brooks/Cole, Thomson Learning.

Kundur P. (1994), Power System Stability and Control (book), McGraw-Hill, Inc..

Lasseter R.H. (2002), MicroGrids, Power Engineering Society Winter Meeting, 2002. IEEE, Volume: 1, 27-31 January 2002

Appendix

1. Simple representation of the flywheel in the MicroGrid

To simplify modelling of the flywheel, two simple representations of the flywheel are presented by using controllable AC and DC voltage sources. The control schemes of the flywheel are still PQ control, Droop control and Frequency/Voltage control, as described in Chapter 2 of this report.

Figures A1 and A2 show the implementations of the control schemes of the flywheel represented by the AC and DC controllable voltage sources, respectively.

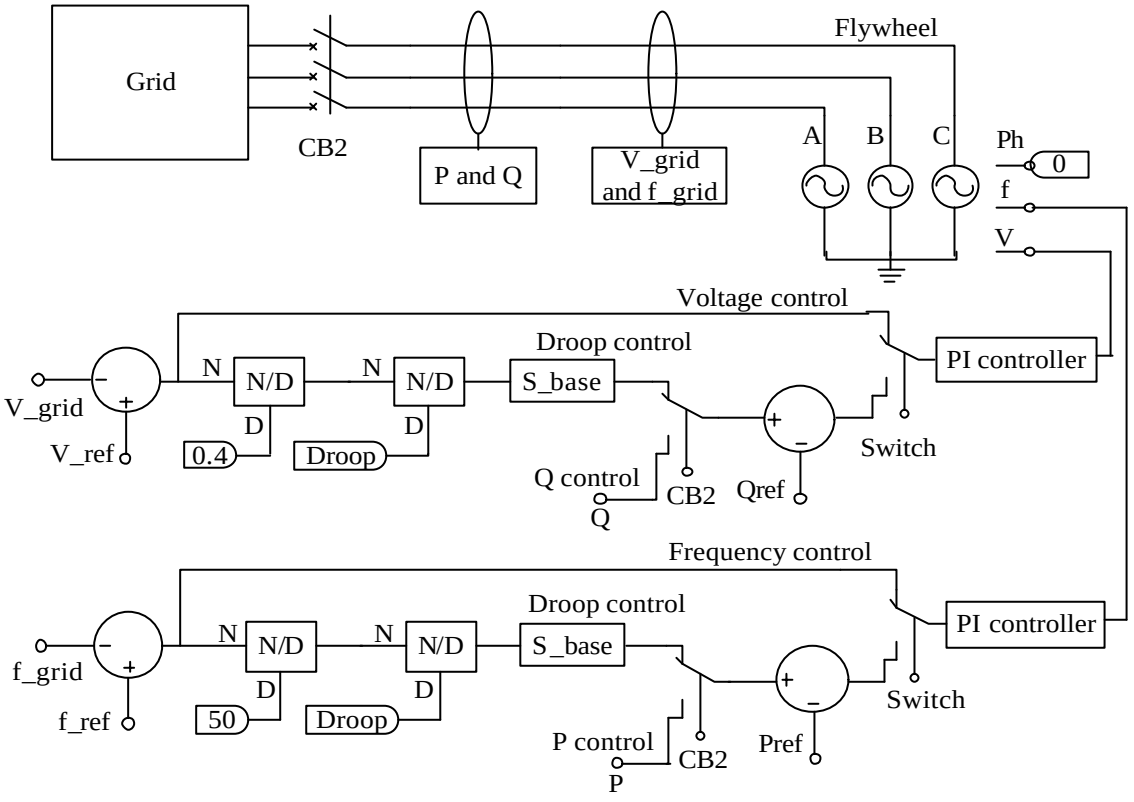

Figure A1 Control schemes of the flywheel represented by a controllable AC voltage source

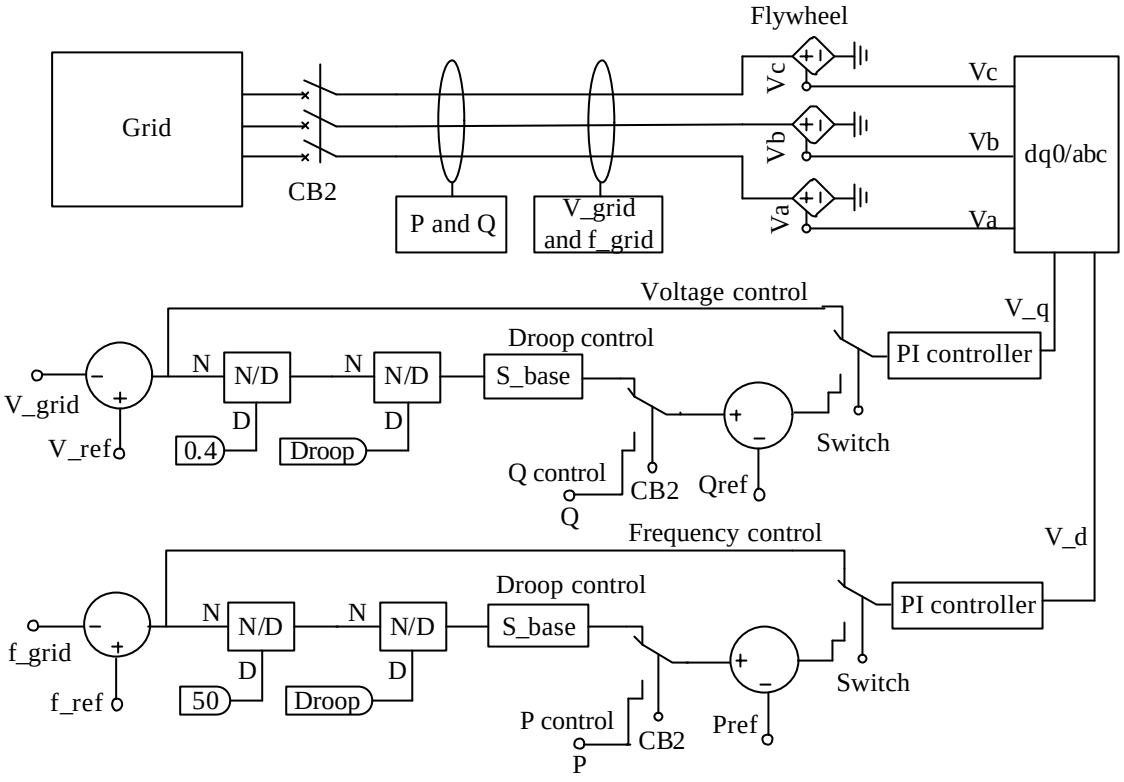

Figure A2 Control schemes of the flywheel represented by a controllable DC voltage source

2. Simulation results

The MicroGrid model used in this study is shown in Figure 14. The flywheel is represented either by a controllable AC voltage source or a controllable DC voltage source. Control strategies of the flywheel are PQ control, Droop control and Frequency/Voltage control. The flywheel uses PQ control only when the MicroGrid is operated in grid-connected mode. After disconnection of the MicroGrid from the main network at 10 seconds, during islanded mode, the control scheme of the flywheel is switched from PQ control to Droop control or Frequency/Voltage control. Simulation results produced in PSCAD/EMTDC are shown in Figures A3, A4, A5 and A6.

Figure A3 shows the dynamic performance of the MicroGrid when the flywheel, represented by a controllable AC voltage source, uses Droop control during islanded mode. The control scheme of the flywheel is switched from PQ control to Droop control after disconnection of the MicroGrid from the main network.

Figure A4 shows the dynamic performance of the MicroGrid when the flywheel, represented by a controllable AC voltage source, uses Frequency/Voltage during islanded mode. The control scheme of the flywheel is switched from PQ control to Frequency/Voltage control after disconnection of the MicroGrid from the main network

Similarly, Figures A5 and A6 show the dynamic performance of the MicroGrid when the flywheel, represented by a controllable DC voltage source, uses Droop control and Frequency/Voltage control during islanded mode.

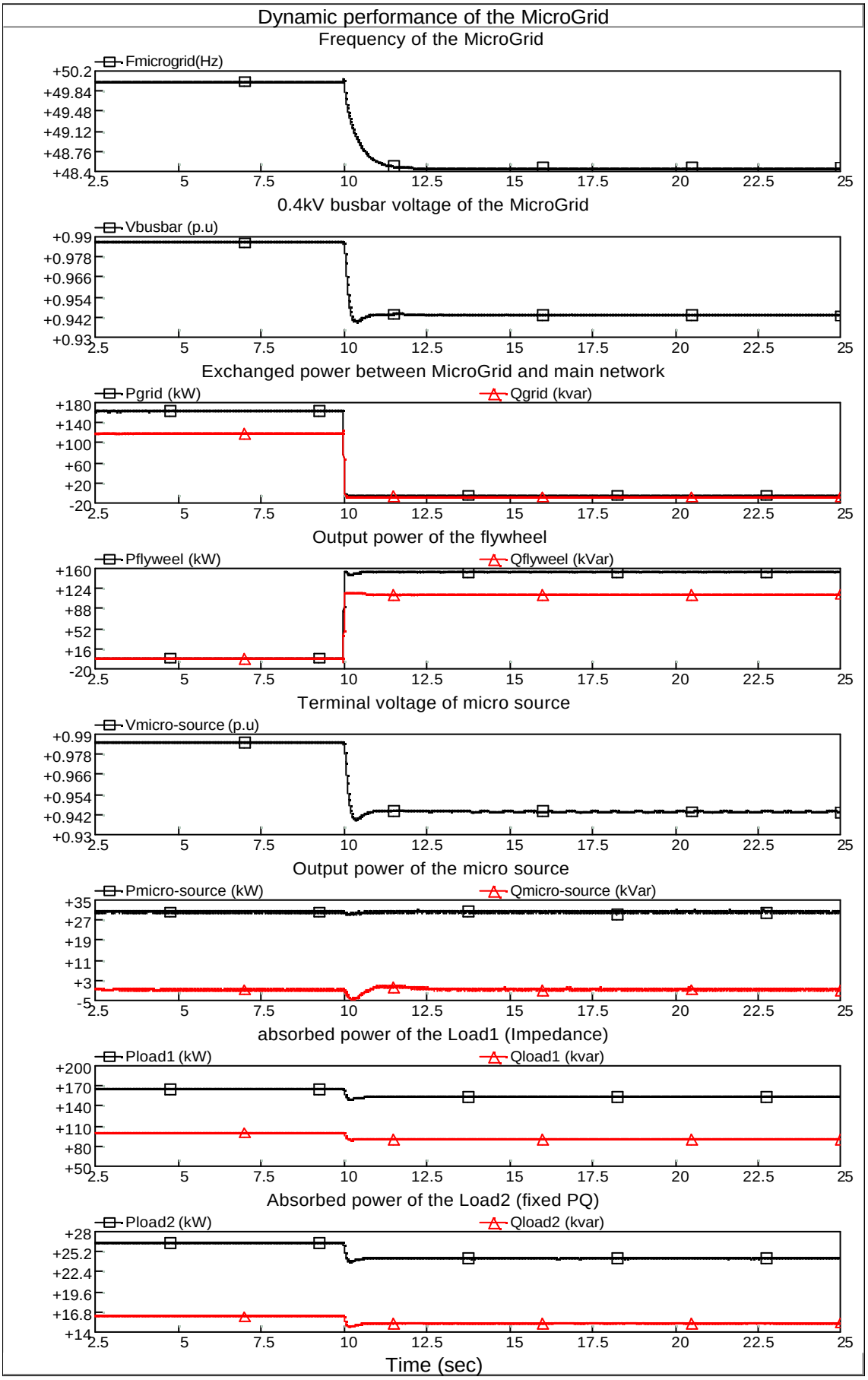

Figure A3 Dynamic performance of the MicroGrid when the flywheel, represented by a controllable AC voltage source, uses Droop control during islanded mode

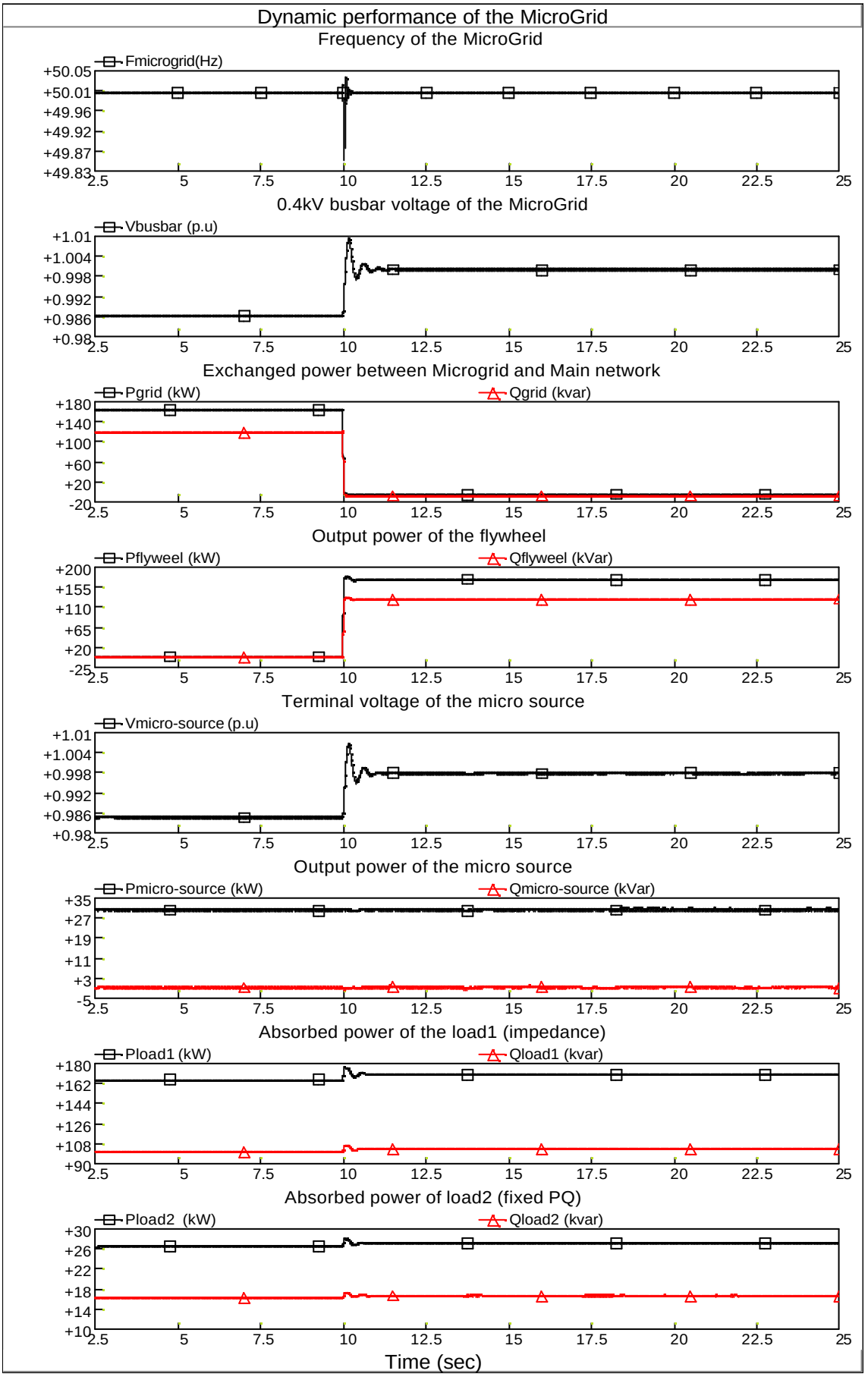

Figure A4 Dynamic performance of the MicroGrid when the flywheel, represented by a controllable AC voltage source, uses Frequency/Voltage control during islanded mode

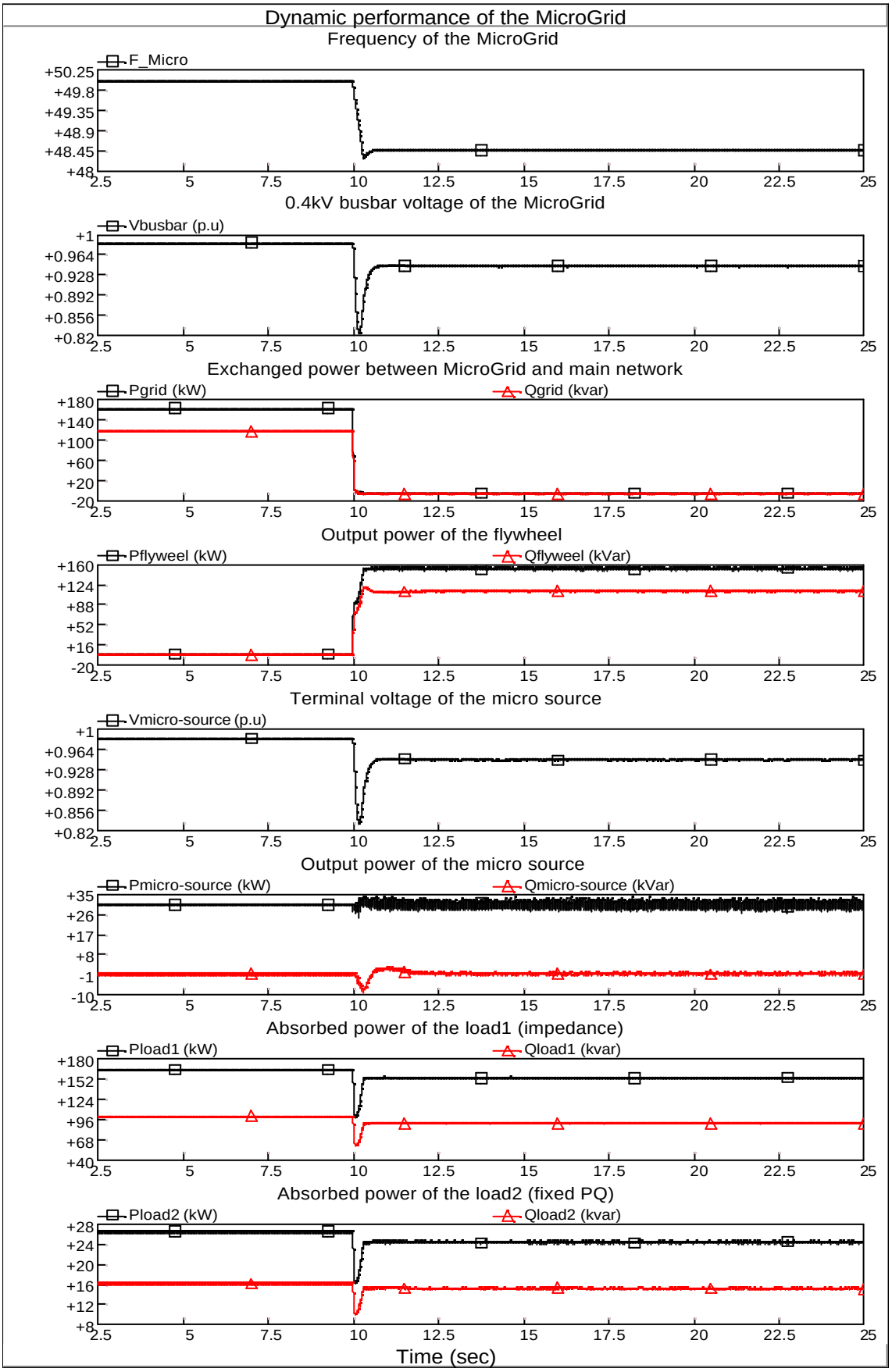

Figure A5 Dynamic performance of the MicroGrid when the flywheel, represented by a controllable DC voltage source, uses Droop control during islanded mode

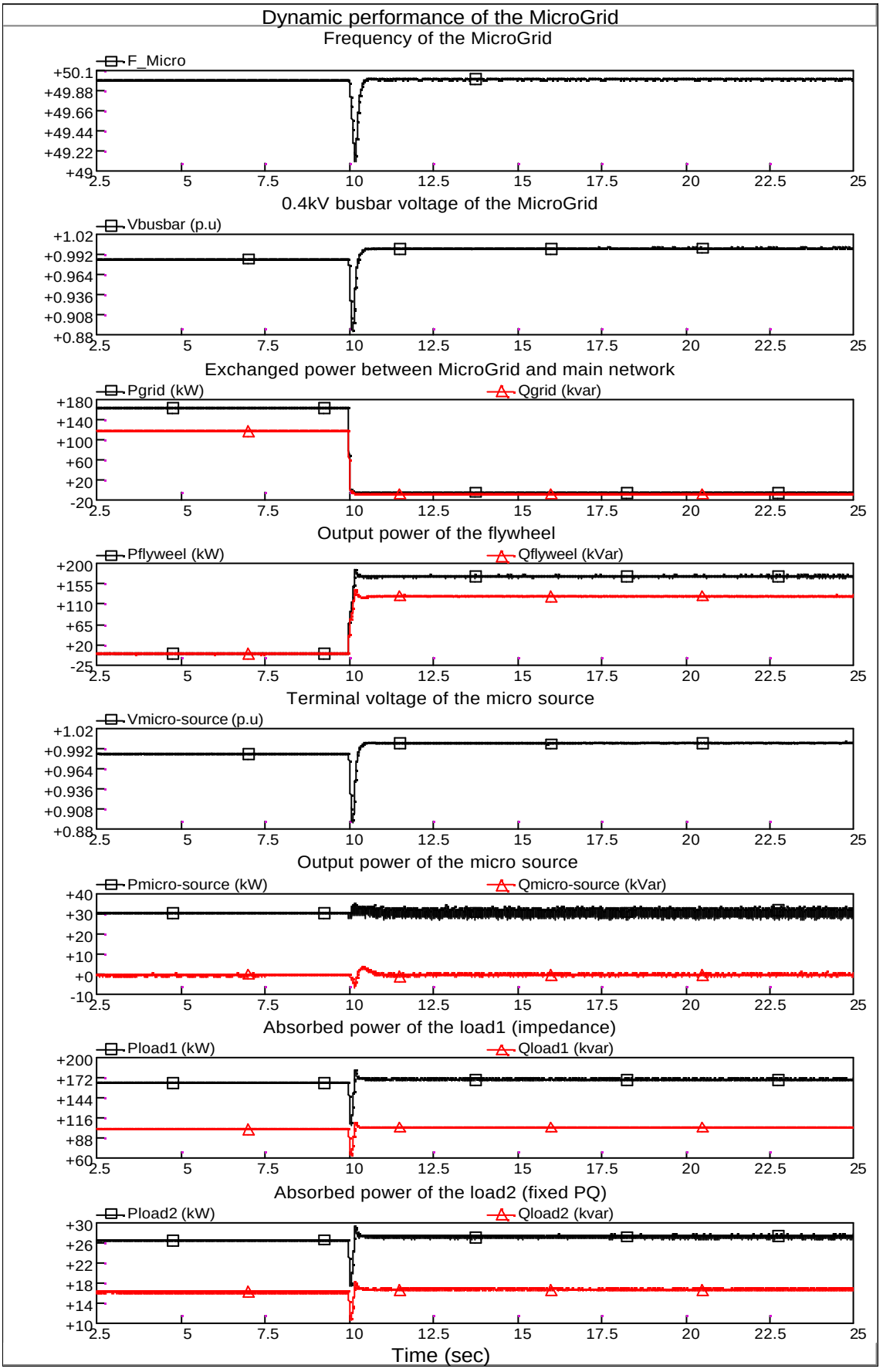

Figure A6 Dynamic performance of the MicroGrid when the flywheel, represented by a controllable DC voltage source, uses Frequency/Voltage control during islanded mode

3. Conclusions

Simulation results show that the dynamic performances of the MicroGrid produced from the simple controllable AC and DC voltage source representations of the flywheel are similar to that from the full STATCOM-BES model. For a simple application of the flywheel to the MicroGrid, the flywheel can be represented by a controllable AC voltage source or a controllable DC voltage source.

Document Information

Title	Stability of a Microgrid
Date	18th November 2004
Version	Draft Issue No 1
Task(s)	

Authors:	Xueguang Wu, Yibin Zhang, Nick Jenkins

Access:	
Project Consortium (for the actual version) European Commission , PUBLIC (for final version)	
Status:	
	Draft Version Final Version (internal document) **X** Submission for Approval (deliverable) Final Version (deliverable, approved on.)

DE2-Appendix IV

MICROGRIDS

Large Scale Integration of Micro-Generation

To Low Voltage Grids

WORK PACKAGE E

TASK TE5

Stability of a MicroGrid

Draft Issue No 1

18th November 2004

Xueguang Wu, Yibin Zhang, Nick Jenkins

UMIST

Access: Restricted to project members

Contents

1. Introduction

Micro-scale distributed generators (DGs), or micro sources, are being considered increasingly to provide electricity for the expanding energy demands in the network. The development of micro DGs also helps to reduce greenhouse gas emissions and increase energy efficiency.

The MicroGrid usually consists of a cluster of micro DGs, energy storage systems (e.g. flywheel) and loads, operating as a single controllable system. The voltage level of the MicroGrid at the load is about 400 Volts or less. The architecture of the MicroGrid is formed to be radial with a few feeders. It often provides both electricity and heat to the local area. It can be operated in both grid-connected mode and islanded mode

The micro DGs existing in the distribution network mainly use rotating machines. They are directly connected to the grid to supply electric power. However, many new technologies (e.g. micro gas turbine, fuel cells, photovoltaic system and several kinds of wind turbines) proposed to be used in MicroGrid are not suitable for supplying energy to the grid directly [Barsali, 2002]. They have to be interfaced with the grid through an inverter stage. Thus, the use of power electronic interfaces in the MicroGrid leads to a series of challenges in the design and operation of the MicroGrid. These major challenges include the safety and stability of the MicroGrid during all operating modes, particularly, islanded mode.

The MicroGrid is subject to the same safety requirements as any other utility electric power system. The protection of the MicroGrid must respond to both main network and MicroGrid faults. If a fault is on the main network, the desired response may be to isolate the MicroGrid from the main network as rapidly as necessary to protect the MicroGrid loads. If a fault is within the MicroGrid, the protection system may only isolate the smallest possible faulted section of the MicroGrid to eliminate the fault.

The inverter based MicroGrid can not normally provide the required levels of short circuit current. In extreme cases, the fault current contribution from the micro sources

may only be twice load current or less [Wall, 2001]. Some conventional overcurrent sensing devices may not even respond to this level of fault current. In addition, undervoltage and frequency protection may fail to detect faults in the MicroGrid due to the voltage and frequency control of the MicroGrid obtained from the flywheel energy storage system. The protection of the MicroGrid may be achieved by using conventional overcurrent protection devices if the flywheel supplies 3-5p.u fault current during islanded mode. However, the protection on the main network may take seconds to respond to the fault on the MicroGrid, rather than the fraction of a second that is necessary for the safety and stability of the MicroGrid operated in islanded mode. The MicroGrid may be unstable due to a long fault clearing time taken by such protection. Thus, to maintain the stability of the MicroGrid, faster protection (e.g. differential protection) is needed to protect the main network.

The control of the micro sources and the flywheel is also very important to maintain the safety and stability of the MicroGrid during all times. For basic operation of the MicroGrid, the controllers should use only local information to control the flywheel and micro sources. Hence, fault communication between the micro sources and the flywheel is unnecessary. For a micro source, the inverter should have plug and play capabilities [Lasseter, 2002]. Plug and play implies that a micro source can be added to the MicroGrid without any changes to the control of the units, which are already a part of the network. For the flywheel, the inverter should be able to respond to the change of load in a predetermined manner automatically. Thus, the possible control strategies of the micro sources and the flywheel are: (a) PQ control (fixed active and reactive power control), (b) Droop control and (c) Frequency/Voltage control. The MicroGrid may be unstable if the flywheel uses PQ control all time. In this case, the flywheel can't supply dynamic active and reactive power compensation to the MicroGrid during islanded mode due to its constant output power. However, the stability of the MicroGrid can be improved by using Droop control or Frequency/Voltage control of the flywheel. With Droop control, the output power of the flywheel is regulated according to the setting droops. With Frequency/Voltage control, the frequency and voltage of the MicroGrid are restored to normal values (e.g. f=50Hz and V=1.0p.u).

PQ control is adopted when the micro sources and the flywheel need to run on constant power output. The electricity, generated by the micro source, may be constant because of the need of the associated thermal load. The power output of the flywheel can be fixed at zero when the MicroGrid is operated in parallel with the main network, grid-connected mode.

After disconnection of the MicroGrid from the main network, operating in islanded mode, the control scheme of the flywheel can be changed from PQ control to Droop control or Frequency/Voltage control. During islanded operation of a MicroGrid, the flywheel should supply dynamic active and reactive power compensation to the MicroGrid. With Droop control of the flywheel, the frequency and voltage of the MicroGrid will be controlled to the steady state values determined by the droop characteristics. With Frequency/Voltage control of the flywheel, the frequency and voltage of the MicroGrid can be brought back to the normal values after a disturbance.

In this report, the three control strategies, (a) PQ control, (b) Droop control and (c) Frequency/Voltage control, of the MicroGrid are described and tested. Based on a simple MicroGrid model in PSCAD/EMTDC, three representations, (1) synchronous generator representation, (2) STATic Synchronous Shunt COMpensator with battery energy storage, STATCOM-BES, representation, and (3) controllable AC or DC voltage source representation, of the MicroGrid are implemented and compared. For different characteristics of load, locations of fault and inertia constants of motors, the stability (critical clearing time, CCT) of the MicroGrid is investigated. Finally, a traditional method (undervoltage load shedding) is used to improve the stability of the MicroGrid. Simulations are demonstrated and discussed with supporting PSCAD/EMTDC results.

2. Control strategies of a MicroGrid

The unique nature of the MicroGrid determines that the control strategies of the MicroGrid can be: (a) PQ control, (b) Droop control and (c) Frequency/Voltage control.

2.1 PQ control

Using this control, the outputs of the micro sources and the flywheel are fixed at their constant values (settings). PQ control consists of a P controller and a Q controller.

The P controller adjusts the frequency-droop characteristic of the generator up or down to maintain the active power output of the generator at a constant value (Pdes, desired active power) when the frequency is changed. Figure 1 shows the effect of frequency-droop characteristic adjustment. A typical droop of the frequency characteristic is about 4% [Kundur, 1994].

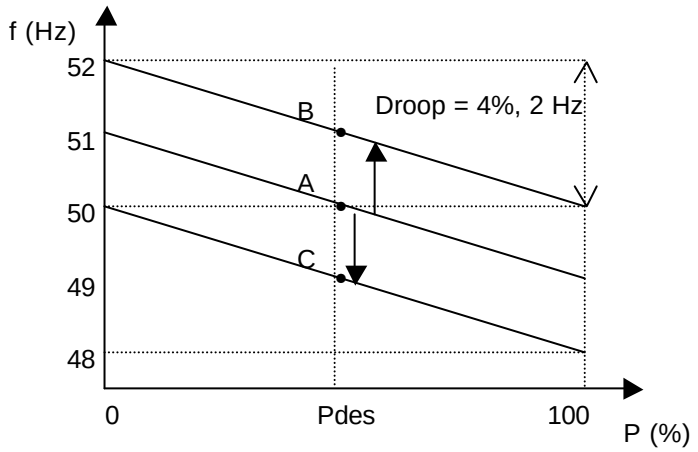

Figure 1 Effect of the frequency-droop characteristic adjustment

At output Pdes, characteristic A corresponds to 50Hz frequency of the grid, characteristic B corresponds to 51Hz frequency of the grid and characteristic C corresponds to 49Hz frequency of the grid. For a frequency change, the power output of the generator can be maintained at the desired value by moving the droop characteristic up or down.

Similarly, the Q controller adjusts the voltage-droop characteristic of the generator by moving the droop lines upon or down to maintain the reactive power output of the generator at a constant value (Qdes, desired reactive power) when the voltage is changed. Figure 2 shows the effect of voltage-droop characteristic adjustment. A typical droop of voltage characteristic is about 10% [Kundur, 1994].

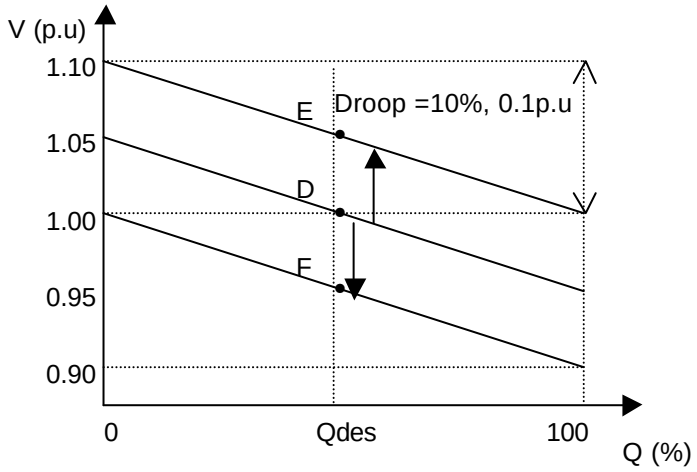

Figure 2 Effect of the voltage-droop characteristic adjustment

At output Qdes, characteristic D corresponds to 1.00 voltage of the network, characteristic E corresponds to 1.05 voltage of the grid and characteristic F corresponds to 0.95 voltage of the grid. For a voltage change, the reactive power output of the generator is maintained at the desired value Qdes by shifting the voltage-droop characteristic up or down.

2.2 Droop control

When the MicroGrid is operated in islanded mode, the control scheme of the micro sources is still PQ control. However, the control scheme of the flywheel needs to be changed to enable local frequency control. With Droop control of the flywheel, the power output of the flywheel is regulated according to the predetermined droop characteristics. Droop control consists of a frequency-droop controller and a voltage-droop controller. Figure 3 shows a frequency-droop characteristic, which would be used in the frequency-droop controller.

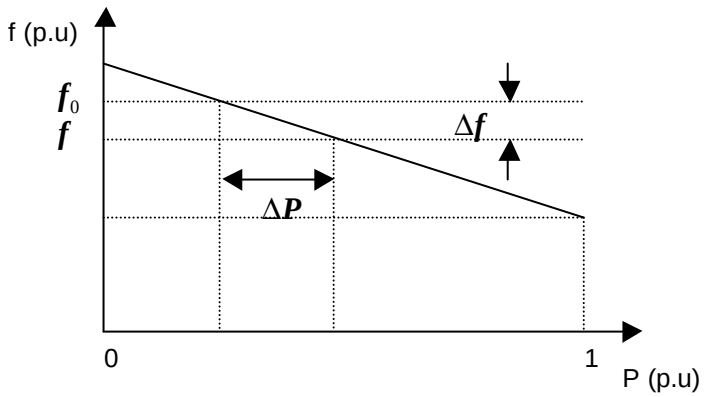

Figure 3 A typical frequency-droop characteristic

The value of droop R_f is the ratio of frequency deviation Δf to change in active power output ΔP. It can be expressed in percentage as equation (1).

$$R_f = \frac{\Delta f(p.u)}{\Delta P(p.u)} \times 100\% \quad (1)$$

Figure 4 shows a typical voltage-droop characteristic used in the voltage-droop controller.

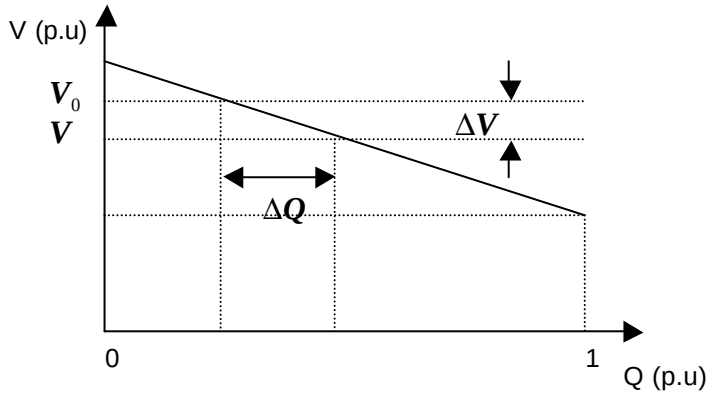

Figure 4 A typical voltage -droop characteristic

The value of droop R_V is a ratio of voltage deviation ΔV to change in reactive power output ΔQ. It can be expressed in percentage as equation (2).

$$R_V = \frac{\Delta V(p.u)}{\Delta Q(p.u)} \times 100\% \quad (2)$$

2.3 Frequency/Voltage control

With droop control action, a load change in the MicroGrid will result in steady-state frequency and voltage deviations, depending on the droop characteristics and Frequency/Voltage sensitivity of the load. The flywheel will contribute to the overall change in generation. Restoration of the Frequency/Voltage of the MicroGrid to their normal values requires a supplementary action to adjust the output of the flywheel. The basic means of the local frequency control of the MicroGrid is through regulating the output of the flywheel. As the load of the MicroGrid changes continually, it is necessary to automatically change the output of the flywheel.

The objective of the frequency control is to restore the frequency to its normal value. This is accomplished by moving the frequency-droop characteristic left or right to maintain the frequency at a constant value. The frequency control adjusts the output of the flywheel to restore the frequency of the MicroGrid to normal (e.g. 50Hz). Figure 5 shows the effect of this adjustment.

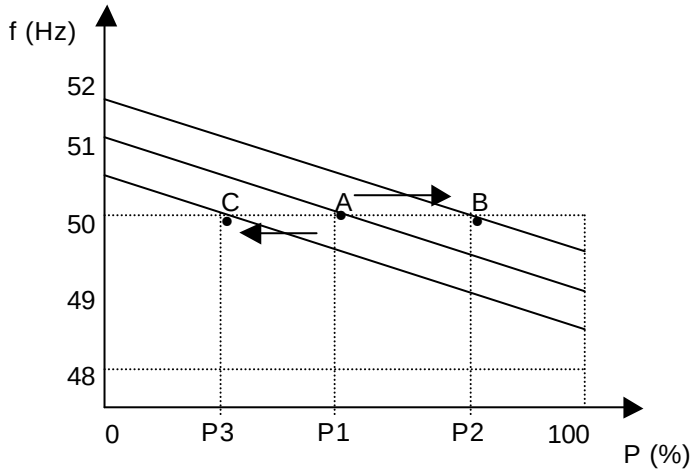

Figure 5 Effect of the adjustment on the frequency-droop characteristic

At 50Hz, characteristic A corresponds to P1 active power output of the flywheel, characteristic B corresponds to P2 active power output and characteristic C corresponds to P3 active power output. The frequency of the MicroGrid is fixed at a constant value (50Hz) by moving the frequency-droop characteristic left or right.

Similarly, the voltage control adjusts the voltage-droop characteristic left or right to maintain a constant voltage when the voltage of the MicroGrid is changed. Thus, the voltage of the MicroGrid is fixed at a desired value (e.g. 1.0p.u). The effect of this adjustment is shown in Figure 6.

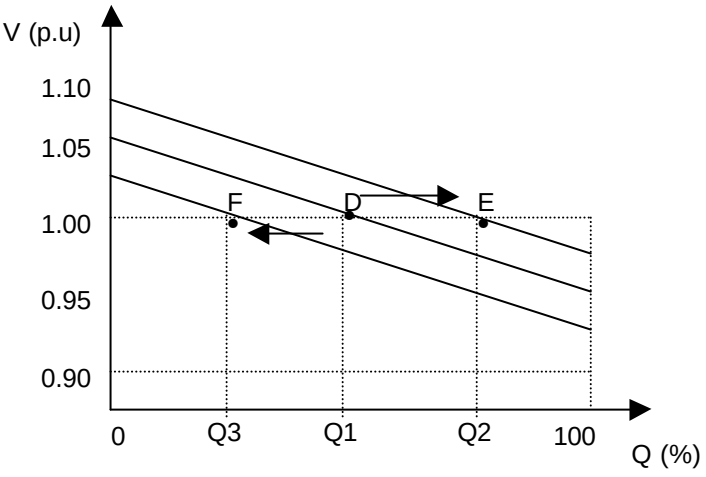

Figure 6 Effect of the adjustment on the voltage-droop characteristic

At 1.0 p.u voltage, characteristic D corresponds to Q1 reactive power output of the flywheel, characteristic E corresponds to Q2 reactive power output and characteristic F corresponds to Q3 reactive power output. The voltage of the MicroGrid is fixed at a constant value (1.0 p.u) by moving the voltage-droop characteristic left or right.

3. Implementation of the control strategies

3.1 For a synchronous generator representation

For this representation of the MicroGrid, the micro sources and the flywheel are represented by synchronous generators. The control schemes of the MicroGrid are implemented as follows:

(1) PQ control

The function of moving droop characteristic of PQ controller is similar to the speed control of a synchronous generator with a supplementary control loop, as shown in Figure 7.

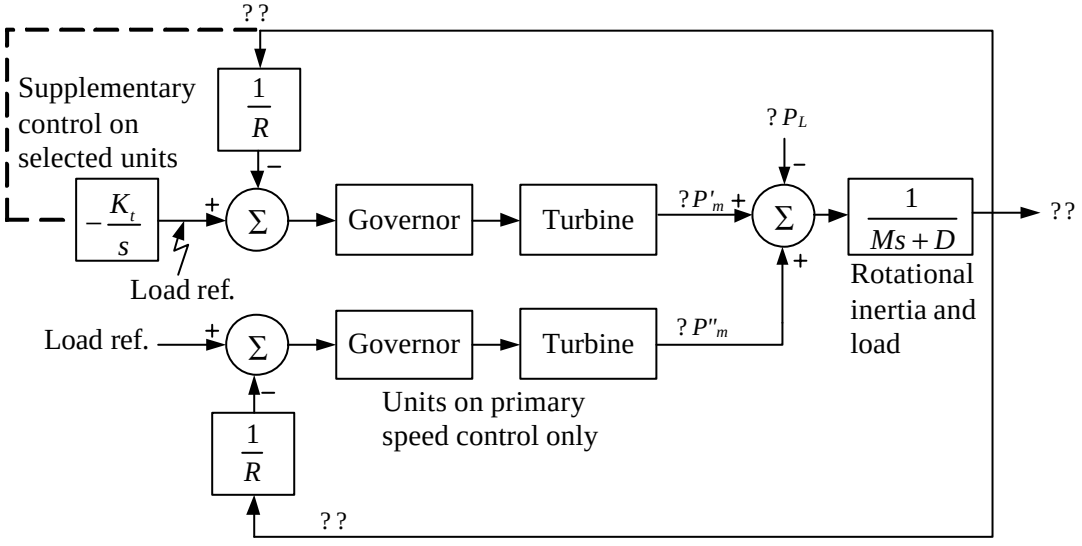

Figure 7 Speed control of synchronous generator with a supplementary control loop [Kundur, 1994]

The movement of the characteristic is achieved through adding an integral control loop, which acts on the load reference settings, to the speed droop control of the generator. The integral control action ensures that the output power of the generator is fixed at a constant value (setting).

Figure 8 shows the configuration of P controller for a synchronous generator representation of the MicroGrid.

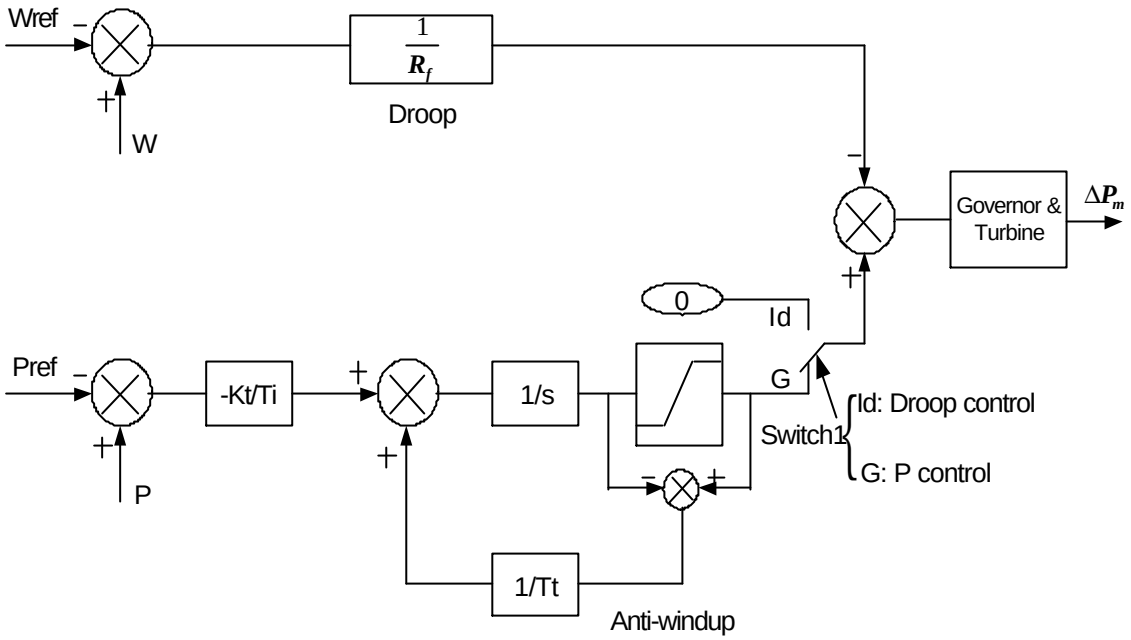

Figure 8 Configuration of P controller for
a synchronous generator representation

Figure 9 shows the implementation of Q controller for a synchronous generator representation.

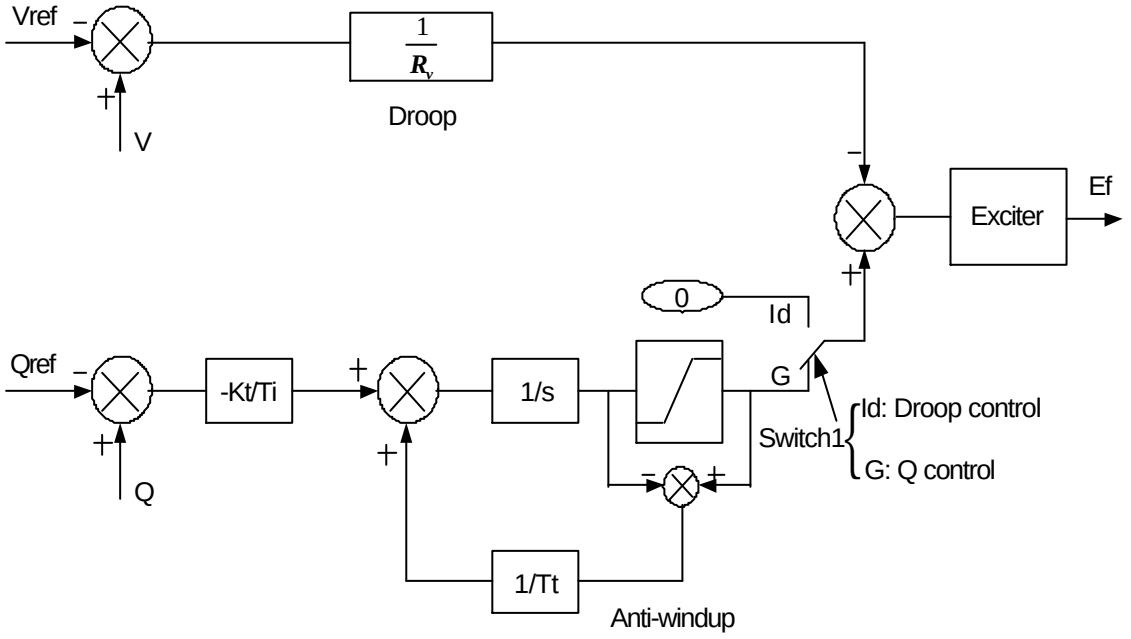

Figure 9 Implementation of Q controller for
a synchronous generator representation

(2) Droop control

From Figures 8 and 9, the implementation of Droop control was achieved by changing position of Switch 1 from G to Id.

(3) Frequency/Voltage control

The implementation of Frequency control is similar to P control in Figure 8. However, the connection of the supplementary control loop needs to be changed from position Gp of Switch 2 to If and from Id of Switch 1 to G.

Figure 10 shows the layout of Frequency control for a synchronous generator representation.

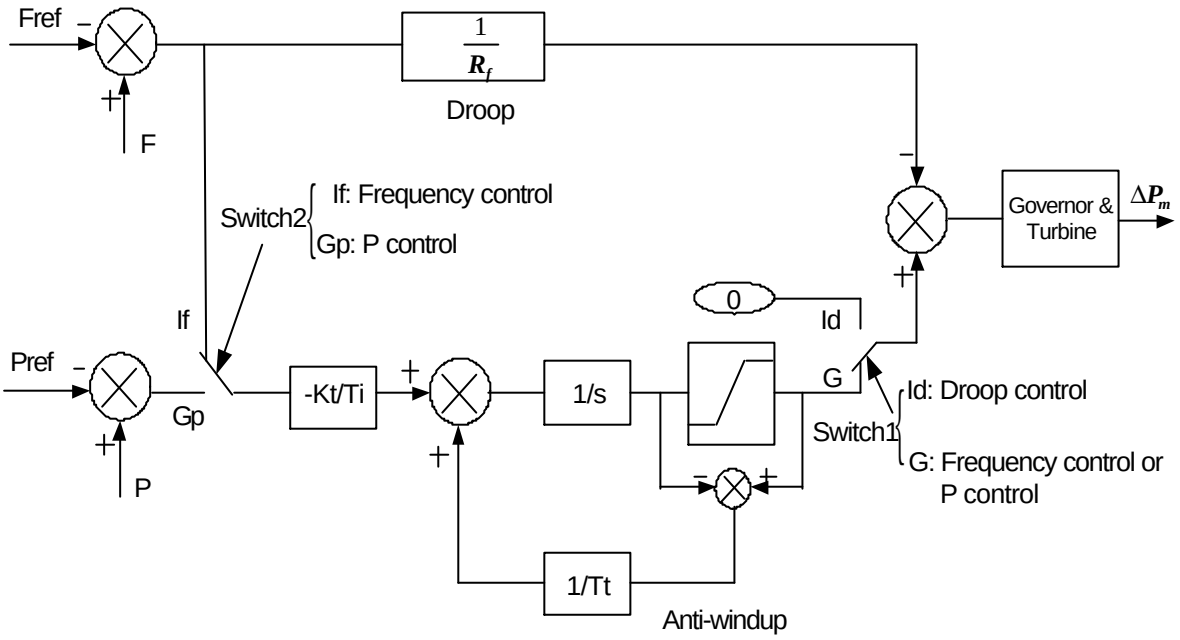

Figure 10 Layout of Frequency control for a synchronous generator representation

Figure 11 shows the implementation of Voltage control for a synchronous generator representation.

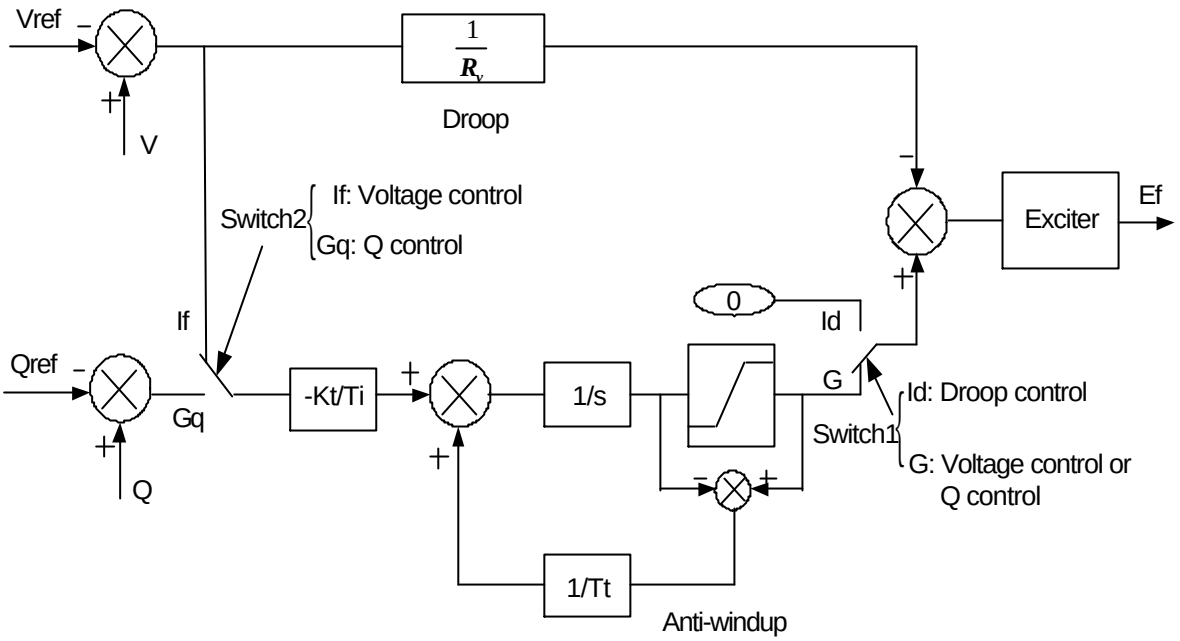

Figure 11 Implementation of Voltage control for
a synchronous generator representation

3.2 For a STATCOM-BES representation

In this representation, the micro sources and flywheel of the MicroGrid are represented by STATCOM-BES. The control schemes of the MicroGrid consist of PQ control, Droop control and Frequency/Voltage. Figure 12 shows the implementation of these control strategies of the flywheel in a STATCOM-BES representation.

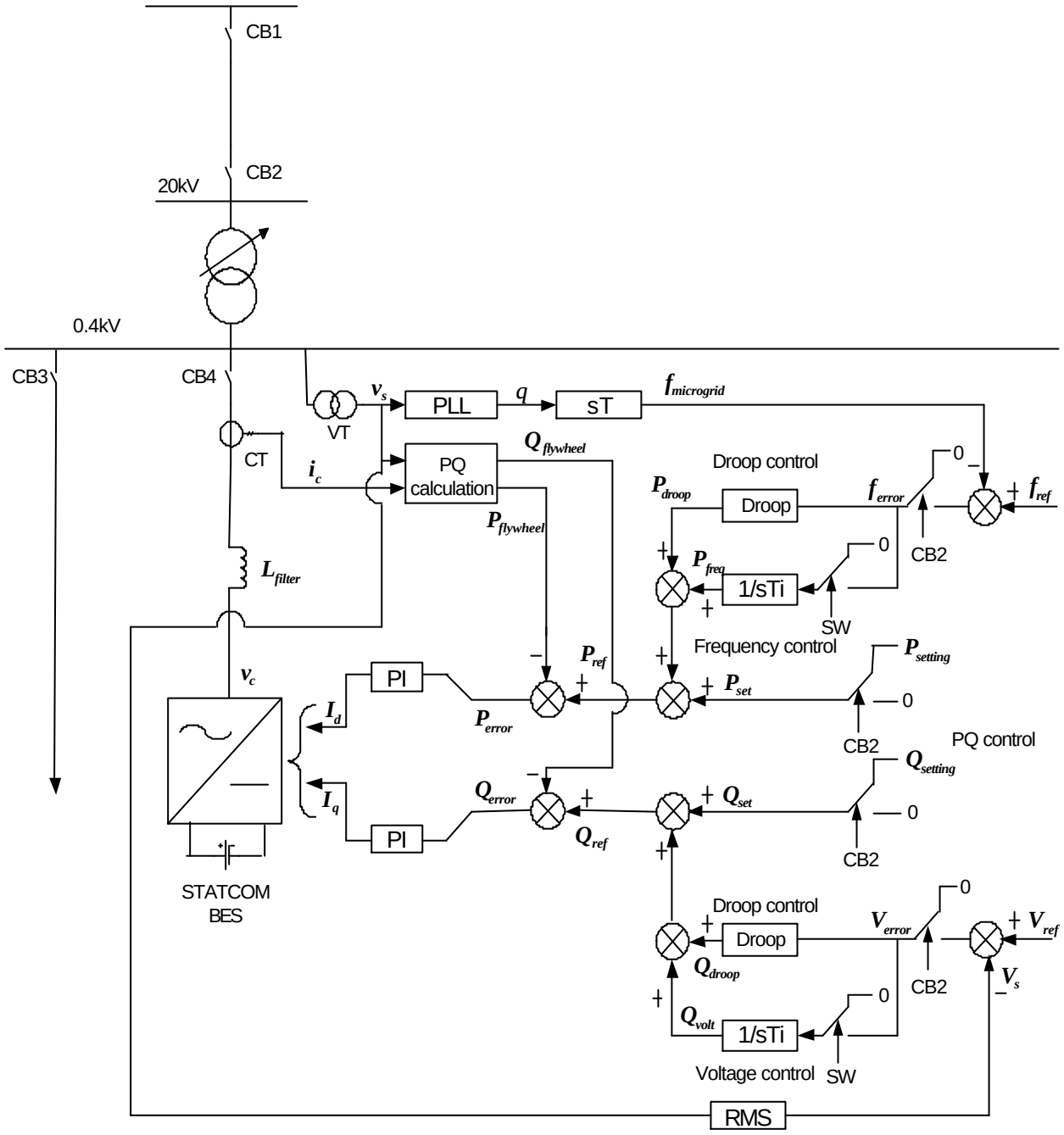

Figure 12 Control schemes of the flywheel represented by STATCOM-BES

During grid-connected mode, the state of circuit breaker CB2 is closed. The control scheme of the flywheel is PQ control. The output P_{droop} and Q_{droop} of Droop control are zero. The output P_{freq} and Q_{volt} of Frequency/Voltage control are also zero. The output P_{set} and Q_{set} of PQ control are set to $P_{setting}$ and $Q_{setting}$. The reference values

of active powers P_{ref} and reactive power Q_{ref} of the STATCOM-BES are $P_{setting}$ and $Q_{setting}$, acting on PQ control.

After disconnection of the MicroGrid from the main network, during islanded mode, CB2 is open. The outputs P_{set} and Q_{set} of PQ control are set to zero by a state signal coming from CB2. The reference values of active power P_{ref} and reactive power Q_{ref} are P_{droop} and Q_{droop}, acting on Droop control. The integral control loops are switched off to zero by SW. The control scheme of the flywheel is thus changed from PQ control to Droop control.

If the integral control loops are added to Droop control by SW, the reference value of the active power P_{ref} is a sum of P_{droop} and P_{freq}. The reference value of the reactive power Q_{ref} is also a sum of Q_{droop} and Q_{volt}. Finally, the control scheme of the flywheel is switched from PQ control to Frequency/Voltage control.

3.3 For a controllable AC or DC voltage source representation

To simplify modelling of the flywheel, two simple representations of the flywheel are presented by using controllable AC or DC voltage sources. The control schemes of the flywheel are still PQ control, Droop control and Frequency/Voltage control, which are similar to that in the STATCOM-BES representation.

Figures 13 and 14 show the implementations of the control schemes of the flywheel represented by the AC and DC controllable voltage sources.

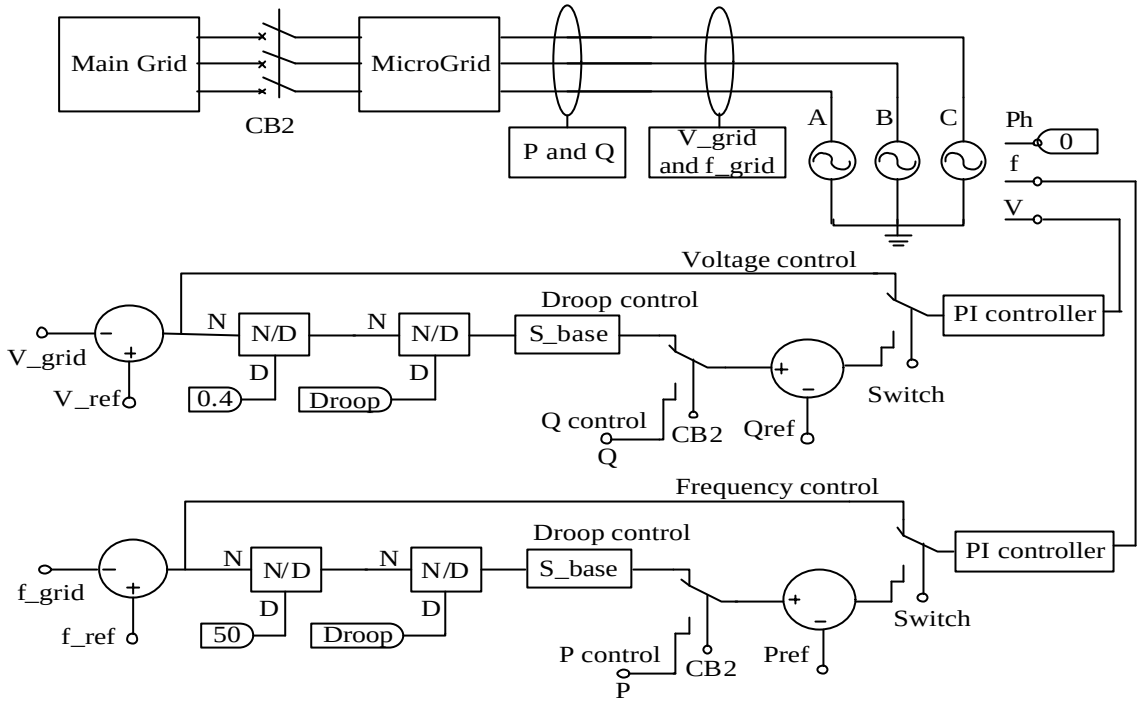

Figure 13 Control schemes of the flywheel represented by a controllable AC voltage source

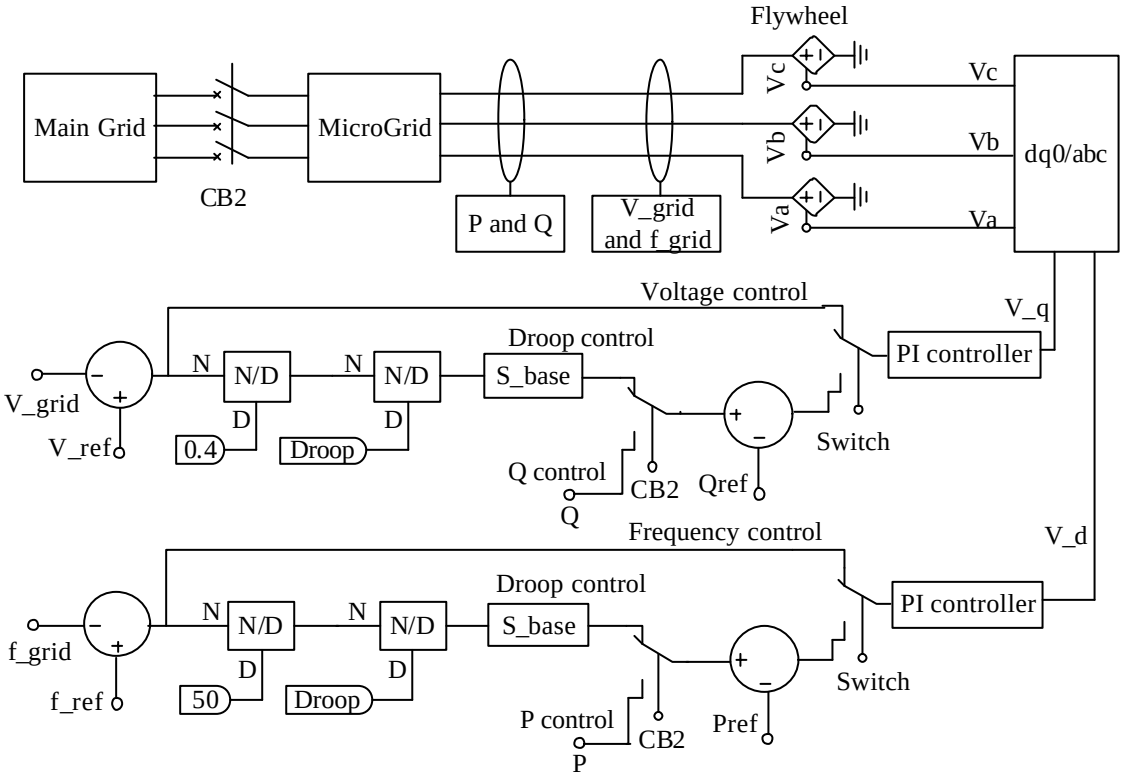

Figure 14 Control schemes of the flywheel represented by a controllable DC voltage source

4. Comparison of the three representations of a MicroGrid

4.1 Modelling of a simple MicroGrid in PSCAD/EMTDC

It is assumed that the micro sources and the flywheel of the MicroGrid are represented by the synchronous generators, the STATCOM-BES, and the controllable AC and DC voltage sources. The three representation modes of the MicroGrid are implemented in PSCAD/EMTDC and shown in Figures 15, 16 and 17.

Figure 15 shows a simple MicroGrid mode, in which the micro source and the flywheel are represented by synchronous generators.

Figure 16 shows a simple MicroGrid mode, in which the micro source and the flywheel are represented by STATCOMs-BES.

Figure 17 shows a simple MicroGrid mode, in which the micro source and the flywheel are represented either by controllable AC or DC voltage sources.

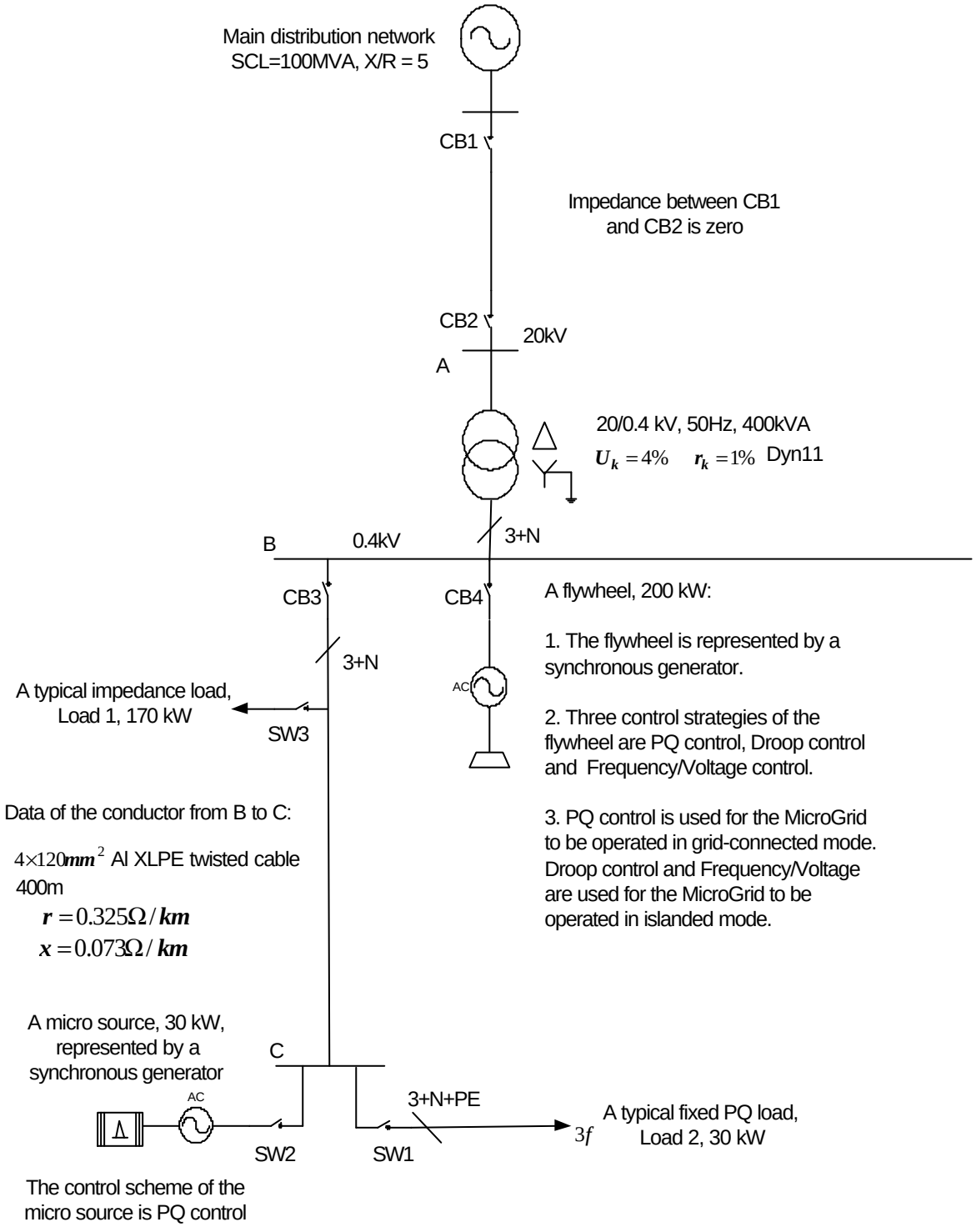

Figure 15 A simple MicroGrid model represented by synchronous generators

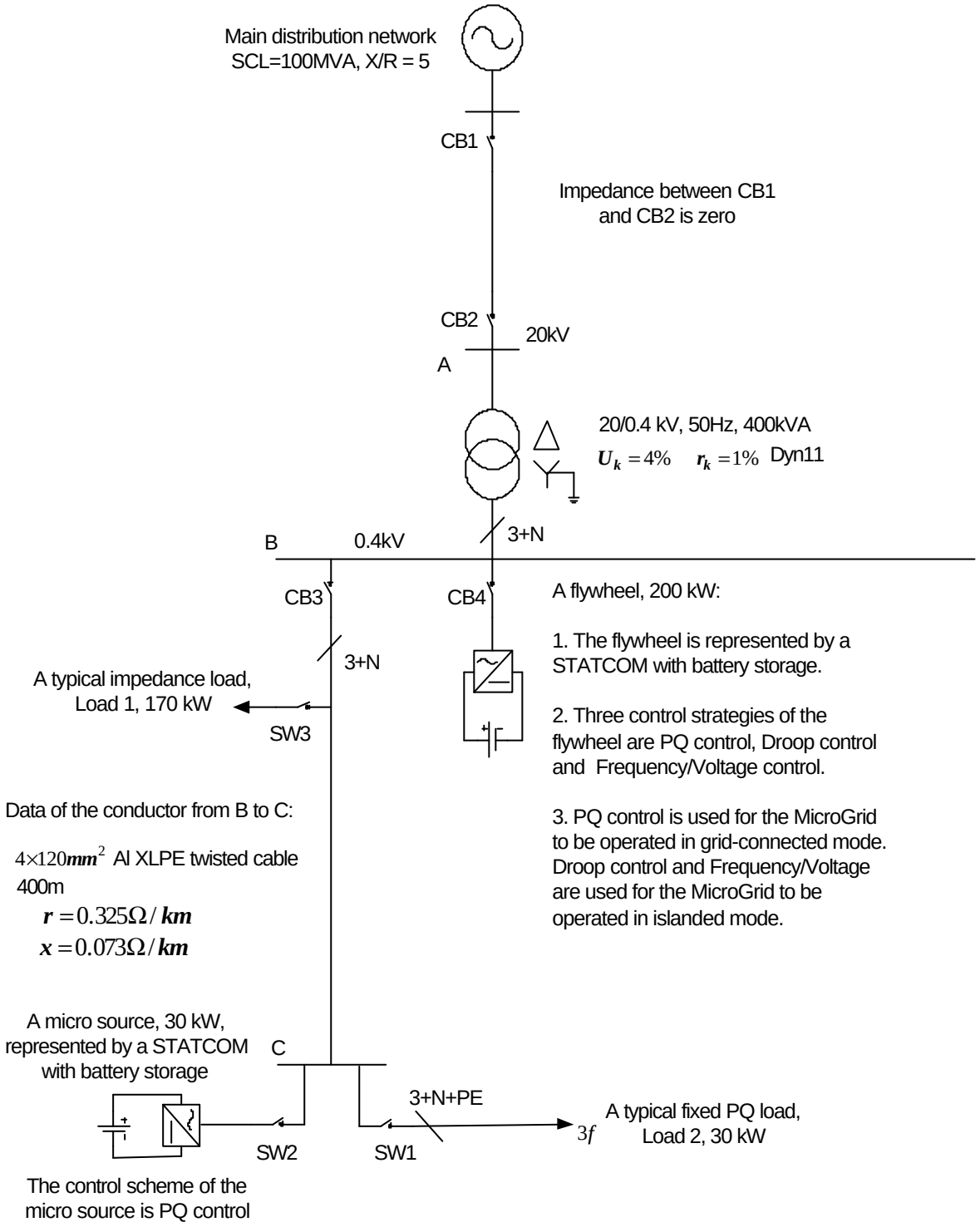

Figure 16 A simple MicroGrid model represented by STATCOM-BES

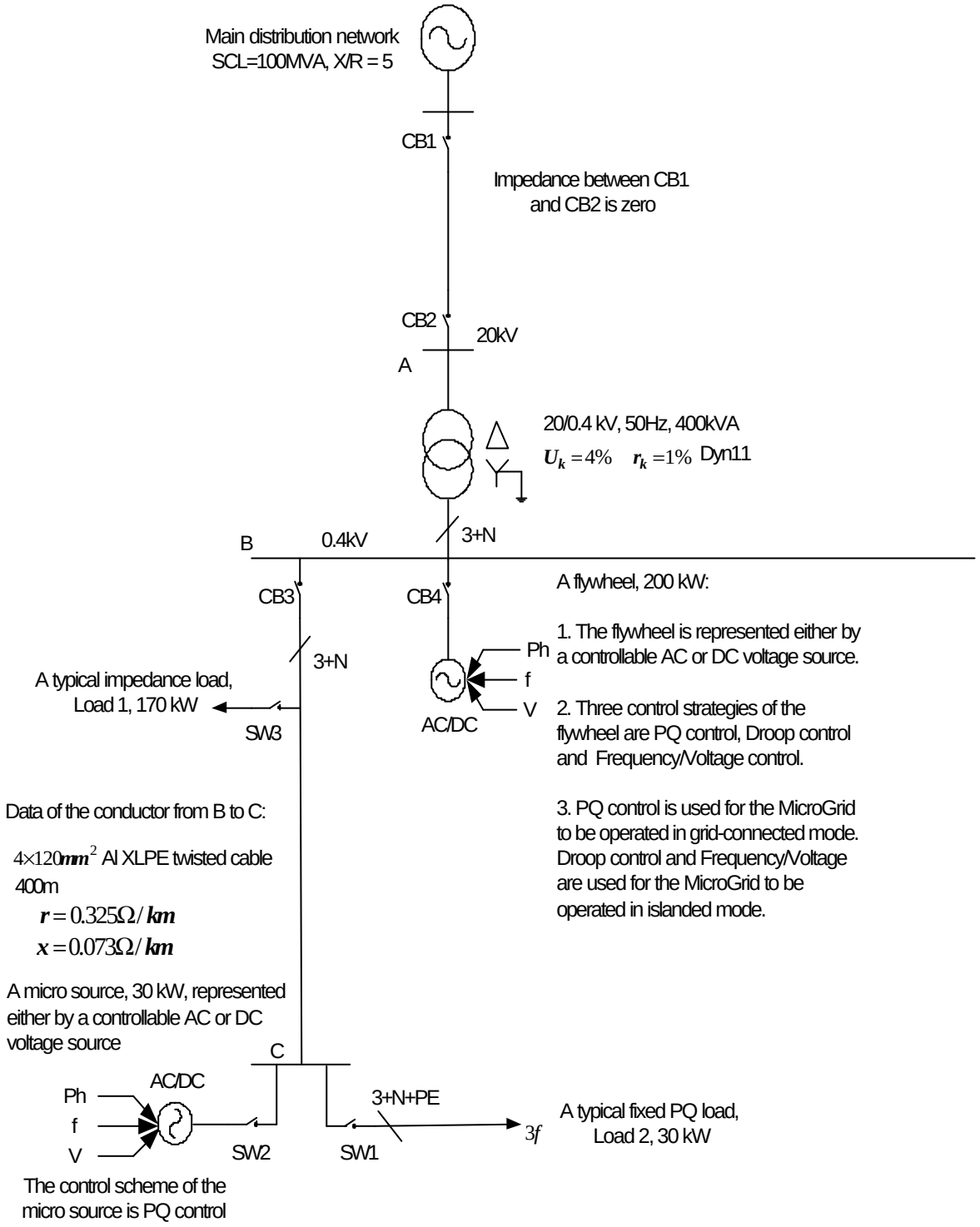

Figure 17 A simple MicroGrid model represented either by controllable AC or DC voltage source

For the three representations of the MicroGrid, the fault level at the 20kV main distribution network is 100MVA, with a X/R ratio of 5. One transformer (400kVA, 20/0.4kV) is installed at the substation between the main network and the MicroGrid. The impedance of the transformer is 0.01+j0.04 p.u. The MicroGrid consists of a flywheel and a feeder. The flywheel is connected to the 0.4kV busbar, which is near to the substation. The capacity of the flywheel is 200kW (assuming the flywheel supplies 4MJ energy for 20 seconds continuously). The feeder is connected to a micro source and two loads (Load 1 and Load 2) through 400 meters of ALXLPE twisted cable ($4\times120mm^2$). The impedance of the cable is 0.325+j0.073 ohms per kilometre [Bungay, 1990]. The capacity of the micro source is 30kW. Load 1 is an impedance load, with capacity of 170kW. Load 2 is a fixed PQ load, with capacity of 30kW.

In the synchronous generator representation, the parameters of the synchronous generators are the typical average values of the synchronous turbine generator constants [Glover, 2002]:

- Synchronous d-axis reactance (X_d): 1.10 [p.u];
- Synchronous q-axis reactance (X_q): 1.08 [p.u];
- Transient d-axis reactance (X'_d): 0.23 [p.u];
- Transient q-axis reactance (X'_q): 0.23 [p.u];
- Sub-transient d-axis reactance (X''_d): 0.12 [p.u];
- Sub-transient q-axis reactance (X''_q): 0.15 [p.u];
- Negative sequence reactance (X_2): 0.13 [p.u];
- Zero sequence reactance (X_0): 0.05 [p.u];
- Stator armature resistance (R_a): 0.005 [p.u];
- Transient time constant (T'_{do}): 5.60 [sec.];
- Sub- transient time constant ($T''_d = T''_q$): 0.035 [sec.];
- Inertia constant (H): 1.05 [MW/MVA].

In the STATCOM-BES and controllable AC or DC voltage source representations, the ratings of the STATCOMs-BES and the voltage sources are the same as the capacities of the micro source and flywheel, 30kW and 200kW.

The control scheme of the micro source is PQ control at all times. The control strategies of the flywheel are PQ control, Droop control or Frequency/Voltage control. The flywheel uses PQ control only when the MicroGrid is operated in grid-connected mode. During islanded mode, the control of the flywheel is switched from PQ control to Droop control or Frequency/Voltage control.

4.2 Simulation results

Based on the three representations of the MicroGrid (synchronous generator representation, STATCOM-BES representation, and controllable AC or DC voltage source representation), the dynamic performance of the MicroGrid was investigated and demonstrated in PSCAD/EMTDC under three control strategies (PQ control, Droop control and Frequency/Voltage control) of the flywheel. In all cases, circuit breaker CB2 is tripped at 10 seconds without a fault on the network. Following the trip of CB2, the MicroGrid is disconnected from the main network and operated in islanded mode.

(1) Synchronous generator representation

In this representation, the micro sources and flywheel in the MicroGrid are represented by synchronous generator representation, as shown in Figure 15. The control scheme of the micro source is PQ control all time. The control strategies of the flywheel are PQ control, Droop control and Frequency/Voltage control. For the three control schemes of the flywheel, simulation results show as follows:

(a) PQ control

Figure 18 shows the dynamic performance of the MicroGrid when the flywheel uses PQ control during islanded mode. The control schemes of the micro source and the flywheel are PQ control. The implementation of PQ control is shown in Figures 8 and 9.

Obviously, the flywheel makes no contribution to the local frequency and voltage control of the MicroGrid. The frequency and voltage of the MicroGrid are unstable

after disconnection of the MicroGrid from the main network. The frequency and voltage of the MicroGrid collapse so that the MicroGrid can not be operated in islanded mode.

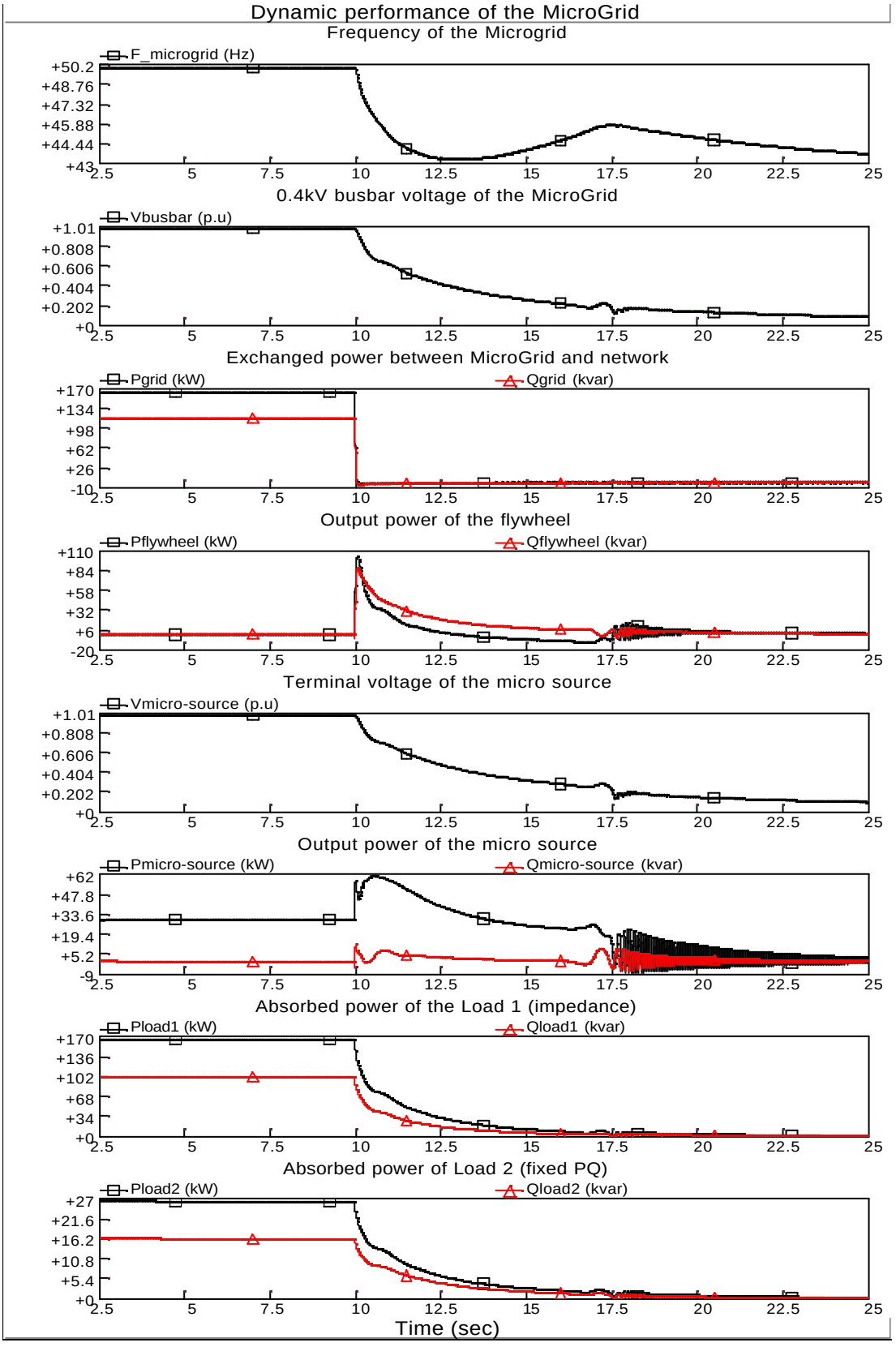

Figure 18 Dynamic performance of the MicroGrid (synchronous generator representation) when the flywheel uses PQ control during islanded mode

(b) Droop control

Figure 19 shows the dynamic performance of the MicroGrid when the flywheel uses Droop control (shown in Figures 8 and 9, changed position of Switch 1 from G to Id) during islanded mode. The control scheme of the micro source is still PQ control.

After disconnection of the MicroGrid from the main network, the output of the micro source is still retained at 30kW. But, the output of flywheel is changed from zero to the value of 149kW+j110kVar according to the droop settings ($\boldsymbol{R}_f = 4\%$ and $\boldsymbol{R}_v = 10\%$). Thus, the frequency and voltage of the MicroGrid drop to their steady state values (48.35Hz and 0.9325p.u) associated with the droop characteristics.

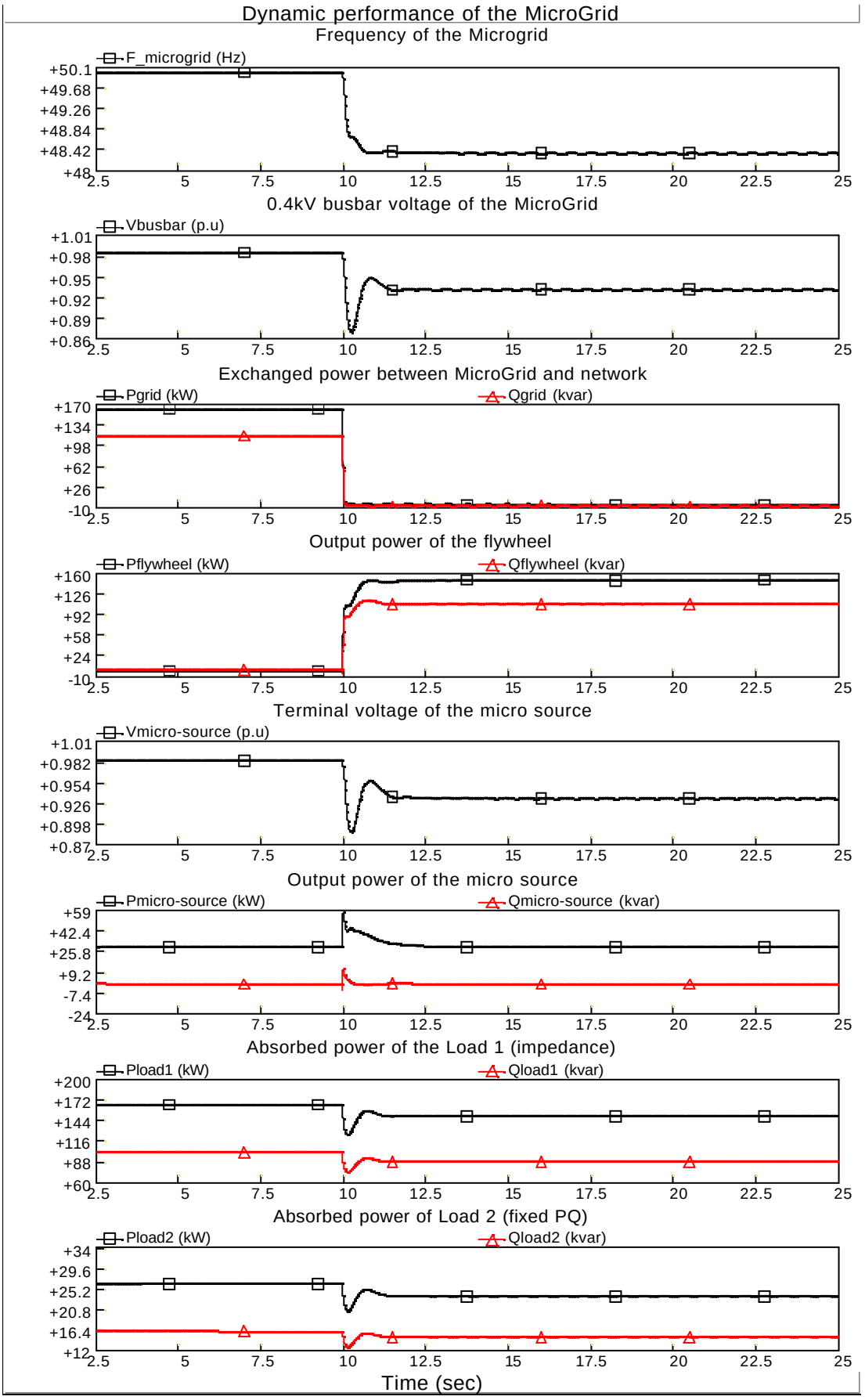

Figure 19 Dynamic performance of the MicroGrid (synchronous generator representation) when the flywheel uses Droop control during islanded mode

(c) Frequency/Voltage control

Figure 20 shows the dynamic performance of the MicroGrid when the flywheel uses Frequency/Voltage control (shown in Figures 10 and 11) during islanded mode. The control of the micro source is PQ control all time. The control of the flywheel is switched from PQ control to Frequency/Voltage.

During islanded mode of the MicroGrid, the output of the micro source is maintained at a constant value of 30kW. However, the output of the flywheel is changed from zero to the value of 171kW+j127kVar. Consequently, the frequency and voltage of the MicroGrid are both brought back to the normal values (50Hz and 1.0p.u). It should be noted that the energy export of the flywheel using Frequency/Voltage control is larger than when using Droop control.

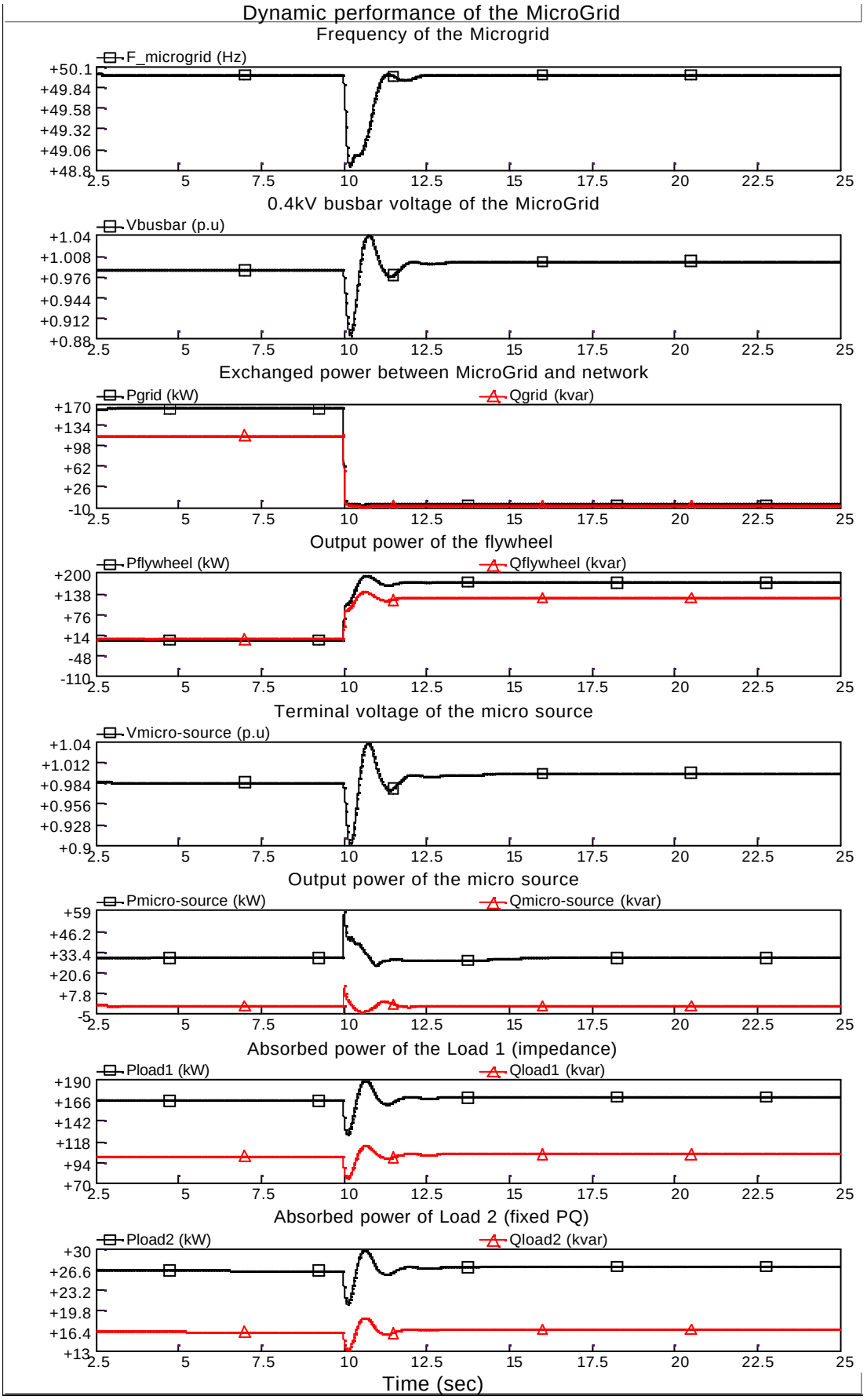

Figure 20 Dynamic performance of the MicroGrid (synchronous generator representation) when the flywheel uses Frequency/Voltage control during islanded mode

(2) STATCOM-BES representation

The MicroGrid, used in PSCAD/EMTDC modelling, is a STATCOM-BES representation, as shown in Figure 16. The implementation of the three control schemes (PQ control, Droop control and Frequency/Voltage control) is shown in Figure 12.

Figures 21, 22 and 23 show the dynamic performances of the MicroGrid when the flywheel uses PQ control, Droop control and Frequency/Voltage control during islanded mode, respectively. The deviations of the frequency and voltage depend on the mismatch between generation and demand in the MicroGrid.

Comparisons with Figures 18, 19 and 20 show that the simulation results of the STATCOM-BES representation are similar to the synchronous generator representation. However, after a disturbance, the dynamic response of the frequency and voltage of the STATCOM-BES representation MicroGrid is faster than the synchronous generator representation due to the zero inertia value of the STATCOM-BES.

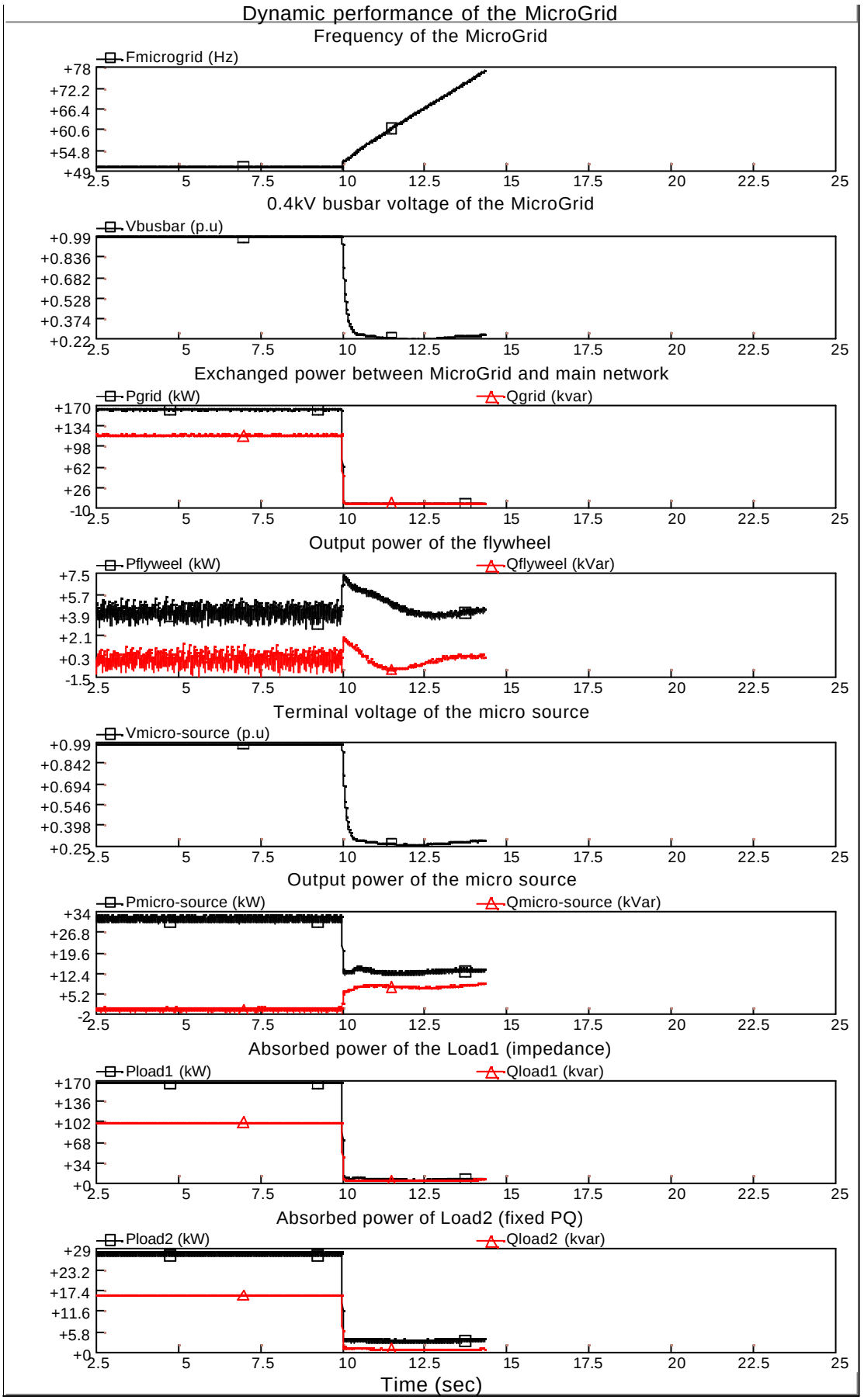

Figure 21 Dynamic performance of the MicroGrid (STATCOM-BES representation) when the flywheel uses PQ control during islanded mode

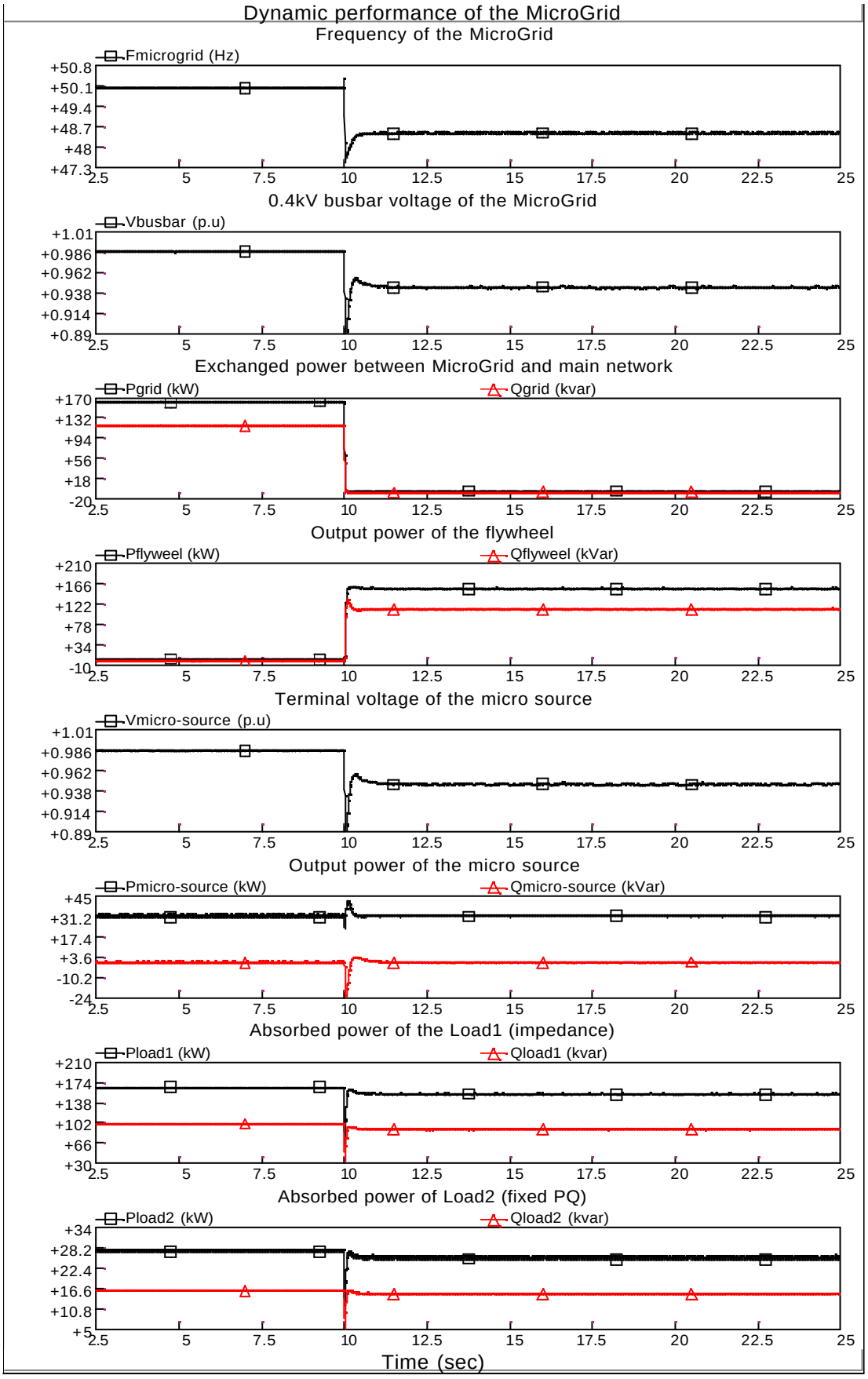

Figure 22 Dynamic performance of the MicroGrid (STATCOM-BES representation) when the flywheel uses Droop control during islanded mode

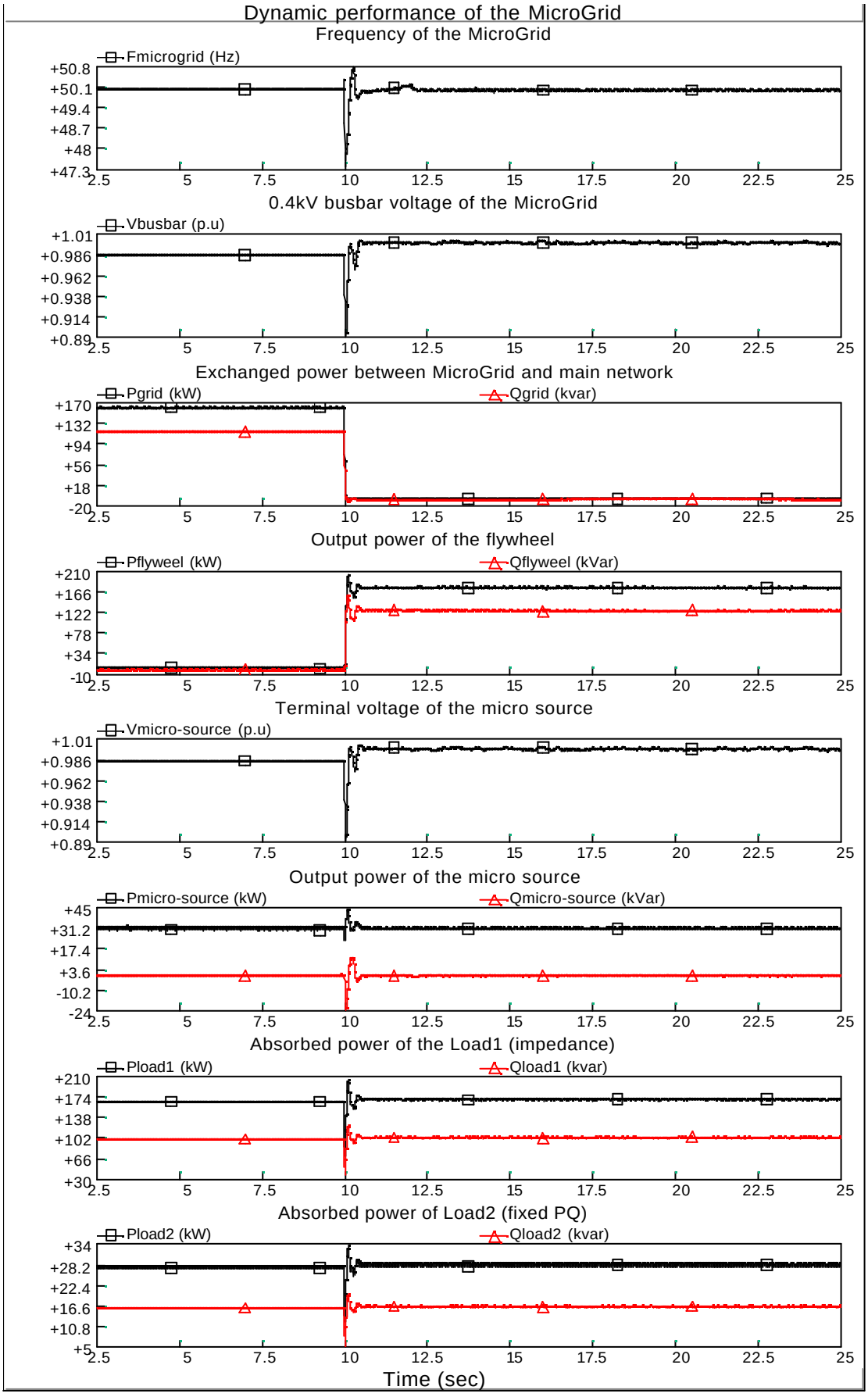

Figure 23 Dynamic performance of the MicroGrid (STATCOM-BES representation) when the flywheel uses Frequency/Voltage control during islanded mode

(3) Controllable AC and DC voltage source representations

The MicroGrid model used in this study is shown in Figure 17. The flywheel is represented either by the controllable AC or DC voltage sources. The control strategies of the flywheel are implemented and shown in Figures 13 and 14. Simulation results produced in PSCAD/EMTDC are shown in Figures 24, 25, 26 and 27.

Figure 24 shows the dynamic performance of the MicroGrid when the flywheel, represented by a controllable AC voltage source, uses Droop control during islanded mode. The control scheme of the flywheel is switched from PQ control to Droop control after disconnection of the MicroGrid from the main network.

Figure 25 shows the dynamic performance of the MicroGrid when the flywheel, represented by a controllable AC voltage source, uses Frequency/Voltage during islanded mode. The control scheme of the flywheel is switched from PQ control to Frequency/Voltage control after disconnection of the MicroGrid from the main network.

Similarly, Figures 26 and 27 show the dynamic performance of the MicroGrid when the flywheel, represented by a controllable DC voltage source, uses Droop control and Frequency/Voltage control during islanded mode.

Simulation results show that the dynamic performances of the MicroGrid produced from the simple controllable AC and DC voltage source representations of the flywheel are similar to that from the full STATCOM-BES model. For a simple application of the flywheel to the MicroGrid, the flywheel can be represented either by a controllable AC voltage source or a controllable DC voltage source.

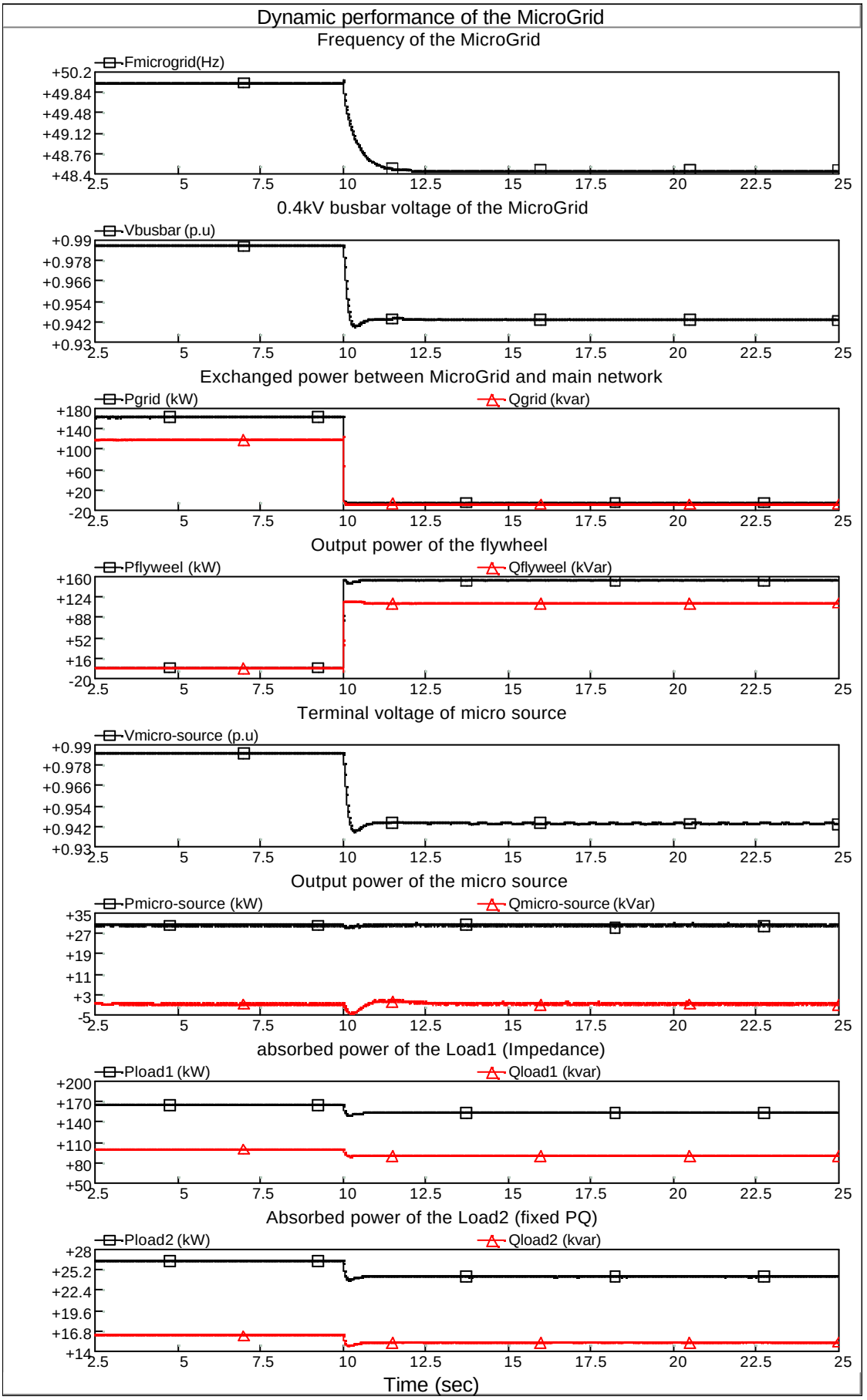

Figure 24 Dynamic performance of the MicroGrid when the flywheel, represented by a controllable AC voltage source, uses Droop control during islanded mode

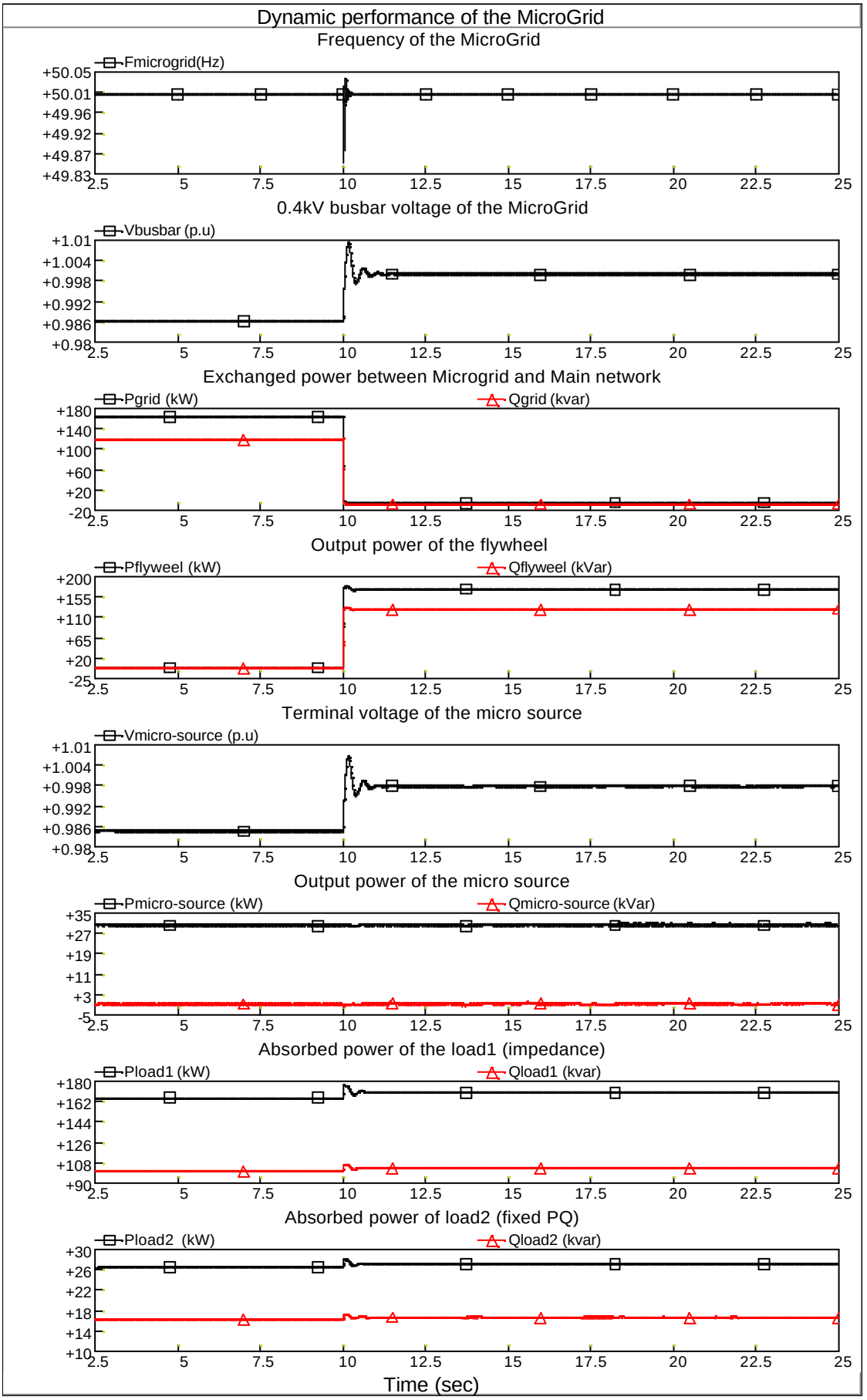

Figure 25 Dynamic performance of the MicroGrid when the flywheel, represented by a controllable AC voltage source, uses Frequency/Voltage control during islanded mode

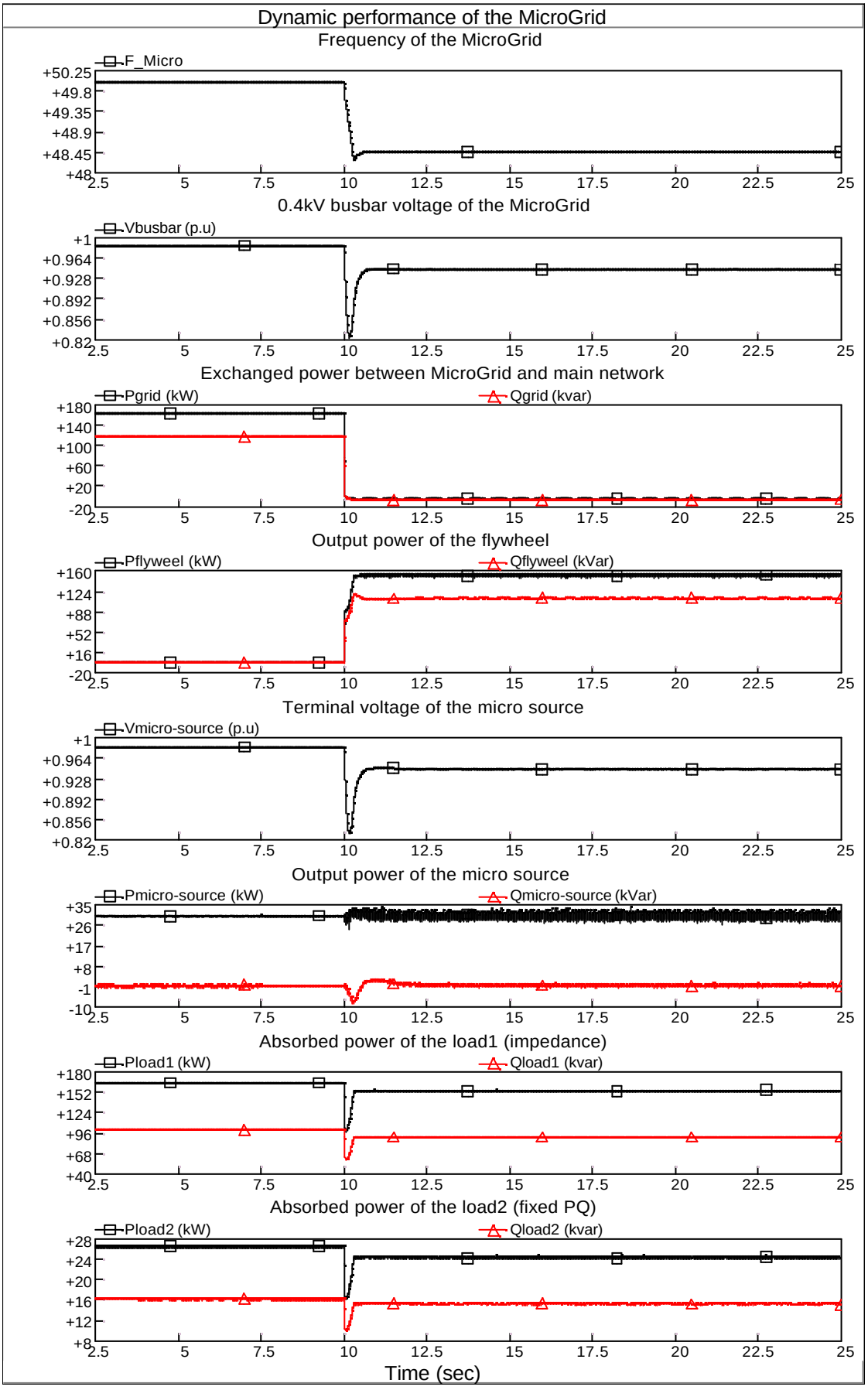

Figure 26 Dynamic performance of the MicroGrid when the flywheel, represented by a controllable DC voltage source, uses Droop control during islanded mode

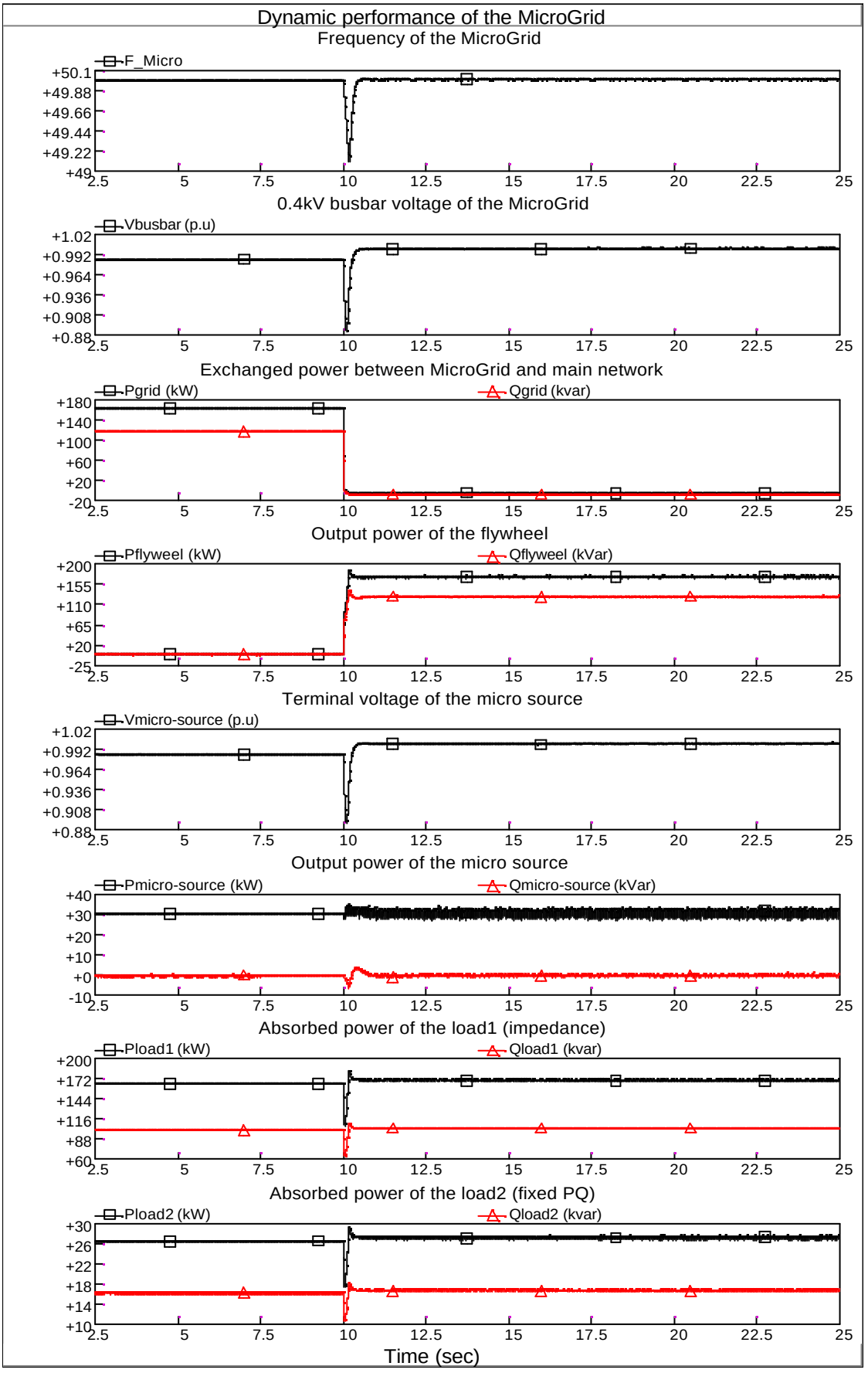

Figure 27 Dynamic performance of the MicroGrid when the flywheel, represented by a controllable DC voltage source, uses Frequency/Voltage control during islanded mode

5. Investigation of the stability of a MicroGrid

The stability of the MicroGrid is defined as a property of the MicroGrid that enables it to remain in a state of operating equilibrium under normal operating condition and to regain an acceptable state of equilibrium after being subjected to a disturbance. Being similar to the stability of the conventional system [Kundur, 1994], the stability of the MicroGrid may be divided into two components, namely, small signal stability and transient stability

The MicroGrid is small signal stable if, following small disturbances, it maintains a steady state operating condition. The dynamic simulation results of the MicroGrid produced in PSCAD/EMTDC show no evidences of small signal instability of the MicroGrid. The micro sources and flywheel are interfaced with the MicroGrid through power electronic devices. They are completely decoupled from the MicroGrid by the inverters. Normally, the length of the MicroGrid is short (less than 500meters). Thus, the MicroGrid has no demonstrated small stability problem.

The MicroGrid is transiently stable under large disturbances if, following that disturbances, it reaches an acceptable steady state operating condition. The large disturbance usually considered is a severe contingency, causing a large deviation of the operating state of the MicroGrid (e.g. a three-phase fault on the feeder). Instability of the MicroGrid may result in voltage and/or frequency collapse.

The factors influencing the stability of the MicroGrid include the control strategies of the MicroGrid, types of load in the MicroGrid and inertia constants of the motor. The control schemes of the MicroGrid are PQ control, Droop Control and Frequency/Voltage control. The micro sources and the flywheel use PQ control only when the MicroGrid is operated in grid-connected mode. After disconnection of the MicroGrid from the main network, the control of the flywheel is switched from PQ control to Droop control or Frequency/Voltage control. The types of load in the MicroGrid are fixed PQ, impedance and motor. The absorbed power of the fixed PQ load is constant at all time. The power taken by impedance loads is a function of the frequency and voltage of the MicroGrid. The motor is a rotating machine with a value of inertia.

To indicate the stability of the MicroGrid, a critical clearing time (CCT) is used in the study. The CCT is defined as a maximum fault clearing time, such that when the fault is cleared before this value the MicroGrid is stable. If the CCT is larger than the actual fault clearing time, the MicroGrid is determined to be stable; otherwise, the MicroGrid is unstable. The difference between these two values is an index of stability of the MicroGrid. The larger the CCT is, the higher the stability of the MicroGrid has. The CCT of the MicroGrid is calculated from the time domain off-line simulations by using electrical power system simulation software, PSCAD/EMTDC.

Figure 28 shows a simple MicroGrid represented by STATCOM-BES. It is implemented in PSCAD/EMTDC.

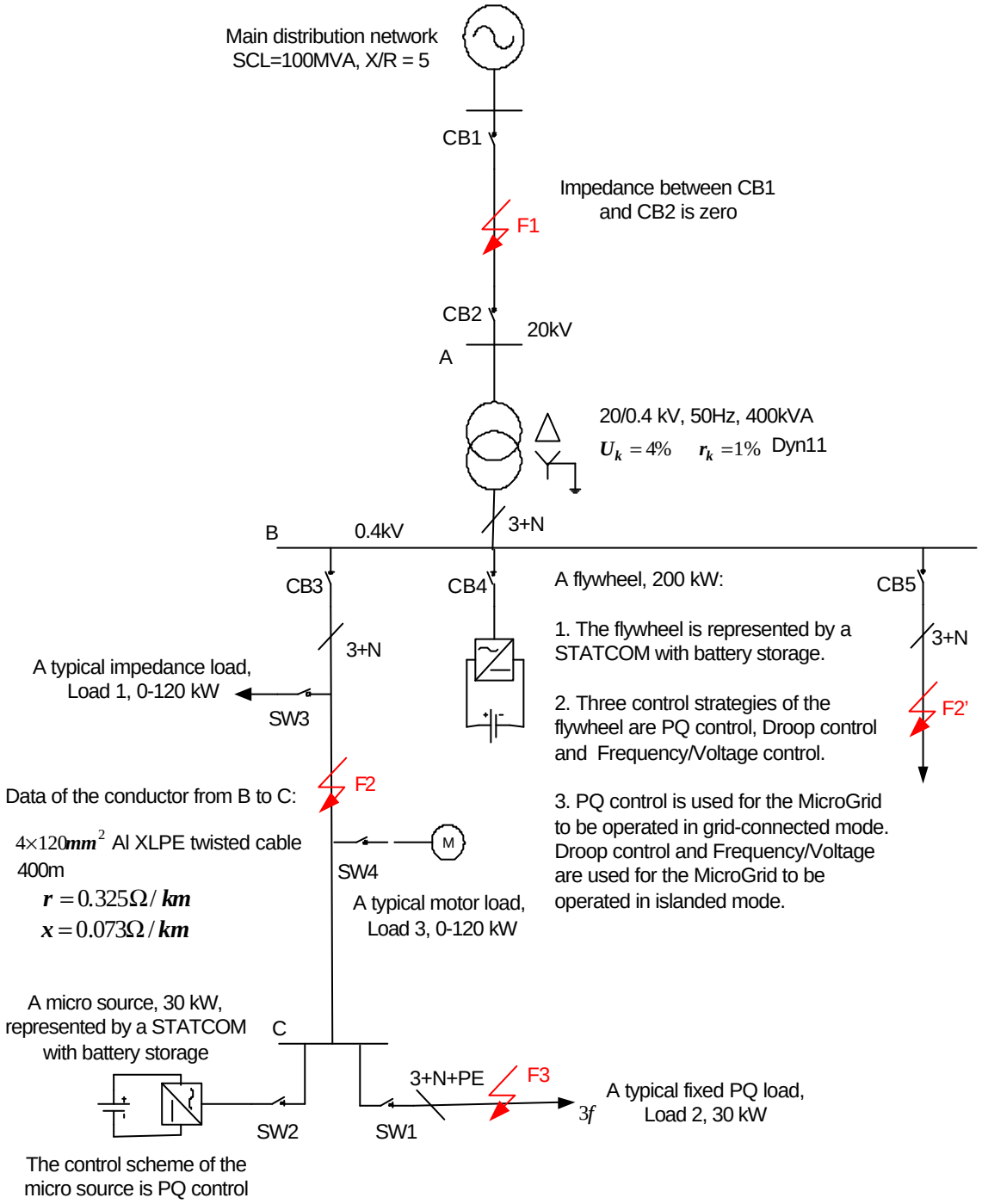

Figure 28 A simple MicroGrid model represented by STATCOM-BES

In Figure 28, the flywheel and micro source are represented by STATCOM-BES. The parameters of the MicroGrid are the same as that described in Section 4. Load 3 is a typical squirrel induction motor. The parameters of the motor are as follows [Smith, 1993]:

- Rated capacity: 100 [kW]
- Rated voltage: 0.4 [kV]
- No. of Poles: 4;
- Power factor: 0.8100;
- Stator resistance (R_s): 0.0267 [p.u];
- Stator unsaturated leakage reactance (X_s): 0.0990 [p.u];
- Mutual unsaturated reactance (X_m): 3.7380 [p.u];
- Rotor resistance (R_r): 0.0126 [p.u];
- Rotor unsaturated mutual reactance (X_r): 0.0665 [p.u];
- Inertia constant (H): 0.6600 [kW sec./kVA].

5.1 Impact of types of load in the MicroGrid

Based on the model shown in Figure 28, three types of load (fixed PQ load, impedance load and motor load) in the MicroGrid are tested in PSCAD/EMTDC. A three-phase fault was applied at F1 at 10 seconds. Following the fault, the MicroGrid was disconnected from the main network and operated in islanded mode when the circuit breaker CB2 was open.

(1) Fixed PQ load

In this case, the type of load in the MicroGrid is a fixed PQ load, with a capacity of 200kW. Figure 29 shows the dynamic performance of the MicroGrid subjected to a long-term (5 seconds) disturbance of the fault at F1. It can be seen that the MicroGrid has no stability problem. During the fault, the voltage of the MicroGrid drops to zero. The frequency of the MicroGrid increases continuously due to the difference of active power between generation and demand in the MicroGrid. Although the frequency of the MicroGrid is high during the fault, it has no influence on the load as the absorbed power of the load is zero during the fault. The load is de-energised during the fault as the applied voltage is zero. After the fault, the MicroGrid is stable. The voltage and frequency of the MicroGrid are both brought back to their normal values.

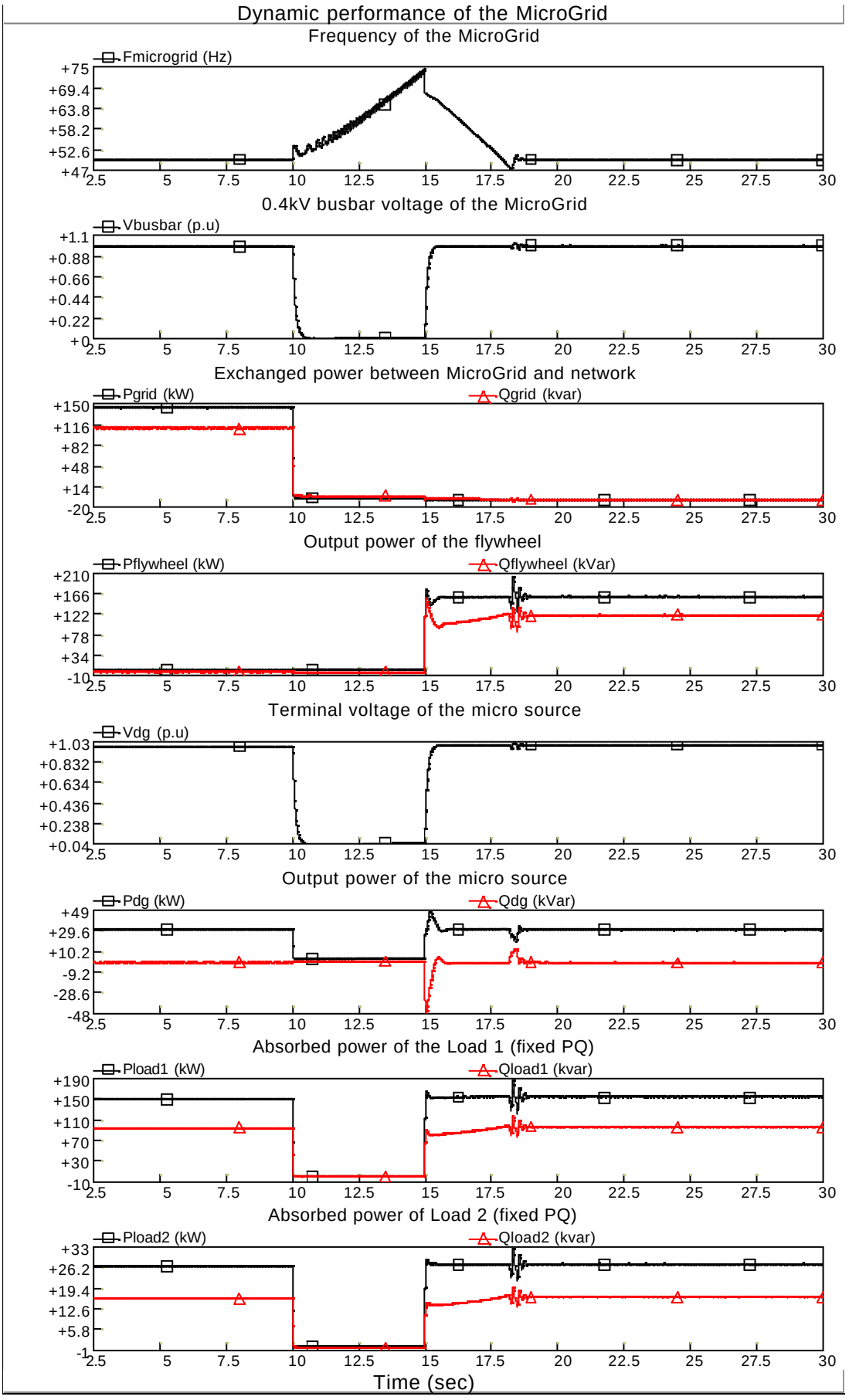

Figure 29 Dynamic performance of the MicroGrid for a type of fixed PQ load

(2) Impedance load

In this scenario, the type of load in the MicroGrid is an impedance load, with a capacity of 200kW. Similarly, Figure 30 shows that the MicroGrid has no stability problem for the impedance load.

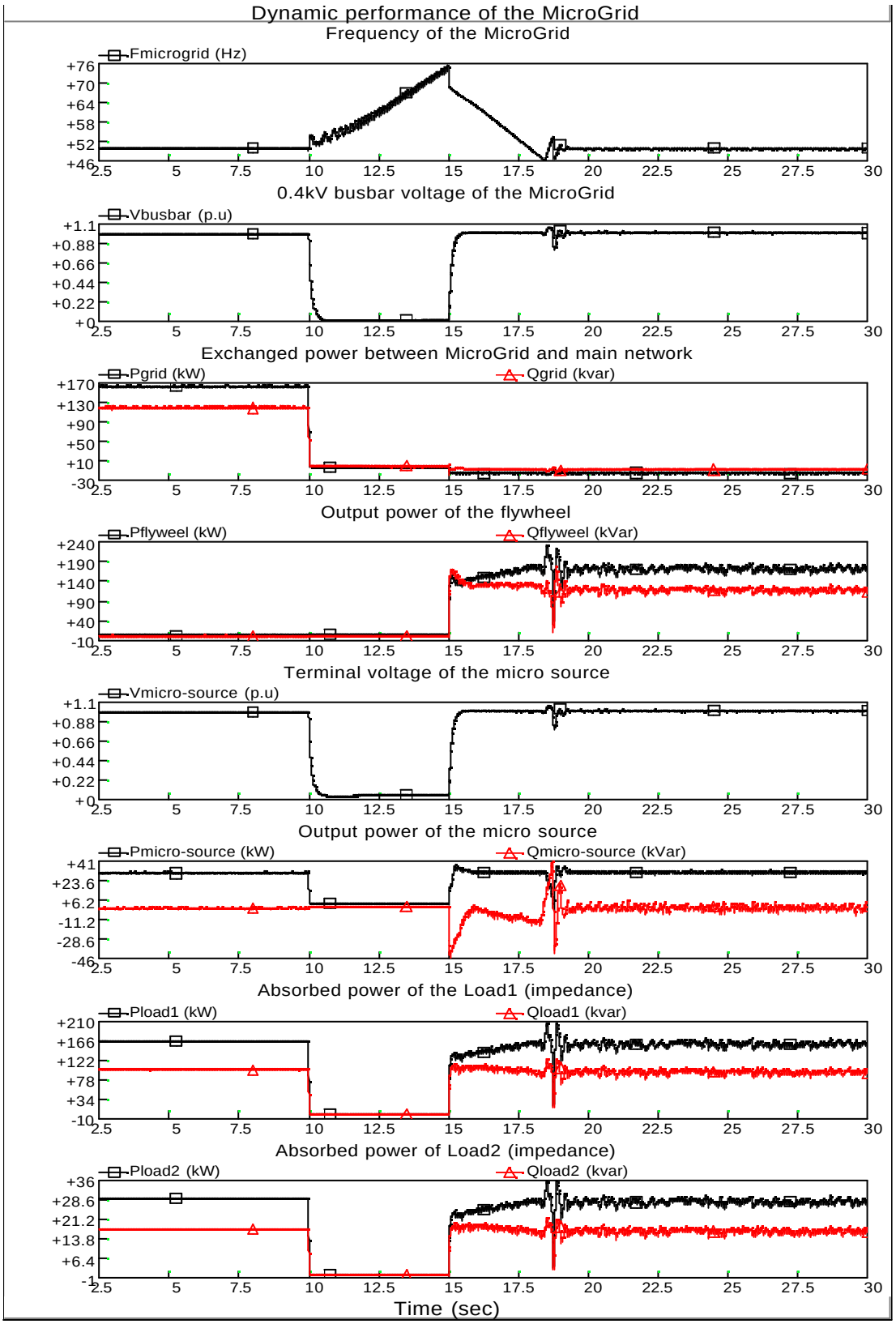

Figure 30 Dynamic performance of the MicroGrid for a type of impedance load

(3) Motor load

In this case, the type of load in the MicroGrid is a squirrel induction motor, with a capacity of 200kW. Figure 31 shows the dynamic performance of the MicroGrid for the fault at F1 with a clearing time of 0.025 seconds. During the fault, the speed of the motor decreases. After the fault, it can be seen that the speed of the motor is reduced continuously, and then, the motor is stalled. The motor tends to absorb large reactive power from the MicroGrid. The MicroGrid is unstable. The voltage of the MicroGrid collapses while the frequency of the MicroGrid is normal. This is a typical transient voltage instability (voltage collapse) of the MicroGrid.

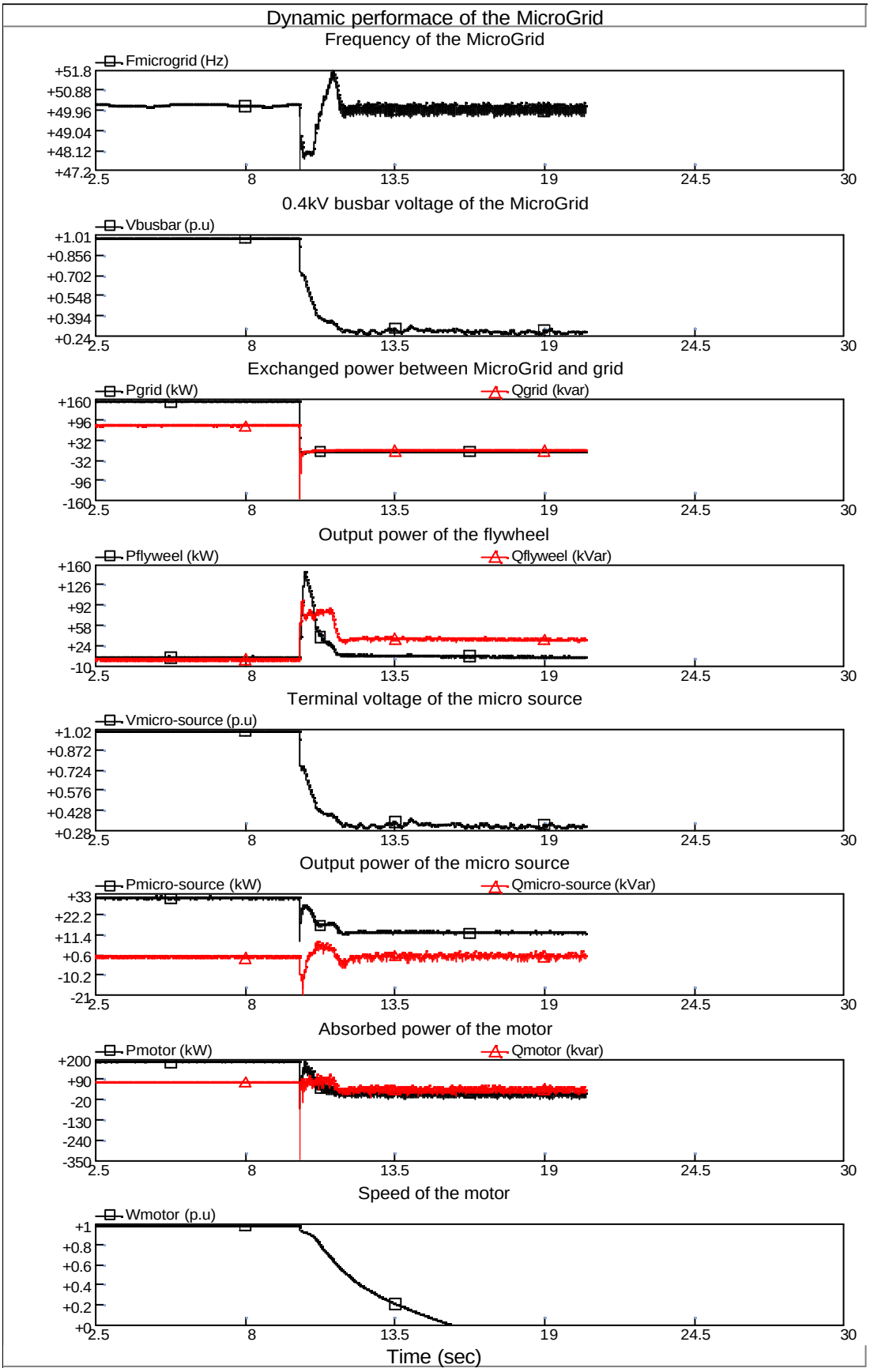

Figure 31 Dynamic performance of the MicroGrid for a type of motor load

The transient stability of the MicroGrid is normally concerned with the effect of large disturbance, a three-phase short circuit fault, on the network and the motor load in the MicroGrid. From motor torque-slip characteristic points of view, when a fault occurs in the network, the electrical torque of the motor decreases as its terminal voltage drops significantly. However, the mechanical torque of the motor is almost constant during the short period of the fault. The rotor speed of the motor is reduced. If the fault remains long enough the speed of the motor will decrease continuously and stability of the motor is lost.

Figure 32 shows a typical motor mechanical torque T_m and the electrical torque-slip (T-S) curves of the motor under three operation conditions: normal T_{e_normal}, during fault T_{e_fault} and post-fault T_{e_post}.

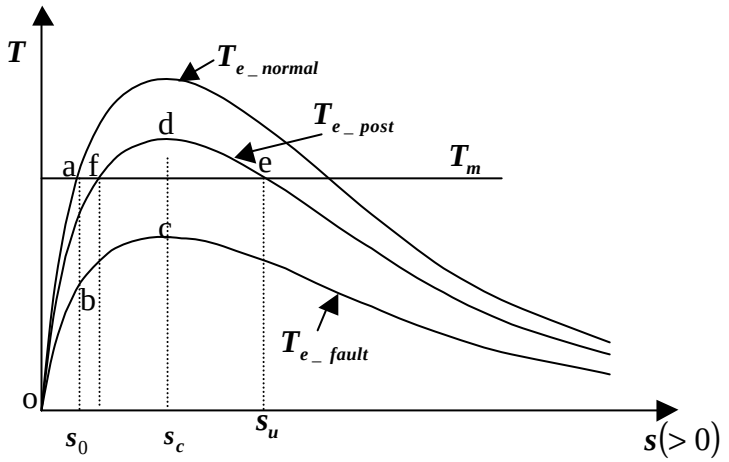

Figure 32 Typical electrical torque-slip curves of a motor as it responds to a fault

From Figure 32, initially, the motor operates at point ***a***, with conditions: $T_{e\_normal} = T_m$ and $s = s_0$. When a fault occurs, the characteristic of the motor suddenly changes from T_{e_normal} to T_{e_fault}, and the operating point immediately shifts from ***a*** to ***b***. Since the mechanical torque T_m is now greater than the electrical torque T_{e_fault}, the motor decelerates from ***b*** to ***c***, hence having a slip s_c. When the fault is cleared by isolating the faulted circuit, the characteristic of the motor immediately changes from T_{e_fault} to T_{e_post}, and the operating point suddenly shifts from ***c*** to ***d***. Now, the electrical torque T_{e_post} is greater than the mechanical torque T_m, which causes an acceleration of the

motor. However, since kinetic energy of the motor has been released during the period of the fault, the speed of the rotor, and hence the reconnected motor speed, will have decreased continuously, so increasing the slip.

The operating point ***e*** is reached when the effective kinetic energy has been completely compensated. However, because the increased slip, T_{e_post} is greater than T_m, the speed of the generator increases, and the operating point retraces the T_{e_post} curve from ***e*** through ***d*** to ***f***. After this whole period of oscillation, the motor now operates at ***f*** and with slip s_s.

If clearance of the fault is delayed, the kinetic energy released during the fault is not compensated completely at point ***e***. As a result, the slip increases beyond a critical value s_u, where T_{e_post} is less than T_m, and the motor continues to decelerate and stalls. The motor becomes unstable.

Figure 33 shows a Torque-Slip curve of the motor (Load 3, in Figure 28) under normal terminal voltage (V = 1 p.u). It can be seen that the pullout torque (maximum electrical torque) of the motor at point C is above 2 per unit. Points A and B correspond to 100kW and 200kW loading values of the motor, respectively. The point A is further away from point C than B. Stability of the motor operating at point A is higher than at point B.

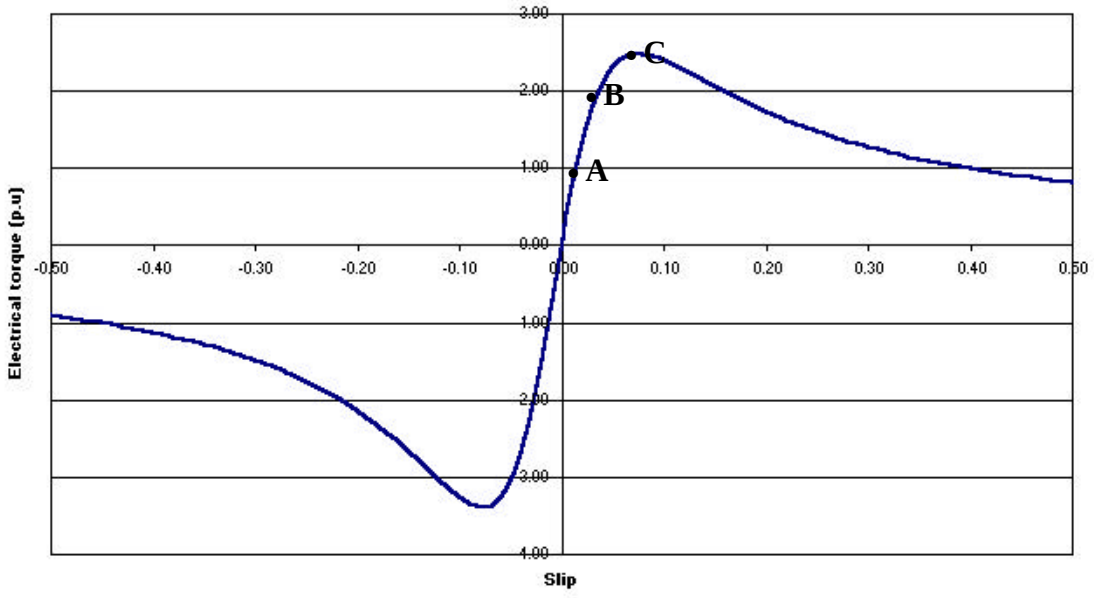

Figure 33 Electrical torque-slip curve of the motor (V =1.0p.u)

Figure 34 shows the reactive power-slip (Q-S) curve of the motor. Under normal conditions, the motor operates at point A. The motor absorbs reactive power (about 30% its rating) from the MicroGrid to establish a magnetic field between the stator and rotor. However, when the slip of the motor increases slightly, the absorbed reactive power of the motor will increase significantly. If the flywheel is not able to supply enough reactive power during islanded mode, the MicroGrid will be unstable due to a large reactive power absorbed by the motor. Thus, the voltage of the MicroGrid will collapse.

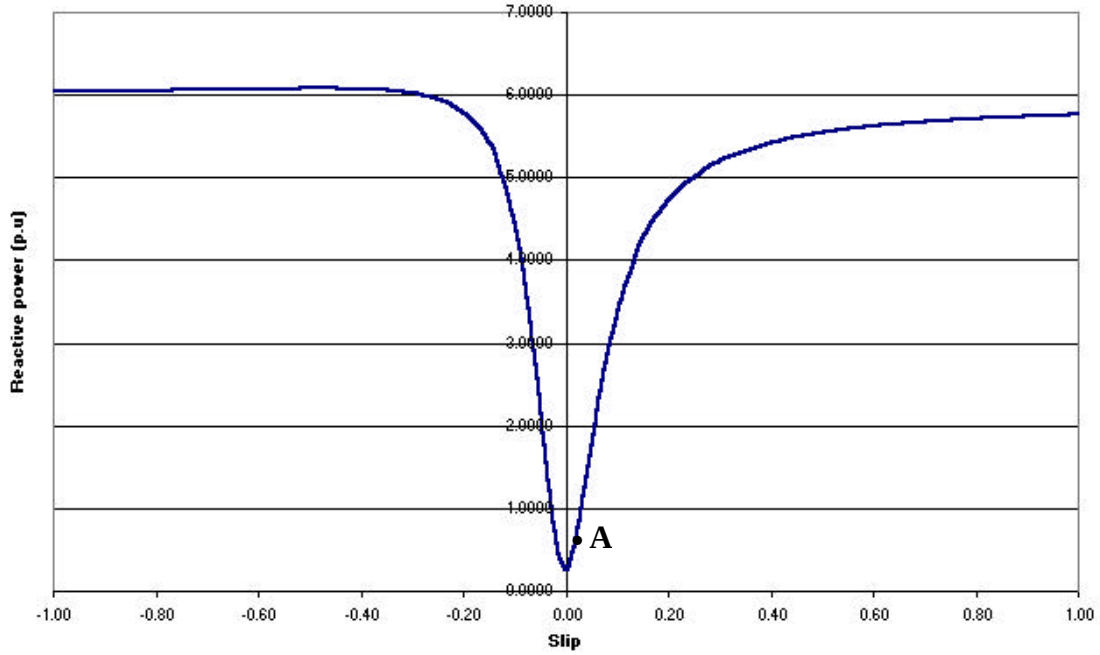

Figure 34 Reactive power-slip curve of the motor (V =1.0p.u)

Figure 34 shows that the stability of the MicroGrid mainly depends on the motor load in the MicroGrid. The larger the capacity of the motor is in the MicroGrid, the lower the stability of the MicroGrid has. In this case, instability of the MicroGrid is usually due to voltage collapse.

5.2 Impact of locations of fault in the MicroGrid

In this study, a combined type load (15% fixed PQ, Load 1; 25% impedance, Load 2; and 60% motor, Load 3) is used in the MicroGrid. A three-phase fault is applied at three different places: F1, F2' and F3 separately, as shown in Figure 28.

(1) Fault F1

For fault F1, the MicroGrid is disconnected from the main network after the fault. The MicroGrid is operated in islanded mode when the circuit breaker CB2 is open. The control scheme of the flywheel is switched from PQ control to Frequency/Voltage. The control of the micro source is still PQ control. Simulation results produced in PSCAD/EMTDC indicate the MicroGrid has a stability problem. The critical clearing time of the MicroGrid mainly depends on the characteristic of the motor in the MicroGrid. Figure 35 shows the CCT characteristic of the MicroGrid for the capacity of the motor changed from 50kW to 120kW.

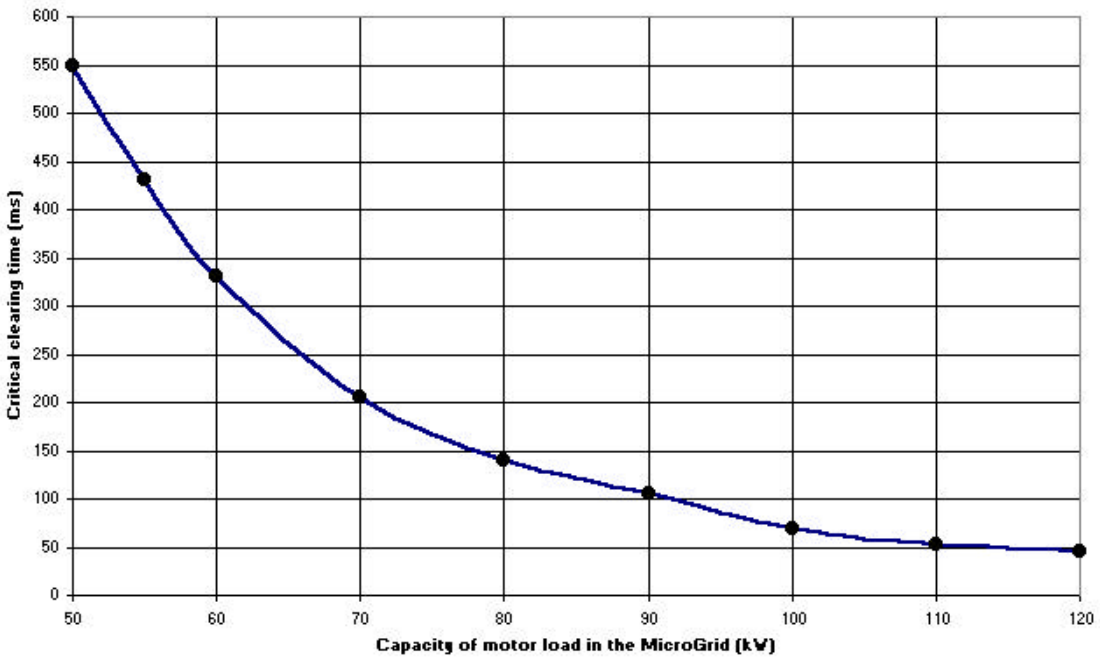

Figure 35 CCT characteristic of the MicroGrid for fault F1

(2) Fault F2' (grid-connected mode)

For fault F2', the circuit breaker CB2 is closed at all times. The MicroGrid is still operated in grid-connected mode after the fault. The control schemes of the micro source and flywheel are PQ control. Figure 36 shows the dynamic performance of the MicroGrid for a long-term fault clearing time of 5 seconds. It can be seen the MicroGrid has no stability problem. The main network is able to supply enough active and reactive power to compensate requirements of the MicroGrid. The voltage and frequency of the MicroGrid can be brought back to the normal values. The speed of the motor is also restored to normal.

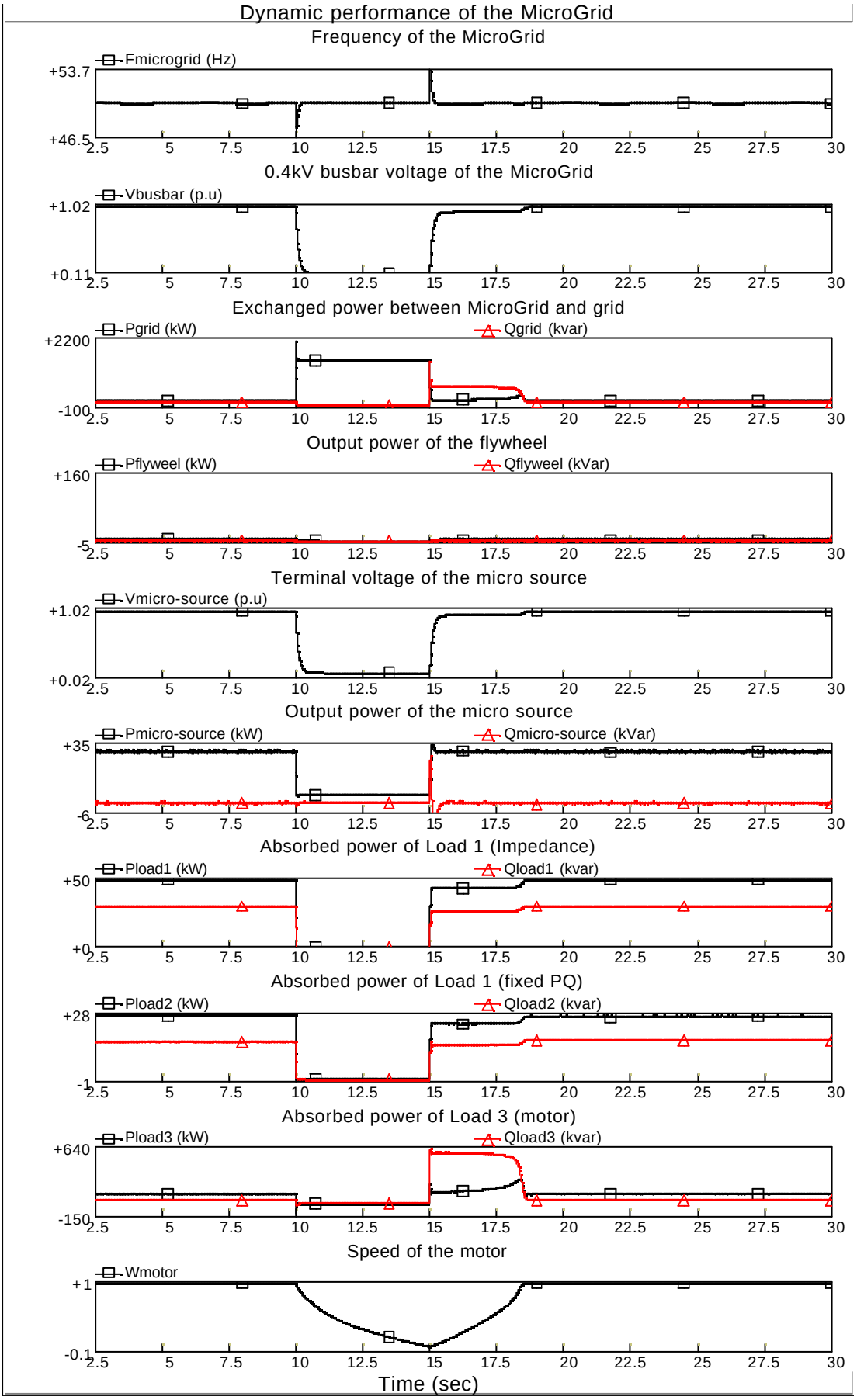

Figure 36 Dynamic performance of the MicroGrid for fault F2'
under grid-connected mode

(3) Fault F3 (grid-connected mode)

For fault F3, similarly, the MicroGrid is still operated in grid-connected mode after the fault. Figure 37 shows the MicroGrid has also no stability problem. During the fault, the speed of the motor decreases slightly. After the fault, the frequency and voltage of the MicroGrid are both restored back to normal quickly.

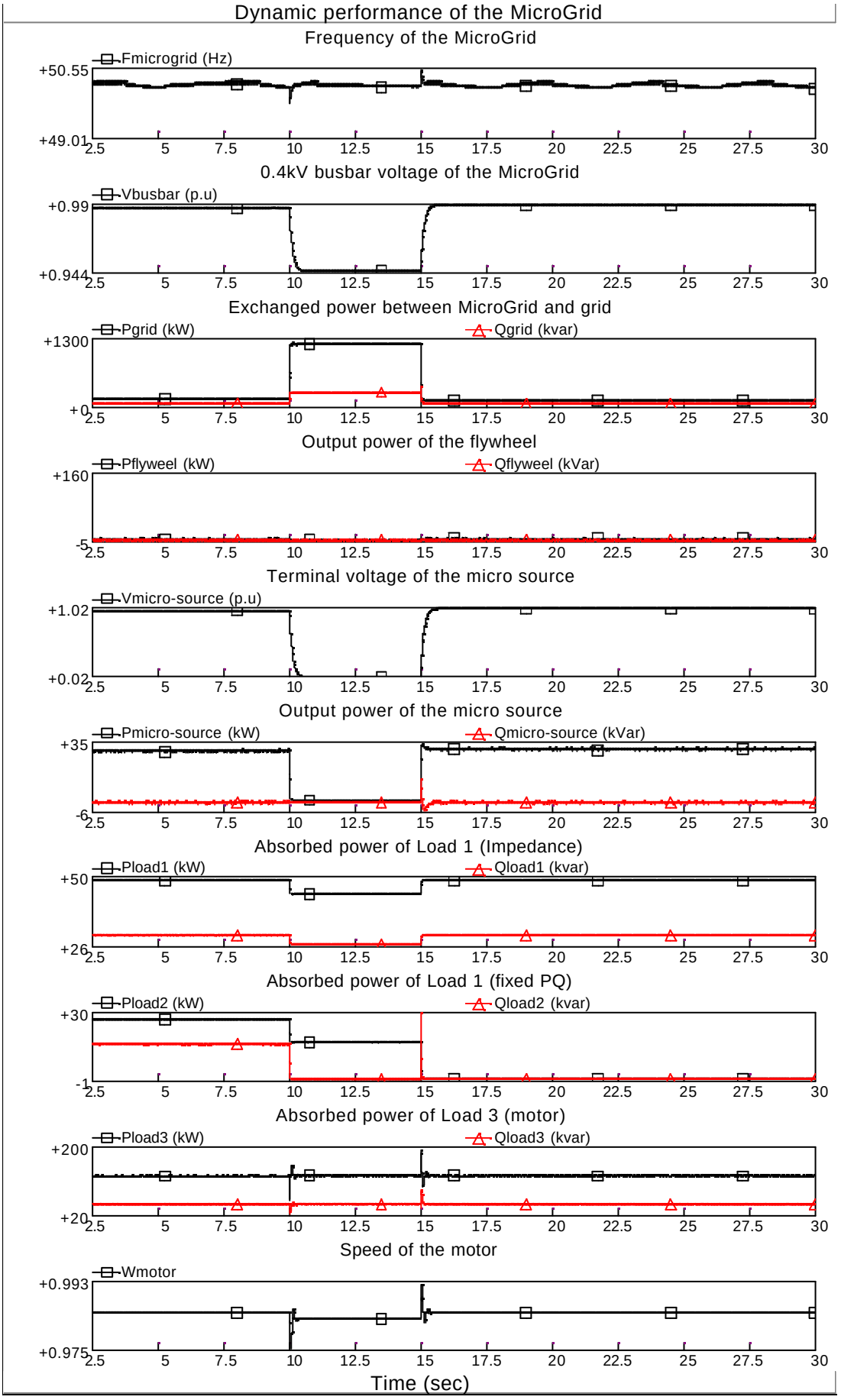

Figure 37 Dynamic performance of the MicroGrid for fault F3 under grid-connected mode

(4) Fault F2' and F3 (islanded mode)

However, for faults F2' and F3, the MicroGrid may be unstable when the MicroGrid is operated in islanded mode. During the islanded mode, the flywheel will compensate the extra power unbalance between generation and demand in the MicroGrid.

Figure 38 shows the CCT characteristics of the MicroGrid operated in islanded mode for faults F2' and F3. The control scheme of the flywheel is Frequency/Voltage control. The capacity of the motor in the MicroGrid is changed from 50kW to 120kW.

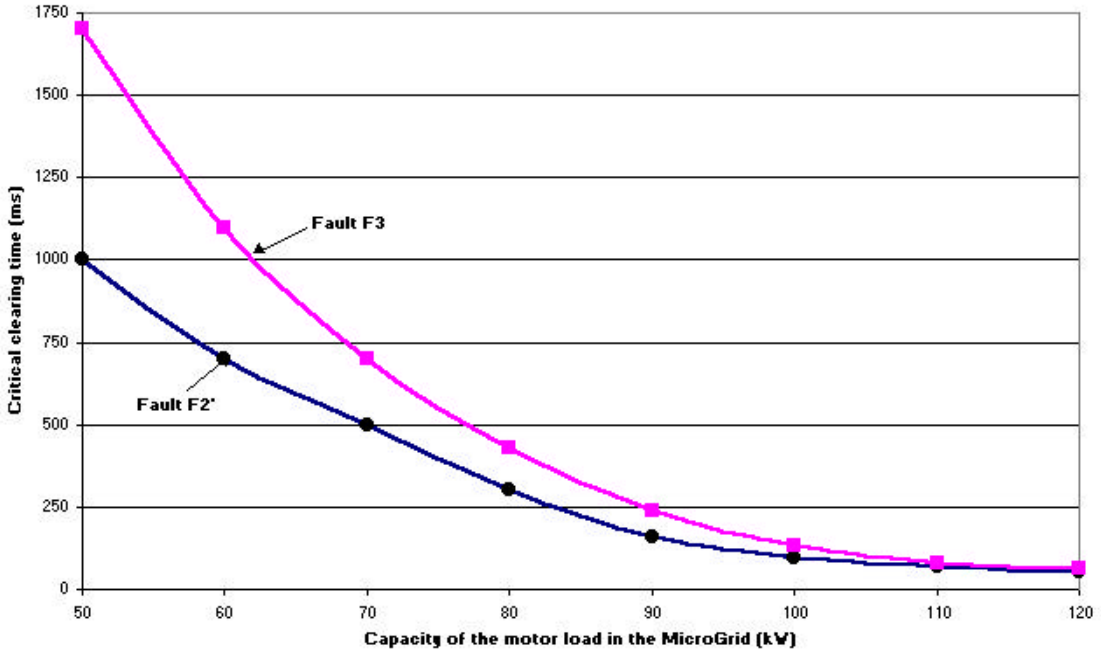

Figure 38 CCT characteristics of the MicroGrid operated in islanded mode for fault F2' and F3

Figure 38 shows that for faults F3 and F2', the CCTs of the MicroGrid operated islanded mode decrease when the capacity of the motor in the MicroGrid increases. The stability of the MicroGrid for fault F2' is more sensitive than for fault F3. The CCTs of the MicroGrid are almost the same when the capacity of the motor increases and reaches to a value of 120kW.

Considering stability of the MicroGrid at different locations of the faults (F1, F2' and F3), the fault at F1 is the severest case to maintain the stable operation of the MicroGrid after the fault. For fault F1, the MicroGrid will be disconnected from the main network and operated in islanded mode. The control strategy of the flywheel is switched from PQ control to Droop control or Frequency/Voltage control. The CCTs of the MicroGrid are quite low when a fault happens at F1. Thus, to maintain the

stability of the MicroGrid after the fault, transition to islanded mode, fast protection (e.g. differential protection) is needed for fault F1.

5.3 Impact of inertia constants of the motor

In this study, three types of loads (Load 1, 15% fixed PQ; Load 2, 25% impedance; and Load3, 60% motor) are used in the MicroGrid. The capacity of the motor (Load 3) is changed from 50kW to 120kW. A three-phase fault is applied at F1 on the main network, as shown in Figure 28. After the fault, the MicroGrid is operated in islanded mode. The control scheme of the micro source is PQ control. The control strategy of the flywheel is switched from the PQ control to Frequency/Voltage control.

Figure 39 shows the CCT characteristics of the MicroGrid for different inertia constants of the motor.

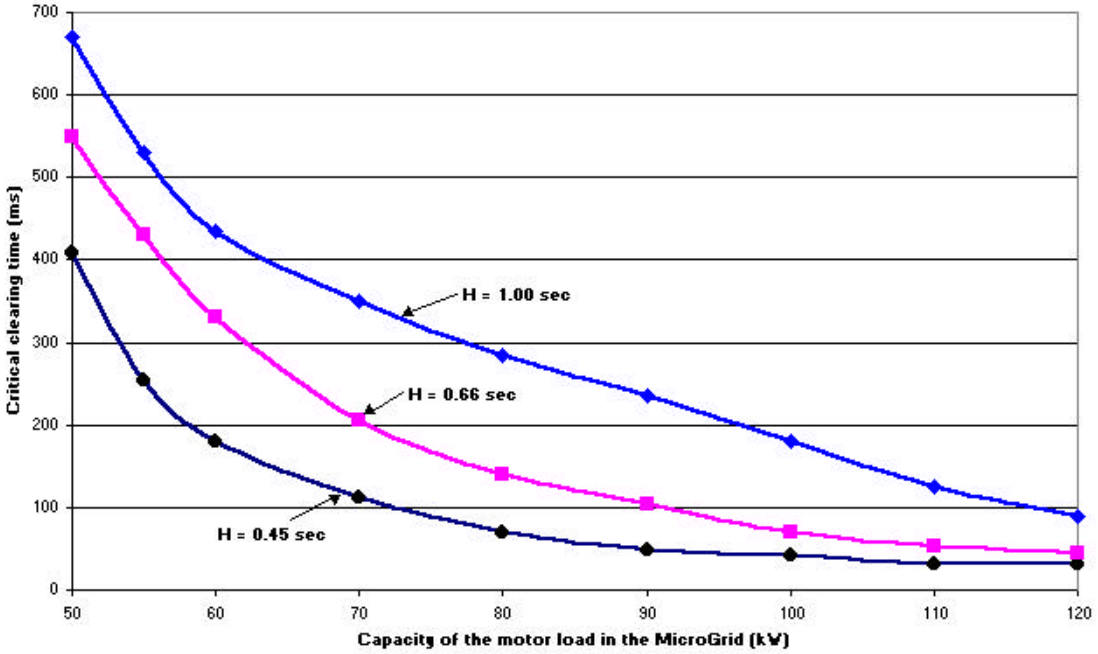

Figure 39 The CCT characteristics of the MicroGrid for different inertia constants of the motor in the MicroGrid

In Figure 39, the three curves correspond to the three inertia constants (H = 0.45sec., 0.66se. and 1.00sec.) of the motor. It can be seen that the inertia constant of the motor has a significant influence on the stability of the MicroGrid. The stability of the MicroGrid is high when the inertia constant of the motor is large.

6. Improvement of the stability of a MicroGrid

The investigation of the stability of the MicroGrid indicates the main issues influencing the stable operation of the MicroGrid are the control strategy of the flywheel and the type of load used in the MicroGrid, particularly motor load. The control scheme of the flywheel is PQ control when the MicroGrid is operated in grid-connected mode. During islanded mode, the control of the flywheel needs to be switched from PQ control to Droop control or Frequency/Voltage. The motors will be stalled when their speeds decrease significantly. The motors will be unstable when the operating point of the motor is beyond its pull-out point, corresponding to the maximum electrical torque of the motor. The motors absorb large reactive power from the MicroGrid during stalling operation. Thus, the voltage of the MicroGrid will collapse. However, the stability of the MicroGrid can be improved by using undervoltage load shedding to trip some less important motor loads in the MicroGrid.

Undervoltage load shedding method is a traditional approach to improve the stability of conventional power systems. The undervoltage load shedding measure can be easily implemented on the motor loads in the MicroGrid. The motor loads are divided into a number of groups according to their importance to the customers. Then undervoltage load shedding devices, with their setting values (e.g. V< 0.7p.u), are installed on the motor loads in the unimportant group. If the voltage of the MicroGrid is below 0.7 per unit, the undervoltage load shedding devices trip the unimportant motor loads in a time delay of 150ms automatically.

In this study, a simple MicroGrid model (see Figure 28) is used. A three-phase fault was applied at F1. The loads in the MicroGrid comprise Load1, Load 2 and Load 3. Load 1 is a fixed PQ load, with a capacity of 30kW. Load 2 is an impedance load, with capacity of 50kW. Load 3 is a motor load. The inertia constant of the motor is 0.66 seconds. The function of undervoltage load shedding is installed on Load 3. Based on three capacities of the motor load (80kW, 100kW and 120kW), the improvement of the stability of the MicroGrid was investigated using the undervoltage load shedding method. The CCT characteristics of the MicroGrid were calculated in PSCAD/EMTDC.

Figure 40 shows the stability improvement of the MicroGrid by applying the undervoltage load shedding measure on the motor load.

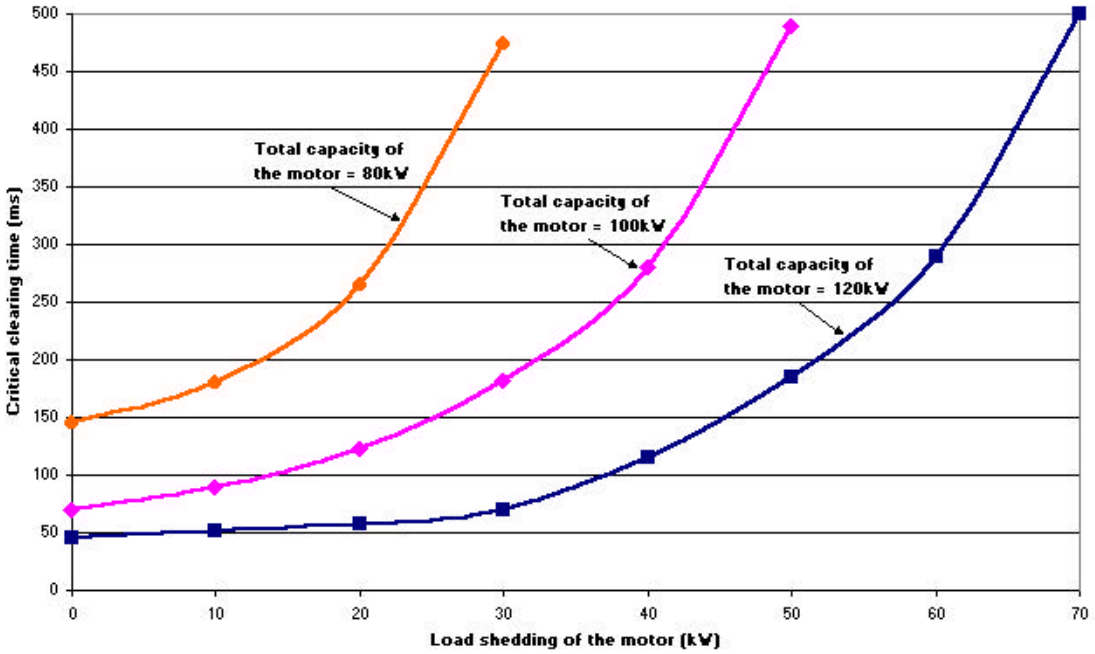

Figure 40 Stability improvement of the MicroGrid through using undervoltage load shedding on the motor in the MicroGrid

From Figure 40, the results show that the stability of the MicroGrid is improved significantly by using the undervoltage load shedding on the motor load. For a 200kW motor in the MicroGrid, the CCT of the MicroGrid increases from 45ms to 500ms when the capacity of the motor load is shed varies from zero to 70kW. For a 100kW and a 80kW motors, the improvement of stability of the MicroGrid has similar results. Therefore, the larger the capacity of the motor load that is shed in the MicroGrid, the higher the stability of the MicroGrid is gained.

7. Conclusions

With increasing penetration levels of the DGs, a number of MicroGrids will exist in the distribution network system in the future. The safety and reliability of the MicroGrid are becoming more and more important. The unique nature of the MicroGrid requires that the MicroGrid is stable operating in both grid-connected mode and islanded mode. The stable operation of the MicroGrid can be maintained through control of the flywheel and using load-shedding measures on the loads in the MicroGrid. The possible control schemes of the flywheel are PQ control, Droop

control and Frequency/Voltage control. One of load shedding methods is undervoltage load shedding.

Three representations (synchronous generator representation, STATCOM-BES representation, and controllable voltage source representation) for a MicroGrid are used. Three control schemes (PQ control, Droop control and Frequency/Voltage control) of the MicroGrid are presented and tested in PSCAD/EMTDC. The control scheme of the micro source is PQ control at all times. The control strategy of the flywheel is PQ control only when the MicroGrid is operated in grid-connected mode. During islanded operation of the MicroGrid, the control of the flywheel has to be switched from PQ control to Droop control or Frequency/Voltage. The major factors influencing the stability of the MicroGrid are the control strategies of the flywheel, types of loads in the MicroGrid and inertia constants of the motors.

The flywheel uses PQ control only when the MicroGrid is operating in grid-connected mode. The active and reactive power outputs of the flywheel are then fixed at the constant values (e.g. zero). After disconnection of the MicroGrid from the main network, during islanded mode, the control of the flywheel should be switched from PQ control to Droop control or Frequency/Voltage control. The output powers of the flywheel are regulated automatically according to the predetermined droop characteristics (Droop control) or errors of the frequency and voltage of the MicroGrid (Frequency/Voltage control).

Three types of load (fixed PQ load, impedance load and motor load) in the MicroGrid are investigated. Simulation results show that the fixed PQ and impedance loads have no effect on the stability of the MicroGrid. The motor load introduces instability to the MicroGrid as it absorbs large amounts of reactive power from the MicroGrid during its stalled operation. The instability mechanism of the MicroGrid is likely to be voltage collapse.

Three different locations (F1, F2' and F3) of the fault are also investigated. The fault at F1 is the severest case to maintain the stable operation of the MicroGrid. For fault F1, the MicroGrid is disconnected from the main network and operated in islanded mode after the fault. The control strategy of the flywheel is switched from PQ control

to Droop control or Frequency/Voltage control during the islanded operation. The CCTs of the MicroGrid have the lowest values when the fault occurs at F1. To maintain the stability of the MicroGrid during the transition to islanded mode, fast protection (e.g. differential protection) is thus needed.

The inertia constants of the motors have significant influence on the stability of the MicroGrid. Motors with high inertia constants used in the MicroGrid will enhance the stability of the MicroGrid.

The stability of the MicroGrid can be improved by using undervoltage load shedding on these motors which are less important loads in the MicroGrid. The larger the capacities of motors that are shed in the MicroGrid, the higher the stability of the MicroGrid.

8. References

Barsali S., et al. (2002), Control Techniques of Dispersed Generators to Improve the Continuity of Electricity Supply, Power Engineering Society Winter Meeting, 2002, IEEE, Volume: 2, 27-37 January 2002.

Bungay E., McAllister D. (1990), Electric Cables Handbook (second edition), BSP Professional Books, Blackwell Scientific Publication Ltd..

Glover J.D., Sarma M.S. (2002), Power System Analysis and Design (third edition), Brooks/Cole, Thomson Learning.

Kundur P. (1994), Power System Stability and Control (book), McGraw-Hill, Inc..

Lasseter R.H. (2002), MicroGrids, Power Engineering Society Winter Meeting, 2002. IEEE, Volume: 1, 27-31 January.

Smith J.R., Chen M.J. (1993), Three-Phase Electrical Machine Systems- computer simulation (book), Research Studies Press LTD.

Wall S.R. (2001), Performance of Inverter Interfaced Distributed Generation, Transmission and Distribution Conference and Exposition, 2001 IEEE/PES, Volume: 2, 28 Oct. – 2 Nov. 2001, Pages: 945 – 950.

MICROGRIDS
ENK5-CT-2002-00610

Status: Final

INESC PORTO
LABORATÓRIO ASSOCIADO

DE2-Appendix VI

MICROGRIDS
Large Scale Integration of Microgeneration to Low Voltage Grids

Contract No: ENK5-CT-2002-00610

Final Version

WORK PACKAGE E

INESC Porto Contribution to Deliverable DE2

Evaluation of MicroGrid Stability for Different Types and Locations of Disturbances

May 2005

Access: Restricted to project members

Document Information

Title	Evaluation of MicroGrid Stability for Different Types and Locations of Disturbances
Date	19th May 2005
Version	Final Version
Task	Deliverable DE2

Coordination:	João Peças Lopes	
Authors:	João Peças Lopes	jpl@fe.up.pt
	Carlos Moreira	cmoreira@inescporto.pt
	André Madureira	agm@inescporto.pt

Access:	
Project Consortium (for the actual version) European Commission, PUBLIC (for final version)	
Status:	
	Draft Version
X	**Final Version**
	Submission for Approval (deliverable)
	Final Version (deliverable approved)

Table of Contents

1. Executive Summary

The main objective of this document is to analyse the dynamic behaviour of a MicroGrid in interconnected (with a main Medium Voltage network) mode and in emergency (islanded) mode under fault conditions, i.e. in case of short-circuit, for instance. Several simulations were performed using the *MatLab*® *Simulink*® simulation platform developed within Work Package D.

A summary of the research conducted is given in the following lines:

A short introduction of MicroGrid operation is made including a description of the main characteristics of this type network and possible operating modes.

A brief description of the dynamic models used for simulation is made with particular incidence on power electronic converters modelling.

The two main modes of operating an inverter and the impact on the control strategies for MicroGrid operation are presented and a short explanation is given.

The study case networks used and the simulation platform chosen are introduced and results of several tests and simulations are presented.

Finally, the main conclusions are detailed and justified, in face of the results obtained.

2. Introduction

A MicroGrid consists of a LV distribution system to which small modular generation systems are connected. Generally speaking, a MicroGrid corresponds to an association of electrical loads and small generation systems through a LV distribution network. In this type of network there is a physical proximity between load and generation.

Addressing currently available technologies, a MicroGrid may contain several types of generation devices, for example fuel-cells, renewable generators such as wind turbines or photovoltaic (PV) systems as well as microturbines powered by natural gas.

Also, some form of storage devices (such as batteries, ultra-capacitors and flywheels) and network control and management systems are included. Storage devices present will play an important role in this kind of network, namely in what concerns fast load-following situations.

At the current research status, it is assumed that a MicroGrid can be operated in two main situations:

- Normal Interconnected Mode – the MicroGrid is electrically connected to the main MV network either being supplied by this network (totally or partially) or injecting power into the main MV grid;
- Emergency Mode – in case of failure of the main MV network (that could be caused by a fault), a MicroGrid must have the ability to operate in isolated mode, i.e., to operate autonomously, similar to power systems of physical islands.

A simulation platform under the *MatLab*® *Simulink*® environment was developed in order to evaluate the dynamic behaviour of several microsources operating together in a MicroGrid network under pre-specified conditions including interconnected and autonomous operation of the MicroGrid.

This simulation platform, including dynamic models of MicroGrid components with control and management systems, has been introduced in deliverable DD1 [1].

3. Dynamic Models

This chapter will discuss the dynamic models used in the simulation platforms that were developed in order to perform these studies.

All the microsource models used for dynamic simulation were detailed in Deliverable DD1 [1] and earlier in Deliverable DA1 [2] and, for that reason, will not be described here. In addition, some devices (such as synchronous and induction generators, loads, breakers, buses and lines) were modelled using the *MatLab*® *Simulink*® library *SimPowerSystems*.

Inverter models were developed independently and will be discussed here in detail since their development holds the basis for the control strategies adopted for an efficient MicroGrid operation. These control strategies will be explained in a later chapter.

3.1. Inverter

Habitually, there are two ways of operating an inverter. Two inverter models were derived from the implementation of the control strategies presented by INESC Porto in deliverable DD1. More details on inverter operation can be found in [3].

The first model is based on a PQ Inverter control logic, where the inverter is used to supply a given active and reactive power set-point. This model differs from the original PQ version of the inverter presented in deliverable DD1 [1].

The second model uses a Voltage Source Inverter (VSI) control logic, where the inverter is controlled in order to "feed" the load a pre-defined value for voltage and frequency. The VSI real and reactive power output is defined based on the load connected to it.

This type of inverter modelling based on their respective control functions assumes several simplifications such as neglecting fast transients, harmonic content and active power losses.

3.1.1. PQ Inverter

A PQ inverter is based on a control scheme of a current-controlled voltage source.

A method for calculating single-phase active and reactive powers is presented in [4] and was adapted for the PQ inverter developed. The instantaneous active and reactive components of inverter current are computed, with the active component in phase with the voltage and the reactive component with a 90º phase-shift lagging, both of them limited to the [-1, 1] interval. The active component is then used to control the DC link voltage and inherently the inverter active power output, balancing microsource and inverter active power levels since all microsource power variations imply a voltage variation on the DC link, which is corrected using a PI regulator. Simultaneously, the reactive component controls the inverter reactive power output. A PQ inverter can be operated using a unit power factor (corresponding to Set Point = 0 in Fig. 1) or receiving a reactive power set-point from the MGCC.

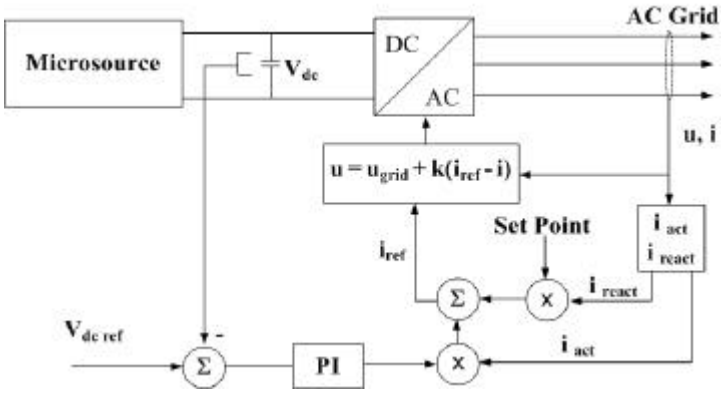

Fig. 1 – PQ inverter control system

3.1.2. Voltage Source Inverter

A VSI utilizes a control concept similar to frequency and voltage control for a conventional synchronous machine.

For a VSI operating in parallel with an AC system with angular frequency ?grid? (as it can be seen in Fig. 2), the VSI output power is defined through the droop equation

derived. In order to change the VSI output power, the idle frequency ($?_0$) is altered. When the AC system is not available, the VSI output power depends only on network load levels and droop settings so that the frequency can reach a new value. The active power is shared amongst all inverters present at the new frequency value. Similar considerations can be made for the voltage/reactive power control [5].

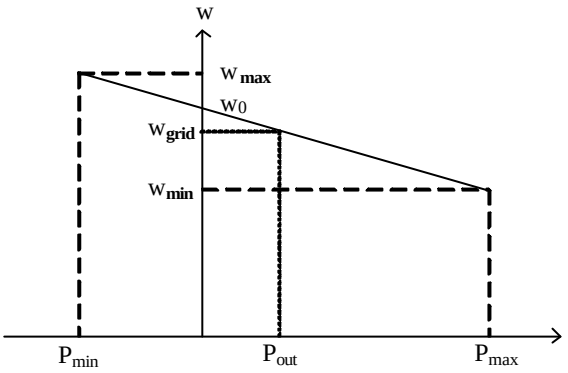

Fig. 2 – Frequency/Active Power droop

A three-phase balanced model of a VSI including the droop concepts was derived from a single-phase version presented in [4] and is shown in Fig. 3.

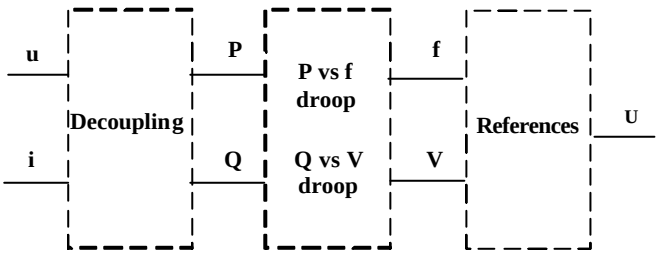

Fig. 3 – VSI control system

From the control scheme it can be seen that VSI voltages and currents are measured and used to compute active and reactive power levels and that a delay is introduced for decoupling purposes. Frequency and voltage are then computed through the droop equations and used as references for a switching sequence for the VSI, using a PWM technique.

3.1.3. Inverter Behaviour Under Short-Circuit Conditions

In conventional power systems containing synchronous machines directly connect to the network, these devices are capable of providing high short-circuit currents that are essential for quick and efficient fault detection and elimination. In a MicroGrid, however, most generating devices are connected to the network through power electronic converters and are not capable of providing such high current values.

According to the MicroGrid protection procedures [6], a protection scheme based on over-current protection will be difficult to implement for islanded operation due to the low short-circuit to load current ratio. The power electronic devices used are usually selected based on voltage, current carrying capability (for a defined switching frequency and under certain cooling conditions) and safe operating areas. Based on these factors, short-circuit handling capability of a power electronic device can be increased only by increasing the respective power rating. The following considerations are made in accordance to the previous points:

- The VSI should be up-rated in order to provide an adequate contribution to short-circuit currents (from 3 to 5 times the nominal current value);
- The PQ inverters can only provide a small total of short-circuit current (around 1.5 pu regarding its nominal current).

During and after the short-circuit, the time interval for which large current values are admissible in the VSI and value of the current itself are strongly dependent on motor load characteristics and asynchronous generator dynamics. The correct dimensioning of the storage capacity available is a very important issue in order to fully benefit from the main features of dispersed generation.

A control scheme developed for PQ inverters enables the control of the inverter current output under short-circuit conditions. In face of a short-circuit, there is a voltage drop at the inverter, leading to an active power output reduction. Consequently, there is an increase of the DC link voltage and a PI controller forces the increase of active current

output of the inverter. By limiting the total gain of the PI controller, the output current of the inverter can also be limited. An increase in the DC link voltage will also be experienced.

Acting as a voltage source, the output current of the inverter is usually very high under fault conditions (similarly to conventional synchronous machines). A control scheme such as the one presented in Fig. 1 is used in order to limit the output current. The main difference lays in the fact that now the current reference has a maximum peak value that depends on the switching devices characteristics and the frequency is imposed by the inverter frequency/active power droop. The output current is continuously monitored and, whenever its value rises above the maximum value, the control scheme is switched in accordance. After fault elimination, the VSI returns to voltage control mode.

4. Operation and Control Modes

This chapter describes the different control modes developed and tested and the main strategies chosen in order to achieve good performance for MicroGrid dynamic behaviour.

For a MicroGrid operating in emergency mode, i.e. in islanded mode, the inverters must be responsible for providing means to control frequency and also voltage. If not, the MicroGrid could experience voltage and/or reactive power oscillations [7].

While the MicroGrid is being operated in interconnected mode, all inverters can be operated as PQ inverters since a frequency and voltage reference is available from the main MV system. However, a disconnection from the main power source would lead to the loss of the MicroGrid as the frequency and voltage references would be lost and there could be no matching for load/generation imbalances. Then, the VSI must provide these requirements. Using VSI control capabilities by adjusting droop settings, a VSI can be operated in parallel with the main power grid without injecting active or reactive power. When disconnection from the main grid occurs, the VSI output is automatically de fined by the load/generation deviation within the MicroGrid. This is a key solution for MG islanded operation. Based on this, two main control strategies are achievable [8]:

- Single Master Operation – in which a VSI or a synchronous machine connected to the grid (using a diesel engine as the prime mover, for example) is used as voltage reference when the main power supply is lost; all other inverters present can be operated in PQ mode;
- Multi Master Operation – in which more than one inverter is operated as a VSI, corresponding to a scenario with dispersed storage devices; eventually, other PQ inverters may also coexist.

The VSI reacts to power system disturbances (for example, load-following situations or wind fluctuations) based only on information available locally [5]. In order to promote adequate secondary control for restoring frequency to the nominal value of 50

Hz after a disturbance, two main strategies can be followed: local secondary control, using a local PI controller located at each microsource, or centralized secondary control mastered by the MGCC, providing set-points for active power outputs of the primary energy sources [9].

These two control strategies were presented in deliverable DD1 [1], and their respective detailed implementation can be found there.

5. Simulation in *MatLab® Simulink®*

This chapter introduces the Low Voltage test system used for simulation purposes considered in this document.

The study case LV network defined by NTUA was the base for the simulation platform that was developed, with some modifications that were later introduced. A single-line diagram of this network can be seen in Fig. 4.

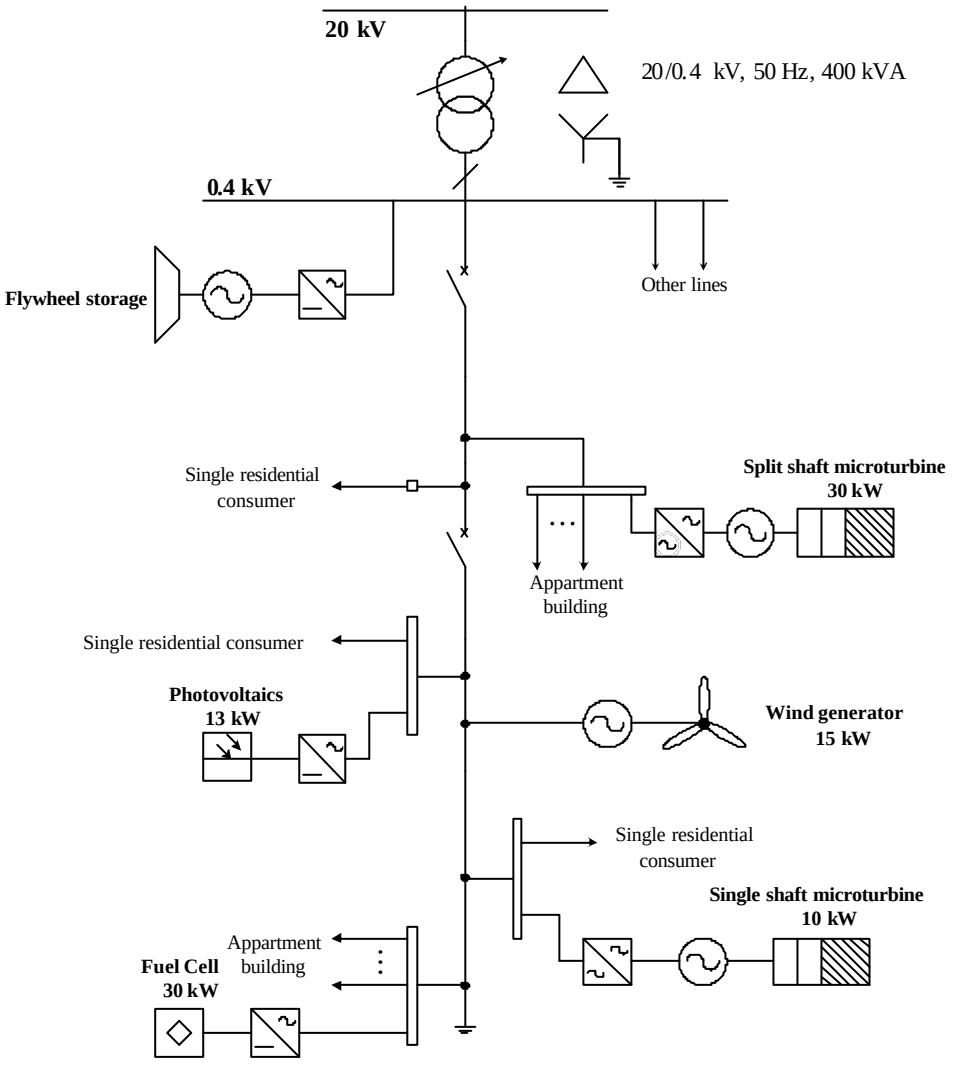

Fig. 4 – Study case LV network

Fig. 5 depicts the LV test network under the *MatLab*® *Simulink*®environment.

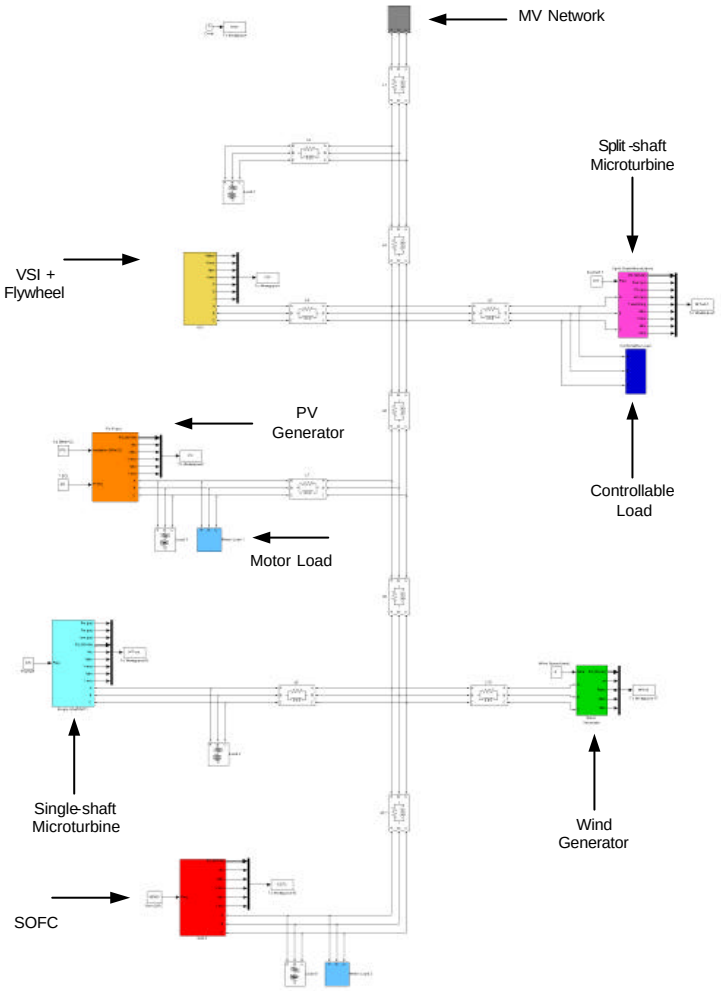

Fig. 5 – Study case LV network under the *MatLab*® *Simulink*® environment

For simplification of the simulation procedure, namely concerning computational execution times, several smaller networks based on the study case network were developed. The structure of these networks will be detailed in the corresponding chapter.

6. Simulation Results

This chapter introduces some of the most interesting results obtained from a large number of simulations performed. The main variables under analysis will be presented and a critical review of the results will be made.

For simulation purposes, two different operating scenarios were considered: In Scenario 1 the Microgrid is connected to the main MV network and in Scenario 2 the Microgrid is operating in islanded mode. Plus, two different fault locations were considered: In Case A a fault on the main MV network was considered and in Case B a fault was applied to the MicroGrid network. Several fault elimination times were considered for the presented situations.

Also, the impact of load types on the dynamic behaviour of the MicroGrid was evaluated.

In addition, for the scenarios and cases described, a comparison between the dynamic behaviour of the MicroGrid with and without the possibility of load-shedding was tested.

For the simulation platform considered, under the *MatLab® Simulink®* environment, only symmetrical three-phase faults were applied.

The control strategy chosen to operate the MicroGrid was the Single Master approach.

6.1. Impact of Types of Loads

It has been observed that constant impedance load types have no significant influence on the dynamic behaviour of the MicroGrid. However, motor loads have very serious implications on the stability of the MicroGrid under fault conditions. The influence of motor loads is due to the fact that the speed of the motor reduces significantly leading to the stalling of the motor. In such a case, the motor absorbs large portions of reactive power which causes voltage stability problems in the MicroGrid that

often lead to Voltage Collapse. Consequently, the stability of the MicroGrid depends on the percentage and characteristics (namely the inertia) of the motor loads present.

6.2. Impact of Fault Locations

The simulation was performed using a simplified network, shown in Fig. 6, based on the one presented in Fig. 4. The simplified network includes a Solid Oxide Fuel-Cell (SOFC), a Single-shaft Microturbine, a Flywheel system with a VSI and several loads (30% of motor loads and 70% of constant impedance loads). The total load of the MicroGrid is around 40 kW.

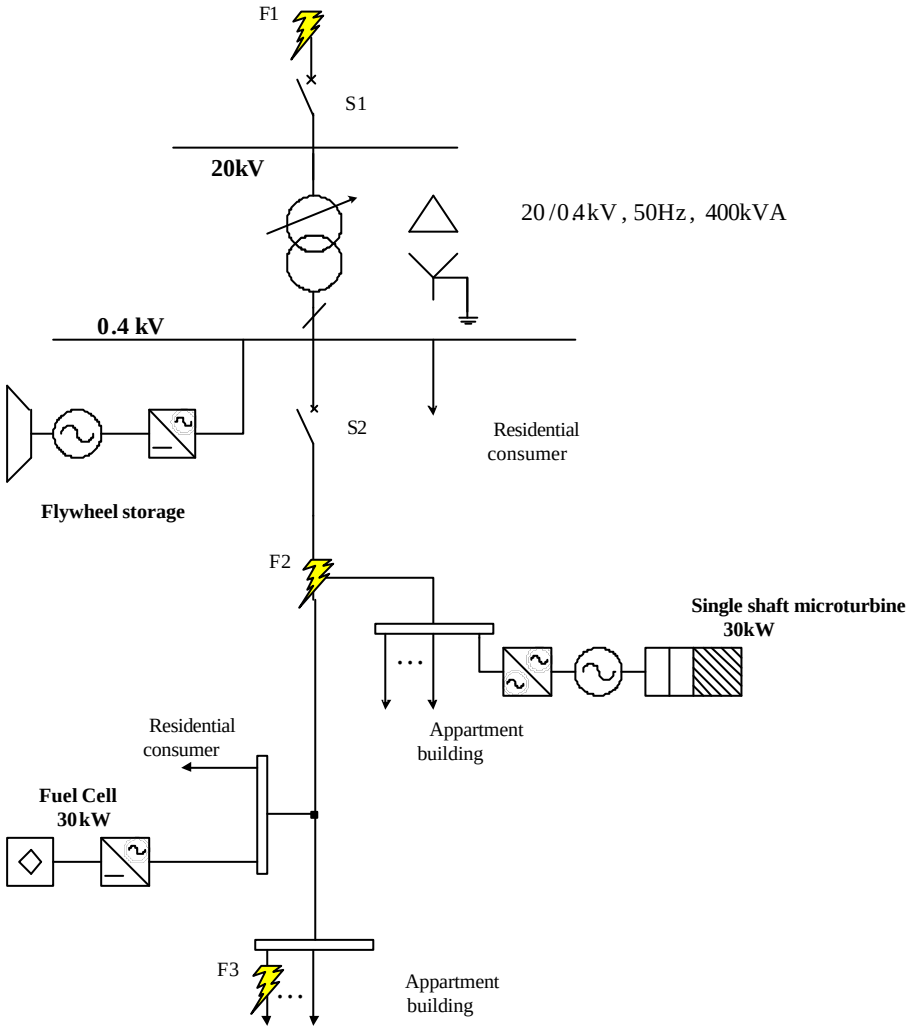

Fig. 6 – Simplified study case LV network

Fig. 7 shows the LV test network under the *MatLab*® *Simulink*®environment.

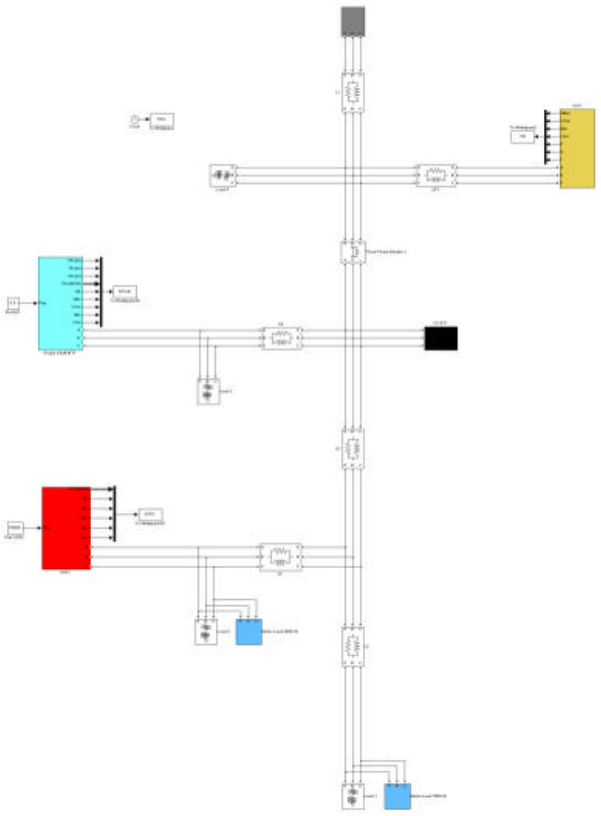

Fig. 7 – Simplified study case LV network under the *MatLab*® *Simulink*® environment

6.2.1. Fault on the Main MV Network

A three-phase fault (F1) is considered to be applied at t = 10 seconds. The MicroGrid is operating in interconnected mode prior to the fault – Scenario 1. The successful elimination of the fault takes 100 milliseconds after the occurrence of the fault, causing the islanding of the MicroGrid. The MicroGrid is importing active power (around 10 kW) from the main MV network prior to the occurrence of the fault. The simulation results are presented for the main electrical variables.

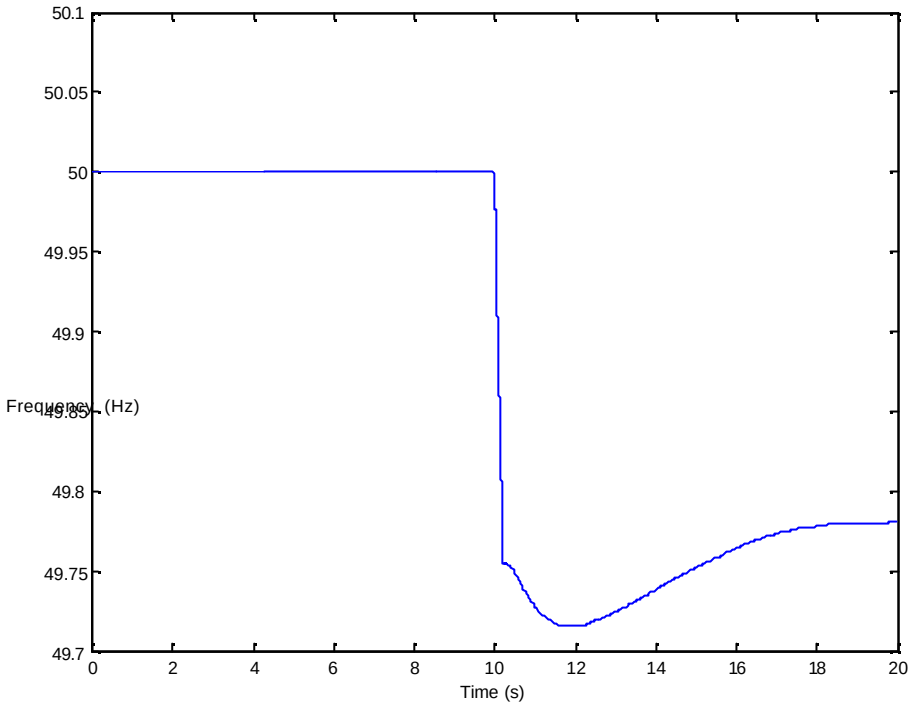

Fig. 8 – MicroGrid frequency for a F1 fault

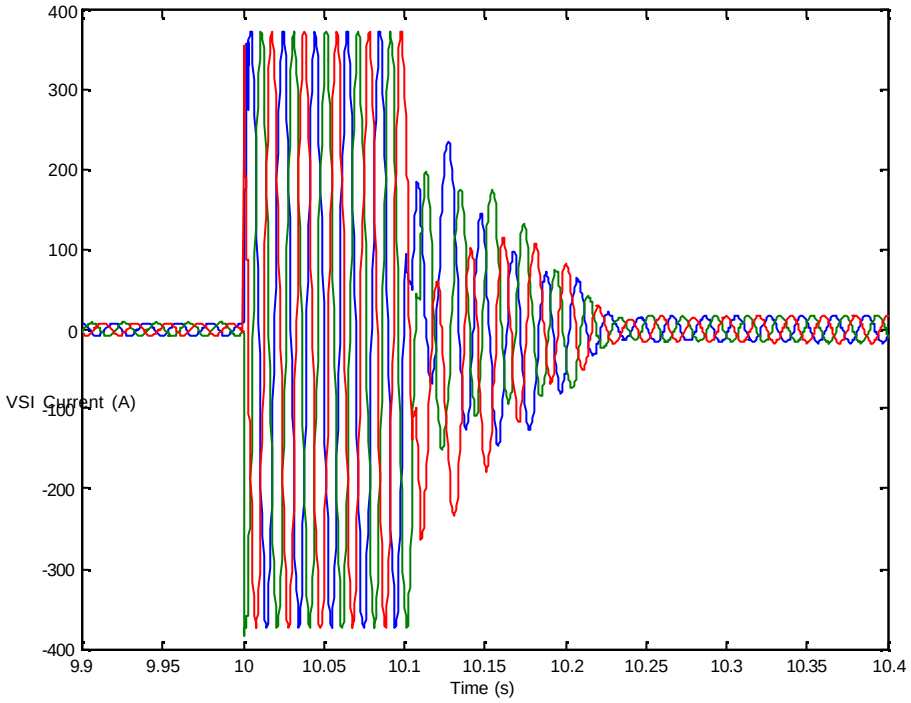

Fig. 9 – VSI current for a F1 fault

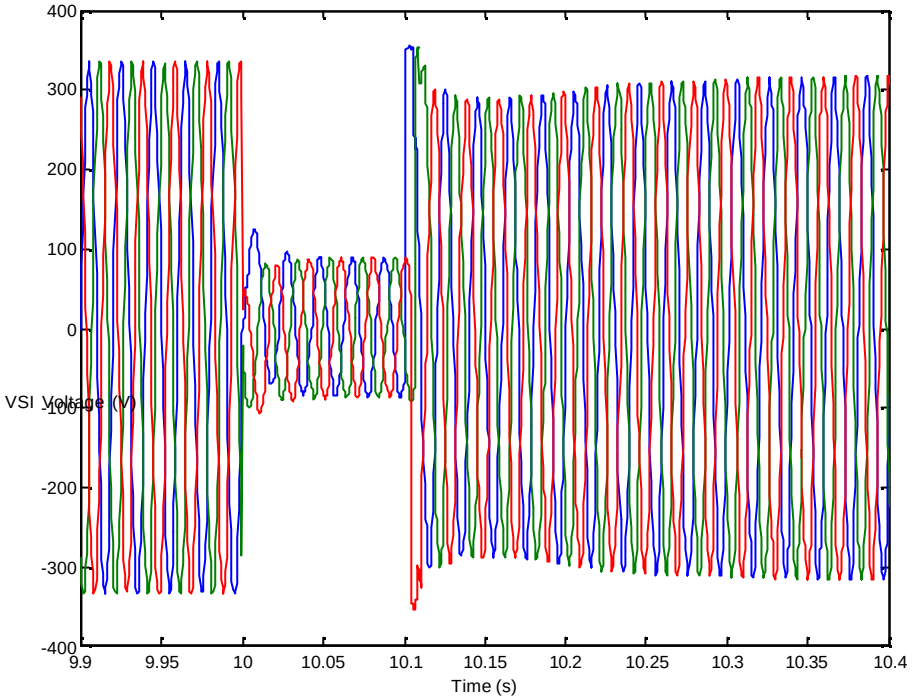

Fig. 10 – VSI voltage for a F1 fault

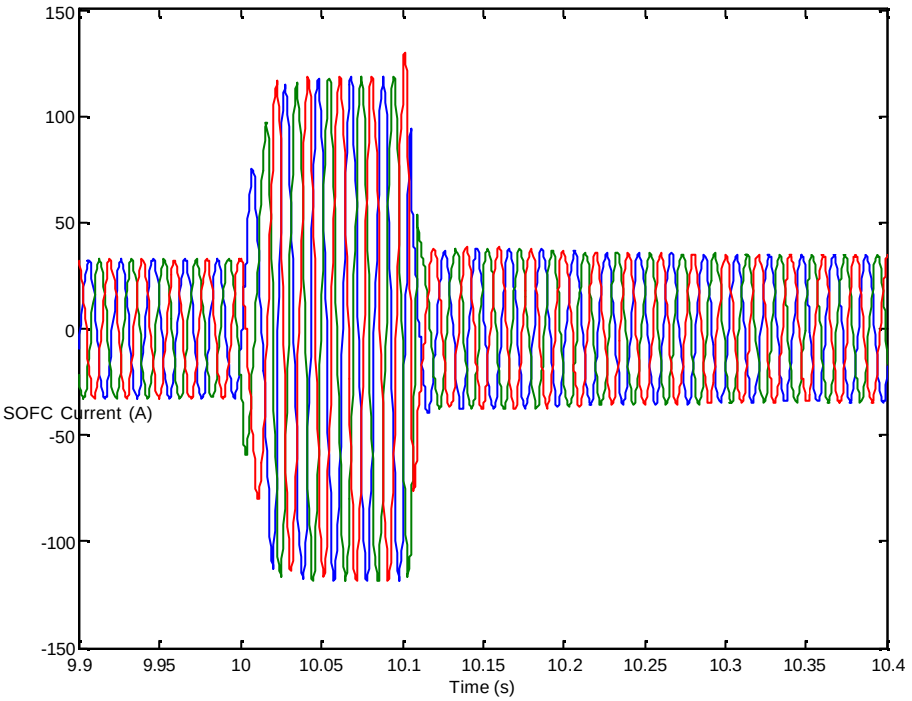

Fig. 11 – SOFC current for a F1 fault

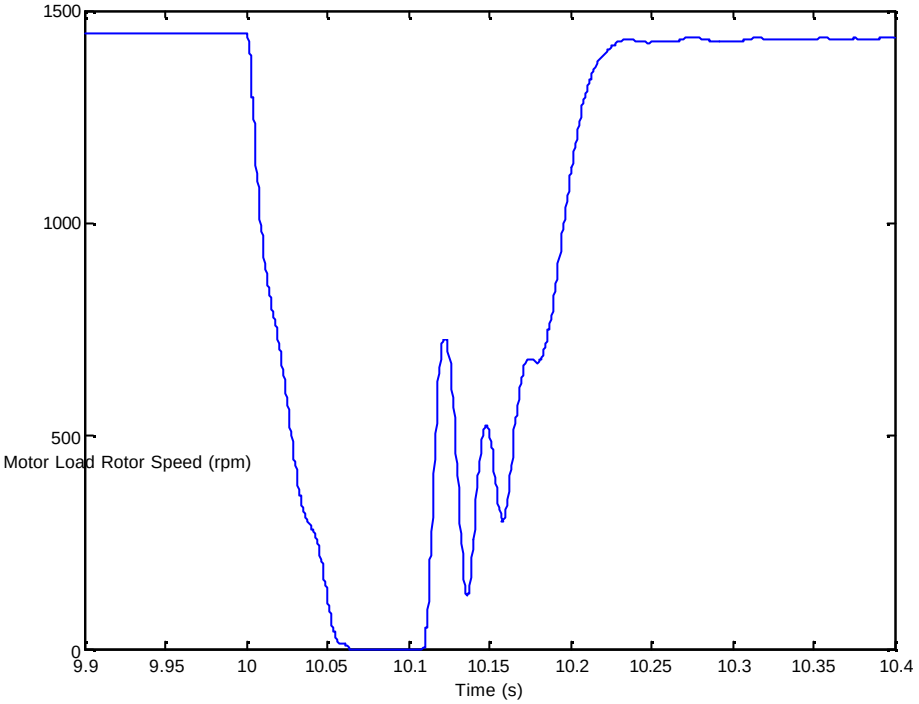

Fig. 12 – Rotor speed of a motor load for a F1 fault

As can be observed, the stability of the MicroGrid is not lost in face of a F1 fault with an elimination time of 100 milliseconds. The frequency (Fig. 8) stabilizes with an offset because secondary control was not yet activated. It can be noticed that, even though stability is preserved, the rotation speed of the motor loads drops leading to the stall of the motors (Fig. 12). The motors will then restart after the fault has been eliminated. Current and voltage waveforms (Fig. 9 and Fig.10, respectively) appear distorted due to the dynamic behaviour of the motor loads during and especially after fault elimination.

The restart of the motor loads is possible even though zero rotation speed is reached due to the speed-torque characteristic of the motors used in this case (data from the *SimPowerSystems* library available in *MatLab*® *Simulink*® was adopted for these motors). This characteristic that can be observed in Fig. 13 is mainly dependent on the size and constructive characteristics of the motors. As can be seen, the electromagnetic torque (Te) is always higher than the mechanical torque (Tm) and therefore the motor is able to restart in any situation.

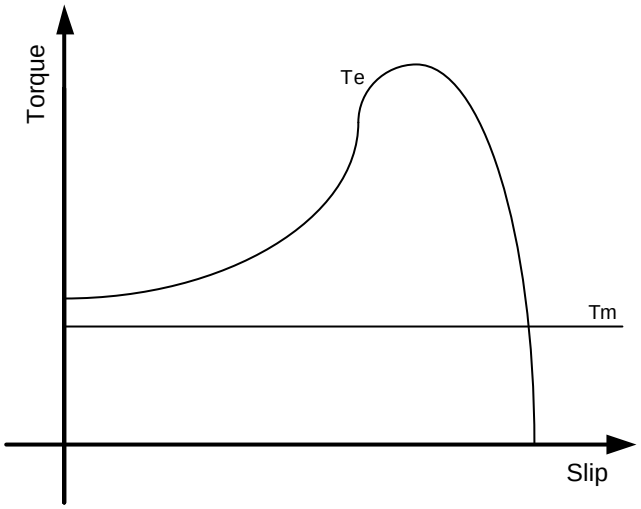

Fig. 13 – Speed-Torque Characteristic of the motor loads used

6.2.2. Fault on the MicroGrid Network

A three-phase fault (F2) is applied at t = 10 seconds. The MicroGrid is operating in islanded mode prior to the fault – Scenario 2. The operating time of protection S2 in the MicroGrid is 100 milliseconds. The simulation results are presented for the main electrical quantities.

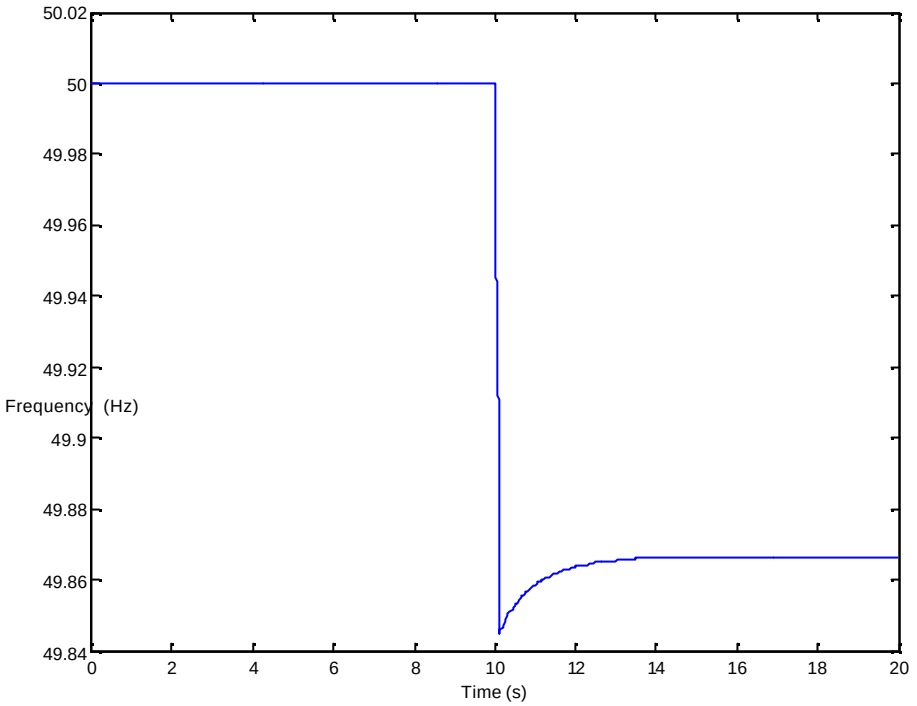

Fig. 14 – MicroGrid frequency for a F2 fault

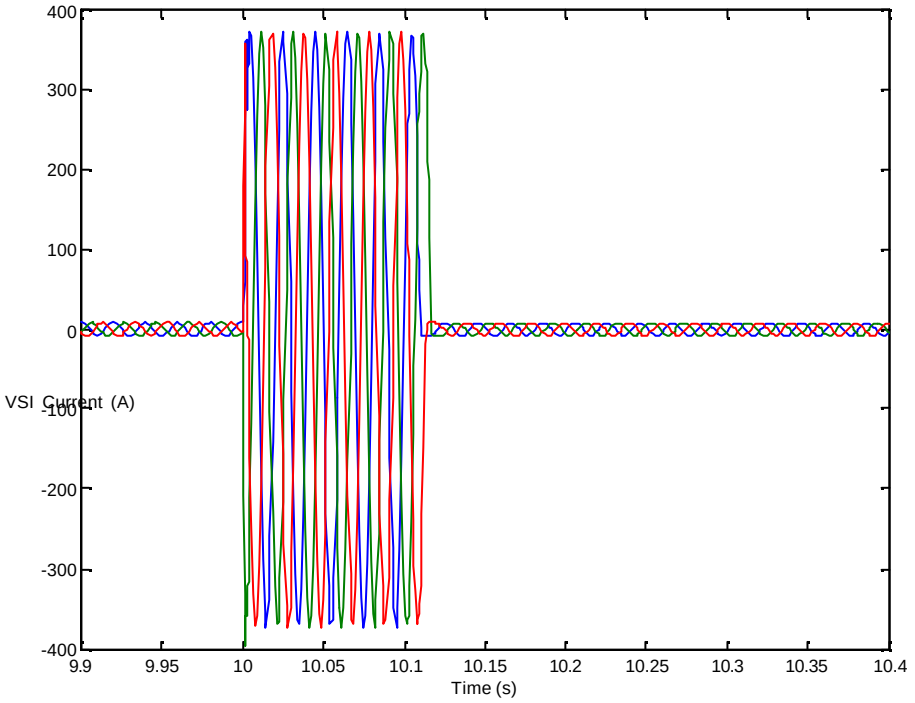

Fig. 15 – VSI current for a F2 fault

As can be seen in Fig. 14 and Fig. 15, the fault did not cause instability to the node where the VSI and the load are connected. The branch of the MicroGrid containing the fault was isolated by the tripping of S2 and all microsources on that branch were safely disconnected.

Another situation was tested, involving a fault near a consumer. For this case, a three-phase fault (F3) is applied at t = 10 seconds. The MicroGrid is operating in islanded mode prior to the occurrence of the fault – Scenario 2. The operating time of the protection located at the load is 100 milliseconds. The main simulation results obtained are presented next.

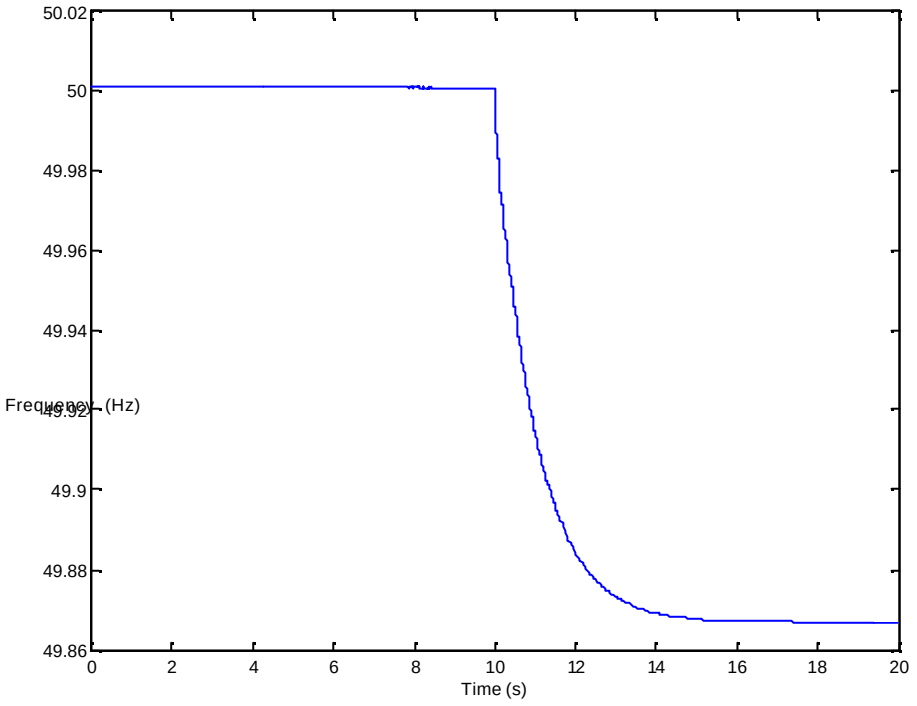

Fig. 16 – MicroGrid frequency for a F3 fault

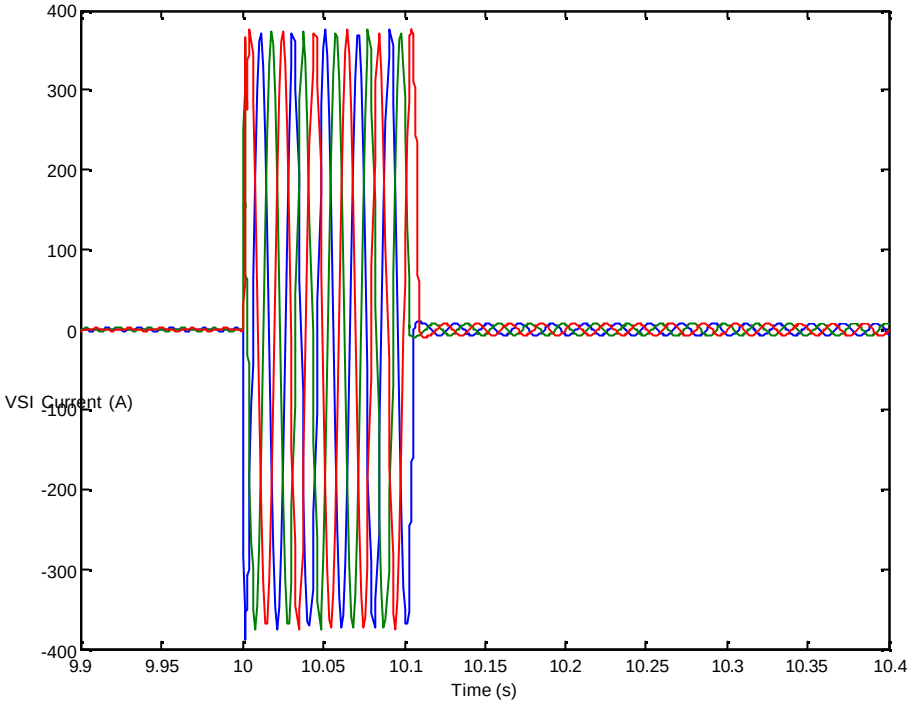

Fig. 17 – VSI current for a F3 fault

As can be seen, the stability of the MicroGrid is not significantly affected by the fault.

6.3. Impact of the Inclusion of Load-Shedding Mechanisms

Load-shedding strategies should be considered as an important resource against severe fault situations. The influence of this control option is confirmed in this section.

The simulation platform used in this section is the same of Section 6.2. A situation considering a F1 fault with an elimination time of 100 milliseconds and Scenario 1 was simulated in order to compare the dynamic behaviour of the MicroGrid with and without the possibility of load-shedding.

Fig. 18 shows the frequency deviation for the two cases: with the action of a load-shedding mechanism and without that possibility.

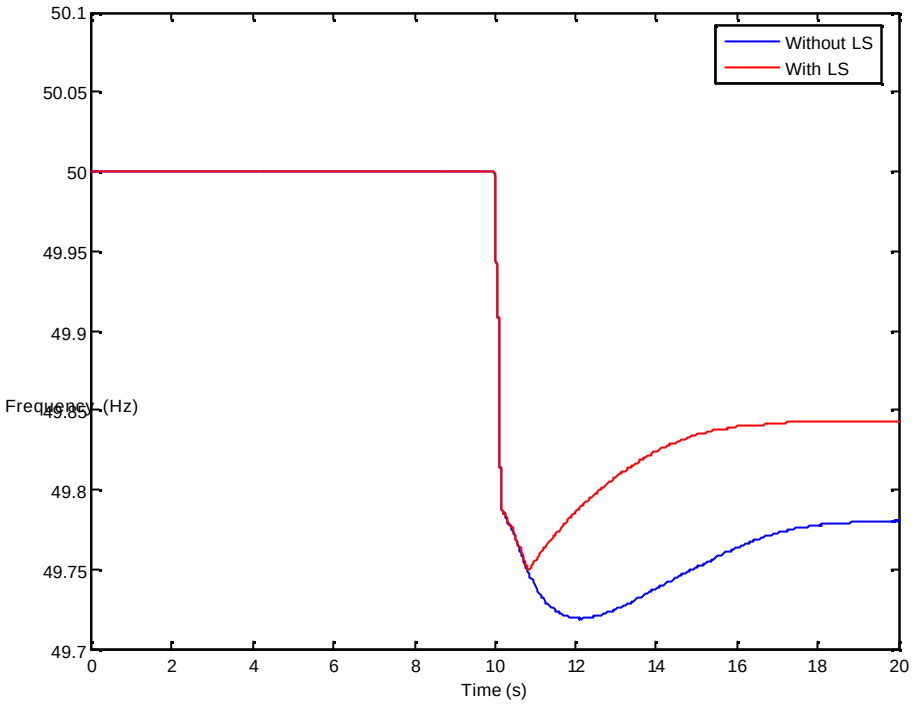

Fig. 18 – Frequency of the MicroGrid with and without Load-Shedding (LS) actions

As it can be observed, there is an improvement on the stability of the MicroGrid when using load-shedding. Using this procedure, it is possible to reduce significantly the frequency deviation caused mainly by the islanding of the MicroGrid after the well-succeeded elimination of the fault. If the load-shedding procedure is furthermore optimized, it will lead to more robust MicroGrid operation.

6.4. Impact of Storage Capacity Sizing

An adequate sizing of the storage capacity can be a decisive issue for maintaining MicroGrid stability after fault occurrence.

The simulation platform used in this section is the same of Section 6.2. A situation based on Scenario 1, considering a F1 fault with an elimination time of 100 milliseconds, was simulated in order to compare the dynamic behaviour of the MicroGrid with two different values of storage capacity of the flywheel system, by adjusting the slope of the frequency droop of the set VSI + flywheel.

Fig. 19 shows the frequency deviation for two cases, considering two different values for the frequency droop of the VSI.

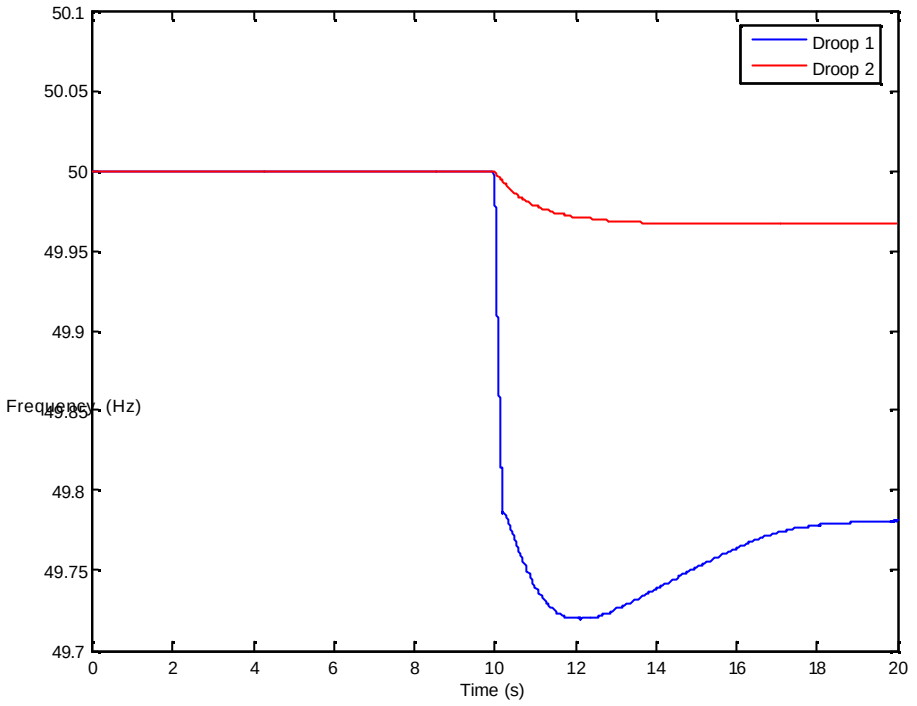

Fig. 19 – Frequency of the MicroGrid for different frequency droop values

The slope of the frequency is given by the following equation:

$$K_p = \frac{\Delta w}{P_{nom}}$$

Where ?? is the frequency deviation admitted and P_{nom} is the nominal active power of the storage device.

In Fig. 19, Droop 1 = 2.094e-4, considering a deviation of 1 Hz; Droop 2 = 2.094e-5, considering a deviation of 0.1 Hz.

A detailed description of the computation of the frequency droop and other VSI parameters can be found in [10].

The figure shows that the frequency deviation can be drastically reduced, acting on the slope of the frequency droop.

Therefore, by combining an adequate sizing of the storage capacity and an efficient load-shedding strategy, it is possible to guarantee a major improvement on the dynamic behaviour of the MicroGrid following the occurrence of faults.

6.5. Impact of Large Fault Clearance Times

Several simulations were performed in order to illustrate the influence of a high percentage of motor loads combined with large fault clearance times on MicroGrid stability.

The simulation platform used in this section is the same of Section 6.2. A situation, using Scenario 1 and considering a F1 fault with several different elimination times, was simulated in order to analyse the dynamic behaviour of the MicroGrid.

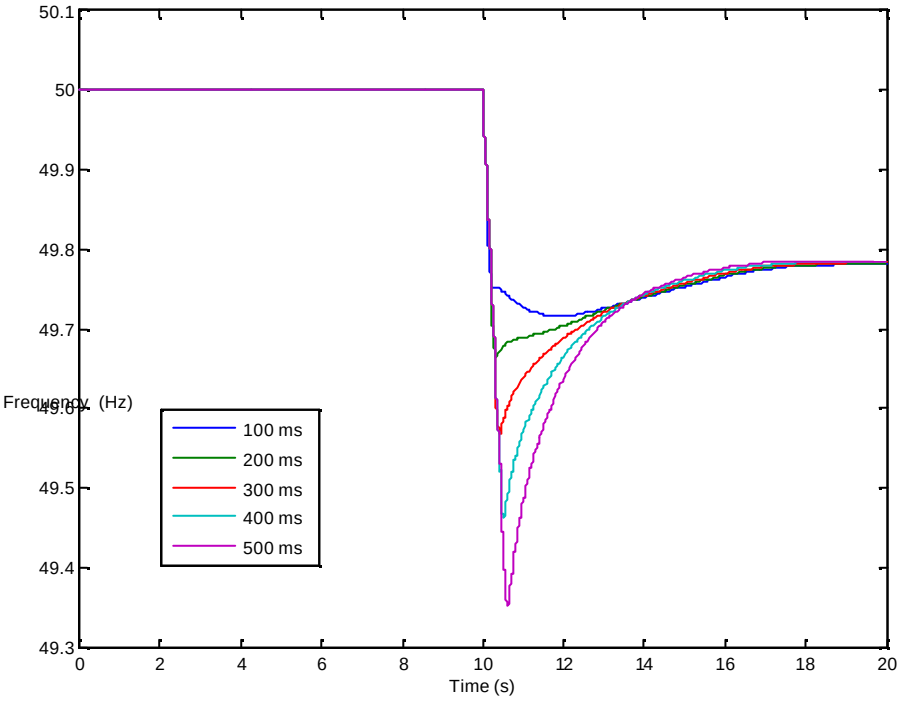

Fig. 20 – Frequency of the MicroGrid for different fault elimination times

It can be observed in Fig. 20 that, considering fault elimination times up to 500 ms, the stability of the MicroGrid is not lost. The maximum frequency deviation observed does not exceed a reference value of 1 Hz.

If the speed-torque characteristic of the motors is not favourable as the one of the motors used in this case, the motors will not be able to have a direct restart and stability would be lost.

6.6. Impact of Fault Resistance

Several simulations were performed in order to show the influence of fault resistance on MicroGrid stability.

The simulation platform used in this section is the same of Section 6.2. A situation, using Scenario 1 and considering a F1 fault with two different values for fault resistance (Rd), was simulated in order to analyse MicroGrid dynamic behaviour.

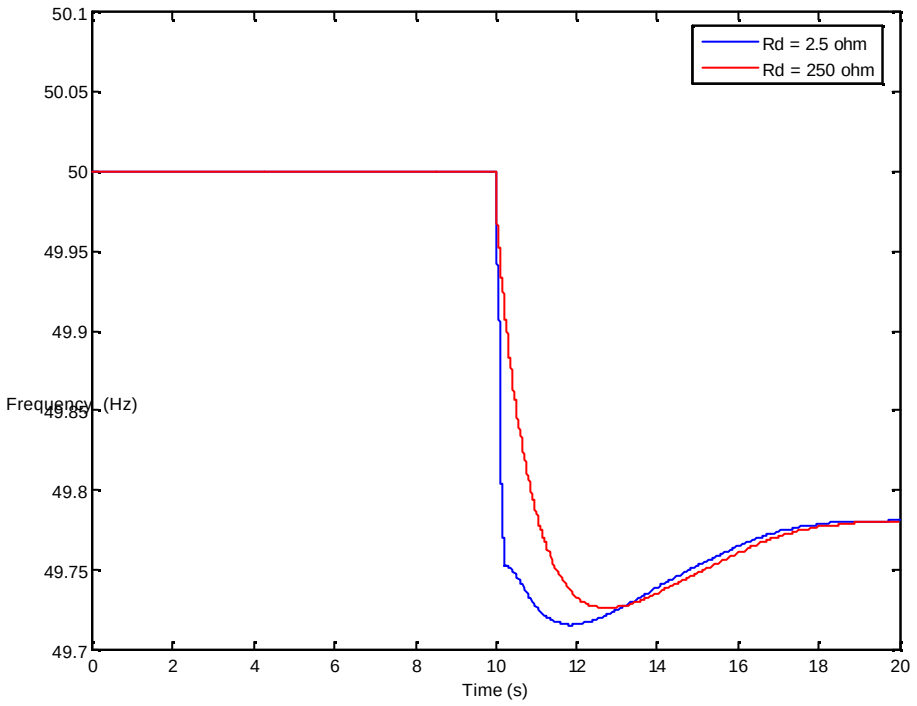

Fig. 21 – Frequency of the MicroGrid for different fault resistance values (Rd)

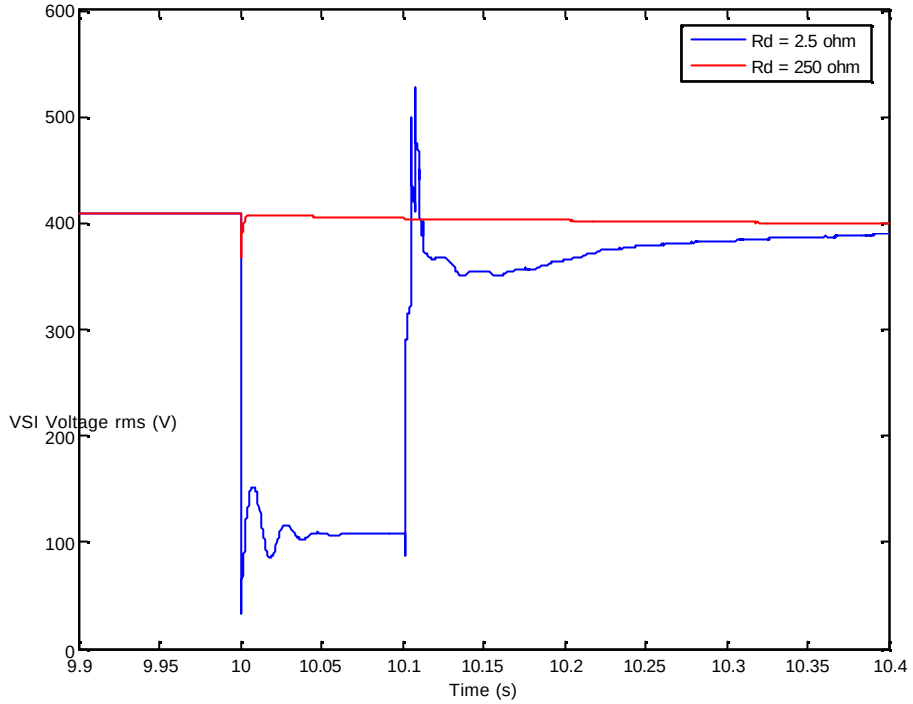

Fig. 22 – VSI voltage for different fault resistance values (Rd)

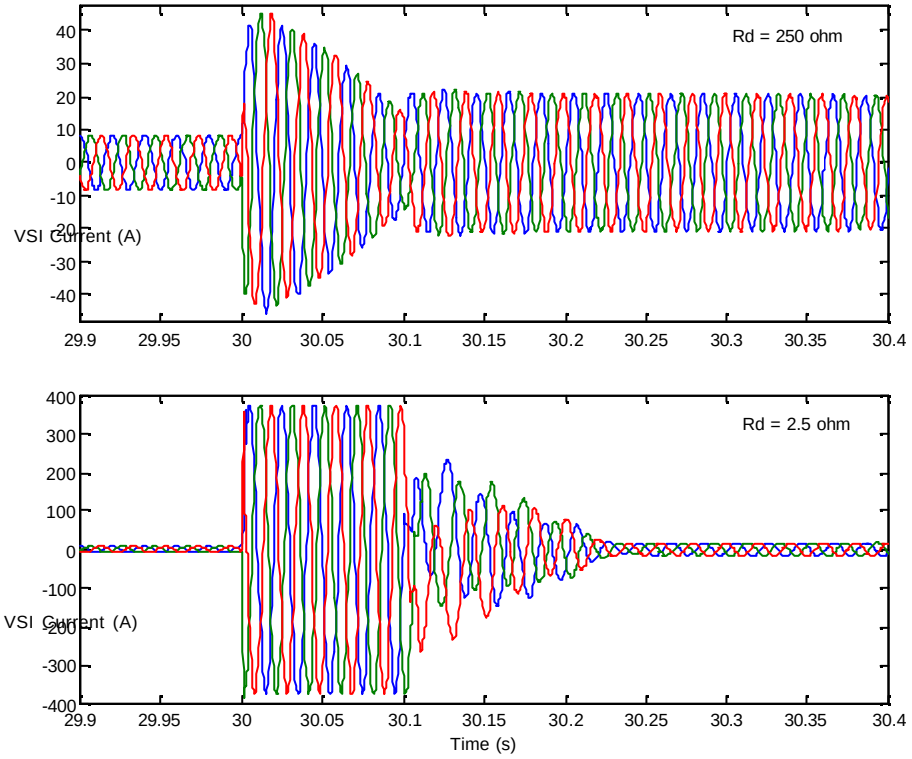

Fig. 23 – VSI current for different fault resistance values (Rd)

It can be observed from Fig. 21 that the frequency fall is much faster considering a small value for the fault resistance, as expected. The amplitude of the frequency deviation, however, is not significantly different.

The voltage drop during the fault was significant for a small value of the fault resistance but almost insignificant for a high value of fault resistance (Fig. 22). The current value is extremely low for a fault with a small resistance value, as can be seen in Fig. 23, endangering an adequate fault detection and elimination.

7. Conclusions

It has been seen that the stability of the MicroGrid is largely influenced by a number of factors, such as:

- The control strategies adopted for the MicroGrid;
- The location of the fault and the operating mode;
- The percentage of motor loads present;
- The inclusion of control strategies such as load-shedding mechanisms;
- The capacity of the storage devices.

Results indicate that a F1 fault appears to be a rather severe fault, not only due to the effects of the fault itself but also due to the islanding of the MicroGrid in order to eliminate the fault. Thus, the severity of the impact on the dynamic behaviour of the MicroGrid is mainly related to the imbalance between generation and consumption at the moment of the islanding procedure.

Results also suggest that a F2 fault with large elimination time endangers the stability of the MicroGrid. This is due to the fact that, when the MicroGrid is already operating in islanded mode, any disturbance can cause large frequency and/or voltage oscillations given the global low inertia of this type of power system.

It has been shown that the implementation of a load-shedding mechanism in the MicroGrid can have a positive impact on the stability of this type of networks.

It has also been shown that a correct sizing of the storage capacity available in the MicroGrid can be very helpful in order to reduce significantly the frequency deviation resulting from the elimination of the fault.

Finally, simulation results suggest that the presence of a large number of motor loads, in particular those with little inertia may be a risk to MicroGrid stability after the occurrence of a fault, especially if the fault elimination time is large.

A recommendation can be issued such that fault elimination must be as fast as possible in order to guarantee MicroGrid stability. However, faults with high resistance

values in the LV network lead to large fault elimination times (due to low short-circuit currents) using fuses, which may provoke stability problems in the MicroGrid.

References

[1] J. Peças Lopes, et al, *DD1 – Emergency Strategies and Algorithms*, MicroGrids project deliverable, 2004

[2] G. Kariniotakis, et al, *DA1 – Digital Models for Microsources*, MicroGrids project deliverable, 2003

[3] S. Barsali; M. Ceraolo, P. Pelacchi, *Control techniques of Dispersed Generators to improve the continuity of electricity supply*, IEEE, 2002

[4] A. Engler, *Regelung von Batteriestromrichtern in modularen und erweiterbaren Inselnetzen*, Ph.D. dissertation, 2002

[5] M. Chandorkar, et al, *Control of Parallel Connected Inverters in Standalone ac Supply Systems*, IEEE Transactions on Industry Applications, Vol. 29, No 1, 1993

[6] N. Jayawarna, et al, *Task TE2 – Fault Current Contribution from Converters*, MicroGrids draft report for task TE2, 2004

[7] R. Lasseter, P. Piagi, *Providing Premium Power through Distributed Resources*, Proc. of the 33rd Hawaiian International Conference on System Science, Vol. 4, 2000

[9] J. Peças Lopes, C. Moreira, A. Madureira, *Defining Control Strategies for Analysing MicroGrids Islanded Operation*, St. Petersburg PowerTech SPPT'05, accepted for publication, 2005

[8] A. Madureira, C. Moreira, J. Peças Lopes, *Secondary Load-Frequency Control for MicroGrids in Islanded Operation*, Proc. of the International Conference on Renewable Energy and Power Quality ICREPQ'05, 2005

[9] A. Engler, et al, *DC1 – Evaluation of the Local Controller Strategies*, MicroGrids project deliverable, 2005